Smithsonian
Scholarly Press

SMITHSONIAN CONTRIBUTIONS TO BOTANY • NUMBER 112

Fortuna Forest Reserve, Panama

Interacting Effects of Climate and Soils on the Biota of a Wet Premontane Tropical Forest

Edited by
James W. Dalling and Benjamin L. Turner

SERIES PUBLICATIONS OF THE SMITHSONIAN INSTITUTION

Emphasis upon publication as a means of “diffusing knowledge” was expressed by the first Secretary of the Smithsonian. In his formal plan for the Institution, Joseph Henry outlined a program that included the following statement: “It is proposed to publish a series of reports, giving an account of the new discoveries in science, and of the changes made from year to year in all branches of knowledge.” This theme of basic research has been adhered to through the years in thousands of titles issued in series publications under the Smithsonian imprint, commencing with Smithsonian Contributions to Knowledge in 1848 and continuing with the following active series:

Smithsonian Contributions to Anthropology
Smithsonian Contributions to Botany
Smithsonian Contributions to History and Technology
Smithsonian Contributions to the Marine Sciences
Smithsonian Contributions to Museum Conservation
Smithsonian Contributions to Paleobiology
Smithsonian Contributions to Zoology

In these series, the Smithsonian Institution Scholarly Press (SISP) publishes small papers and full-scale monographs that report on research and collections of the Institution’s museums and research centers. The Smithsonian Contributions Series are distributed via exchange mailing lists to libraries, universities, and similar institutions throughout the world.

Manuscripts intended for publication in the Contributions Series undergo substantive peer review and evaluation by SISP’s Editorial Board, as well as evaluation by SISP for compliance with manuscript preparation guidelines (available at https://scholarlypress.si.edu). SISP open access publications are licensed under Creative Commons licenses based on copyright status of content. Each is published initially online at https://smithsonian.figshare.com/ScholarlyPress and in print format in limited quantities.

SMITHSONIAN CONTRIBUTIONS TO BOTANY • NUMBER 112

Fortuna Forest Reserve, Panama

Interacting Effects of Climate and Soils on the Biota of a Wet Premontane Tropical Forest

Edited by
James W. Dalling and Benjamin L. Turner

Smithsonian
Scholarly Press
WASHINGTON, D.C.
2021

ABSTRACT

Dalling, James W., and Benjamin L. Turner. Fortuna Forest Reserve, Panama: Interacting Effects of Climate and Soils on the Biota of a Wet Premontane Tropical Forest. *Smithsonian Contributions to Botany*, number 112, x + 302 pages, 66 figures, 23 plates, 125 tables, 2021. — The Fortuna Forest Reserve and adjacent upland areas of the Palo Seco Reserve in western Panama support some of the most extensively studied lower and premontane tropical forests in the world. The forests of Fortuna are among the most diverse in Central America and are therefore of exceptional significance for the preservation of regional biodiversity. This volume brings together more than 50 years of research on the climate, geology, soils, and major plant groups of Fortuna. Spanning the Continental Divide at around 1,000 m above sea level, some parts of the reserve receive more than 6,000 mm of annual rainfall, although there is considerable variation in cloud cover and seasonality. Soil fertility also varies markedly, reflecting the complex regional volcanic geology. The resulting gradients of climate and fertility across the reserve shape the composition, structure, and diversity of plant communities. A network of 12 one-hectare plots at Fortuna contains more than 400 species of trees greater than 5 cm diameter at breast height and reveals extensive compositional turnover across the reserve. One tree species, *Oreomunnea mexicana*, forms monodominant stands in otherwise species-rich forests, while forests on extremely infertile soils are dominated by the canopy palm *Colpothrinax aphanopetala* and include the tropical conifer *Podocarpus oleifolius*. There are also almost 400 species of bryophytes, almost 300 species of ferns and lycophytes, 31 species of palms, 80 species of bromeliads, and more than 200 species of orchids. Many species of ectomycorrhizal fungi identified from fruiting bodies are new to science. Overall, results from Fortuna highlight the remarkable diversity of plants that occur in montane forests and the extent to which their communities are structured by gradients of climate and soil fertility. The chapters in this volume provide a foundation for further research and exploration in this fascinating region.

Cover image: A view across the eastern portion of the Fortuna Forest Reserve from Quijada de Diablo toward Cerro Pata de Macho. Photograph: Cecilia Prada.

Published by SMITHSONIAN INSTITUTION SCHOLARLY PRESS
P.O. Box 37012, MRC 957, Washington, D.C. 20013-7012
https://scholarlypress.si.edu

Library of Congress Control Number: 2020946813

ISSN: 1938-2812 (online); 0081-024X (print)

Publication date (online): 26 March 2021

♾ The paper used in this publication meets the minimum requirements of the American National Standard for Permanence of Paper for Printed Library Materials Z39.48–1992.

Contents

Preface

The Fortuna Reserve and upland portions of the adjacent Palo Seco Protective Reserve in western Panama are among the most studied premontane and montane forests in the world. The reserves range from 700 m to 2,000 m elevation and support perhumid to superhumid aseasonal and seasonal forests on the Caribbean and Pacific slopes of the Continental Divide. The complex geology of these sites, combined with steep local climate gradients, creates a wide range of habitats and exceptional biodiversity. More than 200 studies have been conducted in the reserves, including those associated with an environmental impact study in the 1970s prior to the construction of a dam on the Chiriquí River and the associated creation of Lake Fortuna for hydroelectric power generation. The establishment of the Fortuna reserve in 1976 and the Palo Seco Protected Forest in 1983, coupled with the completion of the David-Chiriquí Grande highway in 1982 and establishment of the Smithsonian Tropical Research Institute Jorge Arauz Field Station in 1996, provides logistical support and unprecedented access to extensive areas of primary forests, representing habitats that have been converted primarily to other land uses elsewhere in the region.

To celebrate the 25th anniversary of the Jorge Arauz Field Station, we bring together information on the climate, geology, soils, and plants that have been studied in the Fortuna area. Although the 19,500 ha Fortuna reserve represents less than 2% of protected area lands in Panama, it harbors approximately a quarter of the country's recorded plant taxa and a relatively intact fauna (Samudio, 2001, 2002). It is therefore essential to the conservation of Panama's biodiversity. In addition to studies of plant and animal taxonomy, systematics, and ecology, Fortuna has been a key site for documenting amphibian die-back resulting from chytrid fungal infection and a natural laboratory for understanding how the loss of amphibian diversity impacts aquatic and terrestrial food webs (e.g., Lips, 1999; Berger et al., 2008; Colón-Gaud et al., 2009).

Fortuna is also one of the only sites in Panama outside the Panama Canal watershed for which long-term ecological and climate data are available. It can therefore play an important role in understanding how plant communities are being altered in response to climate change, and it also has a bearing on the long-term sustainability of hydroelectric energy production in the reserve. Tropical montane forests are predicted to be strongly impacted by changing precipitation regimes as warmer air masses raise the basal elevation of cloud formation. Precipitation regimes can change through a combination of global and regional effects, including conversion of lowland forest to other land uses (e.g., Still et al., 1999; Foster, 2001; van der Molen et al., 2010; Nair et al., 2010). These predicted changes in rainfall and cloud cover are consistent with long-term changes in climate that have already been observed in several Neotropical montane forest sites (Pounds et al., 1999; Barradas et al., 2010). Most recently, region-specific modeling of minimum elevation and humidity for montane cloud forest coverage has predicted that the majority of tropical montane cloud forests will undergo declines in cloud cover in the coming decades, with the greatest severity of declines in the Caribbean and Mesoamerica (Helmer et al., 2019). Detecting early effects of changing cloud regimes on montane forest biota in the face of large interannual variation in rainfall regimes requires long-term monitoring at sites that experience varying seasonal climate conditions such as those on the Caribbean and Pacific slopes in and around Fortuna. In chapter 1, Dalling et al. highlight interannual climate variability for Fortuna based on a 22-year record of rainfall and temperature data collected at the Smithsonian Tropical Research Institute's Jorge Arauz Field Station. They show how rainfall regimes vary over short geographic distances based on records from rain gauges established at a network of 1 ha permanent forest plots distributed through the reserve. Using data from these plots, they also describe the influence of habitat heterogeneity in determining alpha and beta diversity patterns of the tree community. They further review recent work at Fortuna exploring the effects of soil nutrient availability on biogeochemical cycling, ecosystem productivity, and plant performance.

Rainfall patterns reflect variation in topography and exposure that in turn are a consequence of multiple uplift events that have given rise to mountains traversing the north, east, and south of the Fortuna reserve. In chapter 2, Silva et al. describe the geological history of the Fortuna area and present a new geological map of the reserve, including a petrographic description of six major lithological units that outcrop in the area. These consist of gabbro, undifferentiated mafics (an igneous sequence including diabase, basalt, and andesite), pyroclastic flow deposits, quartz-granodiorite, dacite, and vitreous tuff. The distribution of these lithologies provides the most important environmental factor structuring the plant communities present at Fortuna, with particularly notable effects where climate conditions are relatively uniform to the north and east of the Fortuna dam.

Plant species and their associated fauna are expected to undergo upslope migration in response to increases in temperature and solar radiation and a reduction in precipitation resulting from cloud lifting, as has been reported for Andean forests (Fadrique et al., 2018). Successful migration in climate space, however, requires that soils are suitable for plant establishment and growth in newly available habitat. Soils vary markedly at Fortuna, and plant species show strong preferences for sites that vary in nitrogen, phosphorus, base cation availability, and pH. This suggests that climate-driven migration, either by changing temperature or rainfall, might be restricted by soil geography. Nitrogen-limited or colimited forests at Fortuna are also likely to be affected by anthropogenic nitrogen deposition (Phoenix et al., 2006), which is increasing in the tropics (Hietz et al., 2011) and has a disproportionate effect in montane forests because occult deposition from cloud water tends to be elevated in both inorganic and dissolved organic nitrogen relative to rainwater (Vong et al., 1997; Weathers et al., 2000).

In chapter 3, Turner and Dalling review the importance of different state factors (climate, organisms, relief, parent material, and time) on soil development at Fortuna. They highlight the importance of parent material at sites with old (mostly Miocene) substrates and with similar climate and relief. The chapter also provides detailed information on the chemical and physical properties of Fortuna soils and their classification. These data highlight variation in the availability of phosphorus and base cation concentrations, and also illustrate the large organic carbon content of some Fortuna soils, particularly those developed on rhyolitic ash.

Part of the remarkable variation in the composition of plant communities across the Fortuna reserve is related to distinct communities of macrofungi. In chapter 4, Corrales and Ovrebo provide a preliminary list of the fungal taxa of Fortuna based on >1,000 fruiting body collections. The list, composed primarily of Basidiomycota, highlights the presence of diverse groups of ectomycorrhizal (ECM) fungi, which form mutualistic associations with the roots of some tree species, notably those in the Fagales (including the oak and walnut families). Ectomycorrhizal fungi associations benefit their hosts through the acquisition of nutrients from organic sources. In turn, their presence can have ecosystem-level effects on both nitrogen cycling and soil carbon storage (Phillips et al., 2013; Averill et al., 2014). At Fortuna, many ECM species not previously reported from Panama are associated with stands of the locally dominant host tree *Oreomunnea mexicana* (Juglandaceae). The chapter also reviews how differences in soil fertility and rainfall seasonality among stands of *Oreomunnea* trees at Fortuna influence the diversity and composition of ECM fungi, and it describes how long-term nitrogen fertilization in one *Oreomunnea* stand is associated with reduced generic diversity of ECM fungi and declines in species diversity of two key genera: *Russula* and *Cortinarius*. Finally, the authors take a closer look at sequence data from *Russula* collections to illustrate subgeneric diversity and use phylogenetic placement to indicate that most, if not all, of the 40 *Russula* species collected from Fortuna are new to science. Fortuna therefore represents a key unexplored biogeographic region for ECM fungi at the southern limits of the distribution of several host tree species.

A characteristic feature of wet montane forests is a profusion of epiphytic plants associated with high rainfall inputs and frequent cloud cover. In addition to being strongly influenced by the microclimatic conditions that determine their water balance, epiphytes can in turn influence forest hydrology by trapping cloud water that otherwise would not enter the watershed (Veneklaas et al., 1990; Tobón et al., 2010). There is a long history of research on forest hydrology and epiphyte community structure, physiology, and water use at Fortuna (Cavelier, 1996, 1997; Lange, 1994; Zotz, 1997). In chapter 5, Salazar Allen et al. synthesize information from bryophyte collections at Fortuna initiated prior to the construction of the hydroelectric dam in the 1970s. The Fortuna bryophyte community is remarkably species rich, containing 164 genera and a third of the bryophyte species reported from Panama. The chapter also provides detailed descriptions of the broader habitat distributions and biogeographic origins of the Fortuna species assemblage, highlighting continuous migration of taxa from north and south temperate as well as Neotropical origins.

The water retention capacity of epiphytes, much of which is driven by bryophytes, is explored experimentally in chapter 6 by Gómez-Gónzalez et al. The authors quantify the water-holding capacity of epiphytes by extrapolating measurements on 22 tree trunks and 28 canopy branches to the whole-stand level using plot inventories of tree diameters and densities. The estimated total capacity of epiphytic matter of 25,000 L ha^{-1} (2.5 mm rainfall) is largely due to dead organic matter. Nonetheless, bryophytes are responsible for nearly 30% of this capacity despite contributing only 6% of epiphytic matter. Although water retention by epiphytes is small relative to annual rainfall at Fortuna, interception may be important during the dry season and may redirect nutrient fluxes that are otherwise captured by trees via stemflow.

Orchids represent another important component of the epiphyte community at Fortuna. The orchid flora of Panama is particularly species rich (1,432 species), with a substantial fraction (18%) reported from Fortuna. In chapter 7, Silvera discusses the generic composition of the Fortuna orchid flora and uses analyses of tissue total carbon and nitrogen content and their isotopic signatures to provide insight into their photosynthetic pathways and sources of nitrogen.

While orchids and bryophytes are conspicuous components of the epiphyte flora at Fortuna, the forest understory is typically dominated by short-stature palms and ferns. In chapter 8, Viana and Dalling describe the fern and lycophyte flora of Fortuna, consisting of 289 species. They use extensive environmental data to determine which resources underlie the observed habitat associations of the terrestrial taxa, and they highlight the strong concordance between fern composition and parent material. In turn, habitat associations reflect differences in soil conditions (notably phosphorus availability) as well as light availability. Although species richness for terrestrial ferns is highest on intermediate-fertility soils developed on mafic-volcanics, low fertility sites developed on rhyolitic ash are especially important for maintaining tree fern populations.

Palms are the best-studied plant group at Fortuna. The reserve is a diversity hotspot for two tribes: Chamaedoreae and Geonomateae. In chapter 9, Andersen reviews a series of observational and experimental studies that go beyond delineating habitat associations to assess the importance of a constellation of physiological and whole-plant traits, including photosynthetic nutrient-use efficiency, biomass allocation to leaves, herbivory rate, and nitrogen uptake rate that determine performance differences of species associated with sites that differ in soil fertility.

In summary, Fortuna provides an outstanding laboratory to explore the ecological underpinnings of plant performance and distribution. Fortuna and adjacent upland sections of the Palo Seco Protected Forest offer access to areas of species-rich primary forest that have developed on habitats with contrasting climate regimes and with soils that are remarkably variable in fertility. As forest communities respond to climate change, long-term monitoring of plant and animal communities across the range of habitats at Fortuna will reveal the importance of abiotic and biotic factors influencing population growth, as well as the barriers and filters to species migration. We hope that the detailed studies of the flora of Fortuna, and its environmental context described in this volume will provide a baseline to support this endeavor.

James W. Dalling
Department of Plant Biology
University of Illinois at Urbana-Champaign
USA

Benjamin L. Turner
Smithsonian Tropical Research Institute
Apartado 0843-03092, Balboa
Ancón, Republic of Panama

References

Averill, C., B. L. Turner, and A. C. Finzi. 2014. Mycorrhiza-mediated Competition between Plants and Decomposers Drives Soil Carbon Storage. *Nature*, 505:543–545. https://doi.org/10.1038/nature12901

Barradas V. L., J. Cervantes-Pérez, R. Ramos-Palacios, C. Puchet-Anyul, P. Vázquez-Rodriguez, and R. Granados-Ramirez. 2010. Meso-scale Climate Change in the Central Mountain Region of Veracruz State, Mexico. In *Tropical Montane Cloud Forest: Science for Conservation and Management*, ed. L. Bruijnzeel, F. Scatena, and L. Hamilton, pp. 549–556. Cambridge: Cambridge University Press.

Berger, L., R. Speare, P. Daszak, D. E. Green, A. A. Cunningham, C. L. Goggin, and H. Parkes. 1998. Chytridiomycosis Causes Amphibian Mortality Associated with Population Declines in the Rain Forests of Australia and Central America. *Proceedings of the National Academy of Sciences*, 95:9031–9036. https://doi.org/10.1073/pnas.95.15.9031

Cavelier, J., D. Solis, and M. A. Jaramillo. 1996. Fog Interception in Montane Forest Across the Central Cordillera of Panama. *Journal of Tropical Ecology*, 12:357–369. https://doi.org/10.1017/S026646740000955X

Cavelier, J., M. A. Jaramillo, D. Solis, and D. De León. 1997. Water Balance and Nutrient Inputs in Bulk Precipitation in Tropical Montane Cloud Forest in Panama. *Journal of Hydrology*, 193:83–96. https://doi.org/10.1016/S0022-1694(96)03151-4

Colón-Gaud, C., M. R. Whiles, S. S. Kilham, K. R. Lips, C. M. Pringle, S. Connelly, and S. D. Peterson. 2009. Assessing Ecological Responses to Catastrophic Amphibian Declines: Patterns of Macroinvertebrate Production and Food Web Structure in Upland Panamanian Streams. *Limnology and Oceanography*, 54:331–343. https://doi.org/10.4319/lo.2009.54.1.0331

Fadrique, B., S. Báez, A. Duque, A. Malizia, C. Blundo, J. Carilla, O. Osinga-Acosta, L. Malizia, M. Silman, W. Farfan-Ríos, Y. Malhi, K. R. Young, C. Francisco Cuesta, J. Homeier, M. Peralvo, E. Pinto, O. Jadan, N. Aguirre, Z. Aguirre, and K. J. Feeley. 2018. Widespread but Heterogeneous Responses of Andean Forests to Climate Change. *Nature*, 564:207–212. https://doi.org/10.1038/s41586-018-0715-9

Foster, P. 2001. The Potential Negative Impacts of Global Climate Change on Tropical Montane Cloud Forests. *Earth-Science Reviews*, 55:73–106. https://doi.org/10.1016/S0012-8252(01)00056-3

Helmer, E. H., E. A. Gerson, L. S. Baggett, B. J. Bird, T. S. Ruzycki, and S. M. Voggesser. 2019. Neotropical Cloud Forests and Páramo to Contract and Dry from Declines in Cloud Immersion and Frost. *PLOS One*, 14:e0213155. https://doi.org/10.1371/journal.pone.0213155

Hietz, P., B. L. Turner, W. Wanek, A. Richter, C. A. Nock, and S. J. Wright. 2011. Long-term Change in the Nitrogen Cycle of Tropical Forests. *Science*, 334:664–666. https://doi.org/10.1126/science.1211979

Lange, O. L., B. Büdel, H. Zellner, G. Zotz, and A. Meyer. 1994. Field Measurements of Water Relations and CO_2 Exchange of the Tropical, Cyanobacterial Basidiolichen *Dictyonema glabratum* in a Panamanian Rainforest. *Botanica Acta*, 107:279–290. https://doi.org/10.1111/j.1438-8677.1994.tb00797.x

Lips, K. R. 1999. Mass Mortality and Population Declines of Anurans at an Upland Site in Western Panama. *Conservation Biology*, 13:117–125. https://doi.org/10.1046/j.1523-1739.1999.97185.x

Nair, U. S., D. K. Ray, R. O. Lawton, R. M. Welch, R. A. Pielke Sr., and J. Calvo. 2010. The Impact of Deforestation on Orographic Cloud Formation in a Complex Tropical Environment. In *Tropical Montane Cloud Forest: Science for Conservation and Management*, ed. L. Bruijnzeel, F. Scatena, and L. Hamilton, pp. 538–548. Cambridge: Cambridge University Press.

Phillips, R. P., E. Brzostek, and M. G. Midgley. 2013. The Mycorrhizal-Associated Nutrient Economy: A New Framework for Predicting Carbon–Nutrient Couplings in Temperate Forests. *New Phytologist*, 199:41–51. https://doi.org/10.1111/nph.12221

Phoenix, G. K., W. K. Hicks, S. Cinderby, J. C. I. Kuylenstierna, W. D. Stock, F. J. Dentener, K. E. Giller, A. T. Austin, R. D. B. Lefroy, R. Ashmore, and P. Ineson. 2006. Atmospheric Nitrogen Deposition in World Biodiversity Hotspots: The Need for a Greater Global Perspective in Assessing N Deposition Impacts. *Global Change Biology*, 12:470–476. https://doi.org/10.1111/j.1365-2486.2006.01104.x

Pounds, J. A., M. P. L. Fogden, and J. H. Campbell. 1999. Biological Response to Climate Change on a Tropical Mountain. *Nature*, 398:611. https://doi.org/10.1038/19297

Samudio, Jr., R. 2001. Los Bosques Nublados de Panamá [The cloudy forests of Panama]. In *Bosques Nublados del Neotrópico* [Neotropic cloud forests], ed. M. Kapelle and A. Brown, pp. 371–395. Santo Domingo de Heredia, Costa Rica: Editorial INBio.

Samudio, Jr., R. 2002. Mamíferos de Panamá [Mammals of Panama]. In *Diversidad y Conservación de los Mamíferos Neotropicales* [Diversity and conservation of Neotropical mammals], ed. G. Ceballos and J. Simonetti, pp. 415–452. Mexico City: CONABIO-Instituto de Ecología.

Still, C. J., P. N. Foster, and S. H. Schneider. 1999. Simulating the Effects of Climate Change on Tropical Montane Cloud Forests. *Nature*, 389:608–610. https://doi.org/10.1038/19293

Tobón, C., L. Köhler, K. F. A. Frumau, L. A. Bruijnzeel, R. Burkard, and S. Schmid. 2010. Water Dynamics of Epiphytic Vegetation in a Lower Montane Cloud Forest: Fog Interception, Storage, and Evaporation. In *Tropical Montane Cloud Forests: Science for Conservation and Management*, ed. L. Bruijnzeel, F. Scatena, and L. Hamilton, pp. 261–267. Cambridge: Cambridge University Press.

Van der Molen, M. K., H. F. Vugts, L. A. Bruijnzeel, F. N. Scatena, R. A. Pielke Sr., and L. J. M. Kroon. 2006. Meso-scale Climate Change due to Lowland Deforestation in the Maritime Tropics. In *Tropical Montane Cloud Forests: Science for Conservation and Management*, ed. L. Bruijnzeel, F. Scatena, and L. Hamilton, pp. 527–537. Cambridge: Cambridge University Press.

Veneklaas, E. J., and R. Van Ek. 1990. Rainfall Interception in Two Tropical Montane Rain Forests, Colombia. *Hydrological Processes*, 4:311–326. https://doi.org/10.1002/hyp.3360040403

Vong, R. J., B. M. Baker, F. J. Brechtel, R. T. Collier, J. M. Harris, A. S. Kowalski, N. C. McDonald, and L. M. McInnes. 1997. Ionic and Trace Element Composition of Cloud Water Collected on the Olympic Peninsula of Washington State. *Atmospheric Environment*, 31:1991–2001. https://doi.org/10.1016/S1352-2310(96)00337-8

Weathers, K. C., G. M. Lovett, G. E. Likens, and N. F. M. Caraco. 2000. Cloudwater Inputs of Nitrogen to Forest Ecosystems in Southern Chile: Forms, Fluxes and Sources. *Ecosystems*, 3:590–595. https://doi.org/10.1007/s100210000051

Zotz, G., B. Büdel, A. Meyer, H. Zellner, and O. L. Lange. 1997. Water Relations and CO_2 Exchange of Tropical Bryophytes in a Lower Montane Rainforest in Panama. *Botanica Acta* 110:9–17. https://doi.org/10.1111/j.1438-8677.1997.tb00605.x

Acknowledgments

This volume is dedicated to Jorge Luis Araúz (1957–1989), forestry graduate from the University of Panama and the first proponent of research on the use of native species for restoration at Fortuna. He was responsible for the establishment of the Fortuna research station, known as the Centro de Investigaciones Jorge Luis Araúz, which provides an essential base for scientific research, education, and training in the Fortuna Forest Reserve. We thank the Smithsonian Tropical Research Institute (STRI) and Enel Green Power Panama (EGPP) for critical logistic and financial support that has enabled long-term ecological research at Fortuna. In particular, we appreciate the extraordinary dedication of Carlos Espinosa, manager of the Jorge Luis Araúz Field Station, in facilitating research, and Steve Paton for maintaining long-term Fortuna climate data. We are also grateful for the hard work and support of Alberto González, the efforts of many students and interns who have contributed to collection of data presented here, and Professor Pedro Caballero for facilitating collaborations with the Universidad Autónoma de Chiriquí. Finally, we thank a number of anonymous reviewers who provided detailed critical comments on the chapters.

1. Introduction to the Fortuna Forest Reserve: Soil and Climate Effects on the Tree Communities of a Premontane Tropical Forest

James W. Dalling,[1,2] Cecilia M. Prada,[1] Katherine D. Heineman,[1]*
Kelly M. Andersen,[3] Arturo Morris,[4] Juliana Pardo,[1] Emily Hollenbeck,[5]
Pedro Caballero,[4] Carlos Espinosa,[2] Evidelio García,[1] and Benjamin L. Turner[2]

ABSTRACT. The 19,500 ha Fortuna Forest Reserve and adjacent upland portions of the 167,000 ha Palo Seco Forest Reserve are exceptionally well-preserved examples of lower montane and premontane rainforest. Over the last 50 years, this has been an area of extensive botanical research, resulting in detailed locality information for ~20% of Panama's flora. Nonetheless, the true biological diversity of the reserve is likely underestimated, because 40% of the tree species recorded in inventories of just 12 one-hectare plots were not reported in previous surveys. The high plant diversity reflects remarkable habitat diversity. Fortuna experiences heterogeneous rainfall regimes distributed across an array of geologic substrates, resulting in contrasting physical and chemical properties of soil and an almost complete turnover in tree species composition across sites <15 km apart. Over the last decade, Fortuna has emerged as a key site for understanding how nutrient limitation impacts species distributions and ecosystem processes. Ongoing activities include measurements of climate, soils, carbon stocks, forest growth, and plant species composition; plant–fungal interactions; and the impacts of long-term nitrogen addition on forest productivity. We describe the physical environmental setting of Fortuna and the principal plant community types associated with (1) infertile rhyolite tuff (*Colpothrinax* forest), (2) a monodominant ectomycorrhizal tree (*Oreomunnea* forest), and (3) the most widespread parent material (mafic-volcanic forest). Finally, we review recent work at Fortuna that has begun to reveal the impact of nitrogen availability on biogeochemical cycling and ecosystem productivity (the NITROF nitrogen addition experiment), and phosphorus effects on plant performance using seedling transplant and phosphorus addition experiments.

GENERAL INFORMATION ABOUT THE RESERVE

Location, Topography, and Geology

The 19,500 ha Fortuna Forest Reserve (8°42′N, 82°12′W) is located north of the province of Chiriquí in western Panama (Figure 1.1). The adjacent 167,000 ha Palo Seco Forest Reserve forms the northern border of the Fortuna reserve along the Continental Divide and covers the upper elevations of the Caribbean slope from ~200 to 2,000 m above sea level (asl). The Holdridge (1967) life zones in the Fortuna reserve and upper elevations of Palo Seco include perhumid to superhumid premontane forest (700–1,000 m asl) and lower montane forest (1,000–2,000 m), as well as small areas of perhumid montane forest (>2,000 m). The northern boundary of the Fortuna reserve, located along the Continental Divide, has a maximal elevation of 1,920 m

---

[1] Department of Plant Biology, University of Illinois at Urbana-Champaign, 265 Morrill Hall, 505 S. Goodwin Ave, Urbana, IL 61801, USA.
[2] Smithsonian Tropical Research Institute, Apartado 0843-03092, Balboa, Ancon, Republic of Panama.
[3] Asian School of the Environment, Nanyang Technological University, Singapore.
[4] Universidad Autónoma de Chiriquí, Calle de la UNACHI, David, Republic of Panama.
[5] Department of Ecology and Evolutionary Biology, Brown University, Providence, RI 02912, USA.
* Correspondence: dalling@illinois.edu

Manuscript received 18 May 2020; accepted 8 September 2020

(Cerro Guayabo) in the northwestern corner of the reserve. Two other mountain ridges inside the Fortuna reserve extend north from Cerro Hornito in the south of the reserve and to the northeast of reserve to include sections of Cerro Chorcha (2,200 m), and Cerro Pata de Macho (1,960 m; Plate 1.1). These mountain ranges are composed of diverse volcanic rocks including andesite, rhyolitic tuff, porphyritic dacite, basalt, and granodiorite (Instituto de Recursos Hidraulicos y Electrificacion [IRHE], 1975; Silva et al., this volume).

The main highway linking the Caribbean and Pacific coasts of Panama runs through the Fortuna and Palo Seco reserves, crossing over the Edwin Fabrega Dam. The road provides access to multiple watersheds containing old-growth forests that drain into Lake Fortuna. Unpaved roads provide access to forest along the Continental Divide between the Fortuna and Palo Seco reserves and west of the dam on the slopes of Cerro Pinola (Plate 1.1). The Smithsonian Tropical Research Institute maintains a field station (the Jorge L. Araúz Field Station; Plate 1.1) inside the Fortuna reserve, close to a main highway, and a set of permanent forest monitoring plots has been established to sample vegetation and soils on contrasting geology at accessible sites in both Fortuna and Palo Seco (Figure 1.1).

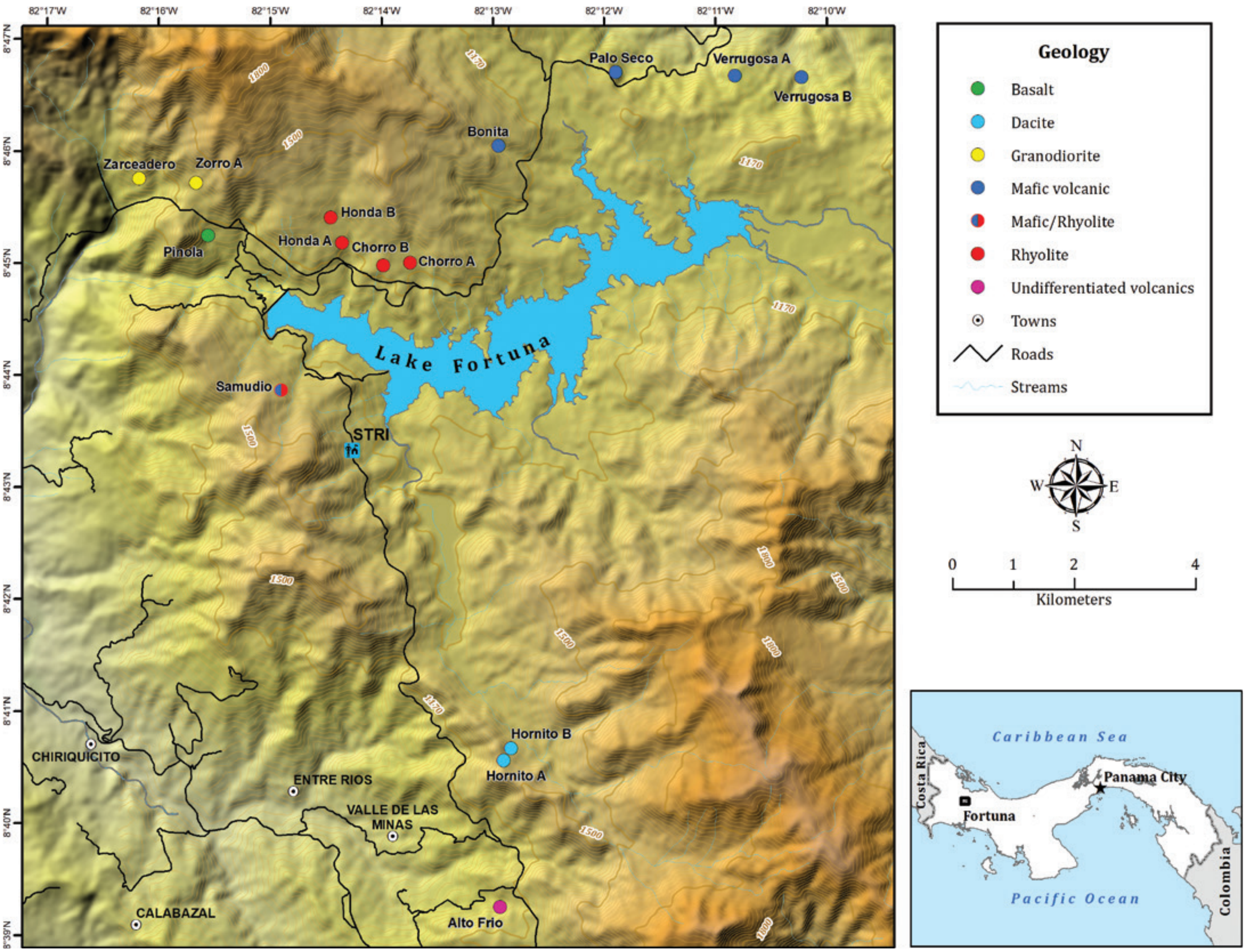

FIGURE 1.1. Location of the Fortuna Forest Reserve in western Panama. Points indicate the locations of permanent forest dynamics plots established between 2003 and 2018 on different parent materials and of the Smithsonian Tropical Research Institute (STRI) Jorge L. Araúz field station. Palo Seco and Verrugosa A and B plots are on the Caribbean slope in Palo Seco Forest Reserve. The Alto Frio plot is on private land on the Pacific slope.

Climate Regime

The complex topography of Fortuna yields locally variable climate regimes (Table 1.1) as well as substantial interannual and intra-annual variation in rainfall and cloud cover. Mean annual maximum temperature from 1997 through 2018 at the Jorge Araúz station varied between 22.3°C and 27.9°C, and mean minimum temperature varied between 15.2°C and 16.6°C (Figure 1.2a), with absolute maximum and minimum recorded temperatures of 36.0°C and 11.0°C respectively. There has been no significant trend of increasing temperature over the last 20 years (Figure 1.2b). Differences in mean annual temperature across a network of permanent plot sites measured from August 2012 to April 2013 were small (17.1°C–19.9°C; Table 1.1).

TABLE 1.1. Climate variables for permanent forest plots in the Fortuna and Palo Seco Forest Reserves (underlying parent material in parentheses). Elev = elevation. MAT = mean annual temperature, measured in the understory from Aug 2012 to Apr 2013. MAP = mean annual precipitation (±1 SE) and DSP = dry season precipitation (1 Jan–30 Apr), measured 2007–2009 and 2011–2014 (Prada et al., 2017). Cloud = mean annual percent probability of midday cloud cover based on 15 years of MODIS imagery (Wilson and Jetz, 2016). W-MAT = WaterWorld model-derived annual temperature. W-Fog = WaterWorld-derived total fog-derived moisture inputs. W-Rain = WaterWorld-derived total water budget. Dash (—) = no data.

Site (Geology)	Lat Long	Elev (m)	MAT (C)	MAP (mm)	DSP (mm)	Cloud (%)	W-MAT (C)	W-Fog (mm)	W-Rain (mm)
Chorro A (Rhyolite)	8.749 –82.229	1,100	17.7	5,507 ±247	351 ±53	96.6	18.7	129	3,015
Chorro B (Rhyolite)	8.749 –82.232	1,240	—	—	—	95.6	18.6	207	3,197
Honda A (Rhyolite)	8.751 –82.239	1,155	18.2	6,255 ±962	381 ±51	96.6	18.5	135	2,897
Honda B (Rhyolite)	8.756 –82.243	1,240	17.9	6,159 ±617	332 ±34	96.6	18.5	206	3,035
Samudio (Rhy/Mafic)[a]	8.731 –82.248	1,215	17.9	4,833 ±219	215 ±30	94.3	16.4	180	2,791
Bonita (Mafic)	8.767 –82.215	1,300	—	—	—	98.3	18.0	131	2,507
Palo Seco (Mafic)	8.778 –82.198	880	19.6	6,257 ±310	445 ±33	96.4	18.6	256	3,884
Verrugosa A (Mafic)	8.778 –82.180	970	—	—	—	95.5	18.7	268	3,616
Verrugosa B (Mafic)	8.777 –82.170	850	—	—	—	95.3	18.7	324	3,733
Pinola (Basalt)	8.754 –82.259	1,135	18.5	4,964[e] ±863	159[e] ±27	91	18.4	117	2,790
Hornito A (Dacite)	8.674 –82.214	1,330	17.2	5,164 ±232	203 ±28	87.5	18.4	274	3,775
Alto Frio (Undiff.)[b]	8.654 –82.215	1,100	—	4,641[e] ±623	94[e] ±27	83.8	18.6	268	3,464
Zorro A (Grano.)[c]	8.760 –82.262	1,249	—	—	—	95.7	18.6	180	2,897
Araúz[d] (-)	8.722 –82.237	1,218	—	4,445 ±427	186 ±28	94.5	17.1	238	2,725

[a] Rhyolite to mafic-volcanic transition.

[b] Undifferentiated volcanics.

[c] Granodiorite.

[d] STRI Jorge Araúz field station.

[e] Data available only from 2013–14.

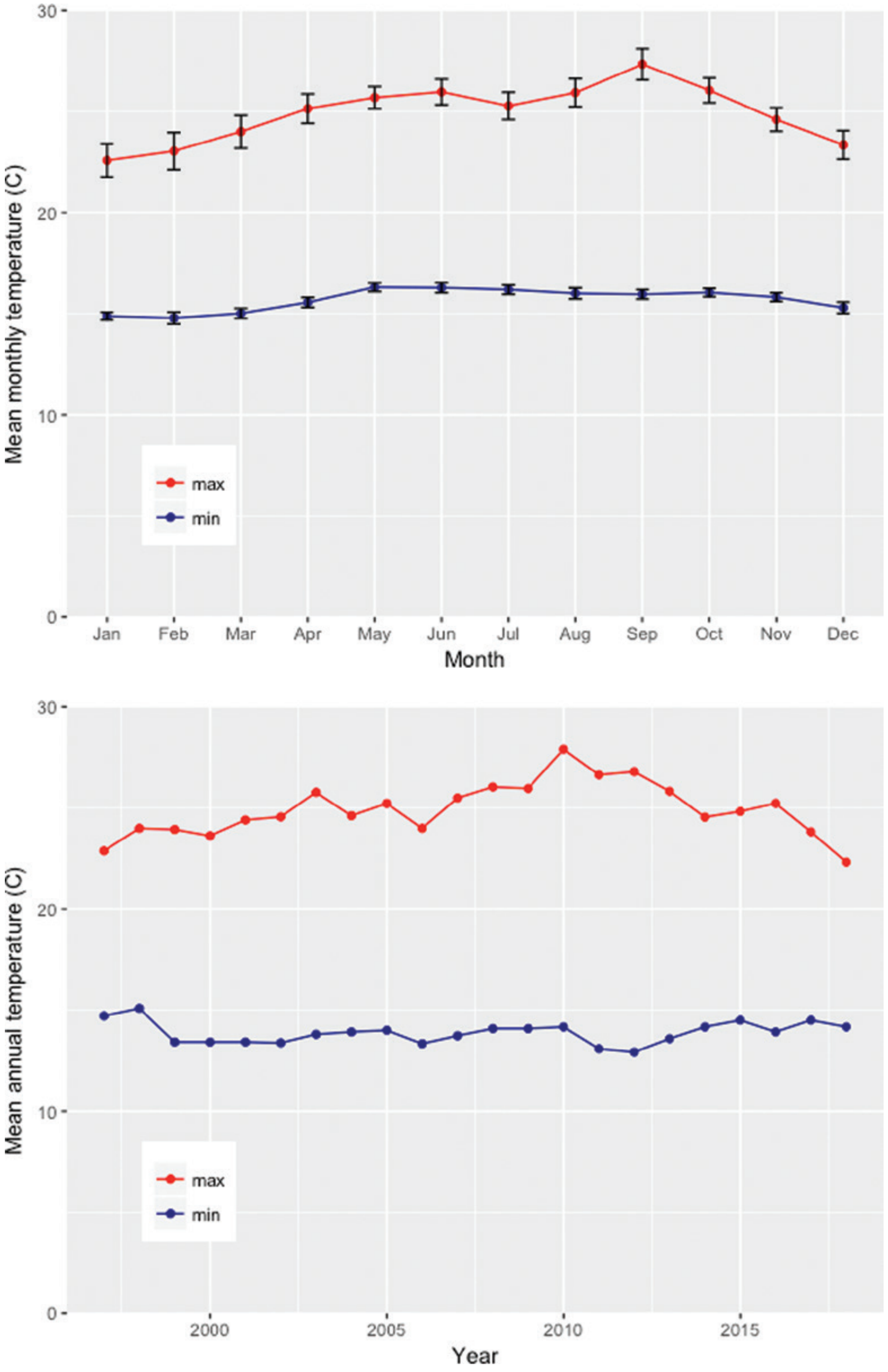

FIGURE 1.2. (Top) Mean monthly maximum and minimum temperatures by month from 1997–2018. Error bars are 95% confidence intervals. (Bottom) Annual mean maximum and mean minimum temperatures by year. All data from the Smithsonian Environmental Science Program, STRI Jorge Araúz field station, Fortuna Forest Reserve.

Long-term mean annual rainfall at the Jorge Araúz field station (1997–2018) is 4,984 mm, SD ±233 mm. However, rainfall is variable interannually (range 2,812–7,728 mm yr^{-1}; Figure 1.3a) and shows seasonality, although average monthly rainfall in the dry season (January–April) is never <100 mm (Figure 1.3b). Rainfall patterns also vary markedly across permanent forest plot sites only a few kilometers apart. Data collected every 2 weeks from 2007 through 2009 and 2011 through 2014 at nine forest plots show that forest on the Caribbean slope (Palo Seco plot) is essentially aseasonal, while the Alto Frio site is as strongly seasonal as sites in the Pacific lowlands (Prada et al., 2017, table 1, appendix S3). Consequently, forest on the northern side of Fortuna lake and on the Caribbean slope of the Palo Seco reserve experience little or no seasonal moisture deficit, whereas those on the southern side of the reserve and on the Pacific slope have one or two months per year with <100 mm of rain (see also Cavelier et al., 1996).

Variation among sites in rainfall seasonality is also reflected in cloud cover patterns. The probability of midday cloud cover for each permanent plot and the Jorge Araúz field station was extracted from an archive of ~1 km resolution cloud cover data (which includes atmospheric and ground-level fog) compiled from 15 years (2000–2014) of daily Moderate Resolution Imaging Spectroradiometer (MODIS) *Terra* and *Aqua* satellite observations (Wilson and Jetz, 2016). The resulting dataset provides a monthly time series of mean midday cloud cover (proportion of days each month with a positive cloud cover assignment). The MODIS dataset indicates that Fortuna includes some of the cloudiest locations on Earth, with annual mean percent cloud cover >95% for 9 out of 14 sites (Table 1.1). In fact, the site at Bonita experienced 100% midday cloud cover for March over the 15 years. For most sites, cloud cover was remarkably invariant across the year, with no evidence of decreased cloud cover during the dry season (January–April), consistent with strong northeasterly trade winds creating orographic cloud cover over the reserve during periods when the intertropical convergence zone lies to the south of Panama. Persistent year-round cloud cover has important implications for gross primary production, which can be light-limited in lowland forests in central Panama during the cloudy wet season (Graham et al., 2003). A notable exception to year-round cloud cover is the southern end of the Fortuna reserve, where the Hornito plots experience reduced dry season cloud cover despite being in the valley of the Rio Hornito and therefore on the windward side of Cerro Chorcha. Similarly, Alto Frio, which is on the leeward Pacific slope, experiences sunny dry season conditions consistent with lower rainfall (Table 1.1).

Given the high cloud cover, a missing component of the Fortuna climatological dataset is the contribution of mist/fog inputs to the forest water budget. MODIS data can provide limited insight because satellite imagery does not indicate the altitude of cloud cover. Ground measurements of fog moisture inputs at gauges across the Continental Divide show that fog inputs are highly heterogeneous (2%–60% of total water inputs), with highest values on the Caribbean slope and lowest values on the Pacific slope (Cavelier et al., 1996). We used the simulation model WaterWorld version 2.92 (Mulligan and Burke 2005; Mulligan 2010, 2013) to predict temperature, total water inputs, and fog-derived moisture inputs for permanent plot sites (Table 1.1). While the WaterWorld model was able to predict mean annual temperature, it substantially underestimated the total water budget by up to a factor of two. Predicted fog inputs from WaterWorld (Table 1.1) matched observations from the field, with higher input rates for plots on the Caribbean slope, but model predictions for plots closer to the Fortuna dam may have been affected by the presence of the lake.

SOILS

A detailed soils analysis has been completed for 13 permanent 1 ha plots established in the Fortuna Forest Reserve, neighboring Palo Seco Forest Reserve, and just south of Fortuna at Alto Frio on the Pacific slope (Figure 1.1). A striking feature of the sites is the highly heterogeneous soils and associated fertility, primarily reflecting variation in parent material. This edaphic heterogeneity yields steep gradients in soil nitrogen (N) and phosphorus (P) availability across the area (Table 1.2), which appears to underlie much of the extraordinary plant diversity at Fortuna (Andersen et al., 2010a; Prada et al., 2017; Andersen, this volume; Viana and Dalling, this volume). The geology and soils are described in detail elsewhere in this volume (Silva et al., this volume; Turner and Dalling, this volume).

FORTUNA BIOLOGICAL DIVERSITY

BOTANICAL INVENTORIES

Fortuna has long been recognized as a key site for botanical research in Panama, with extensive collections made in the 1970s associated with the construction of the Fortuna dam (Adames, 1977; Salazar Allen et al., this volume). A compilation of vascular plant taxa (ferns, gymnosperms, and flowering plants) found 1,880 species collection records for sites around the Fortuna dam (McPherson et al., 2010), representing ~20% of the vascular plant flora of Panama and comprising 137 families of trees and shrubs. An additional 396 bryophytes, representing one-third of the Panama bryoflora, are reported from Fortuna (Salazar Allen et al., this volume). By comparison, tree censuses have recorded 439 taxa with diameter at breast height (DBH) ≥5 cm in 12 one-hectare permanent plots at Fortuna (Prada et al., 2017), representing 73 families (Table 1.3, appendix 1.1, https://fortuna.life.illinois.edu/plants). The overlap in species composition between the McPherson and Prada inventories is remarkably low: only 40% of the 320 woody taxa identified to species in the plot inventory are reported on the McPherson et al. (2010) list. Vascular plant diversity at Fortuna may therefore greatly exceed 2,000 species. For example, the McPherson et al. (2010) collection records report eight species of *Inga* (Fabaceae) at Fortuna, yet 22 species have been tagged and

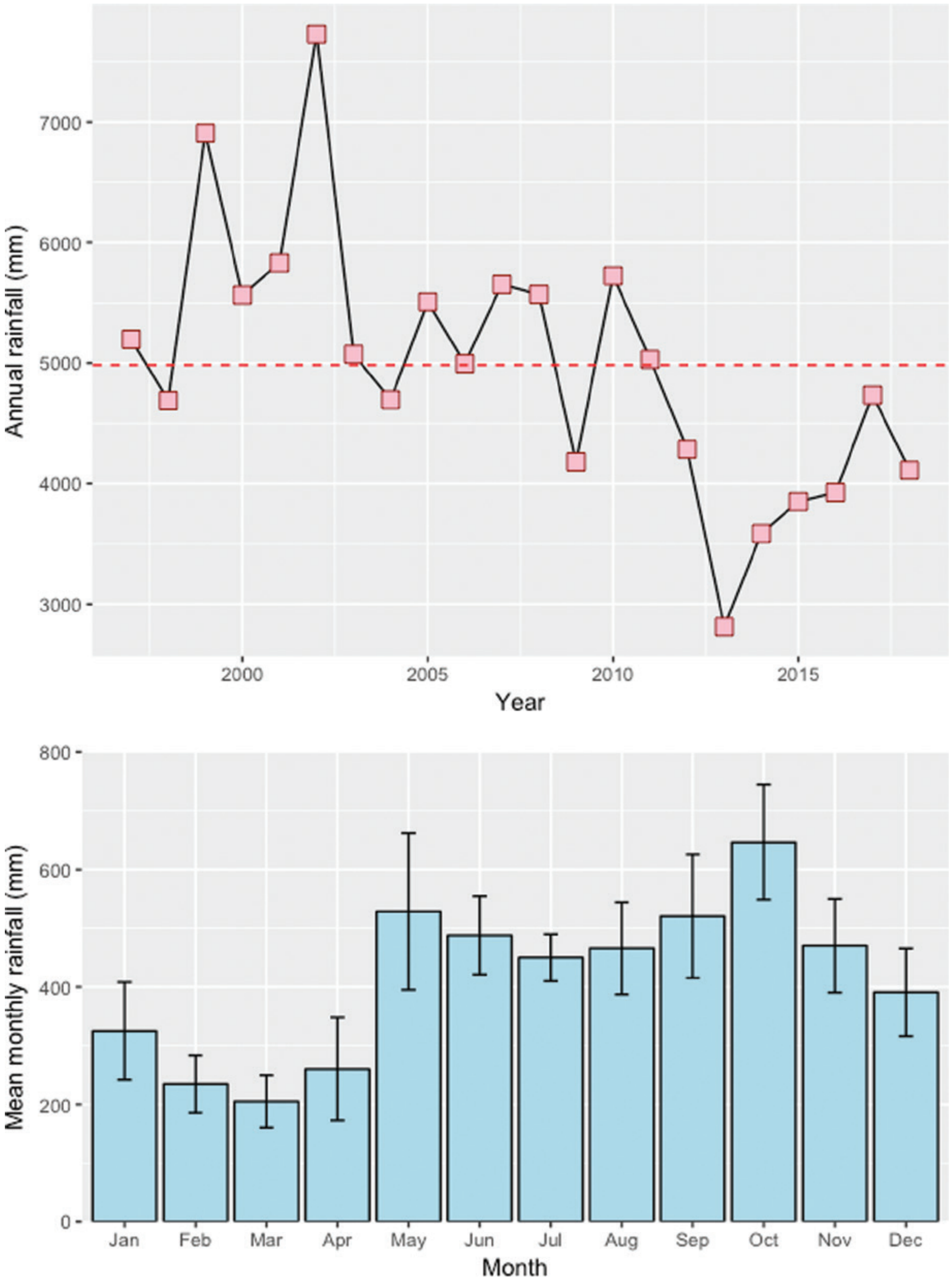

FIGURE 1.3. (Top) Annual rainfall 1997–2018. Red dashed line is the mean rainfall over the 21-year period (4,984 mm). (Bottom) Mean monthly rainfall over the same period ± 95% confidence intervals.

TABLE 1.2. Summary of surface (0–10 cm depth) soil variables measured in 13 locations in 12 permanent forest plots in the Fortuna and Palo Seco Forest Reserves. Values are means (±1 SE). For more information on sample analysis, see Prada et al. (2017).

Site (Geology)	Bulk density = g cm^{-3}	pH	Total N = mg cm^{-3}	Total P = µg cm^{-3}	Total C = mg cm^{-3}	Total N:P	ECEC = $cmol_c$ L^{-1}
Chorro A (Rhyolite)	0.13 ± 0.01	3.7 ± 0.1	1.8 ± 0.1	57.2 ± 8.6	29.6 ± 2.2	26.9 ± 3.0	1.8 ± 0.1
Chorro B (Rhyolite)	0.31 ± 0.04	4.7 ± 0.1	2.7 ± 0.3	86.3 ± 10	50.6 ± 6.1	31.5 ± 2.3	3.1 ± 1.1
Honda A (Rhyolite)	0.29 ± 0.02	3.6 ± 0.05	2.9 ± 0.2	180.6 ± 12	43.9 ± 2	17.5 ± 0.9	1.3 ± 0.2
Honda B (Rhyolite)	0.17 ± 0.02	3.8 ± 0.2	2.3 ± 0.2	127.7 ± 18	40.9 ± 4	16.1 ± 1.9	1.5 ± 0.3
Samudio (Rhy/Mafic)	0.40 ± 0.01	4.2 ± 0.2	3.6 ± 0.2	270 ± 10	51.3 ± 2.5	13.8 ± 0.5	3.4 ± 0.2
Bonita (Mafic)	0.34 ± 0.04	4.5 ± 0.06	3.8 ± 0.6	351 ± 57	47.6 ± 7.2	10.8 ± 0.6	3.4 ± 0.7
Palo Seco (Mafic)	0.41 ± 0.04	4.4 ± 0.1	2.2 ± 0.2	369 ± 23	32.5 ± 4.3	7.7 ± 0.6	2.8 ± 0.2
Verrugosa A (Mafic)	0.42 ± 0.01	4.6 ± 0.1	2.7 ± 0.2	241 ± 23	37.9 ± 3.1	11.2 ± 0.6	2.5 ± 0.1
Verrugosa B (Mafic)	0.40 ± 0.03	5.1 ± 0.04	2.2 ± 0.1	317 ± 35	28.7 ± 1.7	8.0 ± 2.6	1.8 ± 0.1
Pinola (Basalt)	0.50 ± 0.02	5.4 ± 0.1	4.5 ± 0.1	617 ± 20	54.2 ± 1.6	7.5 ± 0.3	8.5 ± 0.1
Hornito A (Dacite)	0.26 ± 0.03	5.0 ± 0.2	2.8 ± 0.1	280 ± 20	35.0 ± 1.6	10.4 ± 0.6	7.4 ± 1.1
Alto Frio (Undiff.)	0.66 ± 0.02	5.6 ± 0.1	4.7 ± 0.2	503 ± 27	51.1 ± 2.3	9.6 ± 0.4	11.4 ± 0.5

identified in permanent plots (appendix 1.1). Similarly, existing inventories undoubtedly underestimate epiphyte diversity. For example, McPherson et al. report 44 bromeliad species, whereas Meisner and Zotz (2012) argue the actual number is closer to 80 species (see also Gómez González et al., this volume). Comparable patterns are likely for other epiphyte groups. Nonetheless, the McPherson list indicates that Fortuna is a key center of diversity for numerous taxa including orchids (224 species; Silvera et al., this volume), Ericaceae (49 species), and understory palms (31 species; Andersen, this volume).

Compositional data from the permanent plots in Fortuna show that 7 to 10 families of woody plants contribute to about half of species richness, number of individuals, and basal area. The dominant families by abundance are Arecaceae, Chloranthaceae, Euphorbiaceae, Fabaceae, Lauraceae, Melastomataceae, Meliaceae, Primulaceae, Rubiaceae, and Sapotaceae, which together account for 57.4% of individuals (appendix 1.1). The most species-rich families, Euphorbiaceae, Fabaceae, Lauraceae, Moraceae, Myrtaceae, Melastomataceae, Meliaceae, Myrsinaceae, Malvaceae, and Rubiaceae, contribute 50.5% of species in the plots. Finally, Arecaceae, Euphorbiaceae, Fabaceae, Juglandaceae, Lauraceae, Meliaceae, Rubiaceae, and Sapotaceae contribute 51.2% of the basal area.

Distribution of Forest Composition and Diversity

The 363 taxa identified at least to genus in the 12 permanent plots (Prada et al., 2017) represent 73 families and account for 17,108 individuals (appendix 1.1). Of these taxa, 37% can be considered rare (<10 individuals recorded) and 44% as having small population sizes or patchy distributions (recorded in no more than two plots). Broadly, species distributions can be grouped into rhyolite-associated species, mafic-volcanic-associated species (classified as andesite in previous site descriptions (Prada et al., 2017), and species associated with fertile soils developed on basalt, dacite, and undifferentiated volcanics (Figure 1.4).

TABLE 1.3. Structural and floristic data for 13 one-hectare forest plots in the Fortuna and Palo Seco Forest reserves. Modified from Prada et al. (2017) with additional unpublished data. Stem number, species counts (Spp), Fisher's α (Div) are for individuals ≥10 cm DBH. Height refers to mean canopy height (±1 SE) for *n* trees >30 cm DBH measured in each plot. Total plot basal area (BA), and percent of BA contributed by species that form ectomycorrhizal associations (EM), by palms, and by potentially nitrogen-fixing taxa (N fixer). Dash (—) = no data.

Site (Geology)	Stems	Spp	Div	BA (m^2)	Height (m)	Height (n)	EM (% BA)	Palm (% BA)	N fixer (% BA)
Chorro A (Rhyolite)	1,015	59	13.7	35.1	18.9 ±0.8	28	8.7	41.9	0.4
Chorro B (Rhyolite)	1,143	53	11.5	40.4	—	—	21.8	25.7	0.1
Honda A (Rhyolite)	787	120	39.4	46.3	24.8 ±0.8	61	24.9	0.7	4.4
Honda B (Rhyolite)	935	102	29.2	47.4	—	—	46.1	0.3	4.2
Samudio (Rhy/Mafic)	754	103	32.3	35.6	24.9 ±1.1	25	1.8	1.6	10.8
Bonita (Mafic)	649	77	22.7	32.6	—	—	0	0.2	10.1
Palo Seco (Mafic)	617	145	59.7	32.5	22.9 ±0.8	45	3.9	4.5	16.0
Verrugosa A (Mafic)	562	114	43.2	30.3	—	—	2.4	3.5	6.9
Verrugosa B (Mafic)	696	126	45.0	30.3	—	—	1.8	4.3	5.9
Pinola (Basalt)	784	80	22.3	43.6	—	—	0.02	0.2	11.5
Hornito A (Dacite)	647	89	28.0	50.3	23.3 ±1.4	31	3.8	0.05	0.3
Alto Frio (Undiff.)	964	75	19.0	42.4	20.8 ±0.9	28	7.4	0.04	13.7

Indicator species analysis (Table 1.4), implemented using the package *indicspecies* in the program R, identified the taxa from appendix 1.1 that were significantly associated with each of these sets of parent material. This revealed considerable numbers of mafic-volcanic specialist species (*n* = 30) and a smaller number of rhyolite-specialist species (*n* = 11). However, separate analysis of the Chorro and Honda watersheds (plots <500 m apart), which have distinct low-fertility soils (Turner and Dalling, this volume), resulted in almost completely nonoverlapping sets of specialist species for these two watersheds (*n* = 18 species). In contrast, few taxa were associated with high-fertility sites, (*n* = 5, Table 1.4). We classified an additional group of 14 taxa with >100 individuals in the census and that occur in eight or more plots as "generalists" (Table 1.4).

Strong environmental filtering across Fortuna is also reflected in plot-level tree diversity, which varies nearly threefold across the plot network (53–145 species ha^{-1} for individuals ≥10 cm DBH, Table 1.3), with the lowest diversity on deep rhyolite deposits in the Chorro watershed and the highest diversity on mafic-volcanic-derived soils with low P and cation availability, and low pH (Palo Seco: 145 species ≥10 cm DBH; Prada et al., 2017). Peak diversity on mafic-volcanics may indicate constraints on species occupancy by resource limitation at the low-fertility sites combined with competitive exclusion on high-fertility sites or perhaps a larger regional species pool associated with the prevalence of mafic-volcanic soils across the Caribbean slope of Panama. It is notable that local diversity at Palo Seco is exceeded in Central America only at two sites further east in Panama, both ever-wet locations on the Caribbean slope at slightly lower elevation than Fortuna (Santa Rita ridge, 400 m asl, 152 species [Pyke et al., 2001]; Nusagandi, 350 m asl, 191 species [Paredes, unpublished data, cited in Leigh, 1999]).

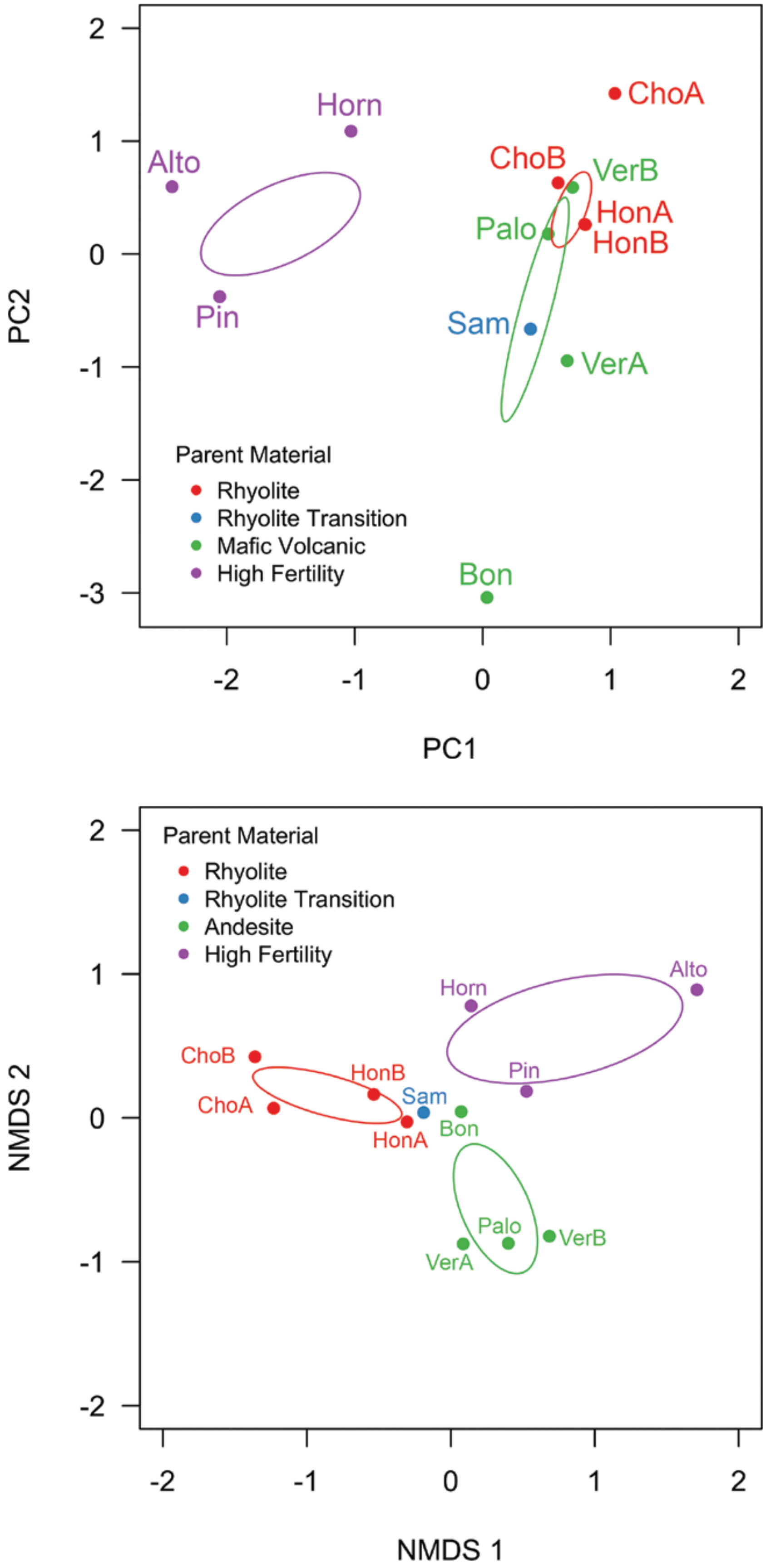

FIGURE 1.4. (Top) Principal components analysis of 21 soil and climate variables (Prada et al., 2017) measured at 12 one-hectare plots results in separation in environmental space of high-fertility plots, mafic-volcanic plots, and rhyolitic plots. (Bottom) Nonmetric multidimensional scaling ordination of tree communities (appendix 1.1) from the same plots shows strong separation of community composition data according to the plot classification. Ellipses represent 1 standard deviation of plot scores relative to the parent material group centroid.

TABLE 1.4. Indicator species analysis for taxa >5 cm DBH in 11 one-hectare plots. Plots are divided into three groups based on parent material: rhyolite plots (Chorro A and B, Honda A and B), mafic-volcanic plots (Bonita, Palo Seco, and Verrugosa A and B), and high-fertility plots (Pinola, Hornito, and Alto Frio). The Samudio plot, which has both rhyolitic and mafic microsites, was excluded from the analysis. In addition, we identified specialist taxa that occurred on the most infertile and deep rhyolite deposits (Chorro plots only) and on the shallow rhyolite deposits (Honda plots only). Specialists were determined using indicator taxon analysis implemented using the package *indicspecies* in R with $p < 0.05$ (De Cáceres and Legendre, 2009) and are ordered by strength of association. Generalist taxa occurred in at least eight plots, all three plot groups, and had more than 100 individuals. Generalist taxa are ordered by abundance.

Rhyolite specialists

Palicourea roseofaucis
Ocotea pullifolia
Cybianthus montanus
Weinmannia pinnata
Hedyosmum bonplandianum
Aniba cinnamomiflora
Pouteria cuspidata
Posoqueria latifolia
Ocotea gomezii
Symphonia globulifera
Cyathea rojasiana

Chorro specialist taxa

Alzatea verticillata
Colpothrinax aphanopetala
Euterpe precatoria
Psychotria luxurians
Alsophila sp1
Tovomita weddelliana
Graffenrieda bella
Podocarpus oleifolius

Honda specialist taxa

Mollinedia cf. *minutiflora*
Clethra lanata
Cecropia cf. *garciae*
Ossaea cf. *acuminata*
Inga exalata
Meliosma allenii
Alibertia garapatica
Ticodendron incognitum
Richeria obovata
Plinia sp1

Mafic-volcanic specialists

Ruagea glabra
Inga jinicuil
Tetrorchidium euryphyllum
Guarea sp4
Conostegia rufescens
Joosia umbellifera
Ardisia hagenii
Pouteria reticulata
Platymiscium pinnatum
Cyathea eggersii
Palicourea sp1
Matisia sp1
Cryosophila warscewiczii
Iriartea deltoidea
Maquira guianensis
Socratea exorrhiza
Inga allenii
Guarea sp5
Myrtaceae sp6
Drypetes brownii
Matisia obliquifolia
Sloanea zuliaensis
Otoba novogranatensis
Inga acrocephala
Lauraceae sp4
Annona sp1
Sapium glandulosum
Henriettella tuberculosa
Conostegia micrantha
Marila jefensis

High-fertility specialists

Sorocea trophoides
Prunus brachybotrya
Perebea sp1
Guarea pterorhachis
Piper sp1

Generalist taxa

Dendropanax arboreus
Hyeronima oblonga
Guarea glabra
Cassipourea elliptica
Eschweilera panamensis
Alchornea glandulosa
Viburnum costaricanum
Micropholis melinoniana
Talauma sp1
Inga alba
Inga marginata
Garcinia marginata
Tapirira guianensis
Alsophila erinacea

FOREST COMPOSITIONAL ASSOCIATIONS AT FORTUNA

Here we describe the most notable compositional associations at Fortuna (Plate 1.2): (1) communities associated with the palm *Colpothrinax aphanopetala*, indicative of deep rhyolite deposits; (2) communities associated with the ectomycorrhizal tree *Oreomunnea mexicana* (Juglandaceae), occurring on a variety of parent materials (except mafic volcanics on the Caribbean slope); and (3) communities associated with mafic-volcanic-derived soils.

Colpothrinax *Forest*

The genus *Colpothrinax* (Arecaceae) occurs in lowland and wet premontane forests through southern and eastern Central America and Cuba (Evans, 2001; Palmweb, 2019). In Panama, populations of *C. aphanopetala* are found in premontane forests (Evans, 2001; Correa et al., 2004) associated with highly infertile soils (e.g., Cerro Jefe and Cerro Azul). Similarly, in Fortuna, adults of *C. aphanopetala* are located in the Chorro A and B plots, with a small number of juveniles in the Honda A plot (Plate 1.3). More broadly, the distinct architecture of emergent individuals of *Colpothrinax* provides a clear visual marker of rhyolite outcrops on slopes north of the Fortuna lake and, to a lesser extent, on the southern shore, sometimes in association with stands of *Vochysia guatemalensis* (Plate 1.3).

Communities associated with *Colpothrinax* are low in diversity compared to the other forest types described in this section. The two Chorro plots harbor 53 and 59 species ≥10 cm DBH, representing 41 tree families (Table 1.3). Canopy palms are especially dominant in this forest, accounting for 33.1% of stems at Chorro (*C. aphanopetala*, 6.5%; *Euterpe precatoria*, 17.1%; *Wettinia quinaria*, 9.5%). Similarly, only five species contribute 54% of the basal area of the two plots (*C. aphanopetala*, 21%; *Hyeronima oblonga* [Euphorbiaceae], 9%; *Euterpe precatoria* [Arecaceae], 9%; *Graffenrieda bella* [Melastomataceae], 8%; *Podocarpus oleifolius* [Podocarpaceae], 7%). *Colpothrinax* forest at Chorro is generally rather short in stature compared to other forests at Fortuna (mean canopy height 18.9 m; Table 1.3), with *Colpothrinax* the dominant emergent species (DBH_{max} = 36 cm; height = 25 m) as well as occasional individuals of *P. oleifolius* (DBH_{max} = 67 cm; height = 27 m). Four additional species, *H. oblonga* (DBH_{max} = 49 cm; height = 26 m), *Quercus* sp5 (DBH_{max} = 57 cm; height = 22 m), and *Pouteria cuspidata* (Sapotaceae) (DBH_{max} = 50 cm), also occur as canopy emergents. In the upper canopy, three species represent 52% of the total basal area: *E. precatoria*, *G. bella*, and *Hedyosmum bonplandianum* (Chloranthaceae), although species such as *Hyeronima oblonga, Clethra coloradensis* (Clethraceae), and *Guatteria acrantha* (Annonaceae) can occur in this layer. In the lower canopy, there are juveniles of *E. precatoria*, *W. quinaria* (Arecaceae), and *Hedyosmum bonplandianum*, and adults of *Psychotria luxurians* (Rubiaceae) and *Cybianthus montanus* (Primulaceae). The understory of this forest is dense, with large numbers of trunkless *Colpothrinax* juveniles. Strangely, although the canopy is dominated by palms, understory palm species are rare (Andersen, Turner, and Dalling 2010). Instead, *Colpothrinax* forest contains a higher density of tree ferns than do other forests at Fortuna, with the abundant species *Cyathea rojasiana* restricted to the Chorro watershed (Viana et al., 2020).

Oreomunnea *Forest*

The genus *Oreomunnea* (Juglandaceae, subfamily Engelhardioideae) has a Central America distribution (Mexico to Panama), with a sister taxon, *Engelhardia*, distributed across Southeast Asia. In Central America, *Oreomunnea* is restricted to premontane and montane forests (Herrera et al., 2014). At Fortuna and elsewhere in Panama, Costa Rica, and southern Mexico, *Oreomunnea mexicana* can form extensive stands spanning hundreds of hectares, occasionally achieving true monodominance (>50% of stems and basal area; Corrales, Ferrer, et al., 2016; Alfonso-Corrado, 2017; Plate 1.3). At Fortuna, *O. mexicana* accounts for up to 43% of stand basal area for trees ≥10 cm DBH across the 12 one-hectare plots (Dalling et al., unpublished data). Notably, patches of *O. mexicana* in Fortuna are distributed across the reserve on a variety of parent materials (Corrales, Ferrer, et al., 2016), including rhyolite-derived soils characterized by low fertility and granodiorite-derived soils of intermediate fertility, and on soils derived from dacite and undifferentiated volcanics, characterized by relatively high fertility (Turner and Dalling, Figure 3.1, this volume). In contrast, *O. mexicana* appears to be rare or absent on mafic-volcanic-derived soils.

Oreomunnea forests are rather consistent in species composition and structure, whether growing on low- or high-fertility soils. This consistency might reflect plant–soil feedbacks beneath *Oreomunnea* stands that reduce inorganic N availability (Corrales, Mangan, et al., 2016). In the best-studied *Oreomunnea* stand at Fortuna (the Honda B plot), where the species accounts for 43% of basal area and 28% of stems ≥10 cm DBH, diversity remains similar to the Honda A plot, where *O. mexicana* is much less abundant (102 vs. 120 species, Table 1.3). Common species associated with *Oreomunnea* include many of the generalist taxa listed in Table 1.4: *Hyeronima oblonga* (Phyllanthaceae), *Pouteria cuspidata* (Sapotaceae), *Eschweilera panamensis* (Lecythidaceae), *Guatteria acrantha* (Annonaceae), *Inga exalata* (Fabaceae), *Talauma* sp. (Magnoliaceae), and *Micropholis melinoniana* (Sapotaceae).

Oreomunnea mexicana dominates the canopy layer of the forests in which it occurs, with emergent individuals reaching 100 cm DBH and 36 m in height occurring alongside the generalist taxa mentioned previously (notably *Eschweilera* and *Micropholis*). The largest trees in these forests include *Quercus insignis* (Fagaceae) (DBH_{max} = 124 cm, height = 43 m), *M. melinoniana* (DBH_{max} = 92 cm, height = 34 m), *H. oblonga* (DBH_{max} = 83 cm, height = 26 m), and *Quercus* cf. *salicifolia* (DBH_{max} = 81 cm). Common trees in the canopy/subcanopy layer include *Posoqueria latifolia*

(Rubiaceae), *E. panamensis*, *Cassipourea elliptica* (Rhizophoraceae), *Talauma* sp. (Magnoliaceae), *Dendropanax arboreus* (Araliaceae), *I. exalata*, *G. acrantha* and *Viburnum costaricanum* (Adoxaceae). In the midstory, the most important species are *Ardisia* sp2 (Primulaceae), juveniles of *O. mexicana*, *Amaioua pedicellata* (Rubiaceae) and individuals of the tree fern *Alsophila cuspidata* (Cyatheaceae). The understory of *O. mexicana*–dominated stands is generally remarkably open, with low densities of palms (Viana et al., 2020), abundant *O. mexicana* seedlings, the climbing fern *Salpichlaena volubilis*, and the terrestrial fern *Lindsaea* (Viana and Dalling, this volume).

Forests on Mafic-Volcanic-Derived Soils

These forests are associated with mafic-volcanic parental material generating soils with relatively high bulk density and clay content and intermediate fertility (Turner and Dalling, table 3.2, this volume). The parent material at these sites was previously classified as andesite on the basis of coarse fragments in profile pits, but here we use the term undifferentiated mafic-volcanics to reflect the difficulty in resolving the small-scale variation in lithology underlying these strongly weathered soils (Silva et al., this volume). Unlike the soils that derive from rhyolite, the soils on the mafic-volcanics lack a strongly developed organic horizon. At Fortuna, mafic-volcanics occur along the Caribbean slope in the Palo Seco reserve and in the valley of the Rio Chiriqui north and east of the Fortuna lake. Mafic-volcanics are represented by four permanent plots: Bonita, Palo Seco, and Verrugosa A and B (Figure 1.1; Plate 1.2). The indicator species analysis revealed that a large number of species ($n = 30$) are specialists to these forests (Table 1.4), in part reflecting the high species richness of mafic-volcanic forests (77–145 spp. ≥10 cm ha^{-1}, Table 1.3).

Mafic-volcanic forests also harbor the highest tree species diversity (Fisher's alpha = 24.5 to 59.6) with 292 species distributed in 62 families. In contrast to the previous forest types, no single species dominates the tree community. Instead, 29 species account for half of the basal area. The top 10 species are *Alchornea glandulosa* (Euphorbiaceae), *Pouteria reticulata* (Sapotaceae), *H. oblonga*, *E. panamensis*, *I. alba* (Fabaceae), *Wercklea insignis* (Malvaceae), *Mortoniodendron anisophyllum* (Malvaceae), *Tetrorchidium euryphyllum* (Euphorbiaceae), and *Dendropanax gonatopodus* (Araliaceae). The most important families are Euphorbiaceae, Fabaceae, Malvaceae, Meliaceae, Sapotaceae, Araliaceae, and Rubiaceae, which collectively account for 52% of the total basal area.

In the canopy layer, the abundant trees are *A. glandulosa*, *Conostegia rufescens* (Melastomataceae), *P. reticulata*, *I. alba*, *Iriartea deltoidei* (Arecaceae), *H. oblonga*, *T. euryphyllum*, *W. insignis*, and *M. anisophyllum*. The largest trees in the plots are *Apeiba membranacea* (Malvaceae) (DBH_{max} = 1.1 m), *Vochysia guatemalensis* (Malvaceae) (DBH_{max} = 98 cm, height = 36 m), *Platymiscium pinnatum* (Fabaceae) (DBH_{max} = 95 cm), *Ocotea mollifolia* (Lauraceae) (DBH_{max} = 86.1 cm), and *Naucleopsis naga* (Moraceae) (DBH_{max} = 83.4 cm, height = 31 m). The 10 most important species in the midstory layer are *C. rufescens*, *A. glandulosa*, *Croton schiedeanus* (Euphorbiaceae), *Calatola costaricensis* (Icacinaceae), *P. reticulata*, *Ardisia hagenii* (Primulaceae), *Ardisia* sp1, and *Maquira guianensis* (Moraceae). In the midstory and understory, there are abundant palms and tree ferns, especially *Alsophila erinacea* (Cyatheaceae). One other palm that also occurs in the *Colpothrinax* forest is also common here: *Wettinia quinaria* accounts for 11% of the total basal area. Two additional palm species, *Cryosophila warscewiczii* and *Socratea exorrhiza*, are common and restricted to mafic-volcanic forests. The tree ferns *A. erinacea*, *Cyathea multiflora*, and *Cyathea eggersii* are typical in this layer. Along with these species, juveniles of *Calatola costaricensis*, *Croton schiedeanus*, and *Joosia umbellifera* (Fabaceae) are common, while dense populations of species-rich palm and fern assemblages can dominate the understory (Viana and Dalling, 2020).

Influence of Soil and Climate Variables on Species Distributions

Strong distributional associations with parent material point at the importance of soil variables in structuring tree communities (Figure 1.4). Analysis of the environmental variables (rainfall and soil parameters) measured in each of the 1 ha forest plot sites has also shown that plots mostly cluster according to parent material (Figure 1.4a), with one principal components analysis (PCA) axis separating the infertile rhyolite plots; intermediate fertility mafic-volcanic plots; and high-fertility plots on basalt, dacite, and undifferentiated volcanics. This first PCA axis is associated with cation exchange capacity, total P, pH, bulk density, and inorganic N availability (Prada et al., 2017, fig. 1.4). Variation in fertility, however, is also correlated with total and dry season rainfall, complicating the separation of nutrient and moisture variables as factors influencing composition and diversity. One exception, however, is in the forests surrounding the Fortuna dam. There, rainfall is high and relatively uniform through the year (Tables 1.1 and 1.2). Despite this, the Pinola plot shares only 64 out of 172 species found in plots in the Honda watershed a few hundred meters away (Figure 1.4b). These differences likely reflect the basalt-derived soils at Pinola that have sixfold higher effective cation exchange capacity, two-unit higher pH, and twofold higher total P than the rhyolite-derived soils of the Honda watershed (Table 1.2).

The relative importance of individual soil nutrients on plant performance and distribution is also difficult to assess, as many soil chemical variables at Fortuna covary (Prada et al., 2017, table 4). Initial work exploring the distribution of palm species highlighted the role of N, cations and aluminum in structuring community composition (Andersen, Turner, and Dalling, 2010), corresponding to directional shifts in functional trait values, including foliar N concentration across the Fortuna soils gradient (Andersen et al., 2012; Andersen, this volume). Experimental work, using both seedling transplant experiments and

N addition, also revealed indirect effects of N on plant performance. While N addition increased foliar N concentration and maximal photosynthetic rates, these potentially positive effects were offset by higher herbivory rates that equalized plant performance (Andersen, Corre, et al., 2010; Andersen et al., 2014; Andersen, this volume).

More recent work, using plots that only partially overlap with Andersen's palm sites, has increasingly highlighted the role of P in structuring plant communities at Fortuna. Across 12 one-hectare permanent plots, the abundance of palms and herbaceous ferns decreases with increasing soil total N:P, reflecting greater abundances in sites with relatively high P availability (Viana et al., 2020; Viana and Dalling, this volume). For tree species, Prada et al. (2017) also showed that N was not a significant correlate of compositional variation in the tree community across the soil gradient, reflecting either a weak influence of N on plant performance or an inability to adequately characterize N availability in soil surveys using conventional extraction procedures. In contrast, there was a strong effect of P availability on compositional variation.

In summary, nutrient limitation by N, P, and potentially base cations, notably potassium (Heineman et al., 2016), appears to structure plant communities and determines plant performance at Fortuna. We summarize evidence for N and P effects in the next section.

Nitrogen Effects on Plant Performance and Ecosystem Productivity

Ecosystem effects of N availability have been explored extensively at Fortuna using a long-term N addition experiment (NITROF) initiated in 2006. Over the last 13 years, urea has been applied at a rate of 125 kg ha^{-1} y^{-1} to four 40 × 40 m plots (with four paired control plots) in the Honda watershed containing a mix of species forming arbuscular mycorrhizal (AM) or ectomycorrhizal (ECM) associations (principally *Oreomunnea mexicana*). Initial work conducted by Marife Corre and colleagues from the University of Göttingen focused on how N addition affects N cycling processes. They showed that N-addition plots had two times higher nitrous oxide emissions, 15 times higher nitrification rates, and higher nitrate leaching losses than control plots. These high nitrification and emission rates were attributed to the high rainfall and deep organic layer at Fortuna compared to lowland forest where losses were smaller (Koehler et al., 2009; Corre et al., 2010). Soil chemistry has been relatively unaffected by prolonged N addition. A decade after applications began, soil pH and resin-extractable phosphate concentrations were unchanged, as were pool sizes of microbial carbon, N, and P (Corrales et al., 2017). However, extractable nitrate and ammonium concentrations increased, and enzyme activity in the soil (phosphomonoesterase and phosphodiesterase, *N*-acetyl-β-glucosaminidase, and β-xylanase) decreased, which was attributed to a reduction in abundance of ECM fungal taxa specialized in organic N and P acquisition (Corrales et al., 2017).

Nitrogen addition has also changed forest productivity. Total litterfall has been consistently higher in the N-addition plots over the last decade (Heineman et al., 2015). In contrast, N addition increased growth rates only for AM trees, with the largest effects for midsized trees (20–40 cm DBH). Furthermore, annual growth rates have declined in N and control treatments by up to 40% over the decade, with especially large declines for ECM species (J. Dalling, unpublished data). Differential responses of ECM versus AM species to N addition highlight the potential for future increases in N deposition to restructure montane forests by favoring lower elevational AM-associated species in ways that may be synergistic with climate warming. Furthermore, because ECM species tend to contribute more to aboveground biomass and are associated with a pronounced organic soil horizon, compositional shifts could also reduce ecosystem carbon storage considerably.

Additional evidence for a key role of N cycling in structuring Fortuna forests comes from studies of the ECM-associated tree species *Oreomunnea mexicana*. At several sites across Fortuna, *Oreomunnea* accounts for at least 30% of stand basal area at sites with a variety of parent material including rhyolite (Honda watershed), granodiorite (Zorro), dacite (Hornito) and undifferentiated volcanics (Alto Frio). *Oreomunnea* associates with diverse ECM fungal communities that differ in composition across the reserve (Corrales, Ferrer, et al., 2016), including numerous new fungal taxa or new records for Panama (Corrales and Ovrebo, this volume). A key feature of *Oreomunnea* stands is the localized reduction in nitrate and ammonium availability determined by in situ resin bags, which are up to three times lower inside than outside *Oreomunnea* stands, and a negative correlation across plots between *Oreomunnea* basal area and nitrate availability (Corrales, Mangan, et al., 2016). It is hypothesized that monodominance, or at least high local abundance, of *Oreomunnea* is achieved by virtue of this species' ECM association. Ectomycorrhizas provide N to the host plant from organic sources, compete with the saprophytes that mineralize organic material, and consequently reduce production rates of inorganic forms of N that AM-associated trees depend on (Corrales, Mangan, et al., 2016). Greatly reduced foliar N concentration in seedlings of *Roupala montana* transplanted into *Oreomunnea* stands relative to seedlings outside the stand provides additional evidence that *Oreomunnea* decreases N availability for competing species (Corrales, Mangan, et al., 2016).

To alleviate competition for N, plants can specialize in uptake of specific chemical forms of N or exhibit flexibility in uptake of different N forms. A series of ^{15}N tracer experiments conducted at low N sites in Fortuna revealed flexibility in N form uptake in seedlings of understory palms with contrasting species distribution patterns (Andersen and Turner, 2013) and coexisting species with contrasting root symbiont associations (Andersen et al., 2017). Understory palm species from high-nutrient sites had higher N uptake rates than species restricted to low-nutrient sites, suggesting uptake rates were related to plant demand. Despite overall plasticity in uptake of N from various chemical sources, seedlings of coexisting species differed in recovery of ^{15}N from nitrate and glycine sources. Nonetheless, most species and root symbiont types showed the highest rates of ^{15}N recovery from nitrate sources, suggesting stronger competition for nitrate compared to other chemical forms of N. Together, the ^{15}N tracer experiments suggest that strong competition for N may be reduced by taking up alternative forms of nitrogen and exploiting whichever N form is most available in the rhizosphere. Furthermore, the importance of plasticity of uptake from various N forms in tropical forests may be driven by weak adaptation for specific N forms in ecosystems with high rates of N turnover and limitation of other soil nutrients (Andersen and Turner, 2013; Russo et al., 2013; Andersen et al., 2017).

Phosphorus Effects on Plant Performance

In addition to correlations between compositional variation in tree and fern communities and total soil P (Prada et al., 2017; Viana et al., 2020; Viana and Dalling, this volume), species tissue P concentrations are strongly correlated with soil P availability across the Fortuna plot network. For understory palms transplanted into five sites, foliar P at Chorro was about half that of more fertile sites (Palo Seco and Hornito) and was accompanied by large shifts in biomass allocation belowground (Andersen et al., 2014). In contrast, an earlier experiment manipulating N availability showed no biomass shift (Andersen, Corre, et al., 2010).

Similar patterns have been observed for leaf, wood, and bark P concentrations in tree species (Heineman et al., 2016; Jones et al., 2019). Wood P concentrations vary enormously at Fortuna (19–300 $\mu g\ g^{-1}$), and P is the wood nutrient most sensitive to soil nutrient availability (Heineman et al., 2016). In addition, differences in the concentration of P between the outermost annulus of wood and inner wood layers suggest that trees conserve P by retranslocating it as sapwood transitions to heartwood. Trees growing on low-P soils at Fortuna also show a greater reduction in their wood P concentration following experimental defoliation compared with trees growing on high-P soils, suggesting that wood P concentration reflects whole plant P reserves (Heineman, 2016).

Species partitioning of a gradient of soil P availability may also reflect among-species differences in P acquisition and use strategies (Turner, 2008). In a first experimental test of whether tree species differ in their ability to use different chemical forms of P, Steidinger et al. (2015) grew seedlings of four Fortuna tree species (*Podocarpus oleifolius* – AM conifer; *Mollinedia darienensis* – AM angiosperm [Monimiaceae]; *Oreomunnea mexicana* – ECM angiosperm [Juglandaceae]; *Roupala montana* – nonmycorrhizal angiosperm [Proteaceae] that forms cluster roots when P availability is extremely low) in the greenhouse in sand with one of four different P sources: inorganic phosphate (sodium phosphate), phosphomonoester (glucose phosphate), phosphodiester (RNA), and phytate (inositol hexakisphosphate). While the AM and ECM tree species showed some differences in enzymatic (esterase) activity, they had similar growth and foliar P responses to the different P sources. In contrast, the nonmycorrhizal tree, *Roupala montana*, was the only species capable of utilizing phytate, the most energetically costly form of P to acquire. Interestingly, *Roupala* does not appear to be restricted to P-poor soils at Fortuna; it is approximately equally abundant on all five parent materials (appendix 1.1). However, *Roupala* is a morphologically highly variable taxon. It reproduces as a small treelet <1 cm DBH at Alto Frio, but reaches >60 cm DBH at Hornito, Palo Seco, and Honda. In conclusion, like N, specialization on particular P sources does not appear to play a critical role in the partitioning of species distributions across the soil P gradient.

CONCLUSIONS

Fortuna provides exceptional opportunities for understanding how species distributions are shaped by environmental factors, with steep gradients in climate and soil conditions resulting in an almost complete turnover in species composition at sites less than 15 km apart and at similar elevations (Prada et al., 2017). Occupying both a climatic transition between lowland forest and montane cloud forest, and between predominantly P-limited lowland forest and N-limited montane forests (Tanner et al., 1998; Ping et al., 2013; Fisher et al., 2013), long-term monitoring plots at Fortuna will become increasingly valuable in understanding how forest communities and biogeochemical processes respond to climate change in one of the most biodiverse areas of Central America. Integrating species edaphic requirements into environmental models will be critical to predicting species' future migration potential. While work at Fortuna has begun to reveal the sensitivity of species to soil properties, additional experimental work is needed to determine the extent to which plant communities either reflect or induce (via plant–soil feedback) the soil conditions where they occur.

APPENDIX 1.1

Woody species >5 cm DBH present in 12 one-hectare forest plots in the Fortuna Forest Reserve and adjacent upland areas of the Palo Seco reserve (see Table 1.1 for full site names and additional site information). Shading indicates parent material (R/M = rhyolite–mafic-volcanic transition, Undif. = undifferentiated volcanics). *n* = total number of individuals across all plots. * indicates taxa recorded from the Missouri Botanic Garden checklist for the Fortuna dam region (http://www.mobot.org/MOBOT/fortuna/fortunaDropdown.aspx). Dash (—) = not present.

		Rhyolite				R/M	Mafic-volcanic				Basalt	Dacite	Undif.	
Family	*Species*	Cho.A	Cho.B	Hon.A	Hon.B	Samu.	Bonita	Palo	Ver.A	Ver.B	Pinola	Horn.	Alto.	*n*
Actinidiaceae	*Saurauia* cf. *montana*	—	—	—	—	3	—	—	—	—	—	1	—	4
	Saurauia cf. *pittieri**	7	—	1	1	—	9	2	—	—	—	—	—	20
	*Saurauia rubiformis**	20	—	—	—	—	11	—	2	—	—	—	—	33
	Saurauia sp2	—	2	—	—	—	—	1	5	—	—	—	—	8
Adoxaceae	*Viburnum costaricanum**	42	48	2	26	1	21	—	—	—	4	3	—	147
Alzateaceae	*Alzatea verticillata*	1	7	—	—	—	—	—	—	—	—	—	—	8
Anacardiaceae	*Tapirira guianensis**	3	12	3	12	4	29	1	3	13	1	5	16	102
Annonaceae	*Annona pittieri**	—	1	13	7	16	—	1	2	—	2	10	—	52
	Annona sp1	—	—	—	—	—	—	2	2	1	—	—	—	5
	*Cymbopetalum rugulosum**	—	—	—	—	—	—	1	2	—	—	—	—	3
	*Desmopsis maxonii**	—	—	—	—	—	—	—	—	—	—	25	—	25
	Guatteria acrantha	17	58	3	36	—	17	—	—	—	—	1	2	134
	Guatteria chiriquiensis	—	—	—	—	—	—	5	7	13	—	—	4	29
	*Guatteria dolichopoda**	—	—	3	—	10	—	—	—	—	—	—	—	13
	*Guatteria talamancana**	—	—	1	—	6	—	—	—	—	—	—	—	7
	Rollinia sp1	—	—	—	—	—	—	—	—	—	—	—	7	7
Apocynaceae	*Rauvolfia aphlebia**	10	—	—	2	—	—	4	1	2	—	73	—	92
	*Tabernaemontana longipes**	—	—	6	—	9	—	—	—	—	—	—	—	15
	Tabernaemontana sp1	—	—	—	—	—	—	8	11	5	—	3	—	27
Araliaceae	*Dendropanax alberti-smithii*	—	—	—	—	—	—	—	—	8	—	—	—	8
	*Dendropanax arboreus**	—	—	71	48	32	71	5	4	7	6	48	37	329
	*Dendropanax capillaris**	—	—	—	—	—	—	—	—	—	1	1	—	2
	*Dendropanax globosus**	—	—	—	—	—	17	—	—	—	—	—	—	17
	*Dendropanax gonatopodus**	2	—	—	—	—	53	—	—	—	39	—	—	94
Arecaceae	*Asterogyne martiana*	—	—	—	—	—	—	7	—	—	—	—	—	7
	*Chamaedorea woodsoniana**	—	—	2	—	1	13	20	2	2	24	8	—	72
	*Colpothrinax aphanopetala**	171	99	1	—	—	—	—	—	—	—	—	—	271
	*Cryosophila warscewiczii **	—	—	—	—	—	—	30	17	15	—	—	—	62
	Euterpe precatoria	283	426	—	10	9	—	—	—	—	—	—	—	728
	Geonoma acuminata	3	—	—	2	—	—	—	1	—	—	1	—	7
	*Iriartea deltoidea**	—	—	—	—	—	—	10	6	35	—	—	—	51

(Continued)

		Rhyolite				R/M	Mafic-volcanic				Basalt	Dacite	Undif.	
Family	*Species*	Cho.A	Cho.B	Hon.A	Hon.B	Samu.	Bonita	Palo	Ver.A	Ver.B	Pinola	Horn.	Alto.	*n*
	Socratea exorrhiza	—	—	—	—	—	—	27	2	7	—	—	—	36
	*Wettinia quinaria**	229	163	45	3	76	—	102	162	22	—	—	—	802
Asteraceae	*Koanophyllon hylonomum**	—	—	14	—	22	—	—	—	—	32	13	—	81
Bignoniaceae	*Amphitecna* cf. *spathicalyx*	—	—	—	—	—	—	1	—	—	—	—	—	1
	Amphitecna kennedyae	—	—	—	—	—	—	1	—	—	—	—	—	1
	Amphitecna sessilifolia	2	3	—	—	—	30	—	—	2	—	—	—	37
Boraginaceae	*Bourreria costaricensis**	—	—	2	—	2	—	—	—	—	3	3	—	10
	Cordia globosa	—	—	—	—	—	3	—	—	—	—	—	—	3
	Cordia lasiocalyx	—	—	7	2	7	6	—	15	4	—	1	—	42
Burseraceae	*Protium glabrum*	—	—	—	—	—	—	2	—	2	—	—	—	4
	*Protium panamense**	—	—	—	9	—	—	12	2	16	—	—	—	39
Calophylaceae	*Marila* cf. *pluricostata*	—	—	—	—	—	—	5	1	—	—	—	—	6
	Marila jefensis	—	—	1	—	—	—	15	13	5	—	—	—	34
	Marila sp1	—	—	—	5	—	—	—	—	—	—	—	—	5
Caricaceae	*Jacaratia dolichaula*	—	—	1	—	7	—	—	—	1	4	—	—	13
	Jacaratia spinosa	—	—	—	—	—	—	—	—	8	1	—	—	9
Celastraceae	*Maytenus recondita*	—	—	—	—	—	—	—	1	—	—	—	—	1
	*Quetzalia occidentalis**	7	11	15	7	12	—	—	—	—	—	1	8	61
	Salacia petenensis	1	—	—	—	—	—	4	—	—	—	13	—	18
	Wimmeria sternii	—	—	—	—	—	—	—	—	—	—	—	28	28
	*Zinowiewia costaricensis**	—	—	1	—	—	—	—	—	—	—	—	138	139
Chloranthaceae	*Hedyosmum bonplandianum**	153	161	46	1	166	—	—	11	—	—	—	—	538
	*Hedyosmum costarricense**	—	—	2	10	—	3	15	6	6	—	—	—	42
Chrysobalanaceae	*Hirtella guatemalensis*	—	—	—	—	—	—	—	2	—	—	—	—	2
	Hirtella latifolia	—	—	—	—	—	—	—	1	—	—	—	—	1
	Licania hypoleuca	—	—	—	—	—	—	1	1	—	—	—	—	2
Clethraceae	*Clethra coloradensis*	—	39	—	—	—	—	—	—	—	—	—	—	39
	Clethra lanata	—	—	14	2	1	—	—	—	—	—	—	—	17
	Clethra sp1	4	—	1	—	1	—	1	—	—	10	—	5	22
	Clethra sp3	—	—	—	2	—	1	—	—	—	—	—	—	3
	Clethra suaveolens	—	—	2	—	—	—	—	—	—	—	—	—	2
	Clethra tutensis	—	—	1	—	—	—	—	—	—	—	—	—	1

		Rhyolite				R/M	Mafic-volcanic				Basalt	Dacite	Undif.	
Family	***Species***	Cho.A	Cho.B	Hon.A	Hon.B	Samu.	Bonita	Palo	Ver.A	Ver.B	Pinola	Horn.	Alto.	***n***
Clusiaceae	*Chrysochlamys psychotriifolia**	1	—	2	—	—	2	6	1	5	16	—	—	33
	*Dystovomita paniculata**	12	5	1	3	3	—	2	1	7	—	—	—	34
	Garcinia madruno	—	—	—	—	—	—	—	4	1	—	—	28	33
	*Garcinia magnifolia**	1	—	52	32	3	—	6	13	1	1	—	—	109
	Symphonia globulifera	26	31	6	12	13	7	—	—	—	—	2	—	97
	*Tovomita croatii**	—	—	—	—	24	—	10	8	3	10	—	—	55
	Tovomita longifolia	—	—	—	—	—	—	1	—	—	—	—	—	1
	*Tovomita weddelliana**	11	23	—	—	—	—	—	4	—	—	—	—	38
Cunoniaceae	*Weinmannia* cf. *balbisiana*	—	5	—	—	—	3	—	—	—	—	—	—	8
	Weinmannia pinnata	7	25	5	2	—	1	—	—	—	—	—	—	40
Cyatheaceae	*Alsophila cuspidata*	—	—	7	25	29	10	5	13	5	2	4	—	100
	Alsophila erinacea	18	—	4	10	47	96	4	19	61	18	—	—	277
	Cyathea eggersii	11	111	—	4	—	—	—	1	—	—	—	—	127
	Cyathea multiflora	—	—	—	—	13	57	1	—	7	—	—	—	78
	Cyathea sp1	1	19	—	—	3	—	5	—	—	2	11	—	41
	Cyathea sp2	—	5	—	2	—	—	—	—	1	11	—	—	19
	Dicksonia sellowiana	—	—	—	—	—	29	—	—	—	—	—	—	29
Dichapetalaceae	*Dichapetalum axillare*	—	—	—	—	—	—	—	—	—	—	23	—	23
Elaeocarpaceae	*Sloanea* aff. *deflexiflora*	—	—	—	—	—	—	—	—	—	—	5	—	5
	Sloanea ampla	1	10	4	—	1	—	1	—	—	—	—	1	18
	Sloanea cf. *meianthera**	—	—	—	1	—	—	—	—	—	—	—	—	1
	Sloanea cf. *brenesii**	—	—	19	—	2	5	—	—	—	4	—	—	30
	Sloanea medusula	—	—	—	—	—	—	—	1	—	—	—	—	1
	Sloanea zuliaensis	—	—	—	—	—	—	2	7	3	—	—	—	12
Erythropalaceae	*Heisteria acuminata*	—	—	—	—	—	—	—	—	—	—	14	—	14
Erythroxylaceae	*Erythroxylum macrophyllum**	—	—	10	4	6	2	1	—	1	6	1	11	42
Euphorbiaceae	*Acalypha diversifolia**	—	—	—	—	—	—	—	—	—	2	—	2	4
	*Alchornea glandulosa**	1	—	14	8	12	—	34	67	46	23	—	—	205
	Alchornea grandis	—	—	—	—	—	17	—	—	—	—	—	17	34
	Alchornea latifolia	—	—	—	—	—	—	—	—	14	—	—	—	14
	Croton billbergianus	—	—	—	—	—	—	—	—	—	—	—	10	10

(*Continued*)

		Rhyolite				R/M	Mafic-volcanic				Basalt	Dacite	Undif.	
Family	*Species*	Cho.A	Cho.B	Hon.A	Hon.B	Samu.	Bonita	Palo	Ver.A	Ver.B	Pinola	Horn.	Alto.	*n*
	*Croton draco**	—	—	—	3	11	—	—	—	2	2	—	2	20
	Croton pachypodus	—	—	—	—	—	—	1	5	—	—	—	—	6
	*Croton schiedeanus**	—	—	59	—	88	—	39	81	16	—	—	—	283
	Euphorbia elata	—	—	—	—	—	—	13	—	—	—	—	—	13
	Hyeronima alchorneoides	—	—	—	—	—	—	1	—	1	—	—	—	2
	*Hyeronima oblonga**	58	131	18	21	10	9	3	23	6	23	7	—	309
	Sapium allenii	—	—	—	—	—	—	—	3	3	—	—	—	6
	*Sapium glandulosum**	—	—	—	—	—	—	1	1	3	—	—	—	5
	*Tetrorchidium euryphyllum**	1	—	—	—	2	8	13	4	42	—	—	—	70
Fabaceae	*Andira inermis*	—	—	—	—	—	—	—	1	—	—	—	—	1
	Cojoba cf. *catenata*	—	—	—	—	—	—	1	—	—	—	—	—	1
	*Cojoba sophorocarpa**	—	—	—	1	2	2	—	—	1	—	1	—	7
	Dussia cuscatlanica	—	—	—	—	—	—	2	—	—	—	1	—	3
	Dussia macroprophyllata	—	—	—	—	—	—	1	—	1	—	—	—	2
	Dussia sp1	—	—	—	—	—	—	—	—	1	—	—	—	1
	Erythrina chiriquensis	—	—	—	—	—	—	—	—	—	—	—	11	11
	*Erythrina gibbosa**	—	—	—	—	—	—	—	—	—	12	—	—	12
	Inga acrocephala	—	—	—	—	—	—	5	2	2	—	—	—	9
	Inga acuminata	1	2	1	1	1	—	1	1	2	—	—	—	10
	Inga alba	—	—	3	4	19	54	12	14	10	18	—	—	134
	Inga allenii	—	—	—	—	—	—	7	8	19	—	—	—	34
	Inga barbourii	—	—	—	—	—	—	14	—	14	—	—	—	28
	Inga cylindrica	—	1	—	—	9	—	—	—	—	—	—	—	10
	Inga densiflora	—	—	—	—	—	—	—	4	—	—	—	—	4
	Inga exalata	—	—	53	43	33	1	—	1	—	3	—	—	134
	Inga jinicuil	—	—	—	—	—	1	23	3	3	—	—	—	30
	Inga leiocalycina	—	—	—	—	—	—	—	—	3	—	—	—	3
	*Inga leonis**	—	—	6	1	4	—	—	—	—	—	4	—	15
	*Inga longispica**	—	—	—	—	—	—	—	—	7	—	—	76	83
	Inga marginata	1	—	2	3	—	8	4	—	5	13	—	84	120
	Inga micheliana	—	—	—	—	—	—	—	9	—	—	—	—	9
	Inga nobilis	2	1	—	—	—	—	—	—	—	2	—	—	5

Family	*Species*	Rhyolite				R/M	Mafic-volcanic				Basalt	Dacite	Undif.	
		Cho.A	Cho.B	Hon.A	Hon.B	Samu.	Bonita	Palo	Ver.A	Ver.B	Pinola	Horn.	Alto.	*n*
	*Inga oerstediana**	—	—	1	—	—	9	—	2	—	10	—	1	23
	Inga pezizifera	—	—	3	1	7	—	—	1	—	1	—	—	13
	*Inga punctata**	1	—	—	4	—	—	1	—	—	—	—	—	6
	Inga sierrae	—	—	—	—	—	—	—	—	—	—	—	18	18
	Inga thibaudiana	—	—	—	—	—	—	—	—	1	—	—	—	1
	Inga umbellifera	—	—	—	—	—	—	—	2	1	—	—	—	3
	*Inga venusta**	5	—	—	4	4	—	1	—	—	—	1	—	15
	Lonchocarpus cf. *heptaphyllus*	—	—	—	—	—	—	1	—	—	—	—	—	1
	Lonchocarpus schiedeanus	—	—	—	—	—	—	—	—	—	—	—	10	10
	Myroxylon balsamum	—	—	—	—	—	—	—	—	—	—	—	1	1
	Ormosia panamensis	—	—	—	—	—	—	—	—	—	—	—	20	20
	Pithecellobium cf. *hymenaeifolium*	—	—	—	—	—	—	11	—	—	—	—	—	11
	Platymiscium pinnatum	—	—	—	—	—	1	6	7	5	—	—	3	22
	Platymiscium sp1	—	—	—	1	—	—	7	7	—	74	—	—	89
	Swartzia simplex	—	—	—	—	—	—	—	—	—	—	—	14	14
Fagaceae	*Quercus* cf. *lancifolia*	—	—	1	1	1	—	—	—	—	—	2	20	25
	Quercus cf. *salicifolia**	16	—	—	6	—	—	—	—	—	—	—	—	22
	Quercus glabra	—	—	—	—	—	—	—	—	—	—	—	4	4
	Quercus gulielmi-treleasei	9	—	—	—	—	—	—	—	—	—	—	—	9
	*Quercus insignis**	—	—	7	2	3	—	—	—	2	—	3	—	17
Icacinaceae	*Calatola costaricensis**	—	1	21	2	43	15	33	68	26	—	—	—	209
Juglandaceae	*Alfaroa costaricensis**	11	13	—	1	9	—	—	—	—	—	10	—	44
	*Oreomunnea mexicana**	—	2	77	354	—	—	—	—	—	—	2	1	436
Lacistemataceae	*Lacistema aggregatum*	—	—	—	—	—	—	—	—	—	—	—	32	32
	*Lozania mutisiana**	—	—	—	4	10	—	1	1	1	—	—	—	17
Lamiaceae	*Aegiphila anomala*	—	1	—	1	6	8	5	3	2	2	5	—	33
	Aegiphila panamensis	—	—	—	—	—	—	—	—	—	—	—	19	19
Lauraceae	*Aiouea costaricensis*	—	—	2	2	—	—	5	3	4	5	—	—	21
	*Aniba cinnamomiflora**	10	56	12	18	2	—	—	3	—	—	—	—	101
	Beilschmiedia sp1	—	—	—	—	—	—	—	—	—	—	—	3	3

(*Continued*)

		Rhyolite				R/M	Mafic-volcanic				Basalt	Dacite	Undif.	
Family	*Species*	Cho.A	Cho.B	Hon.A	Hon.B	Samu.	Bonita	Palo	Ver.A	Ver.B	Pinola	Horn.	Alto.	*n*
	Cinnamomum cf. *paratriplinerve**	—	—	2	1	—	—	—	—	—	—	2	—	5
	*Cinnamomum costaricanum**	1	—	1	1	—	—	—	—	—	—	—	—	3
	Cinnamomum sp2	2	—	—	4	—	—	—	—	—	—	1	—	7
	*Cinnamomum triplinerve**	—	—	1	—	—	—	4	—	—	—	—	—	5
	Endlicheria browniana	—	6	4	—	—	—	—	—	—	—	1	—	11
	Lauraceae sp3	—	—	—	—	—	—	—	—	1	—	—	13	14
	Lauraceae sp4	—	—	—	—	—	—	3	4	1	—	—	—	8
	Licaria cufodontisii	—	—	—	—	—	—	—	—	—	3	—	—	3
	Licaria excelsa	—	—	1	1	1	6	1	1	—	—	2	—	13
	Nectandra globosa	—	4	—	—	—	—	—	—	—	—	—	—	4
	*Nectandra membranacea**	—	—	1	—	—	—	1	1	5	—	—	26	34
	Nectandra purpurea	1	—	—	2	—	3	2	—	—	19	2	1	30
	Ocotea gomezii	4	2	9	10	4	1	1	—	—	—	—	—	31
	*Ocotea insularis**	—	—	2	3	1	18	—	1	—	—	—	—	25
	Ocotea mollifolia	—	—	3	—	3	—	—	—	15	—	—	—	21
	Ocotea oblonga	—	—	16	6	7	—	1	—	—	—	6	—	36
	*Ocotea pullifolia**	2	5	5	1	—	—	—	—	—	—	—	—	13
	Ocotea sp1	—	—	—	—	—	—	1	2	—	1	3	—	7
	Ocotea whitei	6	14	3	7	11	16	4	2	—	2	—	—	65
Lecythidaceae	*Eschweilera panamensis*	16	8	21	79	31	11	3	25	4	—	8	—	206
Magnoliaceae	*Talauma* sp1*	12	28	24	36	6	27	3	2	—	—	1	—	139
Malpighiaceae	*Bunchosia dwyeri**	—	—	—	—	—	—	1	—	—	—	—	—	1
	Bunchosia macrophylla	—	—	1	—	13	4	9	6	2	9	—	—	44
Malvaceae	*Apeiba membranacea*	—	—	—	—	—	—	—	2	—	—	—	—	2
	Goethalsia meiantha	—	—	—	—	—	—	—	4	—	—	—	—	4
	*Hampea appendiculata**	—	—	—	—	—	—	1	—	12	2	2	2	19
	Malvaviscus arboreus	—	—	—	—	—	—	—	—	—	—	2	17	19
	Matisia cf. *exalata*	—	—	—	—	—	—	1	—	—	—	—	—	1
	Matisia obliquifolia	—	—	—	—	—	—	4	1	8	—	—	—	13
	Matisia ochrocalyx	—	—	2	—	—	—	31	6	7	5	—	—	51
	Matisia sp1	—	—	—	—	—	—	13	2	50	—	—	—	65

		Rhyolite				R/M	Mafic-volcanic				Basalt	Dacite	Undif.	
Family	*Species*	Cho.A	Cho.B	Hon.A	Hon.B	Samu.	Bonita	Palo	Ver.A	Ver.B	Pinola	Horn.	Alto.	*n*
	*Mortoniodendron anisophyllum**	—	—	1	2	4	1	12	11	28	8	6	—	73
	Pachira aquatica	—	—	9	—	8	—	4	4	5	1	—	—	31
	Pachira sessilis	—	—	—	—	—	—	—	—	1	—	—	—	1
	Trichospermum galeottii	—	—	—	—	—	—	—	—	2	—	—	—	2
	*Wercklea insignis**	—	—	1	3	—	3	4	—	19	—	—	—	30
Melastomataceae	*Clidemia ombrophila**	—	—	1	—	—	—	—	—	—	—	—	—	1
	Conostegia micrantha	—	—	1	—	—	—	2	2	52	—	—	—	57
	*Conostegia rufescens**	—	—	4	2	8	9	4	4	105	—	—	—	136
	Conostegia sp1	—	—	—	—	—	—	—	—	—	—	31	12	43
	*Graffenrieda bella**	101	202	—	19	—	—	—	—	—	—	—	—	322
	Henriettella tuberculosa	—	—	—	—	—	—	1	1	2	—	—	—	4
	Miconia dissita	—	—	—	—	1	2	1	—	—	—	—	—	4
	Miconia sp1	2	3	—	2	1	—	—	—	—	—	—	—	8
	Miconia sp2	—	—	—	—	—	—	—	—	—	11	—	4	15
	Miconia sp5	—	—	1	—	1	6	—	—	—	—	1	—	9
	*Miconia theaezans**	—	—	—	—	—	—	3	—	2	—	—	—	5
	Ossaea cf. *acuminate*	—	—	11	14	2	1	—	—	—	—	—	—	28
Meliaceae	*Cedrela tonduzii*	—	—	—	—	—	—	—	—	—	—	6	—	6
	Guarea cf. *longifoliola*	—	—	—	—	—	1	—	—	—	—	—	—	1
	*Guarea glabra**	—	—	73	47	56	—	2	7	2	69	10	5	271
	*Guarea grandifolia**	2	—	10	4	9	4	17	3	6	—	12	—	67
	Guarea kunthiana	1	—	—	4	—	—	13	—	—	—	4	—	22
	Guarea pterorhachis	—	—	—	—	—	—	—	—	—	4	39	—	43
	Guarea sp2	—	—	—	6	1	—	—	—	—	—	2	—	9
	Guarea sp4	—	—	—	2	—	48	6	1	6	—	—	—	63
	Guarea sp5	—	—	—	—	—	—	2	20	10	—	—	—	32
	*Ruagea glabra**	—	—	—	—	—	42	18	15	6	—	—	—	81
	*Trichilia havanensis**	3	—	5	1	—	—	—	—	—	—	—	—	9
	*Trichilia martiana**	—	—	2	1	3	28	2	1	—	7	—	—	44
	Trichilia septentrionalis	—	—	—	—	—	—	—	—	—	—	3	—	3

(*Continued*)

		Rhyolite				R/M	Mafic-volcanic				Basalt	Dacite	Undif.	
Family	*Species*	Cho.A	Cho.B	Hon.A	Hon.B	Samu.	Bonita	Palo	Ver.A	Ver.B	Pinola	Horn.	Alto.	*n*
Menispermaceae	*Hyperbaena allenii**	—	—	—	—	—	—	—	—	—	—	30	1	31
Metteniusaceae	*Metteniusa tessmanniana**	—	—	—	—	—	—	28	—	27	—	—	—	55
Monimiaceae	*Mollinedia* cf. *minutiflora**	—	—	1	17	—	—	—	—	—	—	—	—	18
	Mollinedia darienensis	—	—	—	1	9	2	7	—	—	1	15	—	35
Moraceae	*Brosimum guianense*	—	—	—	—	—	—	1	—	1	—	—	—	2
	Ficus insipida	—	—	—	—	—	—	1	—	—	—	—	—	1
	*Ficus pertusa**	—	—	—	—	—	—	—	—	—	—	1	—	1
	Ficus sp3	—	—	—	—	—	4	1	—	4	2	—	—	11
	Ficus tonduzii	—	—	—	—	—	—	—	—	1	—	—	—	1
	*Maquira guianensis**	—	—	—	—	—	—	11	3	25	—	—	—	39
	Naucleopsis naga	—	5	1	—	4	1	10	20	5	2	3	—	51
	Perebea guianensis	—	—	—	—	—	—	—	—	—	—	2	—	2
	Perebea sp1	—	—	—	—	1	—	—	—	—	36	15	—	52
	Poulsenia armata	—	—	—	—	—	—	—	—	1	—	—	—	1
	Pseudolmedia spuria	—	—	10	—	11	—	1	—	—	—	2	—	24
	Sorocea pubivena	—	—	1	—	—	—	2	1	—	—	—	—	4
	*Sorocea trophoides**	—	—	—	—	7	—	4	—	—	33	2	17	63
	Trophis caucana	—	—	—	1	—	—	—	—	—	—	—	—	1
Myristicaceae	*Osteophloeum* cf. *platyspermum*	—	2	11	1	12	2	1	1	20	26	—	—	76
	Otoba novogranatensis	—	—	—	—	—	—	2	4	4	—	—	—	10
	Virola koschnyi	3	—	—	2	—	—	—	—	—	—	—	—	5
Myrtaceae	*Eugenia galalonensis*	—	—	4	—	—	—	—	—	—	4	7	—	15
	*Eugenia siggersii**	—	—	—	3	1	1	—	—	—	—	—	18	23
	Eugenia sp3	—	—	—	—	—	—	—	—	—	—	58	—	58
	Eugenia sp6	—	—	—	—	—	2	—	—	—	—	2	—	4
	Myrcia gatunensis	2	1	6	18	8	6	—	—	—	—	2	—	43
	Myrcianthes fragrans	—	—	—	—	—	—	—	—	—	—	—	4	4
	Myrtaceae sp3	—	—	—	—	—	—	—	7	2	—	—	6	15
	Myrtaceae sp6	—	—	—	—	—	—	2	25	1	—	—	—	28
	Plinia sp1	—	—	16	6	41	—	4	3	—	—	1	—	71

		Rhyolite				R/M	Mafic-volcanic				Basalt	Dacite	Undif.	
Family	*Species*	Cho.A	Cho.B	Hon.A	Hon.B	Samu.	Bonita	Palo	Ver.A	Ver.B	Pinola	Horn.	Alto.	*n*
Nyctaginaceae	*Guapira costaricana*	—	—	—	—	—	2	1	—	3	—	—	58	64
	Guapira sp1	—	—	—	—	—	—	—	5	—	—	—	—	5
	Neea amplifolia	—	—	—	—	1	—	2	—	2	—	—	—	5
	Neea sp1	—	—	—	—	—	—	1	6	2	3	—	—	12
Ochnaceae	*Ouratea lucens**	21	—	—	—	—	—	—	—	—	—	—	13	34
	*Ouratea prominens**	—	—	—	—	—	—	—	1	—	—	—	—	1
	Quiina colonensis	—	—	—	—	—	—	3	—	1	—	—	—	4
Passifloraceae	*Passiflora tica**	—	—	2	—	—	—	—	—	—	—	—	—	2
Phyllanthaceae	*Margaritaria nobilis**	—	—	—	—	—	—	8	2	58	5	—	66	139
	Richeria obovata	—	—	13	6	2	—	—	4	—	—	—	—	25
Picramniaceae	*Picramnia teapensis*	—	—	3	—	1	—	4	7	3	23	3	7	51
Piperaceae	*Piper* cf. *casitense*	—	—	—	—	—	—	1	—	—	—	—	—	1
	Piper imperial	1	—	5	1	2	13	2	—	—	—	10	—	34
	Piper obliquum	—	—	—	—	—	—	—	4	5	—	—	—	9
	Piper sp1	—	—	—	—	—	—	—	—	—	6	1	—	7
	Piper sp2	—	—	—	—	—	—	—	—	—	—	—	33	33
Podocarpaceae	*Podocarpus oleifolius**	7	5	—	1	—	—	—	—	—	—	—	—	13
Polygonaceae	*Coccoloba gentryi**	—	—	—	—	—	—	5	—	6	—	—	—	11
	Coccoloba manzinellensis	—	—	—	—	—	—	1	—	3	—	—	—	4
	*Coccoloba obovata**	—	—	—	—	—	—	3	8	2	—	—	38	51
Primulaceae	*Ardisia gordonii*	—	—	—	—	—	—	1	—	2	—	—	—	3
	Ardisia guianensis	—	—	—	—	—	—	—	—	2	—	—	—	2
	Ardisia hagenii	—	—	—	5	—	40	16	17	12	—	—	—	90
	*Ardisia panamensis**	—	—	—	—	—	—	—	—	—	—	—	10	10
	Ardisia sp2	6	27	54	127	9	—	—	—	—	—	5	26	254
	Ardisia sp4	—	—	—	—	—	14	—	—	—	—	—	—	14
	Ardisia sp5	—	—	—	—	—	—	3	3	—	—	—	—	6
	*Ardisia wedelli**	6	—	6	18	10	—	5	—	1	—	—	—	46
	*Cybianthus montanus**	123	123	3	5	—	1	—	—	—	—	—	—	255
	Myrsine coriacea	—	—	—	—	—	—	—	—	—	—	—	9	9
	Myrsine cubana	—	—	—	—	—	—	1	1	2	—	11	2	17
	*Parathesis amplifolia**	—	—	2	—	3	2	2	7	5	57	—	—	78

(*Continued*)

		Rhyolite				R/M	Mafic-volcanic				Basalt	Dacite	Undif.	
Family	*Species*	Cho.A	Cho.B	Hon.A	Hon.B	Samu.	Bonita	Palo	Ver.A	Ver.B	Pinola	Horn.	Alto.	*n*
Proteaceae	*Panopsis suaveolens*	—	—	5	—	3	—	1	—	—	—	1	—	10
	*Roupala montana**	—	—	11	6	15	—	10	—	2	1	14	8	67
Putranjivaceae	*Drypetes brownii*	—	—	—	—	—	—	17	5	5	—	—	—	27
Rhizophoraceae	*Cassipourea elliptica**	6	—	57	60	61	—	16	8	5	1	19	10	243
Rosaceae	*Prunus brachybotrya*	—	—	3	1	4	—	—	—	—	2	7	22	39
	Prunus cf. *fortunensis**	1	—	1	—	1	—	—	—	—	—	—	72	75
Rubiaceae	*Alibertia garapatica**	—	—	7	7	9	—	1	—	—	1	—	—	25
	*Amaioua pedicellata**	7	—	59	25	3	2	18	26	25	2	—	—	167
	*Bathysa veraguensis**	—	—	—	—	—	—	1	—	—	—	—	—	1
	Chione campanensis	—	—	—	—	—	—	—	—	—	—	4	—	4
	*Chione venosa**	—	8	—	—	—	—	—	—	—	—	—	—	8
	Chomelia sp1	—	—	5	—	5	—	13	7	21	35	21	—	107
	Elaeagia auriculata	—	—	59	11	10	37	1	14	9	—	—	—	141
	Faramea multiflora	—	—	9	6	87	—	—	1	—	39	—	—	142
	*Guettarda crispiflora**	—	—	2	2	3	1	2	1	4	8	—	—	23
	*Joosia umbellifera**	—	—	3	—	5	10	39	7	5	—	—	—	69
	*Palicourea purpurea**	—	—	—	—	—	—	—	—	—	—	1	2	3
	*Palicourea roseofaucis**	11	11	23	18	22	—	—	—	—	—	—	—	85
	Palicourea sp1	—	—	—	—	—	—	14	39	15	—	—	—	68
	*Pentagonia nuciformis**	—	1	11	—	16	—	25	10	27	11	—	—	101
	*Posoqueria latifolia**	38	61	31	71	—	—	11	2	1	—	—	—	215
	*Psychotria chiriquina**	—	—	—	—	—	—	—	—	—	—	—	1	1
	*Psychotria elata**	—	—	4	5	—	3	3	1	2	—	2	—	20
	*Psychotria luxurians**	179	224	1	—	—	9	1	—	17	—	—	—	431
	*Psychotria orosiana**	—	—	—	—	—	—	1	—	—	—	—	—	1
	*Psychotria panamensis**	—	—	11	1	45	7	—	4	—	—	40	—	108
	Psychotria sp1	—	—	12	1	13	—	23	—	42	134	—	—	225
	*Rondeletia buddleioides**	—	—	16	5	23	—	4	5	7	—	—	—	60
	Rondeletia salicifolia	—	—	—	1	—	—	9	—	—	—	—	—	10
	*Rosenbergiodendron formosum**	—	—	—	—	—	—	—	—	—	—	3	—	3
	Rubiaceae sp1	—	—	—	—	—	—	1	1	—	—	—	—	2

		Rhyolite				R/M	Mafic-volcanic				Basalt	Dacite	Undif.	
Family	*Species*	Cho.A	Cho.B	Hon.A	Hon.B	Samu.	Bonita	Palo	Ver.A	Ver.B	Pinola	Horn.	Alto.	*n*
Rutaceae	*Peltostigma guatemalense*	—	—	—	—	—	—	—	—	—	—	97	—	97
	Zanthoxylum acuminatum	—	—	—	—	—	—	—	—	—	—	—	3	3
	*Zanthoxylum melanostictum**	—	—	—	—	—	—	—	—	—	—	—	6	6
	Zanthoxylum panamense	—	—	—	—	1	—	—	—	—	—	—	—	1
	Zanthoxylum setulosum	—	—	—	—	—	—	—	—	—	—	—	3	3
	Zanthoxylum sp1	—	—	—	—	—	—	—	—	—	—	—	8	8
Sabiaceae	*Meliosma allenii*	1	—	16	4	5	—	—	—	—	—	—	—	26
	Meliosma brenesii	—	—	—	—	—	—	1	—	2	—	—	—	3
	*Meliosma occidentalis**	60	—	1	—	—	—	9	4	5	29	15	—	123
	Meliosma sp1	—	—	1	—	1	—	—	—	—	—	—	—	2
Salicaceae	*Casearia arborea**	—	—	16	2	9	—	—	6	—	—	—	—	33
	Casearia arguta	—	—	3	2	—	6	3	—	4	—	1	—	19
	Casearia sylvestris	—	—	2	—	7	2	—	—	—	6	—	—	17
	Casearia tacanensis	—	—	3	—	—	—	—	—	—	—	—	—	3
	Hasseltia floribunda	—	—	—	—	1	—	2	4	1	1	31	—	40
	Pleuranthodendron lindenii	—	—	—	—	18	—	—	—	1	14	—	—	33
	Xylosma chlorantha	—	—	—	—	—	—	2	—	6	—	—	3	11
	*Xylosma oligandra**	—	—	1	—	4	2	—	—	—	—	—	—	7
Sapindaceae	*Allophylus psilospermus*	—	—	—	—	—	—	1	—	7	62	—	—	70
	Billia rosea	18	20	16	22	5	5	—	9	1	9	17	—	122
	Cupania guatemalensis	—	—	—	3	—	—	—	—	—	—	1	—	4
	Cupania latifolia	—	—	2	—	—	—	—	3	10	—	—	—	15
	Cupania rufescens	—	—	—	—	—	—	4	10	3	—	—	4	21
	Cupania seemannii	—	—	—	—	—	—	—	—	—	33	—	—	33
	Talisia hexaphylla	—	—	—	—	—	—	—	—	—	—	—	6	6
Sapotaceae	*Chrysophyllum argenteum*	—	—	—	—	—	—	1	—	—	—	—	57	58
	Chrysophyllum colombianum	—	—	1	—	—	—	1	—	—	—	—	—	2
	Chrysophyllum hirsutum	—	—	—	—	—	—	1	—	—	—	—	—	1
	Manilkara chicle	—	—	—	—	—	—	—	—	—	—	—	6	6
	Micropholis melinoniana	21	27	33	16	32	1	—	—	—	5	9	—	144
	Pouteria cuspidate	13	17	18	19	8	—	—	—	1	—	2	—	78
	*Pouteria fossicola**	—	—	—	—	18	—	—	—	1	13	—	—	32

(Continued)

		Rhyolite				R/M	Mafic-volcanic				Basalt	Dacite	Undif.	
Family	***Species***	**Cho.A**	**Cho.B**	**Hon.A**	**Hon.B**	**Samu.**	**Bonita**	**Palo**	**Ver.A**	**Ver.B**	**Pinola**	**Horn.**	**Alto.**	***n***
	*Pouteria glomerata**	—	—	5	—	9	8	2	1	1	1	—	—	27
	Pouteria glomerata ssp. *stylosa*	—	—	—	—	—	—	2	—	1	4	1	—	8
	Pouteria juruana	—	—	—	—	—	1	5	3	6	1	95	58	169
	*Pouteria reticulata**	15	—	—	2	—	23	42	46	28	—	1	—	157
	*Sarcaulus brasiliensis**	—	—	4	—	4	—	—	—	—	—	4	—	12
Solanaceae	*Witheringia cuneata*	—	—	—	—	—	—	1	—	—	—	—	—	1
Symplocaceae	*Symplocos* cf. *panamensis**	—	—	1	—	—	—	—	—	—	—	—	—	1
	Symplocos limoncello	—	—	—	—	—	—	—	—	—	—	—	43	43
Tapisciaceae	*Turpinia occidentalis**	1	1	—	—	—	9	—	—	—	2	—	20	33
Thymelaeaceae	*Daphnopsis* aff. *correae*	—	—	—	5	4	—	—	1	—	3	—	—	13
	*Daphnopsis americana**	1	—	—	—	—	15	—	1	—	—	1	—	18
	Schoenobiblus panamensis	—	—	—	—	—	—	1	—	—	—	—	—	1
Ticodendraceae	*Ticodendron incognitum**	—	—	11	8	19	—	—	—	1	—	2	—	41
Urticaceae	*Cecropia angustifolia*	1	—	—	3	17	—	—	—	—	—	2	1	24
	Cecropia cf. *garciae*	—	—	3	3	—	—	—	—	—	—	—	—	6
	Cecropia obtusifolia	—	—	4	—	—	—	1	—	—	—	—	—	5
	Pourouma bicolor	—	—	—	—	—	—	—	1	3	—	—	—	4
Verbenaceae	*Callicarpa acuminata*	—	—	—	—	—	—	—	—	—	—	—	26	26
	*Citharexylum gentryi**	—	—	—	—	—	—	1	—	—	—	—	—	1
	*Citharexylum macradenium**	—	—	—	2	1	2	—	—	—	1	8	—	14
Vochysiaceae	*Vochysia guatemalensis*	—	—	28	2	20	—	—	11	—	—	—	—	61
Winteraceae	*Drimys granadensis**	—	15	—	—	—	—	—	—	—	—	—	—	15

References

Adames, A. J. 1977. *Evaluación ambiental y efectos del Proyecto Hidroelectrico Fortuna: Informe final* [Environmental assessment and effects of the Fortuna Hydroelectric Project: Final report]. Panamá: Lotería Nacional de Beneficencia.

Alfonso-Corrado, C., F. Naranjo-Luna, R. Clark-Tapia, J. Campos, O. Rojas-Soto, M. Luna-Krauletz, B. Bodenhorn, M. Gorgonio-Ramírez, and N. Pacheco-Cruz. 2017. Effects of Environmental Changes on the Occurrence of *Oreomunnea mexicana* (Juglandaceae) in a Biodiversity Hotspot Cloud Forest. *Forests*, 8:261. https://doi.org/10.3390/f8080261

Andersen, K. M. 2021. Palm Flora and Drivers of Distributions in Fortuna Forest Reserve. In *Fortuna Forest Reserve, Panama: Interacting Effects of Climate and Soils on the Biota of a Wet Premontane Tropical Forest*, ed. J. W. Dalling and B. L. Turner, pp. 271–287. Smithsonian Contributions to Botany, No. 112. Washington, D.C.: Smithsonian Institution Scholarly Press.

Andersen, K. M., M. D. Corre, B. L. Turner, and J. W. Dalling. 2010. Plant-Soil Associations in Lower Montane Tropical Forest: Physiological Acclimation and Herbivore-Mediated Responses to Nitrogen Addition. *Functional Ecology*, 24:1171–1180. https://doi.org/10.1111/j.1365-2435.2010.01731.x

Andersen, K. M., M.-J. Endara, B. L. Turner, and J. W. Dalling. 2012. Trait-Based Community Assembly of Understory Palms along a Soil Nutrient Gradient in a Lower Montane Tropical Forest. *Oecologia*, 168:519–531. https://doi.org/10.1007/s00442-011-2112-z

Andersen, K. M., J. R. Mayor, and B. L. Turner. 2017. Plasticity in Nitrogen Uptake Among Sympatric Species with Contrasting Nutrient Acquisition Strategies in a Tropical Forest. *Ecology*, 98:1388–1398. https://doi.org/10.1002/ecy.1793

Andersen, K. M., and B. L. Turner. 2013. Preferences or Plasticity in Nitrogen Acquisition by Understory Palms in a Tropical Montane Forest? *Journal of Ecology*, 101:819–825. https://doi.org/10.1111/1365-2745.12070

Andersen, K. M., B. L. Turner, and J. W. Dalling. 2010. Soil-Based Habitat Partitioning in Understorey Palms in Lower Montane Tropical Forests. *Journal of Biogeography*, 37:278–292. https://doi.org/10.1111/j.1365-2699.2009.02192.x

Andersen, K. M., B. L. Turner, and J. W. Dalling. 2014. Seedling Performance Trade-Offs Influencing Habitat Filtering Along a Soil Nutrient Gradient in a Tropical Forest. *Ecology*, 95:3399–3413. https://doi.org/10.1890/13-1688.1

Cavelier, J., D. Solis, and M. A. Jaramillo. 1996. Fog Interception in Montane Forest across the Central Cordillera of Panama. *Journal of Tropical Ecology*, 12:357–369. https://doi.org/10.1017/S026646740000955X

Corrales, A., A. H. Ferrer, A. E. Arnold, and J. W. Dalling. 2016. Variation in Ectomycorrhizal Fungal Communities Associated with *Oreomunnea mexicana* (Juglandaceae) in Tropical Montane Forests. *Mycorrhiza*, 26:1–16. https://doi.org/10.1007/s00572-015-0641-8

Corrales, A., S. A. Mangan, B. L. Turner, and J. W. Dalling. 2016. An Ectomycorrhizal Nitrogen Economy Facilitates Monodominance in a Neotropical Forest. *Ecology Letters*, 19:383–392. https://doi.org/10.1111/ele.12570

Corrales, A., and C. L. Ovrebo. 2021. Fungi of the Fortuna Forest Reserve: Taxonomy and Ecology with Emphasis on Ectomycorrhizal Communities. In *Fortuna Forest Reserve, Panama: Interacting Effects of Climate and Soils on the Biota of a Wet Premontane Tropical Forest*, ed. J. W. Dalling and B. L. Turner, pp. 137–153. Smithsonian Contributions to Botany, No. 112. Washington, D.C.: Smithsonian Institution Scholarly Press.

Corrales, A., B. L. Turner, L. Tedersoo, S, Anslan, and J. W. Dalling. 2017. Nitrogen Addition Alters Ectomycorrhizal Fungal Communities and Soil Enzyme Activities in a Tropical Montane Forest. *Fungal Ecology*, 27:14–23. https://doi.org/10.1111/ele.12570

Corre, M. D., E. Veldkamp, J. Arnold, and S. J. Wright. 2010. Impact of Elevated N Input on Soil N Cycling and Losses in Old-Growth Lowland and Montane Forests of Panama. *Ecology*, 91:1715–1729. https://doi.org/10.1890/09-0274.1

Correa, A. M. D., C. Galdames, and M. S. De Stapf. 2004. *Catálogo de las plantas vasculares de Panamá* [Catalog of vascular plants of Panama]. Balboa, Panamá: Universidad de Panamá.

De Caceres, M., and P. Legendre. 2009. Associations between Species and Groups of Sites: Indices and Statistical Inference. *Ecology*, 90:3566–3574. https://doi.org/10.1890/08-1823.1

Evans, R. J. 2001. Monograph of *Colpothrinax*. *Palms*, 45:177–195.

Fisher, J. B., Y. Malhi, I. C. Torres, D. B. Metcalfe, M. J. van de Weg, P. Meir, J. E. Silva-Espejo, and W. H. Huasco. 2013. Nutrient Limitation in Rainforests and Cloud Forests Along a 3,000-m Elevation Gradient in the Peruvian Andes. *Oecologia*, 172:889–902. https://doi.org/10.1007/s00442-012-2522-6

Gomez, D. C., G. Zotz, and M. Y. Bader. 2021. The Role of Epiphytes in Rainfall Interception by a Lower Montane Tropical Forest in Panama. In *Fortuna Forest Reserve, Panama: Interacting Effects of Climate and Soils on the Biota of a Wet Premontane Tropical Forest*, ed. J. W. Dalling and B. L. Turner, pp. 203–212. Smithsonian Contributions to Botany, No. 112. Washington, D.C.: Smithsonian Institution Scholarly Press.

Graham, E. A., S. S. Mulkey, K. Kitajima, N. G. Phillips, and S. J. Wright. 2003. Cloud Cover Limits Net CO_2 Uptake and Growth of a Rainforest Tree during Tropical Rainy Seasons. *Proceedings of the National Academy of Sciences of the United States of America*, 100:572–576. https://doi.org/10.1073/pnas.0133045100

Heineman, K. D. 2016. *Variation in Tree Species Nutrient Allocation Strategies along a Soil Fertility Gradient in Panama*. PhD thesis, University of Illinois.

Heineman, K. D., P. Caballero, A. Morris, C. Velasquez, K. Serrano, N. Ramos, J. Gonzalez, L. Mayorga, M. D. Corre, and J. W. Dalling. 2015. Variation in Canopy Litterfall along a Precipitation and Soil Fertility Gradient in a Panamanian Lower Montane Forest. *Biotropica*, 47:300–309. https://doi.org/10.1111/btp.12214

Heineman, K. D., B. L. Turner, J. W. Dalling. 2016. Variation in Wood Nutrients along a Tropical Soil Fertility Gradient. *New Phytologist*, 211:440–454. https://doi.org/10.1111/nph.13904

Herrera, F., S. R. Manchester, R. Koll, and C. Jaramillo. 2014. Fruits of *Oreomunnea* (Juglandaceae) in the Early Miocene of Panama. In *Paleobotany and Biogeography: A Festschrift for Alan Graham in His 80th Year*, ed. W. D. Stevens, O. M. Montiel, and P. H. Raven, pp. 124–133. *Monographs in Systematic Botany from the Missouri Botanical Garden*, No. 128. St. Louis: Missouri Botanical Garden Press.

Holdridge, L. R. 1967. *Life Zone Ecology*. San Jose, Costa Rica: Tropical Science Center.

Instituto de Recursos Hidraulicos y Electrificacion (IRHE). 1975. *The Fortuna Hydroelectric Project: Updated Feasibility Report*. Boston: Chas. T. Main International.

Jones, J. M., K. D. Heineman, and J. W. Dalling. 2019. Soil and Species Effects on Bark Nutrient Storage in a Premontane Tropical Forest. *Plant Soil*, 438:347–360. https://doi.org/10.1007/s11104-019-04026-9

Koehler, B., M. D. Corre, E. Veldkamp, H. Wullaert, and S. J. Wright. 2009. Immediate and Long-Term Nitrogen Oxide Emissions from Tropical Forest Soils Exposed to Elevated Nitrogen Input. *Global Change Biology*, 15:2049–2066. https://doi.org/10.1111/j.1365-2486.2008.01826.x

Leigh, E. G. Jr. 1999. *Tropical Forest Ecology: A View from Barro Colorado Island*. New York: Oxford University Press.

McPherson, G., M. Merello, and M. Fica. 2010. A Checklist of the Fortuna Dam Region, Chiriqui/Bocas del Toro, Panama. http://www.mobot.org/MOBOT/Research/fortuna.shtml (accessed 10 October 2019).

Meisner, K., and G. Zotz. 2012. Heteroblasty in Bromeliads: Its Frequency in a Local Flora and the Timing of the Transition from atmospheric to Tank Form in the Field. *International Journal of Plant Sciences*, 173:780–788. https://doi.org/10.1086/666665

Mulligan, M. 2010. Modeling the Tropics-Wide Extent and Distribution of Cloud Forest and Cloud Forest Loss, with Implications for Conservation Priority. In *Tropical Montane Cloud Forests: Science for Conservation and Management*, ed. L. A. Bruijnzeel, F. A. Scatena, and L. S. Hamilton, pp.16–38. Cambridge: Cambridge University Press.

Mulligan, M. 2013. WaterWorld: A Self-Parameterising, Physically Based Model for Application in Data-Poor but Problem-Rich Environments Globally. *Hydrology Research*, 44:748–769. https://doi.org/10.2166/nh.2012.217

Mulligan, M., and S. M. Burke. 2005. FIESTA Fog Interception for the Enhancement of Streamflow in Tropical Areas Final Technical Report for AMBIOTEK/King's College London contribution. DFID-FRP project R7991. Department for International Development, London.

Palmweb. 2019. Palmweb: Palms of the World Online. www.palmweb.org (accessed 10 October 2019).

Ping, C. L., G. J. Michaelson, C. A. Stiles, and G. González. 2013. Soil Characteristics, Carbon Stores, and Nutrient Distribution in Eight Forest Types along an Elevational Gradient, Eastern Puerto Rico. In *Ecological Gradient Analyses in a Tropical Landscape*, ed. G. González, M. R. Willig, and R. B. Waide, pp. 67–86. Ecological Bulletins, No. 54. Hoboken, N.J.: Wiley-Blackwell.

Prada, C. M., A. Morris, K. M. Andersen, B. L. Turner, P. Caballero, and J. W. Dalling. 2017. Soils and Rainfall Drive Landscape-Scale Changes in the Diversity and

Functional Composition of Tree Communities in Premontane Tropical Forest. *Journal of Vegetation Science*, 28:859–870. https://doi.org/10.1111/jvs.12540

Pyke, C. R., R. Condit, S. Aguilar, and S. Lao. 2001. Floristic Composition along a Climatic Gradient in a Neotropical Lowland Forest. *Journal of Vegetation Science*, 12:553–566. https://doi.org/10.2307/3237007

Russo, S. E., A. Kochsiek, J. Olney, L. Thompson, A. E. Miller, and S. Tan. 2013. Nitrogen Uptake Strategies of Edaphically Specialized Bornean Tree Species. *Plant Ecology*, 214:1405–1416. https://doi.org/10.1007/s11258-013-0260-4

Salazar Allen, N., J. Gudiño L., D. Santamaría E., M. B. Johnston, C. Chung, C. Arrocha, E. Rodriguez, and J. Spörle. 2021. The Bryophytes. In *Fortuna Forest Reserve, Panama: Interacting Effects of Climate and Soils on the Biota of a Wet Premontane Tropical Forest*, ed. J. W. Dalling and B. L. Turner, pp. 155–202. Smithsonian Contributions to Botany, No. 112. Washington, D.C.: Smithsonian Institution Scholarly Press.

Silva, C., D. Cárdenas, N. Pardo, L. Londoño, B. L. Turner, and C. Jaramillo. 2021. Geological Map of the Fortuna Forest Reserve. In *Fortuna Forest Reserve, Panama: Interacting Effects of Climate and Soils on the Biota of a Wet Premontane Tropical Forest*, ed. J. W. Dalling and B. L. Turner, pp. 35–46. Smithsonian Contributions to Botany, No. 112. Washington, D.C.: Smithsonian Institution Scholarly Press.

Silvera, K. S. 2021. The Orchids of Fortuna, Panama: A Checklist of Photosynthetic Pathways, Growth Habitat, and Resource Acquisition. In *Fortuna Forest Reserve, Panama: Interacting Effects of Climate and Soils on the Biota of a Wet Premontane Tropical Forest*, ed. J. W. Dalling and B. L. Turner, pp. 213–235. Smithsonian Contributions to Botany, No. 112, Washington, D.C.: Smithsonian Institution Scholarly Press.

Steidinger, B. S., B. L. Turner, A. Corrales, and J. W. Dalling. 2015. Variability in Potential to Exploit Different Soil Organic Phosphorus Compounds among Tropical Montane Tree Species. *Functional Ecology*, 29:121–130. https://doi.org/10.1111/1365-2435.12325

Tanner, E. V. J., P. A. Vitousek, and E. Cuevas. 1998. Experimental Investigation of Nutrient Limitation of Forest Growth on Wet Tropical Mountains. *Ecology*, 79:10–22. https://doi.org/10.1890/0012-9658(1998)079[0010:EIONLO]2.0.CO;2

Turner, B. L. 2008. Resource Partitioning for Soil Phosphorus: A Hypothesis. *Journal of Ecology*, 96:698–702. https://doi.org/10.1111/j.1365-2745.2008.01384.x

Turner, B. L., and J. W. Dalling. 2021. Soils of the Fortuna Forest Reserve. In *Fortuna Forest Reserve, Panama: Interacting Effects of Climate and Soils on the Biota of a Wet Premontane Tropical Forest*, ed. J. W. Dalling and B. L. Turner, pp. 47–135. Smithsonian Contributions to Botany, No. 112. Washington, D.C.: Smithsonian Institution Scholarly Press.

Viana, J. L., and J. W. Dalling. 2021. Diversity and Ecology of the Ferns in Fortuna. In *Fortuna Forest Reserve, Panama: Interacting Effects of Climate and Soils on the Biota of a Wet Premontane Tropical Forest*, ed. J. W. Dalling and B. L. Turner, pp. 237–270. Smithsonian Contributions to Botany, No. 112. Washington, D.C.: Smithsonian Institution Scholarly Press.

Viana, J. L., B. L. Turner, and J. W. Dalling. 2020. Compositional Variation in Understorey Fern and Palm Communities along a Soil Fertility and Rainfall Gradient in a Lower Montane Tropical Forest. *Journal of Vegetation Science*. Published ahead of print, 5 September 2020. https://doi.org/10.1111/jvs.12947

Wilson, A. M., and W. Jetz. 2016. Remotely Sensed High-Resolution Global Cloud Dynamics for Predicting Ecosystem and Biodiversity Distributions. *PLOS Biology*, 14:e1002415. https://doi.org/10.1371/journal.pbio.1002415

PLATE 1.1. (A) Smithsonian Tropical Research Institute Jorge Luis Araúz Field Station. (B) View southeast from the Quijada del Diablo pass up the Rio Hornito Valley, with Cerro Pata de Macho the tallest peak on the left and Cerro Hornito in the background on the right. (C) View eastward across Lake Fortuna from above the dam. (D) View northeast toward the Continental Divide from the same location. The large flat area beneath the divide is the Quebrada Honda watershed supporting monodominant *Oreomunnea* forest. (E) The Fortuna dam with the Continental Divide in the background. (F) View westward below the dam toward Cerro Pinola in the foreground. (G) Canopy of the emergent palm *Colpothrinax aphanopetala*, Quebrada Chorro watershed. (H) View north from the Continental Divide down the Caribbean slope. (I) Locations where photographs A–H were taken.

(*Continued*)

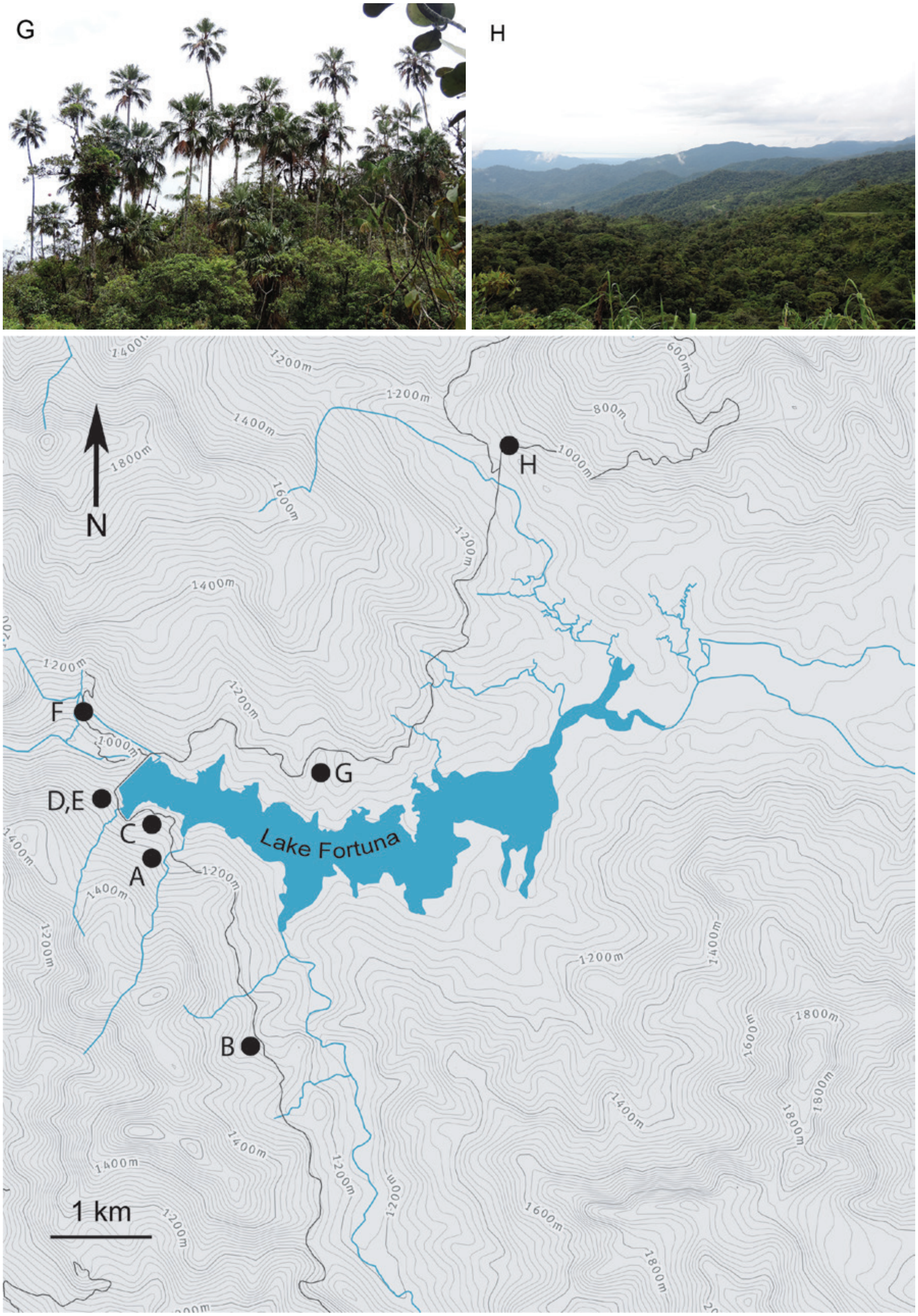

PLATE 1.1. (*Continued*)

PLATE 1.2. (A) View of Alto Frio plot. (B) Hornito A plot. (C) Pinola plot. (D) Zorro A plot. (E) Honda B plot. (F) Chorro A plot. (G) Chorro A soil pit showing rhyolite tuff. (H) Palo Seco plot. (I) Verrugosa B plot.

PLATE 1.3. (A) Individual of *Oreomunnea mexicana* (Juglandaceae), Honda watershed. Note characteristic bark decortication. (B) Abundant *Oreomunnea* seedling regeneration in a monodominant *Oreomunnea* stand, Honda B plot. (C) Understory palm *Chamaedorea verecunda*, endemic to Fortuna, Honda watershed. (D) Juvenile individual of the emergent palm *Colpothrinax aphanopetala* (Arecaceae), Chorro watershed. (E) The conifer *Podocarpus oleifolius* (Podocarpaceae), restricted to Chorro and Honda watershed. (F) Characteristically nodulated roots of *Podocarpus* harboring arbuscular mycorrhizal fungi are distributed on the soil of litter and ascend the trunks of neighboring trees at Chorro. (G) Characteristic flat-topped crowns of *Vochysia guatemalensis* (Vochysiaceae) abundant along the margin of Lake Fortuna and in the Chorro watershed. (H) Cycad, *Zamia lindleyi* (Zamiaceae) found in open wind-disturbed forest at Fortuna, Bonita watershed. (I) Nonmycorrhizal tree *Roupala montana* (Proteaceae) reproductive in the understory, Alto Frio plot, Pacific slope. (J) *Roupala montana* (Proteaceae), a canopy tree on windblown ridges, Palo Seco plot, Caribbean slope.

PLATE 1.3. (*Continued*)

2. Geological Map of the Fortuna Forest Reserve

*Cesar Silva, Damian Cárdenas, Liliana Londoño, Benjamin L. Turner, and Carlos Jaramillo**

ABSTRACT. The Fortuna Forest Reserve is characterized by marked geological variation, which underpins differences in physical and chemical properties of soil and associated forest communities. Here we present a new geologic map of the reserve based on field mapping and the petrographic description of the main units outcropping in the area. The region is dominated by undifferentiated basalts, diabases, and andesites dating from the formation of the Cordilleran arc 11 to 19 million years ago in the Middle Miocene. Other prominent units include an extensive rhyolite/trachyte deposit, a block of porphyritic dacite, and a granodiorite pluton that crops out extensively to the west of the Fortuna lake. The map provides the foundation for future geological, pedological, and biological research in the Fortuna Forest Reserve.

INTRODUCTION

The geology of the southern Caribbean is complex, being the product of at least three colliding tectonic plates and their interactions since the Late Cretaceous (e.g., Mann and Corrigan, 1990; Kolarsky et al., 1995; Mann and Kolarsky, 1995; Coates et al., 2004; Montes et al., 2012; Barat et al., 2014; León et al., 2018; Montes et al., 2019). The landscape of the Isthmus of Panama is derived primarily from the buildup of three magmatic arcs developed by subduction of plates under the trailing edge of the Caribbean Plate. The process began during the Late Cretaceous and culminated with the ongoing collision of the Panama microplate with the South American Plate (Montes et al., 2019). There are also multiple accretions of Pacific-born seamounts that have produced some of the landscape features along the Pacific coast of Panama, including the Azuero Peninsula and Coibita Island (Buchs et al., 2011). An additional phase of Oligocene to Miocene adakitic-like intrusions is also recognized, which were probably produced by extensional tectonics (Whattam et al., 2012; Farris et al., 2011, 2017). The Neogene collision with the South American Plate deformed the entire system, further complicating reconstruction of the regional geological history (e.g., Buchs et al., 2011; Wegner et al., 2011; Montes et al., 2012).

The Fortuna Forest Reserve has been the focus of extensive biological research in recent decades. Plant diversity at Fortuna is influenced by soil composition, which is primarily driven by geology (Dalling et al., this volume; Turner and Dalling, this volume). However, little is known about the geology of Fortuna because of the lack of studies and the scarce rock outcrops. At broad scale, Fortuna is part of the Cordilleran arc of western Panama. This arc formed during the Miocene between 7 and 19 million years (Ma) ago during a magmatic period that created discrete volcanic centers across the Cordillera de Panama. It was followed by a younger magmatic period from about 6 Ma consisting of isolated volcanic centers of adakitic and alkalic composition (Abratis and Wörner, 2001; Wegner et al., 2011). Here, we present a new geologic map for the Fortuna Forest Reserve based on field mapping and the petrographic description of the main units outcropping in the area.

Smithsonian Tropical Research Institute, Apartado 0843-03092, Balboa, Ancon, Republic of Panama.
* Correspondence: jaramilloc@si.edu

GEOLOGIC MAP

The map area is constrained by the Alto Frio forest dynamics plot to the south and the Verrugosa and Palo Seco plots to the north (8°38′30″ – 8°49′0″N and 82°8′30″ – 82°17′30″W; Figure 2.1). The only published geologic map of the region is the Mapa Geológico de Panama (Instituto Geográfico Nacional Tommy Guardia, 1991), which indicates two lithological units for Fortuna: the Virigua Formation (TM-CAvi – andesites, basalts, and volcanoclastic sequences) and the Guayabito Formation (TMPL-TAgy – granodiorites and monzonites). A geological map of Cerro Chorcha, located a few kilometers to the southeast of Fortuna, was developed to prospect copper porphyries (Folk, 2006). This map illustrates Miocene andesitic/basaltic flows and pyroclastic sequences of the Cañazas Group intruded by Miocene to Pliocene monzonite and granodiorite of the Tabasara Group.

An unpublished report on Fortuna geology (Luque, n.d.) describes andesitic and basaltic flows, pyroclastic rocks (tuffs and agglomerates), and an intrusive granodiorite outcropping at Pinola Hill that is interpreted as a *batholith* related to a caldera-like system. However, the granodiorite should be considered as a *pluton*, since the intrusion covers only a few kilometers (~5 km long by 4 km wide). There is petrographic evidence of incipient contact metamorphism of the rocks surrounding the caldera pluton that dates the lava flows and pyroclasts as older than the intrusion. A bedding attitude of 10° to 15° dipping southward was measured by Luque in the lava flows and multiple faults trending northeast to southwest. Luque also describes the Fortuna anticline – a major anticlinal structure that probably

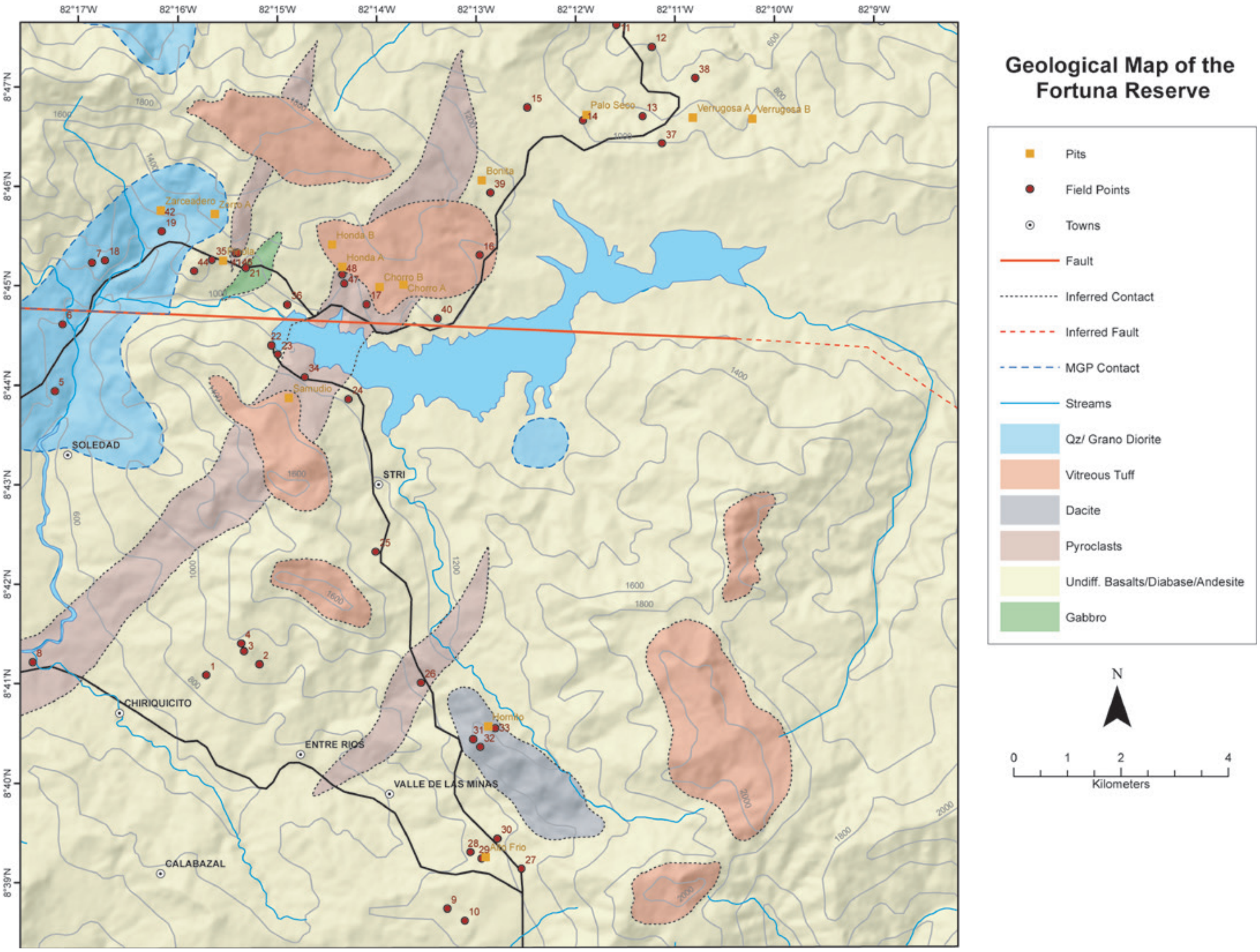

FIGURE 2.1. Geological map of the Fortuna Forest Reserve showing the location of 48 field control points (appendix 2.1) and soil pits associated with 14 permanent forest plots.

formed during the emplacement of the pluton, resulting in the deformation of the surrounding beds.

We produced the geological map of Fortuna by describing 48 exposures along road cuts, creeks, and trails. We collected 32 hand specimens that were labeled using a Smithsonian Tropical Research Institute (STRI) database number (appendix 2.1) and classified using the Streckeisen nomenclature for plutonic and volcanic rocks (Streckeisen, 1976, 1979). Classification for pyroclastic rocks follows Fisher (1996) for the grain-size nomenclature and Schmid (1991) for component attributes. The major geological units were studied petrographically by analyzing six thin sections using a Nikon petrographic microscope. We identified the composition of at least 362 points for each petrographic section using Streckeisen (1976) for igneous rocks and Pettijohn (1975) and Fisher (1966) for type and size of pyroclastic material. The geologic map (Figure 2.1) was digitized in ArcGIS v. 10.1 (ESRI).

LITHOLOGICAL UNITS

We identified six major lithological units (Figure 2.1).

Gabbro

An intrusive mafic fine- to medium-grained gabbro was found in only one exposure associated with basalt and diabase near the Pinola plot. It contains holocrystalline, phaneritic, medium-grained euhedral crystals of plagioclase (59% of total rock; Figure 2.2, sample 41905); *QAPF ratio: plagioclase 100%*. Clinopyroxenes and orthopyroxenes are the only primary mafic minerals (17% and 16%, respectively). The augite and plagioclase have poikilitic textures. An opaque mineral, probably magnetite, represents 5% of the rock volume. Voids and fractures are filled by epidote (2% of total volume) and zeolites (1% of total volume).

Undifferentiated Basalt, Diabase, and Andesite

An extrusive mafic succession, exposing basaltic rocks of different textures, such as porphyritic basalt, amygdular basalt, and diabase. Andesite is also present, but details on the contacts are not exposed. Basaltic lavas are holocrystalline, porphyritic, and fine grained, while plagioclase crystals are the only felsic mineral and the most abundant primary mineral (51% of total rock; Figure 2.3, sample 41898); *QAPF ratio: plagioclase 100%*. Pyroxene is the only mafic primary mineral (17% of total rock), but it is mostly altered to hematite (21% of total rock). Hematite is also present in the glassy groundmass as an alteration mineral (Figure 2.3). Calcite and silica cements fill amygdules (6% and 5%, respectively) and a few vesicles are also present. Diabase subvolcanic bodies are holocrystalline, porphyritic, with plagioclase observed as medium-grained subhedral crystals (27% of total rock), and very fine-grained anhedral crystals within the microcrystalline groundmass (33% of total rock, sample 41907); *QAPF ratio: plagioclase 100%*. Clinopyroxene (augite) is fine grained with subhedral crystals (4% of total rock) and very fine-grained anhedral crystals within the groundmass (11% of total rock). Randomly oriented plagioclase laths enclosed by clinopyroxene in the groundmass show incipient ophitic texture (Figure 2.4). Magnetite is also present in the matrix (12% of total rock), as are amygdules filled by epidote (4%) and sparse silica cement (<1%; Figure 2.4).

Lower Pyroclastic Succession

Pyroclastic rocks are commonly found in the study area in exposures along creeks. These are pyroclastic breccias with abundant block-sized fragments of basaltic lava and lithic-bearing crystalline tuff (sample 41909). The ash matrix comprises glassy and sparse crystalline (plagioclase) fragments (Figure 2.5).

Quartzdiorite/Granodiorite

An igneous intrusive felsic granitoid is exposed in the Zarceadero plot and its surroundings, and it is clearly cropping out along the Chiriquí River and tributaries and along the road to Casita de Piedra. It is holocrystalline, phaneritic, and medium grained (sample 41892). Plagioclase is the most common mineral (63% of total rock; Figure 2.6), followed by quartz (16% of total rock), as the primary and secondary mineral filling voids and veins and surrounding plagioclase crystals; *QAPF ratio: plagioclase 88%, Qz 12%*. Mafic minerals are seen as large euhedral amphibole crystals (hornblende [?] – 10% of total rock; Figure 2.6) and subhedral clinopyroxene crystals (augite [?] – 1% of total rock). Opaque minerals, probably magnetite, represent 3% of the total rock. Alteration minerals such as epidote and sericite replace amphiboles and plagioclases, respectively, and represent 6% of total rock. Enclaves are rare (<1% of total rock).

Dacite

The Fortuna dacite has a porphyritic texture of centimeter-sized phenocrysts of plagioclase > quartz > zeolites within a light gray felsic matrix. It has been observed only in the Hornito plot and its surroundings. It is exposed in several locations on the ridge line above the Hornito plot.

Upper Pyroclastic Succession

The upper pyroclastic succession forms an extensive area around Fortuna Lake, notably at higher elevations in the Honda and Chorro watersheds and above the Samudio plots to the west of the dam wall. It outcrops conspicuously along the road to the east of the dam, forming tall pink and white cliffs. The succession is formed principally of porphyritic tuff, consisting of crystal fragments in a vesicular glass groundmass (similar to pumice). Crystals include quartz xenocrysts within a white cryptocrystalline felsic groundmass. Glassy fragments are trachytic, hypocrystalline, and porphyritic. The ash matrix and most of the glass components of all sizes are devitrified (Figure 2.7, sample 41901). The only felsic

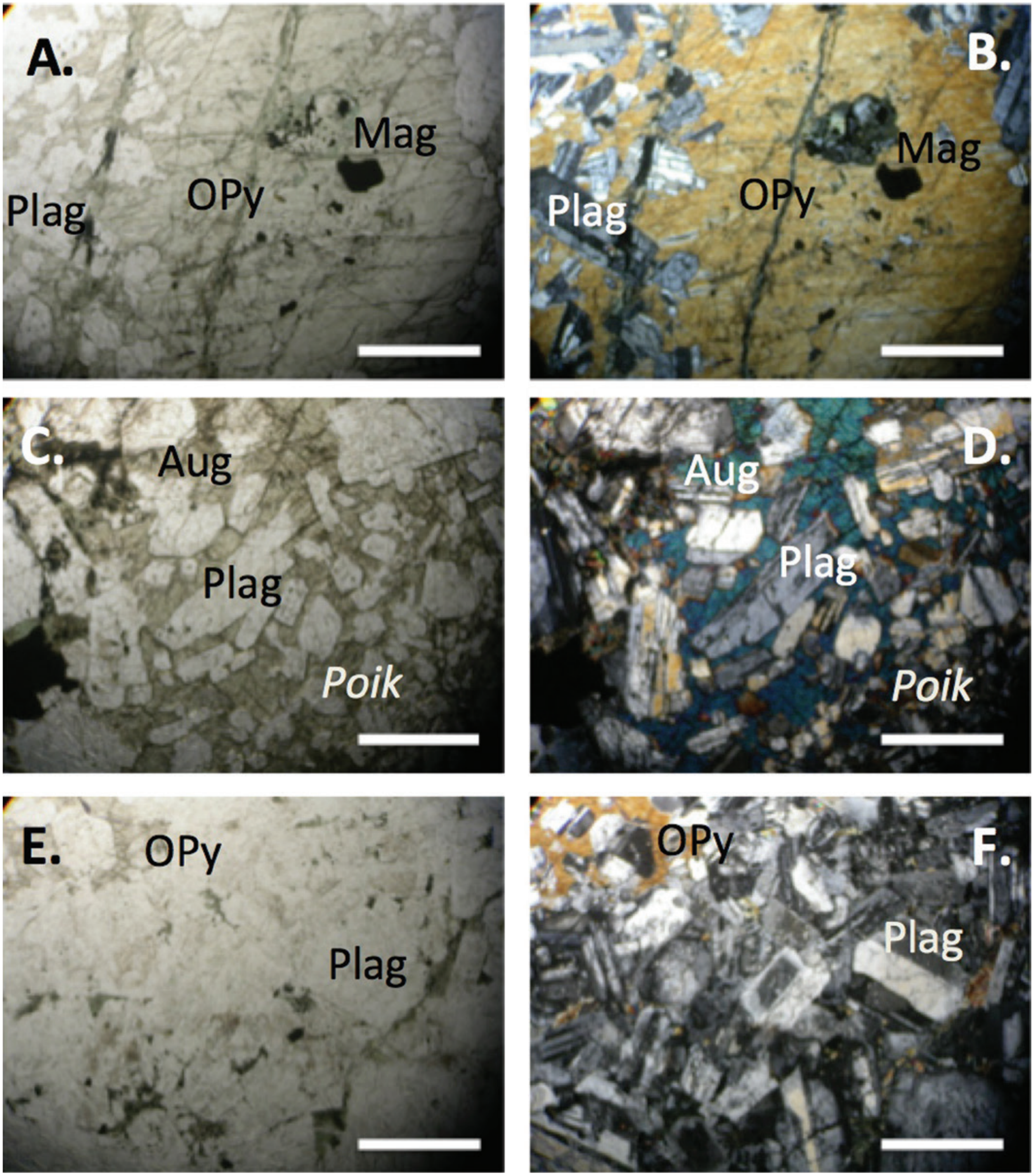

FIGURE 2.2. Petrographic photography of gabbro (sample 41905); plane polarized light (ppl) to the left and cross-polarized light (xpl) to the right. Coarse-grained holocrystalline plagioclase (Plag) (A-F), orthopyroxene (OPy) (A, B, E, F), and clinopyroxene (augite, Aug); (C, D) augite and plagioclase show poikilitic texture (C and D); opaque minerals, probably magnetite (Mag) is also observed (A, B). Scale bar = 1.0 mm.

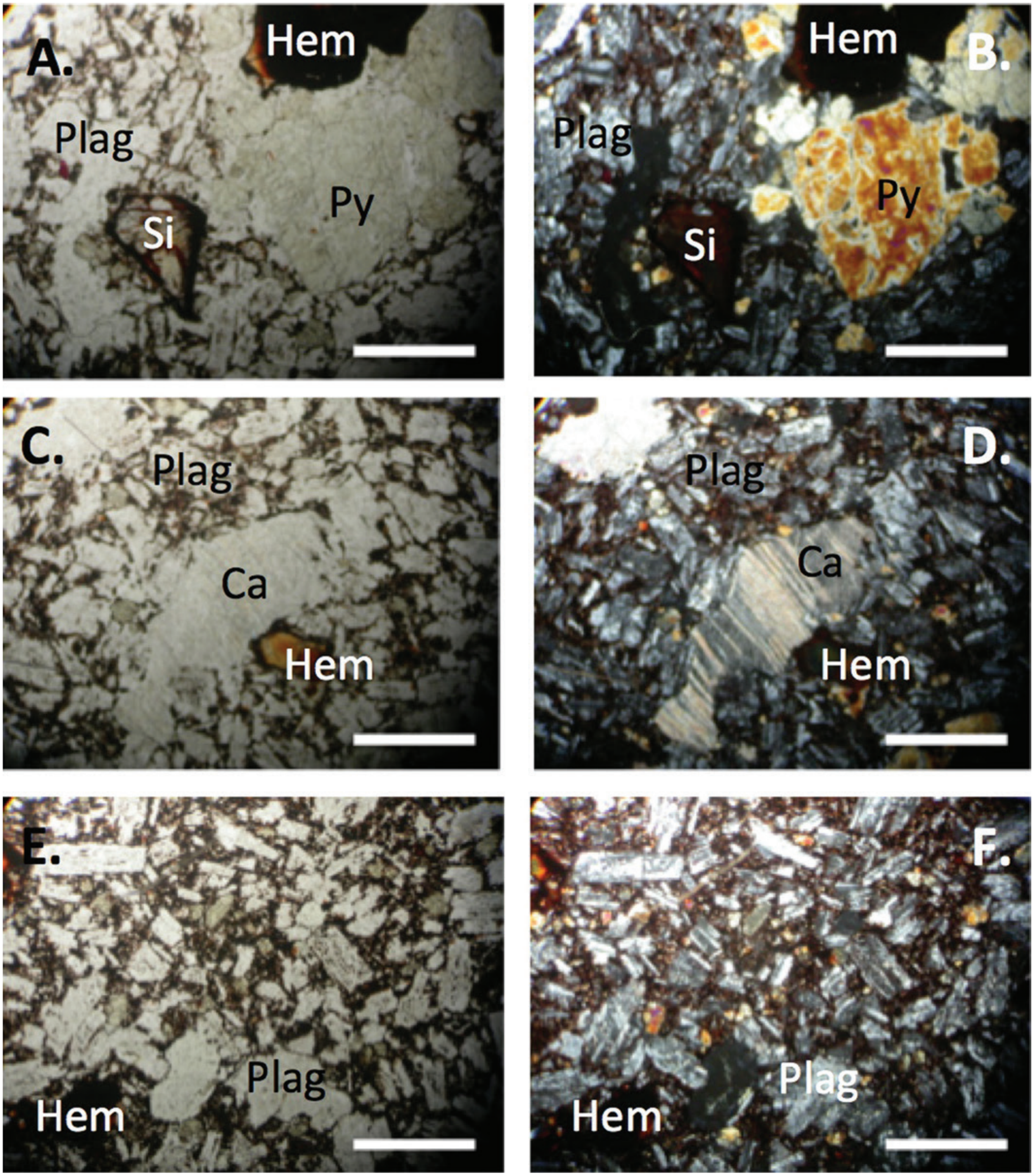

FIGURE 2.3. Petrographic photography of basaltic lava (sample 41898); plane polarized light (ppl) to the left and cross-polarized light (xpl) to the right. Plentiful subhedral to euhedral plagioclase crystals (Plag) (A-F); less common subhedral pyroxene (Py); (A, B) several minerals, such as hematite (Hem) (A-F), and calcite (Ca) (C, D), and silica (Si) cements (A, B), resulted by alteration. Scale bar = 1.5 mm.

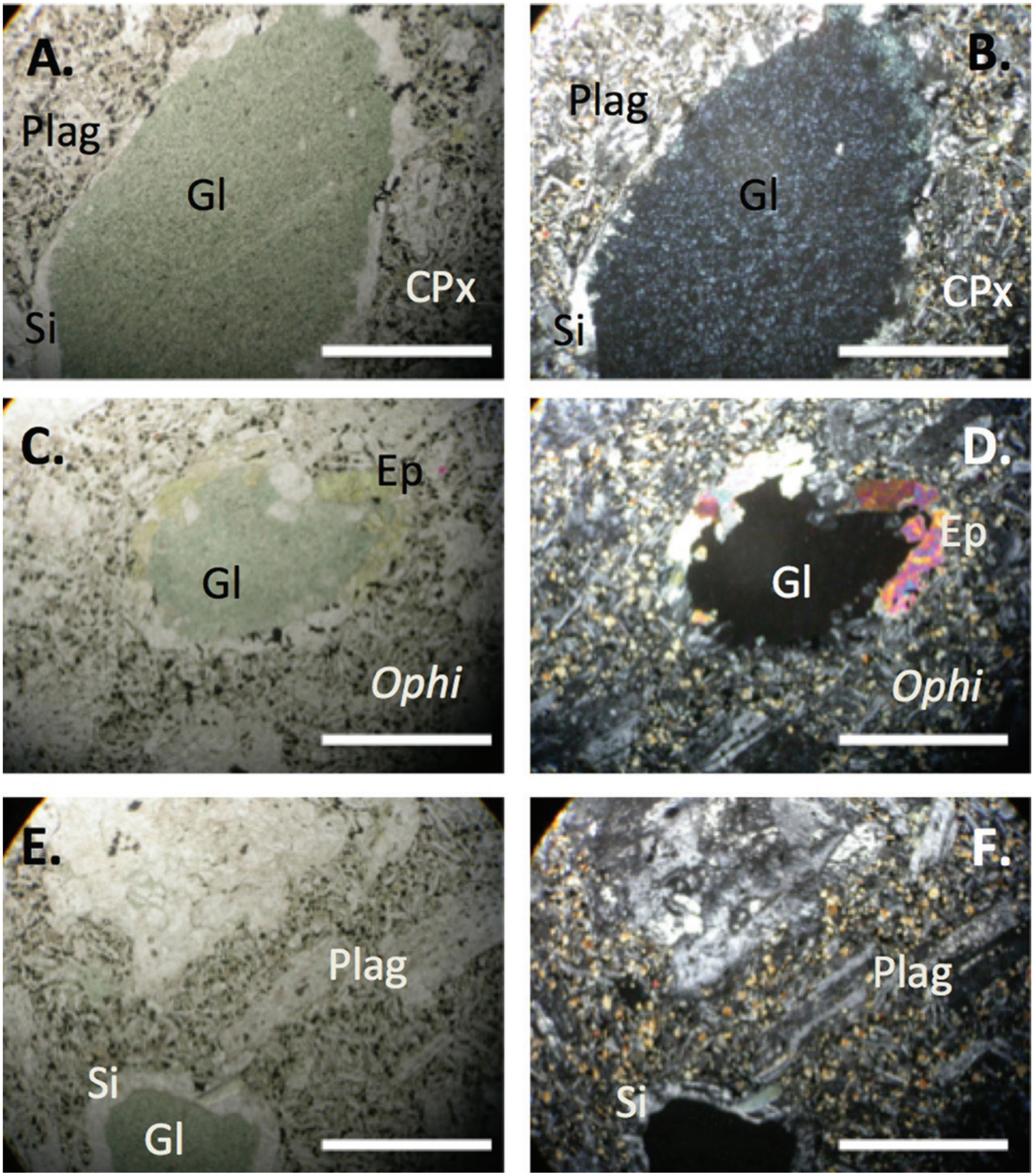

FIGURE 2.4. Petrographic photography of diabase lava (sample 41907); plane polarized light (ppl) to the left and cross-polarized light (xpl) to the right. Porphyritic basaltic lava with large plagioclase (Plag) euhedral crystals (A, B, E, F) and fine-grained plagioclase and clinopyroxene (CPx) crystals (C, D) within the matrix. Ophitic texture (Ophi) is observed in the matrix (C, D). Amygdules are filled by outer silica cement (Si) and epidote (Ep) rims (C-F). Scale bar = 1.0 mm. Volcanic glass (Gl) occurs as large grains (A-D).

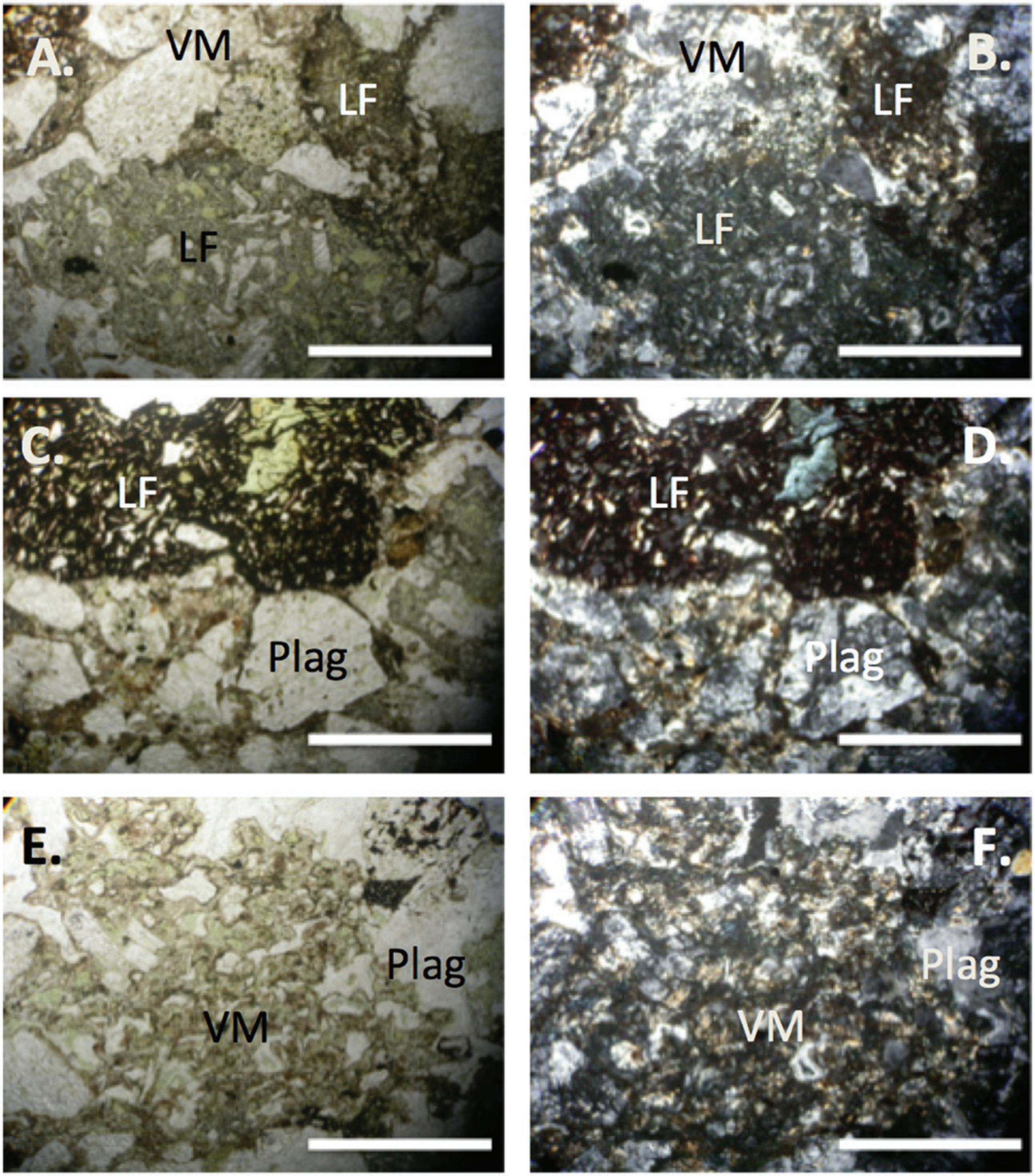

FIGURE 2.5. Petrographic photography of volcanic breccia (sample 41909); plane polarized light (ppl) to the left and cross-polarized light (xpl) to the right. Pyroclastic rock with abundant lithic fragments (LF) of basaltic lavas and tuffs (A-D). Vitreous matrix (VM) with fine-grained anhedral plagioclase crystals (Plag). (E-F) Scale bar = 1.0 mm.

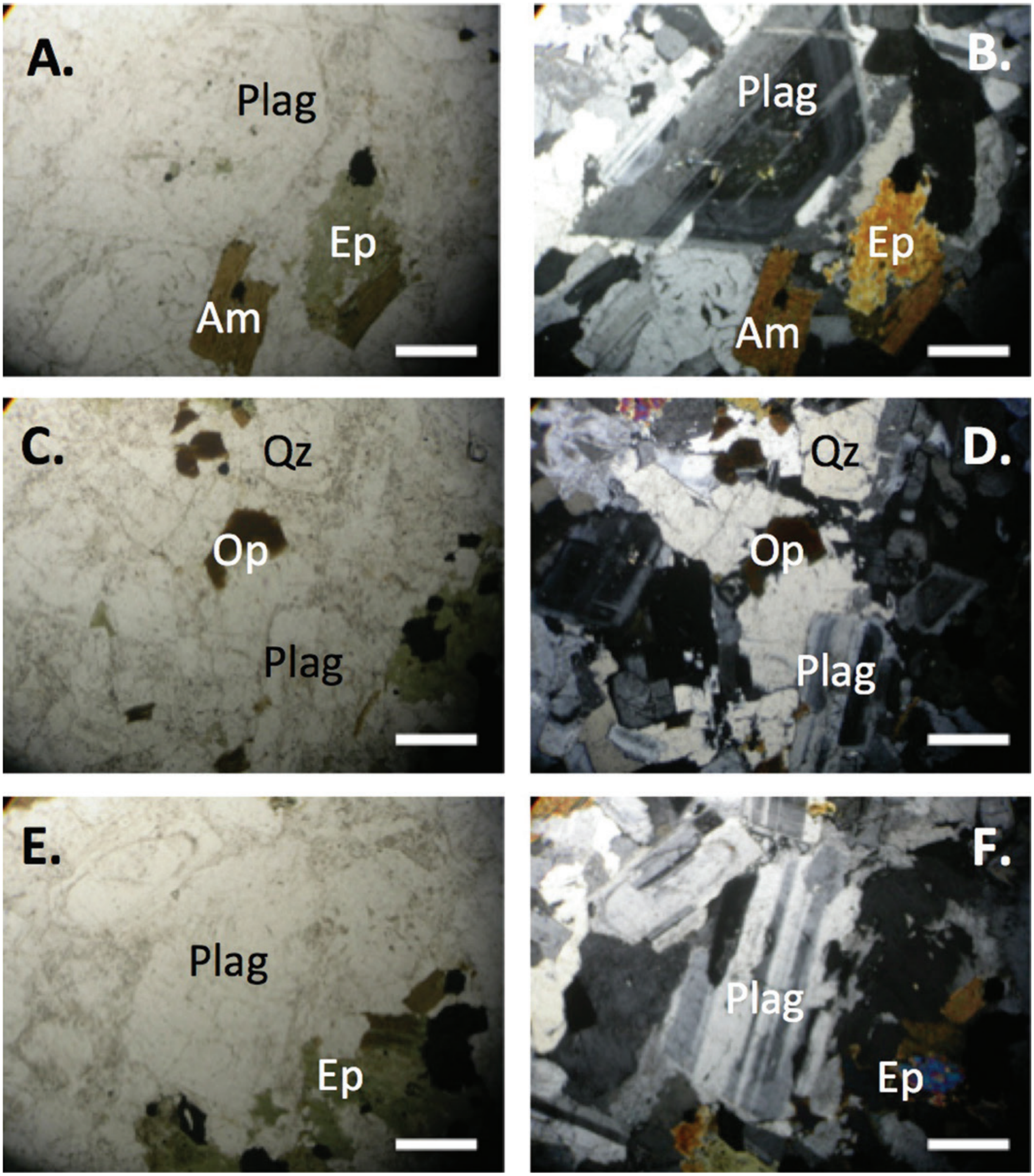

FIGURE 2.6. Petrographic photography of quartz (Qz) diorite (sample 41892); plane polarized light (ppl) to the left and cross-polarized light (xpl) to the right. Abundant euhedral plagioclase crystals (Plag) (A-F); less common Qz (C-D); subhedral to anhedral amphiboles (Am) (A-B), and opaque minerals (Op) (C-D); epidote (Ep) present as alteration of mafic minerals (A, B, E, F). Scale bar = 1.0 mm.

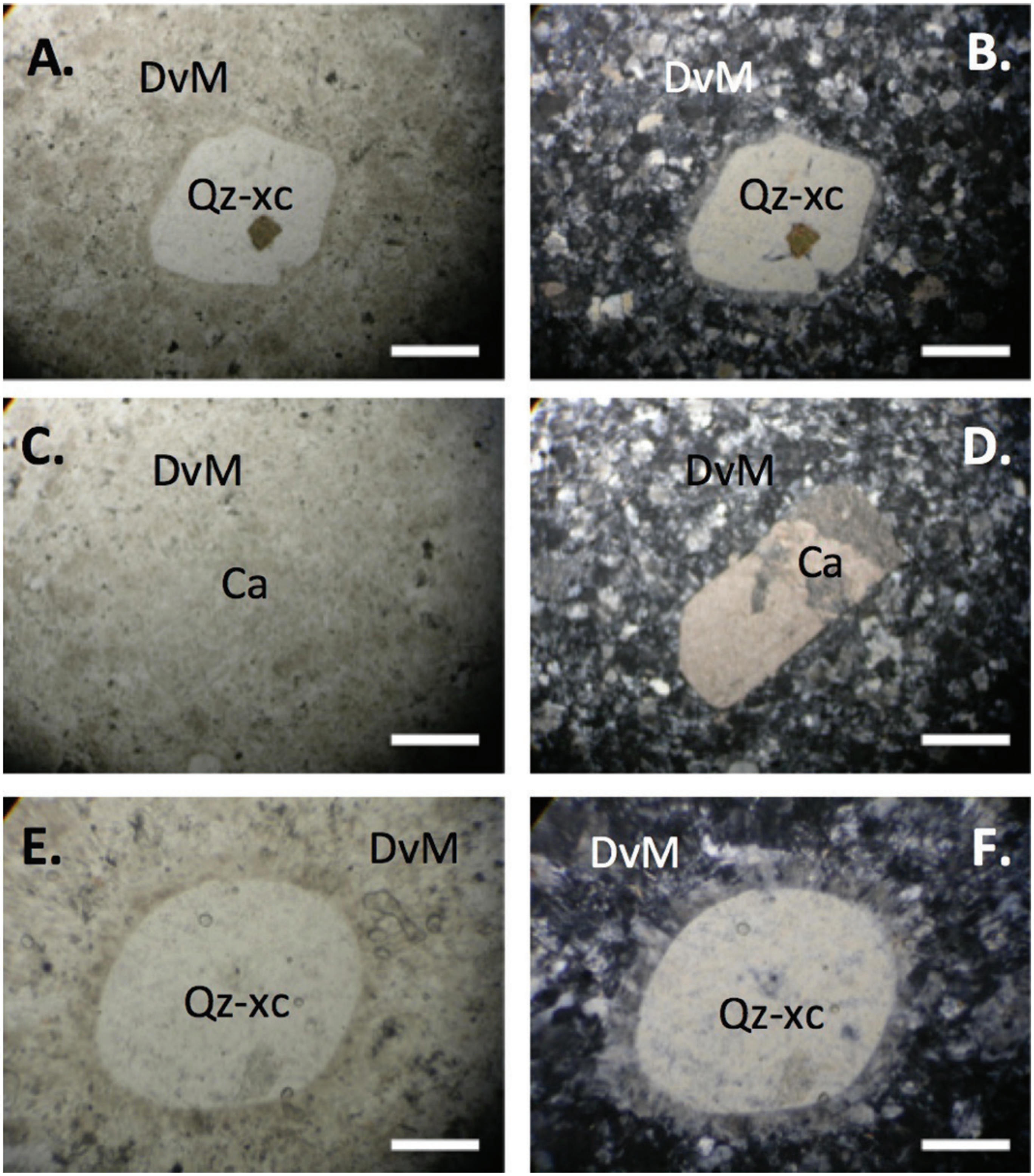

FIGURE 2.7. Petrographic photography of vitreous tuff (sample 41901); plane polarized light (ppl) to the left and cross-polarized light (xpl) to the right. Devitrified hypocrystalline matrix (DvM) (A-F); quartz xenocrysts (Qz-xc) have reacted with the minerals in the matrix forming a vitreous rim surrounding the xenocryst (A, B, E, F); calcite (Ca) completely replacing crystals, probably sanidine, and filling voids (C, D). Scale bar = 0.5 mm.

minerals are euhedral sanidine and orthoclase crystals, which are primary and represent 5% of the total rock volume; *QAPF ratio: alkali feldspar 100%*. The only mafic mineral in the rock is amphibole, likely hornblende, which represents 5% of the rock volume. Quartz occurs as subhedral, medium-grained xenocrysts that are surrounded by a ring of vitreous alteration (7% of total rock; Figure 2.7). This quartz is not considered in the QAPF classification, since the mineral is secondary and is not part of the original pyroclastic composition. Devitrified minerals (58% total rock) and chalcedony (15% total rock) are the main constituents of the matrix, while calcite cement fills the voids (10% of total rock).

BRIEF GEOLOGICAL HISTORY OF THE MAPPED AREA

Most of the lithologies observed at Fortuna were produced during the development of the Miocene Cordilleran arc, which experienced its main period of activity between 11 and 19 Ma ago (MacMillan et al., 2004) during the Middle Miocene Talamanca suite *sensu stricto* (De Boer et al., 1995). There is a subsequent gap in the arc between 6 and 11 Ma ago (MacMillan et al., 2004). The dacite and upper pyroclastic succession may represent a younger volcanic event, with the tuff forming the youngest explosive episode in Fortuna presumably linked to the eruption of a nearby volcano. The rhyolite/trachyte is dated to 7 Ma (Wegner et al., 2007), so is unlikely to have originated from the nearby Volcán Barú, approximately 30 km to the west of Fortuna.

ACKNOWLEDGMENTS

This project was completed with support from the Smithsonian Tropical Research Institute as well as the Anders Foundation, 1923 Fund, and Gregory D. and Jennifer Walston Johnson. We thank Dr Anthony Coates for providing critical comments on the manuscript.

APPENDIX 2.1

Control point	Date	Location	WGS84 coordinates (°)		Elevation (m)	Description	Samples	Photos
			N	W				
1	12/2/15	Road to hydroelectric control house	8.68474	-82.26186	867	Amygdaloidal basalt. Plagioclase phenocrysts in a dark microcrystalline basic matrix. Qz amygdules	41887	0775-0779
2	12/2/15	Road to hydroelectric control house	8.68656	-82.25296	1038	Amygdaloidal basalt. Plagioclase phenocrysts and lithics fragments in a dark microcrystalline basic matrix	41888	0780-0781, 0927
3	12/2/15	Road to hydroelectric control house	8.68874	-82.25552	1177	Basalt. Plagioclase and pyroxene phenocrysts in a dark microcrystalline basic matrix	41889	0786, 0787, 0790-0794
4	12/2/15	Road to hydroelectric control house	8.69004	-82.25601	1134	Amygdaloidal Basalt. Plagioclase and pyroxene phenocrysts in a dark microcrystalline basic matrix, Qz amygdules; andesitic dikes cutting trough basalt at sparse places of the outcrop; weathered	41890	0795-0800, 0923-0924
5	12/2/15	Road from Quebrada Seca to Casita de Piedra	8.73234	-82.28726	791	Qz/Granodiorite. Phenocrysts of quartz + plagioclase + biotite and sparse hornblendes, medium grain size, phaneritic texture	41891	0801-0810
6	12/2/15	Chiriquí river tributary	8.74353	-82.28593	738	Qz/Granodiorite. Phenocrysts of quartz + plagioclase + biotite and sparse hornblendes, medium grain size, phaneritic texture	41892	0811, 0813-0815
7	12/2/15	Trail from Casita de Piedra to Fortuna dam	8.75385	-82.28102	1002	Qz/Granodiorite. Phenocrysts of quartz + plagioclase + biotite and sparse hornblendes, medium grain size, phaneritic texture	41893	0817-0818, 0930
8	12/2/15	Road from Chiriquicito to STRI station	8.68693	-82.29096	502	Volcanic Breccia. Basalt lithic fragments whitin a dark microcrystalline basic matrix	41894	0820-0823, 0933-0934
9	12/2/15	Road from Chiriquicito to STRI station	8.64566	-82.22144	1093	Basalt. Plagioclase phenocrysts in a dark microcrystalline basic matrix	41895	0825-0828, 0936, 0942
10	12/2/15	Road from Chiriquicito to STRI station	8.64361	-82.21849	1143	Basalt. Plagioclase phenocrysts in a dark microcrystalline basic matrix	41896	0829, 0831, 0945, 0950
11	12/3/15	Road from Fortuna dam to Bocas del Toro	8.79369	-82.19310	434	Basalt. Pyroxene phenocrysts in a dark microcrystalline basic matrix	41897	0836-0838
12	12/3/15	Road from Fortuna dam to Bocas del Toro	8.79002	-82.18716	497	Basalt. Plagioclase phenocrysts w/ reddish brown microcrystalline matrix w/ hematite; common quartz veins	41898	0840-0843
13	12/3/15	Cabello de Ángel 2 creek	8.77839	-82.18869	718	Basalt. Pyroxene phenocrysts in a dark microcrystalline basic matrix	41899	0844-0846, 0954
14	12/3/15	Road from Fortuna dam to Bocas del Toro	8.77772	-82.19868	880	Basalt. Pyroxene and plagioclase phenocrysts in a dark microcrystalline basic matrix, sparse Qz veins	41900	0848-0850, 0958
15	12/3/15	Road from Fortuna dam to Bocas del Toro	8.77988	-82.20804	985	Basalt. Plagioclase (?) phenocrysts highly altered to epidote/chlorite (?); andesitic dike (20 cm wide); highly weathered	na	0852-0861
16	12/3/15	Road from Fortuna dam to Bocas del Toro	8.75511	-82.21601	1012	Vitreous ash tuff. Qz + orthoclase + biotite + hornblende subhedral phenocrysts within a white microcrystalline matrix; sparse calcite veins	41901	0863-0865
17	12/3/15	Road from Fortuna dam to Bocas del Toro	8.74689	-82.23498	1058	Lapilli tuff. Lithic fragments and plagioclase phenocrysts (?) highly altered to epidote/chlorite (?)	41902	0871-0872, 0874, 0876
18	12/3/15	Road from Fortuna dam to Casita de Piedra	8.75425	-82.27882	955	Qz/Granodiorite. Phenocrysts of quartz + plagioclase + biotite and sparse hornblendes, phaneritic texture, medium grain size, partially weathered	41903	0877-0880
19	12/3/15	Road from Fortuna dam to Casita de Piedra	8.75911	-82.26936	950	Boulders of Qz diorite within a dark orange soil	na	0882-0883
20	12/3/15	Road from Fortuna dam to Casita de Piedra	8.75553	-82.25666	1128	Volcanic Breccia. Basalt lithic fragments whitin a dark microcrystalline basic matrix	41904	0884-0888
21	12/3/15	Road from Fortuna dam to STRI station	8.75298	-82.25524	1003	Gabbro. Medium grain size phenocrysts of pyroxene and plagioclase, phaneritic texture, holocrystalline	41905	0890-0892, 0894
22	12/4/15	Road from Fortuna dam to STRI station	8.74001	-82.25090	981	Basalt. Pyroxene and plagioclase phenocrysts in a dark microcrystalline basic matrix. Good outcrop near the Fortuna Dam	41906	0895-0896, 0898-0899, 0959
23	12/4/15	Road from Fortuna dam to STRI station	8.73846	-82.24988	984	Amygdaloidal Basalt. Pyroxene and plagioclase phenocrysts in a dark microcrystalline basic matrix; Qz amygdules	41907	0902-0904, 0969

Control point	Date	Location	WGS84 coordinates (°)		Elevation (m)	Description	Samples	Photos
			N	W				
24	12/4/15	Road from Fortuna dam to STRI station	8.73098	-82.23801	1088	Basalt. Pyroxene and plagioclase phenocrysts in a dark microcrystalline basic matrix	41908	0907-0910
25	12/4/15	Road from STRI station to police station	8.70543	-82.23345	1113	Basaltic lava, aphanitic texture, sparse Qz veins, slighltly wheatered	na	0911-0912
26	12/4/15	Road from STRI station to police station	8.68348	-82.22588	1068	Volcanic Breccia. Basalt lithic fragments whitin a dark microcrystalline basic matrix	41909	0913-0917, 0971
27	12/4/15	Road from STRI station to police station	8.65233	-82.20901	1125	Basalt. Plagioclase and pyroxene phenocrysts in a dark microcrystalline basic matrix	41910	0918-0919, 0973
28	1/18/17	Q. Pueblo Nuevo	8.65510	-82.21757	1021	Angular boulders (up to 3m) of dark grey volcanic rocks	na	na
29	1/18/17	Q. Pueblo Nuevo	8.65403	-82.21567	1031	Black porphyritic basalt, green anhedral epidote (?), dark red pyroxene altered to hematite; sparse calcite veins; plagioclase phenocrysts (?) altered to epidote (?)	43883 43884	FOR01, FOR02
30	1/18/17	Pueblo Nuevo	8.65738	-82.21309	1209	Porphyritic basalt, black matrix, white euhedral plagioclase, some twin plagioclase altered to epidote (?), weathered outcrop	na	na
31	1/18/17	Hornito plot	8.67403	-82.21714	1436	Coarse grain porphyritic dacite w/ red&grey lithic fragments, purple aphanitic matrix w/ coarse plagioclase/zeolites (?) crystals	na	na
32	1/18/17	Hornito plot	8.67274	-82.21595	1538	Light grey porphyritic dacite w/ black&red angular lithic fragments, white plagioclase crystals; outcrop not in-place but not transported (eluvium)	na	na
33	1/18/17	Hornito plot	8.67584	-82.21342	1410	Colluvium of porphyritic dacite w/ euhedral plagioclase crystals within a dark purple matrix	na	na
34	1/18/17	Q. Samudio	8.73468	-82.24533	1180	Volcanic breccia, very angular lithic frag from a few cm up to 1m long	na	na
35	1/18/17	Pinola station	8.75431	-82.26092	933	Black basalt, aphanitic text, mm crystals, fractured w/ calcite veins, mm displacement	43885	na
36	1/18/17	Fortuna dam	8.74683	-82.24824	1062	Dark grey porphyritic basalt w/ euhedral plagioclase crystals partially replaced by epidote (?)	43886	na
37	1/19/17	Verrugosa plot	8.77384	-82.18543	786	Porphyritic basalt, brown matrix, white euhedral plagioclase; highly weathered outcrop	na	na
38	1/19/17	Verrugosa plot	8.78480	-82.17990	713	Black aphanitic basalt w/ white silica amygdules, hematite replacing mafic minerals	43887	FOR03
39	1/19/17	Q. Bonita	8.76558	-82.21422	na	STAR OUTCROP - amygdular basalt, black aphanitic matrix, spare (~10%) dark grey pyroxene (?), white concentric silica amygdules w/ euhedral Qz crystals, and greenish white fresh amygdules filled w/ malachite	43888	FOR04, FOR05
40	1/19/17	Q. Chorro	8.74450	-82.22310	na	Black to greenish grey basalt w/ malachite amygdules; fractured	na	FOR06, FOR07
41	1/20/17	Pinola plot	8.75545	-82.25701	na	Boulders of black basalt along the creek, same as the boulders found in the soil pit uphill	na	na
42	1/20/17	Zarceadero plot	8.76261	-82.26948	1356	Light grey Qz diorite, coarse grained, covered by dark orange soil; phenocrystals of Qz, plagioclase, biotite and some hornblendes; phaneritic texture, medium grain size	na	na
43	1/20/17	Q. Pinola	ns	ns	ns	Angular boulders (up to 2m) almost exclusively of basalt	na	na
44	1/20/17	Mirador Pinola	8.75245	-82.26391	1355	Black basalt w/ mm plagioclase crystals, hypabyssal (?), sparse black amygdules (~10%), black aphanitic matrix, not in-place (eluvium)	na	FOR08, FOR09
45	1/20/17	Zarceadero plot	ns	ns	ns	Colluvium of phaneritic Qz diorite (same rock as 42)	na	na
46	1/20/17	Pinola plot	8.75545	-82.25654	1201	GOOD OUTCROP - Dark grey lapilli tuff to volcanic breccia, angular lithic fragments, predominantly basalt	na	na
47	1/20/17	Q. Honda	8.75036	-82.23870	na	STAR OUTCROP - Reddish brown volcanic breccia w/ very angular lithic fragments of basalt>>others; mm white calcite crystals; 2 main perpendicular joints; 'incipient' bedding plane	43889	FOR10, FOR11
48	1/20/17	Q. Honda	8.75186	-82.23906	ns	Dark grey ash-tuff w/ mm lithic frag; relatively clear bedding plane	43890	FOR12

na - not available
ns - no signal (GPS)

REFERENCES

Abratis, M., and G. Wörner. 2001. Ridge Collision, Slab-Window Formation, and the Flux of Pacific Asthenosphere into the Caribbean Realm. *Geology*, 29:127–130. https://doi.org/10.1130/0091-7613(2001)029<0127:RCSWFA>2.0.CO;2

Barat, F., B. Mercier, M. Sosson, C. Müller, P. O. Baumgartner, and C. Baumgartner-Mora. 2014. Transition from the Farallon Plate Subduction to the Collision between South and Central America: Geological Evolution of the Panama Isthmus. *Tectonophysics*, 622:145–167. https://doi.org/10.1016/j.tecto.2014.03.008

Buchs, D. M., R. J. Arculus, P. O. Baumgartner, and A. Ulianov. 2011. Oceanic Intraplate Volcanoes Exposed: Example from Seamounts Accreted in Panama. *Geology*, 39:335–338. https://doi.org/10.1130/G31703.1

Coates, A. G., L. S. Collins, M. P. Aubry, and W. A. Berggren. 2004. The Geology of the Darien, Panama, and the Late Miocene-Pliocene Collision of the Panama Arc with Northwestern South America. *Geological Society of America Bulletin*, 116:1327–1344. https://doi.org/10.1130/B25275.1

Dalling, J. W., C. M. Prada, K. D. Heineman, K. M. Andersen, A. Morris, J. Pardo, E. Hollenbeck, P. Caballero, C. Espinosa, E. García, and B. L. Turner. 2021. Introduction to the Fortuna Forest Reserve: Soil and Climate Effects on the Tree Communities of a Premontane Tropical Forest. In *Fortuna Forest Reserve, Panama: Interacting Effects of Climate and Soils on the Biota of a Wet Premontane Tropical Forest*, ed. J. W. Dalling and B. L. Turner, pp. 1–33. Smithsonian Contributions to Botany, No. 112. Washington, D.C.: Smithsonian Institution Scholarly Press.

De Boer, J. Z., M. S. Drummond, M. J. Bordelon, M. J. Defant, H. Bellon, and R. C. Maury. 1995. Cenozoic Magmatic Phases of the Costa Rican Island Arc (Cordillera de Talamanca). In *Geologic and Tectonic Development of the Caribbean Plate Boundary in Southern Central America*, Special Paper 295, ed. P. Mann, ed., 35–55. Boulder, CO: Geological Society of America.

Farris, D. W., A. Cardona, C. Montes, and C. Jaramillo. 2017. Magmatic Evolution of Panama Canal Volcanic Rocks: A Record of Arc Processes and Tectonic Change. *PLoS ONE*, 12:e0176010. https://doi.org/10.1371/journal.pone.0176010

Farris, D. W., C. Jaramillo, G. Bayona, S. Restrepo-Moreno, C. Montes, A. Cardona, A. Mora, R. J. Speakman, M. D. Glasscock, P. Reiners, and V. Valencia. 2011. Fracturing of the Panamanian Isthmus during Initial Collision with South America. *Geology*, 39:1007–1010. https://doi.org/10.1130/G32237.1

Fisher, R. V. 1966. Rocks Composed of Volcanic Fragments and Their Classification. *Earth Science Reviews*, 1:287–298. https://doi.org/10.1016/0012-8252(66)90010-9

Folk, P. G. 2006. *Technical Report Chorcha Copper Porphyry Project*. Inwood, NY: Bellhaven Ventures Inc.

Instituto Geográfico Nacional Tommy Guardia. 1991. *Mapa Geologico Republica de Panama*, Hoja 1, Region Occidental Bocas – Chiriqui, Escala 1:250,000. Ministerio de Comercio e Industrias, Dirección General de Recursos Minerales, Panama City, Republic of Panama.

Kolarsky, R. A., P. Mann, and S. Monechi. 1995. Stratigraphic Development of Southwestern Panama as Determined from Integration of Marine Seismic Data and Onshore Geology. In *Geologic and tectonic development of the Caribbean plate boundary in southern Central America*, Special Paper 295, ed. P. Mann, ed., 159–200. Boulder, CO: Geological Society of America.

León, S., A. Cardona, M. Parra, E. R. Sobel, J. S. Jaramillo, J. Glodny, V. A. Valencia, D. Chew, C. Montes, G. Posada, G. Monsalve, and A. Pardo-Trujillo. 2018. Transition from Collisional to Subduction-Related Regimes: An Example from Neogene Panama-Nazca-South America Interactions. *Tectonics*, 37:119–139. https://doi.org/10.1002/2017TC004785

Luque, V. n.d. *Análisis geológico adicional sobre el area del embalse y el sitio de presa de Fortuna* [Additional geological analysis on the reservoir area and the Fortuna dam site], Anexo 1, 6 p.

Mann, P., and J. Corrigan. 1990. Model for Late Neogene Deformation in Panama. *Geology*, 18:558–562. https://doi.org/10.1130/0091-7613(1990)018<0558:MFLNDI>2.3.CO;2

Mann, P., and R. A. Kolarsky. 1995. East Panama Deformed Belt: Structure, Age, and Neotectonic Significance. In *Geologic and tectonic development of the Caribbean plate boundary in southern Central America*, Special Paper 295, ed. P. Mann, ed., 111–130. Boulder, CO: Geological Society of America.

MacMillan, I., P. B. Gans, and G. E. Alvarado-Induni. 2004. Middle Miocene to Present Plate Tectonic History of the Southern Central American Volcanic Arc. *Tectonophysics*, 392:325–348. https://doi.org/10.1016/ j.tecto.2004.04.014

Montes, C., G. Bayona, A. Cardona, D. M. Buchs, C. A. Silva, S. E. Moron, N. Hoyos, D. A. Ramirez, C. Jaramillo, and V. Valencia. 2012. Arc-Continent Collision and Orocline Formation: Closing of the Central American Seaway. *Journal of Geophysical Research*, 117:B04105. https://doi.org/10.1029/2011JB008959

Montes, C., A. F. Rodriguez-Corcho, G. Bayona, N. Hoyos, S. Zapata, and A. Cardona. 2019. Continental Margin Response to Multiple Arc-Continent Collisions: The Northern Andes-Caribbean Margin. *Earth Science Reviews*, 198:102903. https://doi.org/10.1016/j.earscirev.2019.102903

Pettijohn, F. J. 1975. *Sedimentary Rocks*. 3rd ed. New York: Harper & Row.

Schmid, R. 1981. Descriptive nomenclature and classification of pyroclastic deposits and fragments: Recommendations of the IUSG Subcommission on the Systematics of Igneous Rocks. *Geology, 9*, 41–43.

Streckeisen, A. 1976. Classification of the Common Igneous Rocks by Means of Their Chemical Composition: A Provisional Attempt. *Neues Jahrbuch fur Mineralogie, Monatshefte*, H.1:1–15.

Streckeisen, A. 1979. Classification and Nomenclature of Volcanic Rocks, Lamprophyres, Carbonatites, and Melilitic Rocks: Recommendations and Suggestions of the IUGS Sub-commission on the Systematics of Igneous Rocks. *Geology*, 7:331–335. https://doi.org/10.1130/0091-7613(1979)7<331:CANOVR>2.0.CO;2

Turner, B. L., and J. W. Dalling. 2021. Soils of the Fortuna Forest Reserve. In *Fortuna Forest Reserve, Panama: Interacting Effects of Climate and Soils on the Biota of a Wet Premontane Tropical Forest*, ed. J. W. Dalling and B. L. Turner, pp. 47–135. Smithsonian Contributions to Botany, No. 112. Washington, D.C.: Smithsonian Institution Scholarly Press.

Wegner, W., G. Wörner, R. S. Harmon, and B. R. Jicha. 2011. Magmatic History and Evolution of the Central America Land Bridge in Panama since Cretaceous Times. *GSA Bulletin*, 123:703–724. https:doi.org/10.1130/B30109.1

Whattam, S. A., C. Montes, R. McFadden, A. Cardona, D. Ramirez, and V. Valencia. 2012. Age and Origin of Earliest Adakitic-like Magmatism in Panama: Implications for the Tectonic Evolution of the Panamanian Magmatic Arc System. *Lithos*, 142–143:226–244. https://doi.org/10.1016/j.lithos.2012.02.017

3. Soils of the Fortuna Forest Reserve

Benjamin L. Turner[1*] *and James W. Dalling*[1,2]

ABSTRACT. Soils vary markedly across the Fortuna Forest Reserve, particularly in terms of fertility. This variation is due primarily to differences in the parent material, which consists of extrusive and intrusive igneous rocks including basalt, andesite, rhyolitic tuff, porphyritic dacite, and granodiorite. In the USDA soil taxonomy system of classification (Soil Survey Staff, 1999), most soils at Fortuna are Andisols, Inceptisols, and Ultisols. One profile on rhyolite has developed into a Spodosol. All soils have an isothermic temperature regime and a perudic moisture regime. Some soils have aquic conditions, while several have andic properties, but soils are sufficiently weathered that few qualify as Andisols. Volcanic glass is present in moderate amounts in only two profiles, both with aquic conditions. In general, Fortuna soils are strongly to extremely acid and fine textured. Kaolinite dominates the clay fraction, although small amounts of vermiculite are common and gibbsite is abundant in some soils. There is marked variation in fertility, particularly for phosphorus and base cations, ranging from extreme infertility in soils formed on rhyolite to relatively fertile soils formed on basalt and undifferentiated mafic-volcanics. Soils at Fortuna also contain large amounts of organic carbon, reflected in the Humult suborder of the Ultisols at Honda, Pinola, and Hornito. The strong edaphic variation has ecological significance because it explains regional vegetation patterns, including in the palm, fern, and tree communities. Fortuna is therefore an important example of the remarkable variation in soils at regional scale in neotropical mountains and how this variation influences plant communities in these threatened ecosystems.

INTRODUCTION

Soils form the basis of the ecosystem, providing the physical material in which plants take root and the fertility that allows life to flourish. In the tropics, soil properties influence the ecology of plant and microbial taxa, determining where they occur and the rates at which they grow and die. In lowland forests of Panama, for example, hundreds of tree species are distributed according to moisture and nutrient availability (Engelbrecht et al., 2007; Condit et al., 2013), while almost all species grow faster where soil phosphorus concentrations are greater (Turner et al., 2018). Understanding the remarkable patterns of diversity in tropical forests therefore depends on a comprehensive understanding of their soils (Committee on Tropical Soils, 1972).

Despite their ecological significance, tropical forest soils remain poorly understood in comparison with temperate forest soils. Most research on tropical soils has been conducted in the context of tropical agriculture, with many undisturbed regions (which are becoming increasingly scarce) receiving little attention. This is particularly true of soils in the tropical mountains.

Soils are shaped by interactions between five key variables, known as state factors. These five variables are captured in the acronym CLORPT, representing climate, organisms, relief, parent material, and time (Jenny, 1941). Each factor has an important

---

[1] Smithsonian Tropical Research Institute, Apartado 0843-03092, Balboa, Ancon, Republic of Panama.

[2] Department of Plant Biology, University of Illinois at Urbana-Champaign, 265 Morrill Hall, 505 S. Goodwin Ave, Urbana, IL 61801, USA.

* Correspondence: blturner@gmail.com

influence on soil development, and soils are often examined along gradients in which four of the five factors remain relatively constant (e.g., soil chronosequences, which consist of a sequence of soils differing only in the time since their formation; Stevens and Walker, 1970; Vitousek, 2004).

At Fortuna, four of the five state factors are relatively constant. Climate is warm and wet, slopes are generally steep, undisturbed mature forest blankets the reserve, and soils have been developing on old substrate without obvious evidence of catastrophic change for several million years. The age of the parent material does not always translate into pedogenic age or weathering state; for example, small landslips appear common in many areas and result in pedogenically young soils. However, given that climate and parent material are the predominant soil forming factors in the tropics (Young, 1976), it is little surprise that variation in parent material is the predominant influence on the chemical and physical properties of soils in the Fortuna region.

This chapter describes the soils in a network of permanent vegetation plots that span the range of geological variation at Fortuna (Figure 3.1). We present descriptions, classifications, and data on the physical, chemical, and mineralogical properties of the soils. The research was conducted in support of our efforts to understand patterns of vegetation in the reserve and is not therefore a conventional soil survey. However, the close relationship between soils and their parent materials means that landscape-level patterns can be identified on the basis of the geological survey map (Figure 3.1; Silva et al., this volume). The findings show that the Fortuna Forest Reserve provides a clear example of the remarkable soil variation that can occur at regional scale in the tropics, particularly on mountains, and how this variation can influence associated plant communities.

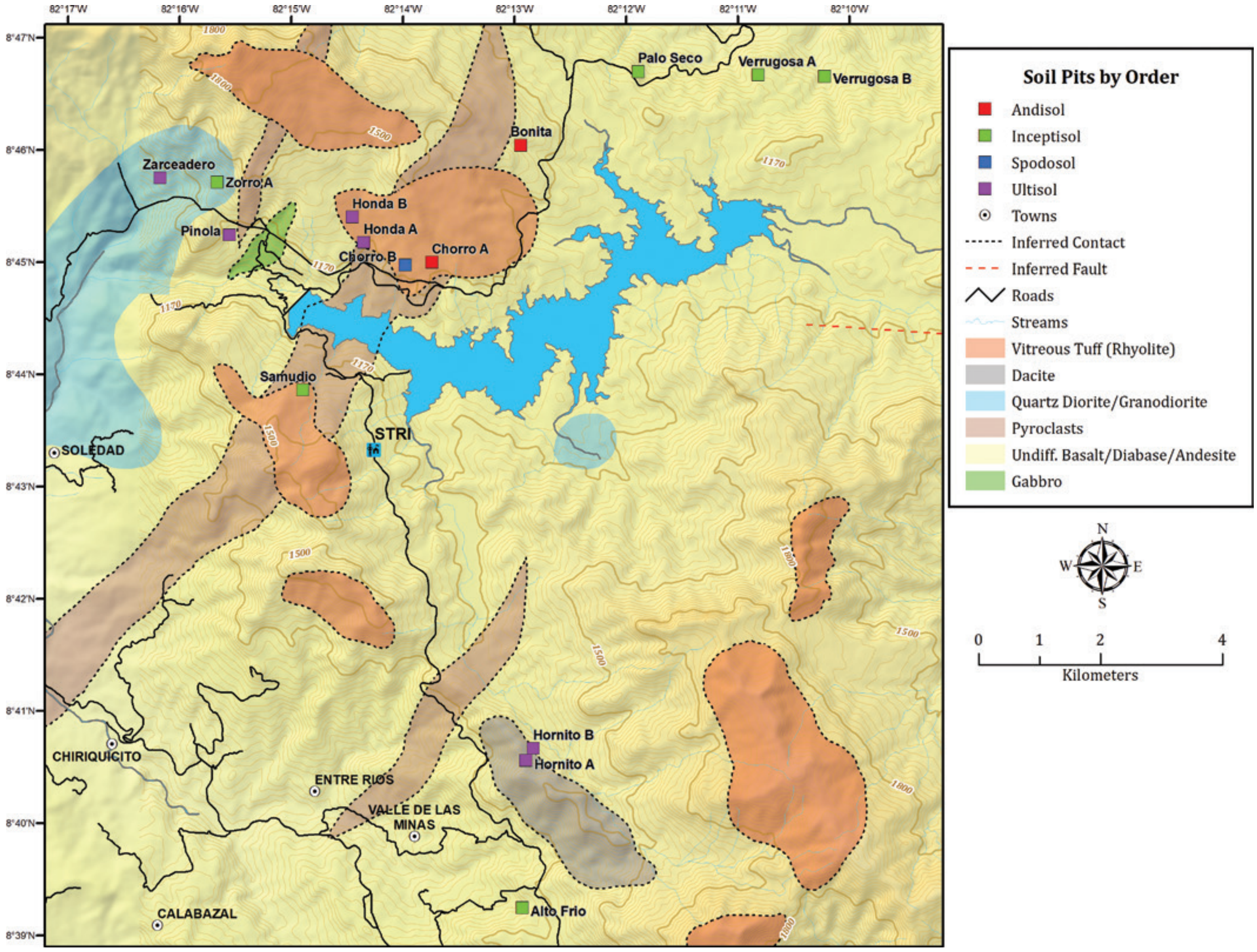

FIGURE 3.1. Map of the Fortuna Forest Reserve showing the locations of the soil profiles and the underlying topography and geology (Silva et al., this volume).

SOIL FORMING FACTORS AT FORTUNA

Climate

The climate is described in detail elsewhere in this volume (Dalling et al.). Fortuna is classed as tropical rainforest (A*f*) in the Köppen-Geiger climate classification scheme (Köppen, 1884; Beck et al., 2018). There is considerable variation in rainfall across the continental divide, with multiyear averages at forest census plots ranging between 4,500 and 6,300 mm per year (Table 3.1). This annual rainfall far exceeds the water demand of the forest, yielding abundant excess water to promote weathering, leaching, and erosion. The highest rainfall occurs in the Honda watershed at about 1,200 m above sea level (asl) and on the Caribbean slopes of the Palo Seco Protected Forest at about 900 m asl. Less rain falls between January and April, but almost all sites still receive an average of more than 100 mm per month during this period (Table 3.1). The exception is the plot at Alto Frio on the drier Pacific slope, which receives 94 ± 27 mm. Based on the rainfall distribution, and assuming that evapotranspiration in montane forests is about 100 mm per month (Leigh, 1999), we estimate that the mean monthly rainfall exceeds evapotranspiration in all months. The soil moisture regime in the soil taxonomy system of soil classification is therefore perudic at all sites, with the possibility that Alto Frio falls into the udic moisture regime.

Temperature is uniform across Fortuna, with mean annual temperature at study sites ranging from 17.2°C to 19.6°C, with little variation (<2°C) in mean monthly temperature across the annual cycle (Table 3.1). Assuming that soil temperature in the control section is about 1°C greater than air temperature (Soil Survey Staff, 1999), the soil temperature regime according to Soil Taxonomy is isothermic at all sites (defined as mean annual temperature between 15°C and 22°C, with <6°C difference between minimum and maximum mean monthly temperatures).

Vegetation

All the soils studied here are under mature superhumid premontane tropical rainforest (Holdridge, 1947, 1967) (Figure 3.2a–d). Details of the vegetation at Fortuna, including the considerable influence of soils and parent material on the distribution of palms and trees, have been reported previously (Andersen et al., 2010; Andersen et al., 2012; Andersen et al., 2014; Prada et al., 2017) and are described elsewhere in this volume (Dalling et al.; Andersen; Viana and Dalling). Table 3.1 shows information on species numbers in a 1 ha plot at each location, the basal area, and the proportion of the basal area that is formed of ectomycorrhizal trees. Basal area of stems >5 cm diameter at breast height (DBH) ranges between 30 and 47 m^2 ha^{-1} (Table 3.1), while stem density ranges between 562 and 1,143 stems ha^{-1} and mean canopy height is between 19 and 25 m (Dalling et al., this volume).

The Fortuna forest is remarkable for its plant diversity. The tree community (stems >5 cm DBH) contains between 53 and 126 species in a hectare of forest (Table 3.1), with approximately 500 tree species in the entire plot network (Prada et al., 2017; Dalling et al., this volume). Only one of those species occurs in all plots, highlighting the remarkable turnover of species across the reserve (Prada et al., 2017). The forest also supports a variety of plant nutrient acquisition strategies, including species colonized by arbuscular, ericoid, orchid, and ectomycorrhizal fungi (Steidinger et al., 2015; Corrales, Arnold et al., 2016; Andersen et al., 2017). Of particular interest is that a member of the walnut family (Juglandaceae), *Oreomunnea mexicana*, with ectomycorrhizal associations forms large monodominant stands at a number of sites in the Fortuna Forest Reserve (Figure 3.2c, Table 3.1). Other ectomycorrhizal trees include several species of oaks, which become considerably more abundant with increasing elevation, for example, on the slopes of the nearby Volcán Barú at elevations up to ~3,000 m asl. The Fortuna forest also contains a tropical conifer, *Podocarpus oleifolius* (Podocarpaceae), with nodulated roots that house arbuscular mycorrhizal fungi (Dalling et al., 2011; Dickie and Holdaway, 2011), as well as a tree that has no mycorrhizal fungi but forms cluster roots at extremely low fertility (*Roupala montana*, Proteaceae) (Steidinger et al., 2015). There are abundant ferns, including tree ferns, and palms, including the canopy palm *Colpothrinax aphanopetala*, which is particularly abundant in the Chorro watershed where, in combination with two other palm species, it accounts for 42% of the basal area (Figure 3.2b; Viana and Dalling, this volume). However, there are generally few lianas except in the more seasonal plot at Alto Frio. The consequences of the various root associations for nutrient acquisition have been studied in detail at Fortuna for both nitrogen and phosphorus (Steidinger et al., 2015; Andersen et al., 2017; Dalling et al., this volume; Andersen, this volume).

The data in Table 3.1 point to three broad effects of soils on the vegetation. First, soils formed on rhyolite support relatively low-diversity tree communities (i.e., at Chorro), unless underlain by mafic-volcanics at relatively shallow depth (i.e., at Honda). Second, species richness is greatest on the infertile soils of the wet Caribbean slope (Palo Seco, Verrugosa A and B; Figure 3.2d). Third, ectomycorrhizal trees are particularly abundant on Ultisols formed on rhyolite in the Honda watershed as well as on other soils developed on rhyolite at Chorro. Although as yet we have no quantitative information on the tree community at Hornito B, Zarceadero, and Zorro A, conspicuous stands of *Oreomunnea mexicana* occur at all three locations, suggesting that ectomycorrhizal trees also favor Ultisols developed on granodiorite and dacite, two rocks with similar chemical composition (Table 3.2).

Relief and Topography

Relief influences soil development in a number of ways, including through its effects on soil hydrology, erosion, and slope stability. The Fortuna Forest Reserve spans the Continental Divide at elevations up to 1,920 m asl, although the soils studied

TABLE 3.1. Locations and soil forming factors for profile pits at the 14 plots in the Fortuna Forest Reserve, western Panama. Values in parentheses are taken from nearby plots. nd = not determined.

Site	Latitude (decimal °N)	Longitude (decimal °E)	Parent material	Mean annual rainfall (mm)	Mean annual temperature (°C)	Elevation (m above sea level)	Topography	Species per ha	Basal area (m^2 ha^{-1})	Ectomycorrhizal trees (% basal area)
Alto Frio	8.654334	–82.215059	Mafic-volcanics	4,641 ± 623	20.5	1,103	Steep slope	75	42.4	7
Bonita	8.767653	–82.215671	Mafic-volcanics	(5,507)[a]	(17.7)[a]	1,296	Steep slope	77	32.6	0
Chorro A	8.750184	–82.228849	Rhyolite	5,507 ± 247	17.7	1,207	Nearly level	59	35.1	9
Chorro B	8.749801	–82.232838	Rhyolite	(5,507)[a]	(17.7)[a]	1,239	Steep slope	53	40.4	22
Honda A	8.753123	–82.239066	Rhyolite over mafic-volcanic	6,255 ± 962	18.2	1,155	Hilly (steep)	120	46.3	25
Honda B	8.756892	–82.240770	Rhyolite over mafic-volcanic	6,159 ± 617	17.9	1,241	Hilly (steep)	102	47.4	46
Hornito A	8.676193	–82.214611	Porphyritic dacite	5,164 ± 232	17.2	1,330	Steep slope	89	50.3	4
Hornito B	8.678430	–82.213501	Porphyritic dacite	(5,164)[b]	(17.2)[b]	1,296	Steep slope	nd	nd	nd
Palo Seco	8.778643	–82.198143	Mafic-volcanics	6,257 ± 310	19.6	878	Steep, narrow interfluve	145	32.5	4
Pinola	8.754164	–82.259095	Basalt	4,964 ± 863	18.5	1,135	Steep slope	80	43.6	<1
Samudio	8.731185	–82.248065	Rhyolite over mafic-volcanic	4,833 ± 219	17.9	1,215	Hilly (steep)	103	35.6	2
Verrugosa A	8.778184	–82.180279	Mafic-volcanics	(6,257)[c]	(19.6)[c]	969	Hilly (steep)	114	30.3	2
Verrugosa B	8.777998	–82.170315	Mafic-volcanics	(6,257)[c]	(19.6)[c]	858	Hilly (steep)	126	30.3	2
Zarceadero	8.762611	–82.269477	Granodiorite	(4,964)[d]	(18.5)[d]	1,150	Steep, narrow interfluve	nd	nd	nd
Zorro A	8.762396	–82.260959	Granodiorite	(4,964)[d]	(18.5)[d]	1,360	Steep, narrow interfluve	nd	nd	nd

[a] Values from the nearby Chorro A plot.
[b] Values from the nearby Hornito A plot.
[c] Values from the nearby Palo Seco plot.
[d] Values from the nearby Pinola plot.

FIGURE 3.2. The landscape and forests of the Fortuna Forest Reserve and Palo Seco Protected Forest. (a) The view north from below the Fortuna Dam Wall toward the plots at Pinola, Zorro, and Zarceadero. (b) The view north from the road into the Chorro watershed showing the canopy dominated by *Colpothrinax* palms. (c) A majestic individual of *Oreomunnea mexicana* in the Hornito B plot; this ectomycorrhizal species forms monodominant stands on Ultisols formed on a variety of parent materials. (d) The dense palm-dominated understory in forest growing on Inceptisols on the wet Caribbean slope (Verrugosa B). (e) A typical boulder-choked stream in the Honda watershed at Fortuna.

TABLE 3.2. Summary of the geological formations in the Fortuna Forest Reserve and Palo Seco Protected Forest, Panama. All rocks are igneous. Mineral composition from Silva et al. (this volume). Sanidine and orthoclase are potassium feldspars; plagioclase includes sodium and calcium feldspars. Intrusive = plutonic; extrusive = volcanic.

Rock	Category	Chemistry	Silica (SiO_2, %)	Grain size	Dominant minerals	Plots
Rhyolite	Extrusive	Felsic	>69	Fine	Quartz, orthoclase, sanidine, amphibole	Chorro A and B, Honda A and B, Samudio
Dacite	Extrusive	Felsic	63–69	Porphyritic	Plagioclase, quartz	Hornito A and B[a]
Granodiorite	Intrusive	Felsic	63–69	Medium	Plagioclase, quartz, amphibole, pyroxene, magnetite	Zarceadero, Zorro A
Andesite	Extrusive	Intermediate	52–63	Fine	Plagioclase, pyroxene	Alto Frio, Bonita, Palo Seco, Verrugosa A and B[b]
Basalt	Extrusive	Mafic	45–52	Fine[c]	Plagioclase, pyroxene	Pinola; as above for andesite
Diabase[d]	Shallow intrusive (sills/dykes)	Mafic	45–52	Porphyritic	Plagioclase, pyroxene, magnetite	As above for andesite
Gabbro	Intrusive	Mafic	45–52	Medium	Plagioclase, pyroxene, magnetite	Present near Pinola but not represented in any plots

[a] Elemental composition of soils of the two Hornito plots suggests a difference in parent material, with a greater mafic contribution to Hornito A.

[b] These plots are on undifferentiated volcanics, including andesite, basalt, and diabase (Silva et al., this volume).

[c] Texture is fine at Pinola but varies in the undifferentiated mafic-volcanic sequence, including porphyritic and amygdular.

[d] Also known as dolerite or microgabbro.

here range between 850 and 1,360 m asl. The topography of Fortuna is characterized by steep slopes dissected by powerful rivers with boulder-choked channels (Figure 3.2a,e). There are flatter areas around the lake, particularly on the soft rhyolite of the Chorro and Honda watersheds. However, most profiles we have studied are on steep slopes, on narrow interfluves or steeply sloping ridge crests (e.g., Palo Seco, Zarceadero), or on hilly terrain characterized by short, steep slopes (e.g., Verrugosa A and B). The steep slopes indicate active erosion, and the jumbled angular, coarse fragments in several profiles suggests that landslides have had considerable influence on soil development (e.g., Alto Frio, Hornito, Palo Seco, Samudio, Zorro A). Despite active erosion and the influence of landslides, several profiles are deeply weathered or have well-developed argillic horizons, indicating relative stability.

Parent Material

Variation in parent material underlies the remarkable differences in soils across the Fortuna region (Figure 3.1). The geology of Fortuna is described in detail elsewhere in this volume (Silva et al.). The main lithological units (Table 3.2) are (1) fine-grained rhyolite formed by pyroclastic flows (the upper pyroclastic unit in Figure 3.1), (2) a series of undifferentiated mafic-volcanic rocks that includes basalt, andesite, and diabase, (3) a plutonic body of granodiorite, (4) a block of porphyritic dacite, and (5) a small area of very fine-grained basalt to the north of the dam wall.

Rhyolite blankets the landscape to the north and west of the lake, including the Honda and Chorro watersheds. It is conspicuous in road cuts to the north of the reservoir, forming thick beds of soft, bright white and pink material many meters deep. The rhyolite is formed of a fine-grained microcrystalline glassy groundmass dated to approximately 7 million years (Wegner et al., 2011). The rhyolite also occurs to the west and south of the dam wall, notably on the upper slopes of the Samudio plot, and in the Chorro area it can be readily delineated from aerial photographs based on the distribution of the canopy palm *Colpothrinax*. At Chorro, the rhyolite includes substantial rhyolite boulders, while at Honda, it forms a thick, well-weathered layer above mafic-volcanic material, with an abrupt boundary clearly visible in profile pits (Figure 3.3f).

The undifferentiated mafic-volcanics include andesite, basalt, and diabase. This sequence forms the bedrock over large areas of the landscape on the Caribbean and Pacific slopes and underlies the rhyolite at relatively shallow depth in the Honda and Samudio watersheds. In most cases, lithic fragments in profile pits were too strongly weathered to infer their lithology other than that they were mafic-volcanics. However, unweathered fragments were typically dark gray medium-grained andesite and quite unlike the very fine-grained black basalt that has so far been identified only at Pinola. As a result, initial publications on the soils described the

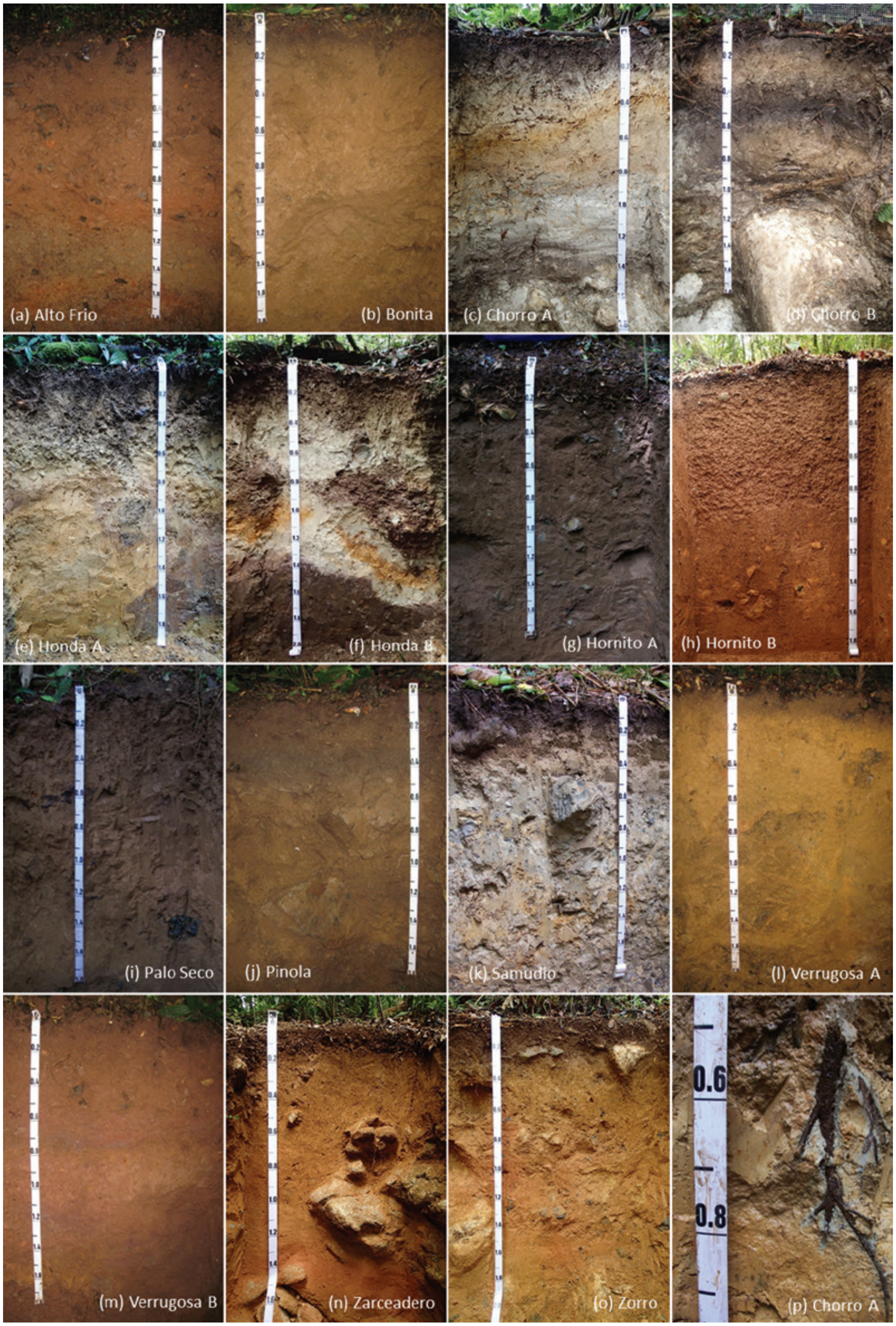

FIGURE 3.3. The soils of the Fortuna Forest Reserve and Palo Seco Protected Forest, showing soils at (a) Alto Frio, (b) Bonita, (c) Chorro A, (d) Chorro B, (e) Honda A, (f) Honda B, (g) Hornito A, (h) Hornito B, (i) Palo Seco, (j) Pinola, (k) Samudio, (l) Verrugosa A, (m) Verrugosa B, (n) Zarceadero, (o) Zorro A, (p) gleying around roots in the subsoil at Honda A.

parent material of a number of plots as andesite (e.g., Andersen et al., 2010), although we now prefer to classify these sites as undifferentiated mafic-volcanics.

Granodiorite and dacite are of similar chemical composition, forming the intrusive and extrusive forms, respectively (Table 3.2). Granodiorite is conspicuous in outcrops below the Fortuna dam. It is medium-grained and relatively rare in Panama (Instituto Geográfico Nacional Tommy Guardia, 1991). Dacite forms a high linear ridge to the south of the reservoir, which rises to the east of the main road through the reserve. Its porphyritic nature indicates slow cooling prior to eruption, dated to approximately 8.7 million years ago (Wegner et al., 2011).

Time

There is little information on soil age at Fortuna. The steep slopes suggest relatively high rates of erosion and therefore pedogenic youth, as is typical of tropical mountains. However, the warm and humid climate promotes rapid weathering, and most soils are strongly weathered to considerable depth. In terms of parent material age, the majority of the lithologies date to the Middle Miocene 11 to 19 million years ago during the rise of the Isthmus of Panama (Silva et al., this volume). In contrast, the pyroclastic rhyolite deposits are dated at about 7 million years (Wegner et al., 2011).

The presence of glass in some profiles, and the predominance of epipedons (i.e., surface horizons) with andic properties, hint at relatively recent inputs of volcanic ash. Significant quantities of volcanic glass were detected in only two profiles (Chorro A, Samudio), in both cases coinciding with the presence of aquic conditions, which suggests that waterlogging impedes glass weathering, with relatively rapid weathering elsewhere (Dahlgren et al., 1997). However, andic properties can also develop where high inputs of organic matter promote the formation of ferrihydrite instead of crystalline iron oxides during pedogenesis (Shoji et al., 1993; Soil Survey Staff, 1999). Given the strongly weathered nature of many of the profiles, with clay mineralogy dominated by kaolinite, it seems possible that the common moderate andic properties arise through this organic matter–related process rather than via recent volcanic ash inputs.

OUTLINE OF FIELD AND ANALYTICAL METHODS

Fieldwork was conducted between 2008 and 2018, almost always during the wet season. At each location, profile pits were excavated around the outside of the plot and close to the southwest corner where possible. The profiles were described according to the USDA's *Soil Taxonomy* (Soil Survey Staff, 1999) and the Natural Resources Conservation Service's *Field Book for Describing and Sampling Soils, Version 3.0* (Schoeneberger et al., 2012), and they were classified using the most recent version of the *Keys to Soil Taxonomy* (Soil Survey Staff, 2014). In profile descriptions, color values are for moist soil and textures are field (hand) textures, with precise laboratory measurements reported in tables. Samples were taken by genetic horizon for laboratory analysis and determination of bulk density. Soils were returned to the Smithsonian Tropical Research Institute for physical and chemical analyses. Samples were air-dried at ambient laboratory conditions (~22°C and 60% relative humidity), sieved (<2 mm), and a subsample ground in a ball mill.

Bulk density was determined by a modified compliant cavity method (Grossman and Reinsch, 2002), removing ~1 L of soil and measuring the volume of water required to fill the plastic-lined excavated hole. The exception was surface organic horizons, for which density was quantified by determining the weight of organic material in a 20 × 20 cm square on the soil surface excavated to the depth of the organic horizon after removing intact or recognizable leaves and roots.

Soil pH was determined in both deionized water and 10 mM calcium chloride ($CaCl_2$) in a 1:2 soil-to-solution ratio, as well as in 0.1 M barium chloride ($BaCl_2$) extracts (described below), in all cases using a glass electrode. Although the pH in water is commonly determined, the value in $CaCl_2$ reflects the true pH in the soil solution and appears robust against seasonal effects of moisture or pretreatment. The pH in $BaCl_2$ is typically similar to that in $CaCl_2$ and can be used to quantify exchangeable acidity.

The concentrations of sand (53 µm–2 mm), silt (2 µm–53 µm), and clay (<2 µm) sized particles were determined by the pipette method following pretreatment to remove soluble salts, organic matter, and iron oxides, the latter involving repeated treatment with buffered dithionite solution (Gee and Or, 2002). Fresh (undried) soil was analyzed from profiles suspected of having andic properties, as drying can cause irreversible changes in the particle-size distribution in such soils.

Total carbon and nitrogen were determined by automated combustion and gas chromatography with thermal conductivity detection using a Thermo Flash 1112 analyzer (CE Elantech, Lakewood, NJ, USA).

Exchangeable cations were determined in all horizons by extraction in 0.1 M $BaCl_2$ (2 h, 1:30 soil-to-solution ratio), with detection by inductively coupled plasma optical-emission spectrometry (ICP–OES) on an Optima 7300 DV (Perkin-Elmer Ltd, Shelton, CT, USA) (Hendershot et al., 2008). Total exchangeable bases (TEB) was calculated as the sum of the charge equivalents of calcium (Ca), potassium (K), magnesium (Mg), and sodium (Na); effective cation exchange capacity (ECEC) was calculated as the sum of aluminum (Al), Ca, iron (Fe), K, Mg, manganese (Mn), and Na; base saturation was calculated by (TEB ÷ ECEC) × 100. We use the values determined in $BaCl_2$ as our primary measures of exchangeable cations, extractable Al, cation exchange capacity (CEC), and base saturation because the extraction approximates these values at the soil pH and therefore reflects conditions experienced by plants and microbes under field conditions.

Additional measurements of cations were made to examine specific criteria for classifications in *Soil Taxonomy* (Soil Survey Staff, 1999). Extractable acidity was quantified by extraction in

0.1 M $BaCl_2$–TEA (triethanolamine) buffered at pH 8.2. Soils were extracted in a 1:16 soil-to-solution ratio by shaking to mix and standing overnight (16 h). Acidity was determined by titration with 0.12 M hydrochloric acid (HCl) to the pink endpoint of bromocresol green–methyl red mixed indicator solution (Seifferlein et al., 2005). Cation exchange capacity by sum of cations (CEC8.2) was calculated as extractable acidity plus TEB extracted in 0.1 M $BaCl_2$ at soil pH, with base saturation by sum of cations calculated as TEB divided by CEC8.2. This value for base saturation is used to separate Ultisols and Alfisols in *Soil Taxonomy* (Soil Survey Staff, 1999).

Cation exchange capacity was also determined by extraction in 1 M ammonium acetate (NH_4AOc) buffered at pH 7 (Sumner and Miller, 1996; Soil Survey Staff, 2014). Soils were extracted in a 1:8 soil-to-solution ratio by shaking for 2 hours, then centrifuged. Exchangeable cations were determined in the supernatant by ICP–OES. Cation exchange capacity (CEC7) was determined in the washed residue by extracting the retained ammonium in 2 M potassium chloride (KCl), with detection by automated colorimetry on a Lachat QuikChem 8500. Base saturation was determined as the sum of Ca, K, Mg, and Na divided by the CEC7. These values are used in a number of criteria in soil taxonomy, including the separation of dystric and eutric Inceptisols, and the definition of umbric and mollic epipedons. Based on many analyses of Panamanian soils, exchangeable cations determined in neutral NH_4AOc are equivalent to those determined in 0.1 M $BaCl_2$. However, CEC in $BaCl_2$ is usually about 75% of that determined in NH_4AOc (CEC7).

Total elements were determined by digestion in concentrated nitric acid for 6 hours under pressure at 180°C in polytetrafluoroethylene (PTFE) vessels (PDS-6 Pressure Digestion System, Loftfields Analytical Solutions, Neu-Eichenberg, Germany), with detection by ICP–OES. Pedogenic Fe was determined by extraction in citrate–dithionite solution. This procedure predominantly quantifies crystalline Fe, such as hematite, magnetite, and goethite, and is used in soil taxonomy to define some mineralogy classes (e.g., parasesquic). Aluminum and manganese were also determined in the extracts. Amorphous (noncrystalline) metal oxides (Al, Fe, Mn) plus silicon were extracted in the dark in acidic ammonium oxalate. These values include metals associated with organic matter and are used to identify andic properties. In both extractions, detection was by ICP–OES spectrometry (Courchesne and Turmel, 2008).

Mineralogy was determined at the USDA–NRCS Kellogg Soil Survey Laboratory in Lincoln, Nebraska, USA, according to methods described in Soil Survey Staff (2014). Clay mineralogy was determined by X-ray diffraction (XRD). Minerals are identified by the spacings between atomic planes, with results reported in semiquantitative classes based on relative peak intensity. These classes are 5, very large (>50%); 4, large (30%–50%); 3, medium (10%–30%); 2, small (3%–10%); 1, very small (<3%); 6, no peaks (amorphous). Clay minerals were also quantified by thermal analysis, involving the measurement of weight loss during gradual heating. Thermal analysis is particularly useful for quantifying kaolinite, gibbsite, and other minerals, with results given in percentage of the clay fraction. Finally, clay mineralogy can be estimated from the CEC determined by extraction in 1 M NH_4AOc at pH 7 divided by the clay concentration in percentage of total mineral mass. Values less than 0.2 represent kaolinitic mineralogy, 0.2 to 0.3 are kaolinitic or mixed, 0.3 to 0.5 are mixed or illitic, 0.5 to 0.7 are mixed or smectitic, and greater than 0.7 are smectitic. Glass content was measured by optical grain counts on samples suspected of having andic properties. Glass grains are identified as either glass, glass-coated grains, or glass aggregates and were measured in the fine sand and coarse silt fractions.

THE SOILS OF FORTUNA: CLASSIFICATION IN SOIL TAXONOMY

There is wide variation in soils across the Fortuna Forest Reserve and Palo Seco Protected Forest (Figure 3.3). The profiles are described here by soil order – the highest level of classification in the soil taxonomy system of soil classification (Table 3.3). Detailed profile descriptions and analytical data by genetic horizon are presented under "Soil Profile Descriptions and Analytical Data."

ANDISOLS

Andisols are characterized by high concentrations of amorphous aluminosilicates, including allophane, imogolite, and ferrihydrite (Shoji et al., 1993; Buol et al., 2011). These amorphous minerals are typically derived from the weathering of volcanic glass, although andic properties can also develop when high concentrations of organic matter prevent formation of crystalline metal oxides such as gibbsite and hematite. Most Andisols have formed in Holocene deposits, while older soils developed on volcanic deposits are typically dominated by crystalline rather than amorphous aluminosilicate minerals and therefore do not qualify as Andisols. Andisols often contain high concentrations of organic matter and have a high capacity to retain phosphorus. Because Andisols are defined by andic properties rather than by the presence of volcanic ash, some Andisols are not formed in ash deposits, and some soils developed in ash are not Andisols.

Despite the abundance of volcanic deposits in the Fortuna region, only two profiles qualify as Andisols. However, several other profiles have moderate andic properties in the upper horizons that are sufficient to qualify for andic subgroups of Inceptisols and Ultisols.

The profile at Bonita (Figure 3.3b) on undifferentiated mafic-volcanics is an Udand. These are the freely draining Andisols of humid regions (Soil Survey Staff, 1999). Diagnostic features of this profile are (1) andic properties in the upper 60 cm of the profile, including low bulk density and a high concentration of noncrystalline Al and Fe oxides; (2) a perudic moisture regime; (3) an argillic horizon (i.e., a subsurface horizon

TABLE 3.3. Soil taxonomy, including family-level classifications for soils in the Fortuna Forest Reserve, western Panama. All profiles have an isothermic temperature regime. n/a = not applicable (cation exchange class used only for soils with mixed mineralogy); nd = not determined.

Site/plot	Particle-size class	Mineralogy	Cation exchange class	Subgroup	Great group, suborder	Pedogenic features
Andisols						
Bonita	Medial	Ferrihydritic	n/a	Acrudoxic Ultic	Hapludand	Andic properties, argillic horizon, low base saturation, extremely low cation exchange capacity
Chorro A	Medial	Amorphic	n/a	Alic	Epiaquand	Shallow organic horizon, andic properties, low base saturation, episaturation, sombric horizon
Inceptisols						
Verrugosa A	Clayey-skeletal	Parasesquic	n/a	Typic	Dystrudept	Cambic horizon, low base saturation
Verrugosa B	Very fine	Mixed	Active	Typic	Dystrudept	Cambic horizon, low base saturation
Palo Seco	Fine	Parasesquic	n/a	Andic	Dystrudept	Cambic horizon, moderate andic properties, low base saturation
Samudio	Fine	Mixed	Superactive	Aquandic	Dystrudept	Shallow organic horizon, moderate andic properties, aquic conditions within 60 cm of the surface
Alto Frio	Clayey-skeletal	Kaolinitic	n/a	Typic	Humudept	Umbric epipedon, cambic horizon, low base saturation
Zorro A	Fine-loamy	Mixed	Active	Typic	Humudept	Umbric epipedon, cambic horizon, low base saturation
Spodosols						
Chorro B	Coarse-loamy	nd	nd	Oxyaquic	Alorthod	Organic horizon, spodic horizon rich in organic matter and amorphous Al, periodic saturation
Ultisols						
Hornito B	Very fine	Parasesquic	n/a	Typic	Haplohumult	Argillic horizon, high organic matter, low base saturation
Zarceadero	Fine	Mixed	Active	Typic	Haplohumult	Argillic horizon, low base saturation, high organic matter
Honda A	Fine	Kaolinitic	n/a	Andic	Haplohumult	Argillic horizon, high organic matter, moderate andic properties, extremely low base saturation
Honda B	Fine	Kaolinitic	n/a	Andic	Haplohumult	Argillic horizon, high organic matter, moderate andic properties, extremely low base saturation
Hornito A	Fine	Kaolinitic	n/a	Andic	Haplohumult	Argillic horizon, high organic matter, low base saturation
Pinola	Fine	Mixed	Superactive	Andic	Palehumult	Argillic horizon, moderate andic properties, low base saturation

enriched in illuvial clay) with low base saturation in the subsoil, and (4) an extremely low CEC. These features qualify the profile as an Acrudoxic Ultic Hapludand. The profile has a ferrihydritic mineralogy class.

The profile at Chorro A (Figure 3.3c) on rhyolite is an Aquand. These are poorly drained Andisols with a water table near the soil surface. They typically occur on relatively flat terrain and have a thin organic surface horizon. This is the case for the profile here, which has a shallow organic horizon over bright white subsoil. The soil appears to become saturated from both above and below, presumably due to the high rainfall, relatively flat topography, and clay-enriched subsurface horizon. Redox concentrations around roots in the upper subsoil indicate oxygenation of a reduced horizon (Figure 3.3p). The profile is very acidic and extremely infertile, and the combination of acidity, infertility, and anaerobic conditions indicates that this environment is particularly challenging for plant growth.

Inceptisols

Inceptisols are moderately weathered soils and occur at Fortuna on three different parent materials: rhyolite (Samudio), granodiorite (Zorro A), and mafic-volcanics (Alto Frio, Palo Seco, Verrugosa A and B). These profiles are all in the Udept suborder, representing well drained Inceptisols of humid regions that typically develop under forest (Soil Survey Staff, 1999).

The Udepts at Fortuna are separated at the great group level into Dystrudepts and Humudepts. Dystrudepts are the typical Udepts of humid regions, being sufficiently leached to reduce base saturation in the subsoil. They occur at all three sites on the wet Caribbean slope, where undulating topography and abundant evidence of small landslides (stone layers, etc.) suggest a relatively youthful landscape. Typic (i.e., typical) Dystrudepts have an ochric epipedon over a cambic horizon (i.e., a moderately developed subsoil horizon) with low base saturation. These soils occur at Verrugosa A and Verrugosa B (Figure 3.3l,m). In contrast, the profile at Palo Seco (Figure 3.3i) has moderate andic properties in the upper 75 cm of the profile, including low bulk density and Al+½Fe concentrations >1.0%, and therefore qualifies as an Andic Dystrudept. The profile on rhyolite at Samudio (Figure 3.3k) has moderate andic properties and aquic conditions within 60 cm of the soil surface and therefore qualifies as an Aquandic Dystrudept. It has insufficient andic properties to qualify as an Andisol despite moderate concentrations of volcanic glass. All the Dystrudepts have extremely low base cation concentrations, suggesting strong weathering and oxic tendencies. However, CEC in neutral ammonium acetate is relatively high, demonstrating substantial pH-dependent charge (see section MINERAL NUTRIENTS below).

The Humudepts are a relatively recent addition to soil taxonomy, being introduced into the 11th edition of the *Keys to Soil Taxonomy* (Soil Survey Staff, 2010). Prior to that time, Humudepts were classified as Humic Dystrudepts. The Humudepts are similar to Dystrudepts but have a dark, organic-rich epipedon, defined as either umbric or mollic depending on base saturation. At Fortuna, Typic Humudepts occur at Alto Frio and Zorro A (Figures 3.3a and 3.2o), with both profiles having an umbric epipedon (i.e., dark colors with low base saturation). Although base saturation by NH_4OAc is low in both profiles, they differ markedly in fertility. For example, the Alto Frio soil has relatively high concentrations of base cations and almost 100% effective base saturation determined in $BaCl_2$ at soil pH, compared to the much lower effective base saturation and extremely low base cation concentrations at Zorro A. The contrast in fertility between taxonomically identical soils highlights a problem with the use of buffered solutions for the determination of CEC in acidic forest soils, which often have considerable pH-dependent charge.

Spodosols

One profile at Fortuna is a Spodosol (also known as a podzol). The soil at Chorro B (Figure 3.3d), developed in rhyolite, has a subsoil horizon enriched by the illuvial accumulation of complexes between organic matter and amorphous Al, which therefore qualifies as a spodic horizon. The spodic horizon contains considerably greater organic carbon (5.6%–6.3% C) and total phosphorus (>100 mg P kg^{-1}) than adjacent horizons. There is little indication that it is a buried A horizon (e.g., caused by a landslide) because, although organic C is high between 36 and 56 cm, there are no clear differences in exchangeable cations, and oxalate and dithionite Fe decrease continuously with depth. Texture is variable throughout the profile, although such measurements can be unreliable in Spodosols (Soil Survey Staff, 1999). The key difference is the greater amorphous Al in the organic-rich subsoil horizon, indicating podzolization and spodic properties. A similar accumulation of amorphous Al has occurred at Chorro A, although it is insufficient to qualify as spodic, perhaps due to the aquic conditions in that profile.

The Chorro B profile is an Oxyaquic Alorthod. Orthods are the most common Spodosols in northern Europe and the United States (Soil Survey Staff, 1999). Alorthods have an accumulation of amorphous Al but little accumulation of amorphous Fe, and they typically have an ochric epipedon and an albic (bleached) subsoil horizon, all of which occur here.

The high concentrations of amorphous metal oxides and organic matter mean that Spodosols have similarities to Andisols (Buol et al., 2003). There is a small amount of volcanic glass in the profile at Chorro B, but neither the glass nor the amorphous metals are sufficient for andic properties. The organic-rich subsoil horizons at Chorro B also have similarities with sombric horizons, defined as dark subsurface mineral horizons formed under free drainage in tropical and subtropical mountains. However, the dark color in a sombric horizon is formed by organic matter that is not associated with aluminum, as in a spodic horizon. A proposal to improve the definition of the sombric horizon (Bockheim,

2014) suggests that it should have at least 0.6% carbon (and 0.2% more than the overlying horizon), be at least 15 cm thick, have color value and chroma <4 (and be 1 unit darker than the overlying horizon), have a pH ≤5, and have a base saturation <50% (by CEC7). To differentiate it from a spodic horizon, a sombric horizon should not be associated with amorphous Al, with an Al+½Fe concentration <0.5%. At Chorro B, the organically enriched subsoil horizons meet all the criteria apart from the Al+½Fe concentration, so these horizons are not sombric.

The low concentrations of Fe in Alorthods can occur through intense leaching and removal of Fe or because of a low-Fe parent material, and both of these appear to be relevant for the Chorro B profile. The absence of redox concentrations at Chorro B, including around root channels (as seen in the profile at Honda A; Fig. 3.3p), suggests no aquic conditions, although the extremely low concentrations of iron oxides mean that it would be difficult to identify redox features if saturation occurs. Redox features are clearly present at Chorro A on the same rhyolitic parent material, although Fe concentrations are greater there. This suggests that long-term reducing conditions have removed Fe from the Chorro B profile, indicating periodic saturation to moderate depth.

Ultisols

Ultisols have an argillic horizon (i.e., subsoil enriched with illuvial clay) and low base saturation at depth. The Ultisols at Fortuna are Humults, which represent free-draining Ultisols rich in organic matter. They typically occur under forest on the steep slopes of mountainous areas with high rainfall (Soil Survey Staff, 1999).

Haplohumults (i.e., Haplo-, from the Greek *haplous*, simple – indicating limited horizon development) occur on three different parent materials at Fortuna: granodiorite at Zarceadero (Figure 3.3n), dacite at Hornito A (Figure 3.3g), and rhyolite in the Honda watershed (Honda A and B, Figure 3.3e,f). These are all felsic (high silica) substrates, with dacite and granodiorite representing the extrusive and intrusive forms of a chemically equivalent magma source (63%–69% SiO_2); see Table 3.2. In all cases, the soils have formed on steep slopes, but the well-defined argillic horizon (with a clay decrease of >20% below the maximum in the upper 150 cm) indicates relative stability.

Typic Haplohumults occur at Hornito B (Figure 3.3h) and Zarceadero (Figure 3.3n). The soils are morphologically similar, although the Zarceadero profile contains less clay and the argillic horizon is more pronounced. This profile also contrasts with the nearby but pedogenically younger Inceptisol on granodiorite at Zorro A, which appears to have formed on a more active slope. The Typic Haplohumults have extremely low concentrations of base cations, particularly Ca, in the subsoil, with TEB cation concentrations <1 $cmol_c kg^{-1}$.

The profile at Hornito B is unusual because it sits on the Ultisol–Oxisol boundary. There is a sufficient clay increase in the subsoil to qualify as an argillic horizon, but although the CEC is low, the clay increase occurs over a distance of >15 cm. The horizon does not therefore qualify as kandic (i.e., an illuvial horizon dominated by low-activity clays), and the profile does not qualify as an Oxisol. Instead, the argillic horizon qualifies the profile as an Ultisol. If the clay increase were just 1% greater in the Bt1 horizon, then the argillic horizon would qualify as a kandic horizon, and the profile would classify as an Oxisol (i.e., a kandic horizon and >40% clay). If the clay concentration in the Bt2 horizon were 1% less, then there would be no argillic horizon, and again, the profile would qualify as an Oxisol (i.e., with an oxic horizon). The profile is therefore transitioning into an Oxisol.

In the Honda watershed and the upper slope at Hornito (Hornito A), the Ultisols are Andic Haplohumults. Unlike the Typic Haplohumults, the Andic subgroup has moderate andic properties in the epipedon, including low bulk density and a moderate concentration of amorphous metals. All three profiles have an organic-rich surface horizon. Although the Honda profiles are developed in rhyolite, this is sufficiently weathered that only traces of glass are detectable, and the clay mineralogy in the control section is kaolinitic, with small amounts of gibbsite (see “Soil Properties: Texture and Mineralogy”). At Honda, mafic-volcanic material occurs at relatively shallow depth (<2 m) beneath the rhyolite mantle, with roots extending through the rhyolite into the mafic subsoil.

Palehumults (i.e., Pale-, from the Greek *paleos*, old – indicating excessive horizon development) are freely draining Ultisols that occur on old, stable surfaces and have little or no clay decrease below the maximum within the upper 150 cm. At Fortuna, the soil at Pinola (Figure 3.3j) qualifies as an Andic Palehumult, having an argillic horizon, low base saturation in the subsoil, and moderate andic properties within the upper 75 cm of the profile. The soil is formed on aphanitic basalt and contains many coarse angular basalt fragments throughout the profile. This dark-colored and fertile soil is rich in organic matter and nutrients, with high concentrations of phosphorus and exchangeable cations, particularly Ca and Mg. However, base saturation by NH_4AOc is low in the subsoil, reflecting high extractable acidity. The basalt, and therefore this soil, appear to be of small extent at Fortuna, although similar soils may occur on the nearby gabbro outcrop (Silva et al., this volume).

SOIL PROPERTIES

Texture and Mineralogy

Soil textures in the upper meter of the profile at Fortuna are predominantly clays and clay loams (Table 3.4). Loams occur only in the Chorro watershed on rhyolitic ash. Clay loams occur on rhyolite at Samudio and Honda and on granodiorite at Zarceadero and Zorro. Verrugosa A has a profile-weighted texture of silty clay, but the remaining soils are clays, with clay concentrations between 41% and 61%. In terms of particle-size classes in soil taxonomy (i.e., based on the particle-size control section, typically subsoil within the upper meter of the profile), the clay-rich soils are fine or very fine (Table 3.3), two soils are classed as

TABLE 3.4. Soil texture and mineralogy for soils across the Fortuna Forest Reserve and Palo Seco Protected Forest, western Panama. Particle size values are profile-weighted for the upper 1 m of soil. Mineralogy was measured in the specific horizon given stated. Grain counts are glass grains as a weighted percentage of the total grains in the coarse silt and fine sand fractions within samples analyzed in the control section. Glass grains include glass, glass-coated grains, and glass aggregates. See individual profile descriptions for details on glass counts by genetic horizon. USDA–NRCS Soil Survey Laboratory mineral codes: KK, kaolinite; GI, gibbsite; HV, hydroxy-interlayer vermiculite; VR, vermiculite; GE, goethite; CR, cristobalite; KH, halloysite; NX, noncrystalline. X-ray diffraction peak sizes: 5 = very large (>50%); 4 = large (30%–50%); 3 = medium (10%–30%); 2 = small (3%–10%); 1 = very small (<3%); 6 = no peaks. ND = not determined.

		Particle-size (% fine earth)								
Soil Taxonomy	Site/Plot	Sand	Silt	Clay	Texture class	Horizon	Depth (cm)	Thermo-gravimetric (%)	X-ray diffraction (peak size)	Volcanic glass (% of total grains), with horizon shown in parentheses
Andisols										
Acrudoxic Ultic Hapludand	Bonita	27	32	41	Clay	Bt2	36–60	ND	GI (2) HV (2) KK (1) GE (1) NX (6)	ND
Alic Epiaquand	Chorro A	37	44	18	Loam	BCg2	90–121	KK 42, GI 06	ND	12–13% (5–31 cm)
Inceptisols										
Typic Dystrudept	Verrugosa A	15	44	41	Silty clay			ND	ND	
Typic Dystrudept	Verrugosa B	18	28	55	Clay			ND	ND	
Andic Dystrudept	Palo Seco	21	36	43	Clay	B1	30–40	KK 56, GI 11	KH (2) GI (2)	
						B3	90–100	KK 55, GI 07	KH (2) GI (1)	
Aquandic Dystrudept	Samudio	26	41	33	Clay loam	B1	25–50	KK 47, GI 09	KK (3) VR (2) GI (2) CR (2)	7% (20–50 cm)
Typic Humudept	Alto Frio	23	31	47	Clay	B1	38–82	KK 59, GI 05	KK (3) HV (2) GI (1) GE (1)	
Typic Humudept	Zorro	42	27	31	Clay loam			ND	ND	
Spodosols										
Oxyaquic Alorthod	Chorro B	45	36	19	Loam			ND	ND	<1%–3% (18–56 cm)
Ultisols										
Typic Haplohumult	Hornito B	9	30	61	Clay			ND	ND	
Typic Haplohumult	Zarceadero	39	24	37	Clay loam	Bt2	39–66	ND	GI (3) KK (1) HV (1) CR (1)	
Andic Haplohumult	Honda A	24	33	44	Clay	A/B	10–20	KK 46, GI 07	KK (2) VR (2) GI (1)	2% (16–51 cm)
						BC	51–75	KK 68, GI 02	KH (3) VR (1) GI (1)	
						BCg	130–180	KK 67, GI 02	KH (2) GI (1) GE (1) HE (1)	
Andic Haplohumult	Honda B	31	38	32	Clay loam	Bt2	25–50	KK 67, GI 03	KH (2) VR (1) GI (1)	1%–4% (10–74 cm)
						2C	150-200	KK 62	KH (2)	
Andic Haplohumult	Hornito A	25	25	50	Clay	Bt1	20–40	KK 62, GI 07	KK (2) VR (2) GI (1)	
						BC	91–100	KK 54, GI 09	KH (2) VR (2) GI (2)	
Andic Palehumult	Pinola	31	26	44	Clay	Bt1	24–49	ND	HV (2) KK (2) GI (1)	

loamy, and the Andisols have a substitute particle-size class of medial (Andisols use substitute particle-size classes to reflect the difficulty in quantifying texture in soils with andic properties; Soil Survey Staff, 1999). Two soils have sufficient coarse fragments to qualify as clayey-skeletal (Alto Frio, Verrugosa A).

Secondary minerals form during pedogenesis and determine soil chemical properties such as sorption and precipitation reactions and metal toxicity (Sposito, 2016). Typical secondary minerals are clay-sized particles and include kaolinite, smectite, vermiculite, allophane, the aluminum oxide mineral gibbsite ($Al(OH)_3$), and iron oxide minerals goethite (FeOOH), hematite (Fe_2O_3), and ferrihydrite (of variable structure) (Sposito, 2016). The iron minerals can be differentiated by their color, goethite giving yellow or brown colors, ferrihydrite yielding yellowish reds, and hematite giving the characteristic red color of strongly weathered tropical soils (Schwertmann, 1993). Manganese minerals also occur, of which birnessite is most common Mn(IV) oxide mineral.

The clay mineralogy of strongly weathered soils are dominated by Al and Fe oxides and kaolinite clay. Almost all soils at Fortuna are strongly weathered, even those with sufficient volcanic glass and amorphous metals to qualify as Andisols. In most cases, kaolinite was the predominant mineral determined by thermogravimetric analysis, ranging from 42% in the Andisol at Chorro A to 67% to 68% in the Ultisols in the Honda watershed (Table 3.3). Gibbsite was typically present at concentrations between 2% and 11% and was the most abundant mineral determined by XRD at Bonita and Zarceadero. Gibbsite is a neutral-charge aluminum hydroxide $Al(OH)_3$ that is abundant in bauxite. The XRD analysis also revealed halloysite, another aluminosilicate similar to kaolinite in its 1:1 structure, in a number of Inceptisols and Ultisols.

Smectite minerals such as vermiculite are more easily lost from soils compared to Al and Fe oxides such as gibbsite and goethite because the silicon in smectites is relatively easily leached. The presence of smectites therefore indicates an intermediate weathering stage. Vermiculite or hydroxy-interlayer vermiculite was detected in almost all profiles, including the Andisol at Bonita, Inceptisols on granodiorite and mafic-volcanics, and most Ultisols. However, vermiculite was not detected at Palo Seco, Verrugosa B, Zorro, or Honda B. Mica was detected in the Inceptisol at Verrugosa B.

A number of soils at Fortuna have moderate andic properties, reflecting the predominance of amorphous metal oxides such as allophane with or without volcanic glass. Volcanic glass was detected in profiles developed on rhyolite (Table 3.4), but typically in small amounts. For example, trace amounts of glass were detected in profiles at Honda (A and B) and the Spodosol at Chorro B. The largest amounts of glass were detected in the profiles at Chorro A and Samudio. Both these profiles have an aquic soil moisture regime, suggesting that waterlogging has reduced the rate of weathering of glass in these profiles.

Allophane ultimately weathers to kaolinite, perhaps explaining the predominance of kaolinite in the clay fraction of soils developed on 7-million-year-old rhyolite (Wegner et al., 2011). In most cases, the rhyolite soils at Fortuna are well-weathered, with argillic horizons (Honda A and B), kaolinitic mineralogy in subsoils, and little remaining volcanic glass. Tephra weathers rapidly even under cool conditions (Dahlgren et al., 1997), so the Miocene age of the rhyolite in road cuts does not preclude more recent deposits at the surface. Indeed, Holocene tephra deposits from Volcán Barú, about 30 km to the west of Fortuna (Sherrod et al., 2008), might be the source of the trace amounts of volcanic glass and moderate andic properties of epipedons in Fortuna soils. However, andic properties are also promoted by the influence of high concentrations of organic matter on secondary metal oxides, leading to the formation of ferrihydrite (i.e., amorphous, noncrystalline) and humus–metal complexes with Al and Fe rather than crystalline forms such as gibbsite and hematite. The large concentrations of organic matter in Fortuna soils suggests that this process is of significance in explaining the moderate andic properties throughout the region.

Cristobalite was detected by XRD in two soils, Zarceadero on granodiorite and Samudio on rhyolite (Table 3.3). This mineral is similar to quartz (SiO_2) and originates from volcanic rocks, being common in pyroclastic flow deposits (Mizota et al., 1987).

Pedogenic Oxides

There is marked variation in pedogenic metal oxides at Fortuna (Table 3.5). Weighted for the upper meter of the soil profile, total pedogenic iron extracted by dithionite (Fe_d) ranged from <0.1% on rhyolite at Chorro B to 10% on mafic-volcanics at Verrugosa A. Dithionite-extractable iron was generally lower on rhyolitic soils at Chorro, Honda, and Samudio. Similarly, amorphous (noncrystalline) iron (Fe_{ox}) accounted for <0.1% of soil mass at Chorro B, but 1.4% in the Andisol at Bonita, reflecting the ferrihydritic mineralogy class there. The ratio of Fe_{ox} to Fe_d, a measure of the proportion of pedogenic iron in amorphous forms and therefore an index of weathering, was relatively low (<16%) in soils developed on dacite, granodiorite, and mafic-volcanics, but much greater (17%–84%) in the Andisol at Bonita and in soils derived from rhyolite, particularly the Spodosol at Chorro B (Table 3.5).

Dithionite-extractable Al (Al_d) ranged from 0.3 to 1.4% of soil mass, with little clear pattern among profiles, although the highest concentrations were in soils developed on dacite and granodiorite, as well as the Andisol at Bonita and the soil on mafic-volcanics at Verrugosa A. Amorphous Al (Al_{ox}) was always <1% of soil mass, being highest in the Andisols at Chorro A and Bonita, as well as in the spodic horizon at Chorro B.

Manganese concentrations were extremely low in soils developed on rhyolite, and this is a diagnostic feature for the distribution of rhyolite in the region. Profile-weighted Mn_d were <0.02 for all soils developed on rhyolite but 0.06 to 2.13 for other soils (Table 3.5). The extremely low Mn in profiles on rhyolite might promote the accumulation of organic matter, as Mn is involved in abiotic and biotic oxidation reactions in soils, which might be suppressed at low Mn (Keiluweit et al., 2015). Low Mn concentrations, particularly Mn_{ox}, occurred on the soils developed in granodiorite (Zorro, Zarceadero) and dacite at

TABLE 3.5. Profile-weighted concentrations of pedogenic oxides in soils across the Fortuna Forest Reserve, western Panama. Values are calculated on an area basis for the organic horizon plus upper 100 cm of the mineral soil using element concentrations and bulk density in genetic horizons. Al_d, Fe_d, and Mn_d are elements extracted in buffered dithionite; Al_{ox}, Fe_{ox}, and Mn_{ox} are elements extracted in acidic ammonium oxalate. The Fe_{ox} to Fe_d ratio indicates the proportion of secondary Fe oxides in amorphous (noncrystalline) forms.

	Oxalate extraction			Dithionite extraction			
Plot	**Al**	**Fe**	**Mn**	**Al**	**Fe**	**Mn**	**Fe_{ox}:Fe_d**
	g kg^{-1}	g kg^{-1}	g kg^{-1}	g kg^{-1}	g kg^{-1}	g kg^{-1}	
Alto Frio	3.6	2.3	1.52	6.1	54.6	2.13	0.04
Bonita	9.6	14.0	0.12	11.5	60.9	0.28	0.23
Chorro A	9.1	2.7	<0.01	6.4	6.8	<0.01	0.41
Chorro B	7.1	0.3	<0.01	5.3	0.4	<0.01	0.84
Honda A	7.6	5.4	<0.01	8.0	30.9	0.02	0.17
Honda B	4.9	1.4	<0.01	3.1	3.9	<0.01	0.36
Hornito A	7.8	6.1	1.11	8.1	64.2	1.74	0.09
Hornito B	3.6	1.5	<0.01	12.7	83.1	0.12	0.02
Palo Seco	5.9	7.4	0.76	9.4	58.1	1.16	0.13
Pinola	6.3	8.2	0.93	9.3	50.1	1.59	0.16
Samudio	6.8	4.6	<0.01	5.4	9.7	<0.01	0.48
Verrugosa A	2.5	3.5	0.44	12.2	100.9	0.82	0.03
Verrugosa B	4.7	4.4	1.18	6.3	62.0	1.52	0.07
Zarceadero	4.3	3.8	0.03	9.7	40.3	0.06	0.09
Zorro	1.2	1.0	<0.01	14.1	51.3	0.09	0.02

Hornito B. However, Mn concentrations were high in the Ultisol at Hornito A, suggesting a difference in parent material between the two Hornito plots. High Mn was also a feature of Inceptisols developed on mafic-volcanics (Alto Frio, Verrugosa B, Palo Seco) and the Ultisol on basalt at Pinola.

Organic Matter

Some of the soils at Fortuna contain relatively large amounts of organic matter (Table 3.6). Total carbon to 1 m depth in the profile ranged between 8.5 and 51.8 kg C m^{-3} (Mg C ha^{-1}). The highest value was in the Spodosol on rhyolite at Chorro B, reflecting organic matter accumulation in the spodic horizon. However, large amounts of organic matter (>20 kg C m^{-3}) also occurred in the Andisol at Bonita, the Ultisol on basalt at Pinola, and the Inceptisol on granodiorite at Zorro A. Lowest amounts occurred in Inceptisols on the wet Caribbean slope.

Total N varied in parallel with total C, but C:N ratios varied systematically according to the abundance of ectomycorrhizal trees (Table 3.6). The C:N ratio was 10–12 in plots with few or no ectomycorrhizal species, including the Inceptisols on mafic-volcanics. However, the ratio was 15–19 in plots with abundant ectomycorrhizal species, including Chorro and Honda on rhyolite, Zorro and Zarceadero on granodiorite, and Hornito B on dacite. This ratio presumably reflects the depletion of nitrogen from organic matter by the ectomycorrhizas, promoting nitrogen limitation of heterotrophic organisms (Orwin et al., 2011; Averill et al., 2014). Indeed, a reduction of nitrogen availability and wide C:N ratios have been observed in monodominant *Oreomunnea mexicana* stands in the Honda watershed (Corrales, Mangan, et al., 2016).

Mineral Nutrients

There is marked variation in fertility across the Fortuna Forest Reserve, particularly for the rock-derived nutrients P and C (Table 3.6). Phosphorus is particularly low in soils developed on rhyolite at Chorro and Samudio (total P = 0.09–0.16 kg P m^{-3}), although values are noticeably greater on rhyolite at Honda (0.26–0.32), perhaps reflecting the proximity to the high P-mafic subsoil there and consequently the uplift of P to the soil surface by trees. Highest total P values are in soils developed on basalt and mafic-volcanics (0.43–0.53 kg P m^{-3}). Corresponding C:P and N:P ratios vary widely but are notably greatest in

TABLE 3.6. Profile-weighted nutrient stocks, total element ratios, and pH in soils across the Fortuna Forest Reserve, western Panama. Values are calculated on an area basis for the organic horizon plus upper 100 cm of the mineral soil using nutrient concentrations and bulk density in genetic horizons. Soil pH values calculated from the depth-weighted pH for each genetic horizon.

	Total elements			Total element ratios			Exchangeable cations				pH
Plot	C	N	P	C:N	C:P	N:P	Al	Ca	K	Mg	$CaCl_2$
	kg m^{-3}						$kmol_c$ m^{-3}				
Alto Frio	16.3	1.63	0.43	10.0	38	3.7	0.5	72.26	0.73	11.87	5.32
Bonita	23.7	2.01	0.50	11.8	47	4.0	26.7	1.07	0.32	0.79	4.28
Chorro A	14.2	0.76	0.09	18.7	156	8.3	49.8	2.14	0.38	1.00	4.54
Chorro B	51.8	2.74	0.12	18.9	433	22.9	29.4	2.08	0.58	1.97	4.63
Honda A	19.3	1.15	0.32	16.8	61	3.6	63.4	3.76	0.20	2.37	4.34
Honda B	15.0	0.99	0.26	15.1	58	3.9	68.9	0.75	0.84	1.46	4.05
Hornito A	15.3	1.37	0.43	11.2	35	3.2	61.4	22.45	0.49	9.38	4.61
Hornito B	15.8	0.90	0.23	17.6	69	3.9	67.4	1.19	0.53	0.67	4.09
Palo Seco	8.5	0.69	0.46	12.3	19	1.5	47.5	1.26	0.11	0.83	4.10
Pinola	20.1	1.63	0.53	12.4	38	3.0	5.7	49.95	1.34	10.97	4.77
Samudio	15.6	1.14	0.16	13.7	101	7.3	47.7	1.75	0.26	0.40	4.15
Verrugosa A	9.3	0.67	0.50	14.0	19	1.3	27.7	0.34	0.08	0.58	4.15
Verrugosa B	16.0	1.61	0.47	9.9	34	3.5	86.1	7.74	0.73	5.07	4.16
Zarceadero	12.6	0.71	0.22	17.8	58	3.3	17.9	1.09	1.10	2.60	4.29
Zorro	23.2	1.47	0.38	15.8	61	3.8	9.3	1.26	0.34	0.41	4.39

soils developed in rhyolite at Chorro and Samudio and lowest on Inceptisols developed in mafic-volcanics on the wet Caribbean slope. Quantification of organic P concentrations in the profiles will facilitate assessment of whether ectomycorrhizal tree species also deplete P from soil organic matter in these forests. The variation in soil P is known to influence the distribution of tree species in the reserve (Prada et al., 2017) and elsewhere in the lowland forests of Panama (Condit et al. 2013).

In moderately weathered soils, the distribution of base cations is assumed to reflect the nature of the soil parent material. Felsic rocks such as rhyolite contain a high relative abundance of potassium-containing feldspars such as orthoclase ($K(AlSi_3O_8)$), leading to relatively high K availability in associated soils. In contrast, feldspars in mafic rocks such as basalt are dominated by plagioclase feldspars ($NaAlSi_3O_8$–$CaAl_2Si_2O_8$) and contain abundant mafic (Fe- and Mn-rich) minerals, yielding soils with relatively high concentrations of Ca and Mg, but low concentrations of K. At Fortuna, exchangeable cations varied markedly among soils (Table 3.6). For example, there is an approximate 200-fold variation in profile-weighted concentrations of exchangeable Ca, which ranged between 0.34 $kmol_c$ m^{-3} in an Inceptisol on mafic-volcanics on the wet Caribbean slope at Verrugosa A and 72.3 $kmol_c$ m^{-3} on mafic-volcanics on the dry Pacific slope at Alto Frio. The concentration of exchangeable Mg was also greatest at Alto Frio but also high on basalt at Pinola and dacite at Hornito A. The high Mg at the latter plot further suggests that the parent material there differs from that at nearby Hornito B, despite the presence of dacite cobbles in the profile pit. Potassium varied less than Ca, ranging from 0.08 $kmol_c$ m^{-3} at Verrugosa A to 1.34 $kmol_c$ m^{-3} at Pinola, despite one of the lowest total K concentrations there.

Extractable Al, which can be toxic to plants, tends to depend on soil pH, with concentrations increasing markedly below pH 5 (measured in 0.01 M $CaCl_2$) (Table 3.6). At Fortuna, extractable Al was low in high pH soils at Alto Frio and Pinola and high in more acidic soils on a variety of other parent materials, including rhyolite at Honda, dacite at Hornito, and mafic-volcanics at Verrugosa B. Exchangeable Al was also moderately high in rhyolite soils at Chorro, where the watershed is characterized by abundant *Vochysia guatemalensis* that hyperaccumulates Al (Jansen et al., 2002). *Vochysia* does not occur in the Chorro plots, but it is common in the plots at Honda A, Samudio, and Verrugosa A (Prada et al., 2017).

Most soils have low base saturation measured in either buffered 1 M NH_4AOc (pH 7) or at soil pH in 0.1 M $BaCl_2$. However, base saturation at soil pH was high in the profiles at Alto Frio and Pinola. A number of profiles also had low ECEC at soil pH, sufficient for kandic or oxic horizons (<12 $cmol_c$ kg^{-1} clay), but markedly higher CEC in buffered solutions. This indicates the importance of pH-dependent charge in the Fortuna soils and therefore the importance of determining CEC at the soil pH to understand the soil exchange complex from the perspective of plant and microbial communities (Committee on Tropical Soils, 1972).

Soil pH and Extractable Acidity

Soil pH is very strongly to strongly acid, between 4.1 and 4.8, in all profiles except the Inceptisol on the relatively dry Pacific slope (Alto Frio, pH 5.3) (Table 3.6). There is considerable exchangeable acidity in most profiles, even when extractable Al at the soil pH is relatively low.

FUTURE WORK

Studies so far at Fortuna reveal a remarkable range of soils and associated fertility that exert a fundamental control on the distribution of plant species across the reserve. This opens up a number of possibilities for further research. The preliminary geological map of the reserve (Silva et al., this volume) provides the basis for a broader soil survey and the opportunity to link findings in the relatively small number of census sites to broader-scale patterns at the landscape level. Currently, census plots span a relatively narrow range in elevation and therefore in temperature, but the higher areas of the reserve offer an important opportunity to identify elevation gradients on similar lithology to examine the influence of temperature on aboveground and belowground communities and processes. Indeed, the apparent homogeneity of parent material and rainfall on the northern Caribbean slope suggests the possibility of elevation gradient from sea level to almost 2,000 m. Given the increase in temperature and associated shifts in tree communities predicted for the coming decades, such elevational gradients present an important opportunity to understand the consequences of climate change on tropical trees. At a smaller spatial scale, the Fortuna Forest Reserve provides an opportunity to examine local scale variation in soils within lithological units. Finally, the marked variation in soils across the reserve will facilitate studies of the influence of soils on belowground microbial communities, as successfully undertaken already for ectomycorrhizas (Corrales, Arnold, et al., 2016; Corrales et al., 2017; Corrales and Ovrebo, this volume).

SOIL PROFILE DESCRIPTIONS AND ANALYTICAL DATA

A. Alto Frio Forest Census Plot, Fortuna Forest Reserve, Panama (Figure 3.4)

Soil taxonomy:	Clayey-skeletal, kaolinitic, isothermic, Typic Humudept
Profile location:	From the STRI station, drive south on the main road through the guard gate and turn off to the right at a blue bus stop. Park 100 m down the hill by a small concrete building and enter the forest on the left. Follow the trail downhill for 10 minutes to the southern boundary of the plot (20,00 marker). The pit was adjacent to the 80,00 marker.
Latitude/longitude:	8.654334°N, –82.215059°E
UTM:	17P 0366314 m E., 0956850 m N.
Date and season:	26 July 2010; wet season
Elevation:	1,103 m asl
Slope and site position:	Steep (~30%) linear backslope, linear lateral, dropping steeply below to a small river
Parent material:	Undifferentiated mafic-volcanics, including andesite, basalt, and diabase
Soil moisture regime:	Perudic: mean annual precipitation 4,641 ± 623 mm, with 94 ± 27 mm mean monthly dry season rainfall (1 January–30 April)
Soil temperature regime:	Isothermic: mean annual temperature 20.5°C
Vegetation:	Lower montane tropical forest; canopy height 20 m; common large trees, including oaks; many small stature trees in the Celastraceae (*Zinowiewia costaricensis*) and Rosaceae (*Prunus fortunensis*); open understory with few palms or ferns
Drainage:	Moderately well drained; water draining into the pit below 150 cm
Surface features:	Thin but complete cover of wet leaves
Faunal activity:	Common earthworms in upper horizons
Coarse fragments:	Hard angular gravel and cobbles throughout the profile
Rooting depth:	Roots throughout the profile to 195 cm
Control section:	Between 25 and 100 cm below the soil surface
Mineralogy class:	Kaolinitic (59% kaolinite by thermal X-ray)
Particle-size class:	Clayey-skeletal (coarse fragments >35% of total volume and clay >35% of the fine earth fraction)
Cation exchange activity class:	Not applicable for kaolinitic mineralogy class
Diagnostic horizons and features:	(1) Perudic moisture regime and isothermic temperature regime (2) Umbric epipedon from 0 to 38 cm (3) Cambic horizon from 38 to 114 cm

---

General Features of the Soil

Despite the classification as an Inceptisol, the kaolinitic mineralogy and a low ratio of amorphous to crystalline Fe throughout the profile indicate that the fine earth is strongly weathered. However, the soil is relatively fertile, with high pH and high concentrations of total P and base cations. The abundant jumbled coarse fragments throughout the subsoil suggest the profile has developed on a landslide deposit. We assume that the moisture regime is perudic (i.e., precipitation always greater than potential evaporation), despite slightly less than 100 mm rainfall per month during the dry season.

Soil Taxonomy

The epipedon is umbric because it has a value and chroma ≤3 moist, and the base saturation by ammonium acetate at pH 7 is <50% in part of the upper 18 cm. There is evidence of clay movement (i.e., clay films), but the clay increase in the B horizon is insufficient to classify it as argillic (requires at least 8% greater than the epipedon when the epipedon contains >40% clay). The soil is therefore an Inceptisol because it has a cambic horizon. It is a Udept because of the perudic moisture regime, and a Humudept because of the umbric epipedon. In the absence of other diagnostic criteria at the subgroup level, the profile qualifies as a Typic Humudept.

Chemical and Physical Properties

The soil is clay-rich and gravelly, with fine subangular blocky structure. The soil is moderately acid (pH 5.8–6.0). The surface mineral soil is relatively rich in organic matter, with a low C:N ratio throughout (<10). Total P is high in the surface soil, with C:P ratios <100. Exchangeable base cations are high, particularly Ca. However, exchangeable K is very low throughout the subsoil, despite relatively high total K. The Ca:Mg ratio is » 1 throughout, and Al saturation is very low. Effective cation exchange capacity

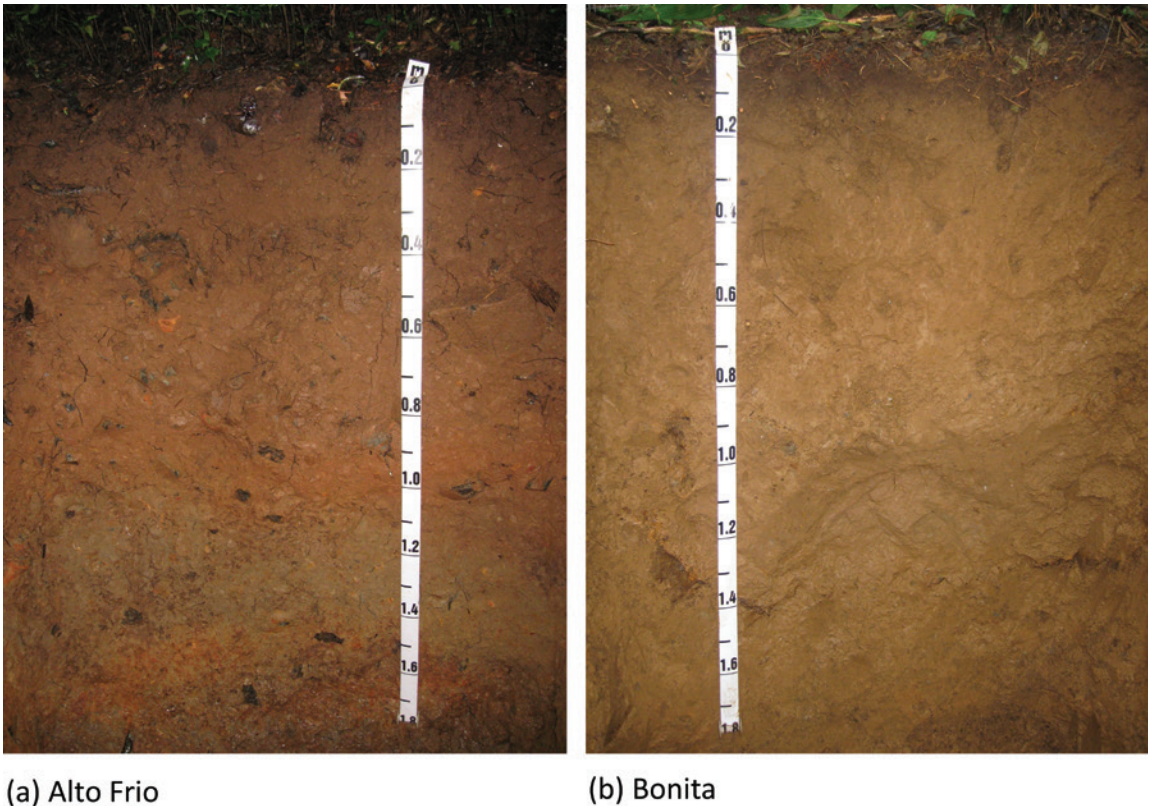

FIGURE 3.4. The profiles at (a) Alto Frio and (b) Bonita. Both images were taken using camera flash due to the particularly dark conditions during sampling.

is relatively high in the subsoil (>18 $\mathrm{cmol_c\ kg^{-1}}$), despite kaolinitic mineralogy, suggesting a considerable contribution of organic matter to the exchange complex. Pedogenic iron oxides are moderately high, with a small proportion (<10%) of amorphous forms. Manganese concentrations are particularly high in this profile, including exchangeable, amorphous, and total Mn, with common black Mn concentrations in the waterlogged subsoil. Effective base saturation (by $BaCl_2$ extraction) is ~100% throughout the profile but is much lower by buffered ammonium acetate (pH 7), indicating considerable pH-dependent charge linked to exchangeable acidity (but not extractable Al).

Horizon Description: Alto Frio

A—0 to 11 cm; very dark brown (7.5YR 2.5/2) sandy clay loam; moderate fine and very fine subangular blocky structure; moist and friable; plastic and slightly sticky; about 5% hard angular coarse gravel; many roots of all sizes; common small earthworms; clear smooth boundary.

AB—11 to 38 cm; dark brown (7.5YR 3/3) sandy clay; moderate fine and very fine subangular blocky structure; moist and friable; sticky and very plastic; about 10% hard angular coarse gravel; many coarse and medium, and common fine and very fine, roots; common medium tubular and common fine interstitial pores; common earthworms; clear smooth boundary.

B1—38 to 82 cm; brown (5YR 4/3) cobbly clay; moderate fine and very fine subangular blocky structure; moist and firm; sticky and very plastic; about 30% hard angular cobbles and about 10% medium angular gravel; faint clay films on ped faces; common coarse and few medium, fine, and very fine roots; clear wavy boundary.

B2—82 to 114 cm; dark reddish-brown (2.5–5 YR 3/4) very gravelly clay; moderate medium, fine, and very fine subangular blocky structure; moist and firm; sticky and very plastic; about 50% hard angular coarse gravel; faint clay films on ped faces; very few fine and medium roots; clear smooth boundary.

BC—114 to 141 cm; brown (10YR 4/3) gravelly clay; moderate medium and fine subangular blocky structure; sticky and very plastic; about 20% hard, angular, medium and coarse gravel; faint gray redox depletions around roots; common round, black, Mn concentrations; few medium and fine roots; clear smooth boundary.

Cg—141 to 195+ cm; brown (10YR 5/3), yellowish-red (5YR 4/6), and red (2.5YR 4/6) gravelly clay; moderate fine and very fine subangular blocky structure; sticky and plastic; common coarse gray redox depletions; common soft, black, medium Mn concentrations; many hard angular coarse gravel and cobbles (~25%); few fine and medium roots; water table at 170 cm draining into the pit.

Laboratory Analysis: Alto Frio

TABLE A.1. Soil physical properties, including bulk density and particle-size distribution, by genetic horizon in the Alto Frio soil. nd = not determined.

Horizon	Designation	Bulk density (fine earth)	Coarse fragments	Sand	Silt	Clay	Textural class	Clay:silt
—cm—		—g cm^{-3}—	—vol%—	—%—	—%—	—%—		
0–11 cm	A	0.66	5	30.0	25.9	44.1	Clay	1.7
11–38 cm	AB	1.06	10	22.6	29.3	48.0	Clay	1.6
38–82 cm	B1	1.22	40	23.3	31.7	44.9	Clay	1.4
82–114 cm	B2	1.19	50	16.0	33.6	50.4	Clay	1.5
114–141 cm	BC	1.40	20	15.7	34.9	49.4	Clay	1.4
141–195+ cm	Cg	nd	25	14.5	36.2	49.3	Clay	1.4

TABLE A.2. Soil pH and total carbon and nitrogen by genetic horizon in the Alto Frio soil.

Horizon	Soil pH			Total C	Total N	C:N	C:P	N:P
	Water	$CaCl_2$	$BaCl_2$	—%—	—%—			
0–11 cm	6.00	5.54	5.05	8.57	0.75	11.5	95.0	8.3
11–38 cm	5.90	5.22	4.74	2.88	0.31	9.2	38.0	4.1
38–82 cm	5.91	5.29	4.84	0.79	0.08	9.4	18.9	1.9
82–114 cm	5.82	5.43	5.09	0.43	0.05	8.7	11.1	1.3
114–141 cm	5.93	5.48	5.04	0.38	0.04	8.6	15.1	1.6
141–195+ cm	6.37	6.01	5.47	0.28	0.03	8.2	7.6	0.8

TABLE A.3. Exchangeable cations and effective cation exchange capacity (ECEC) by extraction in 0.1 M barium chloride ($BaCl_2$) by genetic horizon in the Alto Frio soil. BS = base saturation; sat = saturation; TEB = total exchangeable bases.

Horizon	Al	Ca	Fe	K	Mg	Mn	Na	TEB[a]	ECEC[b]	BS[c]	ECEC per kg clay	Al sat	Ca:Mg
	cmol$_c$ kg^{-1}									—%—	cmol$_c$ kg^{-1}	—%—	
0–11 cm	0.09	24.77	0.01	0.47	2.81	0.35	0.13	28.2	28.6	98.4	64.9	0.3	8.8
11–38 cm	0.11	9.78	<0.01	0.11	1.46	0.23	0.13	11.5	11.8	97.1	24.6	0.9	6.7
38–82 cm	0.04	7.10	<0.01	0.03	1.43	0.15	0.10	8.7	8.8	97.8	19.7	0.4	5.0
82–114 cm	0.02	6.65	<0.01	0.03	1.45	0.22	0.13	8.3	8.5	97.1	16.9	0.2	4.6
114–141 cm	0.01	7.22	<0.01	0.02	1.97	0.18	0.21	9.4	9.6	98.0	19.4	0.1	3.7
141–195+ cm	<0.01	9.32	<0.01	0.03	1.53	0.09	0.21	11.1	11.2	99.2	22.7	<0.1	6.1

[a] TEB determined by extraction in 0.1 M $BaCl_2$.

[b] ECEC determined as the sum of cations extracted in 0.1 M $BaCl_2$.

[c] BS determined as (TEB ÷ ECEC) × 100.

TABLE A.4. Extractable acidity, exchangeable cations, and cation exchange capacity (CEC) determined in buffered solutions by genetic horizon in the Alto Frio soil. BS = base saturation; TEB = total exchangeable bases; dash (—) = not determined.

Horizon	Extractable acidity	CEC by sum of cations[a]	BS by sum of cations[b]	Ca	K	Mg	Na	TEB by CEC7[c]	CEC7[d]	CEC/clay	BS by CEC7[e]
	$\mathrm{cmol_c\ kg^{-1}}$	$\mathrm{cmol_c\ kg^{-1}}$	—%—	$\mathrm{cmol_c\ kg^{-1}}$						$\mathrm{cmol_c\ kg^{-1}}$ clay	—%—
0–11 cm	—	—	—	17.4	0.4	2.6	<0.1	20.5	37.9	86.0	54
11–38 cm	—	—	—	7.9	0.1	1.4	<0.1	9.4	25.6	53.3	37
38–82 cm	—	—	—	6.6	<0.1	1.5	<0.1	8.2	20.8	46.4	39
82–114 cm	—	—	—	6.1	<0.1	1.5	0.1	7.7	19.2	38.1	40
114–141 cm	—	—	—	7.5	<0.1	2.2	0.1	9.8	22.0	44.6	45
141–195+ cm	—	—	—	9.0	<0.1	1.6	0.2	10.7	19.7	40.0	55

[a] Sum of extractable acidity and TEB.

[b] BS determined from TEB ÷ CEC sum of cations × 100.

[c] TEB (sum of Ca, K, Mg, and Na) determined by extraction in ammonium acetate (pH 7).

[d] CEC determined by extraction in ammonium acetate (pH 7).

[e] BS determined as (TEB ÷ ECEC) × 100. (TEB ÷ ECEC) × 100.

TABLE A.5. Pedogenic metal oxides extractable in acid-ammonium oxalate and buffered dithionite by genetic horizon in the Alto Frio soil. $\mathrm{Fe_{ox}:Fe_d}$ ratio, oxalate-extractable iron/dithionite-extractable iron.

	Dithionite extraction			Oxalate extraction						
Horizon	Al	Fe	Mn	Al	Fe	Mn	P	Si	Al+½Fe	$\mathrm{Fe_{ox}:Fe_d}$
	%			$\mathrm{mg\ g^{-1}}$					—%—	
0–11 cm	0.56	4.22	0.26	4.48	2.86	1.99	0.28	0.30	0.59	0.07
11–38 cm	0.70	5.15	0.30	5.23	3.00	2.22	0.20	0.32	0.67	0.06
38–82 cm	0.55	5.57	0.16	2.69	1.83	1.11	0.04	0.31	0.36	0.03
82–114 cm	0.64	6.64	0.12	1.93	1.88	0.74	0.01	0.34	0.29	0.03
114–141 cm	0.57	6.08	0.08	1.77	1.67	0.53	0.01	0.39	0.26	0.03
141–195+ cm	0.65	7.15	0.16	1.21	1.93	1.00	0.01	0.40	0.22	0.03

TABLE A.6. Total elements by nitric acid digestion by genetic horizon in the Alto Frio soil.

Horizon	Al	B	Ca	Cu	Fe	K	Mg	Mn	Na	P	Zn
	$\mathrm{mg\ g^{-1}}$										
0–11 cm	85.2	<0.005	7.58	0.097	74.4	2.31	5.03	2.60	0.91	0.902	0.102
11–38 cm	104.9	<0.005	4.01	0.125	88.9	2.59	5.40	2.88	0.97	0.759	0.108
38–82 cm	116.5	<0.005	3.20	0.128	96.9	3.22	6.53	1.67	1.12	0.418	0.081
82–114 cm	128.5	<0.005	2.23	0.145	98.2	4.03	3.52	1.16	0.77	0.388	0.067
114–141 cm	122.7	<0.005	3.18	0.131	95.1	3.26	4.68	0.95	1.39	0.251	0.077
141–195+ cm	124.4	<0.005	3.14	0.170	93.7	2.58	2.21	1.43	1.08	0.368	0.066

B. Bonita Forest Census Plot, Fortuna Forest Reserve, Panama (Figure 3.4)

Soil taxonomy:	Medial, ferrihydritic, isothermic, Acrudoxic Ultic Hapludand
Profile location:	From the north side of the Quebrada Bonita bridge, follow the trail uphill for ~25 minutes to the plot; the pit was located close to the 00,00 marker.
Latitude/longitude:	8.767653°N, –82.21567°E
UTM:	17P, 0366287 m E., 0969381 m N.
Date and season:	28 July 2010; wet season
Elevation:	1,296 m asl
Slope and site position:	Steep (~30%) upper backslope; convex radial and linear lateral
Parent material:	Undifferentiated mafic-volcanics, including andesite, basalt, and diabase; possibly under a more recent ash deposit
Soil moisture regime:	Perudic: mean annual rainfall at nearby Chorro A 5,507 ± 247 mm, with 351 ± 53 mm mean monthly dry season rainfall (1 January–30 April)
Soil temperature regime:	Isothermic: mean annual temperature 17.7°C at nearby Chorro A
Vegetation:	Lower montane tropical forest; canopy height 20 m; relatively open canopy with many understory ferns, including tree ferns (*Alsophila erinacea, Cyathea darienensis*)
Drainage:	Moderately well drained; lower 30 cm of pit flooded
Surface features:	Shallow incomplete (80%) cover of wet leaves
Faunal activity:	None observed
Coarse fragments:	Many gravel and cobbles between 78 and 100 m
Rooting depth:	Roots throughout the profile to 176 cm but mainly in the upper 10 cm
Control section:	The upper 100 cm of the soil profile
Mineralogy class:	Ferrihydritic
Particle-size class:	Medial (substitute class)
Cation exchange activity class:	Not applicable
Diagnostic horizons/features:	(1) Perudic moisture regime and isothermic temperature regime (2) Umbric epipedon from 0 to 18 cm (3) Andic properties from 18 to 60 cm (4) Argillic horizon from 18 to 78 cm

General Features of the Soil

Although a number of profiles have andic properties at Fortuna, this is one of the few profiles where they are sufficiently expressed to qualify as an Andisol. The upper 60 cm of the profile has low bulk density, high concentrations of amorphous (noncrystalline) metal oxides, and a ferrihydritic mineralogy class. There is an increase in clay concentration with depth and thin clay films on ped faces, indicating illuvial clay accumulation in the subsoil.

Geology in the area of the Bonita plot is classed as undifferentiated volcanics, although an outcrop in the Quebrada Bonita stream is described as amygdular basalt, with a black aphanitic matrix, dark gray pyroxene, white concentric silica amygdules with euhedral quartz crystals, and greenish white fresh amygdules filled with malachite (Silva et al., this volume). However, the clear andic properties in the upper part of the profile suggest that this site might have also been influenced by the rhyolitic ash deposit that covers Chorro and Honda to the west.

Soil Taxonomy

The soil is an Andisol because it has andic properties (organic C <25%, bulk density <0.9 g cm^{-3}, and oxalate-extractable Al+ ½Fe >2%) in more than 50% of the upper 60 cm of the profile (although we did not determine phosphate retention). The soil is a Udand because of the perudic moisture regime, and in the absence of other diagnostic features at the Great Group level (note, some not assessed), the soil qualifies as a Hapludand. The profile qualifies as an Acrudoxic Ultic Hapludand because (1) the sum of bases plus extractable Al is <2.0 $\text{cmol}_c\ \text{kg}^{-1}$ in horizons with a thickness of 30 cm or more between 25 and 100 cm below the soil surface (i.e., the Bt1 and Bt2) and (2) the profile has an argillic horizon with base saturation by sum of cations of <35% throughout its upper 50 cm.

We did not determine water retention at 1,500 kPa, but if it is >70% in 35 cm or more of the upper 100 cm, then the profile could qualify as an Acrudoxic Hydric Hapludand. Water retention also influences whether the mineralogy substitute class is hydrous (>100%) or medial (35%–100%). Moisture content of the upper

60 cm of the profile at the time of sampling (mid–wet season) was ~50% of fresh weight (i.e., ~100% calculated as moisture/dry soil mass). As 1,500 kPa water retention will be much less than field capacity, we classify the mineralogy substitute class as medial.

The profile has a ferrihydritic mineralogy class because $8\times Si_{ox} + 2\times Fe_{ox}$ is ≥5, and $8\times Si_{ox}$ is $<2\times Fe_{ox}$. Organic C in the A horizon is high but insufficient to qualify as organic soil (<20% organic C).

Chemical and Physical Properties

The soil has a loamy epipedon and a clay-rich subsoil. Bulk density is <0.9 cm^{-3} throughout the upper 60 cm of the profile. The soil is very strongly acid throughout, except for the extremely acid and organic-rich surface horizon. Total carbon is high throughout the upper 78 cm of the profile, although C:N ratios are 11 to 12. All base cations are extremely low (<0.3 $cmol_c$ kg^{-1}) below 10 cm, and Al saturation is >80% throughout. Total Al and Fe are high in the deep subsoil, while total Ca is very low (total K and Mg are relatively high). Total P is relatively high throughout. Amorphous Al and Fe are very high in the upper 78 cm of the profile ($Fe_d > Fe_{ox}$).

Horizon Description: Bonita

A—0 to 10 cm; very dark brown (10YR 2/2) silt loam; fine and very fine subangular blocky structure; moist and loose; slightly sticky and not plastic; many very fine, fine, medium, and coarse roots forming a thin surface mat; clear smooth boundary.

AB—10 to 18 cm; dark brown (10YR 3/3) sandy clay loam; medium subangular blocky structure; moist and very friable; sticky and not plastic; many medium, and common coarse, fine, and very fine roots; clear smooth boundary.

Bt1—18 to 36 cm; brown (10YR 4/3) sandy clay loam; coarse subangular blocky structure, breaking to fine and very fine subangular blocky; moist and friable; sticky and slightly plastic; common medium and coarse and few fine and very fine roots; gradual smooth boundary.

Bt2—36 to 60 cm; brown (7.5YR 4/3) silty clay; coarse subangular blocky structure, breaking to medium and fine subangular blocky; moist and friable; sticky and slightly plastic; thin clay films on ped faces; very few fine and very fine roots; gradual smooth boundary.

Bt3—60 to 78 cm; brown (7.5YR 4/3) sandy clay; very coarse subangular blocky structure/medium wedge; moist and firm to friable; sticky and slightly plastic; thin clay films on ped faces; very few fine roots; gradual smooth boundary.

BC1—78 to 100 cm; brown (7.5YR 4/4) gritty clay loam; massive, breaking to very coarse angular blocky; moist and firm; slightly sticky and not plastic; about 40% weathered volcanic cobbles; very few fine roots; gradual smooth boundary.

BC2—100 to 176 cm; brown (7.5YR 4/4) gritty clay loam; massive, breaking to very coarse angular blocky; moist and firm; slightly sticky and not plastic; few continuous clay films on surfaces of major peds; very few fine roots; smooth clear boundary.

C—176 to 190+ cm; brown (7.5YR 4/3) gritty loam; massive; moist and firm; slightly sticky and not plastic; no roots.

Laboratory Analysis: Bonita

TABLE B.1. Soil physical properties, including bulk density and particle-size distribution, by genetic horizon in the Bonita soil. Dash (—) = not determined.

Horizon	Designation	Bulk density (fine earth)	Coarse fragments	Sand	Silt	Clay	Textural class	Clay:silt
—cm—		—g cm^{-3}—	—vol%—	—%—	—%—	—%—		
0–10	A	0.34	0	43.0	35.7	21.3	Loam	0.60
10–18	AB	0.63	0	48.3	19.8	31.9	Sandy clay loam	1.61
18–36	Bt1	0.68	0	38.7	22.9	38.4	Clay loam	1.68
36–60	Bt2	0.76	0	22.6	29.5	47.9	Clay	1.62
60–78	Bt3	1.06	0	20.6	36.9	42.5	Clay	1.15
78–100	BC1	1.40	40	20.4	39.7	39.9	Clay loam	1.01
100–176	BC2	—	0	16.8	50.1	33.0	Silty clay loam	0.66
176–190+	C	—	0	16.7	52.5	30.8	Silty clay loam	0.59

TABLE B.2. Soil pH and total carbon and nitrogen by genetic horizon in the Bonita soil.

Horizon	Soil pH			Total C	Total N	C:N	C:P	N:P
	Water	$CaCl_2$	$BaCl_2$	—%—	—%—			
0–10	4.10	3.61	3.61	18.43	1.70	10.8	131.9	12.2
10–18	4.64	4.30	4.27	5.02	0.43	11.8	71.7	6.1
18–36	4.60	4.53	4.46	4.07	0.34	11.8	62.5	5.2
36–60	4.82	4.48	4.43	3.14	0.25	12.5	44.7	3.6
60–78	4.82	4.31	4.30	1.76	0.14	12.6	29.1	2.3
78–100	4.95	4.11	4.15	0.47	0.04	12.6	9.1	0.8
100–176	4.97	4.06	4.17	0.17	0.02	9.7	3.0	0.4
176–190+	4.88	4.06	4.16	0.12	0.01	9.4	2.2	0.2

TABLE B.3. Exchangeable cations and effective cation exchange capacity (ECEC) by extraction in 0.1 M barium chloride ($BaCl_2$) by genetic horizon in the Bonita soil. BS = base saturation; sat = saturation; TEB = total exchangeable bases.

Horizon	Al	Ca	Fe	K	Mg	Mn	Na	TEB[a]	ECEC[b]	BS[c]	ECEC per kg clay	Al sat	Ca:Mg
	cmol$_c$ kg^{-1}									—%—	cmol$_c$ kg^{-1}	—%—	
0–10	8.78	1.93	0.24	0.52	1.14	0.07	0.10	3.7	12.8	28.9	60.0	68.7	1.7
10–18	2.69	0.12	0.03	0.07	0.14	<0.01	0.01	0.3	3.1	11.1	9.6	87.9	0.9
18–36	1.05	0.09	0.02	0.03	0.07	<0.01	<0.01	0.2	1.3	15.5	3.3	83.3	1.3
36–60	1.25	0.05	0.02	0.03	0.04	<0.01	<0.01	0.1	1.4	8.6	2.9	89.9	1.3
60–78	3.09	0.04	0.01	0.01	0.05	<0.01	0.01	0.1	3.2	3.4	7.6	96.3	0.8
78–100	6.98	0.04	0.01	<0.01	0.04	<0.01	0.02	0.1	7.1	1.4	17.8	98.4	1.0
100–176	8.00	0.05	0.01	0.03	0.07	<0.01	<0.01	0.2	8.2	1.8	24.7	98.0	0.7
176–190+	7.76	0.07	0.02	0.05	0.07	0.01	<0.01	0.2	8.0	2.4	25.9	97.2	1.0

[a] TEB determined by extraction in 0.1 M $BaCl_2$.

[b] ECEC determined as the sum of cations extracted in extraction in 0.1 M $BaCl_2$.

[c] Base saturation determined as (TEB ÷ ECEC) × 100.

TABLE B.4. Extractable acidity, exchangeable cations, and cation exchange capacity (CEC) determined in buffered solutions by genetic horizon in the Bonita soil. BS = base saturation; TEB = total exchangeable bases; dash (—) = not determined.

Horizon	Extractable acidity	CEC by sum of cations[a]	BS by sum of cations[b]	Ca	K	Mg	Na	TEB by CEC7[c]	CEC7[d]	CEC/clay	BS by CEC7[e]
	cmol$_c$ kg^{-1}	cmol$_c$ kg^{-1}	—%—	cmol$_c$ kg^{-1}						cmol$_c$ kg^{-1} clay	—%—
0–10	—	—	—	—	—	—	—	—	—	—	—
10–18	—	—	—	—	—	—	—	—	—	—	—
18–36	39.9	40.1	0.5	—	—	—	—	—	—	—	—
36–60	37.3	37.5	0.3	—	—	—	—	—	—	—	—
60–78	31.5	31.6	0.3	—	—	—	—	—	—	—	—

TABLE B.4. (*Continued*)

Horizon	Extractable acidity	CEC by sum of cations[a]	BS by sum of cations[b]	Ca	K	Mg	Na	TEB by CEC7[c]	CEC7[d]	CEC/clay	BS by CEC7[e]
	$\text{cmol}_c\ \text{kg}^{-1}$	$\text{cmol}_c\ \text{kg}^{-1}$	—%—	$\text{cmol}_c\ \text{kg}^{-1}$						$\text{cmol}_c\ \text{kg}^{-1}$ clay	—%—
78–100	23.6	23.7	0.4	—	—	—	—	—	—	—	—
100–176	24.7	24.8	0.6	—	—	—	—	—	—	—	—
176–190+	—	—	—	—	—	—	—	—	—	—	—

[a] Sum of extractable acidity and TEB.

[b] BS determined from TEB ÷ CEC sum of cations × 100.

[c] TEB (sum of Ca, K, Mg, and Na) determined by extraction in ammonium acetate (pH 7).

[d] CEC determined by extraction in ammonium acetate (pH 7).

[e] BS determined as (TEB ÷ ECEC) × 100.

TABLE B.5. Pedogenic metal oxides extractable in acid-ammonium oxalate and buffered dithionite by genetic horizon in the Bonita soil. Fe_{ox}:Fe_d ratio, oxalate-extractable iron/dithionite-extractable iron.

	Dithionite extraction			Oxalate extraction						
Horizon	Al	Fe	Mn	Al	Fe	Mn	P	Si	Al+½Fe	Fe_{ox}:Fe_d
	%			mg g^{-1}					—%—	
0–10	1.10	3.26	0.01	8.47	10.51	0.06	0.69	0.16	1.37	0.32
10–18	1.11	3.42	0.01	10.57	13.11	0.07	0.40	0.49	1.71	0.38
18–36	1.41	4.93	0.02	12.85	17.88	0.09	0.36	0.98	2.18	0.36
36–60	1.49	7.08	0.03	12.25	20.82	0.12	0.29	0.90	2.27	0.29
60–78	1.15	7.17	0.03	9.17	14.86	0.12	0.17	1.04	1.66	0.21
78–100	0.67	6.03	0.04	5.04	4.53	0.19	0.07	0.60	0.73	0.08
100–176	0.45	5.24	0.07	4.07	2.77	0.36	0.07	0.41	0.55	0.05
176–190+	0.40	5.25	0.11	3.86	2.35	0.63	0.09	0.35	0.50	0.04

TABLE B.6. Total elements by nitric acid digestion by genetic horizon in the Bonita soil.

Horizon	Al	B	Ca	Cu	Fe	K	Mg	Mn	Na	P	Zn
	mg g^{-1}										
0–10	42.0	0.007	2.26	0.039	45.4	1.64	3.00	0.28	0.71	1.397	0.053
10–18	50.9	<0.005	4.56	0.043	62.9	1.39	4.88	0.41	1.53	0.700	0.070
18–36	63.3	<0.005	3.87	0.050	69.4	1.67	4.97	0.42	1.32	0.651	0.073
36–60	93.0	<0.005	1.60	0.071	93.5	2.32	6.09	0.60	0.57	0.702	0.091
60–78	117.7	<0.005	0.38	0.097	105.2	2.51	8.58	0.85	0.17	0.605	0.126
78–100	125.3	<0.005	0.14	0.111	91.2	2.94	8.73	1.05	0.12	0.519	0.143
100–176	125.0	<0.005	0.13	0.114	92.3	1.53	9.91	1.59	0.14	0.563	0.170
176–190+	119.0	<0.005	0.13	0.106	90.1	0.83	10.79	2.12	0.14	0.545	0.159

C. Chorro A Forest Census Plot, Fortuna Forest Reserve, Panama (Figure 3.5)

Soil taxonomy:	Medial, amorphic, isothermic, Alic Epiaquand
Profile location:	From the Quebrada Chorro bridge, enter the forest on the northwest side of the river and climb the trail for ~20 minutes to the plot; the profile pit was located ~20 m west of the 100,50 marker.
Latitude/longitude:	8.750184°N, –82.228849°E
UTM:	17P, 0364831 m E., 0967454 m N.
Date and season:	2 July 2008 (wet season); reassessed 19 January 2014 (early dry season)
Elevation:	1,207 m asl
Slope and site position:	Nearly level, sloping gently (~5%) toward the southeast and then steeply to the Chorro River; the plot is on a relatively flat area below a 1,300 m ridgeline
Soil moisture regime:	Perudic; mean annual rainfall 5,507 ± 247 mm, with 351 ± 53 mm mean monthly dry season rainfall (1 January–30 April)
Soil temperature regime:	Isothermic: mean annual temperature 17.7°C, with mean monthly temperature varying by <2°C)
Parent material:	Rhyolite boulders and fine-grained rhyolitic tuff
Vegetation:	Lower montane tropical rainforest; canopy height 20 m; relatively closed canopy, with a few large *Podocarpus* and oak trees and frequent emergent *Colpothrinax* palms, and *Euterpe* and *Wettinia* canopy palms; understory dominated by juvenile palms
Drainage:	Poorly drained throughout the wet season; water table at ~200 cm during dry season
Surface features:	Thick cover of wet leaf litter
Faunal activity:	A few earthworms in the upper 20 cm
Coarse fragments:	Boulders up to 1 m diameter in the profile pit
Rooting depth:	Throughout the profile to >200 cm, with roots penetrating soft rhyolite
Control section:	The upper 100 cm of the mineral soil
Particle-size class:	Medial (andic properties and a presumed 1,500 KPa water retention capacity of <100%)
Mineralogy class:	Amorphic ($8\times\mathrm{Si}_{ox} + 2\times\mathrm{Fe}_{ox}$ is >5, and $8\times\mathrm{Si}_{ox}$ is $>2\times\mathrm{Fe}_{ox}$)
Cation exchange activity class:	Not applicable
Diagnostic horizons/features:	(1) Perudic moisture regime and isothermic temperature regime (2) Ochric epipedon from 5 to 15 cm (3) Andic soil properties from 15 to 40/60 cm (4) Episaturation between 31 and 45 cm

General Features of the Soil

The profile is an Andisol, with the upper mineral soil dominated by amorphous metal oxides. The profile has a dark, organic surface horizon over bright white subsoil developed in volcanic ash of rhyolitic composition. The soil appears to become saturated from both above and below, presumably due to the high rainfall and clay-enriched subsurface horizon and the relatively flat topography. In particular, redox concentrations around roots in the upper subsoil indicate oxygenation of a reduced horizon. The profile is very acidic and extremely infertile. The combination of acidity, infertility, and saturation indicates that this environment is particularly harsh for plant growth.

Soil Taxonomy

The profile is an Andisol because it has Andic properties in 60% of the upper 60 cm of the mineral soil. Bulk density is <0.9 g cm^{-3} in all horizons to 45 cm depth, although the upper 5 cm does not have andic properties. The A horizon (5–15 cm) qualifies as andic because it contains an Al+½Fe concentration of 0.9% and has 31% glass in the coarse silt fraction (although glass content is small in the fine sand fraction). The Bw horizon (15 to 31 cm) qualifies as andic because the Al+½Fe concentration is 2.3% and the coarse silt and fine sand fractions contain >10% glass. The Bg horizon (31–40/60 cm) has an Al+½Fe of 1.9% and, although we did not quantify glass in this horizon, it is presumably similar to the Bw, in which case the horizon qualifies as andic (i.e., assuming >10% glass; 1.9% Al+½Fe requires >6% glass to qualify as andic).

The profile qualifies as an Aquand because it has aquic conditions and redoximorphic features between 40 and 50 cm below the soil surface. The low Fe concentrations in this profile mean that the expression of redoximorphic features is muted. There is a 1 mm thick iron pan (placic horizon), but this is discontinuous and does not appear to impede root growth, so the profile does not qualify as a Placaquand. The profile appears to saturate from below in the wet season to ~75 cm, as well as

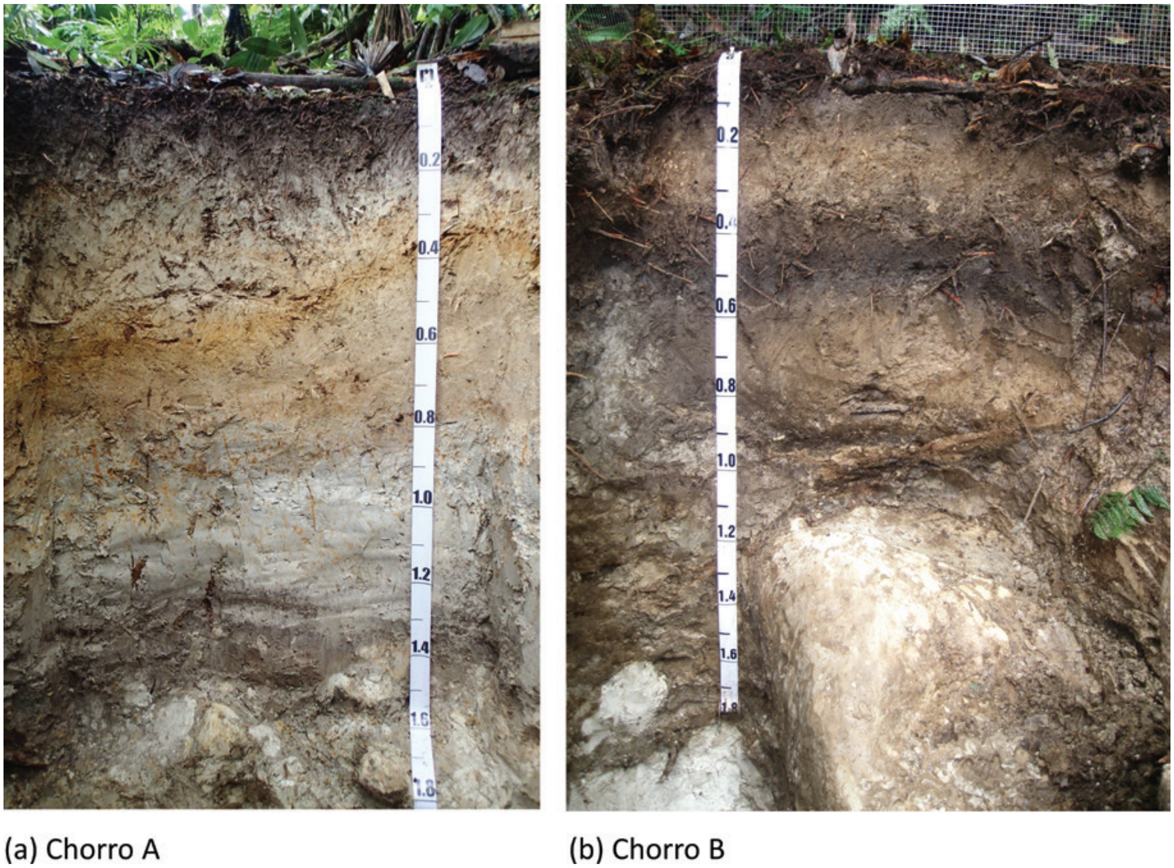
(a) Chorro A (b) Chorro B

FIGURE 3.5. The profiles at (a) Chorro A and (b) Chorro B.

above the clay-rich horizon at 40/60 cm, indicating the possibility of both episaturation and endosaturation. However, episaturation appears earlier in the key, so the profile qualifies as an Epiaquand. With extractable Al >2 $\mathrm{cmol_c\ kg^{-1}}$ between 25 and 50 cm below the mineral soil surface, the profile qualifies as an Alic Epiaquand.

A similar process appears to be operating at Chorro B, where the accumulation of organic matter and amorphous Al is sufficient to qualify the profile as a Spodosol. The Chorro B profile presumably represents a more advanced stage of pedogenesis than Chorro A, despite being formed in the same rhyolitic parent material, perhaps reflecting their different topographic positions.

There is an apparent sombric horizon between 133 and 155 cm, indicated by the darkening caused by organic matter (total C = 1.78%), with abundant fine roots. However, the organic matter appears to be associated with amorphous Al oxides (1.2% by ammonium oxalate extraction), which precludes this horizon from being classified as sombric.

There is a clay increase in the upper part of the mineral soil, but (1) there are only faint clay films, (2) clay concentrations are erratic with depth, and (3) texture analysis is problematic in soils with andic properties. Therefore, we do not consider the measured clay increase to represent an argillic horizon in this profile.

Chemical and Physical Properties

The soil has an organic surface horizon, with a loam surface mineral soil over a clay/silty clay loam B horizon, although the texture is variable in the subsoil and the amorphous mineralogy means that dispersion is unreliable. Bulk density is <1.0 $\mathrm{g\ cm^{-3}}$ throughout the profile. The organic soil is extremely acidic, with a very strongly acidic mineral soil. Carbon to nitrogen ratios are relatively high (17–20). Total P concentrations are relatively low, being <150 $\mathrm{mg\ P\ kg^{-1}}$ in the upper meter of mineral soil. Exchangeable base cation concentrations are extremely low, with ≤0.3 $\mathrm{cmol_c\ kg^{-1}}$ below 15 cm. Aluminum concentrations are high throughout the upper meter of the profile, with corresponding high Al saturation and low base saturation. Amorphous Al and Fe concentrations are relatively high, particularly in the argillic horizon, while dithionite Fe concentrations are ≤1% throughout the profile. Manganese concentrations are extremely low, with undetectable concentrations of exchangeable and extractable (oxalate, dithionite) Mn.

Horizon Description: Chorro A

Oa—0 to 5 cm; black (10YR 2/1) decomposed organic matter; soft, loose, and very moist; many coarse, medium, fine, and very fine roots; slightly sticky; abrupt smooth boundary.

A—5 to 15 cm; very dark grayish-brown (10YR 3/2) silty clay loam; moderate coarse subangular blocky structure, breaking to fine subangular blocky; wet and friable; common fine tubular pores; many medium, and common fine and very fine roots; clear smooth boundary.

Bw—15 to 31 cm; light brownish-gray (2.5Y 6/2) silty clay; moderate medium subangular blocky structure; grayish-brown hypocoats on ped faces; very few fine brownish-yellow (10YR 6/6) redox concentrations, particularly around fine roots; sticky and plastic; faint continuous clay films on ped faces; common medium worm channels infilled with very dark brown (10YR 2/2) organic matter; many coarse, common medium, and few fine and very fine roots; gradual smooth boundary.

Bg—31 to 40/60 cm; pale brown (10YR 6/3) silty clay; sticky and slightly plastic; moderate coarse subangular blocky structure; common medium channels infilled with organic matter; faint mottling throughout, with common brownish-yellow (10YR 6/6) redox concentrations around old root channels; many medium and few fine and very fine roots; wavy clear boundary.

Bs—40/60 to 75 cm; light yellowish-brown (2.5Y 6/4) sandy loam; massive, breaking to granular; wet and friable; brownish-yellow (10YR 6/6) iron enrichment; discontinuous thin (1 mm) hard iron pan in upper part of the horizon; slightly sticky and not plastic; few medium tubular pores infilled with organic matter; common coarse and medium roots clear smooth boundary.

BCg1—75 to 90 cm; light gray (2.5Y7/1) sandy loam; massive, breaking to granular; wet and friable; common fine and medium prominent yellowish-red (5YR 5/8) redox concentrations forming around old root channels; few fine roots; clear smooth boundary.

BCg2—90 to 121 cm; light gray (2.5Y7/1) silty clay; massive, breaking to fine subangular blocky; wet and firm; sticky and plastic; common fine prominent yellowish-red (5YR 5/8) redox concentrations; many fine root channels; very few fine and medium roots; gradual smooth boundary.

Cg1—121 to 133 cm; light brownish-gray (10YR 6/2) silty clay; massive, breaking to fine subangular blocky; grayish-brown (10YR 5/2) organic stains on outside of peds; wet and firm; sticky and plastic; no redox concentrations; very few fine roots; clear smooth boundary.

Cg2—133 to 155 cm; grayish-brown (10YR 5/2) sandy clay loam; massive; sticky and not plastic; wet and slightly firm; abrupt wavy boundary.

Cr—155 to 200+ cm; soft rhyolite and hard rhyolite cobbles, stones, and boulders; roots and root channels in soft rhyolite.

Laboratory Analysis: Chorro A

TABLE C.1. Soil physical properties, including bulk density and particle-size distribution, by genetic horizon in the Chorro A soil. Dash (—) = not determined.

Horizon	Designation	Bulk density (fine earth)	Coarse fragments	Sand	Silt	Clay	Textural class	Clay:silt ratio
—cm—		—g cm^{-3}—	—vol%—	—%—	—%—	—%—		
0–5	Oa	0.12	0	—	—	—	Organic	—
5–15	A	0.54	0	46.2	46.0	7.9	Loam	0.17
15–31	Bw	0.69	0	23.2	47.9	28.9	Clay loam	0.60
31–40/60	Bg	0.76	0	19.5	46.7	33.8	Silty clay loam	0.72
40/60–75	Bs	0.96	0	38.6	45.7	15.7	Loam	0.34
75–90	BCg1	0.90	0	59.1	37.0	3.9	Sandy loam	0.11
90–121	BCg2	0.84	0	32.7	43.7	23.7	Loam	0.54
121–133	Cg1	0.82	0	23.9	47.3	28.8	Clay loam	0.61
133–155	Cg2	0.86	0	43.6	48.0	8.4	Loam	0.18
155–200	Cr	—	100	—	—	—	—	—

TABLE C.2. Soil pH and total carbon and nitrogen by genetic horizon in the Chorro A soil.

Horizon	Soil pH			Total C	Total N	C:N	C:P	N:P
—cm—	Water	$CaCl_2$	$BaCl_2$	—%—	—%—			
0–5	4.26	3.78	3.46	24.24	1.39	17.4	800.3	45.9
5–15	4.64	3.98	4.13	5.89	0.30	19.6	467.6	23.8
15–31	4.96	4.40	4.43	3.47	0.17	19.8	236.0	11.9
31–40/60	4.91	4.30	4.41	1.95	0.11	17.4	158.8	9.1
40/60–75	4.85	4.12	4.25	0.41	0.02	19.6	52.7	2.7
75–90	4.84	4.07	4.23	0.29	0.01	20.5	35.0	1.7
90–121	4.76	4.04	4.17	0.42	0.03	12.3	32.5	2.6
121–133	4.87	4.20	4.30	0.98	0.07	14.5	56.2	3.9
133–155	5.01	4.24	4.60	1.21	0.06	20.7	72.2	3.5
155–200	5.16	4.54	4.63	0.44	0.02	23.4	146.6	6.0

TABLE C.3. Exchangeable cations and effective cation exchange capacity (ECEC) by extraction in 0.1 M barium chloride ($BaCl_2$) by genetic horizon in the Chorro A soil. BS = base saturation; sat = saturation; TEB = total exchangeable bases; dash (—) = not determined.

Horizon	Al	Ca	Fe	K	Mg	Mn	Na	TEB[a]	ECEC[b]	BS[c]	ECEC per kg clay	Al sat	Ca:Mg
—cm—	$cmol_c$ kg^{-1}									—%—	$cmol_c$ kg^{-1}	—%—	
0–5	3.02	12.37	0.08	0.64	3.26	0.28	0.29	16.6	19.9	83.0	—	15	3.8
5–15	4.11	0.79	0.06	0.06	0.26	<0.01	0.04	1.2	5.3	21.6	67.5	77	3.0
15–31	1.93	0.14	<0.01	0.06	0.06	<0.01	0.01	0.3	2.2	12.2	7.6	87	2.4
31–40/60	2.26	0.13	<0.01	0.06	0.08	<0.01	0.02	0.3	2.6	11.2	7.6	89	1.7
40/60–75	5.21	0.10	<0.01	0.02	0.09	<0.01	0.01	0.2	5.4	4.1	34.6	96	1.1
75–90	7.99	0.07	<0.01	0.03	0.07	<0.01	0.01	0.2	8.2	2.3	209.8	98	1.0
90–121	12.65	0.07	<0.01	0.05	0.08	<0.01	0.03	0.2	12.9	1.7	54.3	98	0.9
121–133	6.72	0.07	<0.01	0.06	0.05	<0.01	0.01	0.2	6.9	2.9	24.0	97	1.6
133–155	0.50	0.04	<0.01	0.05	0.01	<0.01	<0.01	<0.1	0.6	15.5	7.2	83	3.1
155–200	0.52	<0.01	<0.01	<0.01	<0.01	<0.01	<0.01	<0.1	0.5	1.0	—	99	<0.1

[a] TEB determined by extraction in 0.1 M $BaCl_2$.

[b] ECEC determined as the sum of cations extracted in extraction in 0.1 M $BaCl_2$.

[c] BS determined as (TEB ÷ ECEC) × 100.

TABLE C.4. Extractable acidity, exchangeable cations, and cation exchange capacity (CEC) determined in buffered solutions by genetic horizon in the Chorro A soil. BS = base saturation; TEB = total exchangeable bases, dash (—) = not determined.

Horizon	Extractable acidity	CEC by sum of cations[a]	BS by sum of cations[b]	Ca	K	Mg	Na	TEB by CEC7[c]	CEC7[d]	CEC/clay	BS by CEC7[e]
	$cmol_c$ kg^{-1}	$cmol_c$ kg^{-1}	—%—	$cmol_c$ kg^{-1}						$cmol_c$ kg^{-1} clay	—%—
0–5	—	—	—	—	—	—	—	—	—	—	—
5–15	—	—	—	0.39	0.07	0.17	0.05	0.7	24.9	314.8	2.7

(*Continued*)

TABLE C.4. (*Continued*)

Horizon	Extractable acidity	CEC by sum of cations[a]	BS by sum of cations[b]	Ca	K	Mg	Na	TEB by CEC7[c]	CEC7[d]	CEC/clay	BS by CEC7[e]
	cmol$_c$ kg^{-1}	cmol$_c$ kg^{-1}	—%—	cmol$_c$ kg^{-1}						cmol$_c$ kg^{-1} clay	—%—
15–31	—	—	—	0.05	0.05	0.03	0.01	0.1	33.5	115.9	0.4
31–40/60	—	—	—	0.07	0.05	0.05	0.02	0.2	27.7	82.1	0.7
40/60–75	—	—	—	0.12	0.04	0.08	0.02	0.3	20.5	130.8	1.2
75–90	—	—	—	—	—	—	—	—	—	—	—

[a] Sum of extractable acidity and TEB.
[b] BS determined from TEB ÷ CEC sum of cations × 100.
[c] TEB (sum of Ca, K, Mg, and Na) determined by extraction in ammonium acetate (pH 7).
[d] CEC determined by extraction in ammonium acetate (pH 7).
[e] BS determined as (TEB ÷ ECEC) × 100.

TABLE C.5. Pedogenic metal oxides extractable in acid-ammonium oxalate and buffered dithionite by genetic horizon in the Chorro A soil. Fe_{ox}:Fe_d ratio, oxalate-extractable iron/dithionite-extractable iron.

	Dithionite extraction			Oxalate extraction						
Horizon	Al	Fe	Mn	Al	Fe	Mn	P	Si	Al+½Fe	Fe_{ox}:Fe_d
—cm—	%			mg g^{-1}					—%—	
0–5	0.19	0.14	<0.01	1.90	1.59	0.04	0.09	0.05	0.27	1.17
5–15	0.52	0.76	<0.01	7.39	5.86	<0.01	0.06	0.29	0.93	0.80
15–31	1.61	0.66	<0.01	18.26	3.21	<0.01	0.07	6.45	2.26	0.58
31–40/60	1.15	1.10	<0.01	18.27	5.10	<0.01	0.03	3.57	1.90	0.43
40/60–75	0.43	0.78	<0.01	8.06	2.50	<0.01	<0.01	0.63	0.78	0.28
75–90	0.28	0.42	<0.01	4.21	0.75	<0.01	<0.01	0.43	0.49	0.24
90–121	0.30	0.33	<0.01	4.93	1.07	<0.01	<0.01	0.29	0.55	0.33
121–133	0.56	0.13	<0.01	8.61	0.82	<0.01	0.06	1.83	0.90	0.63
133–155	0.64	0.06	<0.01	11.92	0.49	<0.01	0.13	4.06	1.22	0.77
155–200	0.33	0.12	<0.01	5.25	0.22	<0.01	0.02	1.73	0.54	0.19

TABLE C.6. Total elements by nitric acid digestion by genetic horizon in the Chorro A soil.

Horizon	Al	B	Ca	Cu	Fe	K	Mg	Mn	Na	P	Zn
—cm—	mg g^{-1}										
0–5	14.8	0.013	3.75	0.012	4.3	0.86	1.28	0.09	0.40	0.303	0.543
5–15	32.5	<0.005	2.22	0.012	16.1	1.42	2.29	0.10	1.06	0.126	0.025
15–31	94.6	0.009	0.75	0.084	14.2	2.37	1.81	0.09	0.57	0.147	0.029
31–40/60	116.8	0.009	0.62	0.115	20.5	2.48	2.17	0.10	0.43	0.123	0.047
40/60–75	103.3	<0.005	0.45	0.067	14.2	1.40	2.08	0.21	0.18	0.078	0.041
75–90	108.6	<0.005	0.35	0.070	11.8	1.02	2.42	0.25	0.14	0.082	0.034
90–121	140.9	<0.005	0.34	0.115	13.2	2.51	2.67	0.18	0.22	0.130	0.038
121–133	102.2	0.006	0.22	0.115	9.6	3.31	2.06	0.08	0.28	0.175	0.034
133–155	60.6	<0.005	0.18	0.085	4.2	1.60	0.86	0.05	0.22	0.168	0.023
155–200	73.5	0.005	0.04	0.018	5.2	1.68	1.26	0.09	0.16	0.081	0.048

TABLE C.7. Detailed particle-size distribution and glass contents in the Chorro A profile. Note that glass includes glass, glass coated grains, and glass aggregates, although the majority were glass grains. For grain counts, 30% of the fine earth must be coarse silt and sand (0.02–2 mm). We did not quantify sand grains coarser than fine sand. GS = glass grains; GC = glass-coated grains; GA = glass aggregates; nd = not determined. Fractions in bold were analyzed for glass content.

	Particle-size distribution (%)								Grain counts (%)		
Horizon	**Clay**	**Fine silt**	**Coarse silt**	**Very fine sand**	**Fine sand**	**Medium sand**	**Coarse sand**	**Very coarse sand**	**Coarse silt**	**Fine sand**	**Mean glass**
—cm—	—%—	—%—	**—%—**	—%—	**—%—**	—%—	—%—	—%—			
5–15	20.5	28.7	**8.9**	7.9	**18.8**	13	1.6	0.6	GS 28, GA 2, GC 1	GS 2, GA 1	12%
15–31	24.1	30.3	**8.8**	11	**14.7**	8	2.9	0.2	GS 10, GA 3, GC, tr	GS 10, GA 3, GC tr	13%
31–40/60	nd	nd	**nd**	nd	**nd**	nd	nd	nd	—	—	—
40/60–75	11.3	19.4	**12.7**	13.7	**19.5**	15.5	5.7	2.2	GC 1, GS 1	GA tr, GC tr	<1%

Additional Data: Chorro A. BS = base saturation; CEC = cation exchange capacity; ECEC = effective CEC; sat = saturation; TEB = total exchangeable bases; nd = not detected; dash (—) = not determined.

	Dithionite–citrate extraction			Ammonium oxalate extraction					
Horizon	**Al**	**Fe**	**Mn**	**Al**	**Fe**	**Si**	**Al+½Fe**	**Mn**	**P**
	%			%				mg kg^{-1}	
15–31	—	—	—	1.60	0.46	0.43	1.83	1.1	46.5
90–121	0.3	0.3	nd	0.59	0.13	0.04	0.59	nd	nd

	Ammonium acetate extraction							
Horizon	**Ca**	**K**	**Mg**	**Na**	**TEB**	**CEC[a]**	**BS**	**CEC per kg clay**
	$\text{cmol}_c\ \text{kg}^{-1}$						%	$\text{cmol}_c\ \text{kg}^{-1}$
15–31	—	—	—	—	—	—	—	—
90–121	nd	0.1	nd	nd	0.1	22.6	0	—

	KCl extraction		Barium chloride–triethanolamine extraction (pH 8.2)				
Horizon	**Al**	**Mn**	**Acidity**	**CEC[b]**	**BS**	**ECEC[c]**	**Al sat**
	$\text{cmol}_c\ \text{kg}^{-1}$	mg kg^{-1}	$\text{cmol}_c\ \text{kg}^{-1}$		%	$\text{cmol}_c\ \text{kg}^{-1}$	%
15–31	—	—	44.5	—	—	—	—
90–121	18.8	nd	25.4	25.5	0	18.9	99

[a] NH_4OAc extraction and measurement of the subsequently displaced NH_4 (i.e., includes bases, exchangeable acidity, etc.).

[b] NH_4OAc bases + acidity (at pH 8.2).

[c] ECEC (NH_4OAc-extractable bases plus KCl-extractable Al).

D. Chorro B Forest Census Plot, Fortuna Forest Reserve, Panama (Figure 3.5)

Soil taxonomy:	Coarse-loamy, isothermic, Oxyaquic Alorthod
Profile location:	Follow the trail through the Chorro A plot for ~10 minutes, crossing two small streams; the pit is located near the 00,60 marker.
Latitude/longitude:	8.749801°N, –82.232838°E
UTM:	17P, 0364392 m E., 0967413 m N.
Date and season:	29 July 2010; wet season
Elevation:	1,239 m asl
Slope and site position:	Steep (30%) lower backslope; concave radial and linear lateral
Soil moisture regime:	Perudic: mean annual rainfall at nearby Chorro A 5,507 ± 247 mm, with 351 ± 53 mm mean monthly dry season rainfall (1 January–30 April)
Soil temperature regime:	Isothermic: mean annual temperature 17.7°C at nearby Chorro A, varying by <2°C over the annual cycle
Parent material:	Rhyolitic boulders and tuff
Vegetation:	Lower montane tropical rainforest; canopy height 20 m; relatively open canopy dominated by emergent *Colpothrinax* palms, canopy *Euterpe* and *Wettinia* palms; a few large *Podocarpus oleifolius*; understory dominated by juvenile palms and tree ferns (*Alsophila* sp.)
Drainage:	Moderately poorly drained; pit half full of water and a large macropore (5 cm diameter) draining into the pit at ~1.5 m depth
Surface features:	Thick layer of moss, ferns, and decomposing leaves
Faunal activity:	None observed
Coarse fragments:	Several large boulders >1 m diameter from 20 cm below the surface extending to the base of the profile pit
Rooting depth:	Throughout the profile to at least 188 cm
Control section:	Between 25 and 100 cm below the soil surface
Particle-size class:	Coarse-loamy (>15% sand and <18% clay)
Mineralogy class:	Not determined
Cation-exchange activity class:	Not applicable
Diagnostic horizons/features:	(1) Perudic moisture regime and isothermic temperature regime (2) Ochric epipedon from 10 to 18 cm (3) Spodic horizon from 36 to 56 cm

General Features of the Soil

There are horizons enriched in organic matter between 36 and 56 cm and between 89 and 100 cm, which appear to be related to the accumulation of illuvial associations between organic matter and amorphous Al. The two organic-rich horizons contain considerably greater organic C (5.6%–6.3% C) and greater total P (>100 mg P kg^{-1}) than adjacent horizons. There is little indication that they are buried A horizons (e.g., caused by landslips) because, although organic C is high between 36 and 56 cm, there are no clear differences in exchangeable cations, and oxalate and dithionite Fe decrease continuously with depth. Texture is variable throughout the profile. The key difference is the greater amorphous Al in the organic-rich subsoil horizon, indicating podzolization and spodic soil properties. The organic-rich horizons also have similarities with sombric horizons but do not qualify because of the high concentrations of amorphous Al.

There is a small amount of volcanic glass in the profile, but neither the glass nor the amorphous metals are sufficient for andic properties.

The absence of redox concentrations, including around root channels, suggests no aquic conditions, although the extremely low concentrations of iron oxides mean that it would be difficult to identify redox features if saturation occurs. Redox features were clearly present at Chorro A on the same rhyolitic parent material, although Fe concentrations are greater there. This suggests that long-term reducing conditions have removed Fe from the Chorro B profile, indicating periodic saturation to moderate depth.

Soil Taxonomy

The organic-rich subsoil horizons contain high concentrations of amorphous Al and therefore meet the requirements for spodic horizons. These include the organic matter, pH, and color requirements, and the horizons have Al+½Fe concentrations >0.5% and twice the concentration in the overlying ochric epipedon. The profile therefore qualifies as a Spodosol. The spodic horizons include a horizon that contains ≥6% carbon, but it is not 10 cm thick (9 cm), so the profile marginally does not qualify as a Humod. Instead, the profile qualifies as an Orthod. The spodic horizon contains <0.1% Fe_{ox}, qualifying it as an Alorthod. Presumed periodic saturation to within 100 cm of the soil surface qualifies the profile as an Oxyaquic Alorthod. However, if it is subsequently found that saturation only occurs to greater depth, then the profile would qualify as a Typic Alorthod. If it is determined that the profile has aquic conditions, it would qualify as a Typic Epiaquod or Endoaquod.

There are insufficient andic properties for the profile to qualify as an Andisol. Specifically, only small amounts of volcanic glass are present in the subsoil, Al+½Fe is >1.0% between 36 and 56 cm, and bulk density is >1 g cm^{-3} below 18 cm. The clay distribution is irregular. There are no redox features, but this might be due to the low concentrations of iron oxides rather than the absence of saturation.

Sombric horizons are dark subsurface mineral horizons formed under free drainage in tropical and subtropical mountains. The dark color is formed by organic matter that is not associated with aluminum (as in a spodic horizon). A proposal to improve the definition of the sombric horizon (Bockheim, 2014) suggests that it should have at least 0.6% carbon (and >0.2% than the overlying horizon), be at least 15 cm thick, have color value and chroma <4 (and be 1 unit darker than the overlying horizon), have a pH ≤5, and have a base saturation <50% (by CEC7). To differentiate it from a spodic horizon, a sombric horizon should not be associated with amorphous Al, with an Al+½Fe concentration <0.5%. Here, the organically enriched subsoil horizons meet all the criteria apart from the Al+½Fe concentration, so these horizons are not sombric. Amorphous (oxalate) Fe is > dithionite Fe throughout the profile.

Chemical and Physical Properties

Texture is predominantly loamy, although the USDA texture analysis yielded much lower concentrations of clay than the STRI analysis, perhaps because the latter analysis was done on air-dried soil. Glass was present in low or trace amounts. Bulk density was ≥1 g cm^{-3} throughout, and the mineral soil is very strongly acid throughout. Total C concentrations are high throughout the profile, between 2.2% and 6.5% through the upper meter, with C:N ratios between 16 and 23. Total P is moderately low in the A and Bh horizons and very low in other mineral horizons, particularly in the deep subsoil. Base cation concentrations are extremely low throughout the mineral soil. Extractable Al concentrations are moderately high throughout, with corresponding very high Al saturation (>95%). Amorphous Al is moderate and is greatest in the organically enriched subsoil horizons between 36 and 56 cm, yielding Al+½Fe of approximately 1.0%. However, all forms of Fe and Mn are extremely low. In particular, all forms of Mn are undetectable in oxalate and dithionite extracts throughout the mineral soil.

Horizon Description: Chorro B

Oe—0 to 10 cm; very dark brown (10YR 2/2) decomposed organic matter; moderate fine and very fine subangular blocky structure; loose; very slightly sticky and not plastic; many coarse and medium, and common fine and very fine roots; abrupt smooth boundary.

A—10 to 18 cm; very dark grayish-brown (10YR 3/2) sandy clay loam; moderate medium and coarse subangular blocky structure; moist and friable; slightly sticky and not plastic; common coarse and fine, and many medium roots; abrupt smooth boundary.

E—18 to 36 cm; brown (10YR 5/3) and pale brown (10YR 6/3) sandy loam; few patches of strong brown (7.5YR 4/6) coarse sand; weak coarse subangular blocky structure; moist and friable; not sticky and not plastic; common medium and few fine roots; abrupt smooth boundary.

Bh1—36 to 47 cm; very dark brown (7.5YR 2.5/2) sandy clay loam; moderate coarse subangular blocky structure; moist and friable; many coarse and medium, and common fine and very fine roots; clear smooth boundary.

Bh2—47 to 56 cm; black (10YR 2/1) silty clay loam; moderate coarse subangular blocky structure; sticky and slightly plastic; firm to friable; many coarse and medium, and common fine and very fine roots; clear smooth boundary.

Bw—56 to 89 cm; patches of very dark grayish-brown (10YR 3/2) silty clay loam, dark brown (10YR 3/3) and yellowish-brown (10YR 5/4) sandy loam, and light gray (2.5Y 7/2) and light brownish-gray (2.5Y 6/2) fine sandy loam; massive and friable; not or slightly plastic and slightly sticky; common medium (<1 cm) patches of organic matter; common fine and medium roots; clear smooth boundary.

Bh3—89 to 100 cm; black (10YR 2/1) silty clay loam; fine patches of lighter-colored sandy material; massive/very coarse subangular blocky; moist and friable; not plastic and slightly sticky; few fine and medium roots; smooth abrupt boundary.

BC—100 to 188 cm; dark brown (10YR 3/3), brown (10YR 5/3), and light yellowish-brown (2.5Y 6/3), extremely bouldery sandy loam; massive; slightly sticky and not plastic; moist and firm; two thin layers a few cm thick of iron-enriched coarse sandy material at 100 cm and 130 cm; about 70% rhyolite boulders; few very coarse, common coarse, and medium, and few fine roots; abrupt smooth boundary.

C—188 to 200+ cm; white (2.5Y 8/1) sand; massive; firm; not sticky and not plastic.

Laboratory Analysis: Chorro B

TABLE D.1. Soil physical properties, including bulk density and particle-size distribution, by genetic horizon in the Chorro B soil. Dash (—) = not determined.

Horizon	Designation	Bulk density (fine earth)	Coarse fragments (>2 mm)	Sand	Silt	Clay	Textural class	Clay:silt ratio
—cm—		—g cm^{-3}—	—vol%—	—%—	—%—	—%—		
0–10	Oa	0.31	0	—	—	—	Organic	—
10–18	A	0.97	0	43.0	35.7	21.3	Loam	0.60
18–36	E	1.13	0	54.5	26.4	19.1	Sandy loam	0.72
36–47	Bh1	ND	0	33.8	48.2	17.9	Loam	0.37
47–56	Bh2	1.25	0	42.8	28.3	28.9	Clay loam	1.02
56–89	Bw	ND	0	48.8	34.4	16.8	Loam	0.49
89–100	Bh3	1.19	0	36.7	46.9	16.5	Loam	0.35
100–188	BC	1.25	70	39.4	48.2	12.4	Loam	0.26
188–200	C	ND	—	43.0	43.3	13.7	Loam	0.32

TABLE D.2. Soil pH and total carbon and nitrogen by genetic horizon in the Chorro B soil. Dash (—) = not determined.

Horizon	Soil pH			Total C	Total N	Total P	C:N	C:P
	Water	$CaCl_2$	$BaCl_2$	—%—	—%—	mg P kg^{-1}		
0–10	4.28	3.46	3.03	38.65	2.33	469	16.6	824
10–18	4.46	3.81	3.96	4.18	0.27	111	15.6	375
18–36	4.69	4.29	4.35	2.14	0.11	71	18.9	301
36–47	4.71	4.27	4.30	5.59	0.31	184	18.2	304
47–56	4.91	4.38	4.39	6.27	0.30	199	20.9	316
56–89	4.97	4.41	4.44	2.18	0.10	60	22.7	364
89–100	4.72	4.19	4.24	6.47	0.32	103	20.1	631
100–188	4.90	4.22	4.29	1.55	0.05	48	31.9	323
188–200	5.62	4.09	4.18	0.06	<0.01	24	—	23

TABLE D.3. Exchangeable cations and effective cation exchange capacity (ECEC) by extraction in 0.1 M barium chloride ($BaCl_2$) by genetic horizon in the Chorro B soil. BS = base saturation; sat = saturation; TEB = total exchangeable bases; dash (—) = not determined.

Horizon	Al	Ca	Fe	K	Mg	Mn	Na	TEB[a]	ECEC[b]	BS[c]	ECEC per kg clay	Ca:Mg	Al sat
	cmol$_c$ kg^{-1}									—%—	cmol$_c$ kg^{-1}		—%—
0–10	2.76	5.78	0.02	1.24	5.95	0.04	0.19	13.2	16.0	82.3	—	1.0	17.3
10–18	5.47	0.05	0.07	0.04	0.07	<0.01	<0.01	0.2	5.7	2.8	26.8	0.8	96.0
18–36	2.37	0.01	0.03	<0.01	0.01	<0.01	<0.01	<0.1	2.4	1.0	12.7	1.2	97.9
36–47	3.18	0.03	0.02	0.01	0.02	<0.01	0.01	<0.1	3.3	2.4	18.3	1.3	97.1
47–56	2.26	0.04	0.02	0.02	0.02	<0.01	0.01	<0.1	2.4	3.9	8.2	2.7	95.5

TABLE D.3. (*Continued*)

Horizon	Al	Ca	Fe	K	Mg	Mn	Na	TEB[a]	ECEC[b]	BS[c]	ECEC per kg clay	Ca:Mg	Al sat
	cmol$_c$ kg^{-1}									—%—	cmol$_c$ kg^{-1}		—%—
56–89	1.63	0.02	0.01	0.02	<0.01	<0.01	<0.01	<0.1	1.7	2.5	10.0	—	96.9
89–100	3.93	0.04	0.01	0.02	<0.01	<0.01	<0.01	<0.1	4.0	1.4	24.3	—	98.3
100–188	2.73	0.02	0.02	0.06	0.01	<0.01	<0.01	<0.1	2.8	3.4	23.0	1.7	96.0
188–200	1.36	0.51	0.25	0.47	0.69	<0.01	0.02	1.7	3.3	51.0	24.0	0.7	41.2

[a] TEB determined by extraction in 0.1 M $BaCl_2$.

[b] ECEC determined as the sum of cations extracted in extraction in 0.1 M $BaCl_2$.

[c] BS determined as (TEB ÷ ECEC) × 100.

TABLE D.4. Pedogenic metal oxides extractable in acid-ammonium oxalate and buffered dithionite by genetic horizon in the Chorro B soil. Fe_{ox}:Fe_d ratio, oxalate-extractable iron/dithionite-extractable iron.

	Dithionite extraction			Oxalate extraction						
Horizon	Al	Fe	Mn	Al	Fe	Mn	P	Si	Al+½Fe	Fe_{ox}:Fe_d
	%			mg g^{-1}					—%—	
0–10	0.28	0.09	<0.01	2.83	0.37	0.02	0.18	0.03	0.30	0.99
10–18	0.34	0.14	<0.01	3.85	1.21	<0.01	0.05	0.21	0.45	1.13
18–36	0.50	0.10	<0.01	7.65	0.92	<0.01	0.04	1.37	0.81	1.53
36–47	0.72	0.02	<0.01	8.91	0.19	<0.01	0.11	0.55	0.90	1.25
47–56	0.80	0.02	<0.01	10.70	0.13	<0.01	0.13	0.81	1.08	1.35
56–89	0.39	<0.01	<0.01	5.65	0.04	<0.01	0.03	0.62	0.57	1.43
89–100	0.67	<0.01	<0.01	8.08	0.05	<0.01	0.05	0.46	0.81	1.20
100–188	0.31	<0.01	<0.01	4.14	0.03	<0.01	0.02	0.45	0.42	1.35
188–200	0.02	0.01	<0.01	0.36	0.08	<0.01	<0.01	0.03	0.04	1.53

TABLE D.5. Total elements by nitric acid digestion by genetic horizon in the Chorro B soil. nd = not determined.

Horizon	Al	B	Ca	Cu	Fe	K	Mg	Mn	Na	P	Zn
	mg g^{-1}										
0–10	9.1	0.005	1.48	0.010	1.3	0.89	0.99	0.04	0.12	0.434	0.018
10–18	56.2	0.009	0.33	0.011	4.9	0.69	0.65	0.03	0.22	0.146	0.016
18–36	69.7	0.010	0.14	0.023	4.5	0.72	0.60	0.03	0.13	0.106	0.024
36–47	63.9	<0.005	1.40	0.019	3.1	0.62	0.94	0.03	0.58	0.205	0.013
47–56	55.7	<0.005	2.41	0.024	3.5	0.92	1.31	0.03	0.98	0.231	0.012
56–89	nd	nd	nd	nd	nd	nd	nd	nd	nd	nd	nd
89–100	63.4	0.021	0.04	0.009	2.0	0.60	0.48	0.02	0.08	0.133	0.011
100–188	65.8	0.011	0.03	0.009	2.4	0.57	0.51	0.02	0.06	0.078	0.013
188–200	57.4	0.008	0.08	0.005	1.7	0.87	0.46	0.01	0.11	0.054	0.013

TABLE D.6. Detailed particle-size distribution and glass contents in the Chorro B profile. Note that glass includes glass, glass coated grains, and glass aggregates, although the majority were glass grains. For grain counts, 30% of the fine earth must be coarse silt and sand (0.02 to 2 mm). We did not quantify sand grains coarser than fine sand. OT = other; GS = glass grains; GC = glass-coated grains; GA = glass aggregates, PO = plant opal. Fractions in bold were analyzed for glass content.

	Particle-size distribution (%)								Grain counts (%)		
Horizon	Clay	Fine silt	Coarse silt	Very fine sand	Fine sand	Medium sand	Coarse sand	Very coarse sand	Coarse silt	Fine sand	Mean glass
		—%—	**—%—**	—%—	**—%—**	—%—	—%—	—%—			
18–36	8.3	18.2	9.0	12.1	17.4	10.7	13.3	11.0	OT 98, GS 2, PO tr	OT 99, PO 1, GA tr	<1
36–47	13.3	29.3	10.3	11.1	22.1	12.7	1.1	0.1	OT 98, GS 2, GA tr, PO tr	OT 98, GA 1, GC tr, GS tr, PO tr	1.3
47–56	17.2	26.4	8.5	8.9	19.5	16.4	2.6	0.5	OT 96, GS 4, GA tr, PO tr	OT 97, GA 1, GC 1, GS 1, PO tr	3.3

E. Honda A Forest Census Plot, Fortuna Forest Reserve, Panama (Figure 3.6)

Soil taxonomy:	Fine, kaolinitic, isothermic, Andic Haplohumult
Profile location:	Park at the Quebrada Honda bridge and enter the forest to the north on the upstream side of the bridge. After ~10 minutes, follow the right fork of the trail and continue a short distance to the plot. The pit is ~30 m downhill to the right of the trail.
Date and season:	3 July 2008 (wet season); reexamined 27 February 2010 (dry season); 18 January 2014 (dry season)
Latitude/longitude:	8.753123°N, –82.239066°E
UTM:	17P, 0363708 m E., 0967783 m N
Elevation:	1,155 m asl
Slope and site position:	Steep (35%) upper backslope, facing southeast; linear radial and lateral
Soil moisture regime:	Perudic: mean annual rainfall 6,255 ± 962 mm, with 381 ± 51 mm mean monthly dry season rainfall (1 January–30 April)
Soil temperature regime:	Isothermic: mean annual temperature 18.2°C
Parent material:	Rhyolite ash over undifferentiated mafic-volcanics
Vegetation:	Lower montane tropical rainforest; canopy height 25 m; relatively open understory under a closed canopy, with the ectomycorrhizal tree *Oreomunnea mexicana* the canopy dominant and emergent individuals of *Quercus insignis*; relatively open understory with many *Oreomunnea* juveniles
Drainage:	Moderately poorly drained; perched water table at ~50 cm draining into profile pit; water table at ~200 cm
Surface features:	Thick layer of wet leaf litter; 100% cover
Faunal activity:	Many earthworms in the upper meter of the profile
Coarse fragments:	Hard subangular gravel and cobbles between 20 and 51 cm
Rooting depth:	Roots to at least 100 cm, although most in upper 10 cm
Control section:	Between 16 and 66 cm below the soil surface (i.e., the upper 50 cm of the argillic horizon)
Particle-size class:	Fine (35%–60% clay)
Mineralogy class:	Kaolinitic (68% kaolinite and 2% gibbsite by thermal X-ray diffraction [XRD])
Cation-exchange activity class:	Not applicable to kaolinitic mineralogy class
Diagnostic horizons/features:	(1) Perudic moisture regime and isothermic temperature regime (2) Ochric epipedon from 4 to 16 cm (3) Argillic horizon from 16 to 51 cm (4) Andic properties in part of the upper 75 cm

General Features of the Soil

The Quebrada Honda watershed supports monodominant forest composed of a member of the walnut family (*Oreomunnea mexicana*, Juglandaceae). The soil is developed in rhyolitic ash over mafic-volcanic material. It has a thick organic horizon over an epipedon with andic soil properties but no volcanic glass (i.e., it is well weathered). The clay-rich subsoil is dominated by kaolinite. The soil is infertile, with low base saturation throughout.

Soil Taxonomy

There are moderate andic properties in the upper part of the profile, but these are insufficient to qualify the profile as an Andisol. In particular, bulk density is >1.0 g cm^{-3} in the entire Bt horizon. The profile is therefore an Ultisol because it has an argillic horizon with a base saturation <35% by sum of cations at 125 cm below the upper boundary of the argillic horizon (i.e., the 135–175 cm horizon). The profile qualifies as a Humult because of the high carbon stock (>25 kg C m^{-2}) in the upper 100 cm of soil as well as >0.9% carbon in the argillic horizon. There is no kandic horizon because, although the ECEC in the argillic horizon by $BaCl_2$ extraction is <12 $cmol_c$ kg^{-1} clay, the CEC by ammonium acetate pH 7 is >16 $cmol_c$ kg^{-1} clay. The profile does not qualify as a Palehumult, as the clay decrease is >20% below the maximum, and there is no apparent sombric horizon (i.e., organic matter rich subsurface horizon). The profile therefore qualifies as a Haplohumult. Andic properties, including Al+½Fe >1.0% and bulk density <1.0 g cm^{-3} (i.e., the A and the upper part of the Bt horizon), qualify the profile as an Andic Haplohumult.

Chemical and Physical Properties

The profile contains coarse fragments of primarily andesitic composition. Clay concentrations are almost 60% in the argillic horizon, with kaolinitic mineralogy and a small amount of vermiculite in the epipedon. The soil is very strongly acid, and the organic matter concentration is high in the epipedon.

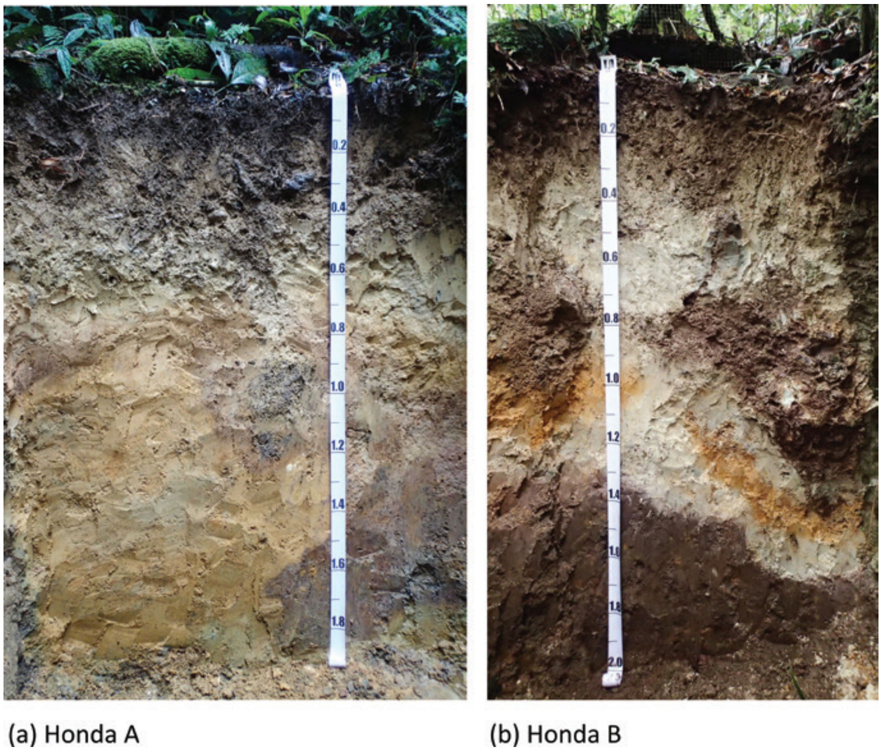

(a) Honda A

(b) Honda B

FIGURE 3.6. The profiles at (a) Honda A and (b) Honda B. Note the contact between overlying rhyolitic material and underlying mafic-volcanic material at approximately 150 cm in profile b.

Exchangeable base cation concentrations are extremely low in the subsoil, with low base saturation and high Al saturation. Amorphous metals are high, with Al+½Fe of >2% in the argillic horizon. Total Al is high (up to 14% in the subsoil), but total Fe is low. There is a small amount of volcanic glass in the subsoil. The mafic material below 180 cm is high in total concentrations of Al, Fe, Mn, and P. It is also rich in base cations, particularly Ca and Mg.

Horizon Description: Honda A

Oa—0 to 4 cm; black (10YR 2/1) decomposed organic matter; moist and friable; very slightly sticky and not plastic; many coarse, medium, fine, and very fine roots, including a thin mat in the surface few millimeters of the horizon; abrupt wavy boundary

A—4 to 16 cm; very dark grayish-brown (10YR 3/2) silty clay loam; moderate medium and fine subangular blocky structure, breaking to fine subangular blocky; moist and friable, sticky and plastic; many earthworms; many fine tubular pores; many coarse and common very fine, fine, and medium roots; gradual wavy boundary.

Bt—16 to 51 cm; yellowish-brown (10YR 5/4) gravelly clay loam; moderate coarse subangular blocky structure, breaking to moderate fine subangular blocky; moist and friable; sticky and plastic; about 20% hard subangular medium and coarse gravel and cobbles with 1 mm thick sesquioxide rinds; continuous clay films on pore linings and ped faces; common earthworms; common fine and medium tubular pores; few very fine, fine, and medium roots; gradual wavy boundary.

BC—51 to 75 cm; light yellowish-brown (10YR 6/4) fine sandy clay loam; massive, breaking to medium angular blocky; moist and friable; plastic and slightly sticky; about 4% hard but weathered subangular gravel; few medium strong brown (7.5YR 5/6) firm redox concentrations around gravel; few light gray (5Y 7/1) redox depletions around roots; faint discontinuous clay films on ped faces; common medium tubular pores; gray redox depletions around dead roots and in old root channels; very few fine and very fine roots; clear wavy boundary.

BCg—75 to 180 cm; strong brown (7.5YR 5/6) fine sandy clay loam; massive, breaking to fine and very fine subangular blocky; moist and firm; slightly sticky and slightly plastic; very coarse, patchy gray redox depletions, with few medium redox depletions inside peds; completely weathered dark yellowish-brown (10YR 4/4) boulders; no clay films; very few fine roots; clear wavy boundary.

C—180 to 275 cm; strong brown (7.5YR 5/8) and then yellowish brown (10YR 5/6); water table at ~190 cm; further augering prevented by rock.

Laboratory Analysis: Honda A

TABLE E.1. Soil physical properties, including bulk density and particle-size distribution, by genetic horizon in the Honda A soil. Dash (—) = not determined.

Horizon	Designation	Bulk density (fine earth)	Coarse fragments (>2 mm)	Sand	Silt	Clay	Textural class	Clay:silt ratio
—cm—		—g cm^{-3}—	—%—	—%—	—%—	—%—		
0–4	Oa	0.29	0	—	—	—	Organic	—
4–16	A	0.56	0	38.6	22.1	39.4	Clay loam	1.8
16–51	Bt	1.13	20	21.0	20.3	58.7	Clay	2.9
51–75	BC	1.32	4	24.3	37.2	38.5	Clay loam	1.0
75–180	BCg	1.42	0	22.7	38.4	38.9	Clay loam	1.0
180–275	C	—	0	35.3	36.6	28.1	Clay loam	0.8

TABLE E.2. Soil pH and total carbon and nitrogen by genetic horizon in the Honda A soil. Dash (—) = not determined.

Horizon	————Soil pH————			Total C	Total N	Total P	C:N	C:P
—cm—	Water	CaCl$_2$	BaCl$_2$	—%—	—%—	mg P kg^{-1}		
0–4	4.91	3.98	3.37	25.98	1.85	634	14.1	410
4–16	4.46	4.00	4.22	8.46	0.52	454	16.3	186
16–51	4.97	4.43	4.46	3.22	0.20	333	16.1	97
51–75	4.92	4.06	4.07	0.45	0.02	61	22.5	74
75–180	5.00	4.04	4.04	0.28	0.01	101	52.8	18
180–275	5.23	4.54	4.20	0.17	<0.01	981	—	2

TABLE E.3. Exchangeable cations and effective cation exchange capacity (ECEC) by extraction in 0.1 M barium chloride (BaCl$_2$) by genetic horizon in the Honda A soil. BS = base saturation; sat = saturation; TEB = total exchangeable bases; dash (—) = not determined.

Horizon	Al	Ca	Fe	K	Mg	Mn	Na	TEB[a]	ECEC[b]	BS[c]	ECEC per kg clay	Ca:Mg ratio	Al sat
—cm—	———cmol$_c$ kg^{-1}———									—%—	cmol$_c$ kg^{-1}		—%—
0–4	2.70	15.33	0.29	1.06	3.97	0.07	0.22	20.6	23.6	87.1	—	3.9	11
4–16	4.54	0.63	0.07	0.07	0.24	0.01	0.05	1.0	5.6	14.7	14.2	2.6	81
16–51	1.54	0.14	0.01	<0.01	0.07	<0.01	<0.01	0.2	1.8	12.2	3.0	2.0	88
51–75	8.61	0.28	<0.01	0.01	0.19	<0.01	0.13	0.6	9.2	6.6	23.9	1.5	93
75–180	7.27	0.09	<0.01	<0.01	0.24	<0.01	0.07	0.4	7.7	5.1	19.7	0.3	95
180–275	1.39	9.05	<0.01	0.15	7.22	0.57	0.31	16.7	18.7	89.5	65.5	1.3	7

[a] TEB determined by extraction in 0.1 M BaCl$_2$.

[b] ECEC determined as the sum of cations extracted in extraction in 0.1 M BaCl$_2$.

[c] BS determined as (TEB ÷ ECEC) × 100.

TABLE E.4. Extractable acidity, exchangeable cations, and cation exchange capacity (CEC) determined in buffered solutions by genetic horizon in the Honda A soil. BS = base saturation; TEB = total exchangeable bases; dash (—) = not determined.

Horizon	Extractable acidity	CEC by sum of cations[a]	BS by sum of cations[b]	Ca	K	Mg	Na	TEB by CEC7[c]	CEC7[d]	CEC/clay	BS by CEC7[e]
—cm—	cmol$_c$ kg^{-1}	cmol$_c$ kg^{-1}	—%—	cmol$_c$ kg^{-1}						cmol$_c$ kg^{-1} clay	—%—
0–4	—	—	—	—	—	—	—	—	—	—	—
4–16	—	—	—	0.19	0.14	0.18	0.07	0.6	34.7	88.2	2
16–51	32.8	33.0	1	0.08	0.06	0.05	0.01	0.2	29.6	50.5	1
51–75	23.9	24.5	2	0.16	0.04	0.17	0.10	0.5	27.6	71.6	2
75–180	25.0	25.4	2	—	—	—	—	—	—	—	—
180–275	—	—	—	—	—	—	—	—	—	—	—

[a] Sum of extractable acidity and TEB.

[b] BS determined from TEB ÷ CEC sum of cations × 100.

[c] TEB (sum of Ca, K, Mg, and Na) determined by extraction in ammonium acetate (pH 7).

[d] CEC determined by extraction in ammonium acetate (pH 7).

[e] BS determined as (TEB ÷ ECEC) × 100.

TABLE E.5. Pedogenic metal oxides extractable in acid-ammonium oxalate and buffered dithionite by genetic horizon in the Honda A soil. Fe$_{ox}$:Fe$_d$ ratio, oxalate-extractable iron/dithionite-extractable iron.

	Dithionite extraction			Oxalate extraction						
Horizon	Al	Fe	Mn	Al	Fe	Mn	P	Si	Al+½Fe	Fe$_{ox}$:Fe$_d$
—cm—	—%—			—mg g^{-1}—					—%—	
0–4	0.29	0.58	<0.01	2.88	2.98	0.01	0.28	0.07	0.44	0.52
4–16	0.94	1.93	<0.01	10.18	12.26	0.01	0.17	0.31	1.63	0.63
16–51	1.13	3.00	<0.01	13.01	14.56	0.01	0.08	1.27	2.03	0.48
51–75	0.58	1.80	<0.01	5.89	1.83	<0.01	0.04	0.79	0.68	0.10
75–180	0.71	4.27	<0.01	5.13	1.25	<0.01	0.03	0.60	0.58	0.03
180–275	0.64	7.89	0.10	2.14	1.42	0.74	0.13	0.42	0.29	0.02

TABLE E.6. Total elements by nitric acid digestion by genetic horizon in the Honda A soil.

Horizon	Al	B	Ca	Cu	Fe	K	Mg	Mn	Na	P	Zn
—cm—	—mg g^{-1}—										
0–4	22.8	0.012	4.95	0.027	12.9	0.89	2.37	0.08	0.70	0.641	0.034
4–16	68.2	<0.005	2.41	0.054	36.4	1.16	3.08	0.13	0.92	0.423	0.062
16–51	109.9	0.011	1.88	0.130	49.2	1.74	4.64	0.22	0.40	0.319	0.077
51–75	149.4	<0.005	0.20	0.282	44.5	0.52	8.41	0.18	0.15	0.224	0.107
75–180	138.2	<0.005	0.09	0.277	69.2	0.20	8.51	0.19	0.14	0.326	0.144
180–275	123.5	<0.005	1.56	0.229	118.1	0.64	7.91	1.32	0.19	1.062	0.134

TABLE E.7. Detailed particle-size distribution and glass contents in the Honda A profile (30–40 cm). Note that glass includes glass, glass coated grains, and glass aggregates, although the majority were glass grains. For grain counts, 30% of the fine earth must be coarse silt and sand (0.02 to 2 mm). GS = glass grains; GC = glass-coated grains; GA = glass aggregates. Fractions in bold were analyzed for glass content; tr = trace.

	Particle-size distribution (%)								Grain counts (%)		
Horizon	Clay	Fine silt	Coarse silt	Very fine sand	Fine sand	Medium sand	Coarse sand	Very coarse sand	Coarse silt	Fine sand	Mean glass[a]
—cm—		—%—	**—%—**	—%—	**—%—**	—%—	—%—	—%—			
16–51	28.2	16.1	3.9	6.0	9.9	12.5	13.8	9.6	GS 3, GC tr, GA, tr	GA 1, GS tr, GC tr	1.5%

[a] Mass-weighted average of coarse silt and fine sand.

Additional Data: Honda A. BS = base saturation; CEC = cation exchange capacity; ECEC = effective CEC; sat = saturation; TEB = total exchangeable bases; nd = not detected: tr = trace.

	Dithionite–citrate extraction			Ammonium oxalate extraction					
Horizon	Al	Fe	Mn	Al	Fe	Si	Al+½Fe	Mn	P
—cm—	%			%				mg kg^{-1}	
4–16	1.5	2.9	nd	1.61	1.87	0.14	2.55	7.7	129.5
51–75	0.5	1.9	nd	0.40	0.14	0.05	0.47	1.1	6.4

	Ammonium acetate extraction							
Horizon	Ca	K	Mg	Na	TEB	CEC[a]	BS	CEC per kg clay
—cm—	$\text{cmol}_c\ \text{kg}^{-1}$						%	$\text{cmol}_c\ \text{kg}^{-1}$
4–16	nd	0.1	0.1	tr	0.2	31.0	1	78.7
51–75	nd	tr	0.2	0.1	0.3	19.7	2	33.6

	KCl extraction		Barium chloride–triethanolamine extraction (pH 8.2)				
Horizon	Al	Mn	Acidity	CEC[b]	BS	ECEC[c]	Al sat
—cm—	$\text{cmol}_c\ \text{kg}^{-1}$	mg kg^{-1}	$\text{cmol}_c\ \text{kg}^{-1}$		%	$\text{cmol}_c\ \text{kg}^{-1}$	%
4–16	2.3	0.1	54.3	54.5	0	2.5	92
51–75	7.5	0.1	18.1	18.4	2	7.8	96

[a] NH_4OAc extraction and measurement of the subsequently displaced NH_4 (i.e., includes bases, exchangeable acidity, etc.).

[b] NH_4OAc bases + acidity (at pH 8.2).

[c] ECEC (NH_4OAc-extractable bases plus KCl-extractable Al).

	X-ray[a]		Thermal	
	4–16 cm	**51–82 cm**	**4–16 cm**	**51–82 cm**
	Peak size		%	
Kaolinite	2	nd	46	68
Goethite	nd	nd	nd	nd
Hematite	nd	nd	nd	nd
Halloysite	nd	3	nd	nd
Gibbsite	1	1	7	2
Vermiculite	2	1	nd	nd
Montmorillonite	nd	nd	nd	nd
Cristobalite	nd	nd	nd	nd
Quartz	nd	nd	nd	nd
Interpretation			Mixed	Kaolinitic

[a] Values refer to relative peak size (5 = very large, 4 = large, 3 = medium, 2 = small, 1 = very small).

F. Honda B Forest Census Plot, Fortuna Forest Reserve, Panama (Figure 3.6)

Soil taxonomy:	Fine, kaolinitic, isothermic, Andic Haplohumult
Profile location:	Park at the Quebrada Honda bridge and enter the forest on the upstream side of the river. Follow the trail uphill for about 20 minutes, taking the right fork. The trail becomes faint and crosses two rivers before reaching the plot. The pit is located to the east and close to the trail (10 m away), downslope ~30 m from the 60,00 marker.
Latitude/longitude:	8.756892°N, –82.240770°E
UTM:	17P, 363522 m E., 968200 m N.
Date and season:	2 July 2008 (wet season); reexamined 27 February 2010 (dry season)
Elevation:	1,241 m asl
Slope and site position:	Steep (53%) linear midslope facing south-southeast; slightly convex lateral
Soil moisture regime:	Perudic: mean annual rainfall 6,159 ± 617 mm, with 332 ± 34 mm mean monthly dry season rainfall (1 January–30 April)
Soil temperature regime:	Isothermic: mean annual temperature 17.9°C
Parent material:	Rhyolitic ash over undifferentiated mafic-volcanics
Vegetation:	Lower montane tropical rainforest; canopy height 25 m; relatively open understory under a closed canopy; common monodominant stands of the ectomycorrhizal tree *Oreomunnea mexicana* plus occasional emergent oaks (*Quercus* spp.)
Drainage:	Moderately well drained
Surface features:	Thick, continuous cover of leaf litter
Faunal activity:	Few earthworms in the upper 10 cm; few small ant nests and tunnels
Coarse fragments:	Weathered cobbles and boulders up to 1 m diameter
Rooting depth:	Throughout the profile to at least 180 cm but mainly in the upper 25 cm
Control section:	Between 10 and 60 cm below the soil surface (i.e., the upper 50 cm of the argillic horizon)
Particle-size class:	Fine (35%–60% clay)
Mineralogy class:	Kaolinitic (67% kaolinite by thermal XRF)
Cation-exchange activity class:	No applicable to kaolinitic mineralogy
Diagnostic horizons/features:	(1) Perudic moisture regime and isothermic temperature regime (2) Ochric epipedon from 0 to 10 cm (3) Moderate andic properties from 0 to 74 cm (4) Argillic horizon from 25 to 74 cm

General Features of the Soil

The Quebrada Honda watershed supports monodominant forest composed of a member of the walnut family (*Oreomunnea mexicana*, Juglandaceae). This soil is similar to Honda A in terms of taxonomy and parent material. It is formed in rhyolitic ash over mafic-volcanics. It has moderate andic properties in the epipedon, but the ash is sufficiently weathered that it classifies as an Ultisol rather than an Andisol. It is organic rich and infertile, with a clay-rich subsoil dominated by kaolinite. Roots extend into the dark subsoil below 134 cm, presumably to obtain cations and phosphorus that are considerably enriched there.

Soil Taxonomy

The profile has moderate andic properties in the upper 25 cm, with bulk density <0.9 g cm^{-3} and oxalate-extractable Al+½Fe >1.0%. (Also, NZ P retention 30–50 cm is <85% and bulk density >1.0 g cm^{-3}.) There is also >0.4% Al+½Fe in the Bt2 horizon and 5% volcanic glass in the coarse silt fraction. However, these are insufficient for Andisols. Instead, the argillic horizon and low base saturation in the subsoil qualifies the profile as an Ultisol. The soil is a Humult because of the high carbon stock (>16 kg C m^{-2}) in the upper 100 cm of soil as well as >0.9% carbon in the upper 15 cm of the argillic horizon. In the absence of other diagnostic features at the great group level, the profile classifies as a Haplohumult. The moderate andic properties in >18 cm of the upper 75 cm of the profile qualify it as an Andic Haplohumult.

Chemical and Physical Properties

The profile contains abundant coarse fragments of primarily andesitic composition. Clay concentrations are almost 40% in the argillic horizon, formed of 67% kaolinite and 3% gibbsite by thermal X-ray diffraction (XRD), with peaks from halloysite, gibbsite, and vermiculite. The deep subsoil contains 62% kaolinite by thermal XRD. The soil is extremely to very strongly acid, and the organic matter concentration is high in the epipedon.

Exchangeable base cation concentrations are extremely low in the subsoil, with low base saturation and high Al saturation. Amorphous metals are moderately high, with Al+½Fe of 1.3% to 1.4% in the upper 25 cm. Total Al is high (12%–13% in the subsoil), but total Fe is low. There are small amounts of volcanic glass throughout the upper 74 cm of the profile.

Horizon Description: Honda B

A—0 to 10 cm; very dark brown (10YR 2.2) silt loam; moderate coarse subangular blocky structure, breaking to fine and very fine subangular blocky; moist and friable; slightly sticky and slightly plastic; few hard subangular medium gravel (<1%); coarse and common medium, fine, and very fine roots, including a thin mat in the surface few mm of the horizon; clear smooth boundary.

Bt1—10 to 25 cm; brown (10YR 5/3) gritty silty clay loam; moderate coarse subangular blocky structure, breaking to moderate fine and very fine subangular blocky; moist and friable; slightly sticky and slightly plastic; faint discontinuous clay films on ped faces; about 15% hard, subangular, medium and coarse andesitic gravel fragments; common medium and few fine and very fine roots; gradual wavy boundary.

Bt2—25 to 74 cm; light gray (2.5Y 7/2) gritty clay loam; massive, breaking to coarse angular blocky and then fine and very fine subangular blocky; moist and firm; sticky and slightly plastic; faint continuous clay films on ped faces and pore linings; about 1% medium weathered gravel fragments; few medium organic-enriched root channels (krotovinas); few medium, fine, and very fine roots; clear wavy boundary.

BC—74 to 134/165 cm; pale brown (2.5Y 7/3) bouldery gritty silty clay loam; massive, breaking to moderate coarse subangular blocky; moist and firm; sticky and plastic; about 20% strongly weathered and fragmented andesitic boulders; about 2% hard fine gravel; common patches of reddish-yellow (7.5YR 6/8) silty clay loam below weathered boulders; no clear clay films; common fine and very fine roots proliferating in weathered boulders, with few fine and medium roots elsewhere; clear wavy boundary.

2C—134/165 to 250 cm; dark brown (7.5YR 3/2) gritty sandy clay loam; very fine subangular blocky structure; upper part (15 cm) firm, sticky, and plastic; remainder friable, slightly sticky, and not plastic; about 3% strongly weathered fine subangular andesitic gravel; very few fine, medium, and coarse roots; water table at 220 cm; bedrock/boulders at 250 cm.

Laboratory Analysis: Honda B

TABLE F.1. Soil physical properties, including bulk density and particle-size distribution, by genetic horizon in the Honda B soil. nd = not determined.

Horizon	Designation	Bulk density (fine earth)	Coarse fragments (>2 mm)	Sand	Silt	Clay	Textural class	Clay:silt ratio
Cm		g cm^{-3}	vol%	%	%	%		
0–10	A	0.53	<1	42.6	34.8	22.6	Loam	0.65
10–25	Bt1	0.95	20	30.8	30.6	38.6	Clay loam	1.26
25–74	Bt2	1.32	1	24.5	38.1	37.5	Clay loam	0.98
74–134/165	BC	nd	20	40.4	39.8	19.8	Loam	0.50
134/165–250	2C	1.29	3	34.0	43.3	22.6	Loam	0.52

TABLE F.2. Soil pH and total carbon and nitrogen by genetic horizon in the Honda B soil. Total P and C:P = nitric digestion.

Horizon	Soil pH			Total C	Total N	Total P	C:N	C:P
—cm—	Water	CaCl$_2$	BaCl$_2$	—%—	—%—	mg P kg^{-1}		
0–10	4.31	3.89	3.56	12.89	0.910	693.0	14.2	197
10–25	4.72	4.33	4.26	3.31	0.209	417.6	15.8	91
25–74	4.61	4.02	4.20	0.60	0.040	275.1	15.1	31
74–134/165	4.68	4.01	4.16	0.28	0.013	239.4	22.2	13
134/165–250	4.80	3.96	4.06	0.26	0.012	553.0	21.9	4

TABLE F.3. Exchangeable cations and effective cation exchange capacity (ECEC) by extraction in 0.1 M barium chloride ($BaCl_2$) by genetic horizon in the Honda B soil. BS = base saturation; sat = saturation; TEB = total exchangeable bases.

Horizon	Al	Ca	Fe	K	Mg	Mn	Na	TEB[a]	ECEC[b]	BS[c]	ECEC per kg clay	Al sat	Ca:Mg
—cm—	$\text{cmol}_c\ \text{kg}^{-1}$									—%—	$\text{cmol}_c\ \text{kg}^{-1}$	—%—	
0–10	6.90	0.94	0.05	0.30	0.72	0.09	0.13	2.09	9.1	22.9	40.4	76	1.31
10–25	2.36	0.24	<0.01	0.20	0.12	0.01	0.03	0.60	3.0	20.1	7.7	79	2.04
25–74	6.24	<0.01	<0.01	0.06	0.11	<0.01	0.07	0.23	6.5	3.6	17.3	96	<0.1
74–134/165	8.23	<0.01	<0.01	0.03	0.09	<0.01	0.06	0.19	8.4	2.3	42.4	98	<0.1
134/165–250	11.36	0.04	<0.01	0.07	0.14	<0.01	0.03	0.27	11.6	2.3	51.4	98	0.29

[a] TEB determined by extraction in 0.1 M $BaCl_2$.

[b] ECEC determined as the sum of cations extracted in extraction in 0.1 M $BaCl_2$.

[c] BS determined as (TEB ÷ ECEC) × 100.

TABLE F.4. Extractable acidity, exchangeable cations, and cation exchange capacity (CEC) determined in buffered solutions by genetic horizon in the Honda B soil. BS = base saturation; TEB = total exchangeable bases; dash (—) = not determined.

Horizon	Extractable acidity	CEC by sum of cations[a]	BS by sum of cations[b]	Ca	K	Mg	Na	TEB by CEC7[c]	CEC7[d]	CEC/clay	BS by CEC7[e]
—cm—	$\text{cmol}_c\ \text{kg}^{-1}$	$\text{cmol}_c\ \text{kg}^{-1}$	—%—	$\text{cmol}_c\ \text{kg}^{-1}$						$\text{cmol}_c\ \text{kg}^{-1}$ clay	—%—
0–10	—	—	—	—	—	—	—	—	—	—	—
10–25	18.1	18.2	0.4	0.13	0.19	0.08	0.04	0.4	31.2	80.3	1.4
25–74	22.2	22.2	0.3	0.02	0.06	0.11	0.08	0.3	24.3	64.8	1.1
74–134/165	25.1	25.2	0.5	0.01	0.04	0.08	0.07	0.2	26.4	133.3	0.8
134/165–250	—	—	—	—	—	—	—	—	—	—	—

[a] Sum of extractable acidity and TEB.

[b] BS determined from TEB ÷ CEC sum of cations × 100.

[c] TEB (sum of Ca, K, Mg, and Na) determined by extraction in ammonium acetate (pH 7).

[d] CEC determined by extraction in ammonium acetate (pH 7).

[e] BS determined as (TEB ÷ ECEC) × 100.

TABLE F.5. Pedogenic metal oxides extractable in acid-ammonium oxalate and buffered dithionite by genetic horizon in the Honda B soil. $Fe_{ox}:Fe_d$ ratio, oxalate-extractable iron/dithionite-extractable iron.

	Dithionite extraction			Oxalate extraction						
Horizon	Al	Fe	Mn	Al	Fe	Mn	P	Si	Al+½Fe	$Fe_{ox}:Fe_d$
—cm—	%			mg g^{-1}					—%—	
0–10	0.83	1.46	<0.01	9.50	7.72	0.02	0.32	0.67	1.34	0.53
10–25	0.76	0.78	<0.01	11.54	4.89	<0.01	0.15	1.80	1.40	0.63
25–74	0.21	0.22	<0.01	3.72	0.70	<0.01	0.02	0.35	0.41	0.32
74–134/165	0.25	0.38	<0.01	3.96	0.42	<0.01	0.03	0.45	0.42	0.11
134/165–250	0.50	6.88	0.02	3.90	1.50	0.02	0.04	0.34	0.47	0.02

TABLE F.6. Total elements by nitric acid digestion by genetic horizon in the Honda B soil.

Horizon	Al	B	Ca	Cu	Fe	K	Mg	Mn	Na	P	Zn
—cm—						mg g^{-1}					
0–10	69.0	<0.005	3.04	0.065	28.4	2.65	3.19	0.25	0.70	0.653	0.112
10–25	118.8	<0.005	0.86	0.163	23.6	4.35	3.26	0.21	0.24	0.365	0.100
25–74	132.0	<0.005	0.06	0.229	17.2	2.78	2.47	0.15	0.08	0.195	0.095
74–134/165	133.8	<0.005	0.07	0.214	21.5	0.40	3.08	0.21	0.09	0.213	0.116
134/165–250	112.4	0.007	0.98	0.177	100.6	0.49	3.82	0.43	0.10	0.663	0.149

TABLE F.7. Detailed particle-size distribution and glass contents in the Honda B profile. Note that glass includes glass, glass coated grains, and glass aggregates, although the majority were glass grains. For grain counts, 30% of the fine earth must be coarse silt and sand (0.02 to 2 mm). GS = glass grains; GC = glass-coated grains; GA = glass aggregates.; tr = trace. Fractions in bold were analyzed for glass content.

	Particle-size distribution (%)								Grain counts (%)		
Horizon	Clay	Fine silt	Coarse silt	Very fine sand	Fine sand	Medium sand	Coarse sand	Very coarse sand	Coarse silt	Fine sand	Mean glass[a]
—cm—		—%—	—%—	—%—	—%—	—%—	—%—	—%—			
10–25	22.9	36.4	**7.2**	6.3	**7.5**	9.3	6.6	3.8	GS 1, GA 1, GC, tr	GS 1, GA 1, GC, tr	1%
25–74	29.0	39.7	**7.9**	5.6	**7.2**	6.4	3.4	0.8	GS 5, GA 2, GC, tr	GA tr	3.7%

[a] Mass-weighted average of coarse silt and fine sand.

Additional Data: Honda B (30–50 cm and 150–200 cm). BS = base saturation; ECEC = effective cation exchange capacity; sat = saturation; TEB = total exchangeable bases; nd = not detected; tr = trace.

	Dithionite–citrate extraction			Ammonium oxalate extraction					
Horizon	Al	Fe	Mn	Al	Fe	Si	Al+½Fe	Mn	P
—cm—		%				%		—mg kg^{-1}—	
25–74	0.5	0.4	nd	0.81	0.22	0.21	0.92	1.1	177.6
134/165–250	0.5	8.6	tr	0.43	0.28	0.06	0.57	26.2	51.2

	Ammonium acetate extraction							
Horizon	Ca	K	Mg	Na	TEB	CEC[a]	BS	CEC per kg clay
—cm—			cmol$_c$ kg^{-1}				%	cmol$_c$ kg^{-1}
25–74	nd	0.1	tr	tr	0.1	17.4	1	46.4
134/165–250	nd	0.1	0.1	tr	0.2	25.9	1	114.6

	KCl extraction		Barium chloride–triethanolamine extraction (pH 8.2)				
Horizon	Al	Mn	Acidity	CEC[b]	BS	ECEC[c]	Al sat
	cmol$_c$ kg^{-1}	mg kg^{-1}	———cmol$_c$ kg^{-1}———		%	cmol$_c$ kg^{-1}	%
3	4.3	tr	23	23.1	0	4.4	98
7	11.4	0.1	23.8	23.8	1	11.6	98

[a] NH_4OAC extraction and measurement of the subsequently displaced NH_4 (i.e., includes bases, exchangeable acidity, etc.).

[b] NH_4OAC bases + acidity (at pH 8.2).

[c] ECEC (NH_4OAC-extractable bases plus KCl-extractable Al).

	X-ray[a]		Thermal	
	30–50 cm	150–200 cm	30–50 cm	150–200 cm
	————Peak size————		————%————	
Kaolinite	nd	nd	67	62
Goethite	nd	nd	nd	nd
Hematite	nd	nd	nd	nd
Halloysite	2	2	nd	nd
Gibbsite	1	nd	3	nd
Vermiculite	1	nd	nd	nd
Montmorillonite	nd	nd	nd	nd
Cristobalite	nd	nd	nd	nd
Quartz	nd	nd	nd	nd
Interpretation			Kaolinitic	Kaolinitic

[a] Values refer to relative peak size (5 = very large, 4 = large, 3 = medium, 2 = small, 1 = very small).

G. Hornito A Forest Census Plot, Fortuna Forest Reserve, Panama (Figure 3.7)

Soil taxonomy:	Fine, kaolinitic, isothermic, Andic Haplohumult
Profile location:	Park at Hornito (south side of Continental Divide) at the entrance to the Jilguera Cabins. Climb the clear trail marked with yellow signs toward the Lost and Found Hostel up and over the ridge (~30 min). As the trail descends on the far side, a marked trail to the left leads to the plot. The pit was located to the west of the plot near the 00,50 marker.
Latitude/longitude:	8.676193°N, –82.214611°E
UTM:	17P, 0366371 m E., 0959267 m N.
Date and season:	4 July 2008, wet season; reexamined 26 February 2010 (dry season) and 23 January 2016
Elevation:	1,330 m asl
Slope and site position:	Steep (~30%) irregular backslope, facing northwest; slightly convex lateral
Soil moisture regime:	Perudic: mean annual rainfall 5,164 ± 232 mm, with 203 ± 28 mm mean monthly dry season rainfall (1 January–30 April)
Soil temperature regime:	Isothermic: mean annual temperature 17.2°C, with mean monthly temperature varying by <2°C over the annual cycle
Parent material:	Porphyritic dacite (intermediate between andesite and rhyolite)
Vegetation:	Lower montane tropical rainforest; canopy height 23 m; closed canopy, with abundant canopy trees in the Myrtaceae, Meliaceae, and Sapotaceae; a few ectomycorrhizal oaks (*Quercus* spp.) and walnuts (Juglandaceae) and large strangler figs (*Ficus* sp.); relatively open understory with small-stemmed bamboo (*Chusquea*)
Drainage:	Moderately well drained
Surface features:	Thick complete cover of leaf litter
Faunal activity:	Some earthworms and other grubs to >1 m
Coarse fragments:	Weathered gravel and cobbles throughout
Rooting depth:	To at least 160 cm, with a thick root mat at the surface
Control section:	Between 16 and 66 cm below the soil surface (i.e., the upper 50 cm of the argillic horizon)
Mineralogy class:	Kaolinitic (>50% kaolinite by thermal XRF)
Particle-size control section:	Fine (35%–60% clay)
Cation-exchange activity class:	Not applicable to kaolinitic mineralogy class
Diagnostic horizons/features:	(1) Perudic moisture regime and isothermic temperature regime (2) Ochric epipedon from 8 to 16 cm (3) Argillic horizon from 16 to 91 cm with a clay decrease of ≥20% below

General Features of the Soil

The soil is formed in porphyritic dacite, which is exposed on the ridgeline above the plot. The profile is dark brown throughout, with abundant weathered gravel and a thick organic horizon composed primarily of fine roots. There are moderate andic properties in the epipedon, which is relatively fertile, particularly in terms of P and base cations. However, subsoil cation concentrations are very low. Augering through the pit floor was stopped at 240 cm by boulders or bedrock.

Soil Taxonomy

The soil is an Ultisol because it has an argillic horizon and low base saturation 125 cm below the upper boundary of the argillic horizon (i.e., <35% by sum of cations at 141 cm). It is a Humult because it contains >0.9% organic C in the upper 15 cm of the argillic horizon and >12 kg C m^{-2} in the upper meter of soil (15.2 g C m^{-2}). There is no kandic horizon, as ECEC is >12 $cmol_c$ kg^{-1} clay, and the clay concentration decreases by >20% below the maximum in the upper 150 cm, so the profile qualifies as a Haplohumult. The profile qualifies as an Andic Haplohumult because it has a bulk density of <1.0 g cm^{-3} and contains Al+½Fe of >1.0% in at least 18 cm of the upper 75 cm of the mineral soil (i.e., 16–40 cm). The soil moisture regime is perudic because rainfall exceeds evapotranspiration in all months.

Chemical and Physical Properties

The soil is clay rich, and there is a marked clay increase, although clay films are clear only in the Bt2 horizon. The soil is strongly acid throughout. Carbon concentrations are relatively high in the upper meter of the profile. Exchangeable base cations are low in the subsoil and dominated by Ca, with low concentrations of K. Base saturation declines with depth through the profile. The subsoil contains high concentrations of dithionite Fe

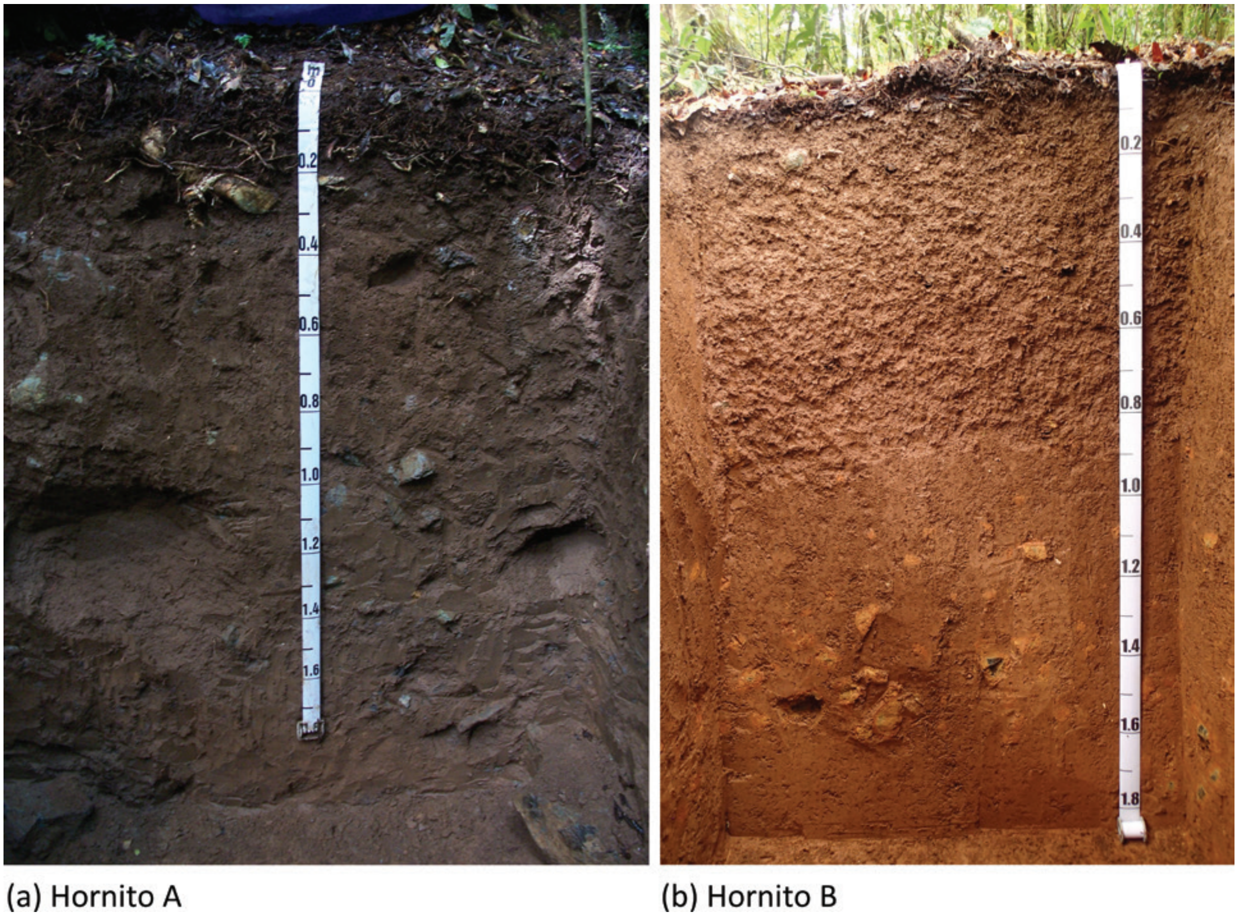

FIGURE 3.7. The profiles at (a) Hornito A and (b) Hornito B.

and very high oxalate Mn concentrations. The profile has moderate andic properties, particularly in the Bt horizon, but like the other Andic Haplohumults (Honda A and Honda B), the clay fraction of the Bt horizon is dominated by kaolinite. Vermiculite is also present in the BC horizon (by XRF). The subsoil contains 8% dithionite Fe and very high Mn_{ox}.

Horizon Description: Hornito A

Oe—0 to 8 cm; black (7.5YR 2.5/1) moderately decomposed organic horizon; many coarse, medium, fine, and very fine roots; abrupt smooth boundary.

A—8 to 16 cm; very dark gray (7.5YR 3/1) gravelly sandy loam; fine granular structure; slightly sticky and not plastic; about 5% weathered cobbles and 11% weathered gravel; many very fine, fine, medium, and coarse roots; clear smooth boundary.

Bt1—16 to 40 cm; dark brown (7.5YR 3/2) gritty clay loam; weak coarse subangular blocky structure, breaking to moderate fine and very fine subangular blocky and fine granular; moist and friable, sticky and plastic; about 10% weathered cobbles and gravel; no clear clay films; common fine and very fine, and few medium and coarse roots; gradual smooth boundary.

Bt2—40 to 91 cm; dark brown (7.5YR 3/2) clay; moderate fine wedge structure, breaking to moderate fine and very fine subangular blocky and fine granular; moist and friable; sticky and very plastic; 4% weathered gravel, identified as andesitic breccia; thin clay films on faces of fine peds; few medium, fine, and very fine roots; gradual smooth boundary.

BC—91 to 180 cm; dark brown (7.5YR 3/3) cobbly clay (loam); moderate coarse wedge structure, breaking to moderate coarse subangular blocky and then fine and very fine subangular blocky and fine granular; friable; about 10% weathered cobbles and 7% weathered gravel; sticky to very sticky and very plastic; thin clay films on faces of fine peds; very few medium, fine, and very fine roots; gradual smooth boundary.

C—180 to 240 cm; dark brown (7.5YR 3/3) sandy clay loam; no stones; no roots.

Laboratory Analysis: Hornito A

TABLE G.1. Soil physical properties, including bulk density and particle-size distribution, by genetic horizon in the Hornito A soil. Dash (—) = not determined.

Horizon	Designation	Bulk density	Stones (>2 mm)	Sand	Silt	Clay	Textural class	Clay:silt ratio
—cm—		—g cm^{-3}—	—%—	—%—	—%—	—%—		
0–8	Oe	0.08	0	—	—	—	Organic	—
8–16	A	0.37	10.5	25.1	30.6	44.4	Clay	1.45
16–40	Bt1	0.52	4.2	24.8	20.1	55.1	Clay	2.74
40–91	Bt2	1.15	3.5	24.4	23.9	51.7	Clay	2.16
91–180	BC	1.37	7.8	26.4	29.6	44.0	Clay	1.49
180–240	C	—	—	36.4	25.8	37.7	Clay loam	1.46

TABLE G.2. Soil pH and total carbon and nitrogen by genetic horizon in the Hornito A soil.

Horizon	Soil pH			Total C	Total N	C:N	C:P	N:P
—cm—	Water	CaCl$_2$	BaCl$_2$	—%—	—%—			
0–8	4.97	4.67	4.19	43.55	3.42	12.7	234	18.4
8–16	5.31	4.80	4.36	7.38	0.68	10.9	73	6.7
16–40	5.08	4.23	4.17	3.05	0.28	10.8	50	4.5
40–91	5.05	4.19	4.13	1.39	0.13	10.5	30	2.8
91–180	5.09	4.09	4.07	0.29	0.02	12.8	10	0.7
180–240	5.27	4.17	4.03	0.40	0.05	8.4	12	1.5

TABLE G.3. Exchangeable cations and effective cation exchange capacity (ECEC) by extraction in 0.1 M barium chloride (BaCl$_2$) by genetic horizon in the Hornito A soil. BS = base saturation; sat = saturation; TEB = total exchangeable bases; dash (—) = not determined.

Horizon	Al	Ca	Fe	K	Mg	Mn	Na	TEB[a]	ECEC[b]	BS[c]	ECEC per kg clay	Al sat	Ca:Mg
—cm—	cmol_c kg^{-1}									—%—	cmol_c kg^{-1}	—%—	
0–8	1.19	51.06	0.02	1.49	9.37	2.03	0.57	62.5	65.7	95.1	—	2	5.4
8–16	1.16	12.25	0.02	0.35	3.67	0.54	0.17	16.4	18.2	90.5	40.9	6	3.3
16–40	4.37	3.16	0.03	0.05	1.29	0.32	0.14	4.6	9.4	49.6	17.0	47	2.4
40–91	6.22	2.10	<0.01	0.04	0.81	0.28	0.16	3.1	9.6	32.3	18.6	65	2.6
91–180	9.78	1.34	0.02	0.04	1.15	0.17	0.22	2.7	12.7	21.6	28.9	77	1.2
180–240	8.26	2.15	0.01	0.03	2.47	0.11	0.17	4.8	13.2	36.5	35.0	63	0.9

[a] TEB determined by extraction in 0.1 M BaCl$_2$.

[b] ECEC determined as the sum of cations extracted in extraction in 0.1 M BaCl$_2$.

[c] BS determined as (TEB ÷ ECEC) × 100.

TABLE G.4. Extractable acidity, exchangeable cations, and cation exchange capacity (CEC) determined in buffered solutions by genetic horizon in the Hornito A soil. BS = base saturation; TEB = total exchangeable bases; dash (—) = not determined.

Horizon	Extractable acidity	CEC by sum of cations[a]	BS by sum of cations[b]	CEC7[c]	Ca	K	Mg	Na	TEB åby CEC7[d]	BS by CEC7[e]
—cm—	cmol$_c$ kg^{-1}	cmol$_c$ kg^{-1}	—%—	cmol$_c$ kg^{-1}	cmol$_c$ kg^{-1}	cmol$_c$ kg^{-1}	cmol$_c$ kg^{-1}	cmol$_c$ kg^{-1}	cmol$_c$ kg^{-1}	—%—
0–8	—	—	—	—	—	—	—	—	—	—
8–16	—	—	—	—	—	—	—	—	—	—
16–40	39.1	43.7	11	—	—	—	—	—	—	—
40–91	33.4	36.5	9	—	—	—	—	—	—	—
91–180	29.3	32.1	9	—	—	—	—	—	—	—
180–240	—	—	—	—	—	—	—	—	—	—

[a] Sum of extractable acidity and TEB.

[b] BS determined from TEB ÷ CEC sum of cations × 100.

[c] CEC determined by extraction in ammonium acetate (pH 7).

[d] TEB (sum of Ca, K, Mg, and Na) determined by extraction in ammonium acetate (pH 7).

[e] BS determined as (TEB ÷ ECEC) × 100.

TABLE G.5. Pedogenic metal oxides extractable in acid-ammonium oxalate and buffered dithionite by genetic horizon in the Hornito A soil. $\mathrm{Fe_{ox}:Fe_d}$ ratio, oxalate-extractable iron/dithionite-extractable iron.

	Dithionite extraction			Oxalate extraction						
Horizon	Al	Fe	Mn	Al	Fe	Mn	P	Si	Al+½Fe	$\mathrm{Fe_{ox}:Fe_d}$
—cm—	%			mg g^{-1}					—%—	
0–8	0.50	0.46	0.09	5.14	0.68	0.53	0.61	0.04	0.55	0.15
8–16	0.94	5.45	0.25	9.97	7.90	1.73	0.42	0.84	1.39	0.14
16–40	0.86	5.97	0.19	9.15	7.92	1.32	0.23	0.79	1.31	0.13
40–91	0.81	6.10	0.18	8.29	6.88	1.14	0.15	0.93	1.17	0.11
91–180	0.79	7.54	0.16	5.56	2.92	0.89	0.06	0.57	0.70	0.04
180–240	0.73	6.05	0.15	6.44	3.65	0.89	0.08	0.68	0.83	0.06

TABLE G.6. Total elements by nitric acid digestion by genetic horizon in the Hornito A soil.

Horizon	Al	B	Ca	Cu	Fe	K	Mg	Mn	Na	P	Zn
—cm—	mg g^{-1}										
0–8	12.1	0.028	13.28	0.027	6.6	0.99	2.17	0.84	0.23	1.554	0.047
8–16	97.6	0.013	3.95	0.111	83.6	2.05	8.90	2.66	0.45	0.940	0.121
16–40	111.7	0.007	1.83	0.160	105.4	1.80	13.28	2.29	0.41	0.556	0.115
40–91	123.6	0.017	1.06	0.172	99.1	1.99	8.14	2.19	0.30	0.480	0.110
91–180	130.1	0.010	0.60	0.160	108.9	1.52	9.18	1.79	0.21	0.377	0.099
180–240	129.2	<0.005	0.44	0.190	101.9	2.22	8.38	1.95	0.23	0.385	0.105

Additional Data (NRCS): Hornito A. BS = base saturation; ECEC = effective cation exchange capacity; sat = saturation; TEB = total exchangeable bases; nd = not detected; tr = trace.

	Dithionite–citrate extraction			Ammonium oxalate extraction					
Horizon	**Al**	**Fe**	**Mn**	**Al**	**Fe**	**Si**	**Al+½Fe**	**Mn**	**P**
—cm—	%			%				mg kg^{-1}	
16–40	1.0	8.0	0.2	1.02	1.10	0.10	1.57	1,834.9	236.2
90–100	0.9	8.1	0.2	0.83	0.65	0.12	1.16	1,290.6	100.5

	Ammonium acetate extraction							
Horizon	**Ca**	**K**	**Mg**	**Na**	**TEB**	**CEC[a]**	**BS**	**CEC per kg clay**
—cm—	$\text{cmol}_c\ \text{kg}^{-1}$						%	$\text{cmol}_c\ \text{kg}^{-1}$
16–40	2.8	0.1	1.4	tr	4.3	27.6	16	50.1
90–100	0.8	0.1	0.8	nd	1.7	25.8	7	58.6

	KCl extraction		Barium chloride–triethanolamine extraction (pH 8.2)				
Horizon	**Al**	**Mn**	**Acidity**	**CEC[b]**	**BS**	**ECEC[c]**	**Al sat**
—cm—	$\text{cmol}_c\ \text{kg}^{-1}$	mg kg^{-1}	$\text{cmol}_c\ \text{kg}^{-1}$		%	$\text{cmol}_c\ \text{kg}^{-1}$	%
16–40	4.6	7.8	38.4	42.7	10	8.9	52
90–100	9.5	3.7	32.1	33.8	5	11.2	85

[a] NH$_4$OAC extraction and measurement of the subsequently displaced NH$_4$ (i.e., includes bases, exchangeable acidity, etc.).

[b] NH$_4$OAC bases + acidity (at pH 8.2).

[c] ECEC (NH$_4$OAC-extractable bases plus KCl-extractable Al).

	X-ray[a]		Thermal	
	16–40 cm	**90–100 cm**	**16–40 cm**	**90–100 cm**
	Peak size		%	
Kaolinite	2	nd	62	54
Goethite	nd	nd	7	9
Hematite	nd	nd	nd	nd
Halloysite	nd	2	nd	nd
Gibbsite	1	2	nd	nd
Vermiculite	2	2	nd	nd
Montmorillonite	nd	nd	nd	nd
Cristobalite	nd	nd	nd	nd
Quartz	nd	nd	nd	nd
Interpretation			Kaolinitic	Kaolinitic

[a] Values refer to relative peak size (5 = very large, 4 = large, 3 = medium, 2 = small, 1 = very small).

H. Hornito B Forest Census Plot, Fortuna Forest Reserve, Panama (Figure 3.7)

Soil taxonomy:	Very fine, parasesquic, isothermic, Typic Haplohumult
Profile location:	From the STRI station, drive south on the main road through the guard gate and park on the left at UTM 17P, 0365570 m E., 0959026 m N., next to a small shop. Follow the track uphill toward the Jilguera Cabins and Lost and Found hostel. Continue up and over the ridge, following the trail downhill toward the river. Take the left trail at the fork and continue for ~5 minutes. The plot is on the left (uphill) side of the trail, and the profile pit is ~50 m uphill from the trail on the end of a broad spur. Hornito B is approximately 200 m downslope of the Hornito A plot.
Date and season:	7 December 2018; late wet season (wet-dry season transition)
Latitude/longitude:	8.678430°N, –82.213501°E
UTM:	17P, 0366494 m E., 0959514 m N.
Elevation:	1,296 m asl
Slope and site position:	Steep (35%) lower backslope, facing east; slightly convex radial and convex lateral
Parent material:	Porphyritic dacite (stones in the pit conform to this)
Soil moisture regime:	Perudic: mean annual rainfall at Hornito A 5,164 ± 232 mm, with 203 ± 28 mm mean monthly dry season rainfall (1 January–30 April) (2 months max with <100 mm during year)
Soil temperature regime:	Isothermic: mean annual temperature at Hornito A 17.2°C, with mean monthly temperature varying by <2°C over the annual cycle
Vegetation:	Lower montane tropical forest; canopy height 20 to 25 m; relatively open, moderately tall canopy (~25 m tall) dominated by the ectomycorrhizal tree *Oreomunnea mexicana* (Juglandanceae); common small stems but relatively open understory with few ferns and very few palms
Drainage:	Moderately well drained
Surface features:	Thin discontinuous cover of wet leaves (~90%)
Faunal activity:	Few small earthworms in upper 36 cm
Coarse fragments:	Common subangular coarse gravel in subsoil, with black cores and yellowish-red (5YR 5/6) weathering rinds, with speckled features characteristic of weathered dacite porphyres
Rooting depth:	Throughout the profile to at least 185 cm, but fine roots predominantly in the upper 6 cm, and coarse roots predominantly in the upper 56 cm
Control section:	Between 20 and 70 cm below the soil surface (i.e., the upper 50 cm of the argillic horizon)
Mineralogy class:	Parasesquic (dithionite Fe × 1.43 >10%)
Particle-size class:	Very fine (>60% clay)
Cation exchange activity class:	Not applicable
Diagnostic horizons and features:	(1) Perudic moisture regime and isothermic temperature regime (2) Ochric epipedon from 6 to 20 cm (3) Argillic horizon from 3,620 to 84 cm (4) Clay decrease >20% below the maximum within 150 cm of the mineral soil surface

General Features of the Soil

This soil is developed on porphyritic dacite, although it is on the boundary with undifferentiated mafic volcanics. It is acidic, clay rich, and has a thin organic horizon over a shallow brown epipedon. The soil is well structured and infertile, with high concentrations of iron oxides. Compared to Hornito A, this profile is more acidic and has much lower Ca, Mg, and Mn and higher Al (and Al saturation). In fact, concentrations of Ca are extremely low in Hornito B. The soil organic matter has a much wider C:N ratio than Hornito A, characteristic of ectomycorrhizal-dominated forest.

Soil Taxonomy

The profile has an argillic horizon, although this is marginal, with the clay concentration increasing from 55% to 63%, the minimum 8% increase allowed for high-clay soils. ECEC and CEC values indicate low activity clays, but the clay increase occurs over more than 15 cm, so the argillic horizon does not qualify as kandic, and the profile therefore does not qualify as an Oxisol. Instead, the argillic horizon and low base saturation at depth qualifies the soil as an Ultisol. The profile is a Humult because of the high concentration of organic matter in the upper 15 cm of the argillic horizon. It does not quite qualify as a Palehumult because the clay concentration decreases by 20% from the maximum in the upper 150 cm. In the absence of other diagnostic features, the profile qualifies as a Typic Haplohumult.

The soil moisture regime is perudic because rainfall exceeds potential evapotranspiration in all months.

The mineralogy class is parasesquic because Fe_d × 1.43 = >12%, and Hornito A contains some gibbsite (mentioned in the parasesquic criteria). If the profile has an oxic horizon or a kandic horizon, the mineralogy class would likely be kaolinitic, based on cation exchange capacity of the clay fraction and XRF analysis of Hornito A.

This profile is on the boundary of Ultisol and Oxisol. If the clay increase were just 1% greater in the 20 to 36 cm horizon, then it would qualify as a kandic horizon, and the profile would classify as an Oxisol (i.e., a kandic horizon and >40% clay). If the clay concentration in the 36 to 56 cm horizon were 1% less, then there would be no argillic horizon and the soil would also qualify as an Oxisol (i.e., with an oxic horizon).

Chemical and Physical Properties

The soil has a thin organic horizon over a clay-rich mineral soil. Cation concentrations are extremely low, and Al saturation is very high (>90% in the mineral soil).

Horizon Description: Hornito B

Oe—0 to 6 cm; very dark brown (10YR 2/2) cohesive but loose mat of moderately decomposed organic matter, including many small leaf fragments, varying from 3 to 6 cm thick around the pit; many very fine, fine, medium, and coarse roots; abrupt wavy boundary.

A—6 to 20 cm; brown (5YR 4/3) clay loam; strong fine and very fine subangular blocky structure; moist and friable to firm; sticky and plastic; few hard subangular mixed gravel (<1%); common fine and medium tubular pores; few very fine and fine, and common medium and coarse roots;

Bt1—20 to 36 cm; dark reddish-brown (5YR 4/4) clay; moderate coarse subangular blocky structure, breaking to strong fine and very fine subangular blocky; moist and firm; sticky and very plastic; about 2% hard subangular fine gravel; faint continuous clay films on ped faces and pore linings; few fine and medium tubular pores; few very fine, fine, and medium roots; gradual smooth boundary.

Bt2—36 to 56 cm; dark reddish-brown (5YR 3/4) clay; moderate very coarse subangular blocky structure, breaking to strong medium, fine, and very fine subangular blocky; moist and firm; sticky and very plastic; few hard subangular fine gravel (<1%); faint continuous clay films on ped faces; very few fine and medium tubular pores; few very fine, fine, and medium, and common coarse roots – appears to be a coarse root threshold at the lower boundary; gradual smooth boundary.

Bt3—56 to 84 cm; dark reddish-brown (5YR 3/4) clay; moderate coarse subangular blocky structure, breaking to strong medium, fine, and very fine subangular blocky; moist and firm; slightly sticky and very plastic; faint continuous clay films on ped faces; very few fine and medium tubular pores; few very fine, fine, medium, and coarse roots; gradual smooth boundary.

BC1—84 to 151 cm; reddish-brown (5YR 4/4) silty clay; weak coarse subangular blocky structure, breaking to strong medium, fine, and very fine subangular blocky; moist and firm to friable; slightly sticky and very plastic; about 20% weathered coarse gravel with black interiors, increasing in abundance with depth; faint continuous clay films on ped faces; very few fine tubular pores; very few very fine, fine, and medium roots; gradual wavy boundary.

BC2—151 to 270+ cm; [includes auger sample] red (2.5YR 4/6) (silty) clay (loam); moderate coarse subangular blocky structure, breaking to strong medium, fine, and very fine subangular blocky; moist and firm; slightly sticky and plastic; few very fine interstitial pores; very few fine and medium roots; about 2% hard black coarse gravel.

Laboratory Analysis: Hornito B

TABLE H.1. Soil physical properties, including bulk density and particle-size distribution, by genetic horizon in the Hornito B soil. Dash (—) = not determined.

Horizon	Designation	Bulk density (fine earth)	Coarse fragments	Sand	Silt	Clay	Textural class	Clay:silt ratio
—cm—		—g cm^{-3}—	—vol%—	—%—	—%—	—%—		
0–6	Oe	0.04	0	—	—	—	—	—
6–20	A	0.80	<1	15.7	29.7	54.6	Clay	1.8
20–36	Bt1	1.15	2	9.5	29.0	61.6	Clay	2.1
36–56	Bt2	1.11	<1	9.3	28.1	62.6	Clay	2.2
56–84	Bt3	1.10	<1	7.5	29.8	62.7	Clay	2.1
84–151	BC1	1.20	20	7.0	34.1	58.9	Clay	1.7
151–185	BC2 (1)	1.25	2	5.2	44.4	50.4	Silty clay	1.1
185–270	BC2 (2)	—	—	5.3	45.9	48.8	Silty clay	1.1

TABLE H.2. Soil pH and total carbon and nitrogen by genetic horizon in the Hornito B soil.

Horizon	Soil pH			Total C	Total N	C:N	C:P	N:P
—cm—	Water	$CaCl_2$	$BaCl_2$	—%—	—%—			
0–6	4.13	3.21	3.10	35.86	1.86	19.3	1064	55.2
6–20	4.36	3.66	4.10	5.22	0.31	16.7	201	11.9
20–36	4.78	3.87	3.94	1.36	0.08	17.1	54	3.2
36–56	4.79	4.00	4.11	1.13	0.06	18.9	67	3.6
56–84	4.81	3.94	4.15	0.90	0.05	17.9	45	2.5
84–151	4.71	3.92	4.12	0.63	0.03	18.4	25	1.2
151–185	4.60	3.90	4.07	0.28	0.01	19.8	10	0.4
185–270	4.64	3.85	4.04	0.28	0.02	18.3	5	0.4

TABLE H.3. Exchangeable cations and effective cation exchange capacity (ECEC) by extraction in 0.1 M barium chloride ($BaCl_2$) by genetic horizon in the Hornito B soil. BS = base saturation; sat = saturation; TEB = total exchangeable bases; dash (—) = not determined.

Horizon	Al	Ca	Fe	K	Mg	Mn	Na	TEB[a]	ECEC[b]	BS[c]	ECEC per kg clay	Al sat	Ca:Mg
—cm—	$\text{cmol}_c\ \text{kg}^{-1}$									—%—	$\text{cmol}_c\ \text{kg}^{-1}$	—%—	
0–6	1.44	10.40	0.14	0.83	3.88	0.80	0.55	15.65	18.0	86.8	—	8	2.7
6–20	5.81	0.12	0.04	0.05	0.05	<0.01	0.11	0.33	6.2	5.3	11.3	94	2.3
20–36	7.32	0.12	0.04	0.06	0.12	<0.01	0.05	0.35	7.7	4.5	12.5	95	1.0
36–56	6.02	0.10	<0.01	0.03	0.05	<0.01	0.03	0.21	6.2	3.3	10.0	96	2.2
56–84	6.26	0.09	<0.01	0.03	0.04	<0.01	0.04	0.19	6.5	3.0	10.3	97	2.3
84–151	7.08	0.05	<0.01	0.01	0.04	<0.01	0.05	0.15	7.2	2.1	12.3	98	1.1
151–185	8.71	0.03	<0.01	0.01	0.04	<0.01	0.04	0.12	8.8	1.4	17.5	99	0.6
185–270	9.68	0.02	<0.01	<0.01	0.05	0.01	0.05	0.13	9.8	1.3	20.1	99	0.5

[a] TEB determined by extraction in 0.1 M $BaCl_2$.

[b] ECEC determined as the sum of cations extracted in extraction in 0.1 M $BaCl_2$.

[c] BS determined as (TEB ÷ ECEC) × 100.

TABLE H.4. Extractable acidity, exchangeable cations, and cation exchange capacity (CEC) determined in buffered solutions by genetic horizon in the Hornito B soil. BS = base saturation; TEB = total exchangeable bases; dash (—) = not determined.

Horizon	Extractable acidity	CEC by sum of cations[a]	BS by sum of cations[b]	CEC7[c]	Ca	K	Mg	Na	TEB by CEC7[d]	BS by CEC7[e]	CEC7 per kg clay
—cm—	$\text{cmol}_c\ \text{kg}^{-1}$	$\text{cmol}_c\ \text{kg}^{-1}$	—%—	$\text{cmol}_c\ \text{kg}^{-1}$						—%—	$\text{cmol}_c\ \text{kg}^{-1}$
0–6	—	—	—	—	—	—	—	—	—	—	—
6–20	—	—	—	—	—	—	—	—	—	—	—
20–36	—	—	—	7.3	0.03	0.07	0.05	0.02	0.17	2.3	11.8
36–56	—	—	—	8.3	0.03	0.05	0.04	0.02	0.13	1.6	13.2

(*Continued*)

TABLE H.4. (*Continued*)

Horizon	Extractable acidity	CEC by sum of cations[a]	BS by sum of cations[b]	CEC7[c]	Ca	K	Mg	Na	TEB by CEC7[d]	BS by CEC7[e]	CEC7 per kg clay
—cm—	$\mathrm{cmol_c\ kg^{-1}}$	$\mathrm{cmol_c\ kg^{-1}}$	—%—	$\mathrm{cmol_c\ kg^{-1}}$						—%—	$\mathrm{cmol_c\ kg^{-1}}$
56–84	—	—	—	8.4	0.02	0.04	0.04	0.02	0.13	1.5	13.4
84–151	—	—	—	6.7	0.01	0.02	0.03	0.02	0.08	1.3	11.4
151–185	—	—	—	—	—	—	—	—	—	—	—
185–270	—	—	—	—	—	—	—	—	—	—	—

[a] Sum of extractable acidity and TEB.

[b] BS determined from TEB ÷ CEC sum of cations × 100.

[c] CEC determined by extraction in ammonium acetate (pH 7).

[d] TEB (sum of Ca, K, Mg, and Na) determined by extraction in ammonium acetate (pH 7).

[e] BS determined as (TEB ÷ ECEC) × 100.

TABLE H.5. Pedogenic metal oxides extractable in acid-ammonium oxalate and buffered dithionite by genetic horizon in the Hornito B soil. $\mathrm{Fe_{ox}{:}Fe_d}$ ratio, oxalate-extractable iron/dithionite-extractable iron.

	Dithionite extraction			Oxalate extraction						
Horizon	Al	Fe	Mn	Al	Fe	Mn	P	Si	Al+½Fe	$\mathrm{Fe_{ox}{:}Fe_d}$
—cm—	%			$\mathrm{mg\ g^{-1}}$					—%—	
0–6	0.27	1.32	0.02	1.08	0.59	0.14	0.11	0.05	0.14	0.05
6–20	1.31	7.23	0.01	4.76	4.41	0.01	0.03	0.19	0.70	0.06
20–36	1.30	7.67	0.01	3.98	1.55	0.01	0.01	0.31	0.48	0.02
36–56	1.34	8.59	0.01	3.52	1.28	0.01	0.01	0.28	0.42	0.01
56–84	1.29	8.76	0.01	3.20	0.96	<0.01	0.01	0.28	0.37	0.01
84–151	1.15	8.47	0.01	3.39	0.88	<0.01	0.01	0.32	0.38	0.01
151–185	0.57	4.77	0.02	3.98	1.10	0.06	0.02	0.40	0.45	0.02
185–270	0.78	6.50	0.03	4.49	1.13	0.13	0.02	0.41	0.51	0.02

TABLE H.6. Total elements by nitric acid digestion by genetic horizon in the Hornito B soil.

Horizon	Al	B	Ca	Cu	Fe	K	Mg	Mn	Na	P	Zn
—cm—	$\mathrm{mg\ g^{-1}}$										
0–6	13.2	0.027	1.33	0.019	11.3	0.58	0.71	0.16	0.15	0.337	0.012
6–20	79.5	<0.005	0.29	0.067	77.0	0.53	2.35	0.13	0.24	0.260	0.037
20–36	108.8	<0.005	0.08	0.102	86.8	0.82	2.64	0.17	0.15	0.253	0.042
36–56	70.3	<0.005	0.03	0.069	58.9	0.62	1.54	0.10	0.05	0.168	0.025
56–84	90.9	0.017	0.02	0.086	74.3	0.79	1.78	0.12	0.15	0.200	0.032
84–151	96.4	<0.005	0.01	0.114	78.8	0.94	1.72	0.13	0.07	0.254	0.031
151–185	72.6	0.018	<0.01	0.137	55.0	0.60	1.11	0.21	0.09	0.267	0.031
185–270	140.4	0.006	0.05	0.317	103.1	0.80	1.96	0.47	0.18	0.558	0.064

I. Palo Seco Forest Census Plot, Palo Seco Forest Reserve, Panama (Figure 3.8)

Soil taxonomy: Fine, parasesquic, isothermic, Andic Dystrudept
Profile location: From the Fortuna Station, cross the dam and continue over the Continental Divide. Park on the left side of the road and follow a trail downhill to the plot. The profile pit was located close to 100,60 marker on the far side of the plot (down the trail and to the left, ~20 m from trail).
Latitude/longitude: 8.778643°N, –82.198143°E
UTM: 17P, 0368219 m E., 0970590 m N.
Date and season: 4 July 2008 (wet season); reexamined 26 February 2010 (dry season)
Elevation: 878 m asl
Slope and site position: Steep (>30%) shoulder on a narrow steeply sloping ridge
Soil moisture regime: Perudic: mean annual rainfall 6,257 ± 310 mm, with 445 ± 33 mm mean monthly dry season rainfall (1 January–30 April)
Soil temperature regime: Isothermic: mean annual temperature 19.6°C, with mean monthly temperature varying by <2°C over the annual cycle
Parent material: Coarse-textured undifferentiated basalt, andesite, and diabase
Vegetation: Species-rich lower montane tropical rainforest; canopy height 23 m; closed canopy and very dense understory almost completely filled with short-stature palms (*Geonoma cuneata* and *Chamaedorea* spp.)
Drainage: Moderately well drained
Surface features: Thick leaf litter layer; 100% cover
Faunal activity: Many earthworms throughout the upper part of the profile
Coarse fragments: Common weathered andesite gravel and cobbles
Rooting depth: Throughout the profile to at least 175 cm
Control section: Between 25 and 100 cm below the soil surface
Particle-size class: Fine (between 35% and 60% clay)
Mineralogy class: Parasesquic
Cation-exchange activity class: N/A
Diagnostic horizons/features: (1) Perudic moisture regime and isothermic temperature regime
(2) Ochric epipedon from 0 to 10 cm
(3) Cambic horizon from 10 to 80 cm

General Features of the Soil

This profile is on a steep slope formed in undifferentiated mafic-volcanics. It supports a thick ground cover including many palms. The soil is infertile, with moderate andic properties.

Soil Taxonomy

The profile is an Inceptisol because it has a cambic horizon and a Udept because of the perudic moisture regime. The low base saturation in the subsoil qualifies the profile as a Dystrudept. Moderate andic properties, including bulk density <1.0 g cm^{-3} and oxalate Al+½Fe >1.0%, in at least 18 cm of the upper 75 cm qualify the profile as an Andic Dystrudept.

The profile has parasesquic mineralogy class because total iron oxides such as Fe_2O_3 (Fe_d × 1.43) plus gibbsite are >10 (Fe_d in the control section = 5.73% × 1.43 = 8.2%, and gibbsite in the clay fraction by thermal XRF = 7%–11% with control section clay = 40.4%, giving gibbsite in the fine earth fraction of 3.6%).

The soil moisture regime is perudic because rainfall exceeds potential evapotranspiration in all months.

Chemical and Physical Properties

The profile has a shallow dark yellowish-brown epipedon over a yellowish-brown subsoil. There are many weathered coarse fragments throughout the profile, covered in thick ferromanganese coatings. The soil has a clay texture in the upper part, over a loamy subsoil. Bulk density is low (<1.0 g cm^{-3}) throughout. Soil pH is very strongly to strongly acid, and organic matter concentrations are moderate, with C:N ratios between 12 and 16. Base cation concentrations are extremely low, with TEB of ≤1.2 $cmol_c$ kg^{-1} throughout the profile. Effective cation exchange capacity and base saturation are also very low, although CEC per kg clay at pH 7 is very high, indicating a considerable pH-dependent charge. Aluminum concentrations and saturation are high. Total Al and Fe are very high, both being >100 mg g^{-1} throughout the subsoil, and total P is moderately high. Secondary Fe (Fe_d) and amorphous Al and Fe are moderate; Al+½Fe

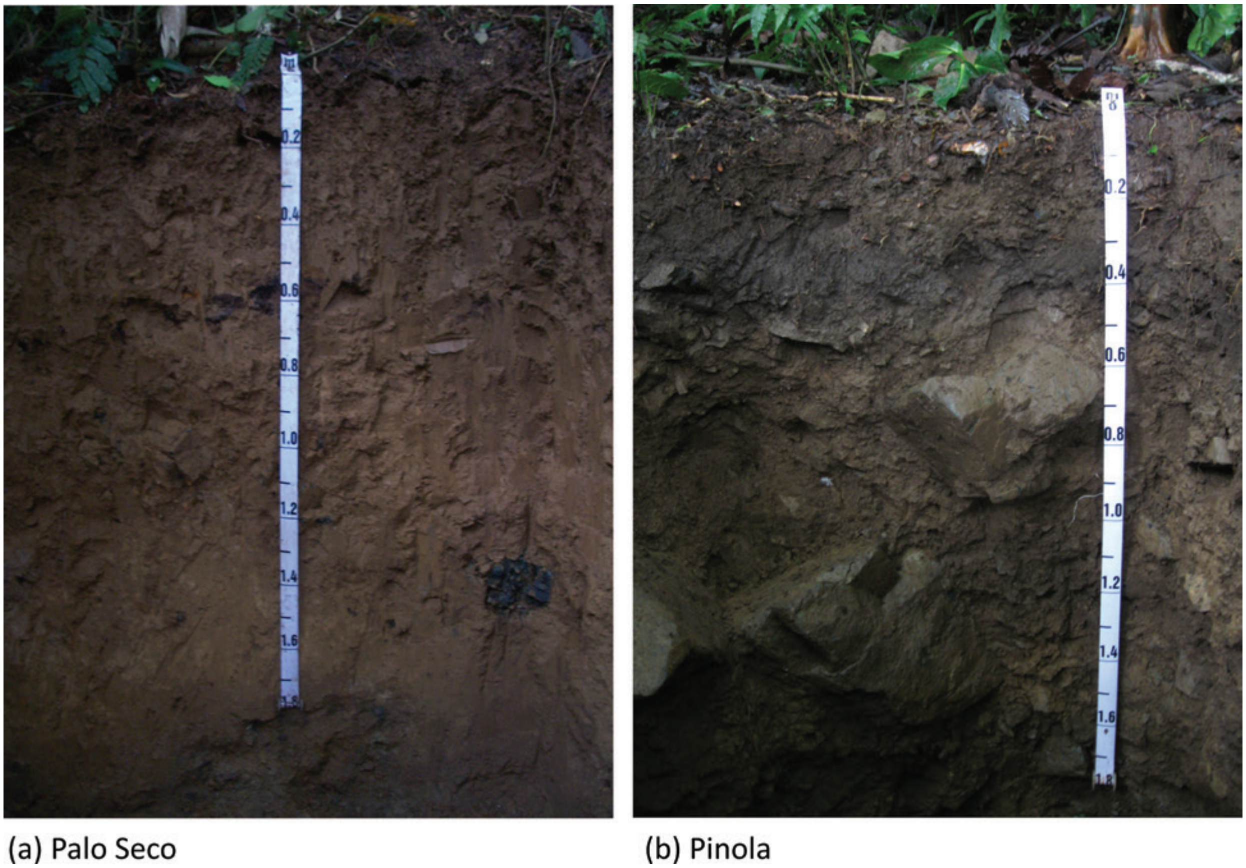

FIGURE 3.8. The profiles at (a) Palo Seco and (b) Pinola.

by oxalate extraction <1.3%. Total Ca is very high in the deep subsoil, but the reason is unclear and is not related to exchangeable Ca.

Horizon Description: Palo Seco

A—0 to 10 cm; dark yellowish-brown (10YR 3/4) sandy clay; moderate coarse subangular blocky structure, breaking to moderate fine subangular blocky; wet and friable; sticky and slightly plastic; many earthworms; common medium and fine tubular pores; many very fine, fine, and medium, and common coarse roots; gradual smooth boundary.

B1—10 to 42 cm; brown (7.5YR 4/4) clay loam; moderate medium subangular blocky structure; wet and friable; sticky and slightly plastic; about 4% angular weathered coarse andesite gravel; common medium and fine tubular pores with clay enriched walls; faint continuous clay films on ped faces; common very fine, fine, and medium, and few coarse roots; clear smooth boundary.

B2—42 to 80 cm; dark yellowish-brown (10YR 4/4) gravelly sandy clay loam; moderate medium and coarse wedge structure, breaking to weak to medium subangular blocky; wet and friable; sticky and slightly plastic; few medium and fine tubular pores; faint discontinuous clay films on ped faces; about 20% angular weathered coarse andesite gravel; few fine and very fine roots; gradual smooth boundary.

BC—80 to 175 cm; dark yellowish-brown (10YR 4/4) gravelly loam; weak medium subangular blocky structure; about 35% weathered subangular andesite coarse gravel and cobbles; very few fine and very fine roots; gradual wavy boundary.

C—175 to 235+ cm; olive brown (2.5Y 4/4) gritty loam; weathered rock prevented further augering.

Laboratory Analysis: Palo Seco

TABLE I.1. Soil physical properties, including bulk density and particle-size distribution, by genetic horizon in the Palo Seco soil. Dash (—) = not determined.

Horizon	Designation	Bulk density (fine earth)	Coarse fragments (>2 mm)	Sand	Silt	Clay	Textural class	Clay:silt ratio
—cm—		—g cm^{-3}—	—%—	—%—	—%—	—%—		
0–10	A	0.41	0	26.6	22.5	50.8	Clay	2.3
10–42	B1	0.72	4	20.3	27.8	51.9	Clay	1.9
42–80	B2	0.89	20	17.0	40.8	42.2	Silty clay	1.0
80–175	BC	0.97	35	30.3	42.6	27.2	Clay loam	0.6
175–235+	C	—	—	49.9	28.8	21.3	Loam	0.7

TABLE I.2. Soil pH and total carbon and nitrogen by genetic horizon in the Palo Seco soil.

Horizon	Soil pH			Total C	Total N	C:N	C:P	N:P
—cm—	Water	$CaCl_2$	$BaCl_2$	—%—	—%—			
0–10	4.36	4.05	4.16	5.54	0.45	12.3	81.7	6.6
10–42	4.74	4.21	4.21	1.85	0.15	12.2	36.4	3.0
42–80	4.94	4.04	4.11	0.70	0.06	12.5	19.1	1.6
80–175	5.05	4.06	4.08	0.18	0.01	15.7	2.2	0.1
175–235+	5.17	4.01	4.36	0.24	0.02	13.5	1.2	0.1

TABLE I.3. Exchangeable cations and effective cation exchange capacity (ECEC) by extraction in 0.1 M barium chloride ($BaCl_2$) by genetic horizon in the Palo Seco soil. BS = base saturation; sat = saturation; TEB = total exchangeable bases.

Horizon	Al	Ca	Fe	K	Mg	Mn	Na	TEB[a]	ECEC[b]	BS[c]	ECEC per kg clay	Al sat	Ca:Mg
—cm—	cmol$_c$ kg^{-1}									—%—	cmol$_c$ kg^{-1}	—%—	
0–10	5.77	0.57	0.03	0.16	0.40	0.09	0.09	1.22	7.1	17.2	14.0	81	1.4
10–42	4.83	0.15	0.02	0.02	0.04	0.05	0.06	0.27	5.2	5.2	10.0	93	3.8
42–80	8.71	0.09	0.02	<0.01	0.04	0.10	0.07	0.20	9.0	2.2	21.4	96	2.3
80–175	8.60	0.36	0.02	<0.01	0.37	0.08	0.10	0.83	9.5	8.7	35.1	90	1.0
175–235+	2.07	0.22	0.02	<0.01	0.14	0.03	0.02	0.38	2.5	15.2	11.7	83	1.6

[a] TEB determined by extraction in 0.1 M $BaCl_2$.

[b] ECEC determined as the sum of cations extracted in extraction in 0.1 M $BaCl_2$.

[c] BS determined as (TEB ÷ ECEC) × 100.

TABLE I.4. Extractable acidity, exchangeable cations, and cation exchange capacity (CEC) determined in buffered solutions by genetic horizon in the Palo Seco soil. BS = base saturation; TEB = total exchangeable bases; dash (—) = not determined.

Horizon	Extractable acidity	CEC by sum of cations[a]	BS by sum of cations[b]	CEC7[c]	Ca	K	Mg	Na	TEB by CEC7[d]	BS by CEC7[e]	CEC7 per kg clay
—cm—	cmol$_c$ kg^{-1}	cmol$_c$ kg^{-1}	—%—	cmol$_c$ kg^{-1}						—%—	cmol$_c$ kg^{-1}
0–10	—	—	—	—	—	—	—	—	—	—	—
10–42	—	—	—	26.7	0.08	0.05	0.09	0.06	0.3	1.0	51.4
42–80	—	—	—	28.4	0.05	0.03	0.11	0.06	0.2	0.8	67.2
80–175	—	—	—	30.3	0.20	0.02	0.32	0.09	0.6	2.1	111.5
175–235+	—	—	—	—	—	—	—	—	—	—	—

[a] Sum of extractable acidity and TEB.

[b] BS determined from TEB ÷ CEC sum of cations × 100.

[c] CEC determined by extraction in ammonium acetate (pH 7).

[d] TEB (sum of Ca, K, Mg, and Na) determined by extraction in ammonium acetate (pH 7).

[e] BS determined as (TEB ÷ ECEC) × 100.

TABLE I.5. Pedogenic metal oxides extractable in acid-ammonium oxalate and buffered dithionite by genetic horizon in the Palo Seco soil. Fe_{ox}:Fe_d ratio, oxalate-extractable iron/dithionite-extractable iron.

	Dithionite extraction			Oxalate extraction						
Horizon	Al	Fe	Mn	Al	Fe	Mn	P	Si	Al+½Fe	Fe_{ox}:Fe_d
—cm—	%			mg g^{-1}					—%—	
0–10	1.07	5.56	0.03	7.38	10.99	0.17	0.18	0.22	1.29	0.20
10–42	1.03	6.08	0.06	6.83	10.02	0.45	0.11	0.35	1.18	0.16
42–80	0.97	6.38	0.15	5.08	5.89	0.93	0.05	0.35	0.80	0.09
80–175	0.68	4.20	0.17	5.56	4.77	1.14	0.22	0.64	0.79	0.11
175–235+	0.43	2.84	0.12	9.19	2.83	0.70	1.06	2.09	1.06	0.10

TABLE I.6. Total elements by nitric acid digestion by genetic horizon in the Palo Seco soil.

	Nitric acid digestion for total elemental analysis										
Horizon	Al	B	Ca	Cu	Fe	K	Mg	Mn	Na	P	Zn
—cm—	mg g^{-1}										
0–10	106.6	0.018	1.35	0.121	99.8	0.68	4.30	0.42	0.52	0.746	0.058
10–42	131.1	0.009	0.87	0.143	103.8	0.59	4.30	0.76	0.37	0.692	0.058
42–80	140.8	0.008	0.13	0.204	111.6	0.64	5.04	1.47	0.17	0.546	0.062
80–175	129.9	0.007	0.15	0.261	100.1	0.25	6.91	1.62	0.17	0.983	0.085
175–235+	124.7	0.010	24.52	0.174	100.4	0.68	15.83	1.61	0.09	1.661	0.190

Additional Data (NRCS): Palo Seco. BS = base saturation; ECEC = effective cation exchange capacity; sat = saturation; TEB = total exchangeable bases; nd = not detected; tr = trace.

	Dithionite–citrate extraction			Ammonium oxalate extraction					
Horizon	**Al**	**Fe**	**Mn**	**Al**	**Fe**	**Si**	**Al+½Fe**	**Mn**	**P**
—cm—	%			%				mg kg^{-1}	
30–40	1.1	8.2	0.1	0.55	1.01	0.04	1.06	365.2	53.9
90–100	0.7	4.0	0.2	0.59	0.68	0.07	0.93	1,262.3	169.7

	Ammonium acetate extraction							
Horizon	**Ca**	**K**	**Mg**	**Na**	**TEB**	**CEC**[a]	**BS**	**CEC per kg clay**
—cm—	$\text{cmol}_c\ \text{kg}^{-1}$						%	$\text{cmol}_c\ \text{kg}^{-1}$
30–40	nd	tr	0.1	tr	0.1	18.3	1	35.3
90–100	nd	tr	0.2	tr	0.2	18.9	1	69.5

	KCl extraction		Barium chloride–triethanolamine extraction (pH 8.2)				
Horizon	**Al**	**Mn**	**Acidity**	**CEC**[b]	**BS**	**ECEC**[c]	**Al sat**
—cm—	$\text{cmol}_c\ \text{kg}^{-1}$	mg kg^{-1}	$\text{cmol}_c\ \text{kg}^{-1}$		%	$\text{cmol}_c\ \text{kg}^{-1}$	%
30–40	5.8	0.8	25.9	26.0	<1	5.9	98
90–100	8.7	1.5	26.9	27.1	1	8.9	98

[a] NH_4OAC extraction and measurement of the subsequently displaced NH_4 (i.e., includes bases, exchangeable acidity, etc.).

[b] NH_4OAC bases + acidity (at pH 8.2).

[c] ECEC (NH_4OAC-extractable bases plus KCl-extractable Al).

	X-ray[a]		Thermal	
	10–42 cm	**82–175 cm**	**10–42 cm**	**82–175 cm**
	Peak size		%	
Kaolinite	nd	nd	56	55
Goethite	nd	nd	nd	nd
Hematite	nd	nd	nd	nd
Halloysite	2	2	nd	nd
Gibbsite	2	1	11	7
Vermiculite	nd	nd	nd	nd
Montmorillonite	nd	nd	nd	nd
Cristobalite	nd	nd	nd	nd
Quartz	nd	nd	nd	nd
Interpretation			Kaolinitic	Kaolinitic

[1] Values refer to relative peak size (5 = very large, 4 = large, 3 = medium, 2 = small, 1 = very small).

J. Pinola Forest Census Plot, Fortuna Forest Reserve, Panama (Figure 3.8)

Soil taxonomy:	Fine, mixed, superactive, isothermic, Andic Palehumult
Profile location:	From the east side of the dam wall, follow the road downhill to the end. Enter the forest on the right (east), following the trail uphill for ~5 minutes to the plot, arriving at the 00,00 marker. The pit is on the far side of the plot close to the 60,100 marker.
Latitude/longitude:	8.754164°N, –82.259095°E
UTM:	17P, 0361505 m E., 0967905 m N.
Date and season:	26 July 2010; wet season
Elevation:	1,135 m asl
Slope and site position:	Steep (~25%) midslope, facing west; concave radial and convex lateral
Soil moisture regime:	Perudic: mean annual rainfall 4,964 ± 863 mm, with 159 ± 27 mm mean monthly dry season rainfall (1 January–30 April)
Soil temperature regime:	Isothermic: mean annual temperature 18.5°C, with mean monthly temperature varying by <2°C over the annual cycle
Parent material:	Basalt
Vegetation:	Lower montane tropical rainforest; canopy height 20 to 25 m; many understory palms (*Chamaedorea* spp.) and small stems; ectomycorrhizal trees absent; abundant Moraceae, Meliaceae (*Guarea*), and Fabaceae (*Platymiscium*)
Drainage:	Moderately well drained
Surface features:	Complete thin cover of wet leaves
Faunal activity:	Common earthworms in upper horizons
Coarse fragments:	Hard angular basalt cobbles and stones in subsoil
Rooting depth:	Throughout the profile to 194 cm
Control section:	Between 24 and 74 cm below the soil surface (i.e., the upper 50 cm of the argillic horizon)
Particle-size class:	Fine (clay between 35% and 60% and coarse fragments <35% of volume)
Mineralogy class:	Mixed (kaolinite, hydroxy-interlayer vermiculite, gibbsite)
Cation-exchange activity class:	Superactive (CEC = 70 cmol_c kg^{-1} clay by ammonium acetate pH 7)
Diagnostic horizons/features:	(1) Perudic moisture regime and isothermic temperature regime (2) Umbric epipedon from 0 to 24 cm (3) Argillic horizon from 24 to 194 cm (4) Moderate andic properties between 8 and 49 cm (5) Base saturation by sum of cations <35% between 49 and 194 cm

General Features of the Soil

This dark colored fertile soil is rich in organic matter and nutrients. Developed on basalt, it contains high concentrations of carbon, phosphorus, and exchangeable cations, particularly Ca and Mg. The clay loam epipedon overlies a clay subsoil containing more than 50% angular basalt cobbles and stones. There appears to be a sombric horizon between 24 and 49 cm, which is much darker than the overlying horizon, but organic C is not greater.

Soil Taxonomy

The soil is an Ultisol because it has an argillic horizon and a base saturation by sum of cations <35% at 125 cm below the top of the argillic horizon. It is a Humult because there is >0.9% organic C in the upper 15 cm of the argillic horizon, and >12 kg C m^{-2} in the upper 100 cm of the profile (20.1 kg C m^{-2}). The profile is a Palehumult because there is no decline in clay concentration with increasing depth in the upper 150 cm of the profile. It is an Andic Palehumult because although there is no volcanic ash, there is >18 cm of the upper 75 cm of the profile with bulk density <1.0 g cm^{-3}, and amorphous Al+½Fe is >1.0% by oxalate extraction. The soil moisture regime is perudic because rainfall exceeds potential evapotranspiration in all months.

Chemical and Physical Properties

The soil has dark colors throughout, including a black upper argillic horizon, matched by relatively high concentrations of organic C (with 1.6% C below >130 cm). Bulk density is low in the upper 49 cm and high below that. The epipedon is clay loam over a clay subsoil. Soil pH is moderately to strongly acid throughout, and so base saturation (at soil pH) is high (≥87%) throughout the profile. Exchangeable Ca and Mg are high, but exchangeable P is relatively low, as expected for a soil developed in basalt. Similarly, total Ca and Mg are high compared to total K. Total P is high, with up to 1,000 mg P kg^{-1} in the epipedon. The soil contains moderate concentrations of dithionite Al and Fe and relatively high concentrations of oxalate Al and Fe, giving moderate andic properties sufficient for the Andic subgroup. Manganese concentrations are high for both dithionite and oxalate extracts.

Horizon Description: Pinola

A1—0 to 8 cm; very dark brown (7.5YR 2.5/2) sandy loam; moderate fine and very fine subangular blocky structure; slightly sticky and slightly plastic; common coarse, many medium, and common fine and very fine roots; clear smooth boundary.

A2—8 to 24 cm; very dark brown (10YR 2/2) sandy clay loam; moderate fine and very fine subangular blocky structure; moist and friable; slightly sticky and slightly plastic; about 4% angular basalt gravel; common earthworms; many coarse and medium, and common fine and very fine roots; clear smooth boundary.

Bt1—24 to 49 cm; black (7.5YR 2.5/1) very fine sandy clay loam; sticky and slightly plastic; moderate coarse subangular blocky structure; moist, friable to firm; few coarse, medium, and fine roots; no clear clay films; clear smooth boundary.

Bt2—49 to 131 cm; brown (10YR 4/3) very stony sandy clay; moderate medium and fine subangular blocky structure; sticky and very plastic; few faint clay films on ped faces; about 50% hard angular cobbles and stones; few fine and medium roots; gradual smooth boundary.

Bt3—131 to 194+ cm; dark yellowish-brown (10YR 4/4) very stony sandy clay loam; moderate fine and very fine subangular blocky structure; sticky and slightly plastic; about 50% hard angular cobbles and stones and about 10% medium and coarse angular gravel; few medium and fine roots.

Laboratory Analysis: Pinola

TABLE J.1. Soil physical properties, including bulk density and particle-size distribution, by genetic horizon in the Pinola soil. Dash (—) = not determined.

Horizon	Designation	Bulk density (fine earth)	Coarse fragments (>2 mm)	Sand	Silt	Clay	Textural class	Clay:silt ratio
—cm—		—g cm^{-3}—	—vol%—	—%—	—%—	—%—		
0–8	A1	0.51	0	43.5	21.8	34.7	Clay loam	1.59
8–24	A2	0.67	4	44.8	21.5	33.7	Clay loam	1.57
24–49	Bt1	0.92	0	29.2	28.5	42.3	Clay	1.48
49–131	Bt2	0.96	50	23.8	25.7	50.5	Clay	1.96
131–194	Bt3	—	65	21.3	29.6	49.1	Clay	1.66

TABLE J.2. Soil pH and total carbon and nitrogen by genetic horizon in the Pinola soil.

Horizon	Soil pH			Total C	Total N	C:N	C:P	N:P
—cm—	Water	$CaCl_2$	$BaCl_2$	—%—	—%—			
0–8	5.64	5.20	4.66	7.88	0.66	12.0	73.4	6.2
8–24	5.45	4.84	4.40	4.16	0.38	10.8	42.8	3.9
24–49	5.37	4.58	4.25	3.25	0.24	13.7	41.6	3.1
49–131	5.48	4.78	4.43	2.11	0.17	12.2	26.4	2.1
131–194	5.53	4.84	4.49	1.60	0.15	10.8	21.7	2.0

TABLE J.3. Exchangeable cations and effective cation exchange capacity (ECEC) by extraction in 0.1 M barium chloride ($BaCl_2$) by genetic horizon in the Pinola soil. BS = base saturation; sat = saturation; TEB = total exchangeable bases.

Horizon	Al	Ca	Fe	K	Mg	Mn	Na	TEB[a]	ECEC[b]	BS[c]	ECEC per kg clay	Al sat	Ca:Mg
—cm—	cmol$_c$ kg^{-1}									—%—	cmol$_c$ kg^{-1}		
0–8	0.17	26.58	0.01	0.91	4.01	0.61	0.08	31.6	32.4	97.6	93.3	0.5	6.6
8–24	0.66	8.68	<0.01	0.48	1.76	0.25	0.07	11.0	11.9	92.3	35.3	5.5	4.9
24–49	1.54	6.28	<0.01	0.10	1.59	0.12	0.07	8.0	9.7	82.9	22.9	15.9	4.0
49–131	0.59	6.42	<0.01	0.10	1.58	0.24	0.09	8.2	9.0	90.8	17.9	6.5	4.1
131–194	0.45	6.12	<0.01	0.15	1.68	0.26	0.07	8.0	8.7	91.9	17.8	5.1	3.6

[a] TEB determined by extraction in 0.1 M $BaCl_2$.

[b] ECEC determined as the sum of cations extracted in extraction in 0.1 M $BaCl_2$.

[c] BS determined as (TEB ÷ ECEC) × 100.

TABLE J.4. Extractable acidity, exchangeable cations, and cation exchange capacity (CEC) determined in buffered solutions by genetic horizon in the Pinola soil. BS = base saturation; TEB = total exchangeable bases; dash (—) = not determined.

Horizon	Extractable acidity	CEC by sum of cations[a]	BS by sum of cations[b]	CEC7[c]	Ca	K	Mg	Na	TEB by CEC7[d]	BS by CEC7[e]	CEC7 per kg clay
—cm—	cmol$_c$ kg^{-1}	cmol$_c$ kg^{-1}	—%—	cmol$_c$ kg^{-1}						—%—	cmol$_c$ kg^{-1}
0–8	—	—	—	46.3	17.47	0.92	3.62	0.07	22.1	47.7	133
8–24	—	—	—	31.8	6.26	0.46	1.60	0.04	8.4	26.3	94
24–49	32.2	41.9	23	32.8	4.53	0.10	1.46	0.06	6.1	18.8	77
49–131	25.6	34.6	26	32.0	5.36	0.10	1.50	0.06	7.0	22.0	63
131–194	23.5	32.3	27	33.0	5.37	0.16	1.66	0.07	7.3	22.0	67

[a] Sum of extractable acidity and TEB.

[b] BS determined from TEB ÷ CEC sum of cations × 100.

[c] CEC determined by extraction in ammonium acetate (pH 7).

[d] TEB (sum of Ca, K, Mg, and Na) determined by extraction in ammonium acetate (pH 7).

[e] BS determined as (TEB ÷ ECEC) × 100.

TABLE J.5. Pedogenic metal oxides extractable in acid-ammonium oxalate and buffered dithionite by genetic horizon in the Pinola soil. Fe_{ox}:Fe_d ratio, oxalate-extractable iron/dithionite-extractable iron.

	Dithionite extraction			Oxalate extraction						
Horizon	Al_d	Fe_d	Mn_d	Al_{ox}	Fe_{ox}	Mn_{ox}	P_{ox}	Si_{ox}	Al+½Fe	Fe_{ox}:Fe_d
—cm—	%			mg g^{-1}					—%—	
0–8	0.58	3.12	0.14	5.35	8.53	1.00	0.56	0.42	1.0	0.27
8–24	0.70	3.52	0.14	6.13	9.60	1.06	0.48	0.54	1.1	0.27
24–49	0.80	4.87	0.13	5.88	7.80	0.54	0.28	0.57	1.0	0.16
49–131	1.22	6.09	0.20	6.82	8.04	1.23	0.22	0.86	1.1	0.13
131–194	1.01	5.84	0.19	6.91	9.06	1.33	0.23	1.08	1.1	0.16

TABLE J.6. Total elements by nitric acid digestion by genetic horizon in the Pinola soil.

	Nitric acid digestion for total elemental analysis										
Horizon	**Al**	**B**	**Ca**	**Cu**	**Fe**	**K**	**Mg**	**Mn**	**Na**	**P**	**Zn**
—cm—	mg g^{-1}										
0–8	51.5	<0.005	12.10	0.092	52.0	0.76	5.02	1.37	1.47	0.864	0.081
8–24	68.6	<0.005	8.70	0.134	57.1	0.67	4.95	1.51	1.33	1.049	0.095
24–49	85.4	<0.005	8.44	0.204	65.1	0.45	5.57	1.42	0.73	0.756	0.089
49–131	123.0	<0.005	6.58	0.267	85.5	0.75	7.69	2.10	0.20	0.890	0.121
131–194	118.5	<0.005	6.94	0.295	85.0	0.75	7.39	2.02	0.17	0.782	0.101

K. Samudio Forest Census Plot, Fortuna Forest Reserve, Panama (Figure 3.9)

Soil taxonomy:	Fine-silty, mixed, superactive, isothermic, Aquandic Dystrudept
Profile location:	Park over the bridge slightly downhill and to the north of the Fortuna station. Follow the trail uphill for ~10 minutes, then follow a faint flagged trail to the left. The trail crosses the plot and rises steeply. The profile pit was ~10 m west of the 00,00 plot marker in the southwest corner.
Latitude/longitude:	8.731185°N, −82.248065°E
UTM:	17P, 0362710 m E., 0965360 m N.
Date and season:	30 June 2008; wet season
Elevation:	1,215 m asl
Slope and site position:	Moderately steep (~20%) midslope facing northeast; slightly convex lateral and linear radial
Soil moisture regime:	Perudic; 4,833 ± 219 mm mean annual rainfall; 215 ± 30 mm mean monthly dry season rainfall
Soil temperature regime:	Isothermic: mean annual temperature 17.9°C, with mean monthly temperature varying by <2°C over the annual cycle
Parent material:	Rhyolite over mafic-volcanics
Vegetation:	Species-rich lower montane tropical rainforest; canopy height 25 m; large amounts of recent canopy disturbance resulting in a very dense understory filled with short-stature palms (*Geonoma cuneata* and *Chamaedorea* spp.) beneath a tall but open canopy
Drainage:	Moderately poorly drained
Surface features:	Thick, continuous cover of wet leaves
Faunal activity:	Common earthworms
Coarse fragments:	Many coarse fragments
Rooting depth:	The upper 75 cm of the profile
Control section:	Between 25 and 100 cm below the soil surface
Particle-size class:	Fine-loamy (>15% sand and between 18 and 35% clay)
Mineralogy class:	Mixed (47% kaolinite, 9% gibbsite); some volcanic glass
Cation-exchange activity class:	Superactive (CEC 70 $\mathrm{cmol_c\ kg^{-1}}$ clay by NH_4AOc)
Diagnostic horizons/features:	(1) Perudic moisture regime and isothermic temperature regime
	(2) Ochric epipedon from 0 to 25 cm
	(3) Cambic horizon from 25 to 80 cm
	(4) Aquic conditions within 60 cm of the soil surface

General Features of the Soil

The profile is formed in rhyolite and has an organic-rich mineral epipedon over a yellowish-brown subsoil. It has moderate andic properties plus some volcanic glass, but this is marginally insufficient to qualify the profile as an Andisol. The profile is gravelly and becomes waterlogged in the upper meter. It is very infertile, particularly in terms of base cations. The gravel is andesitic, indicating a contribution from landslides or volcanic ejecta.

Soil Taxonomy

The profile almost qualifies as an Andisol, but oxalate-extractable is <2.0% throughout the upper 60 cm and there is insufficient volcanic glass to account for the difference. This is based on grain counts of the B1 horizon (25–50 cm), in which coarse silt (representing the silt fraction) contains 15% volcanic glass (including glass-coated grains), but the fine sand fraction (representing the sand fraction) contains only trace amounts. The coarse silt plus fine sand fractions account for 10.8% and 11.8%, respectively, of the total soil particles, so the mean glass content is 7%. This is less than the approximate 11% of glass required given the Al+½Fe concentration. The profile is therefore an Inceptisol because it has a cambic horizon. It is a Udept because of the perudic moisture regime. It does not qualify for Humudepts because the epipedon is ochric rather than umbric (it does not qualify as umbric based on color in the AB horizon). The profile is therefore a Dystrudept because it has a base saturation of <60% by NH_4OAc between 25 and 75 cm below the soil surface. The presence of aquic conditions (including redox depletions with chroma ≤2 in the upper 60 cm) and moderate andic properties (i.e., a bulk density ≤1.0 g $\mathrm{cm^{-3}}$ and oxalate Al+½Fe >1% in at least 18 cm of the upper 75 cm) qualifies the profile as an Aquandic Dystrudept. The soil moisture regime is perudic because rainfall exceeds potential evapotranspiration in all months.

Chemical and Physical Properties

Bulk density is low (<1.0 g $\mathrm{cm^{-3}}$) in the upper 50 cm of the profile. The soil is very strongly acidic and has a clay loam

FIGURE 3.9. The profile at Samudio.

texture throughout the upper 75 cm. Organic matter is high in the upper 50 cm, and C:N ratios are relatively high (13–14). Base cations are extremely low, being ≤0.3 $\text{cmol}_c\ \text{kg}^{-1}$ below 10 cm depth. Effective cation exchange capacity and base saturation are also very low, with very high Al saturation (>90%) in the B and C horizons. However, as is typical for soils with andic properties, CEC is much greater at pH 7 and 8.2. Total P is low (<200 mg P kg^{-1}) in the B horizon. Crystalline Al and Fe are relatively low, but amorphous (noncrystalline) forms are relatively high, with Al+½Fe >1.0 in the upper 50 cm of the profile. As in other rhyolite soils at Fortuna, all forms of extractable Mn are extremely low throughout the profile. The clay fraction contains 47% kaolinite and 9% gibbsite, plus vermiculite and cristobalite.

Horizon Description: Samudio

A—0 to 10 cm; very dark grayish-brown (10YR 3/2) clay loam; moist and friable; many medium, fine, and very fine roots, forming a thin mat in upper few cm of the horizon; clear smooth boundary.

AB—10 to 25 cm; brown (10YR 4/3) clay loam; about 1% subangular andesite gravel; common medium, fine, and very fine roots; clear smooth boundary.

B1—25 to 50 cm; light olive-brown (2.5Y 5/4) clay loam; about 10% subangular andesite gravel and stones; few medium, fine, and very fine roots; gradual smooth boundary.

B2—50 to 75 cm; light yellowish-brown (2.5Y 6/3) gravelly clay loam; few faint brownish-yellow (10YR 6/8) redox concentrations and light gray (2.5Y 7/1) redox depletions; about 10% subangular weathered andesite gravel and cobbles and 10% stones; very few medium roots; gradual smooth boundary.

Cg1—75 to 120 cm; light yellowish-brown (2.5Y 6/4) gravelly loam; common brownish-yellow (10YR 6/8) redox concentrations and light gray (2.5Y 7/1) redox depletions; about 15% subangular and angular weathered andesite gravel and cobbles; gradual smooth boundary.

Cg2—120 to 160 cm; mottled clay loam; many coarse brownish-yellow (10YR 6/8) redox concentrations and light gray (2.5Y 7/1) redox depletions; about 10% subangular weathered andesite gravel and cobbles; gradual smooth boundary.

Cg3—160 to 200+ cm; extremely cobbly loam; about 75% angular gravel and cobbles in a reduced matrix with redox concentrations; augering impeded by coarse fragments.

Laboratory Analysis: Samudio

TABLE K.1. Soil physical properties, including bulk density and particle-size distribution, by genetic horizon in the Samudio soil. Dash (—) = not determined.

Horizon	Designation	Bulk density (fine earth)	Coarse fragments (>2 mm)	Sand	Silt	Clay	Textural class	Clay:silt ratio
—cm—		—g cm^{-3}—	—vol%—	—%—	—%—	—%—		
0–10	A	0.50	0	35.2	29.9	34.9	Clay loam	1.17
10–25	AB	0.71	1	26.1	35.6	38.3	Clay loam	1.08
25–50	B1	0.91	11	21.0	41.7	37.4	Clay loam	0.90
50–75	B2	1.22	20	21.8	42.4	35.8	Clay loam	0.84
75–120	Cg1	1.09	15	31.0	43.3	25.8	Loam	0.60
120–160	Cg2	—	10	20.3	49.8	30.0	Silty clay loam	0.60
160–200	Cg3	—	75	25.6	48.3	26.1	Loam	0.54

TABLE K.2. Soil pH and total carbon and nitrogen by genetic horizon in the Samudio soil.

Horizon	Soil pH			Total C	Total N	C:N	C:P	N:P
—cm—	Water	$CaCl_2$	$BaCl_2$	—%—	—%—			
0–10	4.52	3.91	3.88	12.15	0.86	14.1	281	19.9
10–25	4.79	4.22	4.24	5.24	0.36	13.2	192	13.2
25–50	4.90	4.42	4.37	2.28	0.17	13.6	119	8.9
50–75	4.90	4.16	4.20	0.74	0.06	13.2	66	5.4
75–120	4.96	4.05	4.11	0.39	0.03	12.7	27	2.1
120–160	5.03	4.07	4.13	0.32	0.02	20.9	22	1.4
160–200	5.05	4.12	4.11	0.24	0.02	12.3	15	1.3

TABLE K.3. Exchangeable cations and effective cation exchange capacity (ECEC) by extraction in 0.1 M barium chloride ($BaCl_2$) by genetic horizon in the Samudio soil. BS = base saturation; sat = saturation; TEB = total exchangeable bases; dash (—) = not determined.

Horizon	Al	Ca	Fe	K	Mg	Mn	Na	TEB[a]	ECEC[b]	BS[c]	ECEC per kg clay	Al sat	Ca:Mg
—cm—	cmol$_c$ kg^{-1}									—%—	cmol$_c$ kg^{-1}	—%—	
0–10	8.28	1.41	0.13	0.26	0.53	0.03	0.19	2.4	10.8	22.1	31.0	76.4	2.7
10–25	3.77	0.18	0.04	0.04	0.03	<0.01	0.04	0.3	4.1	7.1	10.7	92.0	6.0
25–50	2.75	0.15	0.06	0.04	<0.01	<0.01	0.07	0.3	3.1	8.3	8.2	89.9	—
50–75	5.26	0.12	0.03	0.01	0.02	<0.01	0.12	0.3	5.6	4.9	15.5	94.5	5.5
75–120	7.96	0.14	0.02	0.01	0.02	<0.01	0.10	0.3	8.3	3.4	32.0	96.4	6.0
120–160	8.89	0.15	<0.01	0.02	0.04	<0.01	0.10	0.3	9.2	3.2	30.7	96.8	4.1
160–200	7.85	0.46	<0.01	0.01	0.30	0.04	0.13	0.9	8.8	10.3	33.7	89.2	1.5

[a] TEB determined by extraction in 0.1 M $BaCl_2$.

[b] ECEC determined as the sum of cations extracted in extraction in 0.1 M $BaCl_2$.

[c] BS determined as (TEB ÷ ECEC) × 100.

TABLE K.4. Extractable acidity, exchangeable cations, and cation exchange capacity (CEC) determined in buffered solutions by genetic horizon in the Samudio soil. BS = base saturation; TEB = total exchangeable bases, dash (—) = not determined.

Horizon	Extractable acidity	CEC by sum of cations[a]	BS by sum of cations[b]	CEC7[c]	Ca	K	Mg	Na	TEB by CEC7[d]	BS by CEC7[e]	CEC7 per kg clay
—cm—	cmol$_c$ kg^{-1}	cmol$_c$ kg^{-1}	—%—	cmol$_c$ kg^{-1}						—%—	cmol$_c$ kg^{-1}
0–10	—	—	—	—	—	—	—	—	—	—	—
10–25	—	—	—	—	—	—	—	—	—	—	—
25–50	—	—	—	23.14	0.04	0.04	0.05	0.03	0.2	0.7	62
50–75	—	—	—	22.01	0.05	0.03	0.08	0.05	0.2	0.9	61
75–120	—	—	—	22.60	0.10	0.03	0.11	0.08	0.3	1.4	88
120–160	—	—	—	—	—	—	—	—	—	—	—
160–200	—	—	—	—	—	—	—	—	—	—	—

[a] Sum of extractable acidity and TEB.

[b] BS determined from TEB ÷ CEC sum of cations × 100.

[c] CEC determined by extraction in ammonium acetate (pH 7).

[d] TEB (sum of Ca, K, Mg, and Na) determined by extraction in ammonium acetate (pH 7).

[e] BS determined as (TEB ÷ ECEC) × 100.

TABLE K.5. Pedogenic metal oxides extractable in acid-ammonium oxalate and buffered dithionite by genetic horizon in the Samudio soil. Fe$_{ox}$:Fe$_d$ ratio, oxalate-extractable iron/dithionite-extractable iron.

	Dithionite extraction			Oxalate extraction						
Horizon	Al	Fe	Mn	Al	Fe	Mn	P	Si	Al+½Fe	Fe$_{ox}$:Fe$_d$
—cm—	%			mg g^{-1}					—%—	
0–10	0.91	1.34	<0.01	8.69	9.15	0.01	0.23	0.16	1.33	0.68
10–25	0.77	1.58	<0.01	8.64	11.16	<0.01	0.13	0.30	1.42	0.71
25–50	0.80	1.49	<0.01	10.32	11.67	<0.01	0.05	1.20	1.61	0.78
50–75	0.43	0.56	<0.01	6.37	2.77	<0.01	0.04	1.15	0.78	0.50
75–120	0.44	1.02	<0.01	5.22	1.41	<0.01	0.06	0.94	0.59	0.14
120–160	0.40	1.24	<0.01	5.05	1.71	<0.01	0.05	0.83	0.59	0.14
160–200	0.43	3.59	0.05	4.31	2.76	0.33	0.03	0.75	0.57	0.08

TABLE K.6. Total elements by nitric acid digestion by genetic horizon in the Samudio soil.

	Nitric acid digestion for total elemental analysis									
Horizon	Al	B	Ca	Cu	Fe	K	Mg	Mn	Na	P	Zn
—cm—	mg g^{-1}										
0–10	56.4	0.016	2.43	0.039	22.85	1.43	2.76	0.20	0.90	0.433	0.031
10–25	70.6	0.008	2.61	0.055	29.88	1.60	3.40	0.26	0.98	0.273	0.039
25–50	92.2	0.020	1.83	0.082	25.89	2.46	3.80	0.26	0.79	0.171	0.050
50–75	126.4	0.011	1.24	0.145	21.76	2.88	9.41	0.50	0.43	0.145	0.084
75–120	136.7	0.007	1.02	0.213	30.62	1.92	13.37	0.64	0.20	0.189	0.094
120–160	147.1	0.013	0.98	0.210	30.97	1.70	9.21	0.50	0.21	0.212	0.099
160–200	133.5	0.009	1.04	0.228	54.70	1.67	9.60	1.01	0.28	0.198	0.111

TABLE K.7. Detailed particle-size distribution and glass contents in the Samudio profile. Note that glass includes glass, glass coated grains, or glass aggregates, although the majority were glass grains. For grain counts, 30% of the fine earth must be coarse silt and sand (0.02–2 mm). GS = glass grains; GC = glass-coated grains; GA = glass aggregates; tr = trace. Fractions in bold were analyzed for glass content.

	Particle-size distribution (%)								Grain counts (%)		
Horizon	Clay	Fine silt	Coarse silt	Very fine sand	Fine sand	Medium sand	Coarse sand	Very coarse sand	Coarse silt	Fine sand	Mean glass[a]
—cm—		—%—	**—%—**	—%—	**—%—**	—%—	—%—	—%—			
20–50	28.2	31.8	10.6	10.8	11.8	4.7	1.5	0.6	GS 14, GC 1, GA, tr	GS tr, GA tr	7.1%

[a] Mass-weighted average of coarse silt and fine sand.

Additional Data: Samudio. BS = base saturation; ECEC = effective cation exchange capacity; sat = saturation; TEB = total exchangeable bases; nd = not detected; tr = trace.

	Dithionite–citrate extraction			Ammonium oxalate extraction					
Horizon	Al	Fe	Mn	Al	Fe	Si	Al+½Fe	Mn	P
—cm—	%			%				mg kg^{-1}	
20–50	0.8	1.7	nd	0.94	1.44	0.09	1.66	3.2	76.8

	Ammonium acetate extraction							
Horizon	Ca	K	Mg	Na	TEB	CEC[a]	BS	CEC per kg clay
—cm—	cmol$_c$ kg^{-1}						%	cmol$_c$ kg^{-1}
20–50	nd	0.1	tr	nd	0.1	18.5	1	44.6

	KCl extraction		Barium chloride–TEA extraction (pH 8.2)				
Horizon	Al	Mn	Acidity	CEC[b]	BS	ECEC[c]	Al sat
—cm—	cmol$_c$ kg^{-1}	mg kg^{-1}	cmol$_c$ kg^{-1}		%	cmol$_c$ kg^{-1}	%
20–50	2.9	tr	33.0	33.1	<1	3.0	97

[a] NH$_4$OAC extraction and measurement of the subsequently displaced NH$_4$ (i.e., includes bases, exchangeable acidity, etc.).

[b] NH$_4$OAC bases + acidity (at pH 8.2).

[c] ECEC (NH$_4$OAC-extractable bases plus KCl-extractable Al).

	X-ray[a]	**Thermal**
	20–50 cm	**20–50 cm**
	—Peak size—	——%——
Kaolinite	3	47
Goethite	nd	nd
Hematite	nd	nd
Halloysite	nd	nd
Gibbsite	2	9
Vermiculite	2	nd
Montmorillonite	nd	nd
Cristobalite	1	nd
Quartz	nd	nd
Interpretation		Mixed

[a] Values refer to relative peak size (5 = very large, 4 = large, 3 = medium, 2 = small, 1 = very small).

L. Verrugosa A Forest Census Plot, Palo Seco Forest Reserve, Panama (Figure 3.10)

Soil taxonomy:	Clayey-skeletal, parasesquic, isothermic, Typic Dystrudept
Profile location:	Cross the dam and continue past the Palo Seco entrance, parking on the right at a small farm. Walk through the farm property and follow a trail uphill to a fork (~30 min). Take the right at the fork in the trail and follow uphill for ~1 hour to the plot. The pit is located at the 100,80 marker.
Latitude/longitude:	8.778184°N, −82.180279°E
UTM:	17P, 370184 m E., 970533 m N.
Date and season:	28 July 2010; wet season
Elevation:	969 m asl
Slope and site position:	Moderately steep (>25%) shoulder in hilly terrain, dropping steeply below; convex radial and complex lateral
Soil moisture regime:	Perudic: mean annual rainfall at nearby Palo Seco 6,257 ± 310 mm, with 445 ± 33 mm mean monthly dry season rainfall (1 January–30 April)
Soil temperature regime:	Isothermic: mean annual temperature at nearby Palo Seco 19.6°C, with mean monthly temperature varying by <2°C over the annual cycle
Parent material:	Undifferentiated mafic-volcanics, including andesite, basalt, and diabase
Vegetation:	Species-rich lower montane tropical rainforest; canopy height 20 to 25 m; *Wettinia quinaria* palms abundant in the canopy; understory filled with short-stature palms (principally *Geonoma cuneata* and *G. deversa*)
Drainage:	Moderately well drained
Surface features:	Discontinuous cover of wet leaves
Faunal activity:	Many earthworms in the upper 50 cm of soil
Coarse fragments:	Strongly weathered subangular cobbles
Rooting depth:	Throughout the profile but mainly the upper 10 cm
Control section:	Between 25 and 100 cm below the soil surface
Particle-size class:	Clayey-skeletal
Mineralogy class:	Parasesquic
Cation-exchange activity class:	N/A
Diagnostic horizons/features:	(1) Perudic moisture regime and isothermic temperature regime (2) Ochric epipedon from 0 to 10 cm (3) Cambic horizon from 10 to 59 cm

General Features of the Soil

This soil is formed in undifferentiated mafic-volcanics. It contains abundant strongly weathered coarse fragments and is extremely infertile, with extremely low concentrations of base cations. In addition, the high Al saturation and low Ca:Mg ratios represent a harsh environment for root growth.

Soil Taxonomy

The B horizon is not oxic because, although ECEC is <12 $\text{cmol}_c\ \text{kg}^{-1}$ clay, CEC by NH_4AOc is >16 $\text{cmol}_c\ \text{kg}^{-1}$ clay. The soil is therefore an Inceptisol because it has a cambic horizon and a Udept because of the perudic moisture regime. It is a Dystrudept because of the extremely low base saturation throughout the profile. The profile does not qualify as Andic because Al+½Fe by oxalate extraction is <1.0% throughout. In the absence of other diagnostic features at the subgroup level, the profile qualifies as a Typic Dystrudept. Mineralogy is parasesquic because Fe_2O_3 is >10% in the control section (measured as $Fe_d \times 1.43$). The clay fraction includes kaolinite, goethite, and hydroxy-interlayer vermiculite determined by x-ray diffraction. The soil moisture regime is perudic because rainfall exceeds potential evapotranspiration in all months.

Chemical and Physical Properties

The profile has a shallow brown epipedon over a yellowish-brown subsoil. There are many strongly weathered coarse fragments throughout; these are hard in the upper 60 cm but are soft below and therefore classed as parabouldery. All coarse fragments are almost entirely weathered and covered in thick ferromanganese coatings. The soil has a clay texture in the upper part over a silty clay loam subsoil. Soil pH is very strongly acid throughout, and organic matter concentrations are moderate, with C:N ratios between 13 and 15. Base cation concentrations are extremely low, with TEB of ≤0.17 $\text{cmol}_c\ \text{kg}^{-1}$ throughout the subsoil. Effective cation exchange capacity and base saturation are also very low, sufficient to qualify for oxic conditions, but CEC at pH 7 is very

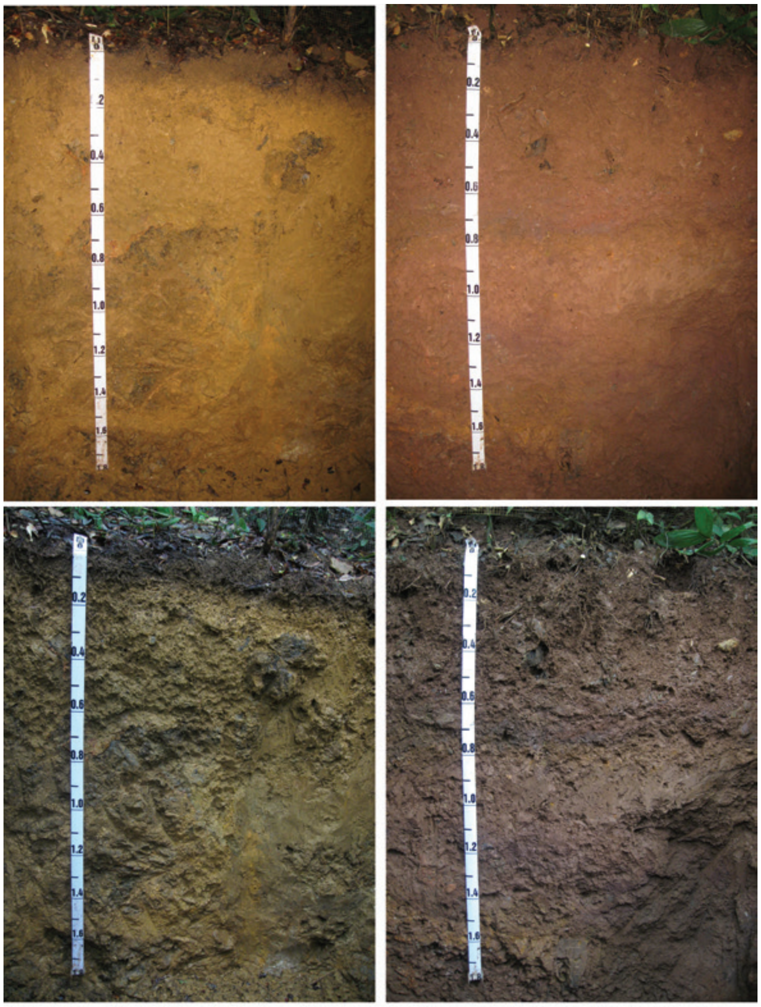
(a) Verrugosa A (b) Verrugosa B

FIGURE 3.10. The profiles at (a) Verrugosa A with (upper) and without (lower) camera flash and (b) Verrugosa B with (upper) and without (lower) camera flash.

high, indicating a considerable pH-dependent charge. Aluminum concentrations and saturation are high, and Ca:Mg ratios are very low throughout the subsoil. Total Al and Fe are very high, and total P is moderately high. Secondary Fe (Fe$_d$) is very high (>10% throughout the upper meter), although amorphous Al and Fe are moderate (Al+½Fe by oxalate extraction <1.0%).

Horizon Description: Verrugosa A

A—0 to 10 cm; dark brown (10YR 3/3) silty clay loam; moderate fine and very fine subangular blocky structure; sticky and plastic; many earthworms; common coarse and very coarse and many medium, fine, and very fine roots; clear smooth boundary.

B1—10 to 24 cm; dark yellowish-brown (10YR 4/6) sandy clay; moderate coarse subangular blocky structure, breaking to moderate medium and fine subangular blocky; sticky and plastic; moist and friable; about 2% hard but strongly weathered gravel fragments; many earthworms; many medium tubular pores with thick clay films enriched with organic C; common medium and few fine and very fine roots; gradual smooth boundary.

B2—24 to 41 cm; brown (7.5YR 4/4) cobbly clay; moderate coarse to very coarse subangular blocky structure; plastic and very sticky; moist and friable; about 25% hard but strongly weathered subangular gravel and cobbles; many earthworms; many medium tubular pores; thick, continuous clay films in pore linings and on faces between rocks and soils; few fine and medium roots; gradual smooth boundary.

Bo3—41 to 59 cm; yellowish-brown (10YR 5/4) very cobbly sandy clay loam; moderate very coarse subangular blocky structure; moist and friable; sticky and slightly plastic; about 10% hard angular medium gravel fragments; about 40% hard but strongly weathered subangular cobbles; common earthworms; common medium tubular pores; thick, continuous clay films in pore linings; few medium and fine roots; gradual smooth boundary.

BC—59 to 110 cm; dark yellowish-brown (10YR 4/4) parabouldery sandy clay loam; weak medium angular blocky structure; slightly sticky and slightly plastic; moist and firm; about 50% strongly weathered rock, with thick black Mn precipitates on surfaces; few fine black Mn nodules; few earthworms; very few fine and medium roots; gradual smooth boundary.

CB—110 to 189 cm dark yellowish-brown (10YR 3/4) parabouldery sandy clay loam; massive; slightly sticky and slightly plastic; moist and friable; very few medium and fine roots; about 50% weathered rock, with thick black Mn precipitates on surfaces.

Laboratory Analysis: Verrugosa A

TABLE L.1. Soil physical properties, including bulk density and particle-size distribution, by genetic horizon in the Verrugosa A soil. Dash (—) = not determined.

Horizon	Designation	Bulk density (fine earth)	Coarse fragments (>2 mm)	Sand	Silt	Clay	Textural class	Clay:silt ratio
—cm—		—g cm^{-3}—	—%—	—%—	—%—	—%—		
0–10	A	—	0	23.0	28.6	48.4	Clay	1.69
10–24	B1	0.94	2	17.9	30.8	51.4	Clay	1.67
24–41	B2	1.20	25	14.1	37.6	48.3	Clay	1.28
41–59	B3	1.18	50	12.1	45.5	42.4	Silty clay	0.93
59–110	BC	—	50	13.0	57.5	29.6	Silty clay loam	0.51
110–189	CB	1.15	50	7.6	58.1	34.3	Silty clay loam	0.59

TABLE L.2. Soil pH and total carbon and nitrogen by genetic horizon in the Verrugosa A soil.

Horizon	Soil pH			Total C	Total N	C:N	C:P	N:P
—cm—	Water	CaCl$_2$	BaCl$_2$	—%—	—%—			
0–10	4.50	3.67	3.65	8.79	0.61	14.5	129	8.9
10–24	4.66	4.13	4.15	2.07	0.15	13.6	60	2.6
24–41	4.84	4.24	4.24	0.98	0.07	14.3	26	1.0
41–59	4.90	4.24	4.24	0.90	0.06	15.4	24	0.9
59–110	4.90	4.19	4.16	0.22	0.02	14.4	4.8	0.2
110–189	4.87	4.12	4.06	0.09	0.01	12.6	1.2	0.1

TABLE L.3. Exchangeable cations and effective cation exchange capacity (ECEC) by extraction in 0.1 M barium chloride (BaCl$_2$) by genetic horizon in the Verrugosa A soil. BS = base saturation; sat = saturation; TEB = total exchangeable bases.

Horizon	Al	Ca	Fe	K	Mg	Mn	Na	TEB[a]	ECEC[b]	BS[c]	ECEC per kg clay	Al sat	Ca:Mg
—cm—	cmol$_c$ kg^{-1}									—%—	cmol$_c$ kg^{-1}	—%—	
0–10	6.29	0.49	0.05	0.14	0.47	0.02	0.05	1.15	7.5	15.3	15.5	83.9	1.1
10–24	3.26	0.06	0.01	0.02	0.09	0.01	<0.01	0.17	3.5	5.0	6.7	94.3	0.7
24–41	3.12	0.02	<0.01	<0.01	0.07	0.03	<0.01	0.09	3.2	2.6	6.7	96.4	0.2
41–59	3.14	0.02	<0.01	<0.01	0.08	0.01	<0.01	0.10	3.3	3.2	7.7	96.4	0.3
59–110	5.35	<0.01	<0.01	<0.01	0.03	<0.01	<0.01	0.03	5.4	0.6	18.2	99.4	0.1
110–189	7.89	<0.01	<0.01	<0.01	0.05	<0.01	0.04	0.09	8.0	1.1	23.3	98.9	0.1

[a] TEB determined by extraction in 0.1 M BaCl$_2$.

[b] ECEC determined as the sum of cations extracted in extraction in 0.1 M BaCl$_2$.

[c] BS determined as (TEB ÷ ECEC) × 100.

TABLE L.4. Extractable acidity, exchangeable cations, and cation exchange capacity (CEC) determined in buffered solutions by genetic horizon in the Verrugosa A soil. BS = base saturation; TEB = total exchangeable bases; dash (—) = not determined.

Horizon	Extractable acidity	CEC by sum of cations[a]	BS by sum of cations[b]	CEC7[c]	Ca	K	Mg	Na	TEB by CEC7[d]	BS by CEC7[e]	CEC7 per kg clay
—cm—	cmol$_c$ kg^{-1}	cmol$_c$ kg^{-1}	—%—	cmol$_c$ kg^{-1}						—%—	cmol$_c$ kg^{-1}
0–10	—	—	—	—	—	—	—	—	—	—	—
10–24	—	—	—	14.95	0.03	0.04	0.07	0.02	0.2	1.1	29.1
24–41	17.4	17.5	1	17.07	0.01	0.02	0.06	0.02	0.1	0.7	35.3
41–59	15.6	15.7	1	15.99	0.01	0.02	0.06	0.02	0.1	0.7	37.7
59–110	12.5	12.5	0	—	—	—	—	—	—	—	—
110–189	—	—	—	—	—	—	—	—	—	—	—

[a] Sum of extractable acidity and TEB.

[b] BS determined from TEB ÷ CEC sum of cations × 100.

[c] CEC determined by extraction in ammonium acetate (pH 7).

[d] TEB (sum of Ca, K, Mg, and Na) determined by extraction in ammonium acetate (pH 7).

[e] BS determined as (TEB ÷ ECEC) × 100.

TABLE L.5. Pedogenic metal oxides extractable in acid-ammonium oxalate and buffered dithionite by genetic horizon in the Verrugosa A soil. Fe$_{ox}$:Fe$_d$ ratio, oxalate-extractable iron/dithionite-extractable iron.

	Dithionite extraction			Oxalate extraction						
Horizon	Al	Fe	Mn	Al	Fe	Mn	P	Si	Al+½Fe	Fe$_{ox}$:Fe$_d$
—cm—	%			mg g^{-1}					—%—	
0–10	1.08	7.51	0.01	4.29	8.96	0.03	0.13	0.07	0.88	0.12
10–24	1.32	10.47	0.04	3.23	7.58	0.25	0.03	0.12	0.70	0.07
24–41	1.36	10.28	0.20	2.83	3.56	1.25	0.01	0.17	0.46	0.03
41–59	1.46	11.77	0.09	2.34	3.07	0.39	0.01	0.14	0.39	0.03
59–110	0.99	9.47	0.04	1.78	0.43	0.10	<0.01	0.15	0.20	<0.01
110–189	0.74	7.57	0.02	2.52	0.49	0.03	0.02	0.24	0.28	<0.01

TABLE L.6. Total elements by nitric acid digestion by genetic horizon in the Verrugosa A soil.

Horizon	Al	B	Ca	Cu	Fe	K	Mg	Mn	Na	P	Zn
—cm—	mg g^{-1}										
0–10	76.0	<0.005	0.95	0.076	89.0	0.58	2.10	0.21	0.36	0.683	0.047
10–24	105.7	<0.005	0.43	0.112	120.6	0.60	2.01	0.51	0.21	0.587	0.062
24–41	120.4	<0.005	0.08	0.144	124.9	0.75	1.98	1.87	0.09	0.680	0.056
41–59	119.5	<0.005	0.08	0.152	139.5	0.79	1.90	0.90	0.08	0.694	0.060
59–110	128.5	<0.005	0.03	0.161	119.0	0.81	2.36	0.39	0.08	0.922	0.058
110–189	133.7	<0.005	0.04	0.238	100.9	0.23	2.92	0.28	0.09	0.876	0.055

M. Verrugosa B Forest Census Plot, Palo Seco Forest Reserve, Panama (Figure 3.10)

Soil taxonomy:	Very fine, mixed, active, isothermic, Typic Dystrudept
Profile location:	Cross the dam and continue past the Palo Seco entrance, parking on the right at a small farm. Walk through the farm property and follow a trail uphill to a fork (~30 min). Take the left fork and follow it downhill, crossing two rivers, then up to the plot. The profile pit was on the far side of the plot at the 20,00 marker.
Latitude/longitude:	8.777998°N, –82.170315°E
UTM:	17P, 0371280 m E., 0970509 m N.
Date and season:	27 July 2010; mid–wet season
Elevation:	858 m asl
Slope and site position:	Steep (35%) foot slope above a relatively flat area; concave radial and convex lateral
Soil moisture regime:	Perudic: mean annual rainfall at nearby Palo Seco 6,257 ± 310 mm, with 445 ± 33 mm mean monthly dry season rainfall (1 January–30 April)
Soil temperature regime:	Isothermic: mean annual temperature at nearby Palo Seco 19.6°C, with mean monthly temperature varying by <2°C over the annual cycle
Parent material:	Undifferentiated mafic-volcanics, including andesite, basalt, and diabase
Vegetation:	Species-rich lower montane tropical rainforest; canopy height 20 to 25 m; compositionally similar to Verrugosa A but with fewer canopy and understory palms and more tree ferns (*Alsophila erinacea*)
Drainage:	Moderately well drained
Surface features:	Incomplete (90%) cover of wet leaves
Faunal activity:	Common medium earthworms in the upper 60 cm
Coarse fragments:	Many weathered gravel and cobbles throughout the profile
Rooting depth:	Throughout the profile to 200 cm
Control section:	Between 25 and 100 cm below the soil surface
Particle-size class:	Very fine (>60% clay)
Mineralogy class:	Mixed (small peaks from kaolinite, gibbsite, mica, and montmorillonite determined by XRD)
Cation-exchange activity class:	Active (CEC by NH$_4$AOc = 42.6 cmolc kg^{-1} clay)
Diagnostic horizons/features:	(1) Perudic moisture regime and isothermic temperature regime (2) Ochric epipedon from 0 to 15 cm (3) Cambic horizon between 15 and 86 cm

General Features of the Soil

This soil is formed in undifferentiated mafic-volcanics. It contains abundant strongly weathered coarse fragments and is extremely infertile. In particular, the low base cations and high Al saturation in the subsoil represent a harsh environment for root growth.

Soil Taxonomy

The clay distribution is irregular throughout the profile, so there is no argillic horizon. The profile is therefore an Inceptisol because of the cambic horizon and a Udept because of the perudic moisture regime. It is a Dystrudept because of the very low base saturation throughout the profile. It does not qualify as Andic because Al+½Fe by oxalate extraction is <1.0% throughout the profile. In the absence of other diagnostic features at the subgroup level, the profile qualifies as a Typic Dystrudept. Unlike Verrugosa A, this profile does not have a parasesquic mineralogy class because Fe$_2$O$_3$ (measured as secondary Fe by dithionite extraction × 1.43) in the control section is <10%. Instead, the clay mineralogy is mixed, and includes kaolinite, mica, and gibbsite. The soil moisture regime is perudic because rainfall exceeds potential evapotranspiration in all months.

Chemical and Physical Properties

The profile has a shallow dark reddish-brown epipedon over a reddish-brown subsoil. There are many strongly weathered coarse fragments throughout the profile. The soil has a clay texture throughout the upper 150 cm of the profile. Soil pH is strongly to very strongly acid, and organic matter concentrations are moderate, with C:N ratios between 7 and 12. Base cation concentrations are very low, with TEB of ≤1.4 cmol$_c$ kg^{-1} throughout the subsoil. Effective cation exchange capacity and base saturation are also low, but CEC at pH 7 is very high, indicating a considerable pH-dependent charge. Aluminum concentrations and saturation are high (>80%) throughout the subsoil. Total Al and Fe are very high, and total P is moderately high.

Horizon Description: Verrugosa B

A—0 to 15 cm; dark reddish-brown (5YR 3/3) silty clay loam; moderate fine and very fine subangular blocky structure; slightly sticky and slightly plastic; about 2% hard angular coarse gravel fragments; common coarse and many medium, fine, and very fine roots; clear smooth boundary.

B1—15 to 46 cm; dark reddish-brown (5YR 3/3) sandy clay loam; moderate coarse subangular blocky structure, breaking to fine and very fine blocky; moist and friable; slightly sticky and slightly plastic; about 2% hard angular coarse gravel; common earthworms; common coarse, medium, fine, and very fine roots; clear smooth boundary.

B2—46 to 68 cm; reddish-brown to dark reddish-brown (5YR 4/3 to 3/3) gravelly sandy clay loam; moderate medium and fine subangular blocky structure; sticky; about 25% hard but weathered (crushable) medium gravel; common medium earthworms; common coarse and medium and few fine and very fine roots; clear smooth boundary.

B3—68 to 77 cm; dark reddish-brown (2.5YR 3/3) gravelly sandy loam; fine and very fine subangular blocky structure; moist and friable; about 30% hard angular medium and coarse gravel; very few fine roots; clear smooth boundary.

B4—77 to 86 cm; yellowish-red (5YR 4/6) gravelly sandy clay loam; moderate fine and very fine subangular blocky structure; moist and firm; slightly sticky; about 35% medium hard angular gravel; thick, continuous black Mn films on gravel faces; few fine and very fine roots; clear wavy boundary.

BC—86 to 119 cm; reddish-brown (5YR 4/3) massive clay; very sticky and very plastic; about 2% hard angular fine gravel fragments at the base of the horizon; very few fine and very fine roots; clear wavy boundary.

CB—119 to 150 cm; dark reddish-brown (2.5YR 3/3) gravelly sandy clay loam; massive; moist and friable; sticky and plastic; very few fine and very fine roots; about 35% hard but crushable fine, medium, and coarse gravel; gradual wavy boundary

C—150 to 201+ cm; extremely gravelly clay loam; about 90% hard angular coarse gravel and cobbles; thick black Mn films on gravel surfaces; bright yellow precipitate in upper part of the horizon.

Laboratory Analysis: Verrugosa B

TABLE M.1. Soil physical properties, including bulk density and particle-size distribution, by genetic horizon in the Verrugosa B soil. Dash (—) = not determined.

Horizon	Designation	Bulk density (fine earth)	Coarse fragments (>2 mm)	Sand	Silt	Clay	Textural class	Clay:silt ratio
—cm—		—g cm^{-3}—	—%—	—%—	—%—	—%—		
0–15	A	—	2	18.8	29.0	52.2	Clay	1.80
15–46	B1	1.03	2	23.4	29.6	47.0	Clay	1.59
46–68	B2	1.35	25	17.9	20.2	61.9	Clay	3.06
68–77	B3	—	30	12.0	35.2	52.9	Clay	1.50
77–86	B4	—	35	18.2	25.8	55.9	Clay	2.17
86–119	BC	1.11	2	8.4	29.9	61.7	Clay	2.06
119–150	CB	—	35	14.5	31.6	53.9	Clay	1.71
150–201+	C	—	90	30.4	31.2	38.4	Clay loam	1.23

TABLE M.2. Soil pH and total carbon and nitrogen by genetic horizon in the Verrugosa B soil.

Horizon	Soil pH			Total C	Total N	C:N	C:P	N:P
—cm—	Water	$CaCl_2$	$BaCl_2$	—%—	—%—			
0–15	5.01	4.28	4.03	7.03	0.58	12.2	111.8	9.2
15–46	4.76	4.15	4.11	2.82	0.30	9.4	44.1	4.7
46–68	4.98	4.24	4.16	0.95	0.10	9.1	20.6	2.2
68–77	5.14	4.14	4.12	0.20	0.03	7.7	7.6	1.1

(*Continued*)

TABLE M.2. (*Continued*)

Horizon	Soil pH			Total C	Total N	C:N	C:P	N:P
—cm—	Water	$CaCl_2$	$BaCl_2$	—%—	—%—			
77–86	4.99	4.14	4.09	0.34	0.04	8.6	7.6	0.9
86–119	4.99	3.93	3.97	0.36	0.04	8.0	27.7	3.1
119–150	5.09	4.06	4.10	0.19	0.03	7.3	7.1	1.1
150–201+	5.05	4.20	4.15	0.21	0.03	8.0	2.2	0.3

TABLE M.3. Exchangeable cations and effective cation exchange capacity (ECEC) by extraction in 0.1 M barium chloride ($BaCl_2$) by genetic horizon in the Verrugosa B soil. BS = base saturation; sat = saturation; TEB = total exchangeable bases.

Horizon	Al	Ca	Fe	K	Mg	Mn	Na	TEB[a]	ECEC[b]	BS[c]	ECEC per kg clay	Al sat	Ca:Mg
—cm—	$\text{cmol}_c\ \text{kg}^{-1}$									—%—	$\text{cmol}_c\ \text{kg}^{-1}$	—%—	
0–15	4.66	6.27	0.01	0.20	1.96	0.29	0.15	8.6	13.5	63.4	25.9	34.4	3.2
15–46	7.58	0.27	0.01	0.07	0.38	0.10	0.07	0.8	8.5	9.2	18.0	89.4	0.7
46–68	7.35	0.90	0.01	0.14	0.38	0.07	0.02	1.4	8.9	16.2	14.3	82.9	2.3
68–77	12.11	0.64	0.01	0.05	0.65	0.03	0.04	1.4	13.5	10.2	25.6	89.5	1.0
77–86	10.29	0.43	0.01	0.02	0.55	0.06	0.08	1.1	11.4	9.4	20.4	90.0	0.8
86–119	17.25	0.25	<0.01	0.02	0.64	0.02	0.05	1.0	18.2	5.3	29.5	94.6	0.4
119–150	13.19	0.17	0.01	0.03	0.35	0.02	0.02	0.6	13.8	4.2	25.6	95.6	0.5
150–201+	4.84	0.13	0.01	<0.01	0.17	0.03	0.03	0.3	5.2	6.4	13.6	93.0	0.8

[a] TEB determined by extraction in 0.1 M $BaCl_2$.

[b] ECEC determined as the sum of cations extracted in extraction in 0.1 M $BaCl_2$.

[c] BS determined as (TEB ÷ ECEC) × 100.

TABLE M.4. Extractable acidity, exchangeable cations, and cation exchange capacity (CEC) determined in buffered solutions by genetic horizon in the Verrugosa B soil. BS = base saturation; TEB = total exchangeable bases, dash (—) = not determined.

Horizon	Extractable acidity	CEC by sum of cations[a]	BS by sum of cations[b]	CEC7[c]	Ca	K	Mg	Na	TEB by CEC7[d]	BS by CEC7[e]	CEC7 per kg clay
—cm—	$\text{cmol}_c\ \text{kg}^{-1}$	$\text{cmol}_c\ \text{kg}^{-1}$	—%—	$\text{cmol}_c\ \text{kg}^{-1}$						—%—	$\text{cmol}_c\ \text{kg}^{-1}$
0–15	—	—	—	—	—	—	—	—	—	—	—
15–46	28.7	29.5	3	24.1	0.16	0.08	0.35	0.07	0.7	2.7	51.3
46–68	21.7	23.1	6	20.6	0.78	0.17	0.39	0.03	1.4	6.7	33.2
68–77	21.0	22.4	6	22.9	0.36	0.04	0.51	0.07	1.0	4.3	43.3
77–86	23.2	24.3	4	—	—	—	—	—	—	—	—
86–119	—	—	—	—	—	—	—	—	—	—	—
119–150	—	—	—	—	—	—	—	—	—	—	—
150–201+	—	—	—	—	—	—	—	—	—	—	—

[a] Sum of extractable acidity and TEB.

[b] BS determined from TEB ÷ CEC sum of cations × 100.

[c] CEC determined by extraction in ammonium acetate (pH 7).

[d] TEB (sum of Ca, K, Mg, and Na) determined by extraction in ammonium acetate (pH 7).

[e] BS determined as (TEB ÷ ECEC) × 100.

TABLE M.5. Pedogenic metal oxides extractable in acid-ammonium oxalate and buffered dithionite by genetic horizon in the Verrugosa B soil. Fe_{ox}:Fe_d ratio, oxalate-extractable iron/dithionite-extractable iron.

	Dithionite extraction			Oxalate extraction						
Horizon	**Al**	**Fe**	**Mn**	**Al**	**Fe**	**Mn**	**P**	**Si**	**Al+½Fe**	**Fe_{ox}:Fe_d**
—cm—	—%—			—mg g^{-1}—					—%—	
0–15	0.66	4.55	0.17	5.01	5.59	1.29	0.26	0.10	0.78	0.12
15–46	0.70	5.26	0.15	5.19	6.51	1.19	0.20	0.19	0.84	0.12
46–68	0.60	5.96	0.20	5.53	3.92	1.61	0.11	0.30	0.75	0.07
68–77	0.44	6.63	0.12	3.50	1.08	0.84	0.03	0.10	0.40	0.02
77–86	0.83	7.34	0.24	4.09	2.64	1.58	0.03	0.25	0.54	0.04
86–119	0.56	8.40	0.06	3.54	2.87	0.49	0.01	0.08	0.50	0.03
119–150	0.55	6.45	0.16	3.79	1.63	1.05	0.03	0.11	0.46	0.03
150–201+	1.04	6.83	0.72	5.17	4.04	5.05	0.24	0.38	0.72	0.06

TABLE M.6. Total elements by nitric acid digestion by genetic horizon in the Verrugosa B soil.

Horizon	Al	B	Ca	Cu	Fe	K	Mg	Mn	Na	P	Zn
—cm—	—mg g^{-1}—										
0–15	77.8	0.008	2.39	0.130	65.8	6.87	3.53	1.76	3.51	0.817	0.068
15–46	92.6	0.006	1.09	0.152	75.9	9.52	3.80	1.70	3.97	0.742	0.064
46–68	113.5	0.006	0.66	0.232	80.9	18.06	4.64	1.89	5.34	0.455	0.086
68–77	111.9	0.007	0.44	0.157	87.1	21.25	3.47	1.25	5.29	0.309	0.071
77–86	109.9	<0.005	0.29	0.261	94.3	8.38	3.87	2.20	3.44	0.575	0.080
86–119	110.2	<0.005	0.52	0.087	99.8	12.47	2.02	0.59	8.23	0.144	0.052
119–150	111.0	0.007	0.39	0.154	82.9	16.54	2.64	1.47	5.70	0.332	0.052
150–201+	106.7	<0.005	0.21	0.254	92.4	5.43	7.11	6.65	2.20	1.265	0.129

N. Zarceadero, Fortuna Forest Reserve, Panama (Figure 3.11)

Soil taxonomy:	Fine, mixed, active, isothermic, Typic Haplohumult
Profile location:	Follow the gravel road down from the dam on the north side, following the right fork (left fork goes to the Pinola plot) and park at the spillway after about 3 km. Cross the river and follow the steep trail up the ridge line to the profile pit.
Latitude/longitude:	8.762611°N, –82.269477°E
UTM:	17P, 0360366 m E., 0968843 m N.
Date and season:	20 January 2014; early dry season
Elevation:	1,150 m asl
Slope and site position:	Crest of a moderately steep (22%) narrow linear SSE trending interfluve ridge
Soil moisture regime:	Perudic: mean annual rainfall at nearby Pinola 4,964 ± 863 mm, with 159 ± 27 mm mean monthly dry season rainfall (1 January–30 April)
Soil temperature regime:	Isothermic: mean annual temperature at nearby Pinola 18.5°C, with mean monthly temperature varying by <2°C over the annual cycle
Parent material:	Granodiorite
Vegetation:	Montane tropical rainforest; canopy height 20 to 25 m; patches dominated by the ectomycorrhizal tree *Oreomunnea mexicana* (Juglandaceae) and frequent small stems, including tree ferns
Drainage:	Well drained
Surface features:	Incomplete cover of dry leaves and twigs
Faunal activity:	Common earthworms and grubs in the upper horizons
Coarse fragments:	Granodiorite boulders in subsoil
Rooting depth:	Throughout the profile, but mainly in the upper 10 cm
Control section:	Between 20 and 66 cm (i.e., the entire argillic horizon)
Particle-size class:	Fine (35%–60% clay)
Mineralogy class:	Mixed (predominantly gibbsite, with kaolinite, hydroxy-interlayer vermiculite, and cristobalite)
Cation-exchange activity class:	Active (CEC by NH$_4$AOc = 42 cmol$_c$ kg^{-1} clay)
Diagnostic horizons/features:	(1) Perudic moisture regime and isothermic temperature regime (2) Ochric epipedon from 0 to 20 cm (3) Argillic horizon from 20 to 66 cm (4) Clay decrease of >20% below the maximum in the upper 150 cm

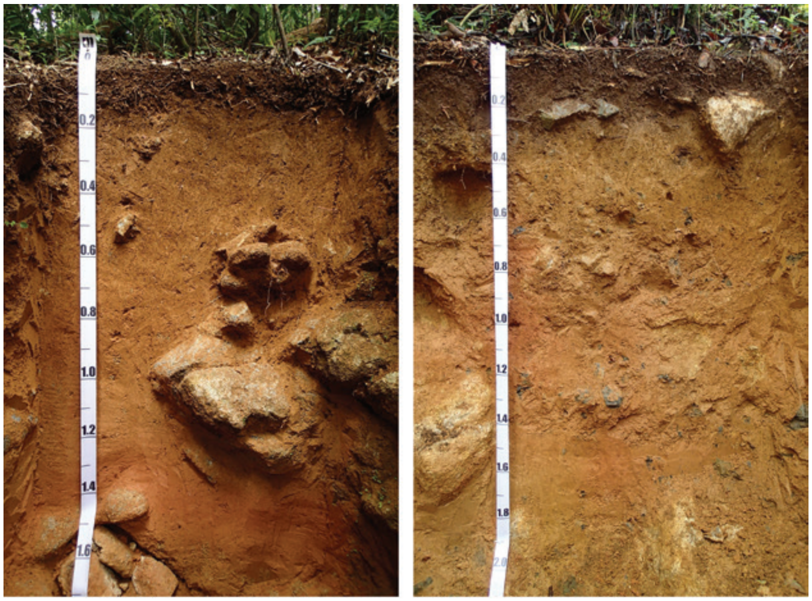

(a) Zarceadero

(b) Zorro A

FIGURE 3.11. The profiles at (a) Zarceadero and (b) Zorro A.

General Features of the Soil

This profile is representative of soils formed on granodiorite on relatively stable slopes. It is the same taxonomic class as the profiles at Hornito, developed on dacite, which is the volcanic equivalent (chemically) of granodiorite. However, the Zarceadero profile contains less clay and has a more pronounced argillic horizon. It contrasts with the pedogenically younger Zorro profile that appears to have formed on a more active slope. Soil C:N ratios are high, typical of soils supporting ectomycorrhizal forest.

Soil Taxonomy

The soil is an Ultisol because it has an argillic horizon with low base saturation at depth (i.e., <35% by sum of cations at 125 cm below the top of the argillic horizon). The soil is a Humult because the upper 15 cm of the argillic horizon contains >0.9% C, and there is >12 kg C m^{-2} in the upper 100 cm of the profile. Although ECEC is <12 cmol$_c$ kg^{-1} clay in the argillic horizon, CEC by NH$_4$OAc is high (>40 cmol$_c$ kg^{-1} clay), so there is no kandic horizon. The clay decrease of >20% below the maximum in the upper 150 cm of the profile means it does not qualify as a Palehumult. The profile is therefore a Haplohumult. In the absence of other diagnostic features at the subgroup level, the profile qualifies as a Typic Haplohumult. The soil moisture regime is perudic because rainfall exceeds potential evapotranspiration in all months.

Chemical and Physical Properties

Despite the strong red colors, the subsoil contains only moderate concentrations of crystalline Fe, although Al$_d$ is high. Indeed, the largest identified clay mineral is gibbsite (large peak) with small peaks from kaolinite and others minerals, giving a mixed mineralogy class. The soil is acidic and contains extremely low concentrations of base cations in the subsoil.

Horizon Description: Zarceadero

A—0 to 10 cm; dark brown (7.5YR 3/2) sandy clay loam; strong fine subangular blocky structure; slightly dry and friable; sticky and very plastic; many interstitial pores; few small earthworms; clear smooth boundary.

AB—10 to 20 cm; dark brown (7.5YR 3/4) sandy clay loam; strong medium subangular blocky structure, breaking to fine and very fine subangular blocky; slightly dry and friable; about 2% medium and coarse weathered granodiorite gravel; sticky and plastic; no clay films; few earthworms and grubs; few fine charcoal fragments; clear smooth boundary.

Bt1—20 to 39 cm; brown (7.5YR 4/4) sandy clay; moderate medium subangular blocky structure, breaking to very fine subangular blocky and fine granular; slightly moist and firm; sticky and very plastic; about 2% medium and coarse moderately weathered granodiorite gravel; faint continuous clay films on ped faces and pore linings; gradual smooth boundary.

Bt2—39 to 66 cm; strong brown (7.5YR 4/6) sandy clay loam; strong medium and coarse subangular blocky structure, breaking to very fine subangular blocky and fine granular; slightly moist and firm; sticky and slightly plastic; no clear clay films; about 12% hard but slightly weathered granodiorite cobbles and about 2% medium weathered granodiorite gravel; gradual smooth boundary.

Bo1—66 to 124 cm; yellowish-red (5YR 5/6) stony sandy clay loam; strong coarse subangular blocky structure, breaking to strong fine subangular blocky and fine granular; slightly moist and firm; no clay films; sticky and slightly plastic; about 60% hard but slightly weathered granodiorite cobbles and stones; gradual smooth boundary.

Bo2—124 to 152 cm; red (2.5YR 5/6) sandy clay loam; moderate medium subangular blocky structure, breaking to strong fine subangular blocky and fine granular; slightly moist and friable; sticky and slightly plastic; common flat golden shiny mineral grains; clear wavy boundary.

C—152+ cm; strong brown (7.5YR 5/6) stony coarse sandy loam; about 90% hard granodiorite cobbles and stones; fine granular structure; slightly moist and friable.

Laboratory Analysis: Zarceadero

TABLE N.1. Soil physical properties, including bulk density and particle-size distribution, by genetic horizon in the Zarceadero soil. Dash (—) = not determined.

Horizon	Designation	Bulk density (fine earth)	Coarse fragments (>2 mm)	Sand	Silt	Clay	Textural class	Clay:silt ratio
—cm—		—g cm^{-3}—	—vol%—	—%—	—%—	—%—		
0–10	A	0.62	0	42.8	27.8	29.4	Clay loam	1.06
10–20	AB	0.99	1	43.9	21.1	35.0	Clay loam	1.66

(*Continued*)

TABLE N.1. (*Continued*)

Horizon	Designation	Bulk density (fine earth)	Coarse fragments (>2 mm)	Sand	Silt	Clay	Textural class	Clay:silt ratio
—cm—		—$g\ cm^{-3}$—	—vol%—	—%—	—%—	—%—		
20–39	Bt1	0.99	1	38.0	20.7	41.2	Clay	1.99
39–66	Bt2	1.14	13	33.9	24.9	41.2	Clay	1.65
66–124	Bw1	1.16	60	44.0	26.4	29.6	Clay loam	1.12
124–152	Bw2	1.26	0	46.6	29.5	23.9	Loam	0.81
152+	C	—	90	58.1	23.6	18.3	Sandy loam	0.78

TABLE N.2. Soil pH and total carbon and nitrogen by genetic horizon in the Zarceadero soil.

Horizon	Soil pH			Total C	Total N	C:N	C:P	N:P
—cm—	Water	$CaCl_2$	$BaCl_2$	—%—	—%—			
0–10	4.93	4.16	3.85	5.91	0.37	16.0	168.9	10.6
10–20	4.98	4.42	4.17	3.08	0.19	16.2	98.0	6.0
20–39	5.02	4.41	4.40	1.69	0.09	18.8	60.8	3.2
39–66	4.95	4.30	4.36	0.83	0.04	20.8	30.4	1.5
66–124	5.12	4.21	4.35	0.32	0.01	32.0	13.3	0.4
124–152	5.03	4.09	4.22	0.12	0.01	12.0	6.3	0.5
152+	5.01	4.22	4.16	0.17	0.01	17.0	3.6	0.2

TABLE N.3. Exchangeable cations and effective cation exchange capacity (ECEC) by extraction in 0.1 M barium chloride ($BaCl_2$) by genetic horizon in the Zarceadero soil. BS = base saturation; sat = saturation; TEB = total exchangeable bases.

Horizon	Al	Ca	Fe	K	Mg	Mn	Na	TEB[a]	ECEC[b]	BS[c]	ECEC per kg clay	Al sat	Ca:Mg
—cm—	$cmol_c\ kg^{-1}$									—%—	$cmol_c\ kg^{-1}$	—%—	
0–10	3.45	0.82	0.04	0.19	0.72	0.05	0.04	1.8	5.3	33.4	18.0	64.9	1.1
10–20	1.79	0.11	<0.01	0.08	0.16	0.01	0.02	0.4	2.2	17.1	6.2	82.1	0.7
20–39	1.62	0.07	<0.01	0.05	0.13	0.02	<0.01	0.3	1.9	13.4	4.6	85.4	0.6
39–66	2.28	0.08	<0.01	0.06	0.49	0.01	0.01	0.6	2.9	21.6	7.1	78.2	0.2
66–124	3.11	0.08	<0.01	0.41	0.28	0.02	<0.01	0.8	3.9	19.8	13.1	79.8	0.3
124–152	5.14	0.21	<0.01	0.29	0.33	0.03	0.01	0.8	6.0	14.0	25.2	85.4	0.6
152+	2.36	0.07	<0.01	0.16	0.19	0.04	0.01	0.4	2.8	15.2	15.5	83.3	0.4

[a] TEB determined by extraction in 0.1 M $BaCl_2$.

[b] ECEC determined as the sum of cations extracted in extraction in 0.1 M $BaCl_2$.

[c] BS determined as (TEB ÷ ECEC) × 100.

TABLE N.4. Extractable acidity, exchangeable cations, and cation exchange capacity (CEC) determined in buffered solutions by genetic horizon in the Zarceadero soil. BS = base saturation; TEB = total exchangeable bases; dash (—) = not determined.

Horizon	Extractable acidity	CEC by sum of cations[a]	BS by sum of cations[b]	CEC7[c]	Ca	K	Mg	Na	TEB by CEC7[d]	BS by CEC7[e]	CEC7 per kg clay
—cm—	$\text{cmol}_c\ \text{kg}^{-1}$	$\text{cmol}_c\ \text{kg}^{-1}$	—%—	$\text{cmol}_c\ \text{kg}^{-1}$						—%—	$\text{cmol}_c\ \text{kg}^{-1}$
0–10	—	—	—	—	—	—	—	—	—	—	—
10–20	—	—	—	21.21	0.05	0.07	0.09	0.03	0.2	1.1	60.6
20–39	21.4	21.6	1	17.39	0.05	0.05	0.08	0.02	0.2	1.1	42.2
39–66	16.0	16.7	4	17.15	0.05	0.05	0.38	0.02	0.5	3.0	41.6
66–124	12.4	13.2	6	—	—	—	—	—	—	—	—
124–152	11.4	12.2	7	—	—	—	—	—	—	—	—
152+	—	—	—	—	—	—	—	—	—	—	—

[a] Sum of extractable acidity and TEB.

[b] BS determined from TEB ÷ CEC sum of cations × 100.

[c] CEC determined by extraction in ammonium acetate (pH 7).

[d] TEB (sum of Ca, K, Mg, and Na) determined by extraction in ammonium acetate (pH 7).

[e] BS determined as (TEB ÷ ECEC) × 100.

TABLE N.5. Pedogenic metal oxides extractable in acid-ammonium oxalate and buffered dithionite by genetic horizon in the Zarceadero soil. $Fe_{ox}:Fe_d$ ratio, oxalate-extractable iron/dithionite-extractable iron.

	Dithionite extraction			Oxalate extraction						
Horizon	Al	Fe	Mn	Al	Fe	Mn	P	Si	Al+½Fe	$Fe_{ox}:Fe_d$
—cm—	%			mg g^{-1}					—%—	
0–10	0.86	3.02	<0.01	5.48	6.83	0.04	0.09	0.23	0.89	0.23
10–20	1.10	3.74	<0.01	6.96	6.90	0.03	0.06	0.56	1.04	0.18
20–39	1.14	4.37	<0.01	5.28	5.23	0.03	0.03	0.47	0.79	0.12
39–66	1.04	4.63	<0.01	3.46	2.43	0.01	0.02	0.37	0.47	0.05
66–124	0.60	3.16	<0.01	2.64	1.43	0.04	0.01	0.33	0.34	0.05
124–152	0.34	2.31	0.02	2.03	0.55	0.11	<0.01	0.19	0.23	0.02
152+	0.36	2.31	0.02	1.76	0.74	0.15	0.02	0.23	0.21	0.03

TABLE N.6. Total elements by nitric acid digestion by genetic horizon in the Zarceadero soil.

Horizon	Al	B	Ca	Cu	Fe	K	Mg	Mn	Na	P	Zn
—cm—	mg g^{-1}										
0–10	74.6	<0.005	1.54	0.068	48.8	0.51	2.74	0.17	0.47	0.350	0.036
10–20	93.2	0.010	1.18	0.086	54.7	0.54	2.78	0.18	0.41	0.314	0.040
20–39	108.7	<0.005	0.66	0.105	61.4	0.59	2.98	0.18	0.23	0.278	0.045
39–66	124.1	<0.005	0.24	0.138	65.8	1.06	4.42	0.19	0.08	0.273	0.052
66–124	112.8	<0.005	0.17	0.143	64.2	1.92	5.88	0.24	0.04	0.240	0.065
124–152	106.0	<0.005	0.10	0.124	61.2	2.60	5.26	0.33	0.07	0.190	0.065
152+	106.0	<0.005	0.15	0.156	63.3	3.13	7.41	0.40	0.07	0.473	0.086

O. Zorro A Forest Census Plot, Fortuna Forest Reserve, Panama (Figure 3.11)

Soil taxonomy:	Fine-loamy, mixed, active, isothermic, Typic Humudept
Profile location:	Park car at small cabin on road below dam and follow the trail 500 m to the plot. The pit is located close to the 100,80 marker (00,00 in SW corner)
Latitude/longitude:	8.762396°N, –82.260959°E
UTM:	17P, 0361303 m E., 0968816 m N.
Date and season:	8 May 2016; early wet season
Elevation:	1,360 m asl
Slope and site position:	Steep (32%) linear narrow interfluve, running up to a peak on the Continental Divide; dropping 70% toward the valley below
Soil moisture regime:	Perudic: mean annual rainfall at nearby Pinola 4,964 ± 863 mm, with 159 ± 27 mm mean monthly dry season rainfall (1 January–30 April)
Soil temperature regime:	Isothermic: mean annual temperature at nearby Pinola 18.5°C, with mean monthly temperature varying by <2°C over the annual cycle
Parent material:	Granodiorite with common angular mafic-volcanic gravel
Vegetation:	Montane tropical rainforest; canopy height 15 to 20 m; open understory with patches dominated by the ectomycorrhizal tree *Oreomunnea mexicana* (Juglandaceae), although none near pit; mainly smaller stems (~10 cm DBH) reflecting past human disturbance or landslide; abundant tree ferns; few understory palms
Drainage:	Well drained
Surface features:	Complete thin cover of wet leaves and twigs
Faunal activity:	Common small and medium earthworms in the upper horizons
Coarse fragments:	Granodiorite cobbles and boulders; common basaltic/volcanic angular fragments
Rooting depth:	Mainly the upper 1 m, with none observed below 145 cm
Control section:	Between 25 and 100 cm below the mineral surface
Particle-size class:	Fine-loamy (>15% sand and between 18% and 35% clay; 32% clay in the control section)
Mineralogy class:	Mixed (predominantly gibbsite, with smaller amounts of goethite and kaolinite by x-ray diffraction)
Cation-exchange activity class:	Active (CEC by NH_4AOc = 42 $cmol_c$ kg^{-1} clay)
Diagnostic horizons/features:	(1) Perudic moisture regime and isothermic temperature regime (2) Umbric epipedon from 0 to 26 cm (3) Cambic horizon from 26 to 145 cm

General Features of the Soil

This profile represents soils developed on relatively unstable slopes on granodiorite. It contrasts with the Zarceadero profile on a more stable slope that has developed into an Ultisol. The Zorro profile shows evidence of clay enrichment, including clay films, but this is insufficient for Ultisols. The profile has an organic-rich mineral epipedon over a reddish subsoil and is infertile, with very low base cation concentrations. However, CEC at pH 7 is very high, indicating a considerable pH-dependent charge. The profile contains dark gray volcanic angular coarse gravel and cobbles, which are of different lithology to the parent granodiorite and might therefore be linked to landslide activity or volcanic ejecta.

Soil Taxonomy

The clay increase is insufficient for an argillic horizon, so the profile qualifies as an Inceptisol because it has a cambic horizon. The profile is therefore a Udept because of the perudic moisture regime. The epipedon is umbric because the upper 18 cm has moist color value and chroma ≤3, >0.6% organic C, and base saturation by NH_4OAc at pH 7 of <50%. The profile therefore qualifies as a Humudept because of the umbric epipedon. In the absence of other diagnostic features, the profile qualifies as a Typic Humudept. This is a relatively recent addition to soil taxonomy, appearing in the 11th edition of *Keys to Soil Taxonomy* (Soil Survey Staff, 2010). Prior to 2010, the profile would have been classified as a Humic Dystrudept. The soil moisture regime is perudic because rainfall exceeds potential evapotranspiration in all months.

Chemical and Physical Properties

The profile has a brown epipedon over a reddish subsoil. There are gravel and cobbles throughout the profile. The soil has a sandy clay loam texture in the epipedon over a clay loam subsoil. Soil pH is very strongly acid, and organic matter concentrations are high in the upper 50 cm, with wide C:N ratios between 13 and 23, reflecting the dominance of ectomycorrhizal trees at this site. Base cation concentrations are extremely low, with TEB of ≤0.10 $cmol_c$ kg^{-1} throughout the subsoil to 183 cm. Effective cation exchange capacity and base saturation are also low, but CEC at pH 7 is high, indicating a considerable pH-dependent charge. Extractable Al concentrations are moderate in the B horizon, but the extremely low base cation concentrations mean that Al saturation is high (>80%) throughout the subsoil. Calcium concentrations are particularly low, including exchangeable and total Ca. Total P is moderate. Clay mineralogy was not determined but is presumed to be similar to nearby Zarceadero on identical lithology. In particular, the Zorro profile contains very high total Al (about 16% in the deep subsoil), which is reflected in the predominance of gibbsite in the clay fraction.

Horizon Description: Zorro A

A—0 to 10 cm; very dark brown (7.5YR 2.5/2) moist, dark brown (10YR 3/3) dry, silt loam; strong fine and very fine subangular blocky structure, breaking to very fine granular; moist and friable; slightly sticky and very plastic; common very fine, fine, and coarse, and many medium roots; many fine interstitial pores; about 2% granodiorite cobbles; clear smooth boundary.

AB—10 to 26 cm; dark brown (7.5YR 3/3) moist, dark yellowish-brown (10YR 4/4) dry, silty clay loam; strong fine subangular blocky structure, breaking to fine granular; moist and friable; sticky and plastic; common very fine, fine, medium, and coarse roots; no clay films; about 10% granodiorite and dark gray cobbles and boulders; clear smooth boundary.

B1—26 to 50 cm; strong brown (7.5YR 4/6) moist, brownish-yellow (10YR 6/6) dry, clay loam; moderate medium and coarse subangular blocky structure, breaking to very fine subangular blocky and fine granular; moist and friable; slightly sticky and plastic; common very fine and fine and few medium and coarse roots; common small and medium earthworms; faint clay films on ped faces; about 5% granodiorite and dark gray angular coarse gravel; gradual smooth boundary.

B2—50 to 94 cm; [jumbled stone layer of coarse gravel and cobbles] strong brown (7.5YR 5/6) moist, brownish-yellow (10YR 6/6) dry, sandy clay; moderate medium subangular blocky structure, breaking to very fine subangular blocky and fine granular; moist and friable; sticky and very plastic; few very fine, fine, and medium roots; faint clay films on ped faces and pore linings; about 10% rounded granodiorite cobbles and 10% angular dark gray andesite coarse gravel; wavy gradual boundary.

B3—94 to 145 cm; yellowish-red (5YR 5/6) moist, reddish-yellow (7.5YR 6/6) dry, sandy clay; moderate coarse subangular blocky structure, breaking to very fine subangular blocky and fine granular; moist and friable; slightly sticky and plastic; very few very fine, fine, and medium roots; faint clay films on ped faces and pore linings; about 10% granodiorite cobbles and 5% dark gray angular andesite coarse gravel; wavy gradual boundary.

B4—145 to 183 cm; red (2.5YR 5/6) moist, reddish-yellow (7.5YR 7/6) dry, sandy clay (loam); moderate medium subangular blocky structure, breaking to very fine subangular blocky and fine granular; moist and firm; slightly sticky and slightly plastic; no roots; faint clay films on ped faces; about 10% angular dark gray andesite coarse gravel and cobbles; wavy gradual boundary.

BC—183 to 210 cm; yellowish-brown (10YR 6/6) moist, very pale brown (10YR 8/4) dry, sandy clay loam; moderate medium subangular blocky structure, breaking to moderate very fine subangular blocky and fine granular; moist and firm; slightly sticky and not plastic; no roots; very few fine tubular pores; faint clay films in pore linings; about 50% rounded weathered granodiorite boulders and 2% angular dark gray andesite coarse gravel.

R—210+ cm; weathered granodiorite.

Laboratory Analysis: Zorro A

TABLE O.1. Soil physical properties, including bulk density and particle-size distribution, by genetic horizon in the Zorro soil.

Horizon	Designation	Bulk density (fine earth)	Stones (>2 mm)	Sand	Silt	Clay	Textural class	Clay:silt ratio
—cm—		—g cm^{-3}—	—%—	—%—	—%—	—%—		
0–10	A	0.42	2	48.4	24.3	27.3	Sandy clay loam	1.12
10–26	AB	0.81	10	47.6	22.0	30.5	Sandy clay loam	1.39
26–50	B1	1.08	5	41.8	27.4	30.8	Clay loam	1.12
50–94	B2	1.27	20	39.7	28.3	32.0	Clay loam	1.13
94–145	B3	1.60	15	44.9	23.4	31.7	Clay loam	1.36
145–183	B4	1.50	10	40.4	23.1	36.5	Clay loam	1.58
183–210	BC	1.61	50	35.9	25.1	39.0	Clay loam	1.56

TABLE O.2. Soil pH and total carbon and nitrogen by genetic horizon in the Zorro soil.

Horizon	Soil pH			Total C	Total N	C:N	C:P	N:P
—cm—	Water	CaCl$_2$	BaCl$_2$	—%—	—%—			
0–10	4.80	3.95	3.85	9.80	0.73	13.3	158.3	11.9
10–26	4.96	4.29	4.17	6.67	0.46	14.6	124.7	8.5
26–50	4.98	4.63	4.40	2.89	0.17	17.0	63.5	3.7
50–94	4.85	4.39	4.36	0.85	0.04	19.6	24.4	1.2
94–145	4.80	4.37	4.35	0.55	0.03	19.6	16.8	0.9
145–183	4.79	4.27	4.22	0.32	0.01	22.8	11.4	0.5
183–210	4.75	4.14	4.16	0.40	0.02	17.9	12.8	0.7

TABLE O.3. Exchangeable cations and effective cation exchange capacity (ECEC) by extraction in 0.1 M barium chloride (BaCl$_2$) by genetic horizon in the Zorro soil. BS = base saturation; sat = saturation; TEB = total exchangeable bases.

Horizon	Al	Ca	Fe	K	Mg	Mn	Na	TEB[a]	ECEC[b]	BS[c]	ECEC per kg clay	Al sat	Ca:Mg
—cm—	cmol$_c$ kg^{-1}									—%—	cmol$_c$ kg^{-1}	—%—	
0–10	4.54	1.83	0.08	0.25	0.40	0.02	0.07	2.56	7.2	35.5	26.4	63	4.5
10–26	2.48	0.27	0.06	0.09	0.10	<0.01	0.03	0.48	3.0	16.0	9.9	82	2.7
26–50	0.54	0.03	0.02	0.03	0.02	<0.01	0.01	0.10	0.7	14.6	2.1	82	1.3
50–94	0.58	0.02	<0.01	0.01	0.01	<0.01	0.02	0.06	0.7	9.8	2.0	90	1.8
94–145	0.69	0.01	<0.01	0.03	0.01	<0.01	0.01	0.07	0.8	9.1	2.4	90	0.8
145–183	1.17	<0.01	<0.01	0.03	0.02	<0.01	0.02	0.08	1.3	6.2	3.4	93	0.2
183–210	2.37	0.06	<0.01	0.04	0.03	<0.01	0.02	0.16	2.5	6.4	6.5	93	1.9

[a] TEB determined by extraction in 0.1 M BaCl$_2$.

[b] ECEC determined as the sum of cations extracted in extraction in 0.1 M BaCl$_2$.

[c] BS determined as (TEB ÷ ECEC) × 100.

TABLE O.4. Extractable acidity, exchangeable cations, and cation exchange capacity (CEC) determined in buffered solutions by genetic horizon in the Zorro soil. BS = base saturation; TEB = total exchangeable bases; dash (—) = not determined.

Horizon	Extractable acidity	CEC by sum of cations[a]	BS by sum of cations[b]	CEC7[c]	Ca	K	Mg	Na	TEB by CEC7[d]	BS by CEC7[e]	CEC7 per kg clay
—cm—	cmol$_c$ kg^{-1}	cmol$_c$ kg^{-1}	—%—	cmol$_c$ kg^{-1}						—%—	cmol$_c$ kg^{-1}
0–10	—	—	—	36.5	0.86	0.21	0.32	0.05	1.4	3.9	133.6
10–26	—	—	—	26.8	0.10	0.08	0.08	0.02	0.3	1.0	87.8
26–50	—	—	—	18.0	0.01	0.03	0.02	0.01	<0.1	0.4	58.4
50–94	—	—	—	10.9	0.01	0.02	0.01	0.01	<0.1	0.4	34.2
94–145	—	—	—	8.9	0.01	0.02	0.01	0.01	<0.1	0.6	28.1
145–183	—	—	—	—	—	—	—	—	—	—	—
183–210	—	—	—	—	—	—	—	—	—	—	—

[a] Sum of extractable acidity and TEB.

[b] BS determined from TEB ÷ CEC sum of cations × 100.

[c] CEC determined by extraction in ammonium acetate (pH 7).

[d] TEB (sum of Ca, K, Mg, and Na) determined by extraction in ammonium acetate (pH 7).

[e] BS determined as (TEB ÷ ECEC) × 100.

TABLE O.5. Pedogenic metal oxides extractable in acid-ammonium oxalate and buffered dithionite by genetic horizon in the Zorro soil. Fe_{ox}:Fe_d ratio, oxalate-extractable iron/dithionite-extractable iron.

	Dithionite extraction			Oxalate extraction						
Horizon	Al	Fe	Mn	Al	Fe	Mn	P	Si	Al+½Fe	Fe_{ox}:Fe_d
—cm—	—%—			mg g^{-1}					—%—	
0–10	1.43	3.42	0.004	1.81	1.72	<0.01	0.04	0.07	0.27	0.05
10–26	1.99	4.16	0.003	2.30	1.82	<0.01	0.03	0.14	0.32	0.04
26–50	1.82	5.04	0.005	2.12	1.89	<0.01	0.02	0.26	0.31	0.04
50–94	1.13	5.52	0.011	0.56	0.44	0.01	<0.01	0.04	0.08	0.01
94–145	0.91	5.48	0.018	0.30	0.22	0.02	<0.01	0.03	0.04	<0.01
145–183	0.88	5.28	0.012	0.33	0.20	0.01	<0.01	0.04	0.04	<0.01
183–210	0.69	4.55	0.009	0.36	0.11	<0.01	<0.01	0.03	0.04	<0.01

TABLE O.6. Total elements by nitric acid digestion by genetic horizon in the Zorro soil.

Horizon	Al	B	Ca	Cu	Fe	K	Mg	Mn	Na	P	Zn
—cm—	mg g^{-1}										
0–10	83.8	0.020	1.74	0.056	50.6	0.52	1.64	0.10	0.72	0.619	0.029
10–26	96.5	<0.005	1.34	0.071	62.1	0.46	1.55	0.12	0.71	0.535	0.039
26–50	131.6	0.013	0.65	0.095	67.4	0.66	1.62	0.14	0.42	0.455	0.039
50–94	147.6	<0.005	0.08	0.094	69.3	0.97	1.09	0.21	0.23	0.346	0.040
94–145	159.7	<0.005	0.06	0.088	73.1	1.00	1.67	0.20	0.22	0.329	0.041
145–183	157.2	<0.005	0.03	0.104	72.9	0.78	1.42	0.17	0.17	0.283	0.048
183–210	144.9	<0.005	0.05	0.126	60.5	1.04	1.98	0.15	0.19	0.309	0.052

Acknowledgements

We thank Dayana Agudo, Aleksandra Bielnicka, and Irene Torres for analytical support, Didimo Urena, Julio Rodriguez, Fredy Miranda, Ignacio del Cid, Fernando Garcia and Evidelio Garcia for field support, and Ian Baillie for comments on the manuscript.

References

Andersen, K. M. 2021. Palm Flora and Drivers of Distributions in Fortuna Forest Reserve. In *Fortuna Forest Reserve, Panama: Interacting Effects of Climate and Soils on the Biota of a Wet Premontane Tropical Forest*, ed. J. W. Dalling and B. L. Turner, pp. 271–287. Smithsonian Contributions to Botany, No. 112. Washington, D.C.: Smithsonian Institution Scholarly Press.

Andersen, K. M., M. J. Endara, B. L. Turner, and J. W. Dalling. 2012. Trait-Based Community Assembly of Understory Palms along a Soil Nutrient Gradient in a Lower Montane Tropical Forest. *Oecologia*, 168:519–531. https://doi.org/10.1007/s00442-011-2112-z

Andersen, K. M., J. R. Mayor, and B. L. Turner. 2017. Plasticity in Nitrogen Uptake among Sympatric Species with Contrasting Nutrient Acquisition Strategies in a Tropical Forest. *Ecology*, 98:1388–1398. https://doi.org/10.1002/ecy.1793

Andersen, K. M., B. L. Turner, and J. W. Dalling. 2010. Soil-Based Habitat Partitioning in Understorey Palms in Lower Montane Tropical Forests. *Journal of Biogeography*, 37:278–292. https://doi.org/10.1111/j.1365-2699.2009.02192.x

Andersen, K. M., B. L. Turner, and J. W. Dalling. 2014. Seedling Performance Trade-offs Influencing Habitat Filtering along a Soil Nutrient Gradient in a Tropical Forest. *Ecology*, 95:3399–3413. https://doi.org/10.1890/13-1688.1

Averill, C., B. L. Turner, and A. C. Finzi. 2014. Mycorrhiza-Mediated Competition between Plants and Decomposers Drives Soil Carbon Storage. *Nature*, 505:543–545. https://doi.org/10.1038/nature12901

Beck, H. E., N. E. Zimmermann, T. R. McVicar, N. Vergopolan, A. Berg, and E. F. Wood. 2018. Present and Future Köppen-Geiger Climate Classification Maps at 1-km Resolution. *Scientific Data*, 5:180–214. https://doi.org/10.1038/sdata.2018.214

Bockheim, J. G. 2014. Sombric Horizon. In *Soil Geography of the USA: A Diagnostic-Horizon Approach*, pp. 237–255. London: Springer International.

Buol, S. W., R. J. Southard, R. C. Graham, and P. A. McDaniel. 2003. Spodosols: Soils with Subsoil Accumulations of Humus and Sesquioxides. In *Soil Genesis and Classification*. 5th ed., pp. 327–338. Ames, IA: Blackwell Publishing. https://doi.org/10.1002/9780470960622.ch9

Buol, S. W., R. J. Southard, R. C. Graham, and P. A. McDaniel. 2011. Andisols: Soils with Andic Soil Properties. In *Soil Genesis and Classification*. 6th ed., pp. 249–264. Ames, IA: Wiley-Blackwell.

Committee on Tropical Soils. 1972. *Soils of the Humid Tropics*. Washington, D.C.: National Academy of Sciences.

Condit, R., B. M. J. Engelbrecht, D. Pino, R. Pérez, and B. L. Turner. 2013. Species Distributions in Response to Individual Soil Nutrients and Seasonal Drought across a Community of Tropical Trees. *Proceedings of the National Academy of Sciences*, 110:5064–5068. https://doi.org/10.1073/pnas.1218042110

Corrales, A., and C. L. Ovrebo. 2021. Fungi of the Fortuna Forest Reserve: Taxonomy and Ecology with Emphasis on Ectomycorrhizal Communities. In *Fortuna Forest Reserve, Panama: Interacting Effects of Climate and Soils on the Biota of a Wet Premontane Tropical Forest*, ed. J. W. Dalling and B. L. Turner, pp. 137–153. Smithsonian Contributions to Botany, No. 112. Washington, D.C.: Smithsonian Institution Scholarly Press.

Corrales, A., A. E. Arnold, A. Ferrer, B. L. Turner, and J. W. Dalling. 2016. Variation in Ectomycorrhizal Fungal Communities Associated with *Oreomunnea Mexicana* (Juglandaceae) in a Neotropical Montane Forest. *Mycorrhiza*, 26:1–17. https://doi.org/10.1007/s00572-015-0641-8

Corrales, A., S. A. Mangan, B. L. Turner, and J. W. Dalling. 2016. An Ectomycorrhizal Nitrogen Economy Facilitates Monodominance in a Neotropical Forest. *Ecology Letters*, 19:383–392. https://doi.org/10.1111/ele.12570

Corrales, A., B. L. Turner, L. Tedersoo, S. Anslan, and J. W. Dalling. 2017. Nitrogen Addition Alters Ectomycorrhizal Fungal Communities and Soil Enzyme Activities in a Tropical Montane Forest. *Fungal Ecology*, 27:14–23. https://doi.org/10.1016/j.funeco.2017.02.004

Courchesne, F., and M.-C. Turmel. 2008. Extractable Al, Fe, Mn, and Si. In *Soil Sampling and Methods of Analysis*, ed. M. R. Carter and E. G. Gregorich, pp. 307–316. Boca Raton, FL: Canadian Society of Soil Science and CRC Press.

Dahlgren, R. A., J. P. Dragoo, and F. C. Ugolini. 1997. Weathering of Mt. St. Helens Tephra under a Cryic-Udic Climatic Regime. *Soil Science Society of America Journal*, 61:1519–1525. https://doi.org/10.2136/sssaj1997.03615995006100050032x

Dalling, J. W., P. Barkan, P. J. Bellingham, J. R. Healey, and E. V. J. Tanner. 2011. Ecology and Distribution of Neotropical Podocarpaceae. In *Ecology of the Podocarpaceae in Tropical Forests*, ed. B. L. Turner and L. A. Cernusak, pp. 43–56. Smithsonian Contributions to Botany, No. 95. Washington, D.C.: Smithsonian Institution Scholarly Press.

Dalling, J. W., C. M. Prada, K. D. Heineman, K. M. Andersen, A. Morris, J. Pardo, E. Hollenbeck, P. Caballero, C. Espinosa, E. García, and B. L. Turner. 2021. Introduction to the Fortuna Forest Reserve: Soil and Climate Effects on the Tree Communities of a Premontane Tropical Forest. In *Fortuna Forest Reserve, Panama: Interacting Effects of Climate and Soils on the Biota of a Wet Premontane Tropical Forest*, ed. J. W. Dalling and B. L. Turner, pp. 1–33. Smithsonian Contributions to Botany, No. 112. Washington, D.C.: Smithsonian Institution Scholarly Press.

Dickie, I. A., and R. J. Holdaway. 2011. Podocarp Roots, Mycorrhizas, and Nodules. In *Ecology of the Podocarpaceae in Tropical Forests*, ed. B. L. Turner and L. A. Cernusak, pp. 175–187. Smithsonian Contributions to Botany, No. 95. Washington, D.C.: Smithsonian Institution Scholarly Press.

Engelbrecht, B. M. J., L. S. Comita, R. Condit, T. A. Kursar, M. T. Tyree, B. L. Turner, and S. Hubbell. 2007. Drought Sensitivity Shapes Species Distribution Patterns in Tropical Forests. *Nature*, 447:80–82. https://doi.org/10.1038/nature05747

Gee, G. W., and D. Or. 2002. Particle-Size Analysis. In *Methods of Soil Analysis, Part 4: Physical Methods*, ed. J. H. Dane and C. Topp, pp. 255–293. Madison, WI: Soil Science Society of America.

Grossman, R. B., and T. G. Reinsch. 2002. The Solid Phase. In *Methods of Soil Analysis, Part 4: Physical Methods*, ed. J. H. Dane and C. Topp, pp. 201–293. Madison, WI: Soil Society of America.

Hendershot, W. H., H. Lalande, and M. Duquette. 2008. Ion Exchange and Exchangeable Cations. In *Soil Sampling and Methods of Analysis*, ed. M. R. Carter and E. Gregorich, pp. 173–178. Boca Raton, FL: Canadian Society of Soil Science and CRC Press.

Holdridge, L. R. 1947. Determination of World Plant Formations from Simple Climatic Data. *Science*, 105:367–368. https://doi.org/10.1126/science.105.2727.367

Holdridge, L. R. 1967. *Life Zone Ecology*. San Jose, Costa Rica: Tropical Science Center.

Instituto Geográfico Nacional Tommy Guardia. 1991. Mapa Geologico Republica de Panama, Hoja 1, Region Occidental Bocas – Chiriqui, Escala 1:250,000. Ministerio de Comercio e Industrias, Dirección General de Recursos Minerales, Panama City, Republic of Panama.

Jansen, S., M. R. Broadley, E. Robbrecht, and E. Smets. 2002. Aluminum Hyperaccumulation in Angiosperms: A Review of Its Phylogenetic Significance. *The Botanical Review*, 68:235–269. https://doi.org/10.1663/0006-8101(2002)068[0235:AHIAAR]2.0.CO;2

Jenny, H. 1941. *Factors of Soil Formation: A System of Quantitative Pedology*. New York: McGraw-Hill.

Keiluweit, M., P. Nico, M. E. Harmon, J. Mao, J. Pett-Ridge, and M. Kleber. 2015. Long-Term Litter Decomposition Controlled by Manganese Redox Cycling. *Proceedings of the National Academy of Sciences*, 112:E5253–E5260. https://doi.org/10.1073/pnas.1508945112

Köppen, W. 1884. Die Wärmezonen der Erde, nach der Dauer der heissen, gemässigten und kalten Zeit und nach der Wirkung der Wärme auf die organische Welt betrachtet [The thermal zones of the earth according to the duration of hot, moderate and cold periods and to the impact of heat on the organic world]. *Meteorologische Zeitschrift*, 20:351–360. https://doi.org/10.1127/0941-2948/2011/105

Leigh, E. G. J. 1999. *Tropical Forest Ecology: A View from Barro Colorado Island*. New York: Oxford University Press.

Mizota, C., N. Toh, and Y. Matsuhisa. 1987. Origin of Cristobalite in Soils Derived from Volcanic Ash in Temperate and Tropical Regions. *Geoderma*, 39:323–330. https://doi.org/10.1016/0016-7061(87)90051-6

Orwin, K. H., M. U. F. Kirschbaum, M. G. St John, and I. A. Dickie. 2011. Organic Nutrient Uptake by Mycorrhizal Fungi Enhances Ecosystem Carbon Storage:

A Model-Based Assessment. *Ecology Letters*, 14:493–502. https://doi.org/10.1111/j.1461-0248.2011.01611.x

Prada, C. M., A. Morris, K. M. Andersen, B. L. Turner, P. Caballero, and J. W. Dalling. 2017. Soils and Rainfall Drive Landscape-Scale Changes in the Diversity and Functional Composition of Tree Communities in Premontane Tropical Forest. *Journal of Vegetation Science*, 28:859–870. https://doi.org/10.1111/jvs.12540

Schoeneberger, P. J., D. A. Wysocki, E. C. Benham, and Soil Survey Staff. 2012. *Field Book for Describing and Sampling Soils*. Version 3.0. Lincoln, NE: Natural Resources Conservation Service, National Soil Survey Center.

Schwertmann, U. 1993. Relations between Iron Oxides, Soil Color, and Soil Formation. In *Soil Color*, ed. J. M. Bingham and E. J. Ciolkosz, pp. 51–69. Madison, WI: Soil Science Society of America.

Seifferlein, E. R., P. Jones, R. Ferguson, R. Burt, and D. Mays. 2005. Extractable Acidity by a Centrifuge Method. *Communications in Soil Science and Plant Analysis*, 36:2067–2083. https://doi.org/10.1080/00103620500194353

Sherrod, D. R., J. W. Vallance, A. Tapia Espinosa, and J. P. McGeehin. 2008. Volcán Barú—Eruptive History and Volcano-Hazards Assessment. U.S. Geological Survey Open-File Report 2007–1401, p. 33. Reston, VA: U.S. Geological Survey.

Shoji, S., M. Nanzyo, and R. A. Dahlgren. 1993. *Volcanic Ash Soils: Genesis, Properties and Utilization*. Amsterdam: Elsevier.

Silva, C., D. Cárdenas, L. Londoño, B. L. Turner, and C. Jaramillo. 2021. Geological Map of the Fortuna Forest Reserve. In *Fortuna Forest Reserve, Panama: Interacting Effects of Climate and Soils on the Biota of a Wet Premontane Tropical Forest*, ed. J. W. Dalling and B. L. Turner, pp. 35–46. Smithsonian Contributions to Botany, No. 112. Washington, D.C.: Smithsonian Institution Scholarly Press.

Soil Survey Staff. 1999. *Soil Taxonomy: A Basic System of Soil Classification for Making and Interpreting Soil Surveys*. 2nd ed. Washington, D.C.: Soil Conservation Service, U.S. Department of Agriculture–Natural Resources Conservation Service.

Soil Survey Staff. 2010. *Keys to Soil Taxonomy*. 11th ed. Washington, D.C.: Soil Conservation Service, U.S. Department of Agriculture.

Soil Survey Staff. 2014. Soil Survey Laboratory Methods Manual. Soil Survey Investigations Report No. 42, Version 5.0, ed. R. Burt and Soil Survey Staff. Lincoln, NE: U.S. Department of Agriculture, National Resources Conservation Service.

Sposito, G. 2016. *The Chemistry of Soils*. 3rd ed. Oxford: Oxford University Press.

Steidinger, B. S., B. L. Turner, A. Corrales, and J. W. Dalling. 2015. Variability in Potential to Exploit Different Soil Organic Phosphorus Compounds among Tropical Montane Tree Species. *Functional Ecology*, 29:121–130. https://doi.org/10.1111/1365-2435.12325

Stevens, P. R., and T. W. Walker. 1970. The Chronosequence Concept and Soil Formation. *Quarterly Review of Biology*, 45:333–350. https://doi.org/10.1086/406646

Sumner, M. E., and W. P. Miller. 1996. Cation Exchange Capacity and Exchange Coefficients. In *Methods of Soil Analysis: Part 3, Chemical Methods*, ed. D. L. Sparks, A. L. Page, P. A. Helmke, R. H. Loeppert, P. N. Soltanpour, M. A. Tabatabai, C. T. Johnston, and M. E. Sumner, pp. 1201–1230. SSSA Book Series 5.3. Madison, WI: Soil Science Society of America.

Turner, B. L., T. Brenes-Arguedas, and R. Condit. 2018. Pervasive Phosphorus Limitation of Tree Species but not Communities in Tropical Forests. *Nature*, 555:367. https://doi.org/10.1038/nature25789

Viana, J. L., and J. W. Dalling. 2021. Diversity and Ecology of the Ferns in Fortuna. In *Fortuna Forest Reserve, Panama: Interacting Effects of Climate and Soils on the Biota of a Wet Premontane Tropical Forest*, ed. J. W. Dalling and B. L. Turner, pp. 237–270. Smithsonian Contributions to Botany, No. 112. Washington, D.C.: Smithsonian Institution Scholarly Press.

Vitousek, P. M. 2004. *Nutrient Cycling and Limitation*. Princeton, NJ: Princeton University Press.

Wegner, W., G. Wörner, R. S. Harmon, and B. R. Jicha. 2011. Magmatic History and Evolution of the Central American Land Bridge in Panama since Cretaceous Times. *gsapubs.org*, pp. 701–724.

Young, A. 1976. *Tropical Soils and Soil Survey*. Cambridge: Cambridge University Press.

4. Fungi of the Fortuna Forest Reserve: Taxonomy and Ecology with Emphasis on Ectomycorrhizal Communities

Adriana Corrales[1*] *and Clark L. Ovrebo*[2]

ABSTRACT. Panamanian montane forests harbor a high diversity of fungi, particularly of ectomycorrhizal (ECM) fungi; however their taxonomy and diversity patterns remain for the most part unexplored. We present state of the art fungal taxonomy and diversity patterns at Fortuna Forest Reserve based on morphological and molecular identification of more than 1,000 fruiting body collections of macromycetes made over a period of 5 years. We compare these new results with previously published work based on environmental sampling of *Oreomunnea mexicana* root tips. We compiled a preliminary list of species and report new records of 22 genera and 33 species for Panama. Based on fruiting body collection data, we compare the species composition of ECM fungal communities associated with *Oreomunnea* stands across sites differing in soil fertility and amount of rainfall. We also examine the effect of a long-term nitrogen addition treatment on the fruiting body production of ECM fungi. Finally, we discuss the biogeographic importance of Panama collections, which fill in the knowledge gap of ECM fungal records between Costa Rica and Colombia. Given that the Isthmus of Panama was an important migration route of ECM tree and fungal species from northern temperate areas to South America, the ECM fungal communities of Panama might show a high degree of isolation and therefore a high level of endemism. We expect that the forests at Fortuna will continue to yield new ECM macromycete data as we continue to study the collected specimens and describe new species.

INTRODUCTION

Fungi play essential roles in tropical ecosystems. They are involved in organic matter decomposition, plant nutrition, nutrient cycling, and in some cases can regulate the local abundances of plants (Tedersoo et al., 2014). In neotropical montane cloud forests, fungi are highly diverse and show strong endemism patterns (Del Olmo-Ruiz et al., 2017). In a recent review of fungal species associated with tropical montane cloud forests, Del Olmo-Ruiz et al. (2017) found 2,962 fungal species distributed within the neotropics. Of that total, only 220 species were originally described from neotropical montane forests, while many others species were shared mostly with the northern temperate region (Del Olmo-Ruiz et al., 2017). This study suggests a large gap in the knowledge of fungal species from underexplored areas in Central and South America where a great part of their diversity likely remains unknown. In the case of Panama, Del Olmo-Ruiz et al. (2017) only report 23 species of fungi from montane cloud forests. Even though Panama has a detailed checklist of fungi containing records of 2,772 species for the country (based on Piepenbring, 2006, 2007; maintained at http://biogeodb.stri.si.edu/fungi), most of the species are from lowland forests, and therefore there is a lack of knowledge of fungal communities from Panamanian montane forests.

In forested ecosystems, saprotrophic and mycorrhizal fungi are the most abundant functional groups of fungi. Saprotrophic fungi decompose organic matter into more

---

[1] Programa de Biología, Facultad de Ciencias Naturales, Universidad del Rosario, Cr. 24 #63C-69, Bogotá, D.C., Colombia.

[2] Department of Biology, University of Central Oklahoma. Edmond, OK 73034, USA.

[*] Correspondence: Adriana.corrales@urosario.edu.co; adricorrales33@gmail.com

simple carbohydrates that can be used for energy. Mycorrhizal fungi form symbiotic associations with the roots of plants receiving sugar from their host while helping them to obtain nutrients from the soil. Mycorrhizal fungi can be classified into two main groups: ECM and arbuscular mycorrhizal (AM). Tropical montane forests between 1,500 and 2,500 m above sea level (asl) are particularly rich in ECM fungal species due to high density of ECM host trees, intermediate temperatures, and high precipitation (Corrales et al., 2018; Geml et al., 2014; Gómez-Hernández et al., 2012). The diversity patterns of fungi associated with ECM host plant species have been studied on only a few occasions in montane forests in tropical America. Fungi associated with *Quercus*-dominated forests in Mexico, Costa Rica, and Colombia are the best-known montane ECM systems in the neotropics (Franco-Molano et al., 2010; Halling and Mueller, 2002, 1999; Halling and Ovrebo, 1987; Morris et al., 2008; Mueller and Halling, 1995) starting with the pioneering work of Singer (1963) in oak forest of Colombia. *Alnus*-dominated forests in Mexico, Bolivia, and Argentina have been studied to a lesser extent, for the most part based on sequencing of root symbiotic fungi using metagenomic approaches (Kennedy et al., 2015, 2011; Põlme et al., 2013; Wicaksono et al., 2017).

This chapter summarizes the research done at the Fortuna Forest Reserve (Fortuna) on the taxonomy and ecology of macrofungi. For the most part, we describe the communities associated with the ECM host tree *O. mexicana* (Juglandaceae) based on new data from fruiting body surveys and sequencing of ECM colonized root tips previously published by Corrales et al. (2016, 2017). Other ECM host plants, including *Quercus* spp., *Coccoloba* spp., and *Alfaroa costaricensis*, are also present in Fortuna at lower abundances, and therefore some of the species included in this chapter may be shared or associated with these species as well. To our knowledge, this is the first study that uses fruiting bodies to characterize the fungal communities associated with *O. mexicana*. This work, which focuses on the morphological and molecular identification of voucher specimens, not only constitutes an essential tool to document molecular ecology studies at Fortuna Forest Reserve but also provides a resource for other studies focusing on the ecology and biogeography of macrofungi in tropical montane forests in Central America and northern South America.

METHODS

Fruiting body collections of macromycetes were made mainly in stands of *O. mexicana* located in four watersheds in the Fortuna Forest Reserve (Fortuna): Alto Frio (AF), Hornito (HO), Honda (HA and HB), and Zarceadero (Za) (for a detailed site description of AF, HO, HA, and HB, see Corrales et al., 2016). Two different studies involving collection of fruiting bodies were done at these sites. First, during February to July 2012, we established 50 × 4 m transects that were revisited every 2 weeks to collect fruiting bodies of all the species of macromycetes present. This study aimed to compare mushroom diversity in sites with contrasting soil fertility and rainfall conditions. Second, during September 2013 to January 2014, collections were also made in a nitrogen (N) addition experiment that has been running since 2006 in the Honda watershed (Corre et al., 2010). Transects of 40 × 4 m were established in three N-addition and four control plots containing *Oreomunnea* trees. These transects were revisited every 2 weeks with the aim of determining the effect of N addition on the production of ECM fruiting bodies.

To augment the data from the transects, we collected fruiting bodies opportunistically in areas near the transects and other sites at Fortuna where *O. mexicana* is present along with *Quercus* spp. These collections were made over 5 years, between 2011 and 2015. The intent of this collecting effort was to capture diversity that might have been missed along the transects in order to ensure a more complete inventory.

Macromorphology of fresh fruiting bodies was recorded in the field, and a tissue sample was preserved for DNA extraction. Vouchers of fruiting bodies are deposited at the University of Arizona Robert L. Gilbertson Mycological Herbarium (ARIZ), the herbarium of the University of Central Oklahoma (CSU), and Herbario de la Universidad de Panama (PMA). Genomic DNA was extracted using the REDExtract-N-Amp tissue PCR kit (following the manufacturer's instructions; Sigma-Aldrich). Primers ITS1F, ITS4, and ITS4B were used for DNA amplification. Methods for species molecular identification follows (Corrales et al., 2016). Voucher collections were identified on the basis of their morphology and DNA, with the help of specialists in the group, and names were assigned when possible. Because of the high diversity and challenging taxonomy of many of the groups, and the possibility that collections represent new species, some species names as well as total diversity of certain genera were assigned on the basis of sequence similarity with a 97% threshold used to classify fungal operational taxonomic units (OTUs).

PRELIMINARY LIST OF FUNGAL SPECIES FOR THE FORTUNA FOREST RESERVE WITH NEW REPORTS FOR PANAMA

During 5 years of collection, 1,003 fruiting body collections were made and processed as herbarium specimens. In addition, 400 of these collections were sequenced to obtain fungal barcode data (ITS region). This section summarizes the most up-to-date results that we have for the fungal inventory. The list of fungi of Fortuna is still a work in progress given that many of the collected specimens likely represent new species. Currently, we are in the process of describing more than 20 species in collaboration with the specialists in each taxonomic group.

We have found 157 species (including morphospecies and OTUs), with most species belonging to Basidiomycota and only

4 species belonging to Ascomycota. These species are distributed in 65 genera (29 ECM, 37 saprotrophs, and 2 fungal parasites) and 35 families (14 ECM, 20 saprotrophs, and 1 fungal parasite; appendix 4.1). The most species-rich genus was *Russula*, with about 40 species (defined on the basis of OTUs; Corrales et al., unpublished data) and *Lactarius* with 8 species. The family with the most genera was Boletaceae, with 12 genera, followed by Russulaceae, Entolomataceae, Hymenogastraceae, Marasmiaceae, Mycenaceae, Phallaceae, and Physalacriaceae, all of them with 3 genera (appendix 4.1).

After revising the checklist of Panamanian fungi (http://biogeodb.stri.si.edu/fungi) and recent mycological publications from Panama, we report 22 genera newly reported for the country. For ECM fungi, 13 out of 28 genera were new records for the country, while for saprotrophic fungi, 7 out of 37 genera were new records. Both genera of fungal parasitic fungi were also new records for Panama. From the specimens that were possible to identify to species level, we report 33 new records of fungal species for Panama (21 ECM and 12 saprotrophs; appendix 4.1). This is not surprising given that the checklist maintained on the Smithsonian Tropical Research Institute (STRI) website includes very few ECM genera among the 657 species of Agaricomycetes reported from Panama. Finally, while 12 out of the 28 ECM basidiomycete genera listed in appendix 4.1 are on the STRI checklist, they mostly indicate the presence of only a single species. Exceptions are *Russula* with 7 species and *Ramaria* with 6 species listed.

FIGURE 4.1. Number of collections for the seven most abundant ECM genera in each of the sites sampled along transects at Fortuna using fruiting bodies (left) and root tips (right; using data published by Corrales et al., 2016). Site abbreviations are Alto Frio (AF), Hornito (HO), Honda A (HA), Honda B (HB), and Zarceadero (ZA). Root tip (RT).

GENERIC DIVERSITY PATTERNS OF ECTOMYCORRHIZAL FUNGI ASSOCIATED WITH STANDS OF *OREOMUNNEA MEXICANA* GROWING ON SITES WITH CONTRASTING ABIOTIC CONDITIONS

Based on 297 fruiting body collections, made in sites with contrasting soil fertility and rainfall conditions, we found that, overall, the most abundant genera at Fortuna were *Russula*, *Lactarius*, *Laccaria*, *Cortinarius*, *Cantharellus*, *Boletus*, and *Amanita*. At the genus level, the HA and AF sites show the highest number of genera, with 19 and 18 genera respectively. From the seven most abundant ECM genera, only *Amanita*, *Laccaria*, and *Russula* were found across all sites, while *Cortinarius* (not collected in AF and ZA), *Lactarius* (not collected in ZA), *Boletus* (not collected in HB), and *Cantharellus* (not found in HO) were found in some sites but not in all (Figure 4.1). Interestingly, few of the genera missing from some transects were later collected during the opportunistic surveys. It could be that some of these taxa are only symbionts of *Quercus* or other ECM hosts present in low abundance at these sites or that they produced fruiting bodies at times when collecting was not done.

Previous molecular inventories using *O. mexicana* root tips have found that fungal ECM communities at Fortuna show high species richness and compositional turnover among sites with contrasting soil and rainfall conditions (Corrales et al., 2016). Given that most of our fruiting body collections were made at the same transects studied by Corrales et al. (2016), a direct comparison of the results from fruiting body collections (aboveground surveys) with root tips inventories (belowground surveys) is possible. Overall, *Russula*, *Cortinarius*, *Laccaria*, and *Lactarius* were found among the top seven most abundant genera for both aboveground and belowground surveys (Figure 4.1). However, *Tomentella*, *Byssocorticium*, and *Elaphomyces* were either rare or absent from fruiting body surveys, while these genera round out the top seven most abundant genera in root tip inventories. This is an expected finding given that these genera produce inconspicuous or truffle-like fruiting bodies that are usually overlooked in aboveground inventories (Koljalg et al., 2000; Tedersoo et al., 2014). However, *Cantharellus*, the third-most abundant genus in terms of number of fruiting body collections, was also absent from root tip inventories. This could be due to the very long and variable internal transcribed spacer (ITS) region of *Cantharellus* that is usually difficult to amplify using universal fungal primers ITS1F/ITS4 (Buyck et al., 2014).

Based on rarefaction curves constructed using 167 fruiting body collections that have been sequenced and assigned to OTUs (Figure 4.2), we found that the site with the strongest seasonality in moisture availability, AF, had the highest alpha diversity of ECM fungal species, while the continually moist site, HB, had the lowest. This finding contrasts with the results from belowground surveys where AF showed the lowest alpha diversity of OTUs (Corrales et al., 2016). This pattern could be associated with a higher investment in dispersal or reproduction of species growing on sites that are at least temporarily limited

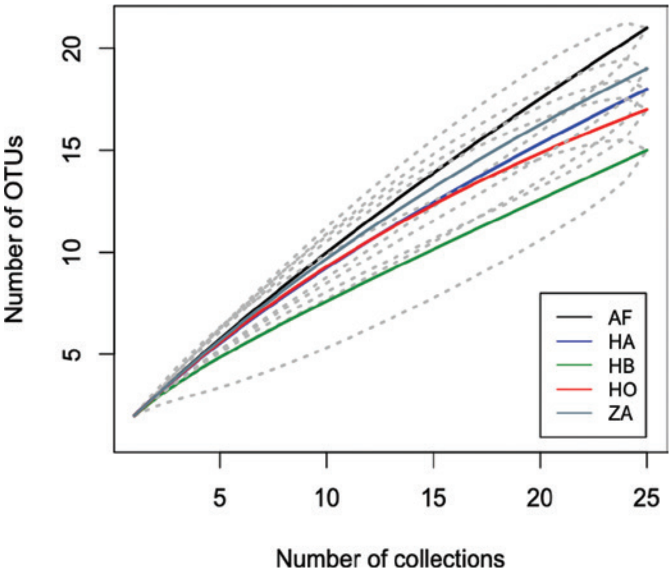

FIGURE 4.2. Ectomycorrhizal species accumulation curves and 95% confidence per site based on operational taxonomic units from fruiting bodies. Site abbreviations are Alto Frio (AF), Hornito (HO), Honda A (HA), Honda B (HB), and Zarceadero (ZA).

by water in contrast with a higher investment on mycelium growth in species that are not limited by this resource (Ekblad et al., 2013).

The timing of fruiting body production, or mushroom phenology, seems to be heavily influenced by differences in the rainfall patterns among sites at Fortuna. Based on fruiting body collections and rainfall data from 2012 (Dalling et al., this volume), sites with a marked dry season between December and April (HO and AF) showed a strong peak of fruiting body production at the beginning of the rainy season between late April and June, similar to phenological observations obtained in nearby lowland vegetation (Piepenbring et al., 2015). This was most noticeable at AF, where more than 50 species were found fruiting in just one week (Figure 4.3A). In sites where the total amount of rainfall is higher and more evenly distributed throughout the year (HA and HB), fruiting body production occurred over the entire collecting period with peaks of fructification in February, April, and June (Figure 4.3B). Even though this is a small window of time to make generalizations about the local mushroom phenology, this is a first approximation to an aspect of fungal ecology that has been little studied in tropical forests. Over the years, we have also observed that the timing of the rainy season and the peak of fruiting body production could be very variable and is becoming more unpredictable due to local climate change. In future research, it would be interesting to monitor these changes over a longer period of time to understand the dynamics of the reproductive cycles of ECM fungi and the potential implications that climate change could have on those dynamics at Fortuna.

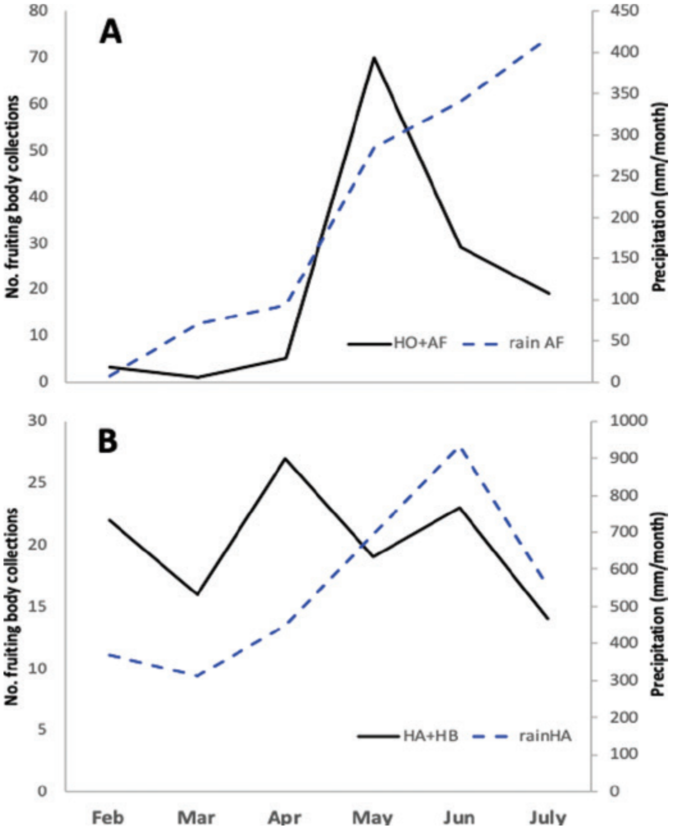

FIGURE 4.3. Number of fruiting body collections (solid line) during February to July 2012 and the local precipitation recorded at each site (dashed line). Number of collections were grouped by sites with differences in rainfall patterns following Corrales et al. (2016). (a) Sites with dry period with <100 mm of rainfall (AF: Alto Frio; HO: Hornito). (b) Sites with no months with <100 mm of rainfall (HA: Honda A; HB: Honda B).

INFLUENCE OF NITROGEN ADDITION ON ECTOMYCORRHIZAL FRUITING BODY PRODUCTION, DIVERSITY, AND SPECIES COMPOSITION

It is well recognized that ECM fungal communities respond to increases in N availability associated with anthropogenic fertilization or N deposition for both aboveground and belowground structures (Lilleskov et al., 2011; van der Linde et al., 2018). However, most of these studies have been done in temperate or boreal forest, and information about tropical ECM communities is scarce or nonexistent. Results from environmental sequencing of O. *mexicana* root tips at Fortuna suggest that N fertilization could be associated with changes in ECM fungal community composition and could cause a reduction in soil enzyme activity and ECM root colonization (Corrales et al., 2017).

Surveys of ECM fruiting bodies done along transects at the same experimental plots used by Corrales et al. (2017) show that N addition could also have an effect on the overall production of fruiting bodies and frequency of fructification of some ECM genera. A total of 313 mushroom collections were made along seven transects. In control plots, we made an average of 44 (SD = 9) collections per plot belonging to 15 (SD = 1) genera, while in N-addition plots, we made an average of 46 (SD = 4) collections per plot belonging to 12 (SD = 0.6) genera. This lower generic diversity found in N-addition plots was also observed in the species-accumulation curves based on OTUs (obtained from sequencing of fruiting body collections) that show a lower species alpha diversity of the mushroom community present in N-addition plots compared with control plots (Figure 4.4A). Community composition, however, did not show significant differences based on ordination and adonis analyses performed using mushroom species presence-absence (Figure 4.4B) and abundance data (not shown) contrasting with results found by Corrales et al. (2017) based on environmental sequencing of *Oreomunnea* root tips that showed a significant change in species composition based on nonmetric multidimensional scaling (NMDS) and adonis analysis.

Russula, *Lactarius*, *Cortinarius*, and *Leotia* were the most abundant genera in plots from both treatments (Figure 4.5), accounting for about 50% of all the collections. *Russula* and *Cortinarius* showed a strong reduction in the number of fruiting body collections between control and N-addition treatments. A total of 41 collections of *Russula* were made in the control plots versus only 17 collections made in the N-addition plots. For *Cortinarius*, there were 18 collections made in control plots and 8 in N-addition plots. In contrast, *Leotia* showed a much higher number of fruiting body collections in N-addition plots compared with control plots with 17 and 10 collections respectively (Figure 4.5). Results based on environmental sequences of

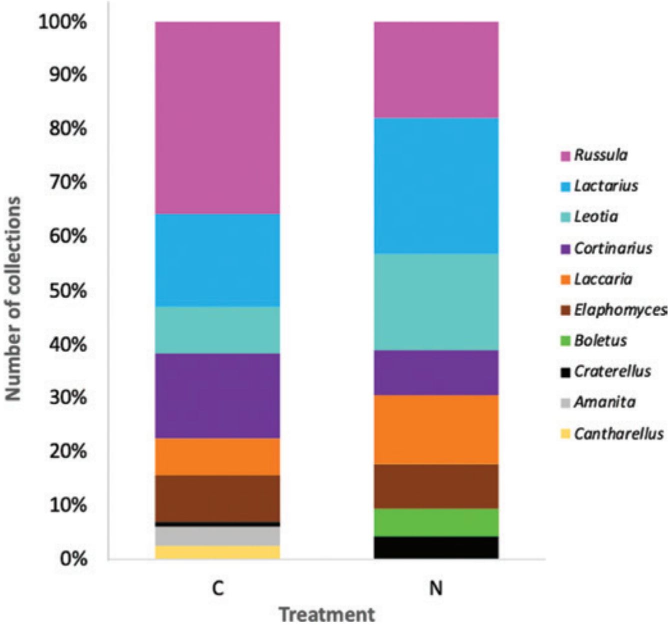

FIGURE 4.5. Number of fruiting body collections for the most abundant ECM genera in control (C) and nitrogen (N) addition plots sampled using transects at Fortuna.

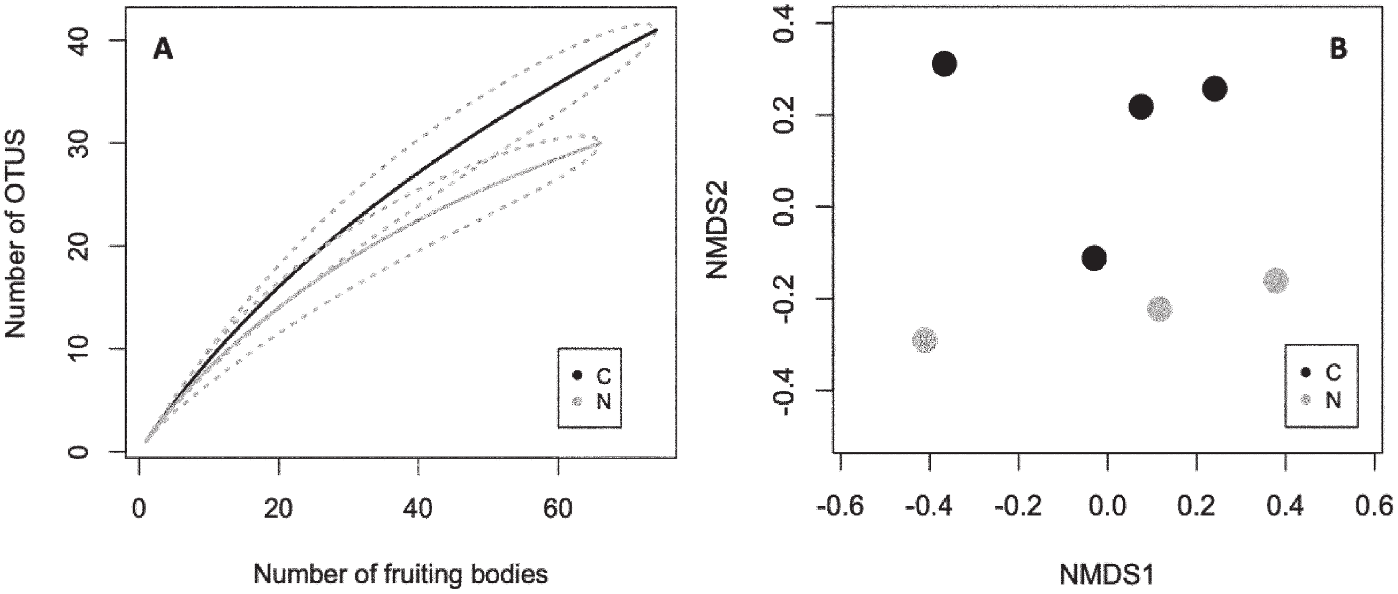

FIGURE 4.4. (a) Species-accumulation curves of ECM fungi for N treatments (C: control; N: nitrogen addition) based on operational taxonomic units obtained from sequencing of fruiting body collections. (b) Nonmetric multidimensional scaling for the mushroom community from C and N plots based on presence-absence data and excluding singletons. Adonis analysis (P(>F) = 0.23, R^2 = 0.244).

Oreomunnea ECM root tips published by Corrales et al. (2017) also showed a lower number of sequences of *Cortinarius* in N-addition plots compared with control plots but showed a higher abundance of *Laccaria* and *Lactarius* in N-addition plots compared with control plots that was not reflected in the production of fruiting bodies.

RUSSULA DIVERSITY AT FORTUNA FOREST RESERVE

Russula has been found to be the most diverse genus of ECM fungi at Fortuna in both aboveground and belowground surveys (Corrales et al., 2016, Corrales et al., 2017). Results from our mushroom inventories show that *Russula* accounted for ~37% of the total number of ECM mushroom species and 25% of total number of species recorded at the study site, including saprotrophs (Table 4.1). Molecular identification of fruiting body collections using Sanger sequencing indicated the existence of 40 OTUs, based on 97% similarity over the whole ITS region. This level of sequence similarity could be interpreted as consistent with species-level variation (Smith et al., 2007). The selected OTUs represented six *Russula* subgenera *sensu* Buyck et al. (2018). The most diverse subgenus was *Russula 2* with 19 OTUs, followed by subgenus *Heterophylla* with 9 OTUs, subgenus *Compactae* and *Crassotunicata* with 5 OTUs each, subgenus *Russula 1* with 2 OTUs, and subgenus *Malodora* with 1 OTU. Preliminary phylogenetic placement of the OTUs suggests that most, if not all, *Russula* spp. from Fortuna are new to science, but more work is required to confirm this finding (B. Buyck, personal communication). So far, only one *Russula* species (*R. fortunae* Corrales) was recently described from Fortuna (Adamčík et al., 2019) and one OTU confirmed by collections Corrales 182 and 626 matched an existing species (*R. nigricans* Fr.) based on morphology and 99% similarity of the ITS region. However, since this is a European species, more sequencing is required to confirm this name.

A remarkable feature of the Fortuna *Russula* community is its high diversity, containing species belonging to six out of eight subgenera recognized by Buyck et al. (2018). The only subgenera as yet uncollected at Fortuna are *Archea* and *Brevipes*. Also remarkable is that the Fortuna dataset is particularly rich in species in the subgenus *Crassotunicata* given that there are only three species described for this subgenus worldwide (Buyck et al., 2018). At present, five OTUs of this subgenus found at Fortuna do not match any of the described species (S. Adamčík, personal communication).

BIOGEOGRAPHIC CONSIDERATIONS OF THE ECTOMYCORRHIZAL COMMUNITIES AT FORTUNA

Many of the ECM host tree species in montane forests in Central and South America are considered relict species with a northern hemisphere temperate origin, and therefore their associated fungal communities show a strong affinity with the ones found in North America (Halling, 2001). Pollen fossil records show that *Oreomunnea* has been present in Panama since the Early Miocene (Graham, 1989; Herrera et al., 2014), while *Quercus* arrived probably much later (Kappelle, 2006). Ectomycorrhizal fungal species associated with these host trees might have a particular evolutionary history given the high degree of isolation and potential speciation that they might have undergone. Mueller and Halling (1995), based on the analysis of the four best-known ECM fungal genera associated with *Quercus* forests, established that in Central and South America, the ECM fungal communities associated with this genus show a high degree of endemism, with most species having limited geographic ranges.

Comparisons of the ECM macromycete community composition of Fortuna with other cloud forests is difficult at this time because of a lack of comparable studies in neotropical montane sites that include intensive multiyear collecting over lengthy periods. Our approach of inventorying all fruiting bodies of the ECM fungi has yielded a wealth of diversity that will require the aid of specialists to assist at arriving at species determinations. Comparisons with fungal inventories from other tropical countries is currently possible only at the genus level. However, future species-level comparisons will yield the most valuable biogeographic information.

Nearly all of the ECM genera that are reported here (Table 4.1, Figures 4.6–4.9) are common genera that can be found from the neotropics to high latitudes in North America (Corrales et al., 2018) as long as their associated ECM tree hosts are present. The only genus found at Fortuna that is likely to have a mainly or exclusively tropical distribution is *Veligaster* (Figure 4.9e; Guzmán et al., 2004; Kasuya and Guzmán, 2007).

As many as 70% of the ECM fungal species in a newly explored area may be undescribed (Henkel et al., 2012). At this point, we can comment on the distribution of only a few species that have been identified at Fortuna (appendix 4.1). *Amanita* spp. were abundant at the study area, and we have confirmed identifications for three species: *A. garabitoana* Tulloss, Halling, and Mueller; *A. flavoconia* var. *inquinata* Tulloss, Ovrebo, and Halling; and *A. brunneolocularis* Tulloss, Ovrebo, and Halling. *Amanita garabitoana* has been recorded from Honduras to Costa Rica (Tulloss et al., 2011), and *A. flavoconia* var. *inquinata* and *A. brunneolocularis* (Figure 4.6a, c) are reported from Colombia and Costa Rica (Tulloss, 2005). Tulloss (2005) reports these species as occurring with *Quercus*, but we are unsure if these species are associated with *Quercus* or *Oreomunnea* in our study area given that they occur in forests where both host taxa are abundant. *Cortinarius* species were also abundant at the study area, and we have identified two species: *C. neotropicus* Harrower and *C. costaricensis* Ammirati, Halling, and Garnica. *Cortinarius neotropicus* (Figure 4.6b) was described from Costa Rica and has also been reported from Colombia (Harrower et al., 2015) as occurring under *Quercus*. At Fortuna, this species was also found growing in *Quercus*-dominated forest. *Cortinarius costaricensis* was described from under *Quercus* on the basis of a single basidiome from Costa Rica; we have now made several additional collections to add to its distribution and to add *Oreomunnea* as a new potential host. We have also confirmed the identity of *Phylloporus*

TABLE 4.1. Estimates of fungal species per family and per genus based on morphology and DNA of fruiting body surveys at Fortuna. *Presumably biotrophic genus **New genus records for Panama

Taxa	No. species	Taxa	No. species	Taxa	No. species
Ectomycorrhizal					
Amanitaceae	**8**	*Tylopilus***	3	**Hydnaceae**	**2**
Amanita	8	*Veloporphyrellus***	1	*Hydnum***	2
Bankeraceae	**2**	**Calostomataceae**	**1**	**Hydnangiaceae**	**4**
*Hydnellum***	1	*Calostoma*	1	*Laccaria*	4
Phellodon	1	**Cantharellaceae**	**4**	**Hymenogastraceae**	**1**
Boletaceae	**20**	*Cantharellus*	2	*Phaeocollybia***	1
*Austroboletus***	1	*Craterellus*	2	**Leotiaceae**	**2**
*Aureoboletus***	1	**Cortinariaceae**	**11**	*Leotia*	2
Boletellus	3	*Cortinarius*	8	**Russulaceae**	**51**
*Boletus***	1	*Inocybe***	3	*Lactarius*	8
Leccinum	2	**Elaphomycetaceae**	**1**	*Lactifluus***	3
Phylloporus	6	*Elaphomyces***	1	*Russula*	40
*Retiboletus***	1	**Gomphaceae**	**1**	**Sclerodermataceae**	**1**
*Strobilomyces***	1	*Ramaria*	1	*Veligaster*	1
Saprotrophic					
Agaricaceae	**2**	**Hymenogastraceae**	**3**	**Phallaceae**	3
Agaricus	1	*Gymnopilus*	1	*Aseroe***	1
Leucocoprinus	1	*Psilocybe*	1	*Laternea*	1
Auriculariaceae	**1**	**Marasmiaceae**	**8**	*Phallus*	1
Auricularia	1	*Crinipellis***	1	**Psathyrellaceae**	1
Auriscalpiaceae	**1**	*Gerronema*	1	*Psathyrella*	1
*Artomyces***	1	*Marasmius*	6	**Physalacriaceae**	3
Entolomataceae	**4**	**Meruliaceae**	**2**	*Armillaria*	1
Alboleptonia	1	*Cymatoderma*	1	*Cyptotrama***	1
*Inocephalus***	1	*Podoscypha*	1	*Xerula*	1
*Entoloma**	2	**Mycenaceae**	**4**	**Polyporaceae**	2
Fistulinaceae	**1**	*Filoboletus*	1	*Lentinus*	1
Fistulina	1	*Mycena*	2	*Polyporus*	1
Ganodermataceae	**1**	*Xeromphalina*	1	**Strophariaceae**	1
Ganoderma	1	**Omphalotaceae**	**4**	*Agrocybe***	1
Hygrophoraceae	**3**	*Gymnopus*	3	**Tapinellaceae**	1
Hygrocybe	3	*Marasmiellus*	1	*Tapinella***	1
Hymenochaetaceae	**1**			**Tricholomataceae**	1
Hymenochaete	1			*Clitocybe*	1
Fungal parasite					
Boletaceae	**1**	**Ophiocordycipitaceae**	**1**		
*Chalciporus***	1	*Tolypocladium***	1		

FIGURE 4.6. (A) *Amanita brunneolocularis*. (B) *Cortinarius neotropicus*. (C) *Amanita flavoconia* var. *inquinita*. (D) *Lactarius* aff. *piperatus*. (E) *Amanita* sp. (F) *Lactarius* sp.

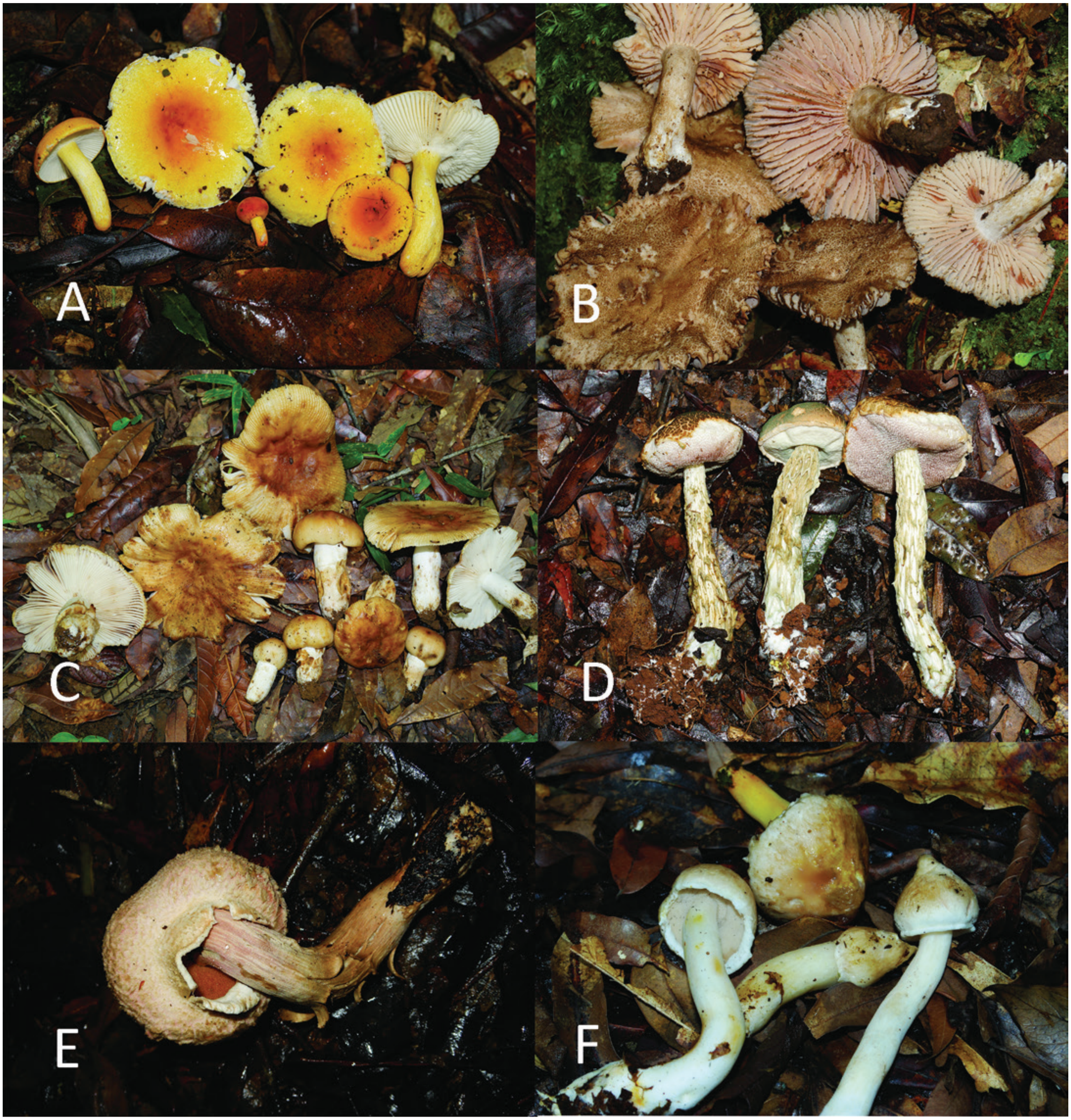

FIGURE 4.7. (A) *Russula* sp. (B) *Russula* sp. (C) *Russula* sp. (D) *Austroboletus neotropicalis*. (E) *Boletellus ananas*. (F) *Veloporphyrellus pantoleucus*.

FIGURE 4.8. (A, B) *Phylloporus centroamericanus*. (C) *Craterellus* sp. (D) *Calostoma cinnabarina*. (E) *Gymnopus omphalodes*. (F) *Aseroe rubra*.

FIGURE 4.9. (A) *Marasmius heliomyces*. (B) *Mycena margarita*. (C) *Crinipellis* sp. (D) *Laternea pusilla*. (E) *Veligaster nitidus*. (F) *Hygrocybe* sp.

centroamericanus (Figure 4.8a, b), previously known only from the oak forests of Costa Rica (Neves and Halling, 2010), and *Phylloporus caballeroi* Singer described from Argentina and also reported for Bolivia, Costa Rica, and Panama growing under *Alnus acuminata* forest (Neves and Halling, 2010). In Panama, this species has been previously collected in the Parque Internacional La Amistad, Chiriquí, by R. Halling (REH 7906, NYBG). *Phellodon niger* (Fr.) P. Karst occurs at Fortuna and is also known from the temperate forests of North America. For boletes, *Leccinum talamancae* Halling, Gómez, and Lannoy and *L. tablense* Halling and G. M. Mueller were described from Costa Rica from under *Quercus*, and we have now collected them at Fortuna. Notably, the ECM genus *Hebeloma*, reported for Panama based on the STRI fungi checklist, has not yet been encountered at Fortuna. Also absent from the STRI checklist and yet to be collected at Fortuna or sequenced from roots is the genus *Tricholoma*, known to occur in the oak forests of Colombia and Costa Rica (Halling and Mueller, 2005; Mueller et al., 2006; Ovrebo et al., 2019).

The new species and genus records from Fortuna are biogeographically relevant because they fill a gap of ECM records between the montane forests of Costa Rica and Colombia. Several ECM host plants, including *Quercus*, *Oreomunnea*, and *Alfaroa*, reach their most southern latitudinal distribution in Colombia, and the Panama isthmus must have been an important bridge for migration of these species and their associated fungi. Research on the occurrence of fungi in Panama therefore provides important insights into the factors that control the diversity and biogeographical patterns of fungi in northern South America. The forests at Fortuna should continue to yield new ECM macromycete data in a number of ways that will help to improve our understanding of macromycete biodiversity and biogeography, including (1) information on the fungal associates of *O. mexicana* and *Quercus* spp.; (2) data on the occurrence of fungi in the cloud forest ecosystem; (3) comparisons with the biodiversity of adjacent countries such as Colombia and Costa Rica, where more fieldwork has been done, especially in the oak forests; and (4) contribution to the knowledge of fungal biodiversity of Panama. Finally, while ECM fungi have been the main focus of our work, saprotrophic macromycetes (and micromycetes) should not be neglected because they might be a source of important information on fungal biogeography and biodiversity, especially compared to AM-dominated forests where saprotrophs are generally the most abundant group of Agaricomycete fungi.

CONCLUSIONS AND FUTURE DIRECTIONS

Based on our preliminary list of macrofungi in the Fortuna Forest Reserve, we conclude that this area harbors a high diversity of ECM fungi, and although not a particular focus of our work, there may be a rich diversity of saprotrophic fungi that future fieldwork will reveal. Here we report 22 new records of genera and 33 species records for Panama. In the near future, we expect the number of species at Fortuna to grow considerably as we work closely with specialists to describe new species. These long-term taxonomic efforts will be important in improving the growing database of fungal records that is being compiled for Panama. Furthermore, exploring undersampled ecosystems and new host species will improve the quality of reference voucher and DNA collections needed to inform environmental next-generation sequencing methods.

We hope that our work continues to fill in the gap of knowledge regarding fungal diversity in montane cloud forests and also contributes to the database of knowledge of oak forest ECM fungi, particularly in comparison to Costa Rica and Colombia, where more intensive oak forest inventories have been made. Upon completion of the identification of our collections, we should be able to make more accurate statements about the degree of endemism in the Fortuna region as well.

Given the functional importance of fungi in ecosystems and the high susceptibility of tropical montane forest to climate change, characterizing the fungal communities associated with this ecosystem and their variability along environmental gradients is essential for a better understanding of the microbial drivers of key ecosystems functions. Fungi play a key role in soil nutrient cycling and in the adaptation of plants to novel environmental conditions, two processes that are crucial under a global change scenery particularly in tropical montane forests.

ACKNOWLEDGMENTS

Funding from the Smithsonian Tropical Research Institute predoctoral Fellowship, NSF Dissertation Improvement Grant (Award ID 1501483), Colciencias (497-2009), Robert L. Gilbertson Mycological Herbarium Grant (University of Arizona), Tinker Summer Research Fellowship, Francis M. and Harlie M. Clark Research support grant, and the Graduate College at University of Illinois are gratefully acknowledged. We thank Kayla Arendt, Jana U'Ren, Betsy Arnold, Katy Heath, and Pat Burke for assistance with molecular work and also Fredy Miranda, Jan Miranda, Evidelio Garcia, Carmen Velasquez, Carlos Espinosa, Marggie Rodriguez, Katie Heineman, Carlos Espinosa, Cecilia Prada, and ENEL green power for help with fieldwork and logistic support. Finally, we thank Jim Dalling and Ben Turner for their help throughout the development of this project and Meike Piepenbring for her helpful comments on a previous draft of the chapter.

We would also like to thank all the specialists who have helped us to identify the species from Fortuna: Michael A. Castellano (U.S. Forest Service), Andrew Wilson (Denver Botanic Gardens), Gregory Mueller (Chicago Botanic Garden), Brandon Matheny and Rachel Sweenie (University of Tennessee), Slavomir Adamčík (Slovak Academy of Science), Bart Buyck (Muséum national d'histoire naturelle, Paris), Donald H. Pfister (Harvard University), Roberto Garibay-Orijel (Universidad Nacional Autónoma de México) and Leticia Montoya (Institute of Ecology), Ed Lickey (Bridgewater College), Roy Halling (New York Botanical Garden), Joe Ammirati (University of Washington), Kare Liimatainen and Tuula Niskanen (Kew Royal Botanic Gardens). Special thanks to Slavomir Adamčík for his input on the *Russula* taxonomy section of this chapter.

APPENDIX 4.1

Preliminary list of fungal species from Fortuna Forest Reserve. The column "New record or literature report" correspond to new records for Panama ("Yes"), new species described from Fortuna ("New species"), or "Unknown" in cases when the species were not fully identified. Species that have been already reported for the country have references to the original publication. Selected collection numbers with herbarium codes indicating where the collections are currently housed are given for vouchered specimens. For genera such as *Boletus*, *Cantharellus*, *Russula*, *Lactarius*, and others, "spp." indicates more than one unidentified species, and no collections are cited—replaced by "Numerous." Guild abbreviations are as follows: ectomycorrhizal (EM), saprotroph (SAP), and fungal parasite (FP). Ectomycorrhizal guild assignment is based on Tedersoo et al. (2010).

Guild	Family	Genus	Species	Voucher collection	New record or literature report
EM	Amanitaceae	*Amanita*	aff. *bisporigera*	Corrales 87 (ARIZ)	Unknown
EM	Amanitaceae	*Amanita*	*brunneolocularis*	Ovrebo 5284, 5520, 5302 (CSU)	Yes
EM	Amanitaceae	*Amanita*	*garabitoana*	Corrales 151 (ARIZ)	Yes
EM	Amanitaceae	*Amanita*	*flavoconia* var. *inquinata*	Ovrebo 5268 (CSU)	Yes
EM	Boletaceae	*Aureoboletus*	*auriporus*	Corrales 370 (ARIZ)	Yes
EM	Boletaceae	*Austroboletus*	*neotropicalis*	Corrales 311 (ARIZ), Ovrebo 5533 (CSU)	Yes
EM	Boletaceae	*Boletus*	spp.	Numerous	Yes
EM	Boletaceae	*Boletellus*	*ananas*	Corrales 179 (ARIZ), 771 (PMA)	Mayor et al., 2008
EM	Boletaceae	*Boletellus*	sp.	Ovrebo 5506 (CSU)	Unknown
EM	Calostomataceae	*Calostoma*	cf. *cinnabarinum*	Ovrebo 5354 (PMA) Corrales 765 PMA	Guzmán and Piepenbring, 2011
EM	Cantharellaceae	*Cantharellus*	spp.	Numerous	Guzmán and Piepenbring, 2011
EM	Cantharellaceae	*Cantharellus*	*atrolilacinus*	Corrales 195 (ARIZ), Ovrebo 5245 (CSU)	Yes
EM	Cortinariaceae	*Cortinarius*	*bolaris*	Ovrebo 5252, 5311 (CSU)	Yes
EM	Cortinariaceae	*Cortinarius*	*neotropicus*	Ovrebo 5342 (CSU)	Yes
EM	Cortinariaceae	*Cortinarius*	*costaricensis*	Ovrebo 5331, 5262 (CSU)	Yes
EM	Cortinariaceae	*Cortinarius*	spp.	Numerous	Unknown
EM	Cantharellaceae	*Craterellus*	sp.	Corrales 178 (ARIZ), Ovrebo 5260 (CSU)	Unknown
EM	Cantharellaceae	*Craterellus*	cf. *boyacensis*	Corrales 519 (CSU)	Unknown
EM	Elaphomycetaceae	*Elaphomyces*	sp.	Corrales 388 (CSU)	Yes
EM	Bankeraceae	*Hydnellum*	spp.	Ovrebo 5347, 5348 (CSU)	Yes
EM	Hydnaceae	*Hydnum*	spp.	Numerous	Yes
EM	Cortinariaceae	*Inocybe*	spp.	Numerous	Yes
EM	Hydnangiaceae	*Laccaria*	*dallingii*	See publication	New species (Corrales et al., 2020)
EM	Hydnangiaceae	*Laccaria*	*fortunensis*	See publication	New species (Corrales et al., 2020)
EM	Hydnangiaceae	*Laccaria*	*nitrophila*	See publication	New species (Corrales et al., 2020)
EM	Hydnangiaceae	*Laccaria*	*stellata*	Corrales 27 (ARIZ), 576 (CSU)	New species (Popa et al., 2016)
EM	Russulaceae	*Lactarius*	aff. *piperatus*	Ovrebo 5338, 5454 (CSU)	Yes

(*Continued*)

Guild	Family	Genus	Species	Voucher collection	New record or literature report
EM	Russulaceae	*Lactarius*	aff. *indigo*	Corrales 319 (ARIZ), Ovrebo 5240 (CSU)	Guzmán and Piepenbring, 2011
EM	Russulaceae	*Lactarius*	spp.	Numerous	Unknown
EM	Russulaceae	*Lactarius*	*hygrophoroides*	Ovrebo 5500 (CSU)	Yes
EM	Boletaceae	*Leccinum*	*tablense*	Ovrebo 5235 (CSU)	Yes
EM	Boletaceae	*Leccinum*	*talamancae*	Ovrebo 5239 (CSU)	Yes
EM	Leotiaceae	*Leotia*	sp.	Corrales 288, 333 (ARIZ), 358, (CSU)	Yes
EM	Leotiaceae	*Leotia*	*lubrica*	Corrales 483, 486, 650 (CSU)	Guzmán and Piepenbring, 2011
EM	Hymenogastraceae	*Phaeocollybia*	spp.	Numerous	Yes
EM	Bankeraceae	*Phellodon*	*niger*	Ovrebo 5348 (CSU)	Yes
EM	Boletaceae	*Phylloporus*	*centroamericanus*	Ovrebo 5265 (CSU)	Yes
EM	Boletaceae	*Phylloporus*	*caballeroi*	Corrales 378 (CSU)	Yes
EM	Boletaceae	*Phylloporus*	aff. *leucomycelinus*	Numerous	Unknown
EM	Boletaceae	*Phylloporus*	spp.	Numerous	Unknown
EM	Boletaceae	*Xerocomus*	cf. *subtomentosus*	Corrales 308 (ARIZ)	Yes
EM	Gomphaceae	*Ramaria*	sp.	Ovrebo 5353 (CSU)	Unknown
EM	Boletaceae	*Retiboletus*	*ornatipes*	Ovrebo 5508 (CSU)	Yes
EM	Russulaceae	*Russula*	*fortunae*	See publication	New species (Adamčík et al., 2019)
EM	Russulaceae	*Russula*	spp.	Numerous	Unknown
EM	Boletaceae	*Strobilomyces*	sp.	Corrales 152 (ARIZ), Ovrebo 5343 (CSU)	Yes
EM	Boletaceae	*Tylopilus*	spp.	Numerous	Yes
EM	Boletaceae	*Tylopilus*	*oradivensis*	Ovrebo 5480 (CSU)	Yes
EM	Sclerodermataceae	*Veligaster*	*nitidus*	Corrales 200 (ARIZ), Ovrebo 5266 (CSU)	Guzmán and Piepenbring, 2011
EM	Boletaceae	*Veloporphyrellus*	*pantoleucus*	Corrales 89 (ARIZ), Ovrebo 5304 (CSU)	Yes
SAP	Agaricaceae	*Agaricus*	sp.	Ovrebo 5505 (CSU)	Unknown
SAP	Strophariaceae	*Agrocybe*	sp.	Ovrebo 5291 (CSU)	Yes
SAP	Entolomataceae	*Alboleptonia*	sp.	Ovrebo 5499 (CSU)	Unknown
SAP	Polyporaceae	*Amauroderma*	sp.	Corrales 269 (ARIZ)	Guzmán and Piepenbring, 2011
SAP	Physalacriaceae	*Armillaria*	spp.	Numerous	Guzmán and Piepenbring, 2011
SAP	Auriculariaceae	*Auricularia*	*delicata*	Ovrebo 5537 (CSU)	Guzmán and Piepenbring, 2011
SAP	Auriscalpiaceae	*Artomyces*	*stephenii*	Ovrebo 5450 (CSU)	Yes
SAP	Phallaceae	*Aseroë*	*rubra*	Ovrebo 5314 (CSU)	Yes
SAP	Tricholomataceae	*Clitocybe*	sp.	Ovrebo 5344 (CSU)	Unknown
SAP	Marasmiaceae	*Crinipellis*	sp.	Ovrebo 5528 (CSU)	Yes
SAP	Meruliaceae	*Cymatoderma*	sp.	Ovrebo 5448 (CSU)	Unknown

Guild	Family	Genus	Species	Voucher collection	New record or literature report
SAP	Physalacriaceae	*Cyptotrama*	*asprata*	Ovrebo 5497 (CSU)	Yes
SAP	Entolomataceae	*Entoloma*	*nitidum*	Corrales 434, 451 (CSU)	Yes
SAP	Entolomataceae	*Entoloma*	sp.	Ovrebo 5280 (CSU)	Unknown
SAP	Mycenaceae	*Filoboletus*	*gracilis*	Ovrebo 5492 (CSU)	Guzmán and Piepenbring, 2011
SAP	Fistulinaceae	*Fistulina*	*hepatica*	Ovrebo 5362 (CSU)	Yes
SAP	Ganodermataceae	*Ganoderma*	sp.	Corrales 269 (ARIZ)	Unknown
SAP	Marasmiaceae	*Gerronema*	sp.	Ovrebo 5523 (CSU)	Unknown
SAP	Omphalotaceae	*Gymnopus*	*omphalodes*	Ovrebo 5357 (CSU)	Mata and Ovrebo, 2009
SAP	Omphalotaceae	*Gymnopus*	*pseudolodgeae*	Ovrebo 5306 (CSU)	Yes
SAP	Omphalotaceae	*Gymnopus*	spp.	Numerous	Unknown
SAP	Hymenogastraceae	*Gymnopilus*	sp.	Ovrebo 5512 (CSU)	Unknown
SAP	Hygrophoraceae	*Hygrocybe*	spp.	Numerous	Unknown
SAP	Hymenochaetaceae	*Hymenochaete*	*damaecornis*	Ovrebo 5220 (CSU)	Parmasto, 2001
SAP	Entolomataceae	*Inocephalus*	sp.	Ovrebo 5233 (CSU)	Yes
SAP	Phallaceae	*Laternea*	*pusilla*	Ovrebo 5251 (CSU)	Guzmán and Piepenbring, 2011
SAP	Polyporaceae	*Lentinus*	sp.	Ovrebo 5471 (CSU)	Unknown
SAP	Agaricaceae	*Lepiota*	sp.	Corrales 115 (ARIZ)	Unknown
SAP	Agaricaceae	*Leucocoprinus*	*fragilissimus*	Photo, anecdotal record	Guzmán and Piepenbring, 2011; Piepenbring et al., 2015, appendix C
SAP	Omphalotaceae	*Marasmiellus*	sp.	Ovrebo 5295 (CSU)	Unknown
SAP	Marasmiaceae	*Marasmius*	*berteroi*	Ovrebo 5317 (CSU)	Yes
SAP	Marasmiaceae	*Marasmius*	*cladophyllus*	Ovrebo 5217 (PMA)	Guzmán and Piepenbring, 2011
SAP	Marasmiaceae	*Marasmius*	*niveus*	Ovrebo 5215 (CSU)	Yes
SAP	Marasmiaceae	*Marasmius*	spp.	Numerous	Unknown
SAP	Marasmiaceae	*Marasmius*	*heliomyces*	Ovrebo 5212 (CSU)	Yes
SAP	Mycenaceae	*Mycena*	cf. *holoporphyra*	Ovrebo 5358 (CSU)	Unknown
SAP	Mycenaceae	*Mycena*	*margarita*	Ovrebo 5346 (CSU)	Yes
SAP	Phallaceae	*Phallus*	*indusiatus*	Ovrebo 5313 (CSU)	Piepenbring et al., 2011
SAP	Meruliaceae	*Podoscypha*	*venustula*	Ovrebo 5535 (CSU)	Welden, 2010
SAP	Polyporaceae	*Polyporus*	*tenuiculus*	Ovrebo 5323 (CSU)	STRI check list
SAP	Psathyrellaceae	*Psathyrella*	sp.	Corrales 58 (ARIZ)	Guzmán and Piepenbring, 2011
SAP	Hymenogastraceae	*Psilocybe*	sp.	Corrales 154 (ARIZ)	Unknown
SAP	Tapinellaceae	*Tapinella*	*atrotomentosa*	Ovrebo 5339 (CSU)	Yes
SAP	Mycenaceae	*Xeromphalina*	*tenuipes*	Ovrebo 5474 (CSU)	Yes
SAP	Physalacriaceae	*Xerula*	*hispida*	Corrales 276 (ARIZ), Ovrebo 5283 (CSU)	Yes
FP	Boletaceae	*Chalciporus*	cf. *piperatus*	Corrales 8, 117, 160 (ARIZ)	Yes
FP	Ophiocordycipitaceae	*Tolypocladium*	sp.	Corrales 420 (CSU)	Yes

References

Adamčík, S., B. Looney, M. Caboň, S. Jančovičová, K. Adamčíková, P. G. Avis, M. Barajas, R. P. Bhatt, A. Corrales, K. Das, F. Hampe, A. Ghosh, G. Gates, V. Kälviäinen, A. N. Khalid, M. Kiran, R. De Lange, H. Lee, Y. W. Lim, A. Kong, C. Manz, C. Ovrebo, M. Saba, T. Taipale, A. Verbeken, K. Wisitrassameewong, and B. Buyck. 2019. The Quest for a Globally Comprehensible *Russula* Language. *Fungal Diversity*, 99:369–449. https://doi.org/10.1007/s13225-019-00437-2

Buyck, B., F. Kauff, G. Eyssartier, A. Couloux, and V. Hofstetter. 2014. A Multilocus Phylogeny for Worldwide *Cantharellus* (Cantharellales, Agaricomycetidae). *Fungal Diversity*, 64:101–121. https://doi.org/10.1007/s13225-013-0272-3

Buyck, B., S. Zoller, and V. Hofstetter. 2018. Walking the Thin Line . . . Ten Years Later: The Dilemma of Above- versus Below-ground Features to Support Phylogenies in the Russulaceae (Basidiomycota). *Fungal Diversity*, 89:267–292. https://doi.org/10.1007/s13225-018-0397-5

Corrales, A., A. E. Arnold, A. Ferrer, B. L. Turner, and J. W. Dalling. 2016. Variation in Ectomycorrhizal Fungal Communities Associated with *Oreomunnea mexicana* (Juglandaceae) in a Neotropical Montane Forest. *Mycorrhiza*, 26:1–17. https://doi.org/10.1007/s00572-015-0641-8

Corrales, A., T. W. Henkel, and M. E. Smith. 2018. Ectomycorrhizal Associations in the Tropics: Biogeography, Diversity Patterns and Ecosystem Roles. *New Phytologist*, 220:1076–1091. https://doi.org/10.1111/nph.15151

Corrales, A., B. L. Turner, L. Tedersoo, S. Anslan, and J. W. Dalling. 2017. Nitrogen Addition Alters Ectomycorrhizal Fungal Communities and Soil Enzyme Activities in a Tropical Montane Forest. *Fungal Ecology*, 27:14–23. https://doi.org/10.1016/j.funeco.2017.02.004

Corrales, A., A. W. Wilson, G. M. Mueller, and C. Ovrebo. 2020. Novel *Laccaria* Species from Juglandaceae Forest in Panama with Notes on Their Ecology. *Frontiers of Microbiology*, 11:1–10. https://doi.org/10.3389/fmicb.2020.01597

Corre, M. D., E. Veldkamp, J. Arnold, and S. J. Wright. 2010. Impact of Elevated N Input on Soil N Cycling and Losses in Old-growth Lowland and Montane Forests in Panama. *Ecology*, 91:1715–1729. https://doi.org/10.1890/09-0274.1

Dalling, J. W., C. M. Prada, K. D. Heineman, K. M. Andersen, A. Morris, J. Pardo, E. Hollenbeck, P. Caballero, C. Espinosa, E. García, and B. L. Turner. 2021. Introduction to the Fortuna Forest Reserve: Soil and Climate Effects on the Tree Communities of a Premontane Tropical Forest. In *Fortuna Forest Reserve, Panama: Interacting Effects of Climate and Soils on the Biota of a Wet Premontane Tropical Forest*, ed. J. W. Dalling and B. L. Turner, pp. 1–33. Smithsonian Contributions to Botany, No. 112. Washington, D.C.: Smithsonian Institution Scholarly Press.

Del Olmo-Ruiz, M., R. García-Sandoval, O. Alcántara-Ayala, M. Véliz, and I. Luna-Vega. 2017. Current Knowledge of Fungi from Neotropical Montane Cloud Forests: Distributional Patterns and Composition. *Biodiversity and Conservation*, 26:1919–1942. https://doi.org/10.1007/s10531-017-1337-5

Ekblad, A., H. Wallander, D. L. Godbold, C. Cruz, D. Johnson, P. Baldrian, R. G. Björk, D. Epron, B. Kieliszewska-Rokicka, R. Kjøller, H. Kraigher, E. Matzner, J. Neumann, and C. Plassard. 2013. The Production and Turnover of Extramatrical Mycelium of Ectomycorrhizal Fungi in Forest Soils: Role in Carbon Cycling. *Plant Soil*, 366:1–27. https://doi.org/10.1007/s11104-013-1630-3

Franco-Molano, A. E., A. Corrales, and A. M. Vasco-Palacios. 2010. Macrofungi of Colombia II. Checklist of the Species of Agaricales, Boletales, Cantharellales, and Russulales (Agaricomycetes, Basidiomycota). *Actualidades Biológicas*, 32:89–114.

Geml, J., N. Pastor, L. Fernandez, S. Pacheco, T. A. Semenova, A. G. Becerra, C. Y. Wicaksono, and E. R. Nouhra. 2014. Large-Scale Fungal Diversity Assessment in the Andean Yungas Forests Reveals Strong Community Turnover among Forest Types along an Altitudinal Gradient. *Molecular Ecology*, 23:2452–2472. https://doi.org/10.1111/mec.12765

Gómez-Hernández, M., G. Williams-Linera, R. Guevara, D. J. Lodge. 2012. Patterns of Macromycete Community Assemblage along an Elevation Gradient: Options for Fungal Gradient and Metacommunity Analyse. *Biodiversity and Conservation*, 21:2247–2268. https://doi.org/10.1007/s10531-011-0180-3

Graham, A. 1989. Studies in Neotropical Paleobotany. VII. The Lower Miocene Communities of Panama: The La Boca Formation. *Annals of the Missouri Botanical Garden*, 76:50–66. https://doi.org/10.2307/2399342

Guzmán, G., and M. Piepenbring. 2011. *Hongos de Panamá: Introducción a la identificación de los macroscópicos* [Fungi of Panama: Introduction to macroscopic identification]. Veracruz, México: Instituto de Ecología.

Guzmán, G., F. Ramírez-Guillén, O. K. Miller, D. J. Lodge, and T. J. Baroni. 2004. *Scleroderma stellatum* versus *Scleroderma bermudense*: The Status of *Scleroderma echinatum* and the First Record of *Veligaster nitidum* from the Virgin Islands. *Mycologia*, 96:1370–1379. https://doi.org/10.1080/15572536.2005.11832886

Halling, R. E. 2001. Ectomycorrhizae: Co-Evolution, Significance, and Biogeography. *Annals of the Missouri Botanical Garden*, 88:5–13. https://doi.org/10.2307/2666128

Halling, R. E., and G. M. Mueller. 1999. New Boletes from Costa Rica. *Mycologia*, 91:893–899. https://doi.org/10.1080/00275514.1999.12061095

Halling, R. E., and G. M. Mueller. 2002. Agarics and Boletes of Neotropical Oakwoods. In *Tropical Mycology*, ed. R. Watling, J. C. Frankland, A. M. Ainsworth, S. Isaac, and C. H. Robinson, vol. 1, pp. 1–10. New York: CABI Publishing.

Halling, R. E., and G. M. Mueller. 2005. *Common Mushrooms of the Talamanca Mountains, Costa Rica*. Bronx, NY: New York Botanical Garden.

Halling, R. E., and C. L. Ovrebo. 1987. A New Species of *Rozites* from Oak Forests of Colombia, with Notes on Biogeography. *Mycologia*, 79:674. https://doi.org/10.2307/3807818

Harrower, E., N. L. Bougher, C. Winterbottom, T. W. Henkel, E. Horak, and P. B. Matheny. 2015. New species in *Cortinarius* section *Cortinarius* (Agaricales) from the Americas and Australasia. *MycoKeys*, 11:1–21. https://doi.org/10.3897/mycokeys.11.5409

Henkel, T. W., M. C. Aime, M. M. Chin, S. L. Miller, R. Vilgalys, and M. E. Smith. 2012. Ectomycorrhizal Fungal Sporocarp Diversity and Discovery of New Taxa in *Dicymbe* Monodominant Forests of the Guiana Shield. *Biodiversity and Conservation*, 21:2195–2220. https://doi.org/10.1007/s10531-011-0166-1

Herrera, F., S. R. Manchester, R. Koll, and C. Jaramillo. 2014. Fruits of *Oreomunnea* (Juglandaceae) in the Early Miocene of Panama. *Paleobotany and Biogeography: A Festschrift Alan Graham in His 80th Year*, ed. W. D. Stevens, O. M. Montiel, and P. H. Raven, pp. 124–133. Monographs in Systematic Botany from the Missouri Botanical Garden, No. 128. St. Louis: Missouri Botanical Garden.

Kappelle, M. 2006. *Ecology and Conservation of Neotropical Montane Oak Forests*. Ecological Studies, No. 185. Berlin: Springer-Verlag.

Kasuya, T., and G. Guzmán. 2007. *Veligaster nitidum*, a Pantropical Sclerodermataceous Fungus New to Japan and Thailand. *Mycoscience*, 48:259–262. https://doi.org/10.1007/S10267-007-0359-3

Kennedy, P. G., R. Garibay-Orijel, L. M. Higgins, and R. Angeles-Arguiz. 2011. Ectomycorrhizal Fungi in Mexican *Alnus* Forests Support the Host Co-Migration Hypothesis and Continental-Scale Patterns in Phylogeography. *Mycorrhiza*, 21:559–568. https://doi.org/10.1007/s00572-011-0366-2

Kennedy, P. G., J. K. M. Walker, and L. M. Bogar. 2015. Interspecific Mycorrhizal Networks and Non-Networking Hosts: Exploring the Ecology of the Host Genus *Alnus*. In *Mycorrhizal Networks*, ed. T. R. Horton, pp. 227–254. Ecological Studies, No. 224. Dordrecht, Netherlands: Springer Science.

Koljalg, U., A. Dahlberg, A. F. S. Taylor, E. Larsson, N. Hallenberg, J. Stenlid, K.-H. Larsson, P. M. Fransson, O. Karen, and L. Jonsson. 2000. Diversity and Abundance of Resupinate Thelephoroid Fungi as Ectomycorrhizal Symbionts in Swedish Boreal Forests. *Molecular Ecology*, 9:1985–1996. https://doi.org/10.1046/j.1365-294X.2000.01105.x

Lilleskov, E. A., E. A. Hobbie, and T. R. Horton. 2011. Conservation of Ectomycorrhizal Fungi: Exploring the Linkages between Functional and Taxonomic Responses to Anthropogenic N Deposition. *Fungal Ecology*, 4:174–183. https://doi.org/10.1016/j.funeco.2010.09.008

Mata, J. L., and C. L. Ovrebo. 2009. New reports and illustrations of *Gymnopus* for Costa Rica and Panama. *Fungal Diversity*. 38, 125–131.

Mayor, J. R., T. D. Fulgenzi, T. W. Henkel, and R. E. Halling. 2008. *Boletellus piakaii* sp. nov. and a New Distribution Record for *Boletellus ananas* var. *ananas* from Guyana. *Mycotaxon*, 105:387–398.

Morris, M. H., M. A. Perez-Perez, M. E. Smith, and C. S. Bledsoe. 2008. Multiple Species of Ectomycorrhizal Fungi Are Frequently Detected on Individual Oak Root Tips in a Tropical Cloud Forest. *Mycorrhiza*, 18:375–383. https://doi.org/10.1007/s00572-008-0186-1

Mueller, G. M., and R. E. Halling. 1995. Evidence for High Biodiversity of Agaricales (Fungi) in Neotropical Montane *Quercus* Forests. *Biodiversity and Conservation of Neotropical Montane Forests*, 303–312.

Mueller, G. M., R. E. Halling, J. Carranza, M. Mata, and J. P. Schmit. 2006. Saprotrophic and Ectomycorrhizal Macrofungi of Costa Rican Oak Forests. In *Ecology and Conservation of Neotropical Montane Oak Forests*, ed. M. Kappelle, pp. 55–68. Berlin: Springer-Verlag.

Neves, M. A., and R. E. Halling. 2010. Study on Species of *Phylloporus* I: Neotropics and North America. *Mycologia*, 102:923–943. https://doi.org/10.3852/09-215

Ovrebo, C. L., K. W. Hughes, and R. E. Halling. 2019. Three New Species of *Tricholoma* from Costa Rica. *Phytotaxa*, 392(1):33–44. https://doi.org/10.11646/phytotaxa.392.1.3

Parmasto, E. 2001. Hymenochaetoid fungi (Basidiomycota) of North America. *Mycotaxon*, 79:107–176.

Piepenbring, M. E. 2006. *Checklist of Fungi in Panama, Preliminary Version*. David, Republic of Panamá: Universidad Autónoma de Chiriquí.

Piepenbring, M. E. 2007. Inventoring the Fungi of Panama. *Biodiversity and Conservation*, 16:73–84. https://doi.org/10.1007/s10531-006-9051-8

Piepenbring, M., E. Caballero, J. Fournier, G. Guzmán, C. L. Hou, R. Kirschner, E. Serrano, T. Trampe, and O. Cáceres. 2011. Pioneer Forays for Fungi in the Darién Province in Eastern Panama: Quintuplicating the Knowledge on Fungi in This Area by Five Days of Fieldwork. *Biodiversity and Conservation*, 20:2511–2526. https://doi.org/10.1007/s10531-011-0085-1

Piepenbring, M. E., T. A. Hofmann, E. Miranda, O. Cáceres, M. Unterseher. 2015. Leaf Shedding and Weather in Tropical Dry-Seasonal Forest Shape the Phenology of Fungi: Lessons from Two Years of Monthly Surveys in Southwestern Panama. *Fungal Ecology*, 18:83–92. https://doi.org/10.1016/j.funeco.2015.08.004

Põlme, S., M. Bahram, T. Yamanaka, K. Nara, Y. C. Dai, T. Grebenc, H. Kraigher, M. Toivonen, P.-H. Wang, Y. Matsuda, T. Naadel, P. G. Kennedy, U. Kõljalg, and L. Tedersoo. 2013. Biogeography of Ectomycorrhizal Fungi Associated with Alders (*Alnus* spp.) in Relation to Biotic and Abiotic Variables at the Global Scale. *New Phytologist*, 198:1239–1249. https://doi.org/10.1111/nph.12170

Popa, F., S. Castillo-Jimenez, J. Weisenborn, K. Donges, K. H. Rexer, and M. Piepenbring. 2016. A New Laccaria Species from Cloud Forest of Fortuna, Panama. *Mycological Progress*, 15:1–8. https://doi.org/10.1007/s11557-015-1139-7

Singer, R. 1963. Oak mycorrhiza fungi in Colombia. Mycopathlogia et mycologia applicate 20:239-252.

Smith, M. E., G. W. Douhan, and D. M. Rizzo. 2007. Intra-Specific and Intra-Sporocarp ITS Variation of Ectomycorrhizal Fungi as Assessed by rDNA Sequencing of Sporocarps and Pooled Ectomycorrhizal Roots from a *Quercus* Woodland. *Mycorrhiza*, 18:15–22. https://doi.org/10.1007/s00572-007-0148-z

Tedersoo, L., M. Bahram, S. Polme, U. Koljalg, N. S. Yorou, R. Wijesundera, L. V. Ruiz, A. M. Vasco-Palacios, P. Q. Thu, A. Suija, M. E. Smith, C. Sharp, E. Saluveer, A. Saitta, M. Rosas, T. Riit, D. Ratkowsky, K. Pritsch, K. Poldmaa, M. Piepenbring, C. Phosri, M. Peterson, K. Parts, E. Otsing, E. Nouhra, A. L. Njouonkou, R. H. Nilsson, L. N. Morgado, J. Mayor, T. W. May, L. Majuakim, D. J. Lodge, S. S. Lee, K.-H. H. Larsson, P. Kohout, K. Hosaka, I. Hiiesalu, T. W. Henkel, H. Harend, L. Guo, A. Greslebin, G. Grelet, J. Geml, G. Gates, W. Dunstan, C. Dunk, R. Drenkhan, J. Dearnaley, A. De Kesel, T. Dang, X. Chen, F. Buegger, F. Q. Brearley, G. Bonito, S. Anslan, S. Abell, and K. Abarenkov. 2014. Global Diversity and Geography of Soil Fungi. *Science*, 346:1256688–1256688. https://doi.org/10.1126/science.1256688

Tedersoo, L., T. W. May, M. E. Smith. 2010. Ectomycorrhizal Lifestyle in Fungi: Global Diversity, Distribution, and Evolution of Phylogenetic Lineages. *Mycorrhiza*, 20:217–263. https://doi.org/10.1007/s00572-009-0274-x

Tulloss, R. E. 2005. *Amanita:* Distribution in the Americas with Comparison to Eastern and Southern Asia and Notes on Spore Character Variation with Latitude and Ecology. *Mycotaxon*, 93:189–231.

Tulloss, R. E., R. E. Halling, and G. M. Mueller. 2011. Studies in *Amanita* (Amanitaceae) of Central America. 1. Three new species from Costa Rica and Honduras. *Mycotaxon*, 117:165–205. https://doi.org/10.5248/117.165

van der Linde, S., L. M. Suz, C. D. L. Orme, F. Cox, H. Andreae, E. Asi, B. Atkinson, S. Benham, C. Carroll, N. Cools, B. De Vos, H. P. Dietrich, J. Eichhorn, J. Gehrmann, T. Grebenc, H. S. Gweon, K. Hansen, F. Jacob, F. Kristofel, P. Lech, M. Manninger, J. Martin, H. Meesenburg, P. Merila, M. Nicolas, P. Pavlenda, P. Rautio, M. Schaub, H. W. Schrock, W. Seidling, V. Šramek, A. Thimonier, I. M. Thomsen, H. Titeux, E. Vanguelova, A. Verstraeten, L. Vesterdal, P. Waldner, S. Wijk, Y. Zhang, D. Žlindra, and M. I. Bidartondo. 2018. Environment and Host as Large-Scale Controls of Ectomycorrhizal Fungi. *Nature*, 558:243–248. https://doi.org/10.1038/s41586-018-0189-9

Welden, A. L. 2010. *Flora Neotropica Monograph Stereum s.l.*, No. 106. New York: New York Botanical Garden Press, 1–80.

Wicaksono, C. Y., J. Aguirre-Guiterrez, E. Nouhra, N. Pastor, N. Raes, S. Pacheco, and J. Geml. 2017. Contracting Montane Cloud Forests: A Case Study of the Andean Alder (*Alnus acuminata*) and Associated Fungi in the Yungas. *Biotropica*, 49:141–152. https://doi.org/10.1111/btp.12394

5. The Bryophytes

Noris Salazar Allen,[1] José A. Gudiño L.,[1] Marla B. Johnston,[2]*
Dilia Santamaría E.,[3] Clementina Chung C.,[4] Clotilde Arrocha,[5]
Eyvar Rodriguez,[5] and Jörg Spörle[2]

ABSTRACT. Systematic collections of the vegetation of the Fortuna Forest Reserve, including bryophytes, started in 1976 within the framework of the studies on the environmental and human impacts of the Fortuna Hydroelectric Project. For the lower montane flora of Fortuna, 396 species of bryophytes in 164 genera, 2 subspecies, and 12 varieties are reported. Three taxa (a foliose liverwort, a moss) and a variety of a moss were previously described as new to science from bryophytes of Fortuna. Of these, the liverwort *Plagiochila salazariae* is endemic to Panama. There is a predominance of mosses, with 214 species and 8 varieties, followed by the liverworts, with 174 species, 2 subspecies, and 4 varieties; the hornworts are the smallest group, with 8 species. The most diverse family among the mosses is the Hookeriaceae, with 37 species that grow in very humid to wet places; and among the liverworts, the most diverse is the actively evolving Lejeuneaceae, with 87 species that grow in a variety of environments. The bryoflora of Fortuna accounts for ~32% of the total bryophytes known for Panama, 35.9% of all liverworts and hornworts, and 28.5% of the moss flora of the country. Affinities of the bryoflora are with the Neotropics followed, in descending order, by species with pantropical, African, and subcosmopolitan distribution. Seventeen major collecting sites were distinguished from collectors' notes and literature survey. Quebrada Bonita, the foothills of Cerro Pinola, northeast of the camping site (where members of the University of Panama, Botany Department stayed while surveying the flora of Fortuna during the building of the dam in 1976) and Quebrada Arena account for the highest diversity of bryophytes. The bryoflora of Fortuna is a heterogeneous assemblage of ancestral lowland tropical and north temperate, cool-adapted elements from North (Laurasia, e.g., *Anthoceros*) and South temperate (Gondwana, e.g., *Macromitrium*) and also those of Neotropical origins (e.g., members of the Lejeuneaceae). The bryoflora of Fortuna is another example of the importance of the Isthmus of Panama as a biological corridor for the exchange of biota between the adjacent continental masses.

INTRODUCTION

When collecting for bryophytes, the Province of Chiriquí is one of the most visited areas of Panama besides the provinces of Panama, Coclé, Veraguas, and the Panama Canal. This is due to its accessibility and diverse geographic landscapes with lowland areas including coastal seashores and mountains that range from 1,000 to 3,475 m at the highest mountain in Panama, the Volcán Barú. Bryophytes (mosses, liverworts, and hornworts) are the second-most diverse group of land plants after the angiosperms. The initial transition of plants to land and their earliest diversification dates back to the Ordovician. Bryophytes are among the oldest groups of land plants, having persisted for approximately half a billion years and are considered the closest ancestors of the earliest diverging terrestrial plants (Vanderpoorten and Goffinet, 2009; Renzaglia et al., 2018). Extant bryophytes include three groups (divisions or phyla): mosses (Bryophyta), liverworts (Marchantiophyta), and hornworts (Anthocerotophyta). The mosses include approximately 9,000 to 13,000 species (Magill, 2010);

---

[1] Smithsonian Tropical Research Institute, Apartado 0843-03092, Balboa, Ancón, Republic of Panama.

[2] Martin-Niemöller Straße 72, 64354 Reinheim, Deutschland.

[3] Corregimiento de Ancón, Clayton, Edificio Clayton Tower, Republic of Panama.

[4] Deceased; formerly at the Smithsonian Tropical Research Institute, Ancón, Republic of Panama.

[5] Herbario UCH, Universidad Autónoma de Chiriquí, Chiriquí, Republic of Panamá.

* Correspondence: salazarn@si.edu

the liverworts, 4,000 to 9,000; and the hornworts, approximately 215 (Söderström et al., 2016). Bryophytes are poikilohydric organisms photosynthesizing and growing when moist and becoming "dormant" (suspending their metabolism) when dry (Proctor, 2009; Vanderpoorten and Goffinet, 2009). They take up water and nutrients through the whole surface of their shoots (Proctor, 2009). Bryophytes are found on a variety of substrates (soil, rock, trees, and leaves) and in ecosystems from the most extreme environments of the Arctic and the Antarctic to the tropics, except in the sea. They are more diverse in the tropics where they can be found from dry or seasonally dry rainforests to cloud forests and paramos. Their diversity and biomass increase in forests of higher elevations, particularly in cloud forests where they are an important component of the epiphytic vegetation. In these forests, they grow in soil on riverbanks, creeks, rocks, leaves (epiphylls), and decomposing logs. Bryophytes sometimes form symbioses with cyanobacteria (capable of fixing atmospheric nitrogen) and with various fungi (Bentley, 1987; Adams and Duggan, 2008; Papaefthimiou et al., 2008; Renzaglia et al., 2009; Desirò et al., 2013). These plants are important in the capture, storage, and cycling of water and nutrients (among these, nitrogen) in cloud forests (Pócs, 1980; Clark et al., 1998; Nadkarni and Solano, 2002; Ah-Peng et al., 2017; Horwath et al., 2019; Rodríguez-Quiel et al., 2019). Ecological studies in cloud and elfin forests have estimated that moisture stored by bryophytes from the interception of fog and rainfall exceeds by 50% to 90% the total annual rainfall (Pócs, 1980; Cavalier and Goldstein, 1989; Jarvis and Mulligan, 2011). Bryophytes are also important in the carbon cycling of tropical forests. Carbon budgets for cloud forests remain incomplete unless the epiphytic biomass is included (Horwath et al., 2019). Thus, through their growth and decomposition, bryophytes play a major role in the cycling of carbon and nutrients in the forests (Vanderpoorten and Goffinet, 2009). Bryophytes provide shelter and food to a myriad of invertebrates, such as tardigrades, scorpions, snails; insect nymphs, such as *Disdercus* spiders (e.g., the green spider [Uloboridae] and the tiny money spider [Linifiidae]; D. Quintero, personal communication); and sawflies, among various organisms observed in cloud forests in Panama. For a thorough review of insects associated with bryophytes, see Glime (2017). In addition, the association of bryophytes with microbes could contribute to the nutrient budget of the forests (Alcaraz et al., 2018; Aschenbrenner et al., 2016; Berg et al., 2011; Coxson, 2011; Turetsky, 2003). Because bryophytes absorb water and nutrients exclusively or mostly through their surfaces, they are therefore good indicators of water and air pollution, heavy metal contamination, and radioactivity (Ayrault et al., 2002; Acto et al., 2003; Frahm, 2003; Ares et al., 2018).

Among bryophytes, the liverworts produce a wide array of active secondary metabolites, especially terpenoids and aromatic compounds. They are of taxonomic, chemical, and pharmaceutical importance, and many of these compounds have not been found in any other plants, fungi, or marine organisms (Asakawa, 1982, 1995, 2008; Asakawa et al., 2013).

PREVIOUS STUDIES

One of the first collections of bryophytes reported for Panama are those of Berthold Seemann between 1846 and 1851, published in *Botany of the Voyage of H.M.S. Herald*. W. Wilson identified the mosses and W. Mitten, the liverworts (Seemann, 1852–1854; Crum and Steere, 1950). These collections are mainly from lowland areas with few from Volcán Barú and other unspecified sites. Many foreign botanists have collected in the area of what is now the Fortuna Forest Reserve (Reserva Forestal Fortuna) in the province of Chiriquí (Figure 5.1). Among these are botanists and bryologists from the Missouri Botanical Garden, the New York Botanical Garden, the Field Museum of Natural History, and from the various European herbaria.

In 1976, the government, through the Institute of Hydraulic Resources and Electricity (IRHE) of that time, selected the Gorgas Memorial Laboratory to do a multidisciplinary study of the environment and human ecology of the Fortuna area where two hydroelectric projects, Estrella de los Valles and Fortuna, were going to be constructed. Dr. Abdiel Adames, then a scientist at the Gorgas Memorial Laboratory, directed the project (Adames, 1977). The Department of Botany of the University of Panama was responsible for the botanical part. Vascular plants, bryophytes, and lichens were collected in the area before the logging started.

Salazar Allen was in charge of the bryophyte and lichen part of the survey. Two hundred fifty samples were collected between June and September 1976. Eleven of them were identified to species, genus, or family for the published report (Mayo et al., 1977). Upon request of the Fortuna Hydroelectric Project, in April and May 1987, Salazar Allen and her students, M. Johnston and D. Santamaría, made four field trips to five logging areas that were going to be inundated for the enlargement of the reservoir during the second phase of the hydroelectric project (IRHE, 1986). Most samples were collected along the nature trails of a secondary forest in Quebrada Bonita, Quebrada Arena, Trocha Las Mellizas, along Río Chiriquí, and in the primary forest at the foothills of Cerro Pinola (Johnston, 1990; Santamaría, 1991). Approximately 1,150 samples were gathered during those trips. In May 1988, a German student, J. Spörle, who was working on the chemistry of bryophytes, joined the team and made additional collections in the logged area of Cerro Fortuna, in Palo Seco, and in Quijada del Diablo (Spörle, 1990) (Figures 5.1–5.2). Personnel of the Autonomous University of Chiriquí (UNACHI) contributed with collections made at Quebrada Honda. Some of these collections were identified or revised, for mosses by S. P. Churchill (some *Lepidopilum*), D. Griffin III (Bartramiaceae), H. Ochi (†) (Bryaceae), J.-P. Frahm (†) (*Campylopus*), R. A. Pursell (†) (Fissidentaceae), W. C. Steere (†), R. H. Zander (Pottiaceae), and personnel of the Missouri Botanical Garden (M. R. Crosby and B. H. Allen); and for the liverworts, G. Dauphin (*Ceratolejeunea*), K. Feldberg (*Herbertus*), M. Fulford (†), R. S. Gradstein, J. Heinrich (†) (*Plagiochila*), R. Stotler (†) (*Frullania*), and M. E. Reiner-Drehwald (*Lejeunea*).

In March 1996, participants of the workshop Bryophytes as Non-woody Biodiversity Indicators collected and identified

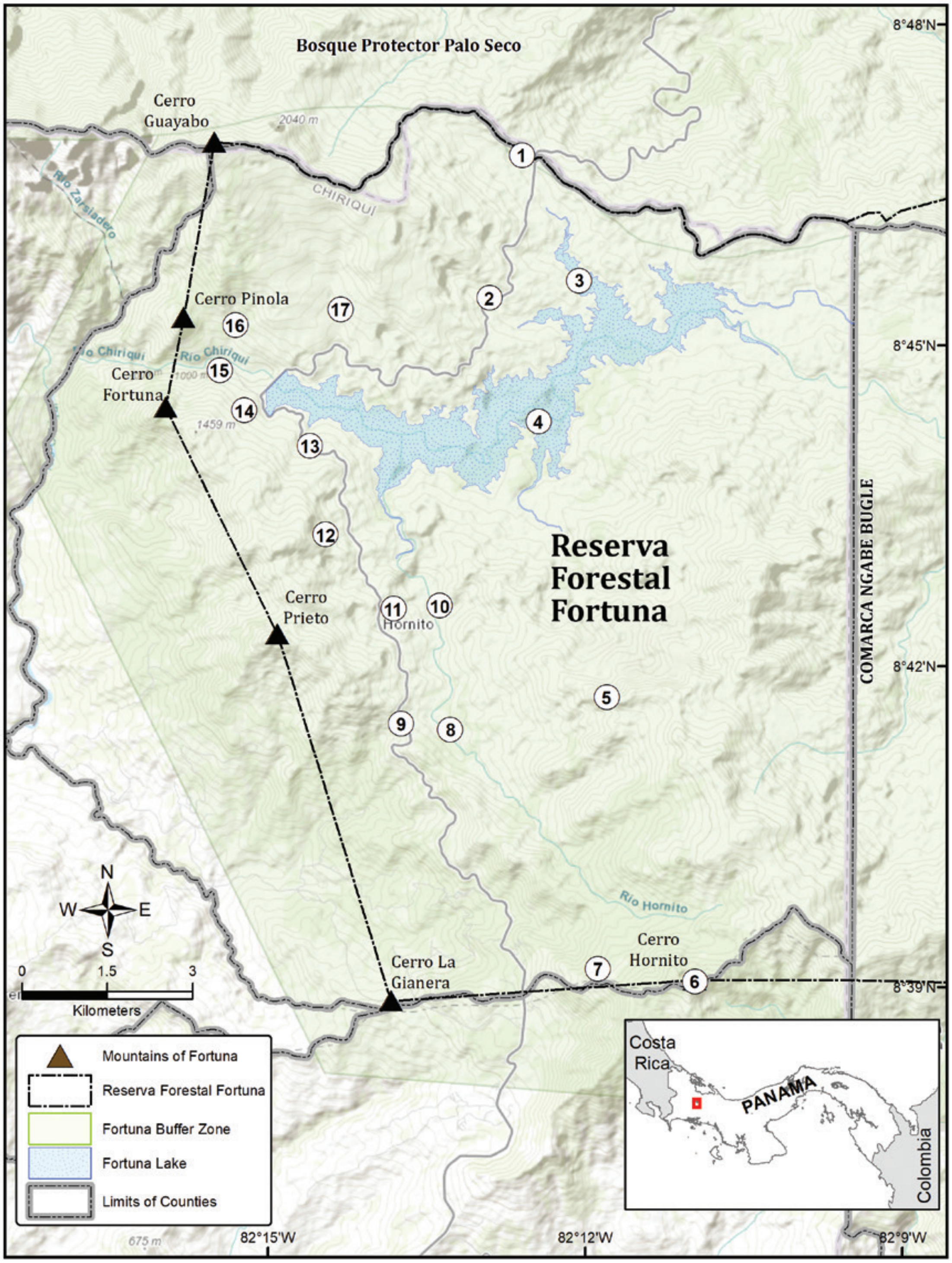

FIGURE 5.1. Main collecting sites: 1 = Continental Divide, Trail to Palo Seco (900–1,200 m); 2 = Quebrada Bonita (920–1,150 m); 3 = Quebrada Arena (900–1,000 m); 4 = Trail to Quebrada Las Mellizas (1,200 m); 5 = Cerro Pata de Macho (1,700–1,800 m); 6 = Cerro Hornito (1,670–2,300 m); 7 = Valle de Hornito (1,300–1,700 m); 8 = Trail along Río Hornito (1,200 m); 9 = Quijada del Diablo (1,200–1,600 m); 10 = Quebrada Mono (1,100–1,300 m); 11 = Quebrada Alemán (1,200–1,400 m); 12 = Institute of Hydraulic Resources and Electricity's plant nursery (1,100 m); 13 = At mouth of Quebrada Samudio (1,100–1,280 m); 14 = SW of camping site, from Finca Pittí to foothills of Cerro Fortuna (1,000–1,270 m); 15 = NW of camping site (1,000–1,200 m); 16 = Foothills of Cerro Pinola (1,280–2,000 m); 17 = NE of camping site (900–1,200 m).

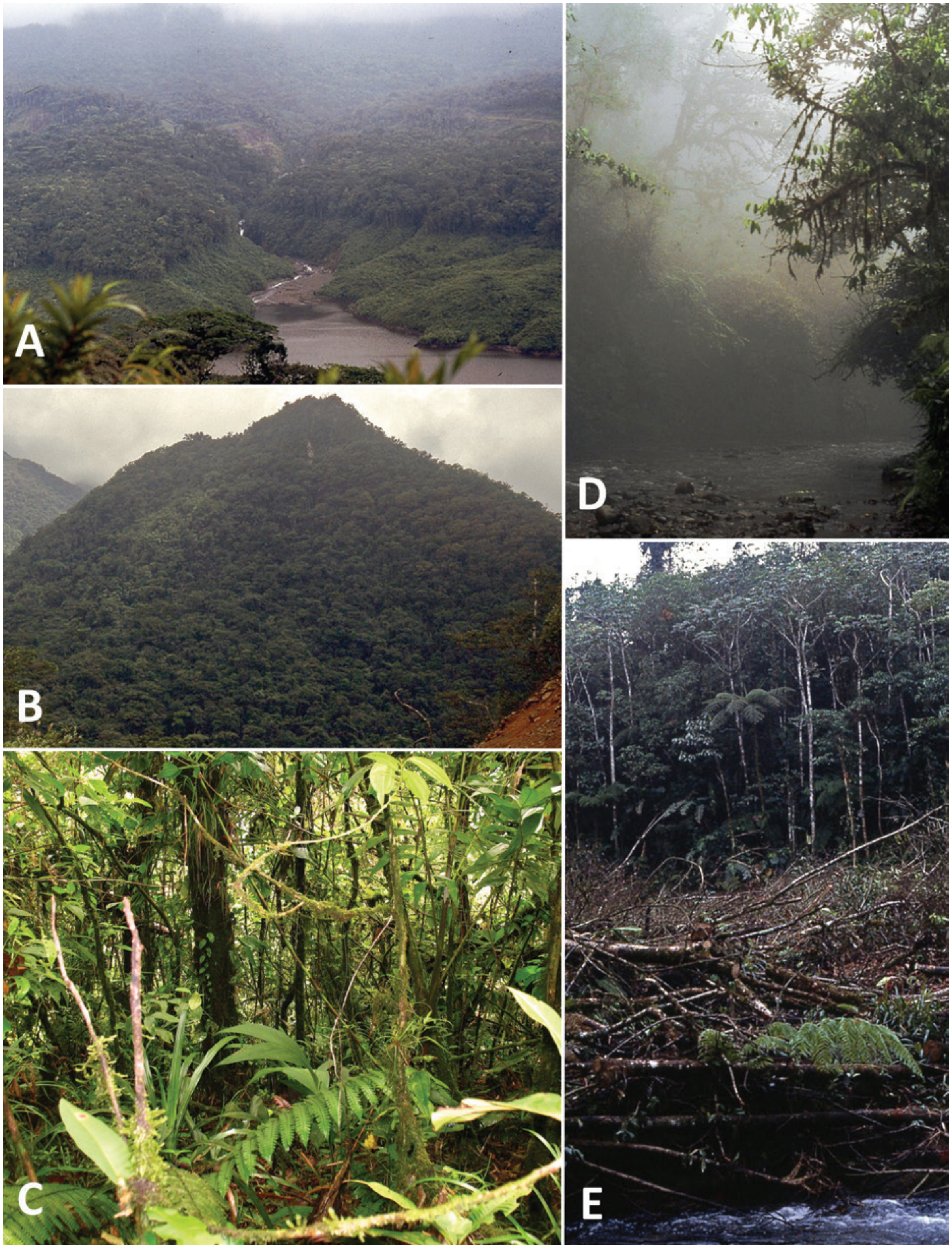

FIGURE 5.2. (A) Cut areas to be flooded during the last part of the construction of the Fortuna Dam Project; in the foreground part of the lake, in the background Río Chiriquí entering the lake (May 1988). (B) Cerro Pinola (May 1988). (C) Vegetation in Trocha Palo Seco. (D) Quebrada Bonita (May 1988). (E) Logging area in Quebrada Bonita (May 1988).

bryophytes of Fortuna. In June 2017, a visit to Fortuna by professors and students of the International Bryophyte Biology Workshop held at Bocas del Toro added new reports.

DATA COLLECTION

The list of bryophytes was compiled from various sources: personal collections and database of Salazar Allen; the database of the University of Panama Herbarium (PMA); the database from the Autonomous University of Chiriquí Herbarium (UCH), and the Missouri Botanical Garden website TROPICOS (accessed 2018–2019). Additional sources included a revision of publications on the flora of Panama (Mayo et al., 1977; Stotler et al., 1998; Spörle, 1990; Dauphin et al., 2006; Dauphin, 2007; Dauphin et al., 2015; Schäfer-Verwimp, 2014); selected monographs (Reese, 1993; Allen, 1994, 2002, 2010, 2018; Reiner-Drehwald and Ilkiu-Borges, 2007; Wei et al., 2014); unpublished BA theses by Johnston (1990), Santamaría E. (1991), and Chung C. (1995); and collections from the workshops described previously. The classification and nomenclature of liverworts is based on Crandall-Stotler et al. (2009), Söderström et al. (2016), and Gradstein and Ilkiu-Borges (2009) for Neotropical *Herbertus*; Söderström et al. (2013) for the Lophocoleaceae; Bastos (2017) for *Cheilolejeunea* of the Americas; Ye et al. (2015) for *Cheilolejeunea* and the former *Omphalanthus*; and Gradstein (2015) for *Plagiochila*. For the mosses, it is based on Goffinet and Buck (2019) and Allen (1994, 2002, 2010, 2018). Collecting sites in the Fortuna Forest Reserve with their approximate coordinates and elevations are based on information in the collectors' notebooks and the database at PMA and UCH.

Monographs and other taxonomic publications and consultation with specialists provided additional information on the geographical distribution of liverworts. Unlike it is for the mosses, information on species distribution of liverworts is not compiled in an international database such as LATMOSS (Delgadillo et al., 2013) or TROPICOS (Missouri Botanical Garden); thus, because of the extensive list of documents revised, this literature and a few for mosses are listed in Appendix 1. Information for the tables on geographical distribution and geographical affinities of the bryophytes of Fortuna is based mainly on Allen (1994, 2002, 2010, 2018), Câmara (2011), LATMOSS, and TROPICOS. When applicable, for the altitudinal range of bryophytes in Panama, comparisons are made with the known flora of Barro Colorado Island (BCI) in the Panama Canal area (liverworts and mosses), the region of Bahía Honda in Veraguas Province (mosses), and the Reserva Natural Privada Chucantí in Darién Province (hornworts and mosses). This last site has both lowland and premontane rainforests.

LATMOSS distribution was modified as follows (Table 5.1):

North America (Greenland, Alaska, Canada, western United States, and unknown sites in the region.)
Mexico (only Mexico)
Central America (Guatemala, Belize, El Salvador, Honduras, Nicaragua, Costa Rica, and Panama)
Northern South America (Colombia, Venezuela, Guyana, Suriname, French Guiana, and Trinidad and Tobago)
Mid-South America (Ecuador, including the Galapagos, Peru, Bolivia, and Brazil)
Southern South America (Chile, Argentina, Paraguay, Uruguay, and Falkland Islands)
Caribbean (Cuba, Haiti, Dominican Republic, Puerto Rico, Virgin Islands, and Lesser Antilles)
Africa (North, West, East, and South Africa, Madagascar and adjacent islands)
Europe (including the Union of Soviet Socialist Republics)
Asia (China, Malesia, Japan, Korea, Thailand, Vietnam, Laos, and Cambodia).
India (Indian subcontinent and Western Indian Ocean)
Hawaii and Eastern and South Pacific Islands
Australia and New Zealand

FLORISTIC RELATIONSHIPS

Based on geographical distribution of the species, the following floristic elements are recognized: NEO (Neotropical) – distributed from southern North American to Central America, the Caribbean and South America; NEO-AF–EU – neotropical species distributed in Africa and Europe; AF–AM – Species distributed in Africa, Madagascar and adjacent islands, and the Americas; PAN (Pantropical) – distributed throughout the Tropics; and SUBCOS (Subcosmopolitan) – with a worldwide distribution. Restricted or disjunct distribution of neotropical species are recognized as follows: NEO-AS – distributed in América and Asia; NEOC – only in continental America, unrecorded for the Caribbean; NEO-CAM – only in Central America; and NEO-PMA – endemic to Panama. To evaluate the total number of species, subspecies, and varieties that were distributed in each geographical area, every name was taken as an individual record (e.g., *Syrrhopodon incompletus* is an African–American species, but its variety *S. incompletus* var. *berteroanus* is Neotropical. The first one was included with the AF–AM species and the second with the NEO species; *Eucamptodontopsis brittoniae* and *E. brittoniae* var. *mcphersonii* both are growing in Central America and were counted as two NEO records).

RESULTS AND DISCUSSION

TAXONOMIC DIVERSITY

To date, the total number of bryophytes recorded for Panama is 1,236 species. Some 752 species are mosses, 484 liverworts and hornworts (Dauphin et al., 2015; N. Salazar Allen, personal communication). Three hundred ninety-six species of bryophytes in 164 genera, 2 subspecies, and 12 varieties are reported for Fortuna (Tables 5.1 and 5.2; Figure 5.3). Before this study, three species and one variety were described as new to science from plants of Fortuna: *Plagiochila salazariae* (Inoue, 1989), *Eucamptodontopsis*

TABLE 5.1. Phytogeographic affinities and world distribution of the bryophytes of Fortuna. Next to the family, in parenthesis, the digits refer to the number of genera/species/subspecies/varieties reported for each family, a dash (–) = unreported. Abbreviations for Affinities: AF, Africa; AM, America; AS, Asia; CAM, Central America; Chocó, Chocó biogeographic region; EU, Europe; N Andes, Northern Andes; NEO, Neotropical; NEOC, Neotropical continental, unreported for the Caribbean; PAN, pantropical; PMA, Panama; SUBCOS, subcosmopolitan. Abbreviations for World distribution: NA, North America; MX, Mexico; CA, Central America; NW, South America; MS, mid–South America; SS, southern South America; CR, Caribbean Antilles; AF, Africa; EU, Europe; AS, Asia; IN, India; PO, Hawaii and South Pacific (Oceania); AU, Australia; NZ, New Zealand. Asterisk (*) = reported for the area; (—) = unreported.

		Worldwide distribution													
Species by division and family	**Affinities**	**NA**	**MX**	**CA**	**NW**	**MS**	**SS**	**WI**	**AF**	**EU**	**AS**	**IN**	**PO**	**AU**	**NZ**
HORNWORTS (ANTHOCEROTOPHYTA)															
Anthocerotaceae (1/2/-/-)															
Anthoceros lamellatus Steph.	NEOC	*	*	*	*	*	*	—	—	—	—	—	—	—	—
A. tuberculatus Lehm. & Lindenb.	NEO	—	*	*	*	*	—	*	—	—	—	—	—	—	—
Dendrocerotaceae (3/5/-/-)															
Dendroceros crispatus (Hook.) Nees	PAN	—	*	*	—	—	—	*	*	—	—	—	—	*	—
D. crispus (Sw.) Nees	PAN	—	*	*	*	*	—	*	*	—	—	—	*	—	—
Nothoceros schizophyllus (Steph.) J.C.Villarreal	NEO	—	—	*	*	—	—	*	—	—	—	—	—	—	—
N. vincentianus (Lehm. & Lindenb.) J.C.Villarreal	NEO	—	*	*	*	*	—	*	—	—	—	—	—	—	—
Phaeomegaceros fimbriatus (Gottsche) R.J.Duff, J.C.Villarreal, Cargill & Renzaglia	NEO	—	—	*	*	*	—	*	—	—	—	—	—	—	—
Notothyladaceae (1/1/-/-)															
Phaeoceros laevis (L.) Prosk.	SUBCOS	*	—	—	*	*	*	*	*	*	*	—	*	*	—
LIVERWORTS (MARCHANTIOPHYTA)															
Acrobolbaceae (1/1/-/-)															
Acrobolbus laxus (Lehm. & Lindenb.) Briscoe	AF–AM	—	*	*	*	*	—	*	*	—	—	—	—	—	—
Aneuraceae (2/3/-/-)															
Aneura pinguis (L.) Dumort.	SUBCOS	*	*	*	*	*	*	—	*	*	*	*	*	*	*
Riccardia fucoidea (Sw.) C.Massal.	NEO	—	*	*	*	*	—	*	—	—	—	—	—	—	—
R. poeppigiana (Lehm. & Lindenb.) Hässel ex Meenks & C.De Jong	NEO	—	*	*	*	*	—	*	—	—	—	—	—	—	—
Balantiopsidaceae (2/2/-/-)															
Isotachis multiceps (Lindenb. & Gottsche) Gottsche	NEO	—	*	*	*	*	—	*	—	—	—	—	—	—	—
Neesioscyphus argillaceus (Nees) Grolle	NEOC	—	—	*	*	*	—	—	—	—	—	—	—	—	—
Calypogeiaceae (2/4/-/-)															
Calypogeia peruviana Nees & Mont.	AF–AM	*	*	*	*	*	—	*	*	—	—	—	—	—	—
C. rhombifolia (Spruce) Steph.	NEO	—	—	*	*	*	—	*	—	—	—	—	—	—	—
Mnioloma cyclostipum (Spruce) R.M.Schust.	NEO	—	—	*	*	*	—	*	—	—	—	—	—	—	—
M. rhynchophyllum Herzog	NEOC	—	—	*	—	—	—	—	—	—	—	—	—	—	—
Cephaloziaceae (3/3/-/-)															
Alobiellopsis dominicensis (Spruce) Fulford	NEO	—	—	*	*	—	—	*	—	—	—	—	—	—	—
Fuscocephaloziopsis crassifolia (Lindenb. & Gottsche) Váňa & L.Söderstr.	NEO	—	*	*	*	*	—	*	—	*	—	—	—	—	—
Odontoschisma variabile (Lindenb. & Gottsche) Trevis.	AF–AM	—	*	*	*	*	—	*	*	—	—	—	—	—	—

TABLE 5.1. (*Continued*)

Species by division and family	Affinities	Worldwide distribution													
		NA	MX	CA	NW	MS	SS	WI	AF	EU	AS	IN	PO	AU	NZ
Dumortieraceae (1/1/-/-)															
Dumortiera hirsuta (Sw.) Nees	PAN	*	*	*	*	*	*	*	*	*	*	*	*	*	*
Frullaniaceae (1/12/-/1)															
Frullania bicornistipula Spruce	NEOC–N. Andes	—	—	*	*	*	—	—	—	—	—	—	—	—	—
F. brasiliensis Raddi	NEO	—	*	*	*	*	*	*	—	—	—	—	—	—	—
F. caulisequa (Nees) Mont.	NEO	*	—	*	*	*	—	*	—	—	—	—	—	—	—
F. dusenii Steph.	NEO	—	—	*	*	*	—	*	—	—	—	—	—	—	—
F. ericoides (Nees) Mont.	PAN	*	—	*	*	*	*	*	*	—	*	*	*	—	—
F. exilis Taylor	NEO	—	*	*	*	*	—	*	—	—	—	—	—	—	—
F. kunzei (Lehm. & Lindenb.) Lehm. & Lindenb.	NEO	*	—	*	*	*	—	*	—	—	—	—	—	—	—
F. macrocephala (Lehm. & Lindenb.) Lehm. & Lindenb.	NEO	—	—	*	*	*	—	*	—	—	—	—	—	—	—
F. mirabilis J.B.Jack & Steph.	NEOC	—	—	*	*	*	—	—	—	—	—	—	—	—	—
F. obscura (Sw.) Mont. var. *spiniloba* (Steph.) Hentschel & von Konrat	NEO	—	—	*	*	*	—	*	—	—	—	—	—	—	—
F. pittieri Steph.	NEOC	—	—	*	*	*	—	—	—	—	—	—	—	—	—
F. uleana Steph.	NEO	—	—	*	—	*	—	*	—	—	—	—	—	—	—
Herbertaceae (2/3/1/-)															
Herbertus bivittatus Spruce	NEO	—	—	*	*	*	—	*	—	—	—	—	—	—	—
H. juniperoideus (Sw.) Grolle	AF–AM	—	*	*	*	*	—	*	*	—	—	—	—	—	—
H. pensilis (Taylor) Spruce	NEO	—	—	*	*	*	—	*	—	—	—	—	—	—	—
Lejeuneaceae (26/87/1/2)															
Acanthocoleus aberrans (Lindenb. & Gottsche) Kruijt var. *laevis* Gradst.	AF–AM	—	*	*	*	*	*	*	*	—	—	—	—	—	—
Anoplolejeunea conferta (C.F.W.Meissn. ex Spreng.) A.Evans	NEO	—	—	*	*	*	—	*	—	—	—	—	—	—	—
Brachiolejeunea laxifolia (Taylor) Schiffn.	NEO	—	*	*	*	*	—	*	—	—	—	—	—	—	—
Bryopteris filicina (Sw.) Nees	NEO	—	*	*	*	*	—	*	—	—	—	—	—	—	—
Ceratolejeunea cornuta (Lindenb.) Steph.	PAN	—	*	*	*	*	—	*	*	—	*	—	—	—	—
C. fallax (Lehm. & Lindenb.) Bonner	AF–AM	—	—	*	*	*	—	*	*	—	—	—	—	—	—
C. filaria (Taylor ex Lehm.) Steph.	NEO	—	*	*	*	*	—	*	—	—	—	—	—	—	—
C. spinosa (Gottsche) Steph.	NEO	—	—	*	*	*	—	*	—	—	—	—	—	—	—
Cheilolejeunea acutangula (Nees) Grolle	NEO	—	*	*	*	*	—	*	—	—	—	—	—	—	—
C. aneogyna (Spruce) A.Evans	NEO	—	—	*	*	*	—	*	—	—	—	—	—	—	—
C. comans (Spruce) R.M.Schust.	NEO	—	—	*	*	*	*	*	—	—	—	—	—	—	—
C. filiformis (Sw.) W.Ye, R.L.Zhu & Gradst.	NEO	—	*	*	*	*	—	*	—	—	—	—	—	—	—
C. holostipa (Spruce) Grolle & R.L.Zhu	NEO	—	—	*	*	*	—	*	—	—	—	—	—	—	—
C. inflexa (Hampe ex Lehm.) Grolle	NEO	—	—	*	*	*	—	*	—	—	—	—	—	—	—
C. lineata (Lehm. & Lindenb.) Steph.	NEO	—	*	*	*	*	—	*	—	—	—	—	—	—	—
C. oncophylla (Ångstr.) Grolle & M.E.Reiner	NEO	—	—	*	*	*	*	*	—	—	—	—	—	—	—

(*Continued*)

TABLE 5.1. (*Continued*)

		Worldwide distribution													
Species by division and family	**Affinities**	**NA**	**MX**	**CA**	**NW**	**MS**	**SS**	**WI**	**AF**	**EU**	**AS**	**IN**	**PO**	**AU**	**NZ**
C. trifaria (Reinw., Blume & Nees) Mizut.	PAN	—	*	*	*	*	*	*	*	—	*	*	*	*	—
C. xanthocarpa (Lehm. & Lindenb.) Malombe	PAN	*	—	*	*	*	*	*	*	—	*	—	*	—	—
Cololejeunea appressa (A.Evans) Benedix	PAN	—	*	*	*	—	—	*	*	—	*	*	*	—	*
C. camillii (Lehm.) A.Evans	NEO	—	*	*	*	*	*	*	—	—	—	—	—	—	—
C. diaphana A.Evans	PAN	*	—	*	*	*	—	*	—	—	*	—	—	—	—
C. gracilis (Jovet-Ast) Pócs	NEO	—	—	*	*	*	—	*	—	—	—	—	—	—	—
C. jamesii (Austin) M.E.Reiner & Pócs	PAN	*	*	*	*	*	*	*	*	—	—	*	—	—	—
C. linopteroides H.Rob.	NEOC	—	—	*	*	—	—	—	—	—	—	—	—	—	—
C. papilliloba (Steph.) Steph.	AF–AM	—	*	*	*	*	—	—	*	—	—	—	—	—	—
C. papillosa (K.I.Goebel) Mizut.	NEO-AS	—	—	*	*	*	—	*	—	—	*	—	—	—	—
C. sicifolia (Gottsche ex A.Evans) Pócs & Bernecker subsp. *jamaicensis* (R.M.Schust.) Bernecker & Pócs	NEO	—	—	*	—	*	—	*	—	—	—	—	—	—	—
C. subcardiocarpa Tixier	NEO	—	*	*	*	*	—	*	—	—	—	—	—	—	—
C. submarginata Tixier	NEO	—	*	*	*	*	—	*	—	—	—	—	—	—	—
C. yelitzae Pócs & Bernecker	NEOC	—	—	*	*	*	—	—	—	—	—	—	—	—	—
Cyclolejeunea accedens (Gottsche) A.Evans	NEO	—	—	*	*	*	—	*	—	—	—	—	—	—	—
C. chitonia (Taylor ex Lehm.) A.Evans	NEO	—	—	*	*	*	—	*	—	—	—	—	—	—	—
C. convexistipa (Lehm. & Lindenb.) A.Evans	NEO	—	*	*	*	*	—	*	—	—	—	—	—	—	—
C. peruviana (Lehm. & Lindenb.) A.Evans	NEO	—	—	*	*	*	—	*	—	—	—	—	—	—	—
Diplasiolejeunea caribea Tixier	NEO	—	—	*	*	*	—	*	—	—	—	—	—	—	—
D. cavifolia Steph.	PAN	—	*	*	*	*	—	*	*	—	*	—	*	—	—
D. johnsonii A.Evans	NEO	—	*	*	—	*	—	*	—	—	—	—	—	—	—
D. pellucida (C.F.W.Meissn. ex Spreng.) Schiffn.	PAN	*	*	*	*	*	—	*	*	—	*	—	—	—	—
D. pluridentata Schäf.-Verw.	NEOC	—	—	*	—	*	—	—	—	—	—	—	—	—	—
D. rudolphiana Steph.	PAN	*	*	*	*	*	—	*	*	—	*	—	—	—	—
D. unidentata (Lehm. & Lindenb.) Schiffn.	NEO	—	*	*	*	*	—	*	—	—	—	—	—	—	—
Drepanolejeunea bidens (Prantl) A.Evans	NEO	—	—	*	*	*	—	*	—	—	—	—	—	—	—
D. orthophylla (Nees & Mont.) Bischl.	NEO	—	*	*	*	*	—	*	—	—	—	—	—	—	—
Fulfordianthus pterobryoides (Spruce) Gradst.	NEOC–Chocó	—	—	*	*	*	—	—	—	—	—	—	—	—	—
Harpalejeunea stricta (Lindenb. & Gottsche) Steph.	NEO	*	*	*	*	*	—	*	—	—	—	—	—	—	—
H. uncinata Steph.	NEO	—	—	*	*	*	—	*	—	—	—	—	—	—	—
Lejeunea adpressa Nees	AF–AM	*	—	*	—	*	*	*	*	—	—	—	—	—	—
L. angusta (Lehm. & Lindenb.) Mont	NEOC	—	*	—	*	*	—	—	—	—	—	—	—	—	—
L. aphanes Spruce	AF–AM	*	—	*	*	*	—	*	*	—	—	—	—	—	—
L. asperrima Spruce	NEO	—	*	*	*	*	—	*	—	—	—	—	—	—	—
L. bermudiana (A.Evans) R.M.Schust.	NEO	*	—	*	—	*	—	*	—	—	—	—	—	—	—
L. caulicalyx (Steph.) M.E.Reiner & Goda	NEO	—	—	*	*	*	—	*	—	—	—	—	—	—	—

TABLE 5.1. (*Continued*)

Species by division and family	Affinities	NA	MX	CA	NW	MS	SS	WI	AF	EU	AS	IN	PO	AU	NZ
		Worldwide distribution													
L. cerina (Lehm. & Lindenb.) Lehm. & Lindenb.	NEO	—	—	*	*	*	—	*	—	—	—	—	—	—	—
L. cristuliflora (Steph.) M.E.Reiner & Goda	NEOC	—	—	*	—	*	—	—	—	—	—	—	—	—	—
L. deplanata Nees	NEO	—	*	*	*	*	—	*	—	—	—	—	—	—	—
L. flava (Sw.) Nees	PAN	*	*	*	*	*	*	*	*	*	*	—	*	*	*
L. cf. *glaucescens* Gottsche	NEO	*	—	*	*	*	—	*	—	—	—	—	—	—	—
L. herminieri (Steph.) R.L.Zhu	NEO	—	*	*	*	*	—	*	—	—	—	—	—	—	—
L. laeta (Lehm. & Lindenb.) Lehm. & Lindenb.	NEO	—	*	*	*	*	*	*	—	—	—	—	—	—	—
L. laetevirens Nees & Mont.	NEO	*	—	*	*	*	*	*	—	—	—	—	—	—	—
L. cf. *lusoria* (Lindenb. et Gottsche) Steph.	NEOC	—	—	*	*	*	—	—	—	—	—	—	—	—	—
L. obtusangula Spruce	NEO	*	*	*	*	*	*	*	—	—	—	—	—	—	—
L. paucidentata (Steph.) Grolle	NEO	—	—	*	—	—	—	*	—	—	—	—	—	—	—
L. rotundifolia Mitt.	NEOC	—	—	*	*	*	—	—	—	—	—	—	—	—	—
L. sulphurea (Lehm. & Lindenb.) Spruce	NEO	—	—	*	*	*	—	*	—	—	—	—	—	—	—
L. venezuelana (R.M.Schust.) R.L.Zhu & W.Ye	NEOC	—	—	*	*	—	—	—	—	—	—	—	—	—	—
Lepidolejeunea cordifissa (Taylor) M.E.Reiner	NEOC	—	—	*	*	*	—	—	—	—	—	—	—	—	—
L. involuta (Gottsche) Grolle	NEO	—	*	*	*	*	—	*	—	—	—	—	—	—	—
Lopholejeunea nigricans (Lindenb.) Schiffn.	PAN	*	*	*	*	*	*	*	*	—	*	*	*	*	—
L. subfusca (Nees) Schiffn.	PAN	*	*	*	*	*	—	*	*	—	*	*	*	*	—
Marchesinia brachiata (Sw.) Schiffn.	AF–AM	—	*	*	*	*	*	*	*	—	—	—	—	—	—
M. robusta (Mitt.) Schiffn.	NEOC	—	—	*	*	*	—	—	—	—	—	—	—	—	—
Microlejeunea bullata (Taylor) Steph.	NEO	*	—	*	*	*	—	*	—	—	—	—	—	—	—
M. crenulifolia (Gottsche) Steph.	NEO	—	—	*	*	*	—	*	—	—	—	—	—	—	—
M. diversiloba (Spruce) Müll. Frib.	NEO	—	*	*	*	*	—	*	—	—	—	—	—	—	—
M. epiphylla Bischl.	NEO	*	—	*	*	*	—	*	—	—	—	—	—	—	—
Neurolejeunea breutelii (Gottsche) A.Evans	NEO	*	*	*	*	*	—	*	—	—	—	—	—	—	—
Odontolejeunea lunulata (F.Weber) Schiffn.	AF–AM	—	*	*	*	*	—	*	*	—	—	—	—	—	—
Otigoniolejeunea huctumalcensis (Lindenb. & Gottsche) Y.M.Wei, R.L.Zhu & Gradst.	NEO	—	*	*	*	*	—	*	—	—	—	—	—	—	—
Prionolejeunea cf. *aemula* (Gottsche) A.Evans	NEO	—	—	*	*	*	—	*	—	—	—	—	—	—	—
P. schlimiana (Gottsche) Steph.	NEOC	—	—	*	*	*	—	—	—	—	—	—	—	—	—
Pycnolejeunea decurviloba Steph.	NEOC	—	—	*	*	*	—	—	—	—	—	—	—	—	—
Schiffneriolejeunea polycarpa (Nees) Gradst.	PAN	—	*	*	*	*	*	*	*	—	*	*	—	—	—
Stictolejeunea squamata (Willd. ex F.Weber) Schiffn. Jong	NEO	—	*	*	*	*	*	*	—	—	—	—	—	—	—
Symbiezidium dentatum Herzog	NEOC–Chocó	—	—	*	*	*	—	—	—	—	—	—	—	—	—

(*Continued*)

TABLE 5.1. (*Continued*)

Species by division and family	Affinities	Worldwide distribution													
		NA	MX	CA	NW	MS	SS	WI	AF	EU	AS	IN	PO	AU	NZ
S. transversale (Sw.) Trevis. var. *hookerianum* (Gottsche, Lindenb. & Nees) Gradst. & J.Beek	NEO	—	—	*	*	*	—	*	—	—	—	—	—	—	—
Thysananthus auriculatus (Wilson & Hook.) Sukkharak & Gradst.	AF–AM	*	*	*	*	*	*	*	*	—	—	—	*	—	—
Lepicoleaceae (1/1/-/-)															
Lepicolea pruinosa (Taylor) Spruce	NEOC	—	*	*	*	*	*	—	—	—	—	—	—	—	—
Lepidoziaceae (7/11/-/-)															
Bazzania cuneistipula (Gottsche & Lindenb.) Trevis.	NEO	—	—	*	*	*	—	*	—	—	—	—	—	—	—
B. hookeri (Lindenb.) Trevis.	NEO	—	*	*	*	*	—	*	—	—	—	—	—	—	—
B. stolonifera (Sw.) Trevis.	NEO	—	*	*	*	*	—	*	—	—	—	—	—	—	—
Kurzia capillaris (Sw.) Grolle	AF–AM	—	*	*	*	*	*	*	*	—	—	—	—	—	—
Lepidozia cupressina (Sw.) Lindenb.	NEO-AF–EU	—	*	*	*	*	*	*	*	*	—	—	—	—	—
L. macrocolea Spruce	NEO	—	*	*	*	—	—	*	—	—	—	—	—	—	—
L. patens Lindenb.	NEO	—	—	*	*	*	—	*	—	—	—	—	—	—	—
Micropterygium cf. *trachyphyllum* Reimers	NEO	—	—	*	*	*	—	*	—	—	—	—	—	—	—
Mytilopsis albifrons Spruce	NEO	—	—	*	*	*	—	*	—	—	—	—	—	—	—
Telaranea nematodes (Gottsche ex Austin) M.Howe	NEO-AF–EU	—	*	*	*	*	*	*	*	*	—	—	—	—	—
Zoopsidella integrifolia (Spruce) R.M.Schust.	NEOC	—	—	*	*	*	—	—	—	—	—	—	—	—	—
Lophocoleaceae (5/8/-/-)															
Chiloscyphus quadridentatus (Spruce) J.J.Engel & R.M.Schust.	NEO	—	—	*	*	*	—	*	—	—	—	—	—	—	—
Cryptolophocolea connata (Sw.) L.Söderstr. & Váňa	NEO	—	*	*	*	*	—	*	—	—	—	—	—	—	—
Heteroscyphus marginatus (Steph.) Fulford	NEOC	—	—	*	*	*	—	—	—	—	—	—	—	—	—
Leptoscyphus gibbosus (Taylor) Mitt.	NEO	—	—	*	*	*	—	*	—	—	—	—	—	—	—
L. porphyrius (Nees) Grolle	NEO	—	—	*	*	*	—	*	—	—	—	—	—	—	—
L. trapezoides (Mont.) L.Söderstr.	NEO	—	*	*	*	*	*	*	—	—	—	—	—	—	—
Lophocolea liebmanniana Gottsche	NEO	—	*	*	*	*	—	*	—	—	—	—	—	—	—
L. muricata (Lehm.) Nees	PAN	*	*	*	*	*	*	*	*	—	*	*	*	—	—
Marchantiaceae (1/2/-/-)															
Marchantia chenopoda L.	NEO	—	*	*	*	*	*	*	—	—	—	—	—	—	—
M. polymorpha L.	SUBCOS	*	*	*	*	*	*	*	—	*	*	—	—	—	—
Metzgeriaceae (1/6/-/-)															
Metzgeria albinea Spruce	AF–AM	—	*	*	*	*	*	*	*	—	—	—	—	—	—
M. attenuata Steph.	AF–AM	—	—	*	*	*	—	*	*	—	—	—	—	—	—
M. ciliata Raddi	PAN	—	*	*	*	*	*	*	*	—	*	—	*	*	*
M. conjugata Lindb.	PAN	*	*	*	*	*	—	*	—	*	*	—	—	*	—
M. leptoneura Spruce	PAN	*	*	*	*	*	—	*	*	*	*	—	*	*	*
M. procera Mitt.	NEO	—	—	*	*	*	—	*	—	—	—	—	—	—	—

TABLE 5.1. (*Continued*)

Species by division and family	Affinities	Worldwide distribution													
		NA	MX	CA	NW	MS	SS	WI	AF	EU	AS	IN	PO	AU	NZ
Monocleaceae (1/1/1/-)															
Monoclea gottschei Lindb. subsp. *gottschei*	NEO	—	*	*	*	*	*	*	—	—	—	—	—	—	—
Pallaviciniaceae (1/3/-/-)															
Symphyogyna aspera Steph. ex F.A.McCormick	NEO	—	*	*	*	*	*	*	—	—	—	—	—	—	—
S. brasiliensis Nees	AF–AM	—	—	*	*	*	—	*	*	—	—	—	—	—	—
S. brongniartii Mont.	NEO	—	—	*	*	*	—	*	—	—	—	—	—	—	—
Plagiochilaceae (1/15/-/1)															
Plagiochila adianthoides (Sw.) Lindenb.	NEO	—	*	*	*	*	*	*	—	—	—	—	—	—	—
P. aerea Taylor	NEO	—	*	*	*	*	—	*	—	—	—	—	—	—	—
P. bifaria (Sw.) Lindenb.	NEO-AF–EU	—	*	*	*	*	—	*	*	*	—	—	—	—	—
P. cristata (Sw.) Lindenb.	NEO	—	—	*	*	*	—	*	—	—	—	—	—	—	—
P. disticha (Lehm. & Lindenb.) Lehm. & Lindenb.	NEO	—	—	*	*	*	—	*	—	—	—	—	—	—	—
P. gymnocalycina (Lehm. & Lindenb.) Mont. & Nees	NEO	—	*	*	—	*	—	*	—	—	—	—	—	—	—
P. laetevirens Lindenb.	NEOC	—	—	*	*	*	—	—	—	—	—	—	—	—	—
P. patula (Sw.) Nees & Mont. ex Lindenb.	NEO	*	—	*	*	*	—	*	—	—	—	—	—	—	—
P. raddiana Lindenb.	NEO	*	*	*	*	*	—	*	—	—	—	—	—	—	—
P. rudischusteri H.Rob.	NEOC–Chocó	—	—	*	*	—	—	—	—	—	—	—	—	—	—
P. rutilans Lindenb.	NEO	—	*	*	*	*	*	*	—	—	—	—	—	—	—
P. rutilans var. *moritziana* (Lindenb. & Gottsche ex Hampe) Heinrichs	NEO	—	—	*	*	*	—	*	—	—	—	—	—	—	—
P. salazariae Inoue	NEO-PMA	—	—	*	—	—	—	—	—	—	—	—	—	—	—
P. simplex (Sw.) Lindenb.	NEO	—	—	*	*	*	—	*	—	—	—	—	—	—	—
P. subplana Lindenb.	NEO-AS	—	*	*	*	*	—	*	—	—	*	—	—	—	—
P. superba (Nees ex Spreng.) Mont. & Nees	NEO	—	*	*	*	*	—	*	—	—	—	—	—	—	—
Radulaceae (1/6/-/-)															
Radula episcia Spruce	NEOC	—	—	*	*	*	*	—	—	—	—	—	—	—	—
R. fendleri Gottsche ex Steph.	NEO	—	—	*	*	*	—	*	—	—	—	—	—	—	—
R. gottscheana Taylor	NEO	—	*	*	*	*	—	*	—	—	—	—	—	—	—
R. kegelii Gottsche ex Steph.	NEO	—	—	*	*	*	*	*	—	—	—	—	—	—	—
R. cf. *sinuata* Gottsche ex Steph.	NEOC	—	—	*	*	*	—	—	—	—	—	—	—	—	—
R. stenocalyx Mont.	PAN	—	—	*	*	*	—	*	*	—	*	—	—	—	—
Scapaniaceae (1/1/-/-)															
Scapania portoricensis Hampe & Gottsche	NEO	—	*	*	*	*	—	*	—	—	—	—	—	—	—
Trichocoleaceae (1/4/-/-)															
Leiomitra flaccida Spruce	NEO	—	*	*	*	*	—	*	—	—	—	—	—	—	—
L. paraphyllina Spruce	NEO	—	*	*	*	*	—	*	—	—	—	—	—	—	—
L. sprucei (Steph) T.Katagiri	NEO	—	—	*	*	*	—	*	—	—	—	—	—	—	—
L. tomentosa (Sw.) Lindb.	NEO	—	*	*	*	*	—	*	—	—	—	—	—	—	—

(*Continued*)

TABLE 5.1. (*Continued*)

		Worldwide distribution													
Species by division and family	**Affinities**	**NA**	**MX**	**CA**	**NW**	**MS**	**SS**	**WI**	**AF**	**EU**	**AS**	**IN**	**PO**	**AU**	**NZ**
MOSSES (BRYOPHYTA)															
Bartramiaceae (3/5/-/-)															
Breutelia tomentosa (Sw. ex Brid.) A.Jaeger	AF–AM	—	*	*	*	*	—	*	*	—	—	—	—	—	—
Leiomela bartramioides (Hook.) Paris	PAN	—	*	*	*	*	—	*	*	—	*	—	—	—	—
Philonotis elongata (Dism.) H.A.Crum & Steere	NEO	—	*	*	*	*	*	*	—	—	—	—	—	—	—
P. sphaericarpa (Hedw.) Brid.	NEO	*	*	*	*	*	*	*	—	—	—	—	—	—	—
P. uncinata (Schwägr.) Brid.	NEO	*	*	*	*	*	—	*	—	—	—	—	—	—	—
Brachytheciaceae (2/2/-/-)															
Eurhynchium cf. *clinocarpum* (Taylor) Paris	NEO	—	*	*	*	*	—	*	—	—	—	—	—	—	—
Rhynchostegium scariosum (Taylor) A.Jaeger	NEO	—	*	*	*	*	—	*	—	—	—	—	—	—	—
Bryaceae (4/9/-/-)															
Anomobryum conicum (Hornsch.) Broth.	NEO	—	*	*	*	*	—	—	—	—	—	—	*	—	—
A. julaceum (Schrad. ex G.Gaertn., B. Mey. & Scherb.) Schimp.	SUBCOS	*	—	*	*	*	*	—	*	*	*	*	—	—	—
Brachymenium columbicum (De Not.) Broth.	NEO	—	*	*	*	*	—	*	—	—	—	—	—	—	—
B. speciosum (Hook. & Wilson) Steere	NEO	*	—	*	*	*	—	*	—	—	—	—	—	—	—
Bryum apiculatum Schwägr.	PAN	*	*	*	*	*	*	*	*	*	*	*	*	*	—
B. argenteum Hedw.	SUBCOS	*	*	*	*	*	*	*	*	*	*	*	*	*	*
B. billarderii Schwägr.	SUBCOS	*	*	*	*	*	*	*	*	—	*	*	*	*	*
B. incrassatolimbatum Cardot	NEO-CAM	*	*	*	—	—	—	—	—	—	—	—	—	—	—
B. limbatum Müll. Hal.	NEO	—	*	*	*	*	*	*	—	—	—	—	—	—	—
Pohlia sp.	—	—	—	—	—	—	—	—	—	—	—	—	—	—	—
Calymperaceae (2/8/-/2)															
Calymperes nicaraguense Renauld & Cardot	NEO	—	*	*	*	*	—	*	—	—	—	—	—	—	—
Syrrhopodon circinatus (Brid.) Mitt.	NEO	—	*	*	*	*	—	*	—	—	—	—	—	—	—
S. hornschuchii Mart.	NEO	—	*	*	*	*	—	*	—	—	—	—	—	—	—
S. incompletus Schwägr.	AF–AM	*	*	*	*	*	—	*	*	—	—	—	—	—	—
S. incompletus var. *berteroanus* (Brid.) W.D.Reese	NEO	—	*	*	*	*	—	*	—	—	—	—	—	—	—
S. leprieurii Mont.	NEO	—	—	*	*	*	—	*	—	—	—	—	—	—	—
S. lycopodioides (Sw. ex Brid.) Müll. Hal.	NEO	—	*	*	*	*	—	*	—	—	—	—	—	—	—
S. parasiticus (Sw. ex Brid.) Besch.	PAN	*	*	*	*	*	*	*	*	—	*	—	—	*	—
S. prolifer Schwägr.	PAN	—	*	*	*	*	*	*	*	—	—	*	*	—	—
S. prolifer var. *cincinnatus* (Hampe) W.D.Reese	NEO	—	—	*	*	*	—	*	—	—	—	—	—	—	—
Daltoniaceae (2/2/-/-)															
Daltonia sp.	—	—	—	—	—	—	—	—	—	—	—	—	—	—	—
Leskeodon andicola (Spruce ex Mitt.) Broth.	NEO	—	*	*	*	*	—	*	—	—	—	—	—	—	—
L. cubensis (Mitt.) Thér.	NEO	—	*	*	*	*	—	*	—	—	—	—	—	—	—

TABLE 5.1. (*Continued*)

		Worldwide distribution													
Species by division and family	**Affinities**	**NA**	**MX**	**CA**	**NW**	**MS**	**SS**	**WI**	**AF**	**EU**	**AS**	**IN**	**PO**	**AU**	**NZ**
Dicranaceae (10/24/-/1)															
Bryohumbertia filifolia (Hornsch.) J.-P.Frahm	NEO	—	*	*	*	*	—	*	—	—	—	—	—	—	—
Campylopus arctocarpus (Hornsch.) Mitt.	AF–AM	*	*	*	*	*	*	*	*	—	—	—	—	—	—
C. asperifolius Mitt.	NEOC	—	—	*	*	*	—	—	—	—	—	—	—	—	—
C. atlanticus B.H.Allen	NEO-CAM	—	—	*	—	—	—	—	—	—	—	—	—	—	—
C. densicoma (Müll. Hal.) Paris	NEOC	—	—	*	*	*	*	—	—	—	—	—	—	—	—
C. flexuosus (Hedw.) Brid.	SUBCOS	*	*	*	*	*	—	*	*	*	*	*	—	*	*
C. fragilis (Brid.) Bruch & Schimp.	SUBCOS	*	*	*	*	*	*	*	*	*	*	*	—	—	—
C. savannarum (Müll. Hal.) Mitt.	AF–AM	—	*	*	*	*	—	*	*	—	—	—	—	—	—
Dicranella harrisii (Müll. Hal.) Broth.	NEO	—	—	*	—	*	—	*	—	—	—	—	—	—	—
D. hilariana (Mont.) Mitt.	NEO	*	*	*	*	*	—	*	—	—	—	—	—	—	—
Dicranodontium pulchroalare Broth.	NEOC	—	—	*	*	*	*	—	—	—	—	—	—	—	—
Dicranum flagellare Hedw.	SUBCOS	*	*	*	*	—	—	*	*	*	*	*	—	—	—
D. frigidum Müll. Hal.	NEO	—	*	*	*	*	—	*	—	—	—	—	—	—	—
Eucamptodontopsis brittoniae (E.B.Bartram) B.H.Allen	NEOC	—	—	*	*	—	—	—	—	—	—	—	—	—	—
E. brittoniae var. *mcphersonii* B.H.Allen	NEO-CAM	—	—	*	—	—	—	—	—	—	—	—	—	—	—
Holomitrium arboretum Mitt.	NEO	—	*	*	*	*	*	*	—	—	—	—	—	—	—
H. flexuosum Mitt.	NEO	—	—	*	*	*	—	—	—	—	—	—	—	—	—
H. longifolium Hampe	NEO	—	—	*	*	*	—	—	—	—	—	—	—	—	—
H. pulchellum Mitt.	NEO	—	*	*	*	*	—	*	—	—	—	—	—	—	—
H. sinuosum B.H.Allen	NEO	—	*	*	*	—	—	—	—	—	—	—	—	—	—
Leucoloma cruegerianum (Müll. Hal.) A.Jaeger	NEO	—	*	*	*	*	—	*	—	—	—	—	—	—	—
L. serrulatum Brid.	NEO	—	*	*	*	*	—	*	—	—	—	—	—	—	—
Microcampylopus leucogaster (Müll. Hal.) B.H.Allen	NEO	—	*	*	*	*	*	*	—	—	—	—	—	—	—
Schliephackea meteorioides (R.S.Williams) Broth.	NEO	—	—	*	*	*	—	—	—	—	—	—	—	—	—
Entodontaceae (1/1/-/-)															
Entodon hampeanus Müll. Hal.	NEO	*	*	*	*	*	—	—	—	—	—	—	—	—	—
Fissidentaceae (1/11/-/5)															
Fissidens anguste-limbatus Mitt. var. *anguste-limbatus*	NEOC	—	*	*	*	*	*	—	—	—	—	—	—	—	—
F. asplenioides Hedw.	PAN	—	*	*	*	*	*	*	*	—	*	*	—	*	*
F. bryoides Hedw.	NEO	—	*	*	*	*	*	*	—	—	—	—	—	—	—
F. crispus Mont.	SUBCOS	*	*	*	*	*	*	*	*	*	—	—	—	—	—
F. flaccidus Mitt.	PAN	—	*	*	*	*	*	*	*	—	*	—	—	*	—
F. guianensis Mont.	NEO	—	*	*	*	*	—	*	—	—	—	—	—	—	—
F. lagenarius Mitt. var. *lagenarius*	NEO	*	*	*	*	*	*	*	—	—	—	—	*	—	—

(*Continued*)

TABLE 5.1. (*Continued*)

		Worldwide distribution													
Species by division and family	**Affinities**	**NA**	**MX**	**CA**	**NW**	**MS**	**SS**	**WI**	**AF**	**EU**	**AS**	**IN**	**PO**	**AU**	**NZ**
F. pellucidus Hornsch. var. *pellucidus*	PAN	*	*	*	*	*	*	*	*	—	*	—	—	*	*
F. polypodioides Hedw.	NEO	*	*	*	*	*	—	*	—	—	—	—	—	—	—
F. weirii Mitt.	AF–AM	—	*	*	*	*	—	*	*	—	—	—	—	—	—
F. weirii var. *hemicraspedophyllus* (Cardot) Pursell	NEO	—	*	*	*	*	—	*	—	—	—	—	—	—	—
F. zollingeri Mont.	SUBCOS	*	*	*	*	*	*	*	*	—	*	—	—	*	—
Funariaceae (1/1/-/-)															
Funaria hygrometrica Hedw.	SUBCOS	*	*	*	*	*	*	—	*	*	*	—	*	*	*
Hookeriaceae (15/37/-/-)															
Actinodontium sprucei (Mitt.) A.Jaeger	NEO	—	*	*	*	*	—	*	—	—	—	—	—	—	—
Amblytropis hispidula (Mitt.) Broth.	NEOC	—	—	*	*	*	—	—	—	—	—	—	—	—	—
Brymela angustiretis (E.B.Bartram) B.H.Allen	NEO-CAM	—	—	*	—	—	—	—	—	—	—	—	—	—	—
B. crosbyi (B.H.Allen) B.H.Allen	NEO-CAM	—	—	*	—	—	—	—	—	—	—	—	—	—	—
B. obtusifolia (E.B.Bartram) W.R.Buck	NEOC	—	—	*	*	—	—	—	—	—	—	—	—	—	—
Callicostella callicostelloides (Herzog & Thér.) B.H.Allen	NEO	—	*	*	—	—	—	*	—	—	—	—	—	—	—
C. oerstediana (Müll. Hal.) A.Jaeger	NEOC	—	—	*	*	*	—	—	—	—	—	—	—	—	—
C. pallida (Hornsch.) Ångstr.	NEO	*	*	*	*	*	*	*	—	—	—	—	—	—	—
Crossomitrium epiphyllum (Mitt.) Müll. Hal.	NEO	—	—	*	*	*	—	*	—	—	—	—	—	—	—
C. patrisiae (Brid.) Müll. Hal.	NEO	—	—	*	*	*	—	*	—	—	—	—	—	—	—
Cyclodictyon albicans (Hedw.) Kuntze	NEO	—	*	*	*	*	*	*	—	—	—	—	—	—	—
C. roridum (Hampe) Kuntze	NEO	—	—	*	*	*	—	*	—	—	—	—	—	—	—
C. rubrisetum (Mitt.) Kuntze	NEOC	—	*	*	*	*	—	—	—	—	—	—	—	—	—
C. subtortifolium (E.B.Bartram) W.R.Buck	NEO	—	*	*	*	*	—	*	—	—	—	—	—	—	—
C. varians (Sull.) Kuntze	NEO	*	*	*	*	*	—	*	—	—	—	—	—	—	—
Hemiragis aurea (Lam. ex Brid.) Kindb.	NEO	—	—	*	*	*	—	*	—	—	—	—	—	—	—
Hookeria acutifolia Hook. & Grev.	PAN	*	*	*	*	*	—	*	—	—	*	*	*	—	—
Hypnella diversifolia (Mitt.) A.Jaeger	NEO	—	—	*	*	*	—	*	—	—	—	—	—	—	—
H. pallescens (Hook.) A.Jaeger	NEO	—	—	*	*	*	—	*	—	—	—	—	—	—	—
Lepidopilidium divaricatum (Dozy & Molk.) Broth.	AF–AM	—	*	*	*	*	*	*	*	—	—	—	—	—	—
Lepidopilum amplirete (Sull.) Mitt.	NEO	*	*	*	*	—	—	*	—	—	—	—	—	—	—
L. brevipes Mitt.	NEO	—	*	*	*	*	—	*	—	—	—	—	—	—	—
L. diaphanum (Sw. ex Hedw.) Mitt.	NEO	—	—	*	*	*	—	*	—	—	—	—	—	—	—
L. longifolium Hampe	NEO	—	*	*	*	*	—	*	—	—	—	—	—	—	—
L. muelleri (Hampe) Hampe	NEO	—	*	*	*	*	*	*	—	—	—	—	—	—	—
L. permarginatum R.S.Williams	NEOC	—	—	*	*	—	—	—	—	—	—	—	—	—	—
L. polytrichoides (Hedw.) Brid.	NEO	*	*	*	*	*	—	*	—	—	—	—	—	—	—
L. scabrisetum (Schwägr.) Steere	NEO	—	*	*	*	*	—	*	—	—	—	—	—	—	—
L. tortifolium Mitt.	NEO	—	*	*	*	*	—	*	—	—	—	—	—	—	—
Pilotrichidium callicostatum (Müll. Hal.) A.Jaeger	NEO	—	*	*	*	*	—	*	—	—	—	—	—	—	—

TABLE 5.1. (*Continued*)

Species by division and family	Affinities	Worldwide distribution													
		NA	MX	CA	NW	MS	SS	WI	AF	EU	AS	IN	PO	AU	NZ
Stenodictyon wrightii (Sull. & Lesq.) Crosby	NEOC	—	—	*	*	*	—	—	—	—	—	—	—	—	—
Thamniopsis cruegeriana (Müll. Hal.) W.R.Buck	NEOC	—	*	*	*	*	*	—	—	—	—	—	—	—	—
T. pendula (Hook.) M.Fleisch.	NEOC	—	—	*	*	*	—	—	—	—	—	—	—	—	—
T. undata (Hedw.) W.R.Buck	NEO	—	*	*	*	*	*	*	—	—	—	—	—	—	—
Trachyxiphium guadalupense (Brid.) W.R.Buck	NEO	—	*	*	*	*	—	*	—	—	—	—	—	—	—
T. subfalcatum (Hampe) W.R.Buck	NEOC	—	*	*	*	*	—	—	—	—	—	—	—	—	—
T. variabile (Hornsch. ex Mitt.) W.R.Buck	NEOC	—	—	*	*	*	—	—	—	—	—	—	—	—	—
Hypnaceae (11/14/-/1)															
Caribaeohypnum polypterum (Mitt.) Ando & Higuchi	NEO	—	*	*	*	*	—	*	—	—	—	—	—	—	—
Chryso-hypnum diminutivum (Hampe) W.R.Buck	NEO	*	*	*	*	*	*	*	—	—	—	—	—	—	—
Ctenidium malacodes Mitt.	NEO	—	*	*	*	*	—	*	—	—	—	—	—	—	—
Ectropothecium leptochaeton (Schwägr.) W.R.Buck	NEO	—	*	*	*	*	*	*	—	—	—	—	—	—	—
Mittenothamnium langsdorffii (Hook.) Cardot	NEO	—	—	*	*	*	—	*	—	—	—	—	—	—	—
M. reduncum (Schimp. ex Mitt.) Ochyra	NEOC	—	—	*	*	*	—	—	—	—	—	—	—	—	—
M. reptans (Hedw.) Cardot	PAN	—	*	*	*	*	*	*	*	—	—	*	—	—	—
M. substriatum (Mitt.) Cardot	NEO	—	—	*	*	*	—	*	—	—	—	—	—	—	—
Phyllodon truncatulus (Müll. Hal.) W.R.Buck	NEO	—	—	*	*	*	—	*	—	—	—	—	—	—	—
Puiggariopsis aurifolia (Mitt.) M.Menzel	NEOC	—	*	*	*	*	—	—	—	—	—	—	—	—	—
Pylaisiadelpha tenuirostris (Bruch & Schimp. ex Sull.) W.R.Buck	SUBCOS	*	*	*	—	*	—	*	—	—	*	—	—	—	*
Rhacopilopsis trinitensis (Müll. Hal.) E.Britton & Dixon	PAN	—	*	*	*	*	—	*	*	—	—	*	—	—	—
Taxiphyllum laevifolium (Mitt.) W.R.Buck	NEO	—	*	*	*	*	—	*	—	—	—	—	—	—	—
Vesicularia vesicularis (Schwägr.) Broth. var. *rutilans* (Brid.) W.R.Buck	NEO	*	*	*	*	*	*	*	—	—	—	—	—	—	—
Hypopterygiaceae (1/1/-/-)															
Hypopterygium tamarisci (Sw.) Brid. ex Müll. Hal.	PAN	*	*	*	*	*	*	*	*	—	*	*	—	*	*
Lembophyllaceae (2/2/-/-)															
Lepyrodontopsis trichophylla (Sw. ex Hedw.) Broth.	NEO	—	—	*	*	*	—	*	—	—	—	—	—	—	—
Pilotrichella flexilis (Hedw.) Ångstr.	PAN	—	*	*	*	*	—	*	*	—	—	*	—	—	—
Leskeaceae (2/5/-/-)															
Pelekium minutulum (Hedw.) Touw	NEO-AF–EU	*	*	*	*	*	*	*	*	*	—	—	—	—	—
Thuidium carantae (Müll. Hal.) A.Jaeger	NEOC	—	—	*	*	*	—	—	—	—	—	—	—	—	—
T. delicatulum (Hedw.) Schimp.	SUBCOS	*	*	*	*	*	*	*	—	*	*	—	—	—	—
T. pseudoprotensum (Müll. Hal.) Mitt.	NEO	—	—	*	*	*	—	*	—	—	—	—	—	—	—
T. tomentosum Schimp.	NEO	—	*	*	*	*	*	*	—	—	—	—	—	—	—

(*Continued*)

TABLE 5.1. (*Continued*)

		Worldwide distribution													
Species by division and family	**Affinities**	**NA**	**MX**	**CA**	**NW**	**MS**	**SS**	**WI**	**AF**	**EU**	**AS**	**IN**	**PO**	**AU**	**NZ**
Leucobryaceae (1/5/-/-)															
Leucobryum antillarum Schimp. ex Besch.	NEO	*	*	*	*	*	—	*	—	—	—	—	—	—	—
L. crispum Müll. Hal.	NEO	—	*	*	*	*	—	*	—	—	—	—	—	—	—
L. giganteum Müll. Hal.	NEO	—	*	*	*	*	—	*	—	—	—	—	—	—	—
L. martianum (Hornsch.) Hampe ex Müll. Hal.	NEO	—	*	*	*	*	—	*	—	—	—	—	—	—	—
L. polakowskyi (Müll. Hal. ex Besch.) Cardot	NEO	—	*	*	*	*	—	*	—	—	—	—	—	—	—
Leucomiaceae (2/2/-/-)															
Leucomium strumosum (Hornsch.) Mitt.	PAN	—	*	*	*	*	—	*	*	—	*	*	*	—	—
Rhynchostegiopsis flexuosa (Sull.) Müll. Hal.	NEO	—	*	*	*	—	—	*	—	—	—	—	—	—	—
Meteoriaceae (6/9/-/-)															
Barbella sp.	—	—	—	—	—	—	—	—	—	—	—	—	—	—	—
Meteoridium remotifolium (Müll. Hal.) Manuel	NEO	—	*	*	*	*	*	*	—	—	—	—	—	—	—
Meteorium deppei (Hornsch. ex Müll. Hal.) Mitt.	NEO	—	*	*	*	*	*	*	—	—	—	—	—	—	—
Squamidium isocladum (Renauld & Cardot) Broth.	NEO	—	*	*	*	*	—	*	—	—	—	—	—	—	—
S. leucotrichum (Taylor) Broth.	NEO	—	*	*	*	*	—	*	—	—	—	—	—	—	—
S. livens (Schwägr.) Broth.	NEO	—	—	*	*	*	—	*	—	—	—	—	—	—	—
Toloxis imponderosa (Taylor) W.R.Buck	NEO	—	*	*	*	*	—	*	—	—	—	—	—	—	—
Zelometeorium ambiguum (Hornsch.) Manuel	AF–AM	—	—	*	—	*	*	—	*	—	—	—	—	—	—
Z. patulum (Hedw.) Manuel	NEO	*	*	*	*	*	*	*	—	—	—	—	—	—	—
Z. recurvifolium (Hornsch. in Mart.) Manuel	NEOC	—	—	*	*	*	—	—	—	—	—	—	—	—	—
Mniaceae (3/3/-/-)															
Plagiomnium rhynchophorum (Hook.) T.J.Kop.	SUBCOS	*	*	*	*	*	*	*	*	—	*	*	—	—	—
Pyrrhobryum spiniforme (Hedw.) Mitt.	PAN	*	*	*	*	*	*	*	*	—	*	*	—	*	*
Rhizogonium lindigii (Hampe) Mitt.	NEO	—	*	*	*	*	*	*	—	—	—	—	—	—	—
Neckeraceae (7/12/-/-)															
Homaliodendron piniforme (Brid.) Enroth	PAN	—	*	*	*	*	—	*	*	—	—	*	—	—	—
Isodrepanium lentulum (Wilson) E.Britton	NEO	—	*	*	*	*	—	*	—	—	—	—	—	—	—
Neckeropsis undulata (Hedw.) Reichardt	NEO	*	*	*	*	*	*	*	—	—	—	—	—	—	—
Orthostichella rigida (Müll. Hal.) B.H.Allen & Magill	PAN	—	*	*	*	*	—	—	*	—	—	*	—	—	—
O. versicolor (Müll. Hal.) B.H.Allen & W.R.Buck	PAN	—	*	*	*	*	*	*	*	—	—	*	—	—	—
Porotrichodendron lindigii (Hampe) W.R.Buck	NEO	—	*	*	*	*	—	*	—	—	—	—	—	—	—
Porotrichum brevifolium E.B.Bartram	NEO-CAM	—	—	*	—	—	—	—	—	—	—	—	—	—	—
P. korthalsianum (Dozy & Molk.) Mitt.	NEO	—	*	*	*	*	—	*	—	—	—	—	—	—	—
P. longirostre (Hook.) Mitt.	NEO	—	*	*	*	*	—	*	—	—	—	—	—	—	—

TABLE 5.1. (*Continued*)

Species by division and family	Affinities	Worldwide distribution													
		NA	MX	CA	NW	MS	SS	WI	AF	EU	AS	IN	PO	AU	NZ
P. mutabile Hampe	NEO	—	*	*	*	*	—	*	—	—	—	—	—	—	—
P. substriatum (Hampe) Mitt.	AF–AM	—	*	*	*	*	—	*	*	—	—	—	—	—	—
Thamnomalia glabella (Hedw.) S.Olsson, Enroth & D.Quandt	NEO	—	*	*	*	*	—	*	—	—	—	—	—	—	—
Octoblepharaceae (1/3/-/-)															
Octoblepharum cocuiense Mitt.	NEO	—	*	*	*	*	—	*	—	—	—	—	—	—	—
O. erectifolium Mitt. ex R.S.Williams	NEO	—	*	*	*	*	—	*	—	—	—	—	—	—	—
O. pulvinatum (Dozy & Molk.) Mitt.	NEO	—	*	*	*	*	—	*	—	—	—	—	—	—	—
Orthotrichaceae (3/18/-/-)															
Groutiella apiculata (Hook.) H.A.Crum & Steere	NEO	—	*	*	*	*	—	*	—	—	—	—	—	—	—
G. chimborazensis (Spruce ex Mitt.) Florsch.	NEO	—	*	*	*	*	—	*	—	—	—	—	—	—	—
G. mucronifolia (Hook. & Grev.) H.A.Crum & Steere	NEO	—	*	*	*	*	—	*	—	—	—	—	—	—	—
G. tomentosa (Hornsch.) Wijk & Margad.	PAN	*	*	*	*	*	—	*	*	—	*	*	—	*	—
Macromitrium cirrosum (Hedw.) Brid.	NEO	—	*	*	*	*	—	*	—	—	—	—	—	—	—
M. echinatum B.H.Allen	NEOC	—	—	*	*	*	—	—	—	—	—	—	—	—	—
M. fuscoaureum E.B.Bartram	NEOC	—	—	*	*	*	—	—	—	—	—	—	—	—	—
M. guatemalense Müll. Hal.	NEO	—	*	*	*	*	—	*	—	—	—	—	—	—	—
M. leprieurii Mont.	NEO	—	—	*	*	—	—	*	—	—	—	—	—	—	—
M. longifolium (Hook.) Brid.	NEO	—	*	*	*	*	—	*	—	—	—	—	—	—	—
M. mcphersonii B.H.Allen	NEO-CAM	—	—	*	—	—	—	—	—	—	—	—	—	—	—
M. punctatum (Hook. & Grev.) Brid.	NEO	—	*	*	*	*	—	*	—	—	—	—	—	—	—
M. scoparium Mitt.	NEO	—	—	*	*	*	—	*	—	—	—	—	—	—	—
M. standleyi E.B.Bartram	NEOC	—	—	*	*	—	—	—	—	—	—	—	—	—	—
M. subcirrhosum Müll. Hal.	NEO	—	—	*	*	—	—	*	—	—	—	—	—	—	—
M. ulophyllum Mitt.	NEOC	—	—	*	*	*	—	—	—	—	—	—	—	—	—
Schlotheimia jamesonii (Arnott) Brid.	NEO	—	*	*	*	*	—	*	—	—	—	—	—	—	—
S. rugifolia (Arn.) Brid.	NEO	*	*	*	*	*	*	*	—	—	—	—	—	—	—
Phyllogoniaceae (1/2/-/-)															
Phyllogonium fulgens (Hedw.) Brid.	NEO	—	*	*	*	*	—	*	—	—	—	—	—	—	—
P. viscosum (P.Beauv.) Mitt.	AF–AM	—	*	*	*	*	—	*	*	—	—	—	—	—	—
Pilotrichaceae (1/5/-/-)															
Pilotrichum andersonii Crosby	NEOC	—	—	*	*	*	—	—	—	—	—	—	—	—	—
P. bipinnatum (Schwägr.) Brid.	NEO	—	—	*	*	*	—	*	—	—	—	—	—	—	—
P. evanescens (Müll. Hal.) Crosby	NEO	—	*	*	*	*	—	*	—	—	—	—	—	—	—
P. fendleri Müll. Hal.	NEO	—	*	*	*	*	—	*	—	—	—	—	—	—	—
P. ramosissimum Mitt.	NEOC	—	*	*	*	*	—	—	—	—	—	—	—	—	—
Polytrichaceae (4/7/-/-)															
Atrichum oerstedianum (Müll. Hal.) Mitt.	NEO	—	*	*	*	*	—	*	—	—	—	—	—	—	—
A. polycarpum (Müll. Hal.) Mitt.	NEO	—	—	*	*	*	*	*	—	—	—	—	—	—	—

(*Continued*)

TABLE 5.1. (*Continued*)

		Worldwide distribution													
Species by division and family	Affinities	NA	MX	CA	NW	MS	SS	WI	AF	EU	AS	IN	PO	AU	NZ
Pogonatum campylocarpum (Müll. Hal.) Mitt.	NEO	—	*	*	*	*	*	*	—	—	—	—	—	—	—
P. procerum (Lindb.) Schimp.	NEO	—	*	*	—	*	—	*	—	—	—	—	—	—	—
P. tortile (Sw.) Brid.	NEO	—	*	*	*	*	—	*	—	—	—	—	—	—	—
Polytrichum juniperinum Hedw.	SUBCOS	*	*	*	*	*	*	*	*	*	*	—	—	*	*
Steereobryon subulirostrum (Schimp. ex Besch.) G.L.Sm.	NEO	—	*	*	*	*	—	*	—	—	—	—	—	—	—
Pottiaceae (1/1/-/-)															
Hyophila involuta (Hook.) A.Jaeger	SUBCOS	*	*	*	*	*	*	*	*	*	*	*	—	*	—
Pterobryaceae (6/7/-/-)															
Orthostichidium quadrangulare (Schwägr.) B.H.Allen & Magill	NEO	—	*	*	*	*	—	*	—	—	—	—	—	—	—
Orthostichopsis tetragona (Sw. ex Hedw.) Broth.	NEO	—	*	*	*	*	—	*	—	—	—	—	—	—	—
Pireella angustifolia (Müll. Hal.) Arzeni	NEO	—	*	*	*	*	—	*	—	—	—	—	—	—	—
P. pycnothallodes (Müll. Hal.) M.Fleisch.	NEO	—	*	*	—	—	—	*	—	—	—	—	—	—	—
Pterobryon densum Hornsch.	NEO	—	*	*	*	*	*	*	—	—	—	—	—	—	—
Pterobryopsis mexicana (Renauld & Cardot) M.Fleisch.	NEOC	—	*	*	—	—	—	—	—	—	—	—	—	—	—
Renauldia paradoxica B.H.Allen	NEOC	—	—	*	*	—	—	—	—	—	—	—	—	—	—
Pylaisiadelphaceae (2/2/-/-)															
Isopterygium tenerum (Sw.) Mitt.	SUBCOS	*	*	*	*	*	*	*	*	*	*	—	—	*	—
Taxithelium planum (Brid.) Mitt.	AF–AM	*	*	*	*	*	—	*	*	—	—	—	—	—	—
Racopilaceae (1/1/-/-)															
Racopilum tomentosum (Hedw.) Brid.	NEO	*	*	*	*	*	*	*	—	—	—	—	—	*	—
Sematophyllaceae (3/16/-/-)															
Acroporium caespitosum (Hedw.) W.R.Buck	NEO-AS	—	—	*	—	—	—	*	—	—	*	—	—	—	—
A. longirostre (Brid.) W.R.Buck	NEO	—	*	*	—	—	—	*	—	—	—	—	—	—	—
A. pungens (Hedw.) Broth.	PAN	—	*	*	*	*	—	*	*	—	*	—	—	—	—
Sematophyllum adnatum (Michx.) E.Britton	PAN	*	*	*	*	*	*	*	—	—	*	—	—	—	—
S. cochleatum (Broth.) Broth.	NEOC	—	—	*	*	*	—	—	—	—	—	—	—	—	—
S. cuspidiferum Mitt.	NEOC	—	*	*	*	*	—	—	—	—	—	—	—	—	—
S. galipense (Müll. Hal.) Mitt.	AF–AM	—	*	*	*	*	*	*	*	—	—	—	—	—	—
S. cf. *hampei* (Besch.) Broth.	NEO	—	*	*	*	—	—	*	—	—	—	—	—	—	—
S. marylandicum (Müll. Hal.) E.Britton	NEOC	*	*	*	—	—	—	—	—	—	—	—	—	—	—
S. squarrosum W.R.Buck	AF–AM	—	—	*	*	—	—	—	*	—	—	—	—	—	—
S. subpinnatum (Brid.) E.Britton	PAN	*	*	*	*	*	*	*	*	—	*	*	*	*	—
S. cf. *subsimplex* (Hedw.) Mitt.	AF–AM	—	*	*	*	*	—	*	*	—	—	—	—	—	—
S. swartzii (Schwägr.) W.H.Welch & H.A.Crum	NEO	—	*	*	*	*	—	*	—	—	—	—	—	—	—
Trichosteleum fluviale (Mitt.) A.Jaeger	AF–AM	—	*	*	*	*	—	—	*	—	—	—	—	—	—
T. papillosum (Hornsch.) A.Jaeger	AF–AM	—	*	*	*	*	—	—	*	—	—	—	—	—	—
T. sentosum (Sull.) A.Jaeger	NEO	—	—	*	—	*	—	*	—	—	—	—	—	—	—

TABLE 5.2. Summary of families, genera, species, subspecies and varieties of bryophytes reported for Fortuna and their geographic affinities. NEO = Neotropical; AF–AM = affinities with Africa; PAN = pantropical; SUBCOS = subcosmopolitan.

Family	Genera	Species	Subspecies	Variety	NEO	AF–AM	PAN	SUBCOS
HORNWORTS (ANTHOCEROTOPHYTA)								
Anthocerotaceae	1	2			2			
Dendrocerotaceae	3	5			3		2	
Notothyladaceae	1	1						1
Subtotals	**5**	**8**			**5**		**2**	**1**
LIVERWORTS (MARCHANTIOPHYTA)								
Acrobolbaceae	1	1				1		
Aneuraceae	2	3			2			1
Balantiopsidaceae	2	2			2			
Calypogeiaceae	2	4			3	1		
Cephaloziaceae	3	3			2	1		
Dumortieraceae	1	1					1	
Frullaniaceae	1	12		1	11		1	
Herbertaceae	1	3			2	1		
Lejeuneaceae	26	87	1	2	66	8	13	
Lepicoleaceae	1	1			1			
Lepidoziaceae	7	11			10	1		
Lophocoleaceae	5	8			7		1	
Marchantiaceae	1	2			1			1
Metzgeriaceae	1	6			1	2	3	
Monocleaceae	1	1	1		1			
Pallaviciniaceae	1	3			2	1		
Plagiochilaceae	1	15		1	16			
Radulaceae	1	6			5		1	
Scapaniaceae	1	1			1			
Trichocoleaceae	1	4			4			
Subtotals	**60**	**174**	**2**	**4**	**137**	**16**	**20**	**2**
MOSSES (BRYOPHYTA)								
Bartramiaceae	3	5			3	1	1	
Brachytheciaceae	2	2			2			
Bryaceae	4	9			5		1	3
Calymperaceae	2	8		2	7	1	2	
Daltoniaceae	2	2			2			
Dicranaceae	10	23		1	19	2		3
Entodontaceae	1	1			1			
Fissidentaceae	1	11		4	6	1	3	2
Funariaceae	1	1						1
Hookeriaceae	15	37			35	1	1	
Hypnaceae	11	14		1	11		2	1
Hypopterygiaceae	1	1					1	

(*Continued*)

TABLE 5.2. (*Continued*)

Family	Genera	Species	Subspecies	Variety	NEO	AF–AM	PAN	SUBCOS
Lembophyllaceae	2	2			1		1	
Leskeaceae	2	5			4			1
Leucobryaceae	1	5			5			
Leucomiaceae	2	2			1		1	
Meteoriaceae	6	9			8	1		
Mniaceae	3	3			1		1	1
Neckeraceae	7	12			8	1	3	
Octoblepharaceae	1	3			3			
Orthotrichaceae	3	18			17		1	
Phyllogoniaceae	1	2			1	1		
Pilotrichaceae	1	5			5			
Polytrichaceae	4	7			6			1
Pottiaceae	1	1						1
Pterobryaceae	6	7			7			
Pylaisiadelphaceae	2	2				1		1
Racopilaceae	1	1			1			
Sematophyllaceae	3	16			8	5	3	
Subtotals	**99**	**214**	**0**	**8**	**167**	**15**	**21**	**15**
Totals for all taxa	**164**	**396**	**2**	**12**	**309**	**31**	**43**	**18**

brittoniae, *E. brittoniae* var. *mcphersonii* (Allen, 1994), and *Macromitrium mcphersonii* (Allen, 2002). Most bryophytes collected in Fortuna are epiphytes on trunks, branches, and leaves and epipetric on rocks. A small number grow in soil, particularly thallose liverworts, some hornworts, and, for mosses, some members of Bartramiaceae, Dicranaceae, Fissidentaceae, Polytrichaceae, and Sematophyllaceae. According to Gradstein (1995a), montane forests have approximately 2.5 times as many bryophyte families as lowland forests have. Fortuna has twice the number of bryophyte families (52) that the lowland forest of BCI has (26). It is interesting to note that the state of Rhode Island in the United States, approximately 1.6 times the size of the Reserva Forestal Fortuna, has only 118 species of bryophytes (97 mosses and 21 liverworts; Miller and Buck, 2008).

Bryophytes inventories in tropical montane forests have shown that liverworts species outnumber those found in the lowland forests (Richards, 1984; Gradstein et al., 1989; Dauphin, 1999; Horwath et al., 2019), although less than previously assumed if canopy flora is fully accounted (Gradstein et al., 1990; Gradstein, 1995b; Gehrig-Downie et al., 2013). In Fortuna, the highest number of mosses compared to liverworts may indicate that the forests in the areas studied comprise many more species from the humid lowlands that extend their ranges into the humid premontane to montane forest and fewer species characteristic of high montane forests that descend to this humid forest. However, this difference may also be related, at least in part, to collecting sites that are generally close to roads (accessibility), in secondary forests, in disturbed forests, and at the foothills of the mountains, with less intense collections in the primary forests at higher elevations and the canopy areas.

In the account that follows, only the main families in richness of species are discussed for each bryophyte division found in Fortuna.

Hornworts (Anthocerotophyta)

The hornworts (Anthocerotophyta) are the smallest taxon in number of species (8) and genera (5) of the bryophytes of Fortuna (Tables 5.1 and 5.2, Figures 5.3 and 5.4). The hornworts are a lineage of Paleozoic origin (Villarreal et al., 2015) with approximately 215 species worldwide (Söderström et al., 2016). Although with few species compared to other bryophytes, the hornworts are very important morphologically and genetically for understanding the transition of plants to land. Unlike all other land plants, the hornworts are the only terrestrial taxon with species having a pyrenoid (carbon-concentrating organelle) in their chloroplasts, as occurs in green algae. Most hornworts grow in soil or rocks in very moist to wet environments, near creeks, waterfalls, and some even in indoor and outdoor gardens (e.g., *Notothylas*). Collections of Fortuna were from rocks near rivers or creeks or from soil in the forest floor. The paucity of species of hornworts in Fortuna is related, in part, to difficulties in identifying sterile

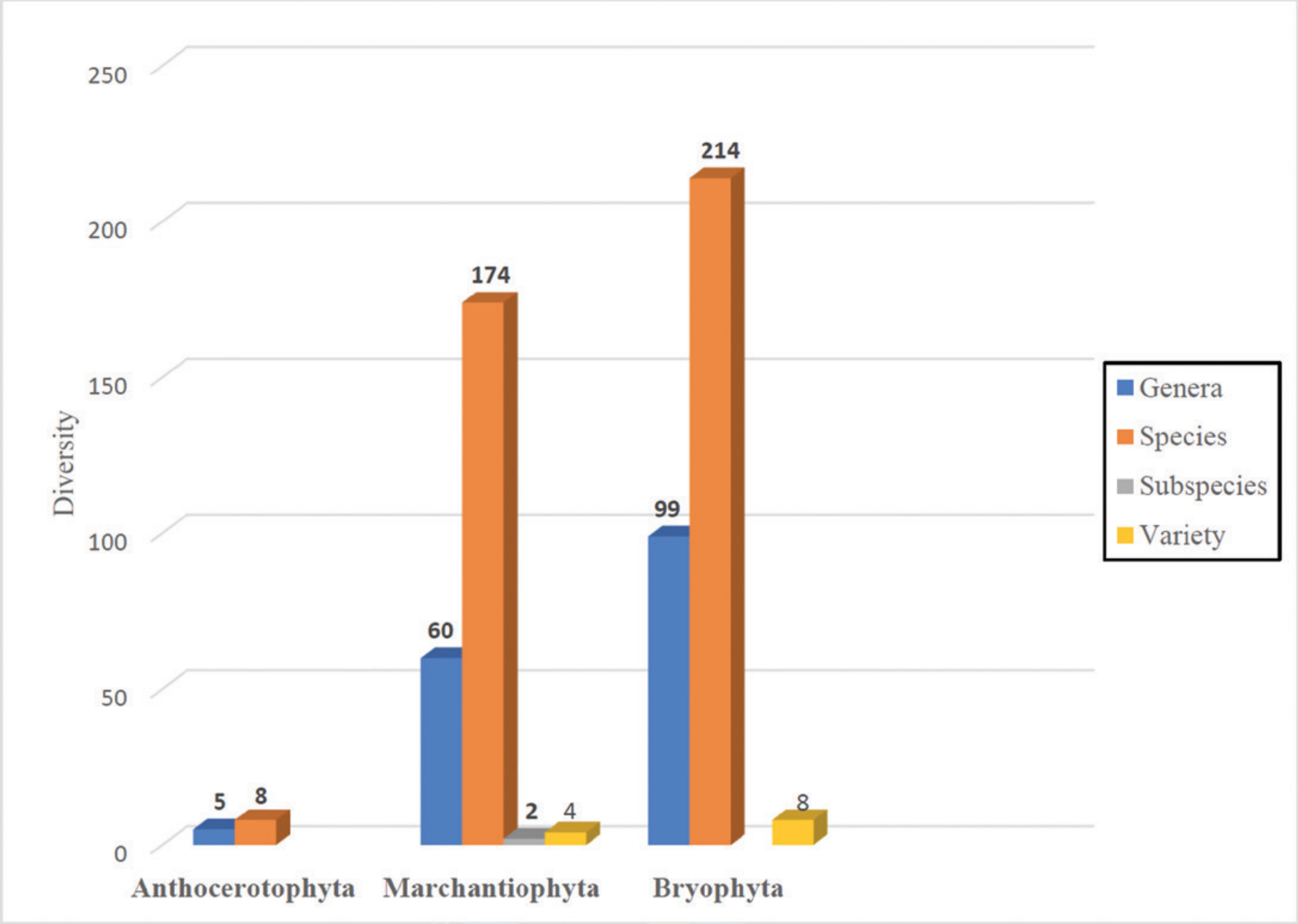

FIGURE 5.3. Number of genera, species, subspecies and varieties of the hornworts (Anthocerotophyta), liverworts (Marchantiophyta) and mosses (Bryophyta) of Fortuna.

dried material and to the small number of fertile collections. Of the eight species found in Fortuna, only two, *Dendroceros crispatus* and *Phaeoceros laevis*, have a wide distribution in tropical and temperate regions (Tables 5.1 and 5.2). The Neotropical *Anthoceros lamellatus*, *A. tuberculatus*, and *Phaeoceros laevis*, like some mosses (*Atrichum*, *Dicranum*, and *Pelekium*), are ancestrally derived from northern temperate (Laurasian) elements that radiated south into temperate and tropical areas of the Americas. Unlike these species, the ancestral region for *Nothoceros*, *Phaeomegaceros* (Villarreal et al., 2015), some liverworts such as *Monoclea* (Gradstein et al., 1996), and the mosses *Macromitrium* (Vitt and Ramsay, 1985a, 1985b), *Campylopus* (Frahm, 1988), and *Leucoloma* (La Farge-England, 1998) are considered to be southern temperate (Gondwana) with northern dispersal to tropical America. Of the hornworts reported for Fortuna, only the genus *Nothoceros* has been found in Chucantí (J. Gudiño, personal communication). None of the species of hornworts of Fortuna is reported for BCI.

Liverworts (Marchantiophyta)

Liverworts (Marchantiophyta; Figure 5.4) include 174 species, 60 genera, 2 subspecies, and 4 varieties (Figure 5.3). Important families in richness of species are the Lejeuneaceae (87 spp., 26 gen.), Plagiochilaceae (15 spp., 1 gen.), Frullaniaceae (12 spp., 1 gen.), and Lepidoziaceae (11 spp., 7 gen.) (Tables 5.1 and 5.2). All of these are leafy liverworts. Nevertheless, the diversity of leafy liverworts is incomplete. Many samples of the large tropical family Lejeuneaceae and other liverwort families still need to be identified. Thalloid liverworts are comparatively few in number of species and genera and include the families Metzgeriaceae (6 spp., 1 gen.), Aneuraceae (3 spp., 2 gen.), Pallaviciniaceae (3 spp.,

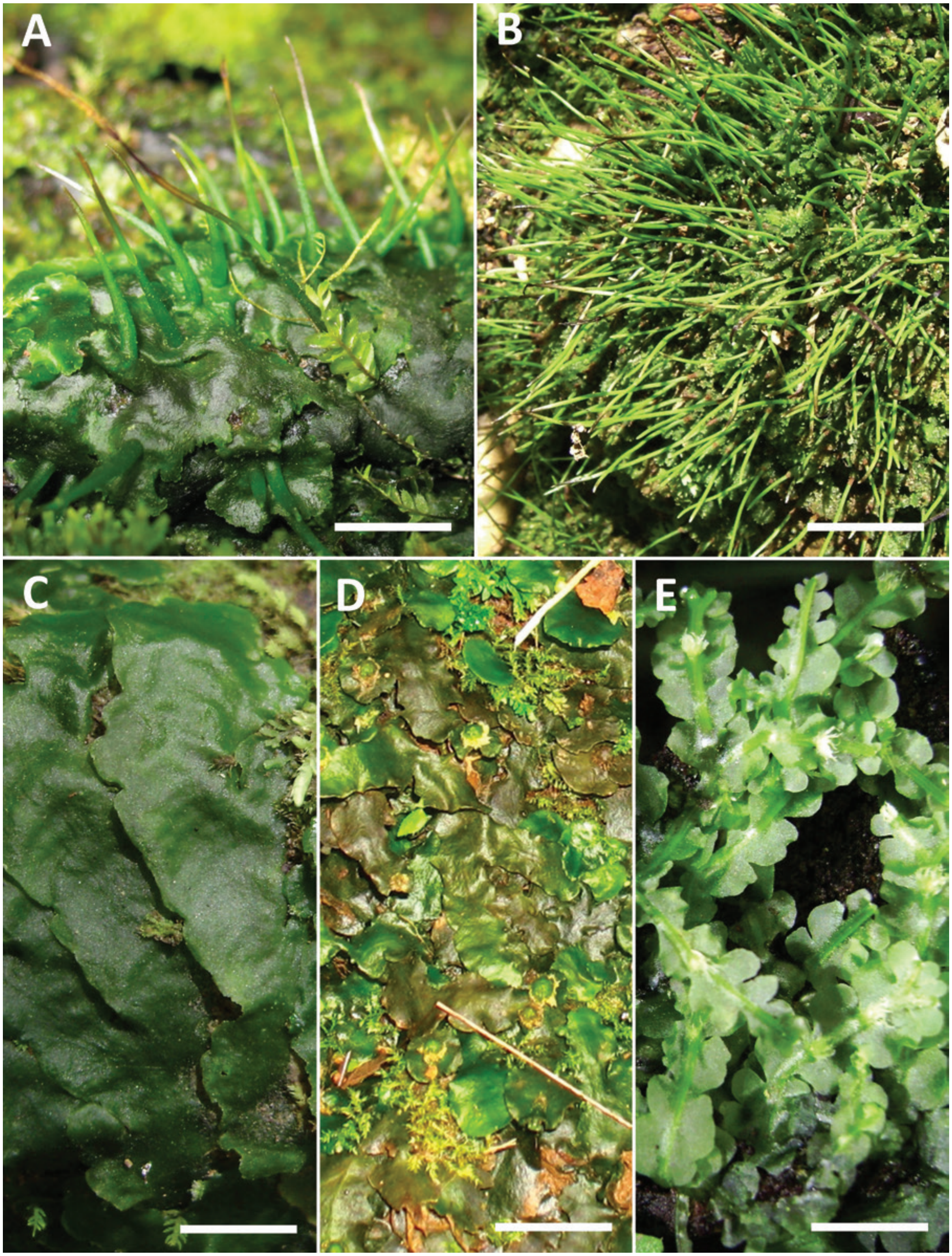

FIGURE 5.4. HORNWORTS: (A) *Nothoceros vincentianus* (Lehm. & Lindenb.) J. C. Villarreal (scale bar = 7.1 mm); (B) *Anthoceros tuberculatus* Lehm. & Lindenb. (scale bar = 15.8 mm). THALLOID LIVERWORTS: (C) *Aneura pinguis* (L.) Dumort. (scale bar = 8.6 mm); (D) *Dumortiera hirsuta* (Sw.) Nees (scale bar = 26.5 mm); (E) *Symphyogyna aspera* Steph. *ex* F. A. McCormick (scale bar = 5.2 mm).

1 gen.), Marchantiaceae (2 spp., 1 gen.), Dumortieraceae (1 sp., 1 gen.), and Monocleaceae (1 sp., 1 gen.) (Figure 5.3). Twenty-five species of liverworts are shared between the lowland forests of BCI and Fortuna (Salazar Allen et al., n.d.).

The Lejeuneaceae (Figure 5.5a–c) is one of the largest families of liverworts with 1,000 species and 68 currently accepted genera. The number of genera has been reduced on the basis of recent molecular studies (Gradstein, 2013a). It is the most important family in the lowland rain forests; more than three-quarters of the liverwort's species are members of this family (Gradstein et al., 2003). They inhabit many niches, tree trunks and branches, twigs, lianas, stones, boulders, and the surface of leaves (epiphylls) (Gradstein et al., 2003). Species diversity in *Lejeunea* accounts for 300 currently accepted species (Lee and Gradstein, 2013), but the precise number of species is unclear due to the unavailability of modern taxonomic studies (Heinrichs et al., 2013). Molecular phylogenetic studies have shown that *Lejeunea* is a pantropical genus with origins in the Neotropics. From the Neotropical lineages, there was a postcolonization into tropical and temperate regions (Heinrichs et al., 2013). In Fortuna, the most diverse genus in the family is *Lejeunea* with 20 species, that is, 23% of the species of the Lejeuneaceae.

The Lejeuneaceae accounts for ~70% of the lowland flora and ~20% to 45% of flora in montane forests (Gradstein, 1995a). In the lowland forest of BCI, the Lejeuneaceae accounts for ~39% of the bryoflora (Salazar Allen et al., n.d.), while in Fortuna, the family accounts for 22%. However, taking into account only the liverwort flora, the Lejeuneaceae represents 75.5% of the liverworts of BCI, while in Fortuna, it is 50%. A decrease in the diversity of Lejeuneaceae in submontane, montane, and subalpine forests has been reported in previous studies (Gradstein et al., 1989; Gradstein and Salazar Allen, 1992; Gradstein, 1995b, 2006; Horwath et al., 2019). This phenomenon probably can be explained by the reduced surface area in terms of habitats available in the mountains as compared to in the lowland forests (Aryanti and Gradstein, 2007) or to the sexuality and dispersal capacities of Lejeuneaceae. About two-thirds of the liverworts are dioicous (Vanderpoorten and Goffinet, 2009), but this varies in different genera, and only few have been studied (Heinrichs et al., 2013). Several authors have suggested that autoicous species have wider ranges than dioicous species (van Zanten and Pócs, 1981; Longton and Schuster, 1983); however, the importance of long-distance dispersal and monoicy for an epiphytic mode of life is still unclear for many taxa (Heinrich et al., 2013).

Common lowland Neotropical genera of Lejeuneaceae (Gradstein, 1995a) that are not present in Fortuna are *Acrolejeunea*, *Aphanolejeunea*, *Archilejeunea*, *Caudalejeunea*, *Leptolejeunea*, *Mastigolejeunea*, *Rectolejeunea*, *Thysananthus*, and *Trachylejeunea*. These genera plus *Lopholejeunea* and *Neurolejeunea* are absent or rare in the mountains (Gradstein, 1995a). Species of six of these genera have been found in BCI. In Fortuna, there are two species of *Lopholejeunea*; one of them, *L. subfusca*, is also known for BCI, while *L. nigricans* is a montane element (Gradstein, 1994). *Lopholejeunea subfusca* is a pioneer, xerotolerant species growing on bark in the high canopy, most common in lowland environments (Gradstein, 1994). Its presence in Fortuna (Quebrada Bonita; Table 5.3) may reflect its adaptation to grow in humid cool environments.

The Plagiochilaceae is also a predominant liverwort family in moist and very humid lowland to lower and montane forests. In Fortuna, *Plagiochila* is the only genus in this family (Figure 5.5d). It is considered monophyletic with the exclusion of *P. radiculosa*, which was transferred to a new genus (*Cryptoplagiochila* gen. nov.; Patzak et al., 2016). *Plagiochila* is the largest genus of liverworts (Inoue, 1984; Gradstein, 2001). Species of the genus are common from lowland to mountain forests and alpine regions (Gradstein, 2001). It is the most abundant and conspicuous bryophyte genus in montane cloud forests (Gradstein, 2001). Three of the 16 species of *Plagiochila* found in Fortuna occur in the lowland forests of BCI (*P. disticha*, *P. laetevirens*, and *P. raddiana*). Of the Neotropical species of *Plagiochila*, *P. bifaria* is the only species distributed in America, Africa, and southern Europe while *P. subplana* is known for the Americas (Heinrichs et al., 1999) and Asia (Pócs 1971; Bakalin and Nguyen, 2016). *Plagiochila rudischusteri* is a species that also occurs in the northern half of the Chocó biogeographical region (S. R. Gradstein, personal communication). *Plagiochila salazariae* (Inoue, 1989), described from a specimen from Fortuna, is the only species endemic to Fortuna and the second endemic liverwort for Panama. Nevertheless, after its description, it has not been revised on a worldwide basis; thus, it is unknown whether it can be found in other countries (Söderström, 2016).

The Frullaniaceae, like the Lejeuneaceae, is a very important epiphytic family in tropical rainforests. In Fortuna, *Frullania* is the only genus known for the family (Figure 5.5e). It is a large genus with 300 to 375 species. It includes nearly cosmopolitan species to narrow endemics (Hentschel et al., 2009). It is a predominantly epiphytic genus on bark of trees from mid-trunk to the canopy, branches, and twigs and is less frequently found on rocks and living leaves (Schuster, 1992; Gradstein, 2001). Many species of *Frullania* occur not only in moist but also in rather dry forests (Hentschel et al., 2009). There is a high concentration of species in the tropics; the humid montane areas adjacent to the tropics; the warm temperate regions; and geologically "old" regions, particularly those that have not been recently glaciated or submerged (Schuster, 1992). Most species of *Frullania* from Fortuna (e.g., *Frullania caulisequa*, also reported for BCI) have a wide elevation range from lowlands to submontane and montane forests (Salazar Allen et al., n.d.). Of the 12 species and one variety found in Fortuna, 11 are Neotropical and only one is pantropical in distribution (*F. ericoides*) (Tables 5.1 and 5.2). Gradstein (2006) considered *F. brasiliensis*, *F. caulisequa*, and *F. kunzei* to be canopy specialists. Molecular studies suggest that the distribution patterns within *Frullania* may reflect dispersal events rather than Gondwanan vicariance (Hentschel et al., 2009). A similar scenario was proposed for the genus *Plagiochila* (Heinrichs et al., 2006).

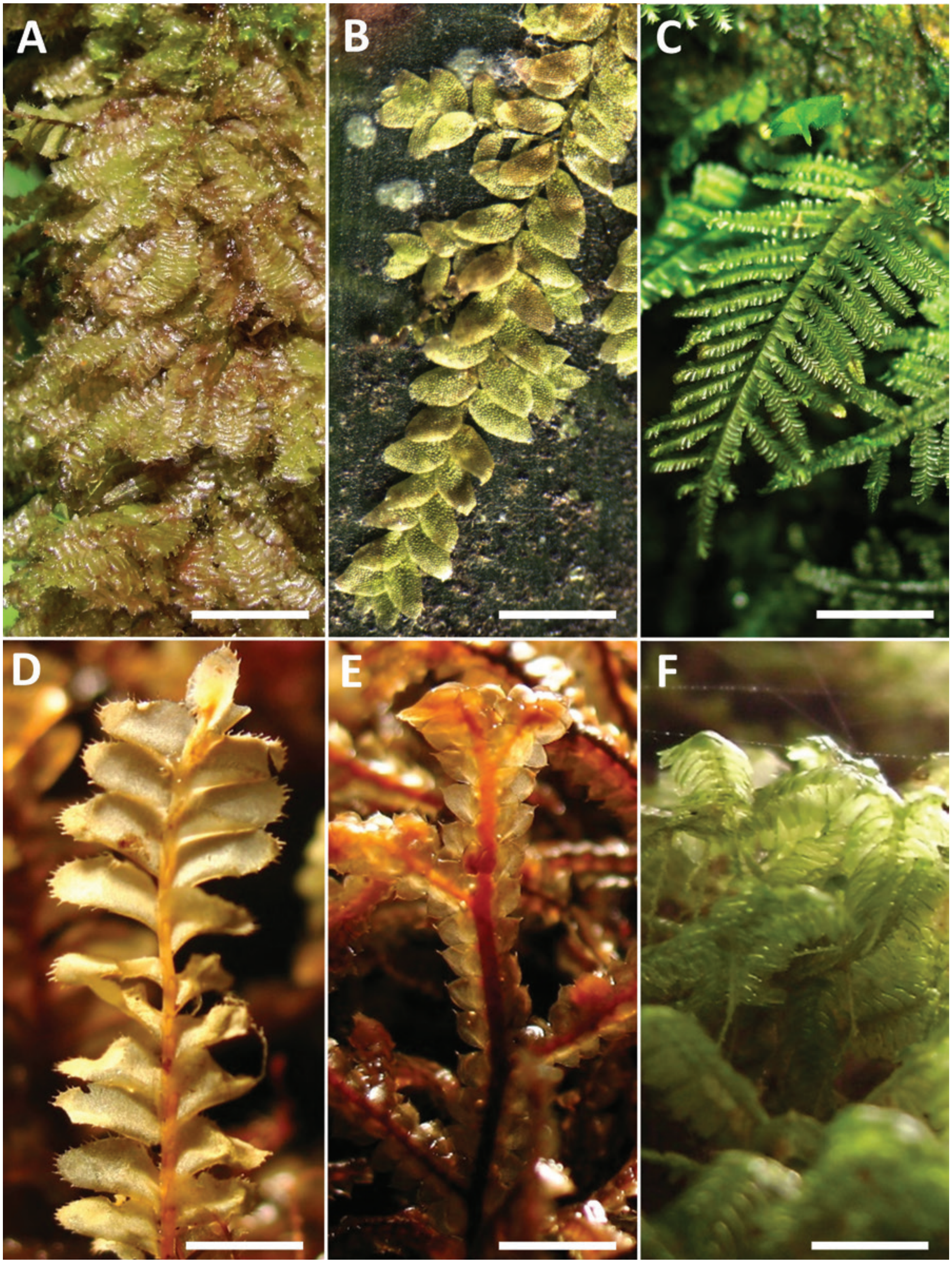

FIGURE 5.5. Foliose liverworts: (A) *Cyclolejeunea convexistipa* (Lehm. & Lindenb.) A. Evans (scale bar = 5.4 mm). (B) *Cololejeunea subcardiocarpa* Tixier (scale bar = 0.7 mm). (C) *Fulfordianthus pterobryoides* (Spruce) Gradst. (scale bar = 9.7 mm). (D) *Plagiochila adianthoides* (Sw.) Lindenb. (scale bar = 2.5 mm). (E) *Frullania bicornistipula* Spruce (scale bar = 2.3 mm). (F) *Bazzania stolonifera* (Sw.) Trevis (scale bar = 4.5 mm).

The Lepidoziaceae, Lophocoleaceae, Marchantiaceae, Monocleaceae, Pallaviciniaceae, Scapaniaceae, and Trichocoleaceae of Fortuna are composed of species characteristic of the lower montane to montane forests (Gradstein, 1995a). Species of these families have not been reported for BCI, and only one species of Lepidoziaceae (*Zoopsidella antillana*) unknown for Fortuna was reported for Bahía Honda. In the Lepidoziaceae, all species of *Bazzania* are Neotropical, occurring from Mexico to Central America, northwest to mid–South America and the Caribbean, while other genera of the family have wider distributions (Table 5.1, Figure 5.5f). Gradstein (2017) suggested that the scarcity of intercontinental ranges of *Bazzania* may have to do with the absence of asexual propagules suitable for long-distance dispersal, the rarity of sexual reproduction, and thus spore production. This may apply also to other liverworts with restricted distribution.

The Metzgeriaceae are thalloid liverworts represented in America by species of the genus *Metzgeria* (Costa, 2008). The family has a cosmopolitan distribution with a concentration of species in the Neotropics. The species grow in mountain coastal and continental areas (Costa, 2008). Of the six species of *Metzgeria* reported for Fortuna, only one, *M. procera*, is neotropical. *Metzgeria albinea* and *M. attenuata* are AF–AM species, while *M. ciliata*, *M. conjugata* and *M. leptoneura* are pantropical (Table 5.1).

In the Radulaceae, there are species that grow in lowlands to lower and montane forests, such as *R. kegelii*. One species, *R. episcia*, is reported for Central America and southern South America. It is unknown for the Caribbean (Table 5.1). None of the species of *Radula* from Fortuna have been found in BCI.

Mosses (Bryophyta)

There is a predominance of mosses (Bryophyta) in the bryoflora of Fortuna, with 214 species and 8 varieties (Figure 5.3). The most speciose families are the Hookeriaceae (37 spp., 15 gen.), Dicranaceae (23 spp., 10 gen.), Orthotrichaceae (18 spp., 3 gen.), Sematophyllaceae (16 spp., 3 gen.), and Neckeraceae (12 spp., 7 gen.) (Tables 5.1 and 5.2). Most species of mosses are Neotropical except for some widely distributed (SUBCOS) species, such as *Bryum argenteum*, *Fissidens crispus*, *F. flaccidus*, *Funaria hygrometrica*, *Hyophila involuta*, and *Polytrichum juniperinum*, among them (Tables 5.1 and 5.2). A variety of the Dicranaceae, *Eucamptodontopsis brittoniae* var. *mcphersonii* and a species of Orthotrichaceae, *Macromitrium mcphersonii*, were described as new to science from collections from Fortuna (Allen 1994, 2002). Due to space and time constraint, the five most diverse families are discussed with only few comments on additional selected families.

The Hookeriaceae is a family of pantropical and Southern Hemisphere elements with approximately 200 species in the Neotropics (Churchill and Salazar Allen, 2001) (Table 5.1). Members of this family grow in very moist lowland to lower and montane forests. They can be recognized by the double costa (nerve) in their leaf, although there are few species (e.g., *Hookeria*) that lack it. All genera in Fortuna are Neotropical except for the American, African, and Asiatic *Lepidopilidium* (Churchill and Salazar Allen, 2001; Atwood, 2015). *Hookeria acutifolia*, the only species of *Hookeria* in the Neotropics, is widespread in the Americas and Asia. It is a genus with northern temperate affinities (Churchill and Salazar Allen, 2001). Two species of the Neotropical *Brymela*, *B. angustiretis* and *B. crosbyi*, have a restricted distribution known only for Central America (NEOCAM), while *B. obtusifolia* is distributed in Central America and northern South America, and all three are unrecorded for the Caribbean (NEOC) (Table 5.1). These species grow in very humid to wet lowland to lower and montane forests (Churchill and Salazar Allen, 2001; Allen, 2010). Although *Callicostella* is a pantropical genus (Churchill and Salazar Allen, 2001), all species in Fortuna are Neotropical. *Callicostella callicostelloides* and *C. pallida*, known for Fortuna, have also been recorded from the humid lowland forests of BCI (Salazar Allen et al., 1991), Bahía Honda (Salazar Allen and Chung, 2005), and Chucantí (Darién) (Gudiño and Salazar Allen, 2017). Similarly, *Lepidopilum polytrichoides*, *L. scabrisetum*, and *Pilotrichidium callicostatum*, found in Fortuna, are reported from those lowland areas. These species grow from lowlands to approximately 1,000 m. *Crossomitrium* is a Neotropical genus widespread in continental and Caribbean areas (Churchill and Salazar Allen, 2001). It is one of the few epiphyllous mosses, although it can also grow on twigs, lianas, tree branches, and trunks (Allen, 2010). The genus *Cyclodictyon*, although widely distributed in tropical Africa, is best represented in the Neotropics (Buck, 1998). Of the five species that occur in Fortuna, only *C. rubrisetum* is continental (NEOC) in distribution and does not occur in the Caribbean (Table 5.1). *Hemiragis* is a monospecific genus (*H. aurea*) distributed in Central America, western and northern South America, and the Caribbean (Buck, 1998; Allen, 2018) (Table 5.1). *Lepidopilum* is primarily a Neotropical genus with few species in mountain habitats of Africa (Churchill and Salazar Allen, 2001) (Figure 5.6a). The species in this genus are mainly epiphytic on tree trunks, branches, lianas, and bamboo nodes from near sea level to 3,700 m (Churchill and Salazar Allen, 2001). Species of *Amblytropis*, *Brymela* (not common), *Stenodictyon*, and *Thamniopsis* were considered by Gradstein and Raeymaekers (2000) as indicators of undisturbed submontane rainforests from 500 to 1,500 m. Likewise, species of *Holomitrium* (usually those in the canopy), *Macromitrium* (widespread), *Meteoridium remotifolium*, *Mittenothamnium*, *Toloxis*, *Pilotrichella flexilis*, and species of *Porotrichum* grow frequently in undisturbed montane rainforest (1,500–3,000 m). Gradstein and Raeymaekers (2000) considered these species indicators of this type of forest.

The Dicranaceae is one of the largest families in tropical America (Churchill and Salazar Allen, 2001) and the largest in number of species in Central America (Allen, 1990). It is the main component of the open montane and alpine environments (Churchill and Salazar Allen, 2001), although it has species that can grow in lowland forests, among them, for example,

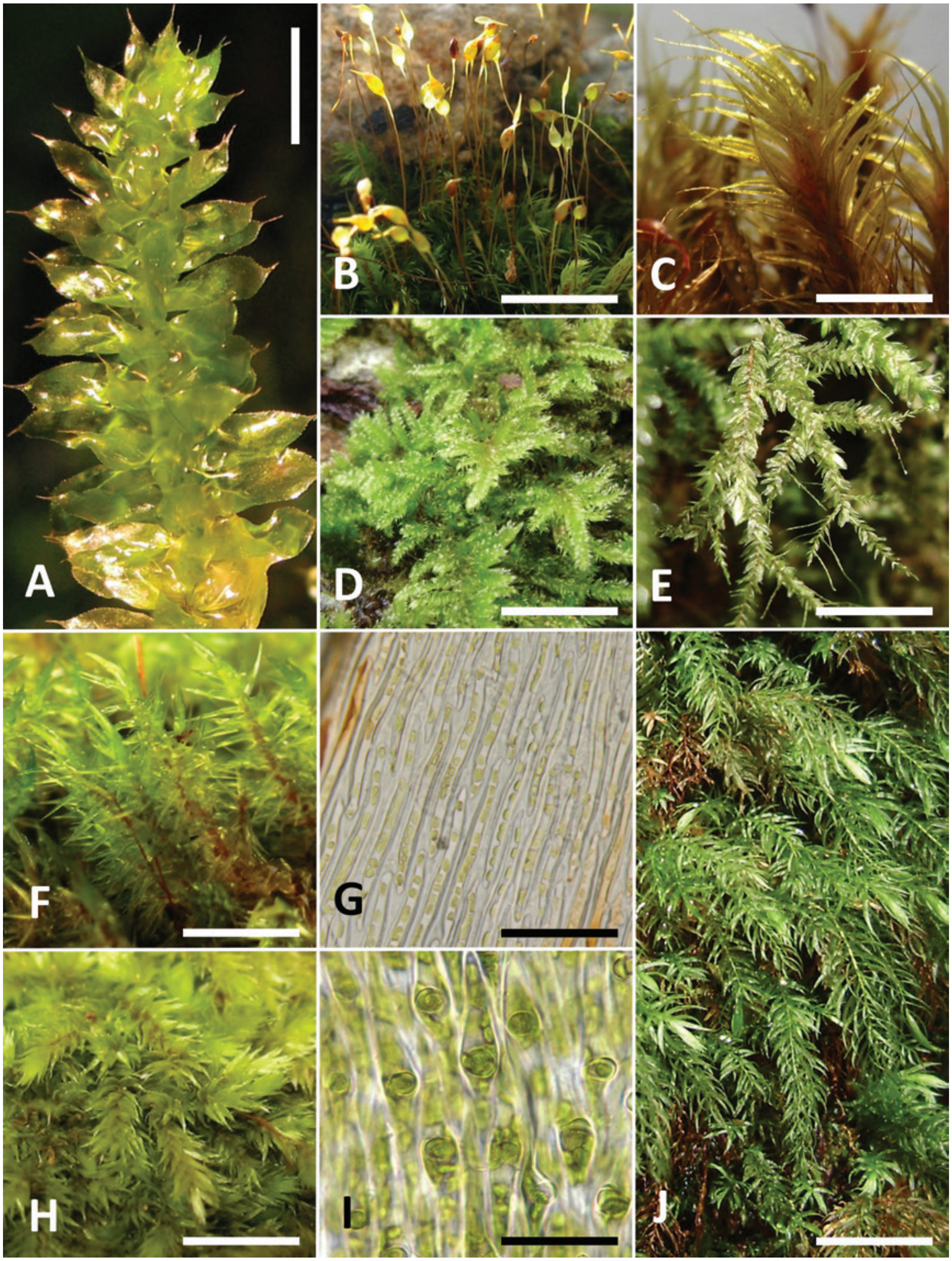

FIGURE 5.6. Mosses: (A) *Lepidopilum polytrichoides* (Hedw.) Brid. (scale bar = 3.8 mm). (B) *Dicranella hilariana* (Mont.) Mitt. (scale bar = 4.7 mm). (C) *Macromitrium fuscoaureum* E. B. Bartram (scale bar = 4.9 mm). (D) *Ectropothecium leptochaeton* (Schwägr.) W. R. Buck (scale bar = 10.8 mm). (E) *Porotrichum mutabile* Hampe (scale bar = 7.1 mm). (F) *Acroporium pungens* (Hedw.) Broth. (scale bar = 3.3 mm). (G) apical leaf cells (scale bar = 35.8 µm). (H) *Trichosteleum fluviale* (Mitt.) A. Jaeger (scale bar = 3.8 mm). (I) unipapillose apical leaf cells (scale bar = 44.6 µm). (J) *Pyrrhobryum spiniforme* (Hedw.) Mitt. (scale bar = 1.8 mm).

Dicranella hilariana, *D. harrisii*, *Leucoloma cruegerianum*, and *Holomitrium arboreum* (Allen, 1994) (Figure 5.6b). They grow epiphytic on tree trunks, branches, in soil, and on rocks. Of the 24 species in Fortuna, 19 are Neotropical, 3 are subcosmopolitan, and two are African–American elements (Tables 5.1 and 5.2). *Campylopus* is a genus of tropical and warm temperate areas and one of the largest genera of mosses (Frahm, 1990, 2002). It is assumed that the genus is of Gondwanan origin with recent diversification (Frahm, 1988, 1990). Taxa of this genus have a wide ecological range in habitats that extend from the subantarctic to the subarctic and from sea level to more than 4,500 m. All species prefer acidic substrates (Frahm, 1990). Five species of the Neotropical *Campylopus* and *Schliephackea* are distributed in the American continent (NEOC) and do not occur in the Caribbean (Table 5.1). The species of *Campylopus* from Fortuna include two subcosmopolitan species, two African–American species, and four Neotropicals, with one of them, *C. atlanticus*, restricted to Central America (NEO-CAM) (Allen, 1994) (Table 5.1). The type specimen of this species was collected near Fortuna Dam, in Bocas del Toro province (Allen, 1994). In the genus *Dicranum*, according to Allen (1994), the two species known for Fortuna, *D. flagellare* and *D. frigidum*, represent two phytogeographic groups. The first one belongs to the Northern Hemisphere and the second to the Southern Hemisphere group. Both species grow in cloud forests of premontane to montane forests at higher elevations, from 1,000 m to 3,700 m (Allen, 1994). In Fortuna, *D. flagellare* was collected between 1,000 and 1,200 m at the northwest camping site (Site 15, Figure 5.1, Table 5.3), and *D. frigidum* was collected at 1,670 to 2,300 m at Cerro Hornito (Site 6, Figure 5.1, Table 5.3). Two species of *Leucoloma*, *L. cruegerianum* and *L. serrulatum*, are Neotropical from Mexico to northern South America and the Caribbean. None of the Neotropical species occur in Africa (Table 5.1). The genus *Leucoloma* is pantropical with its center of diversity in Madagascar

TABLE 5.3. Species distribution in the main collecting sites of Fortuna. Sites: 1 = Continental Divide, Trail Palo Seco (900–1,200 m); 2 = Quebrada Bonita (920–1,150 m); 3 = Quebrada Arena (900–1,100 m); 4 = trail to Quebrada Las Mellizas; 5 = Cerro Pata de Macho (1,700–1,800 m); 6 = Cerro Hornito (1,670–2,300 m); 7 = Valle de Hornito (1,300–1,700 m); 8 = trail along Río Hornito (1,200 m); 9 = Quijada del Diablo (1,200–1,600 m); 10 = Quebrada Mono (1,100–1,300 m); 11 = Quebrada Alemán (1,200–1,400 m); 12 = Institute of Hydraulic Resources and Electricity's plant nursery (1,100 m); 13 = at mouth of Quebrada Samudio (1,100–1,280 m); 14 = SW of camping site, from Finca Pittí to foothills of Cerro Fortuna (1,000–1,270 m); 15 = NW of camping site (1,000–1,200 m); 16 = foothills of Cerro Pinola (1,280–2,000 m); 17 = NE of camping site (900–1,200 m). Asterisk (*) = presence of the species; dash (—) = absence of the species.

	Main collecting sites																
Species by division and family	1	2	3	4	5	6	7	8	9	10	11	12	13	14	15	16	17
HORNWORTS (ANTHOCEROTOPHYTA)																	
Anthocerotaceae																	
Anthoceros lamellatus	—	—	*	—	—	—	—	—	—	—	—	—	—	—	—	—	—
A. tuberculatus	*	*	—	—	—	—	—	—	—	—	—	—	—	—	—	—	—
Dendrocerotaceae																	
Dendroceros crispatus	*	—	*	—	—	—	—	—	—	—	—	—	—	—	—	—	—
D. crispus	—	*	—	—	—	—	—	—	—	—	—	—	—	—	—	—	—
Nothoceros schizophyllus	—	*	—	—	—	—	—	—	—	—	—	—	—	—	—	—	—
N. vincentianus	—	*	—	—	—	—	—	—	*	—	—	—	—	—	—	—	*
Phaeomegaceros fimbriatus	—	—	—	—	—	—	—	—	—	—	—	*	—	—	—	—	—
Notothyladaceae																	
Phaeoceros laevis	—	—	—	—	—	—	—	—	—	—	—	—	—	—	—	—	*
LIVERWORTS (MARCHANTIOPHYTA)																	
Acrobolbaceae																	
Acrobolbus laxus	—	—	—	—	—	—	*	—	—	—	—	—	—	—	—	—	—
Aneuraceae																	
Aneura pinguis	—	—	—	—	—	—	—	—	—	—	—	—	—	—	—	—	*
Riccardia fucoidea	—	*	—	—	—	—	—	—	—	—	—	—	—	*	*	—	*
R. poeppigiana	—	*	—	—	—	—	—	—	—	—	—	—	—	—	—	—	—

(*Continued*)

TABLE 5.3. (*Continued*)

Species by division and family	Main collecting sites 1	2	3	4	5	6	7	8	9	10	11	12	13	14	15	16	17
Balantiopsidaceae																	
Isotachis multiceps	—	—	—	—	—	—	—	—	—	—	—	—	—	—	—	—	*
Neesioscyphus argillaceus	—	—	—	—	—	—	—	—	—	—	—	—	—	—	—	—	—
Calypogeiaceae																	
Calypogeia peruviana	—	*	—	—	—	—	—	—	—	—	—	—	—	—	*	*	*
C. rhombifolia	—	—	—	—	—	—	—	—	—	—	*	—	—	—	—	—	—
Mnioloma cyclostipum	—	—	—	—	—	—	—	—	—	—	—	—	—	—	—	—	*
M. rhynchophyllum	—	—	—	—	—	—	—	—	—	—	—	*	—	—	—	—	—
Cephaloziaceae																	
Alobiellopsis dominicensis	—	—	—	—	—	—	—	—	—	—	—	—	—	—	—	—	—
Fuscocephaloziopsis crassifolia	—	—	—	—	—	—	—	—	—	—	—	—	—	*	—	—	—
Odontoschisma variabile	—	—	—	—	—	—	*	—	—	—	—	—	—	—	—	—	—
Dumortieraceae																	
Dumortiera hirsuta	—	—	*	—	—	—	—	—	—	—	—	*	—	—	*	—	*
Frullaniaceae																	
Frullania bicornistipula	*	*	—	—	—	—	—	—	—	—	—	—	—	—	—	—	—
F. brasiliensis	—	—	—	—	—	—	—	—	—	—	—	—	—	—	*	—	—
F. caulisequa	—	—	—	—	—	—	*	—	—	—	—	—	*	—	—	—	—
F. dusenii	—	—	—	—	—	—	*	—	—	—	—	—	—	—	—	—	—
F. ericoides	—	—	—	—	—	—	*	—	—	—	—	—	*	—	—	—	—
F. exilis	—	—	—	—	—	—	—	—	—	—	—	—	—	*	*	—	—
F. kunzei	—	—	—	—	—	—	*	—	—	—	—	—	*	—	—	—	—
F. macrocephala	—	—	—	—	—	—	—	—	—	—	—	—	—	*	—	—	—
F. mirabilis	—	—	—	—	—	—	—	—	—	—	—	—	*	—	—	—	—
F. obscura var. *spiniloba*	—	—	—	—	—	—	—	—	—	—	—	—	*	—	—	—	—
F. pittieri	—	—	—	—	—	—	—	—	—	—	—	—	—	—	*	—	—
F. uleana	—	—	—	—	—	—	—	—	*	—	—	—	—	*	—	—	—
Herbertaceae																	
Herbertus bivittatus	—	—	—	—	—	—	—	—	—	—	—	—	—	—	—	—	—
H. juniperoideus	—	*	—	—	*	—	—	—	—	*	*	—	—	—	—	—	*
H. pensilis	—	*	—	—	*	—	—	—	—	*	*	—	—	—	—	—	*
Lejeuneaceae																	
Acanthocoleus aberrans var. *laevis*	—	—	—	—	—	—	*	—	—	—	—	—	—	—	—	—	—
Anoplolejeunea conferta	—	—	—	—	—	—	—	—	—	—	—	—	—	—	*	—	*
Brachiolejeunea laxifolia	—	—	—	—	—	—	*	—	—	—	—	—	—	—	—	—	—
Bryopteris filicina	—	*	—	—	—	—	—	—	—	—	—	—	—	—	—	*	—
Ceratolejeunea cornuta	—	*	—	—	—	—	—	—	*	—	—	—	—	*	*	—	*
C. fallax	—	—	—	—	—	—	—	—	—	—	—	—	—	—	—	—	—
C. filaria	—	—	—	—	—	—	—	—	—	—	—	—	—	*	—	—	—
C. spinosa	—	—	—	—	—	—	—	—	—	—	—	—	—	—	—	—	—
Cheilolejeunea acutangula	—	—	—	—	—	—	—	—	—	—	—	—	—	—	*	*	—

TABLE 5.3. (*Continued*)

	Main collecting sites																
Species by division and family	**1**	**2**	**3**	**4**	**5**	**6**	**7**	**8**	**9**	**10**	**11**	**12**	**13**	**14**	**15**	**16**	**17**
C. aneogyna	—	—	—	—	—	—	*	—	—	—	—	—	—	—	—	—	—
C. comans	—	—	—	—	—	—	—	—	—	—	—	—	—	—	—	*	—
C. filiformis	—	*	*	—	—	—	—	—	—	—	—	—	—	*	*	*	—
C. holostipa	—	—	—	—	—	—	*	—	—	—	—	—	—	—	—	—	—
C. inflexa	—	—	—	—	—	—	—	—	—	—	—	—	—	—	—	—	*
C. lineata	—	*	—	—	—	—	—	—	—	—	—	—	—	—	—	—	—
C. oncophylla	—	—	—	—	—	—	*	—	—	—	—	—	—	—	—	—	—
C. trifaria	—	—	—	—	—	*	—	—	—	—	—	—	*	—	—	—	—
C. xanthocarpa	—	—	—	—	—	—	—	—	—	—	—	—	*	—	—	—	—
Cololejeunea appressa	—	—	—	—	—	—	*	—	—	—	—	—	—	—	—	—	—
C. camillii	—	—	—	—	—	—	*	—	—	—	—	—	—	—	—	—	—
C. diaphana	—	—	—	—	—	—	*	—	—	—	—	—	—	—	—	—	—
C. gracilis	—	—	—	—	—	—	*	—	—	—	—	—	—	—	—	—	—
C. jamesii	—	—	—	—	—	—	*	—	—	—	—	—	—	—	—	—	—
C. linopteroides	—	—	—	—	—	—	*	—	—	—	—	—	—	—	—	—	—
C. papilliloba	—	—	—	—	—	—	*	—	—	—	—	—	—	—	—	—	—
C. papillosa	—	—	—	—	—	—	*	—	—	—	—	—	—	—	—	—	—
C. sicifolia subsp. *jamaicensis*	—	—	—	—	—	—	*	—	—	—	—	—	—	—	—	—	—
C. subcardiocarpa	—	—	—	—	—	—	*	—	—	—	—	—	—	—	—	—	—
C. submarginata	—	—	—	—	—	—	*	—	—	—	—	—	—	—	—	—	—
C. yelitzae	—	—	—	—	—	—	*	—	—	—	—	—	—	—	—	—	—
Cyclolejeunea accedens	—	*	—	—	—	—	—	—	—	—	—	—	*	—	—	—	—
C. chitonia	—	—	—	—	—	—	—	—	*	—	—	—	*	—	—	—	—
C. convexistipa	—	*	*	—	—	—	—	—	—	—	*	—	*	—	—	—	—
C. peruviana	—	*	*	—	—	—	—	—	—	—	*	—	*	—	—	—	—
Diplasiolejeunea caribea	—	—	—	—	—	—	—	—	—	—	—	—	*	—	—	—	—
D. cavifolia	—	—	—	—	—	—	—	—	*	—	—	—	*	—	—	—	—
D. johnsonii	—	—	—	—	—	—	*	—	—	—	—	—	*	—	—	—	—
D. pellucida	—	—	—	—	—	—	*	—	—	—	—	—	—	—	—	—	—
D. pluridentata	—	—	—	—	—	—	—	—	—	—	—	—	*	—	—	—	—
D. rudolphiana	—	—	—	—	—	—	*	—	—	—	—	—	—	—	—	—	—
D. unidentata	—	—	—	—	—	—	*	—	*	—	—	—	*	—	—	—	—
Drepanolejeunea bidens	—	—	—	—	—	—	*	—	—	—	—	—	*	—	—	—	—
D. orthophylla	—	—	—	—	—	—	*	—	—	—	—	—	—	—	—	—	—
Fulfordianthus pterobryoides	—	*	—	—	—	—	—	—	—	—	*	—	—	—	—	—	—
Harpalejeunea stricta	—	—	—	—	—	—	—	—	—	—	—	—	—	—	—	*	—
H. uncinata	—	—	—	—	—	—	*	—	—	—	—	—	—	—	—	—	—
Lejeunea adpressa	—	—	—	—	—	—	—	—	—	—	—	—	*	—	—	—	—
L. angusta	—	—	—	—	—	—	—	—	—	—	—	—	—	—	*	—	—
L. aphanes	—	—	—	—	—	—	*	—	—	—	—	—	—	—	—	—	—

(*Continued*)

TABLE 5.3. (*Continued*)

	Main collecting sites																
Species by division and family	1	2	3	4	5	6	7	8	9	10	11	12	13	14	15	16	17
L. asperrima	—	*	—	—	—	*	—	—	—	—	—	—	—	—	—	—	*
L. bermudiana	—	—	—	—	—	—	*	—	—	—	—	—	—	—	—	—	—
L. caulicalyx	—	—	—	—	—	—	*	—	—	—	—	—	—	—	—	—	—
L. cerina	—	—	—	—	—	—	—	—	*	—	—	—	—	—	—	—	—
L. cristuliflora	—	—	—	—	—	—	*	—	—	—	—	—	—	—	—	—	—
L. deplanata	—	—	—	—	—	—	—	—	—	—	—	—	*	—	—	—	—
L. flava	—	—	—	—	—	—	—	—	—	—	—	—	—	—	—	*	—
L. cf. *glaucescens*	—	*	—	—	—	—	—	—	—	—	—	—	—	—	—	—	—
L. herminieri	—	—	—	—	—	—	*	—	—	—	—	—	—	—	—	—	—
L. laeta	—	—	—	—	—	*	—	—	—	—	—	—	—	—	—	*	—
L. laetevirens	—	—	—	—	—	—	—	—	*	—	—	—	—	—	—	—	—
L. cf. *lusoria*	—	—	—	—	—	—	—	—	—	—	—	—	—	—	—	*	—
L. obtusangula	—	—	—	—	—	—	*	—	—	—	—	—	—	—	—	—	—
L. paucidentata	—	—	—	—	—	—	—	—	—	—	—	—	—	—	—	*	—
L. rotundifolia	—	—	—	—	—	—	—	—	*	—	—	—	*	—	—	—	—
L. sulphurea	—	*	—	—	—	—	—	—	*	—	—	—	*	*	—	—	—
L. venezuelana	—	—	—	—	—	—	*	—	—	—	—	—	—	—	—	—	—
Lepidolejeunea cordifissa	—	—	—	—	—	—	—	—	—	—	—	—	—	*	*	—	*
L. involuta	—	—	—	—	—	*	—	—	*	—	—	—	*	—	—	—	—
Lopholejeunea nigricans	—	—	—	—	—	—	—	—	—	—	—	—	—	—	—	—	—
L. subfusca	—	*	—	—	—	—	—	—	—	—	—	—	—	—	—	—	—
Marchesinia brachiata	—	—	—	—	—	—	—	—	—	—	*	—	—	*	—	*	—
M. robusta	—	—	—	—	—	—	*	—	—	—	—	—	—	—	—	—	—
Microlejeunea bullata	—	—	—	—	—	—	—	—	—	—	—	—	*	—	—	—	—
M. crenulifolia	—	—	—	—	—	—	—	—	—	—	—	—	—	—	—	*	—
M. diversiloba	—	—	—	—	—	*	—	—	—	—	—	—	—	—	—	*	—
M. epiphylla	—	—	—	—	—	—	*	—	—	—	—	—	—	—	—	—	—
Neurolejeunea breutelii	—	—	—	—	—	—	—	—	—	—	—	—	—	—	—	—	*
Odontolejeunea lunulata	—	*	—	—	—	*	—	—	*	—	—	—	*	—	—	—	—
Otigoniolejeunea huctumalcensis	—	—	—	—	—	—	*	—	—	—	—	—	*	—	—	—	—
Prionolejeunea cf. *aemula*	—	*	—	—	—	—	—	—	—	—	—	—	—	—	—	—	—
P. schlimiana	—	—	—	—	—	—	—	—	—	—	—	—	*	*	*	—	—
Pycnolejeunea decurviloba	—	*	—	—	—	—	—	—	—	—	—	—	—	—	—	—	—
Schiffneriolejeunea polycarpa	—	—	—	—	—	—	*	—	—	—	—	—	—	—	—	—	—
Stictolejeunea squamata	*	*	*	—	—	*	—	—	—	—	—	—	—	*	*	*	—
Symbiezidium dentatum	—	—	*	—	—	—	—	—	—	—	—	—	—	—	—	—	—
S. transversale var. *hookerianum*	—	*	—	—	—	—	—	—	—	—	—	—	—	—	—	—	*
Thysananthus auriculatus	—	—	—	—	—	—	—	—	—	—	—	—	—	—	—	—	*
Lepicoleaceae																	
Lepicolea pruinosa	—	—	—	—	—	*	—	—	—	—	—	—	—	—	—	—	—

TABLE 5.3. (*Continued*)

	Main collecting sites																
Species by division and family	**1**	**2**	**3**	**4**	**5**	**6**	**7**	**8**	**9**	**10**	**11**	**12**	**13**	**14**	**15**	**16**	**17**
Lepidoziaceae																	
Bazzania cuneistipula	—	—	—	—	—	—	*	—	—	—	—	—	—	—	—	—	—
B. hookeri	—	—	—	—	—	—	—	—	—	—	—	—	—	—	*	—	—
B. stolonifera	*	—	—	—	—	—	—	—	—	—	—	—	—	—	—	—	—
Kurzia capillaris	—	*	—	—	—	—	—	—	—	—	—	—	—	—	*	—	—
Lepidozia cupressina	—	—	—	—	—	—	*	—	—	—	—	—	—	—	—	—	—
L. macrocolea	—	*	—	—	—	—	—	—	—	—	—	—	—	—	—	—	—
L. patens	—	—	—	—	—	—	—	—	—	—	—	—	—	—	—	*	—
Micropterygium cf. *trachyphyllum*	—	—	—	—	—	—	—	—	—	—	—	—	—	—	—	*	—
Mytilopsis albifrons	—	—	—	—	—	—	—	*	—	—	—	—	—	—	—	—	—
Telaranea nematodes	—	*	—	—	—	—	—	—	—	—	—	—	—	—	—	—	—
Zoopsidella integrifolia	—	—	—	—	—	—	—	—	—	—	—	—	—	*	—	—	—
Lophocoleaceae																	
Chiloscyphus quadridentatus	—	—	—	—	—	—	—	—	—	*	—	—	—	—	—	—	—
Cryptolophocolea connata	—	—	—	—	—	—	—	—	—	—	—	—	—	—	*	—	*
Heteroscyphus marginatus	—	—	—	—	—	—	*	—	—	—	—	—	—	—	—	—	—
Leptoscyphus gibbosus	—	*	*	—	—	—	—	—	—	—	—	—	*	*	*	—	—
L. porphyrius	—	—	—	—	—	—	*	—	—	—	—	—	—	—	—	—	—
L. trapezoides	—	—	—	—	—	—	—	—	—	—	—	—	—	—	—	—	—
Lophocolea liebmanniana	—	—	—	—	—	—	—	—	—	—	—	—	—	—	—	—	*
L. muricata	—	—	—	—	—	—	*	—	—	—	—	—	—	—	—	—	—
Marchantiaceae																	
Marchantia chenopoda	—	—	—	—	—	—	—	—	—	—	*	—	—	—	*	—	—
M. polymorpha	—	—	—	—	—	—	—	—	—	—	—	—	—	—	—	—	—
Metzgeriaceae																	
Metzgeria albinea	—	—	—	—	—	—	—	—	*	—	—	*	—	—	—	—	—
M. attenuata	—	—	—	—	—	—	—	—	—	—	—	—	—	—	—	—	—
M. ciliata	—	—	—	—	—	—	—	—	*	—	—	—	—	—	—	—	—
M. conjugata	—	—	—	—	—	—	—	—	—	—	—	—	—	—	—	—	—
M. leptoneura	—	*	—	—	—	*	—	—	—	—	—	—	—	—	—	—	—
M. procera	—	—	*	—	—	—	—	—	—	—	—	—	—	—	—	—	—
Monocleaceae																	
Monoclea gottschei subsp. *gottschei*	—	*	*	—	—	—	—	—	*	—	—	*	—	—	—	*	—
Pallaviciniaceae																	
Symphyogyna aspera	—	—	—	—	—	—	—	—	—	—	—	—	—	—	—	*	—
S. brasiliensis	—	—	—	—	—	—	—	—	—	—	—	—	—	—	*	—	—
S. brongniartii	—	*	—	—	*	—	—	—	—	—	—	—	*	—	—	—	*
Plagiochilaceae																	
Plagiochila adianthoides	—	—	—	*	—	—	—	—	—	—	—	—	—	—	—	—	*
P. aerea	—	*	—	—	—	—	—	—	—	—	*	—	—	*	—	—	—

(*Continued*)

TABLE 5.3. (*Continued*)

	Main collecting sites																
Species by division and family	**1**	**2**	**3**	**4**	**5**	**6**	**7**	**8**	**9**	**10**	**11**	**12**	**13**	**14**	**15**	**16**	**17**
P. bifaria	—	—	—	—	—	*	—	—	—	—	—	—	—	—	—	*	—
P. cristata	—	—	—	—	—	*	—	—	*	—	—	—	—	—	—	—	—
P. disticha	—	—	—	—	—	—	—	—	—	—	—	—	—	—	—	—	—
P. gymnocalycina	—	—	—	—	—	—	—	—	—	—	*	—	—	—	—	—	—
P. laetevirens	—	—	—	—	—	—	—	—	—	—	—	—	—	—	—	—	—
P. patula	—	—	—	—	—	—	*	—	—	—	—	—	—	—	—	—	—
P. raddiana	—	—	—	—	—	—	*	—	—	—	—	—	—	—	—	—	—
P. rudischusteri	—	—	—	—	—	—	—	—	*	—	*	—	—	—	—	—	—
P. rutilans	—	—	—	—	—	—	—	—	*	—	—	—	—	—	—	—	—
P. rutilans var. *moritziana*	—	—	*	—	—	—	—	—	*	—	—	—	—	—	—	—	—
P. salazariae	*	—	—	—	—	—	—	—	—	—	—	—	—	—	—	—	—
P. simplex	—	—	—	—	—	—	—	—	—	—	—	—	—	—	—	—	—
P. subplana	—	—	—	—	—	—	—	—	—	—	—	—	—	—	—	*	—
P. superba	—	—	—	—	—	—	—	—	—	—	*	—	—	—	—	—	—
Radulaceae																	
Radula episcia	—	—	—	—	—	—	—	—	—	—	—	—	—	—	*	—	*
R. fendleri	—	—	—	—	—	—	*	—	—	—	—	—	—	—	—	*	—
R. gottscheana	—	—	—	—	—	*	—	—	—	—	—	—	—	—	—	—	—
R. kegelii	—	—	—	—	—	*	—	—	—	—	—	—	*	—	—	—	—
R. cf. *sinuata*	—	—	—	—	—	—	—	—	—	—	—	—	—	—	—	*	—
R. stenocalyx	—	—	—	—	—	*	—	—	—	—	—	—	*	—	—	—	—
Scapaniaceae																	
Scapania portoricensis	—	—	—	—	—	—	—	—	—	—	—	—	—	—	—	—	—
Trichocoleaceae																	
Leiomitra flaccida	—	—	—	—	—	—	—	—	—	—	—	—	—	*	—	—	*
L. paraphyllina	—	—	—	—	—	—	—	—	—	—	—	—	—	—	—	—	*
L. sprucei	—	—	—	—	—	*	—	—	—	—	—	—	*	—	—	—	—
L. tomentosa	—	*	—	—	—	—	—	—	—	—	—	—	—	—	—	—	*
MOSSES (BRYOPHYTA)																	
Bartramiaceae																	
Breutelia tomentosa	—	—	—	—	—	—	—	—	—	—	—	—	—	—	—	—	—
Leiomela bartramioides	—	—	—	—	—	—	—	—	—	—	—	—	—	—	—	*	—
Philonotis elongata	—	—	*	—	—	—	—	—	—	—	—	—	—	—	—	—	—
P. sphaericarpa	—	*	—	—	—	—	—	—	—	—	—	—	—	—	—	—	—
P. uncinata	—	*	*	—	—	—	—	—	—	—	—	—	—	—	*	*	*
Brachytheciaceae																	
Eurhynchium cf. *clinocarpum*	—	*	—	—	—	—	—	—	—	—	—	—	—	—	—	—	—
Rhynchostegium scariosum	—	*	—	—	—	—	—	—	—	—	—	—	—	—	—	*	—
Bryaceae																	
Anomobryum conicum	*	—	—	—	—	—	—	—	—	—	—	—	—	—	—	—	—
A. julaceum	—	*	*	—	—	—	—	—	—	—	—	—	—	—	—	—	—

TABLE 5.3. (*Continued*)

	Main collecting sites																
Species by division and family	**1**	**2**	**3**	**4**	**5**	**6**	**7**	**8**	**9**	**10**	**11**	**12**	**13**	**14**	**15**	**16**	**17**
Brachymenium columbicum	—	—	—	—	—	—	—	—	—	—	—	—	—	—	—	—	—
B. speciosum	—	—	—	—	—	—	—	—	—	—	—	—	—	*	—	—	—
Bryum apiculatum	—	—	—	—	—	—	—	—	—	—	—	—	—	—	—	—	—
B. argenteum	—	*	—	—	—	—	—	—	—	—	—	—	—	—	—	—	*
B. billarderii	—	—	—	—	*	—	—	—	—	—	—	—	—	—	—	—	—
B. incrassatolimbatum	—	*	*	—	—	—	—	—	—	—	—	—	—	—	—	—	—
B. limbatum	—	—	—	—	—	—	—	—	—	—	—	—	—	—	—	—	—
Pohlia sp.	—	—	—	—	—	—	—	—	—	—	—	—	—	—	—	—	—
Calymperaceae																	
Calymperes nicaraguense	—	—	—	—	—	—	—	—	—	—	—	—	—	—	*	—	—
Syrrhopodon circinatus	—	—	—	—	—	—	—	—	—	—	—	—	—	—	—	—	*
S. hornschuchii	—	—	—	—	—	—	—	—	—	—	—	—	—	—	—	—	—
S. incompletus	—	*	—	*	—	—	—	—	—	—	—	—	—	—	—	—	*
S. incompletus var. *berteroanus*	—	*	—	—	—	—	—	—	—	—	—	—	—	*	—	—	—
S. leprieurii	*	*	—	—	—	—	—	—	—	—	—	—	—	—	—	—	—
S. lycopodioides	*	*	*	—	*	—	—	—	—	—	—	—	—	—	—	—	—
S. parasiticus	—	*	—	—	—	—	—	—	—	—	—	—	—	—	—	—	—
S. prolifer	*	*	*	—	—	—	—	—	—	—	—	—	—	—	*	*	—
S. prolifer var. *cincinnatus*	—	*	—	—	—	—	—	—	—	—	—	—	—	—	—	—	—
Daltoniaceae																	
Daltonia sp.	—	—	—	—	—	—	—	—	—	—	—	—	—	—	—	—	—
Leskeodon andicola	—	*	—	—	—	—	—	—	—	—	—	—	—	—	—	—	—
L. cubensis	—	*	—	—	—	—	—	—	—	—	—	—	—	—	—	—	—
Dicranaceae																	
Bryohumbertia filifolia	—	*	—	—	—	—	—	—	—	—	—	—	—	—	—	—	—
Campylopus arctocarpus	—	*	—	*	—	—	—	—	—	—	—	—	—	—	—	*	—
C. asperifolius	—	—	—	—	—	—	—	—	—	—	—	—	—	—	*	—	—
C. atlanticus	*	—	—	—	—	—	—	—	—	—	—	—	—	—	—	—	—
C. densicoma	—	*	—	—	—	—	—	—	—	—	—	—	—	—	—	—	—
C. flexuosus	—	*	—	—	—	—	—	—	—	—	—	—	—	*	*	—	—
C. fragilis	—	—	—	—	—	—	—	—	—	—	—	—	—	—	—	—	—
C. savannarum	—	—	—	—	—	—	—	—	—	—	—	—	—	—	—	—	—
Dicranella harrisii	—	*	*	—	—	—	—	—	—	—	—	—	—	—	—	—	—
D. hilariana	—	*	*	—	—	—	—	—	—	—	—	—	—	—	—	—	*
Dicranodontium pulchroalare	*	—	—	—	—	—	—	—	—	—	—	—	—	—	—	—	—
Dicranum flagellare	—	—	—	—	—	—	—	—	—	—	—	—	—	*	—	—	—
D. frigidum	—	—	—	—	—	*	—	—	—	—	—	—	—	—	—	—	—
Eucamptodontopsis brittoniae	—	—	—	—	*	—	—	—	—	—	—	—	—	—	—	—	—
E. brittoniae var. *mcphersonii*	—	—	—	—	*	—	—	—	—	—	—	—	—	—	—	—	—
Holomitrium arboretum	—	*	—	—	—	—	—	—	—	—	—	*	—	*	—	—	—
H. flexuosum	—	—	—	—	—	—	—	—	—	—	—	—	—	—	—	—	—

(*Continued*)

TABLE 5.3. (*Continued*)

	Main collecting sites																
Species by division and family	**1**	**2**	**3**	**4**	**5**	**6**	**7**	**8**	**9**	**10**	**11**	**12**	**13**	**14**	**15**	**16**	**17**
H. longifolium	—	—	—	—	—	—	—	—	—	—	—	—	—	*	—	—	—
H. pulchellum	—	—	—	—	—	—	—	—	—	—	—	—	—	—	—	—	—
H. sinuosum	—	—	—	—	—	—	—	—	—	—	—	—	—	—	—	—	—
Leucoloma cruegerianum	—	*	*	—	—	—	—	—	—	—	—	—	—	—	—	*	—
L. serrulatum	—	*	*	—	—	—	—	—	—	—	—	—	—	*	—	—	*
Microcampylopus leucogaster	—	—	—	—	—	—	—	—	—	—	—	—	—	—	*	—	—
Schliephackea meteorioides	*	—	—	—	—	—	—	—	—	—	—	—	—	—	—	—	—
Entodontaceae																	
Entodon hampeanus	—	—	—	—	—	*	—	—	—	—	—	—	—	—	—	—	*
Fissidentaceae																	
Fissidens anguste-limbatus var. *anguste-limbatus*	—	—	—	—	—	—	—	—	—	—	—	—	—	—	—	—	*
F. asplenioides	*	*	*	*	—	—	—	—	—	—	—	—	—	—	—	*	*
F. bryoides	—	—	*	—	—	—	—	—	—	—	—	—	—	—	—	—	—
F. crispus	—	—	*	—	—	—	—	—	—	—	—	—	—	—	—	*	—
F. flaccidus	—	—	—	—	—	—	—	—	—	—	—	—	—	—	—	—	*
F. guianensis	—	—	—	—	—	—	—	—	—	—	—	—	—	—	—	*	—
F. lagenarius var. *lagenarius*	—	—	—	—	—	—	—	—	—	—	—	—	—	—	—	—	—
F. pellucidus var. *pellucidus*	—	*	*	—	—	—	—	—	—	—	—	—	—	*	—	—	—
F. polypodioides	—	*	*	—	—	—	—	—	—	—	—	—	—	—	—	—	—
F. weirii	*	*	—	*	—	—	—	—	—	—	—	—	—	—	—	—	—
F. weirii var. *hemicraspedophyllus*	—	*	—	—	—	—	—	—	—	—	—	—	—	—	—	—	—
F. zollingeri	—	—	*	—	—	—	—	—	—	—	—	—	—	—	—	—	—
Funariaceae																	
Funaria hygrometrica	—	—	—	—	—	—	—	—	—	—	—	—	—	—	—	—	*
Hookeriaceae																	
Actinodontium sprucei	—	*	—	—	—	—	—	—	—	—	—	—	—	—	—	—	—
Amblytropis hispidula	—	—	—	*	—	—	—	—	—	—	—	—	—	—	—	—	—
Brymela angustiretis	—	*	—	—	—	—	—	—	—	—	—	—	—	—	—	—	—
B. crosbyi	—	*	—	—	—	—	—	—	—	—	—	—	—	—	—	—	—
B. obtusifolia	—	*	*	—	—	—	—	—	—	—	—	—	—	—	—	—	—
Callicostella callicostelloides	—	*	—	—	—	—	—	—	—	—	—	—	—	—	—	—	*
C. oerstediana	—	—	—	—	—	—	—	—	—	—	—	—	—	—	—	—	—
C. pallida	—	*	—	—	—	—	—	—	—	—	—	—	—	*	—	*	*
Crossomitrium epiphyllum	—	—	—	—	—	—	—	—	—	—	—	—	—	—	—	*	—
C. patrisiae	—	—	*	—	—	—	—	—	—	—	—	—	—	—	—	—	—
Cyclodictyon albicans	—	—	—	—	—	—	—	—	—	—	—	—	—	—	*	—	*
C. roridum	—	—	—	—	—	—	—	—	—	—	—	—	—	—	—	—	—
C. rubrisetum	—	—	—	—	—	—	—	—	—	—	—	—	—	—	—	—	*
C. subtortifolium	—	*	—	—	—	—	—	—	—	—	—	—	—	—	—	—	—
C. varians	—	—	*	—	—	—	—	—	—	—	—	—	—	—	—	*	*

TABLE 5.3. (*Continued*)

Species by division and family	Main collecting sites 1	2	3	4	5	6	7	8	9	10	11	12	13	14	15	16	17
Hemiragis aurea	*	*	*	—	—	—	—	—	—	—	*	—	—	—	—	—	—
Hookeria acutifolia	—	*	—	—	—	—	—	—	—	—	—	—	—	—	—	*	—
Hypnella diversifolia	—	*	*	—	—	—	—	—	—	—	—	—	—	—	—	—	*
H. pallescens	—	*	—	—	—	—	—	—	—	—	—	—	—	—	—	—	—
Lepidopilidium divaricatum	—	*	—	—	—	—	—	—	—	—	—	—	—	—	—	—	—
Lepidopilum amplirete	—	*	—	—	—	—	—	—	—	—	—	—	—	—	—	*	—
L. brevipes	—	*	—	—	—	—	—	—	—	—	—	—	—	—	—	—	—
L. diaphanum	—	—	—	—	—	—	—	—	—	—	—	—	—	*	—	—	—
L. longifolium	—	*	—	—	—	—	—	—	—	—	—	—	—	—	—	—	—
L. muelleri	—	*	—	—	—	—	—	—	—	—	—	—	—	—	—	—	—
L. permarginatum	—	*	—	—	—	—	—	—	—	—	—	—	—	—	—	—	—
L. polytrichoides	—	*	—	—	—	—	—	—	—	—	—	—	—	—	—	*	—
L. scabrisetum	—	*	—	*	—	—	—	—	—	—	—	—	—	—	—	*	—
L. tortifolium	—	*	—	—	—	—	—	—	—	—	—	—	—	—	—	—	—
Pilotrichidium callicostatum	—	—	—	—	—	—	—	—	—	—	—	—	—	—	—	*	—
Stenodictyon wrightii	*	*	*	—	—	—	—	—	—	—	—	—	—	—	—	—	—
Thamniopsis cruegeriana	—	*	*	—	—	—	—	—	—	—	—	—	—	—	—	—	*
T. pendula	—	*	*	—	—	—	—	—	—	—	—	—	—	—	—	—	*
T. undata	—	*	*	—	—	—	—	—	—	—	—	—	—	—	—	—	*
Trachyxiphium guadalupense	—	—	—	—	—	—	—	—	—	—	—	—	—	—	—	*	—
T. subfalcatum	—	*	—	—	—	—	—	—	—	—	—	—	—	*	—	*	—
T. variabile	—	—	—	—	—	—	—	—	—	—	—	—	—	—	—	*	—
Hypnaceae																	
Caribaeohypnum polypterum	—	*	—	—	—	—	—	—	—	—	—	—	—	—	—	—	—
Chryso-hypnum diminutivum	—	*	—	—	—	—	—	—	—	—	—	—	—	—	—	*	*
Ctenidium malacodes	—	*	*	—	—	—	—	—	—	—	—	—	—	—	—	*	—
Ectropothecium leptochaeton	—	—	—	—	—	—	—	—	—	—	—	—	—	—	*	—	*
Mittenothamnium langsdorffii	—	—	—	—	—	—	—	—	—	—	—	—	—	—	*	—	—
M. reduncum	—	—	—	—	—	—	—	—	—	—	—	—	—	—	—	—	*
M. reptans	—	*	—	—	—	—	—	—	—	—	—	—	—	—	*	*	*
M. substriatum	—	—	*	—	—	—	—	—	—	—	—	—	—	—	—	—	—
Phyllodon truncatulus	—	—	*	—	—	—	—	—	—	—	—	—	—	—	—	*	—
Puiggariopsis aurifolia	—	—	—	—	—	—	—	—	—	—	—	—	—	—	—	*	—
Pylaisiadelpha tenuirostris	—	—	—	—	—	—	—	—	—	—	—	—	—	—	—	—	*
Rhacopilopsis trinitensis	—	—	—	—	—	—	—	—	—	—	—	—	—	—	*	*	—
Taxiphyllum laevifolium	—	*	*	—	—	—	—	—	—	—	—	—	—	—	—	—	—
Vesicularia vesicularis var. *rutilans*	—	*	—	—	—	—	—	—	—	—	—	—	—	—	—	*	—
Hypopterygiaceae																	
Hypopterygium tamarisci	—	—	—	—	—	—	—	—	*	—	—	—	—	—	—	*	*

(*Continued*)

TABLE 5.3. (*Continued*)

	Main collecting sites																
Species by division and family	**1**	**2**	**3**	**4**	**5**	**6**	**7**	**8**	**9**	**10**	**11**	**12**	**13**	**14**	**15**	**16**	**17**
Lembophyllaceae																	
Lepyrodontopsis trichophylla	—	—	—	—	—	—	—	—	—	—	—	—	—	*	—	—	—
Pilotrichella flexilis	—	*	—	—	*	*	—	—	—	—	—	—	—	*	—	*	*
Leskeaceae																	
Pelekium minutulum	—	—	—	—	—	—	—	—	—	—	—	—	—	*	*	—	—
Thuidium carantae	—	—	—	—	—	—	—	—	—	—	—	—	—	—	—	—	—
T. delicatulum	—	*	—	—	—	—	—	—	—	—	—	—	—	—	—	—	—
T. pseudoprotensum	—	—	—	—	—	—	—	—	—	—	—	—	—	—	—	—	—
T. tomentosum	—	—	—	—	—	—	—	—	—	—	—	—	—	—	—	—	*
Leucobryaceae																	
Leucobryum antillarum	—	*	—	—	—	—	—	—	—	—	*	—	—	—	*	*	—
L. crispum	*	*	*	*	—	—	—	—	—	—	—	—	—	*	—	*	—
L. giganteum	—	*	*	—	*	—	—	*	—	—	*	—	—	—	—	—	*
L. martianum	—	*	—	—	—	—	—	—	—	—	—	—	—	—	*	*	—
L. polakowskyi	—	—	—	—	—	—	—	—	—	—	—	—	—	—	*	—	—
Leucomiaceae																	
Leucomium strumosum	—	*	—	—	—	—	—	—	—	—	—	—	—	—	*	*	*
Rhynchostegiopsis flexuosa	—	—	—	—	—	—	—	—	—	—	—	—	—	—	—	—	*
Meteoriaceae																	
Barbella sp.	—	—	—	—	—	—	—	—	—	—	—	—	—	—	—	—	—
Meteoridium remotifolium	*	—	*	—	—	—	—	—	—	—	—	—	—	*	—	*	—
Meteorium deppei	—	—	—	*	—	—	—	—	—	—	—	—	—	*	—	*	*
Squamidium isocladum	—	*	*	—	—	—	—	—	—	—	—	—	—	*	*	—	—
S. leucotrichum	*	*	—	—	—	—	—	—	—	—	—	—	—	*	*	*	*
S. livens	—	*	—	*	—	—	—	—	—	—	—	—	—	—	—	—	—
Toloxis imponderosa	*	—	—	*	—	—	—	—	*	—	—	—	—	*	—	*	—
Zelometeorium ambiguum	—	—	—	—	—	—	*	—	—	—	—	—	—	—	—	—	—
Z. patulum	—	*	*	*	—	—	—	—	—	—	—	—	—	*	—	*	—
Z. recurvifolium	—	—	*	—	—	—	—	—	—	—	—	—	—	—	—	*	—
Mniaceae																	
Plagiomnium rhynchophorum	—	—	*	—	—	—	—	—	—	—	—	—	—	—	—	—	—
Pyrrhobryum spiniforme	—	*	*	—	—	—	—	—	*	—	*	*	—	*	*	*	*
Rhizogonium lindigii	*	—	—	—	—	—	—	—	—	—	—	—	—	—	—	—	—
Neckeraceae																	
Homaliodendron piniforme	—	—	—	—	—	—	—	—	—	—	—	—	—	—	—	—	—
Isodrepanium lentulum	*	*	*	—	—	—	—	—	—	—	—	—	—	—	*	—	*
Neckeropsis undulata	—	—	—	—	—	—	—	—	—	—	—	—	—	—	*	*	—
Orthostichella rigida	—	—	—	—	—	—	—	—	—	—	—	—	—	—	—	*	—
O. versicolor	*	—	—	—	—	—	—	—	—	—	—	—	—	—	—	—	—
Porotrichodendron lindigii	—	—	—	—	—	—	—	—	—	—	—	—	—	—	—	*	—
Porotrichum brevifolium	—	—	—	—	—	—	—	—	—	—	—	—	—	—	—	—	—

TABLE 5.3. (*Continued*)

	Main collecting sites																
Species by division and family	**1**	**2**	**3**	**4**	**5**	**6**	**7**	**8**	**9**	**10**	**11**	**12**	**13**	**14**	**15**	**16**	**17**
P. korthalsianum	—	*	—	—	—	—	—	—	—	—	—	—	—	—	—	*	—
P. longirostre	—	*	*	—	—	—	—	—	*	—	—	—	—	—	—	—	*
P. mutabile	—	*	*	—	—	—	—	—	—	—	—	—	—	—	—	*	—
P. substriatum	—	—	—	—	—	—	—	—	—	—	—	—	—	—	—	*	—
Thamnomalia glabella	—	—	—	—	—	—	—	—	*	—	—	—	*	—	—	*	*
Octoblepharaceae																	
Octoblepharum cocuiense Mitt.	*	*	—	—	—	—	—	—	—	—	—	*	—	—	—	—	—
O. erectifolium	—	*	—	—	—	—	—	—	—	—	—	*	—	—	—	—	—
O. pulvinatum	*	*	—	—	—	—	—	—	—	—	—	*	—	—	—	*	—
Orthotrichaceae																	
Groutiella apiculata	—	—	—	—	—	—	—	—	—	—	—	—	—	*	*	—	—
G. chimborazensis	—	—	—	—	—	—	—	—	—	—	—	—	—	*	—	—	—
G. mucronifolia	—	—	—	—	—	—	—	—	—	—	—	—	—	—	*	—	—
G. tomentosa	—	—	—	—	—	—	—	—	—	—	—	—	—	—	—	—	—
Macromitrium cirrosum	—	*	*	—	—	*	—	—	—	—	—	—	—	*	—	—	—
M. echinatum	—	—	—	—	—	—	—	—	—	—	—	—	—	—	—	—	—
M. fuscoaureum	*	*	—	—	—	—	—	—	—	—	—	—	—	—	—	—	—
M. guatemalense	*	*	—	—	—	—	—	—	—	—	—	—	—	*	—	*	*
M. leprieurii	—	*	—	—	—	—	—	—	—	—	—	—	—	—	—	—	—
M. longifolium	—	—	—	—	—	—	—	—	—	—	—	—	—	—	—	—	—
M. mcphersonii	—	—	—	—	*	—	—	—	—	—	—	—	—	—	—	—	—
M. punctatum	—	*	—	—	—	—	—	—	—	—	—	—	—	—	—	—	—
M. scoparium	—	—	—	—	—	—	—	—	—	—	—	—	—	—	—	—	*
M. standleyi	*	—	—	—	—	—	—	—	—	—	—	—	—	—	—	—	—
M. subcirrhosum	—	*	—	—	*	—	—	—	—	—	—	—	—	—	—	—	—
M. ulophyllum	—	*	—	—	—	*	—	—	—	—	—	—	—	—	—	—	—
Schlotheimia jamesonii	—	—	—	—	—	*	—	—	—	—	—	—	—	—	—	—	—
S. rugifolia	—	—	—	—	—	—	—	—	—	—	—	—	—	—	—	—	—
Phyllogoniaceae																	
Phyllogonium fulgens	*	*	*	*	—	—	—	—	*	—	—	—	—	*	—	—	—
P. viscosum	*	*	—	—	—	—	—	—	*	—	—	—	—	*	—	*	—
Pilotrichaceae																	
Pilotrichum andersonii	—	—	—	—	—	—	—	—	—	—	—	—	—	—	—	—	—
P. bipinnatum	—	*	—	—	—	—	—	—	—	—	—	—	—	—	—	*	—
P. evanescens	—	—	—	—	—	—	—	—	—	—	—	—	—	—	—	—	*
P. fendleri	—	—	—	—	—	—	—	*	—	—	—	—	—	—	—	*	—
P. ramosissimum	—	—	—	—	—	—	—	—	—	—	—	—	—	—	—	—	*
Polytrichaceae																	
Atrichum oerstedianum	—	—	—	—	—	—	—	—	—	—	—	—	—	—	*	—	*
A. polycarpum	—	—	—	—	—	—	—	—	—	—	—	—	—	—	—	—	*

(*Continued*)

TABLE 5.3. (*Continued*)

	Main collecting sites																
Species by division and family	**1**	**2**	**3**	**4**	**5**	**6**	**7**	**8**	**9**	**10**	**11**	**12**	**13**	**14**	**15**	**16**	**17**
Pogonatum campylocarpum	—	*	—	—	—	—	—	—	—	—	—	—	—	—	—	—	—
P. procerum	—	*	—	—	—	—	—	—	—	—	—	—	—	—	—	—	—
P. tortile	—	*	*	—	—	—	—	—	*	—	—	—	—	—	*	*	*
Polytrichum juniperinum	—	—	—	—	—	—	—	—	—	—	—	—	—	—	—	—	*
Steereobryon subulirostrum	—	*	*	—	—	—	—	—	—	—	—	—	—	—	—	—	—
Pottiaceae																	
Hyophila involuta	—	—	—	—	—	—	—	—	—	—	—	—	—	—	—	—	*
Pterobryaceae																	
Orthostichidium quadrangulare	—	*	*	—	—	—	—	—	—	—	—	—	—	—	—	—	—
Orthostichopsis tetragona	—	—	—	—	—	—	—	—	—	—	—	—	—	—	*	—	—
Pireella angustifolia	—	—	—	—	—	—	—	—	—	—	—	—	—	—	—	—	—
P. pycnothallodes	—	—	—	—	—	—	—	—	—	—	—	—	—	—	—	*	—
Pterobryon densum	—	—	—	—	—	—	—	—	*	—	—	—	—	—	—	*	—
Pterobryopsis mexicana	—	—	—	—	—	—	—	—	—	—	—	—	—	—	—	*	—
Renauldia paradoxica	—	—	—	—	—	—	—	—	—	—	—	—	—	—	—	—	—
Pylaisiadelphaceae																	
Isopterygium tenerum	—	*	—	—	—	—	—	—	—	—	—	—	—	—	—	*	—
Taxithelium planum	—	—	—	—	—	—	—	—	—	—	—	—	—	—	—	*	—
Racopilaceae																	
Racopilum tomentosum	—	—	—	—	—	—	—	—	—	—	—	—	—	*	—	*	*
Sematophyllaceae																	
Acroporium caespitosum	—	—	—	—	—	—	—	—	—	—	—	—	—	—	—	—	*
A. longirostre	—	—	—	—	—	—	—	—	—	—	—	—	—	—	—	—	*
A. pungens	*	*	*	—	—	—	—	—	—	—	—	—	—	*	—	*	*
Sematophyllum adnatum	—	—	—	—	—	—	—	—	—	—	—	—	—	—	—	—	—
S. cochleatum	—	—	*	—	—	—	—	—	—	—	—	—	—	—	—	—	—
S. cuspidiferum	—	—	*	—	—	—	—	—	—	—	—	—	—	—	—	*	*
S. galipense	—	*	*	—	—	—	—	—	—	—	—	—	—	—	—	*	*
S. cf. *hampei*	—	—	—	—	—	—	—	—	—	—	—	—	—	—	—	—	—
S. marylandicum	*	—	—	—	—	—	—	—	—	—	—	—	—	—	—	—	—
S. squarrosum	*	—	—	—	—	—	—	—	—	—	*	—	—	—	—	—	*
S. subpinnatum	—	—	*	—	—	—	—	—	—	—	—	—	—	—	—	—	*
S. cf. *subsimplex*	—	—	—	—	—	—	—	—	—	—	—	—	—	—	—	—	*
S. swartzii	—	—	—	—	—	—	—	—	—	—	—	—	—	*	*	*	—
Trichosteleum fluviale	—	*	—	—	—	—	—	—	—	—	—	—	—	—	—	*	—
T. papillosum	—	—	—	—	—	—	—	—	—	—	—	—	—	—	—	—	—
T. sentosum	—	*	—	—	—	—	—	—	—	—	—	—	—	*	—	—	*

(La Farge-England, 1998). The genus has primarily a Gondwana distribution, and thus, it is presumed that its ancestors originated in Gondwana (La Farge-England, 1998). Without fossil record, it is hypothesized that *Leucoloma* diversified in the last 100 million years and that speciation took place after the breakup of Gondwana followed by few dispersal events (La Farge-England, 1998). *Schliephackea* is an element of the Chocó biogeographical region, although it extends to submontane and upper montane regions (Churchill and Salazar Allen, 2001). *Holomitrium* is a genus of approximately 50 species associated with the Southern Hemisphere (Suárez et al., 2014). Fifteen of these species occur in the Neotropics. The species are common elements of the lower and upper montane forests (Churchill and Salazar Allen, 2001). They are uncommon in the lowlands except for *Holomitrium arboreum*. This species is the most common species of the genus in Central America (Allen, 1990) and grows from sea level to 3,950 m (Churchill and Salazar Allen, 2001).

The Orthotrichaceae are widely distributed in the world, including continental Antarctica (Allen, 2002). Most genera contain few species, but two of them, *Macromitrium* and *Orthotrichum*, have many species (Figure 5.6c; Allen, 2002). In Fortuna, 18 species in 3 genera have been collected: *Macromitrium* with 12 species, *Groutiella* with 4, and *Schlotheimia* with 2 (Table 5.1). *Groutiella* is a genus with distribution primarily in the Neotropics and various species recorded for the Paleotropics (Churchill and Salazar Allen, 2001). The species grow from humid lowland to submontane and montane forests and are mostly epiphytic on branches, trunks, and decomposing logs. One of the species, *Groutiella apiculata*, was recorded for BCI (Salazar Allen et al., 1991). In Fortuna, *Groutiella* was collected from 1,000 to 1,200 m. Species of *Groutiella* grow at lower elevations than most species of *Macromitrium*. Species of *Macromitrium* are highly adapted to situations of high light intensities where periodic events of wetting and drying may cause extremes in the water regime (Vitt and Ramsay, 1985a). The evolution of physiological ability to tolerate the extreme fluctuations in the water content due to their poikilohydry is considered a feature of all species of *Macromitrium* (Vitt and Ramsay, 1985a; see also experiments with *M. cirrosum* in Fortuna by Zotz et al., 1997). *Macromitrium* is more diverse at higher elevations in submontane to montane forests. In Fortuna, it grows from 900 to 2,300 m. In the cloud forests of Cerro Chucantí in Darién, the two species of *Groutiella* that it shares with Fortuna (*G. chimborazensis* and *G. tomentosa*) grow at lower elevations (730–900 m), and three species of *Macromitrium* (*M. cirrosum*, *M. punctatum*, and *M. scoparium*) are found at 1,150 to 1,328 m (Gudiño et al., n.d.). However, only *M. guatemalense* was reported for Bahía Honda (Salazar Allen and Chung, 2005). In the submontane forest of Cerro Pirre (Darién), *Macromitrium* was found at 800 to 1100 m (Gradstein and Salazar Allen, 1992). Vitt and Ramsay (1985b) suggested that *Macromitrium* as a genus differentiated on the intact continent of Gondwana and that the extant species of *Macromitrium* evolved after the breakup of this continental mass approximately 80 to 100 million years ago in middle to late Cretaceous. Nevertheless, they added that, if Australasian species were to be found in either the Paleotropics or Neotropics, they would suspect that they originated from a "wide-ranging stock" of recent origin (Vitt and Ramsay, 1995b). Today, none of the neotropical species found in Fortuna has been reported for the Paleotropics.

The Sematophyllaceae is primarily a family of tropical and subtropical species with 30 to 40 genera (Allen, 2018). The family is widespread in the Neotropics and the Asian Paleotropics, although it can be found in some temperate regions (Tusbota et al., 2001). Its members generally occupy epiphytic habitats (trunk, branches, even rocks). The family is deemed to be "comparatively young" and still evolving (O'Shea, 1999) with considerably plasticity in gametophytic characters (Ramsay, 2012). Two genera widely distributed in the Neotropics are *Acroporium* and *Sematophyllum* (Figure 5.6f). These two genera differ from the third genus, *Trichosteleum*, in their smooth leaf cells, although a few species of *Acroporium* can also have unipapillose leaf cells, but the papillae tend to be rather small and in the upper third of the leaf (Ramsay, 2012) instead of in the center of the leaf lumen, as occurs in *Trichosteleum* (Figure 5.6f–i). In Fortuna, there are 3 species of *Acroporium* and 10 of *Sematophyllum* (Table 5.1). Based on molecular studies (chloroplast *rbcL* sequences), *Acroporium* is considered a monophyletic genus (Tsubota et al., 2001). The genus is pantropical with many species in the Paleotropics. Two species of *Acroporium* are Neotropical, while *A. pungens* is pantropical in distribution (Table 5.1). According to Allen (2018), there are eight species of *Acroporium* in the Neotropics. *Acroporium caespitosum* is a high-elevation moss in Central America that is often epiphytic on twigs, although Buck (1998) found it at 500 m in the Caribbean. In Fortuna, it was collected at 1,000 m on humid rocks and decomposing logs. The other two species, *A. longirostre* and *A. pungens*, grow from near sea level to 2,000 m (Buck, 1998; Allen, 2018). Three species of *Sematophyllum* (*S. cuspidiferum*, *S. cochleatum*, and *S. marylandicum*) are Neotropical (Allen, 2018), distributed from eastern United States to Mexico and northern South America (Table 5.1). They are absent in the Caribbean. Although *Sematophyllum marylandicum* is a common eastern North America species, it is less frequently found in Central America. It grows at higher elevations (Allen, 2018). It was collected at the Continental Divide at 1,250–1,550 m (Table 5.3). *Sematophyllum adnatum* and *S. subpinnatum* are pantropical with the first species having a narrower distribution range (Table 5.1). Three species are African–American elements: *S. galipense*, *S. squarrosum*, and *S. subsimplex*. *Sematophyllum cochleatum* was collected in Quebrada Arena at 1,100 m growing on boulders and rocks in the stream (Table 5.3). *Trichosteleum* is a pantropical genus of approximately 130 species, with the greatest diversity in the Paleotropics (Churchill and Salazar Allen, 2001; Allen, 2018). Two species, *T. fluviale* and *T. papillosum*, are African–American elements, while *T. sentosum* has a distribution in Central America, South America, and the Caribbean (Allen, 2018) (Table 5.1). Seven species of

Sematophyllaceae are shared with Chucantí (Gudiño et al., n.d.), five with Parque Nacional de Coiba (Salazar Allen and Chung, 1997) and three (*Sematophyllum subsimplex*, *Trichosteleum fluviale,* and *T. sentosum*) are shared with the lowlands of BCI (Salazar Allen et al., 1991) and Bahía Honda (Salazar Allen and Chung, 2005).

The Hypnaceae is one of the oldest families of mosses, and its circumscription has changed in time (Allen, 2018). There have been many taxonomic changes resulting in some members transferred to other families. In his treatment of the moss flora of Central America, Allen (2018) considered that the Hypnaceae are closely related to the Sematophyllaceae and Pylaisiadelphaceae. Allen's treatment of the Hypnaceae is followed in this work. Fourteen species are registered for Fortuna (Table 5.1). Eleven species are Neotropical elements, with two of them, *Mittenothamnium reduncum* and *Puiggariopsis aurifolia*, occurring only in continental Neotropics (Table 5.1). *Mittenothamnium* is a pantropical genus with a large number of species, showing plasticity in many of their characters. The genus is in need of a taxonomic revision (Allen, 2018). Most species are concentrated in the Neotropics and tropical Africa, with few in Asia and Oceania (Allen, 2018). Three species are registered for Fortuna, two of them Neotropical and one, *Mittenothamnium reptans*, pantropical. *Mittenothamnium reduncum* is documented by a single collection (Correa 2461A) and growing on humid rock at 1,000 to 1,200 m in what is now the dam site (Table 5.3). According to Allen (2018), the substrate on which it grows is wet rocks or boulders near waterfalls and in or along streams. The second Neotropical species, *M. substriatum*, is a high-elevation moss in Central America mostly growing as an epiphyte on tree trunks, vines, and in soil (Allen, 2018). Gradstein and Raeymaekers (2000) considered the last two species to be indicators of undisturbed submontane to montane rainforests. *Chryso-hypnum diminutivum* grows in humid lowland forests of BCI (Salazar Allen et al., 1991), Parque Nacional de Coiba (Salazar Allen and Chung, 1997), Bahía Honda (Salazar Allen and Chung, 2005), and Chucantí at 732 to 870 m (Gudiño et al., n.d.). *Rhacopilopsis trinitensis* has been collected at sea level in Bahía Honda (Salazar Allen and Chung, 2005) and at 1,055 to 1,340 m in Chucantí (Gudiño et al., n.d.).

Neckeraceae is a family of 10 genera in the Neotropics (Churchill and Salazar Allen, 2001; Allen, 2018), and seven of these occur in Fortuna. Of the 12 species registered for Fortuna, three are pantropical in distribution, one is an African–America element, and eight are Neotropical (Tables 5.1 and 5.2). Of the species with a pantropical distribution, only *Orthostichella rigida* does not occur in the Caribbean (Table 5.1), although the species is frequent in Central America and most common in Africa (Allen, 2018). It grows from 350 to 3,175 m. Allen (2018) considered *Orthostichella versicolor* the most common species of the genus in Central America. It grows from lowland humid forests to over 2,000 m (Allen, 2018). This species has been reported for BCI (Salazar Allen et al., 1991) and the forests of Chucantí (Darién) from 850 to 1,155 m (Gudiño et al., n.d.). Another species of Neckeraceae that occurs only in the continent (NEOC) is the Neotropical *Porotrichum brevifolium*, which is known only for Central America (Table 5.1). This species grows in lowland humid forests to 1,100 m (Allen, 2018; Buck, 1998). *Porotrichum korthalsianum* and *P. substriatum* (an African–American species) have been reported for BCI (Salazar Allen et al., 1991) and Chucantí (Gudiño et al., n.d.). *Porotrichum mutabile* (Figure 5.6e) is also present in Chucantí at elevations above 1,100 m. In Central America, it occurs from 400 to 2,480 m (Allen, 2018). *Neckeropsis* is a genus primarily of tropical regions of the world (Allen, 2018). Sastre (1987) treated the Neotropical *Neckeropsis*. There have been other treatments of the Neckeraceae of Africa and Asia with further taxonomic revisions (see Allen, 2018, for details). *Neckeropsis undulata* grows in moist forests from near sea level to lower montane forests (Buck, 1998), from southern United States to northeastern and northwestern South America to Brazil (Allen, 2018) (Table 5.1). In Panama, the species has been reported for BCI (Salazar Allen et al., 1991), Parque Nacional Altos de Campana (Panamá Oeste) (Chung, 1995), Parque Nacional de Coiba (Salazar Allen and Chung, 1997), Chucantí (Darién) at 800 to 1,105 m (Gudiño et al., n.d.), and Bahía Honda (Salazar Allen and Chung, 2005). *Thamnomalia glabella* is a species of wet and shaded habitats from lowlands to 3,000 m (Allen, 2010).

Taxonomic note: Recent molecular studies (Enroth et al., 2019) have separated *Orthostichella* into its own family, Orthostichellaceae. However, due to time constraints, the species is here treated in the Neckeraceae.

PHYTOGEOGRAPHIC PATTERNS

Approximately 77% of the flora of Fortuna is Neotropical, 11% pantropical, 8% African–American, and 4% subcosmopolitan. Seventy-one of the Neotropical species, including 46 mosses, are restricted to continental America (NEOC) and have not been reported for the Caribbean (Table 5.1). An endemic liverwort (*Plagiochila salazariae*) and five species and one variety of mosses have been reported only for Central America. These are *Campylopus atlanticus*, *Brymela angustirete*, *B. crosbyi*, *Macromitrium mcphersonii*, *Porotrichum brevifolium*, and *Eucamptodontopsis brittoniae* subsp. *mcphersonii* (Allen, 1994, 2002, 2010) (Table 5.1). A liverwort, *Cololejeunea papillosa*, has a circum-Pacific distribution (T. Pócs, personal communication) (Table 5.1). *Plagiochila subplana*, a widespread Neotropical species occurring in lowland and lower montane rainforests to approximately 1,900 m (Heinrichs et al., 1999) have been reported for Vietnam (Pócs, 1971; Bakalin and Nguyen, 2016) (Table 5.1). This species has asexual reproduction by caducous leaves (Heinrichs et al., 1999). A similar case is known for *Acroporium caespitosum* distributed in Central America, the Caribbean (Allen, 2018), and Vietnam (TROPICOS, He and Nguyen 42098) (Table 5.1). This mostly epiphytic, autoicous species produces abundant sporophytes on a rather long seta (8–17 mm) and lacks asexual reproductive propagules (Buck, 1998; Allen, 2018). As has been suggested for other taxa, they may have arrived in Asia and the South Pacific via long-distance dispersal (van Zanten, 1978; van Zanten and Pócs, 1981; Reese, 1987; Gradstein and Vàňa 1987; Gradstein, 2013b, 2018).

Due to its recent geological history, the bryophytes of Panama and of Fortuna arrived from the two adjacent continental masses most probably by long-distance dispersal of spores and/or asexual propagules. The near absence of endemism in the bryoflora of Panama and Fortuna may reflect the continuous exchange of plants and animals from the adjacent landmasses since the emergence of the Isthmus. Vanderpoorten and Goffinet (2009) have suggested that the low global rates of endemism in bryophytes may be due to the strong floristic exchange that may prevent diversification of bryophytes. Gradstein et al. (1989) have indicated that understories of the submontane and lower montane forests, below 3,000 m, are composed of a wide range of tropical (Neotropical and widely distributed) species. This appears to be the case for the bryoflora of Fortuna.

Distribution of Species per Site

Seventeen collecting sites were determined with information obtained from collectors' notes, TROPICOS, and published and unpublished records (e.g., Stotler et al., 1998; Johnston, 1990; Santamaría, 1991; Schäfer-Verwimp, 2014) (Table 5.3; Figure 5.2). Most of the sites are close to the highway and along the creeks and major rivers. The eastern and southeast areas of the Fortuna Forest Reserve, as well as the buffer zone, have been sparsely botanized.

Among the sites studied (Figure 5.1; Table 5.3), the highest species diversities were found in Quebrada Bonita (Site 2, 136 spp.); foothills of Cerro Pinola (Site 16, 85 spp.); northeast of the camping site (Site 17, 82 spp.); Quebrada Arena (Site 3, 59 spp.); southwest of the camping site (Site 14, 49 spp.), southeast of the camping site from Finca Pittí to foothills of Cerro Fortuna, (Site 14, 49 spp.), and northwest of the camping site (Site 15, 48 spp.). The camping site was located close to where the dam is today. There were no geographic coordinates recorded for this site. Thus, the geographic location of the sites that appear in Figure 5.1 and in Table 5.3 as NE, NW, and SW of the camping site are approximate.

The first collections for the environmental evaluation (botanical part) of the Fortuna Dam area in 1976 were gathered northeast, northwest, and southwest of the camping site. Description of the forest in these areas is taken from Adames (1977). The northeast forest was a dense forest rich in species with a good representation of epiphytes (Araceae, ferns, and mosses). Mosses were frequent in more humid areas, near the creeks and even on rocks in the creeks. Large trees were well represented but not as many as in the area northwest of the camping site. Those in the northeast were considered remnants of the original vegetation. The rest of the vegetation was considered to have appeared after a regrowth of the area that was possibly used for agriculture or livestock. Heading north, in front of the camping site, the understory was dense, although not as rich in species as the previous one. Epiphytes, particularly mosses and liverworts, were well represented when compared with the northeast area. Large trees in the north forest were more numerous than in the northeast forest.

Northwest of the camping site, the understory was sparse and large trees were numerous. Epiphytes, including mosses, liverworts, and Araceae, were found in less quantity than in the north and northeast forests. Members of the Bromeliaceae were frequent and more numerous than in the other forests. In the southwest site, known as Sitio Pittí or Finca Pittí, the forest was cut for livestock activities. However, beyond this area, in the same southwest direction, there were areas of forest rich in trees with epiphytes, and the understory was quite dense.

The description of the vegetation agrees with the diversity of bryophytes found in those areas. Bryophytes are more diverse in the forests northeast of the camping site (82 spp.) than in the northwest forests (48 spp.). In the southwest site, the diversity in the areas from Finca Pittí to the foothills of Cerro Fortuna has similar diversity (49 spp.) to that in the northwest. Because of the distance between the Pittí site and Cerro Fortuna, only forests at the foothills were surveyed. If bryophytes at higher elevations in Cerro Fortuna had been collected, it is most probable that they would have increased the diversity of bryophytes in that area.

Species diversity of sites reflects, in part, the collecting efforts centered in selected areas and also the emphasis on the identification of mosses. Quebrada Bonita, Quebrada Arena, and the foothills of Cerro Pinola were the sites where Salazar Allen and her students (i.e., Santamaría and Johnston) collected during April and May 1987 (Figure 5.1, Sites 2, 3, and 16). The students used part of the collections for their baccalaureate research theses in the University of Panama's Department of Botany. Likewise, the high diversity of liverwort species at Valle de Hornito (Site 7) reflects, to a great extent, the intense collection made in that area by Schäfer-Verwimp and his wife during tourist trips in 2010 and 2013 (Schäfer-Verwimp, 2014).

None of the species reported are distributed in all sites. The pantropical *Pyrrhobryum spiniforme* is the most widely distributed bryophyte. It is registered in 9 of the 17 sites (Table 5.3). The species grows in wet lowlands to upper montane forests from nearly sea level to above 3,000 m (Churchill and Salazar Allen, 2001). Fossils of this species dating from the Miocene have been found in amber of the Dominican Republic (Frahm, 2008).

Many collections at PMA are still in need of identification and verification, particularly of liverworts. With the advances in molecular studies, species concepts and distribution are in flux, particularly in tropical taxa (see taxonomic note in the earlier discussion of Neckeraceae). Communities of tropical bryophytes, unlike those of temperate areas, are very heterogeneous in composition. When unidentified collections remaining at PMA are studied, species diversity and distribution as well as similarities among sites, most probably, will be properly assessed.

CONCLUSIONS

This contribution includes the first systematic studies of the bryoflora of Fortuna ever accomplished in Panama. Because of these efforts, the country counts, with a database, information of the species and their distribution in the Fortuna Forest Reserve. In addition, the documentation of new species described from bryophytes of the area include the second endemic liverwort of Panama.

The bryophytes of Fortuna are very diverse with 214 species of mosses, 174 of liverworts, and 8 of hornworts. One-third of the total bryoflora of Panama is found in Fortuna. One-third of all mosses and more than one-third of the liverworts and hornworts reported for Panama occur in Fortuna. The bryoflora of the Fortuna Forest Reserve is a heterogeneous assemblage of species with a mixture of lowland tropical and temperate species, cool-adapted bryophytes from north and south temperate origins, and additional Neotropical species. Phytogeographically, the major component of the bryoflora of Fortuna is neotropical, followed in order by pantropical, African-related, and subcosmopolitan elements. There has been a concentration of collecting activities on the northern and southern sides of the reservoir along and on the sides of the highway. There is a need for expanding the bryophyte surveys to the eastern and southeastern sides of the reserve, the adjacent mountains, and the buffer zone. The occurrence of new species and varieties described from Fortuna suggests that this forest, with additional surveys of the vegetation, could be a cradle of new species, varieties, or forms as the bryophytes adapt morphologically, physiological, and genetically to cooler climates (lowland species) and the highland species adapt to warmer conditions.

In addition, bryophytes, with their overall capacity to intercept and retain water and nutrients from clouds and fog, provide important ecosystem services for Fortuna. These include protection against erosion that deposit sediments in the lake, endangering the operation of the hydroelectric dam and threatening its capacity to provide energy for the country. Bryophytes also contribute to stabilization of streamflow and provide water and nutrients to downstream areas as well as shelter and water for small animals.

The government of Panama must prioritize the protection of the Biological Corridor of the Atlantic of Panama, of which the Fortuna Forest Reserve is a part, to assure the connectivity for the continuous exchange of biota and the potential of these forests as biological laboratories for studies of climate change at the macro and micro scales.

The recent geological age of the Isthmus as a consolidated biological corridor for the exchange of flora and fauna from adjacent landmasses accounts for the diversity of the bryoflora of Panama and Fortuna. The circumscription of the bryophyte flora of Fortuna still requires a finer definition through systematic and ecological studies, identification and revision of collections remaining at PMA, and canopy sampling. It is our hope that this working list will stimulate further research on the bryophytes of the Fortuna Forest Reserve.

ACKNOWLEDGMENTS

N. Salazar Allen, M. Johnston, and D. Santamaría E. acknowledge financial support by the University of Panama (research and travel funds), the former Institute of Hydraulic Resources and Electricity of Panama, and the Smithsonian Tropical Research Institute (research funds to Salazar Allen). C. Arrocha and E. Rodríguez acknowledge support by the Autonomous University of Chiriquí. We are very much indebted to Ing. Batista, Lic. G. Crócamo, Dr. R. Dressler, Dr. M. D. Correa, Magister M. Meléndez (†), Magister N. Escobar (†), and our former students Dr. T. Béliz J., Magister F. Farnum, Dr. C. Garibaldi, and Lic. R. Mendoza for help in the field; to students of the two International Bryophyte Workshops held in Panama for collecting and identifying bryophytes; to Lic. C. Galdames and Lic. J. Aranda for field assistance in Cerro Hornito; and to Magister J. A. De Gracia for help identifying some liverworts. Our acknowledgments go to Lic. M. Solano for help with location of sites and the making of the digital map; Magister N. Flores, curator of the Bryophyte and Lichen herbarium at PMA; and J. Valdés for providing support with the database of PMA and revision of collections at PMA. Special thanks to the following colleagues for help with identification of bryophytes: Dr. S. P. Churchill, Dr. M. R. Crosby, and Dr. B. H. Allen (mosses) of the Missouri Botanical Garden; and Dr. R. A. Pursell (†) (*Fissidens*), Dr. J.-P. Frahm (†) (*Campylopus*), Dr. D. Grifin III (mosses), Dr. I. Sastre De Jesús (Neckeraceae), Dr. M. Fulford (†) (liverworts), Dr. R. Stotler (†) (*Frullania*), Dr. S. R. Gradstein (liverworts), and Dr. G. Dauphin (*Ceratolejeunea*). We gratefully acknowledge Dr. A. Aiello for revision of the English and observations to improve the first part of the manuscript, J. Vargas Y. for help searching for species in the literature, Dr. R. S. Gradstein for revision of the liverworts (nomenclature and geographical distribution), Dr. T. Pócs for revision of *Cololejeunea*, Dr. I. A. Valdespino for critical revision of the manuscript, and Dr. W. R. Buck for revision of the manuscript and constructive comments. Last but not least, our thanks to personnel of the Autoridad Nacional del Ambiente, now Ministerio de Ambiente (MiAmbiente), and park rangers for collecting permits and help in the field.

APPENDIX 5.1. LITERATURE ON LIVERWORTS AND HORNWORTS SPECIES DISTRIBUTION

Acebey, A., S. R. Gradstein, and T. Krömer. 2003. Species Richness and Habitat Diversification of Bryophytes in Submontane Rain Forest and Fallows of Bolivia. *Journal of Tropical Ecology* 19(1):9–18.

Alvarenga, L. D. P., M. P. P. Silva, J. R. P. M Oliveira, and K. C. Pôrto. 2007. Novas Ocorrências de Briófitas para Pernambuco, Brasil. *Acta Botanica Brasilica,* 21(2):349–360.

Arnell, S. 1956. Hepaticae Collected in Cuba and Hispaniola by E. L. Ekman. *Bryologist*, 59(4):271–276.

Bączkiewicz, A., and K. Buczkowska. 2016. Differentiation and Genetic Variability of Three Cryptic Species within the *Aneura pinguis* Complex (Jungermanniidae, Marchantiophyta). *Cryptogamie Bryologie*, 37(1):3–18.

Barbosa-C., I., J. Uribe M., and L. Campos. 2007. Las hepáticas de Santa María (Boyacá, Colombia) y alrededores [The liverworts of Santa María (Boyacá, Colombia) and surrounding area]. *Caldasia*, 29(1):39–49.

Barillas K., R., M. E. Pérez, A. Fajardo, V. Ríos, and S. Guerra. 2007. *Composición y distribución geográfica de las hepáticas epifílicas presentes en los especímenes de herbario de las familias Lauraceae y Arecaceae de Guatemala* [Composition and geographical distribution of epiphyllous liverworts present in herbarium specimens of the Lauraceae and Arecaceae families of Guatemala]. Herbario USCG, Centro de Estudios Conservacionistas (CECON).

Bischler-Causse, H., S. R. Gradstein, S. Jovet-Ast, D. G. Long, and N. Salazar Allen. 2005. *Marchantiidae*. Flora Neotropica Monograph, No. 97. Bronx: New York Botanical Garden Press.

Boggan, J., V. Funk, C. Kellof, M. Hoff, G. Cremers, and C. Feuillet. 1997. *Checklist of the Plants of the Guianas (Guyana, Surinam, French Guiana)*. 2nd ed. Georgetown, Guyana: Centre for the Study of Biological Diversity, University of Guyana.

Burghardt, M., and R. Gradstein. 2008. Chapter Eighteen: A Revision of *Tylimanthus* (Acrobolbaceae, Marchantiophyta) in Tropical America, Africa, and Macaronesia. *Fieldiana Botany*, 47:199–210.

Campos, L. V., S. R. Gradstein, J. Uribe M., and H. ter Steege. 2014. Additions to the Catalogue of Hepaticae of Colombia II. *Cryptogamie Bryologie*, 35(1):77–92.

Campos, L. V., H. ter Steege, and J. Uribe. 2015. The Epiphytic Bryophyte Flora of the Colombian Amazon: Los Briófitos Epífitos de la Región Amazónica de Colombia. *Caldasia*, 37(1):47–59.

Cañiza, B. D., D. F. Peralta, and G. M. Suárez. 2017. New Records and Range Extension of Bryophytes for Paraguay. *Cryptogamie Bryologie*, 38(4):393–410.

Cargill, D. C., and B. A. Fuhrer. 2008. Chapter Twenty: Taxonomic Studies of the Australian Anthocerotophyta II: The Genus *Phaeoceros*. *Fieldiana Botany*, 47:239–253.

Castle, H. 1959. A Revision of the Genus *Radula*. Part 2. Subgenus *Acroradula*. Section 3. *Dichotomae*. *Journal of the Hattori Botanical Laboratory*, 21:1–52.

Castle, H. 1963. A Revision of the Genus *Radula*. Part 2. Subgenus *Acroradula*. Section 6. *Saccatae*. *Revue Bryologie Liquénologie*, 32(1–4):1–48.

Clark, L., and T. C. Frye. 1952. *Frullania pittieri*. *Bryologist*, 55(2):130–133.

Clark, L., and R. D. Svihla. 1944. *Frullania brasiliensis*. *Bryologist*, 47(3):108–112

Clark, L., and R. D. Svihla. 1947. *Frullania arecae*. *Bryologist*, 50(1):82–85.

Clark, L., and R. D. Svihla. 1948. *Frullania mirabilis*. *Bryologist*, 51(3):189–191.

Clark, L., and R. D. Svihla. 1948. Provisional Keys to the Frullanias of Middle America. *Bryologist*, 51(1):17–27.

Crosby, M. R. 1971. Additional Panamanian Bryophytes. *Annals of the Missouri Botanical Garden*, 58(2):258–260.

Cykowska, B. 2014. *Phaeomegaceros fimbriatus* (Gottsche) Duff, J. C. Villarreal, Cargill et Renzaglia New to Bolivia. *Cryptogamie Bryologie*, 35(1):99–103.

Dauphin, G. 2003. *Ceratolejeunea*. Flora Neotropica Monograph, No. 90. Bronx: New York Botanical Garden Press.

Dauphin, G. 2005. Catalogue of Costa Rican Hepaticae and Anthocerotae. *Tropical Bryology*, 26:141–218.

Dauphin, G., S. R. Gradstein, A. Bernecker-Lücking, and M. Morales. 1998. Additions to the Hepatic Flora of Costa Rica II. *Lindbergia*, 23(2):74–80.

Dauphin, G., and A. L. Ilkiu-Borges. 2002. Hepaticae of Cerro Venamo, Venezuela, collected by J. Steyermark. *Tropical Bryology*, 22:115–123.

Dauphin, G., N. Salazar Allen, J. A. Gudiño, A. Sierra, and D. Reyes. 2015. Nuevas Adiciones de Especies de Hepáticas (Marchantiophyta) para la Flora de Panamá. II [New additions of liverwort species (Marchantiophyta) for the flora of Panama]. *Brenesia*, 83–84:16–21.

de Lange P. J., D. Glenny, J. Braggins, M. Renner, M. von Konrat, J. Engel, C. Reeb, and J. Rolfe. 2015. *Conservation Status of New Zealand Hornworts and Liverworts, 2014*. New Zealand Threat Classification Series, No. 11. Wellington, New Zealand: Department of Conservation.

Dirkse, G. M., J. A. W. Nieuwkoop, A. Vanderpoorten, A. Losada-Lima, J. M. González-Mancebo, J. Patiño, A. Sotiaux, R. Hernández-Hernández, and A. Rodríguez-Romero. 2018. New Bryophyte Records from Macaronesia. *Cryptogamie Bryologie*, 39(1):61–76.

Duncan, B., and N. G. Slack. 2017. New York State Liverworts and Hornworts: A Distributional Checklist by Counties. *Evansia*, 34(3):114–133.

Eggers, J., M. Infante, and P. Heras. 2004. New Bryophyte Taxon Records for Tropical Countries 5. *Tropical Bryology*, 25:19–23.

Engel, J. J., and G. L. Smith Merrill. 2004. Austral Hepaticae. 35. A Taxonomic and Phylogenetic Study of *Telaranea* (Lepidoziaceae), with a Monograph of the Genus in Temperate Australasia and Commentary on Extra–Australasian Taxa. *Fieldiana Botany*, 44:1–265.

Equihua, C., and T. Pócs. 1999. Epiphyllous Bryophytes from the Lacandon Forest, Chiapas, Mexico. *Bryologist*, 102(4):747–752.

Evans A. W. 1919. A Taxonomic Study of *Dumortiera*. *Bulletin of the Torrey Botanical Club*, 46(5):167–182.

Feldberg, K., and J. Heinrichs. 2006. A Taxonomic Revision of *Herbertus* (Jungermanniidae: Herbertaceae) in the Neotropics Based on Nuclear and Chloroplast DNA and Morphology. *Botanical Journal of the Linnean Society*, 151:309–332.

Fuertes, E., and S. Manzano. 2017. New and Interesting Records of Argentinian Ricciaceae (Marchantiophyta) and Hornworts (Anthocerotophyta). *Cryptogamie Bryologie*, 38(2):213–222.

Fuertes, E., and C. Prada. 2014. New Record and Additions to the Argentinean Bryophyte Flora. *Darwiniana*, 2(1):68–73.

Fulford, M. 1959. Studies on American Hepaticae. 7. A Supplement to "The Genus *Bazzania* in Central and South America." Part 1. Introduction and the Subgenus *Bidentatae*. *Bulletin of the Torrey Botanical Club*, 86(5):308–341.

Fulford, M. H. 1963. *Manual of the Leafy Hepaticae of Latin America*. Part I. Memoirs of the New York Botanical Garden, Vol. 11. Bronx: New York Botanical Garden Press.

Fulford, M. H. 1966. *Manual of the Leafy Hepaticae of Latin America*. Part II. Memoirs of the New York Botanical Garden, Vol. 11. Bronx: New York Botanical Garden Press.

Fulford, M. H. 1968. *Manual of the Leafy Hepaticae of Latin America*. Part III. Memoirs of the New York Botanical Garden, Vol. 11. Bronx: New York Botanical Garden Press.

Fulford, M. H. 1976. *Manual of the Leafy Hepaticae of Latin America*. Part IV. Memoirs of the New York Botanical Garden, Bronx: New York Botanical Garden Press.

Fulford, M. H., B. Crandall, and R. Stotler. 1970. The Ecology of an Elfin Forest in Puerto Rico, 11. The Leafy Hepaticae of Picodel Oeste. *Journal of the Arnold Arboretum*, 51(1):56–69.

Fulford, M. H., B. Crandall, and R. Stotler. 1971. The Ecology of an Elfin Forest in Puerto Rico, 15. A Study of the Leafy Hepatic Flora of the Luquillo Mountains. *Journal of the Arnold Arboretum*, 52(3):435–458.

Fulford, M. H., and A. J. Sharp. 1990. *The Leafy Hepaticae of Mexico: One Hundred and Twenty-Seven Years after C. M. Gottsche*. Memoirs of the New York Botanical Garden, Vol. 63. Bronx: New York Botanical Garden Press.

Garcia, C., C. Sérgio, J. C. Villarreal, M. Sim-Sim, and F. Lara. 2012. The Hornworts *Dendroceros* Nees and *Megaceros* Campb. in São Tomé e Príncipe (Africa, Gulf of Guinea) with the Description of *Dendroceros paivae* sp. nov. *Cryptogamie Bryologie*, 33(1):3–21.

Glenny, D., A. J. Fife, P. J. Brownsey, M. A. M. Renner, J. E. Braggins, J. E. Beever, and R. Hitchmough. 2011. Threatened and Uncommon Bryophytes of New Zealand (2010 revision). *New Zealand Journal of Botany*, 49(2):305–327.

Gradstein, S. R. 1989. A Key to the Hepaticae and Anthocerotae of Puerto Rico and the Virgin Islands. *Bryologist*, (92)3:329–348.

Gradstein, S. R. 1991. A Key to the Colombian Species of Holostipous Lejeuneaceae (Hepaticae). *Caldasia*, 16(79):429–437.

Gradstein, S. R. 1994. *Lejeuneaceae: Ptychantheae, Brachiolejeuneae*. Flora Neotropica Monograph, No. 62. Bronx: New York Botanical Garden Press.

Gradstein, S. R. 2013. Afro-American Hepatics Revisited. *Polish Botanical Journal*, 58(1):149–177.

Gradstein, S. R. 2016. Nueva Clave para los Géneros de Hepáticas de Colombia [A new key to the genera of liverworts of Colombia]. *Caldasia*, 38(2):225–249.

Gradstein, S. R. 2016. The Genus *Plagiochila* (Marchantiophyta) in Colombia. *Revista de la Academia Colombiana de Ciencias Exactas, Físicas y Naturales*, 40(154):104–136.

Gradstein, S. R. 2017. *Bazzania* (Marchantiophyta) in South America. *Nova Hedwigia*, 105(1–2):243–266.

Gradstein, S. R., and D. P. Costa. 2003. *The Hepaticae and Anthocerotae of Brazil*. Memoirs of the New York Botanical Garden, Vol. 87. Bronx: New York Botanical Garden Press.

Gradstein, S. R., D. Griffin III, M. I. Morales, and N. M. Nadkarni. 2001. Diversity and Habitat Differentiation of Mosses and Liverworts in the Cloudforest of Monteverde, Costa Rica. *Caldasia*, 23(1):203–212.

Gradstein, S. R., and A. L. Ilkiu-Borges. 2015. A Taxonomic Revision of the Genus *Odontoschisma* (Marchantiophyta: Cephaloziaceae). *Nova Hedwigia*, 100(1–2):15–100.

Gradstein, S. R., A. Lücking, M. I. Morales Z., and G. Dauphin. 1994. Additions to the Hepatic Flora of Costa Rica. *Lindbergia*, 19(2/3):73–86.

Gradstein, S. R., C. Morales, M. A. Negritto, and J. G. Duckett. 2016. New Records of Liverworts and Hornworts from the Sierra Nevada de Santa Marta, Colombia. *Cryptogamie Bryologie*, 37(4):463–475.

Gradstein, S. R., T. Pócs, and J. Váňa. 1983. Disjunct Hepaticae in Tropical America and Africa. *Acta Botanica Hungarica*, 29 (1–4):127–171.

Gradstein, S. R., and J. Uribe M. 2011. A Synopsis of the Frullaniaceae (Marchantiophyta) from Colombia/Sinopsis de la Familia Frullaniaceae (Marchantiophyta) para Colombia. *Caldasia*, 33(2):367–396.

Gradstein, S. R., J. Uribe M, J. E. Gil-N, C. Morales, and M. A. Negritto. 2018. Hepáticas Nuevas para Colombia [Liverworts new to Colombia]. *Caldasia*, 40(1):82–90.

Griffin III, D. 1977. Un Informe Sobre la Briología del Estado Zulia, Venezuela [A report on Zulia State Briology, Venezuela]. *Acta Botanica Venezuelica*, 12(1/4):285–292.

Grolle, R. 1964. *Neesioscyphus* – eine neue Lebermoosgattung mit Gedrehten Sporogonklappen [*Neesioscyphus* – a new genus of liverwort with twisted sporogon valves]. *Oesterreichische Botanische Zeitschrift*, 111(1):19–36.

Grolle, R. 2002. The Hepaticae of the Easter Island (Chile). *Bryologist*, 105(1):126–127.

Grolle, R., R.-L. Zhu, and S. R. Gradstein. 2001. On *Cyrtolejeunea* A. Evans (Lejeuneaceae, Hepaticae). *Taxon*, 50(4):1067–1074.

Haughian, S. R., B. A. Bagnell, E. Daley, K. A. Frego, L. Smith, and S. R. Clayden. 2016. A Checklist of the Marchantiophyta and Anthocerotophyta of New Brunswick, Canada. *Northeastern Naturalist*, 23(M13):1–35.

He, X.-L. 1996. Type Studies on *Pycnolejeunea* (Lejeuneaceae, Hepaticae), II. *Annales Botanici Fennici*, 33:51–58.

Heinrichs, J. 2002. A Taxonomic Revision of *Plagiochila* sect. *Hylacoetes*, sect. *Adiantoideae* and sect. *Fuscoluteae* in the Neotropics with a Preliminary Subdivision of Neotropical Plagiochilaceae into Nine Lineages. *Bryophytorum Bibliotheca*, 58:1–184.

Heinrichs, J., A. Czumaj, S. Dong, A. Scheben, A. Schäfer-Verwimp, D. F. Peralta, K. Feldberg, A. R. Schmidt, and H. Schneider. 2014. The Bromeliaceae Tank Dweller *Bromeliophila* (Lejeuneaceae, Porellales) Is a Member of the *Cyclolejeunea–Prionolejeunea* Clade. *Plant Systematics and Evolution*, 300:63–73.

Heinrichs, J., and S. R. Gradstein. 2000. A Revision of *Plagiochila* sect. *Crispatae* and sect. *Hypnoides* (Hepaticae) in the Neotropics. I. *Plagiochila disticha*, *P. montagnei* and *P. raddiana*. *Nova Hedwigia*, 70(1–2):161–184.

Heinrichs, J., H. Groth, S. R. Gradstein, D. S. Rycroft, W. J. Cole, and H. Anton. 2001. *Plagiochila rutilans* (Hepaticae): A Poorly Known Species from Tropical America. *Bryologist*, 104(3):350–361.

Heinrichs, J., H. Groth, I. Holz, D. S. Rycroft, C. Renker, and T. Pröschold. 2002. The Systematic Position of *Plagiochila moritziana*, *P. trichostoma*, and *P. deflexa* based on ITS Sequence Variation of Nuclear Ribosomal DNA, Morphology, and Lipophilic Secondary Metabolites. *Bryologist*, 105(2):189–203.

Heinrichs, J., H. Groth, M. Lindner, K. Feldberg, and D. S. Rycroft. 2004. Molecular, Morphological, and Phytochemical Evidence for a Broad Species Concept of *Plagiochila bifaria* (Hepaticae). *Bryologist*, 107(1):28–40.

Heinrichs, J., C. Renker, and S. R. Gradstein. 1999. A Taxonomic Revision of *Plagiochila subplana* Lindenb., a Widespread Liverwort of Tropical America. *Haussknechtia. Beiheft* 9:171–181.

Holz, I., and S. R. Gradstein. 2005. Phytogeography of the Bryophyte Floras of Oak Forests and Páramo of the Cordillera de Talamanca, Costa Rica. *Journal of Biogeography*, 32(9):1591–1609.

Hong, W. S. 1988. Studies on *Scapania portoricensis* Hampe et Gott. of Latin America. *Lindbergia*, 14(1):69–72.

Ilkiu-Borges, A. L. 2005. *A Taxonomic Monograph of the Genus Prionolejeunea (Lejeuneaceae, Jungermanniopsida)*. Götting, Germany: Cuvillier Verlag.

Ilkiu-Borges, A. L. 2005. A Taxonomic Revision of *Echinocolea* (Lejeuneaceae, Hepaticae). *Nova Hedwigia*, 80(1–2):45–71.

Ilkiu-Borges, A. L., and R. C. L. Lisboa. 2004. Os Gêneros *Cyclolejeunea*, *Haplolejeunea*, *Harpalejeunea*, *Lepidolejeunea* e *Rectolejeunea* (Lejeuneaceae, Hepaticae) na Estação Científica Ferreira Penna, Pará, Brasil [The genres Cyclolejeunea, Haplolejeunea, Harpalejeunea, Lepidolejeunea, and Rectolejeunea (Lejeuneaceae, Hepaticae) at Estação Científica Ferreira Penna, Pará, Brazil]. *Acta Botanica Brasilica*, 18(3):537–553.

Ilkiu-Borges, A. L., and R. C. L. Lisboa. 2004. *Cololejeuneae* (Lejeuneaceae, Hepaticae) na Estação Científica Ferreira Penna, Melgaço, PA, Brasil. *Acta Botanica Brasilica*, 18(4):887–902.

Ilkiu-Borges, A. L., and F. R. O. Silva. 2018. Flora das Cangas da Serra dos Carajás, Pará, Brasil: Lejeuneaceae [Flora of the Canga of the Serra dos Carajás, Pará, Brazil: Lejeuneaceae]. *Rodriguésia*, 69(3):989–1012.

Inoue, H. 1989. Two New Species of *Plagiochila* (Dum.) Dum. from Panama, Central America. *Bulletin of the National Museum of Nature and Science, Series B, Tokyo*, 15:91–96.

Juárez-Martínez, C., and C. Delgadillo-Moya. 2017. The Leafy Liverworts (Marchantiophyta) of the Valley of Mexico. *Revista Mexicana de Biodiversidad*, 88(3):502–518.

Kelly, D. L., G. O'Donovan, J. Feehan, S. Murphy, S. O. Drangeid, and L. Marcano-Berti. 2004. The Epiphyte Communities of a Montane Rain Forest in the Andes of Venezuela: Patterns in the Distribution of the Flora. *Journal of Tropical Ecology* 20(6):643–666.

Kornochalert, S., K. Santanachote, and J. Wang. 2012. Lejeuneaceae Subfamily Ptychanthoideae (Marchantiophyta) in Thailand. *Cryptogamie Bryologie*, 33(1):39–63.

Lavocat B., E., and A. Schäfer-Verwimp. 2011. Checklist of the Bryophytes of the Guadeloupe Archipelago and Martinique (French West Indies). *Cryptogamie Bryologie*, 32(3):233–272.

León-Yánez, S., S. R. Gradstein, and C. Wegner. 2006. *Catálogo de Hepáticas (Marchantiophyta) y Antoceros (Anthocerotophyta) del Ecuador* [Catalog of liverworts (Marchantiophyta) and *Anthoceros* (Anthocerotophyta) from Ecuador]. Quito, Ecuador: Herbario QCA.

Lücking, A. 1997. Diversity and Distribution of Epiphyllous Bryophytes in a Tropical Rainforest in Costa Rica. In *Cryptogams in the Phyllosphere: Systematics, Distribution, Ecology and Use*, ed. E. Farkas and T. Pócs, pp. 79–87. Abstracta Botanica, No. 21. Budapest: Department of Plant Taxonomy and Ecology.

McAvoy, W. A., L. T. Biechele, and W. M. Knapp. 2006. New Records for the Leafy Liverwort *Calypogeia peruviana* Nees et Mont. (Calypogeiaceae) on the Delmarva Peninsula. *Evansia*, 23:19–20.

Meenks J. 1987. Studies on Colombian Cryptogams XXVIII. A Guide to the Tropical Andean Species of *Riccardia* (Hepaticae). *Journal of the Hattori Botanical Laboratory*, 62:161–182.

Menzel, M. 1985. Katalog der Lebermoose von Peru. *Willdenowia*, 14(2):473–523.

Morales, T., E. Moreno, R. Ghinaglia, and A. Ángel. 2014. Inventario y Estado de Conservación de la Brioflora del Parque Nacional Yurubí (Estado Yaracuy, Venezuela) [Inventory and conservation status of the bryophyte flora in Yurubí National Park (Yaracuy State, Venezuela)]. *Acta Botanica Venezuelica*, 37(1):1–30.

Mustelier M., K. 2012. Hepáticas Foliosas en los Bosques Pluviales de la Región Oriental de Cuba [Foliose liverworts in the rainforests of the eastern region of Cuba]. *Boletín de la Sociedad Española de Briología*, 38–39:51–68.

Oliveira, H. C., and C. J. P. Bastos. 2014. Briófitas Epífitas de Fragmentos de Floresta Atlântica da Reserva Ecológica Michelin, Estado da Bahia, Brasil [Epiphytic bryophytes of Atlantic forest fragments of Reserva Ecológica Michelin, Bahia State, Brazil]. *Hoehnea* 41(4):631–646.

Opisso M., J., and S. P. Churchill. 2008. Bryophytes from the Environs of Yanachaga–Chemillén National Park, Department of Pasco, Peru. *Bryologist*, 111(2):310–317.

Pagán, F. M. 1939. A Preliminary List of the Hepaticae of Puerto Rico including Vieques and Mona Island. *Bryologist*, 42(2):37–50.

Pérez, M. E. 2009. Catálogo de las Hepáticas (Marchantiophyta) de Guatemala: Una Actualización [Catalog of the liverworts (Marchantiophyta) of Guatemala: an update]. *Brenesia*, 71–72:3–12.

Piippo, S. 1986. A Monograph of the Genera *Lepidolejeunea* and *Luteolejeunea* (Lejeuneaceae, Hepaticae). *Acta Botanica Fennica*, 132:1–69.

Pócs, T. 2008. Liverwort Floristics and Revisions – Asia and Australasia. Chapter 13: Bryophytes from the Fiji Islands, IV. The Genus *Frullania* Raddi (Jungermanniopsida), I., with Description of *F. vivip*ara Pócs, spec. nov. *Fieldiana Botany*, 47:147–158.

Pócs, T., and S. Chantanaorrapint. 2015. *Ceratolejeunea tahitensis*, a New Synonym of *C. cornuta* (Lejeuneaceae, Marchantiophyta). *Phytotaxa*, 207(2):213–214.

Pócs, T., and G. E. Lee. 2016. Data to the Malaysian Liverwort Flora, II. *Cryptogamie Bryologie*, 37(1):39–52.

Pócs, T., F. Müller, and J. R. Shevock. 2015. Additions to the Liverwort and Hornwort Flora of São Tomé and Príncipe II, with *Neurolejeunea*, a Genus New to Africa. *Herzogia*, 28(1):50–69.

Pócs, T., R. Ochyra, and H. Bednarek-Ochyra. 2016. *Lepidozia cupressina* (Marchantiopsida, Lepidoziaceae) in Sub-Saharan Africa, with a Note on the Taxonomic Status of *L. chordulifera*. *Cryptogamie Bryologie*, 37(2):125–147.

Preußing, M., S. Olsson, A. Schäfer-Verwimp, N. J. Wickett, S. Wicke, D. Quandt, and M. Nebel. 2010. New Insights in the Evolution of the Liverwort Family Aneuraceae (Metzgeriales, Marchantiophyta), with Emphasis on the Genus *Lobatiriccardia*. *Taxon*, 59(5):1424–1440.

Promma, C., and S. Chantanaorrapint. 2015. The Epiphyllous *Radula* (Radulaceae, Marchantiophyta) in Thailand, with the Description of *Radula grandilobula* sp. nov. *Cryptogamie Bryologie*, 36(3):217–234.

Reiner-Drehwald, M. E. 1994. El Género *Radula* (Radulaceae, Hepaticae) en el Noreste de Argentina [The genus Radula (Radulaceae, Hepaticae) in northeast Argentina]. *Tropical Bryology*, 9:5–22.

Reiner-Drehwald, M. E. 1998. Las Lejeuneaceae (Hepaticae) de Misiones, Argentina V. *Cheilolejeunea* y *Lepidolejeunea* [The Lejeuneaceae (Hepaticae) of Misiones, Argentina V. Cheilolejeunea and Lepidolejeunea]. *Tropical Bryology*, 14:53–68.

Reiner-Drehwald, M. E. 2006. Type Studies on Neotropical Lejeuneaceae (Jungermanniopsida). *Cheilolejeunea* and *Lepidolejeunea*. *Nova Hedwigia*, 83(3–4):473–482.

Reiner-Drehwald, M. E. 2010. A Taxonomic Revision of *Lejeunea deplanata* (Lejeuneaceae, Marchantiophyta) from Tropical America. *Nova Hedwigia*, 91(3–4):519–532.

Reiner-Drehwald, M. E., and A. L. Ilkiu-Borges. 2007. *Lejeunea huctumalcensis*, a Widely Distributed Lejeuneaceae from the Neotropics, and Its Relation to *Ceratolejeunea*. *Bryologist*, 110(3):465–474.

Reis, L. C., H. C. de Oliveira, and C. J. P. Bastos. 2015. Hepáticas (Marchantiophyta) Epífitas de duas Áreas de Floresta Atlântica no Estado da Bahia, Brasil [Liverwort (Marchantiophyta) epiphytes of two areas of Atlantic forest in Estado da Bahia, Brazil]. *Pesquisas Botânica*, 67:225–241.

Santos, N. D., and D. P. Costa. 2010. Altitudinal Zonation of Liverworts in the Atlantic Forest, Southeastern Brazil. *Bryologist*, 113(3):631–645.

Schäfer-Verwimp, A. 2004. The Genus *Diplasiolejeunea* (Lejeuneaceae, Marchantiopsida) in the Tropical Andes, with Description of Two New Species. *Cryptogamie Bryologie*, 25(1):3–17.

Schäfer-Verwimp, A. 2014. Towards a More Complete Knowledge of the Liverwort Flora of Panama. *Phytotaxa*, 172(3):201–234.

Schäfer-Verwimp, A., M. Lehnert, and M. Nebel. 2013. Contribution to the Knowledge of the Bryophyte Flora of Ecuador. *Phytotaxa*, 128(1):1–63.

Schäfer-Verwimp, A., and T. Pócs. 2009. Contributions to the Hepatic Flora of the Dominican Republic, West Indies. *Acta Botanica Hungarica*, 51(3–4):367–425.

Schäfer-Verwimp, A., and H. M. H. van Melick. 2016. A Contribution to the Bryophyte Flora of Jamaica. *Cryptogamie Bryologie*, 37(3):305–348.

Schuster, R. M. 1957. North American Lejeuneaceae VI. *Lejeunea*: Introduction and Keys; Subgenus *Lejeunea* (I). *Journal of the Elisha Mitchell Scientific Society,* 73(1):122–197.

Schuster, R. M. 1965. North American Lejeuneaceae. IX. *Taxilejeunea*. *Journal of the Elisha Mitchell Scientific Society*, 81(1):32–50.

Sérgio, C., and C. Garcia. 2011. Bryophyte Flora of São Tomé e Príncipe Archipelago (West Africa): Annotated Catalogue. *Cryptogamie Bryologie*, 32(2):145–196.

Shu, L., Y.-L. Xiang, X.-F. Cheng, Y.-M. Wei, J. Wang, L.-N. Zhang, W. Li, X.-B. Yin, W.-P. Zhang, C.-X. Zhao, T. Peng, T. V. Do, T. N. Lu, and R.-L. Zhu. 2017. New Liverwort and Hornwort Records for Vietnam. *Cryptogamie Bryologie*, 38(4):411–445.

Sierra, A. M., A. Vanderpoorten, S. R. Gradstein, M. R. Pereira, C. J. P. Bastos, and C. E. Zartman. 2018. Bryophytes of Jaú National Park (Amazonas, Brazil): Estimating Species Detectability and Richness in a Lowland Amazonian Megareserve. *Bryologist*, 121(4):571–588.

Singh, A. P., D. Kumar, and V. Nath. 2008. *Lophocolea fragrans* (Moris & De Not.) Gottsche *et al.* (Bryophyta: Hepaticae): An Addition to India from Eastern Himalaya. *Evansia*, 25(2):40–46.

Singh, A. P., D. Kumar, and V. Nath. 2008. Studies on the Genera *Frullania* Raddi and *Jubula* Dum. from Meghalaya (India): Eastern Himalayas. *Taiwania*, 53(1):51–84.

Singh, D. 2012. A Note on *Cheilolejeunea trifaria* (Reinw. et al.) Mizut. from Indian Himalayan Region. *Lindbergia*, 35:18–21.

Singh, S. K., and H. A. Barbhuiya. 2012. A Compendium to Marchantiophyta and Anthocerotophyta of Assam, India. *Archive for Bryology*, 149:1–30.

Smith, C. W., Gardner, and W. J. Hoe. 1997. Foliicolous Hawaiian Cryptogams. *Abstracta Botanica*, 21(1):163–167.

Söderström, L., A. Hagborg, J. Váňa, and M. von Konrat. 2011. Land of Wood and Water: A Checklist of Liverworts and Hornworts of Jamaica. *Bryologist*, 114(1):67–91.

Söderström, L., E. Urmi, and J. Váňa. 2002. Distribution of Hepaticae and Anthocerotae in Europe and Macaronesia. *Lindbergia* 27(1):3–48.

Spruce, R. 1890. HEPATICÆ BOLIVIANÆ. In Andibus Boliviæ Orientalis, Annis 1885–6, a cl. H. H. Rusby lectæ. *Memoirs of the Torrey Botanical Club*, 1(3):113–140.

Staples, G. W., and C. T. Imada. 2006. Checklist of Hawaiian Anthocerotes and Hepatics. *Tropical Bryology*, 28:15–47.

Steyermark, J. A., and B. Maguire. 1984. Flora de la Guayana Venezolana. *Acta Botanica Venezuelica*, 14(3):3, 5–89, 91–117.

Stotler, R., and B. Crandall–Stotler. 2017. A Synopsis of the Liverwort Flora of North America North of Mexico. *Annals of the Missouri Botanical Garden*, 102(4):574–709.

Sukkharak, P., and S. R. Gradstein. 2014. A Taxonomic Revision of the Genus *Mastigolejeunea* (Marchantiophyta: Lejeuneaceae). *Nova Hedwigia*, 99(3–4):279–345.

Thouvenot, L., S. R. Gradstein, A. Hagborg, L. Söderström, and J. Bardat. 2011. Checklist of the Liverworts and Hornworts of New Caledonia. *Cryptogamie Bryologie*, 32(4):287–390.

Tixier, P. 1985. Contribution à la Connaissance des *Cololejeunoideae* [Contribution to the knowledge of Cololejeunoideae]. *Bryophytorum Bibliotheca*, 27:1–439.

Uribe M., J., and J. Aguirre C. 1995. Las Especies Colombianas del Género *Symphyogyna* (Hepaticae: Pallaviciniaceae) [Colombian species of the genus Symphyogyna (Hepaticae: Pallaviciniaceae)]. *Caldasia*, 17(82–85):429–458.

Uribe M., J., and S. R. Gradstein. 1998. Catalogue of the Hepaticae and Anthocerotae of Colombia. *Bryophytorum Bibliotheca*, 53:1–99.

Uribe M., J., and S. R. Gradstein. 2003. Type Studies on *Frullania* Subgenus *Meteoriopsis* (Hepaticae). I. The Lectotypification of the Genus *Frullania*, *F.* subgen. *Thyopsiella* and *F.* subgen. *Meteoriopsis*, and Some Species Transferred from subgen. *Meteoriopsis* to subgen. *Thyopsiella*. *Cryptogamie Bryologie*, 24 (3):193–207.

Villarreal, J. C., B. Goffinet, R. J. Duff, and D. C. Cargill. 2010. Phylogenetic Delineation of *Nothoceros* and *Megaceros* (Dendrocerotaceae). *Bryologist*, 113(1):106–113.

Villarreal, J. C., and S. S. Renner. 2014. A Review of Molecular-Clock Calibrations and Substitution Rates in Liverworts, Mosses, and Hornworts, and a Timeframe for a Taxonomically Cleaned–up Genus *Nothoceros*. *Molecular Phylogenetics and Evolution*, 78:25–35.

Villarreal, J. C., and K. S. Renzaglia. 2006. Sporophyte Structure in the Neotropical Hornwort *Phaeomegaceros fimbriatus*: Implications for Phylogeny, Taxonomy, and Character Evolution. *International Journal of Plant Sciences*, 167(3):413–427.

Wang, J., M.-J. Lai, and R.-L. Zhu. 2011. Liverworts and Hornworts of Taiwan: An Updated Checklist and Floristic Accounts. *Annales Botanici Fennici*, 48(5):369–395.

Wei, Y.-M., R.-L. Zhu, and S. R. Gradstein. 2014. Notes on Early Land Plants Today. 49. On *Lejeunea huctumalcensis* Lindenb. & Gottsche and the Resurrection of *Otigoniolejeunea* (Spruce) Schiffn., an Older Name for *Physantholejeunea* R. M. Schust. (Marchantiophyta, Lejeuneaceae). *Phytotaxa*, 162(4):236–238.

Welch, W. H. 1950. A Contribution to the Bryophyte Flora of Cuba. *Bryologist*, 53(3):238–243.

Whittemore, A. T., and B. Allen. 1996. The Liverworts and Hornworts of Belize. *Bryologist*, 99(1):64–67.

Windolf, J. 1987. Annotated Checklist of Queensland Hepaticae. *Austrobaileya*, 2(4):380–400.

Yamada, K., and S. R. Gradstein. 1991. The Genus *Radula* (Hepaticae) in the Galapagos Islands. *Tropical Bryology*, 4:63–68.

Yano, O., and P. E. A. S. Câmara. 2004. Briófitas de Manaus, Amazonas, Brasil [Bryophytes from Manaus, Amazonas, Brazil]. *Acta Amazonica*, 34(3):445–457.

Ye, W., S. R. Gradstein, A. J. Shaw, B. Shaw, B.-C. Ho, A. Schäfer-Verwimp, T. Pócs, J. Heinrichs, and R.-L. Zhu. 2015. Phylogeny and Classification of Lejeuneaceae Subtribe Cheilolejeuneinae (Marchantiophyta) Based on Nuclear and Plastid Molecular Markers. *Cryptogamie Bryologie*, 36(4):313–333.

Zhu, R.-L., and S. R. Gradstein. 2005. Monograph of *Lopholejeunea* (Lejeuneaceae, Hepaticae) in Asia. *Systematic Botany Monographs*, 74:1–98.

References

Acto, M., O. Abollino, R. Conca, M. Malandrino, E. Mentasti, and C. Sarzanini. 2003. The Use of Mosses as Environmental Metal Pollution Indicators. *Chemosphere* 50:333–342. https://doi.org/10.1016/S0045-6535(02)00533-7

Adames, A. J. 1977. *Evaluación Ambiental y Efectos del Proyecto Hidroeléctrico Fortuna. Informe Final* [Environmental assessment and effects of the Fortuna Hydroelectric Project. Final report]. Revista Lotería 254-255-256. Panama City, Panama: Lotería Nacional de Beneficencia.

Adams, D. G., and P. S. Duggan. 2008. Cyanobacteria-Bryophyte Symbiosis. *Journal of Experimental Botany*, 59:1047–1058. https://doi.org/10.1093/jxb/ern005

Ah-Peng, C., A. W. Cardoso, O. Flores, A. West, N. Wilding, D. Strasberg, and T. A. Hedderson. 2017. The Role of Epiphytic Bryophytes in Interception, Storage, and the Regulated Release of Atmospheric Moisture in a Tropical Montane Cloud Forest. *Journal of Hydrology*, 548:665–673. https://doi.org/10.1016/j.jhydrol.2017.03.043

Alcaraz, L. D., M. Peimbert, H. R. Barajas, A. E. Dorantes-acosta, J. L. Bowman, and M. A. Arteaga-Vázquez. 2018. *Marchantia* Liverworts as a Proxy to Plant's Basal Microbiomes. *Scientific Reports*, 8:12712. https://doi.org/10.1038/s41598-018-31168-0

Allen, B. H. 1990. A Preliminary Treatment of the *Holomitrium* Complex (Musci: Dicranaceae) in Central America. *Tropical Bryology*, 3:59–71. https://doi.org/10.11646/bde.3.1.7

Allen, B. H. 1994. *Moss Flora of Central America, Part 1. Sphagnaceae–Calymperaceae*. Monographs in Systematic Botany from the Missouri Botanical Garden, No. 49. St. Louis: Missouri Botanical Garden Press.

Allen, B. H. 2002. *Moss Flora of Central America, Part 2. Encalyptaceae–Orthotrichaceae*. Monographs in Systematic Botany from the Missouri Botanical Garden, No. 90. St. Louis: Missouri Botanical Garden Press.

Allen, B. H. 2010. *Moss Flora of Central America, Part 3. Anomodontaceae–Symphyodontaceae*. Monographs in Systematic Botany from the Missouri Botanical Garden, No. 117. St. Louis: Missouri Botanical Garden Press, St. Louis.

Allen, B. H. 2018. *Moss Flora of Central America, Part 4. Fabroniaceae–Polytrichaceae*. Monographs in Systematic Botany from the Missouri Botanical Garden, No. 132. St. Louis: Missouri Botanical Garden Press.

Ares, A., M. Itouga, Y. Kato, and H. Sakakibara. 2018. Differential Metal Tolerance and Accumulation Patterns of Cd, Cu, Pb and Zn in the Liverwort *Marchantia polymorpha* L. *Bulletin of Environmental Contamination and Toxicology*, 100:444–450. https://doi.org/10.1007/s00128-017-2241-0

Aryanti, N. S., and R. S. Gradstein. 2007. Wallace's Line and the Distribution of the Liverworts of Sulawesi. *Cryptogamie Bryologie*, 28:3–14.

Asakawa Y., 1982. Chemical Constituents of the Hepaticae. In *Progress in the Chemistry of Organic Natural Products*, ed. W. Herz, H. Grisebach, and G. W. Kirby, vol. 42. Vienna: Springer-Verlag.

Asakawa, Y. 1995. Chemical Constituents of the Bryophytes. In *Progress in the Chemistry of Organic Natural Products*, ed. W. Herz, G. W. Kirby, R. E. Moore, W. Steglich, and C. Tamm, vol. 65. Vienna: Springer-Verlag.

Asakawa, Y. 2008. Liverworts-Potential Source of Medicinal Compounds. *Current Pharmaceutical Design*, 14:3067–3088. https://doi.org/10.2174/138161208786404272

Asakawa, Y., A. Ludwiczuk, and F. Nagashima. 2013. Chemical Constituents of Bryophytes. Bio- and Chemical Diversity, Biological Activity and Chemosystematics. In *Progress in the Chemistry of Organic Compounds*, ed. A. D. Kinghorn, H. Falk, and J. Kobayashi, vol. 95. Vienna: Springer-Verlag.

Aschenbrenner, I. A., T. Cernava, G. Berg, and M. Grube. 2016. Understanding Microbial Multi-Species Symbioses. *Frontiers in Microbiology*, 7:180. https://doi.org/10.2989/18142321003714492

Atwood, J. J. 2015. Taxonomic Revision of the Moss Genus *Lepidopilidium* (Pilotrichaceae). *Annals of the Missouri Botanical Garden*, 100:364–392. https://doi.org/10.3417/2014021

Ayrault S., L. Galsomiès, G. Amblard, M. D. Sciarretta, P. Bonhomme, and A. Gaudry. 2002. Instrumental Neutron Activation Analysis (INAA) and Inductively Coupled Plasma/mass Spectrometry (ICP-MS) for Trace Element Biomonitoring Using Mosses. *International Journal of Environmental Analytical Chemistry*, 82:463–473. https://doi.org/10.1080/0306731021000014994

Bakalin, V. A., and S. Nguyen. 2016. The Checklist of Liverworts (Hepaticae) and Hornworts (Anthocerotae) of Vietnam Updated Based on Literature Survey. *Tap Chi Sinh Hoc*, 38:480–491. https://doi.org/10.15625/0866-7160/v38n4.8771

Bastos, C. J. P. 2017. O gênero Cheilolejeunea (Spruce) Steph. (Lejeuneaceae, (Marchantiophyta) nas Américas [The genus Cheilolejeunea (Spruce) Steph. (Lejeuneaceae, (Marchantiophyta) in the Americas]. *Pesquisas Botânica*, 70:5–78.

Bentley, B. L. 1987. Nitrogen Fixation by Epiphylls in a Tropical Rainforest. *Annals of the Missouri Botanical Garden,* 74:234–241. https://doi.org/10.2307/2399396

Berg, G., A. Bragina, M. Cardinale, C. Zachow, H. Müller, C. Berg, A. Shcherbakov, W. Chebotar, and M. Grube. 2011. From Metagenome and Proteome to Biocontrol: Analysis of Moss- and Lichen-Associated Microbial Communities. Conference at 6th IOBC Working Group Meeting on Multitrophic Interactions in Soil, Cordoba, Spain, 4 April.

Buck, W. R. 1998. *Pleurocarpous Mosses of the West Indies*. Memoirs of the New York Botanical Garden, No. 82. New York: New York Botanical Garden Press.

Câmara, P. E. A. S. 2011. A Re-circumscription of the Moss Genus *Taxithelium* (Pylasiadelphaceae) with a Taxonomic Revision of Subgenus *Vernieri*. *Systematic Botany*, 36:7–21. https://doi.org/10.1600/036364411X553081

Cavalier, J., and G. Goldstein. 1989. Mist and Fog Interception in Elfin Cloud Forest in Colombia and Venezuela. *Journal of Tropical Ecology*, 5:309–322. https://doi.org/10.1017/S0266467400003709

Chung C., C. 1995. Estudio Preliminar de los Musgos Corticícolas en Árboles y Arbustos Menores de 10 cm de DAP en el Sendero Panamá, Parque Nacional Altos de Campana [Preliminary study of corticultural mosses in trees and shrubs less than 10 cm from DAP on the Panama Trail, Altos de Campana National Park]. BA thesis, University of Panama, Panama.

Churchill, S. P., and N. Salazar Allen. 2001. Mosses. In *Guide to the Bryophytes of Tropical America*, ed. S. R. Gradstein, S. P. Churchill, and N. Salazar Allen, pp. 240–571. Memoirs of the New York Botanical Garden, No. 86. New York: New York Botanical Garden Press.

Clark, K. E., N. M. Nadkarni, and H. L. Gholz. 1998. Growth, Net Production, Litter Decomposition, and Net Nitrogen Accumulation by Epiphytic Bryophytes in a Tropical Montane Forest. *Biotropica*, 30:12–23. https://doi.org/10.1111/j.1744-7429.1998.tb00365.x

Costa, D. P. 2008. *Metzgeriaceae (Hepaticae)*. Flora Neotropica Monograph, No. 102. Bronx: New York Botanical Garden Press.

Coxson, D. S. 2011. Nutrient Release from Epiphytic Bryophytes in Tropical Montane Forest (Guadeloupe). *Canadian Journal of Botany*, 69:2122–2129. https://doi.org/10.1139/b91-266

Crandall-Stotler, B., R. E. Stotler, and D. G. Long. 2009. Morphology and Classification of the Marchantiophyta. *Edinburgh Journal of Botany*, 66:155–198. https://doi.org/10.1017/S0960428609005393

Crum, H. A., and W. C. Steere. 1950. Additions to the Moss Flora of Panama. *Bryologist*, 53:139–152. https://doi.org/10.2307/3240382

Dauphin, G. 1999. Bryophytes of Cocos Island, Costa Rica: Diversity, Biogeography and Ecology. *Revista de Biología Tropical*, 47:309–328.

Dauphin, G. 2007. Nuevas Adiciones de Especies de Hepáticas para la Flora de Panamá. *Candollea* 62(1):45–51.

Dauphin, G., T. Pócs, J. C. Villarreal, and N. Salazar Allen. 2006. Nuevos Registros de Hepáticas y Anthocerotófitas para Panamá. *Tropical Bryology*, 27:73–85. https://doi.org/10.11646/bde.27.1.10

Dauphin, G., N. Salazar Allen, J. A. Gudiño, A. Sierra and D. Reyes. 2015. Nuevas Adiciones de Especies de Hepáticas para la Flora de Panamá II [New additions of liverwort species for the flora of Panama II]. *Brenesia*, 83–84:16–21.

Delgadillo M., C., B. Bello, and A. Cárdenas. 2013. LATMOSS. A Catalog of Neotropical Mosses [electronic database]. Missouri Botanical Garden.

Desirò, A., J. G. Duckett, S. Pressel, J. C. Villarreal, and M. I. Bidartondo. 2013. Fungal Symbioses in Hornworts: A Chequered History. *Proceedings of the Royal Society of London B*, 280: 20130207. https://doi.org/10.1098/rspb.2013.0207

Enroth, J., S. Olsson, S. Huttunen, V. Buchbender, R. Tangney, M. Stech, L. Hedenäs, and D. Quandt. 2019. Orthostichellaceae fam. nov. and Other Novelties in Pleurocarpous Mosses Revealed by Phylogenetic Analyses. *Bryologist*, 122(2):219–245. https://doi.org/10.1639/0007-2745-122.2.219

Frahm, J.-P. 1988. The Subantarctic and Southern Hemispheric Species of *Campylopus* (Dicranaceae) with Contributions to the Origin and Speciation of the Genus. *Journal of the Hattori Botanical Laboratory*, 64:367–388.

Frahm, J.-P. 1990. The Origin and Distribution of Neotropical Species of *Campylopus*. *Tropical Bryology*, 3:1–18. https://doi.org/10.11646/bde.3.1.2

Frahm, J.-P. 2002. *Campylopus*. Bryophyte Flora of North America, Provisional Publication, Buffalo Museum of Science. Version 2a, 7 January 2005. http://www.mobot.org/plantscience/bfna/v1/DicrCampylopus.htm.

Frahm, J.-P. 2003. Introduction. In *Manual of Tropical Bryology*, pp. 9–11. *Tropical Bryology*, 23.

Frahm, J.-P. 2008. *Echypopterygiopsis dominicensis*, a New Genus and Species, and *Pyrrhobryum spiniforme* from the Miocene of the Dominican Republic. *Tropical Bryology*, 29:48–50. https://doi.org/10.11646/bde.29.1.6

Gehring-Downie, C., A. Obregon, J. Bendix and R. S. Gradstein. 2013. Diversity and vertical distribution of epiphytic liverworts in lowland rain forest and lowland cloud forest of French Guiana. J. Bryol. 35: 243-254. https://doi.org/10.1179/1743282013Y.0000000070

Glime, J. 2017. *Bryophyte Ecology*. Vol. 2, chap. 1–12. Michigan Technological University. https://digitalcommons.mtu.edu/bryophyte-ecology2

Goffinet B., and W. R. Buck. 2019. Classification of the Bryophyta. http://bryology.uconn.edu/classification.

Gradstein, S. R. 1994. *Lejeuneaceae: Ptychantheae, Brachiolejeuneae*. Flora Neotropica Monograph, No. 62. New York: New York Botanical Garden Press.

Gradstein, S. R. 1995a. Diversity of Hepaticae and Anthocerotae in Montane Forests of Tropical Andes. In *Biodiversity and Conservation of Neotropical Montane Forest*, ed. S. P. Churchill, H. Balslev, E. Forero, and J. L. Luteyn, pp. 321–334. New York: New York Botanical Garden Press.

Gradstein, S. R. 1995b. Bryophyte Diversity of the Tropical Rainforest. *Archives des Sciences, Genève*, 48:91–96.

Gradstein, S. R. 2001. Liverworts and Hornworts: Keys and Descriptions. In *Guide to the Bryophytes of Tropical America*, ed. S. R. Gradstein, S. P. Churchill and N. Salazar Allen, pp. 70–239. Memoirs of the New York Botanical Garden, No. 86. New York: New York Botanical Garden Press.

Gradstein, S. R. 2006. The Lowland Cloud Forest of French Guiana – A Liverwort Hotspot. *Cryptogamie Bryologie*, 27:141–152.

Gradstein, S. R. 2013a. A Classification of Lejeuneaceae (Marchantiophyta) Based on Molecular and Morphological Evidence. *Phytotaxa*, 100:6–20. https://doi.org/10.11646/phytotaxa.100.1.2

Gradstein, S. R. 2013b. Afro-American Hepatics Revisited. *Polish Botanical Journal*, 58:149–177. https://doi.org/10.2478/pbj-2013-0016

Gradstein, S. R. 2015. New Synonyms and New Lectotypifications in Neotropical *Plagiochila* (Marchantiophyta). *Cryptogamie Bryologie*, 36:369–379. https://doi.org/10.7872/cryb/v36.iss4.2015.369

Gradstein, S. R., 2017. *Bazzania* (Marchantiophyta) in South America. *Nova Hedwigia*, 105(1):1–24. https://doi.org/10.1127/nova_hedwigia/2017/0409

Gradstein, S. R. 2018. Amphi-Pacific Tropical Disjunctions in the Bryophyte Floras of Asia and the New World. *Philippine Journal of Systematic Biology*, 12(1):1–11. https://doi.org/10.26757/pjsb.2018a12012

Gradstein, S. R., and A. L. Ilkiu-Borges. 2009. *Guide to the Plants of Central French Guiana*. Part 4. Liverworts and Hornworts. Memoirs of the New York Botanical Garden, No. 76. New York: New York Botanical Garden Press.

Gradstein, S. R., R. Klein, L. Kraut, R. Mues, J. Spörle, and H. Becker. 1996. Phytochemical and Morphological Support for the Existence of Two Species in *Monoclea* (Hepaticae). *Plant Systematics and Evolution*, 180:115–135. https://doi.org/10.1007/BF00940401

Gradstein, S. R., D. Montfoort, and J. H. C. Cornelissen. 1990. Species Richness and Phytogeography of the Bryophyte Flora of the Guianas, with Special Reference to the Lowland Forest. *Tropical Bryology*, 2:117–126. https://doi.org/10.11646/bde.2.1.9

Gradstein, S. R., and T. Pócs. 1989. Bryophytes. In *Tropical Rain Forest Ecosystems: Biogeographical and Ecological Studies*, ed. H. Lieth and M. J. A. Werger, pp. 311–325. Ecosystems of the World, No. 14B. Amsterdam: Elsevier.

Gradstein, S. R., and G. Raeymaekers with contribution from S. P. Churchill. 2000. Tropical America (incl. México). In *Mosses, Liverworts and Hornworts. Status Survey and Conservation Action Plan for Bryophytes*, ed. T. Hallingbäck and N. Hodgetts, pp. 38–44. Gland, Switzerland: IUCN/SSC Bryophyte Specialist Group.

Gradstein, S. R., M. E. Reiner-Drehwald, and H. Schneider. 2003. A Phylogenetic Analysis of the Genera of Lejeuneceaceae (Hepaticae). *Botanical Journal of the Linnean Society*, 143:391–410. https://doi.org/10.1111/j.1095-8339.2003.00235.x

Gradstein, S. R., and N. Salazar Allen. 1992. Bryophyte Diversity along an Altitudinal Gradient in Darién National Park, Panama. *Tropical Bryology*, 5:61–71. https://doi.org/10.11646/bde.5.1.10

Gradstein, S. R., G. B. A. van Reenen, and D. Griffin III. 1989. Species Richness and Origin of the Bryophyte Flora of the Colombian Andes. *Acta Botanica Neerlandica*, 84:439–448. https://doi.org/10.1111/j.1438-8677.1989.tb01375.x

Gradstein, S. R., and J. Váňa. 1987. *On the Occurrence of Laurasian Liverworts in the Tropics*. Memoirs of the New York Botanical Garden, No. 45. New York: New York Botanical Garden Press.

Gudiño L., J., and N. Salazar Allen. 2017. Morfología y Distribución de *Dolotortula mniifolia* y *Trachyphyllum dusenii* (Bryophyta) en Panamá [Morphology and distribution of *Dolotortula mniifolia* and *Trachyphyllum dusenii* (Bryophyta) in Panama]. *Boletín de la Sociedad Argentina de Botánica*, 52:331–340. https://doi.org/10.31055/1851.2372.v52.n2.17448

Gudiño L., J., N. Salazar Allen, R. Vergara, and C. Chung C. (†) (n.d.). Contribución a la Brioflora de Panamá: Primer Listado de Musgos de Cerro Chucantí (Reserva Natural Privada), Provincia de Darién [Contribution to the bryoflora of Panama: First list of the mosses of Cerro Chucantí (Private Natural Reserve)].

Heinrichs, J., S. Dong, A. Schäfer-Verwimp, T. Pócs, K. Feldberg, A. Czumaj, A. R. Schmidt, J. Reitner, M. A. M. Renner, J. Hentschel, M. Stech, and H. Schneider. 2013. Molecular Phylogeny of the Leafy Liverwort *Lejeunea* (Porellales): Evidence for a Neotropical Origin, Uneven Distribution of Sexual Systems and Insufficient Taxonomy. *PLoS One*, 8:1–14. https://doi.org/10.1371/journal.pone.0082547

Heinrichs J., M. Lindner, H. Groth, J. Hentschel, K. Feldberg, C. Renker, J. J. Engel, M. von Konrat, D. G. Long, and H. Schneider. 2006. Goodbye or Welcome Gondwana? – Insights into the Phylogenetic Biogeography of the Leafy Liverwort *Plagiochila* with a Description of *Proskauera*, gen. nov. (Plagiochilaceae, Jungermanniales). *Plant Systematics and Evolution*, 258:227–250. https://doi.org/10.1007/s00606-006-0411-3

Heinrichs, J., C. Renker, and S. R. Gradstein. 1999. A Taxonomic Revision of *Plagiochila subplana* Lindenb., a Widespread Liverwort of Tropical America. *Haussknechtia Beiheft*, 9: 171–181.

Hentschel, J., M. J. von Konrat, T. Pócs, A. Schäfer-Verwimp, A. J. Shaw, H. Schneider, and J. Heinrichs. 2009. Molecular Insights into the Phylogeny and Subgeneric Classification of *Frullania* Raddi (Frullaniaceae, Porellales). *Molecular Phylogenetics and Evolution*, 52:142–156. https://doi.org/10.1016/j.ympev.2008.12.021

Horwath, A. B., J. Royles, R. Tito, J. A. Gudiño, N. Salazar Allen, W. Farfan-Ríos, J. M. Rapp, M. R. Silman, Y. Malhi, V. Swamy, J. P. L. Farfan, and H. Griffiths. 2019. Bryophyte Stable Isotope Composition, Diversity and Biomass Define Tropical Montane Cloud Forest Extent. *Proceedings of the Royal Society B: Biological Sciences*, 286. https://doi.org/10.1098/rspb.2018.2284

Inoue, H. 1984. *The Genus* Plagiochila *in Southeast Asia*. Tokyo: Academic Scientific Book.

Inoue, H. 1989. Two New Species of *Plagiochila* (Dum.) Dum. from Panama, Central America. *Bulletin of the National Museum of Nature and Science, Series B. Tokyo*, 15:91–96.

IRHE (Institute of Hydraulic Resources and Electricity). 1986. Mapa del Programa de Tala: Segunda Fase – Área Polanimetrada [Logging program map: Second phase – Polanimetric area]. Dirección de Ingeniería, Departamento de Cuencas.

Jarvis A., and M. Mulligan. 2011 The Climate of Cloud Forests. *Hydrological Processes*, 25:327–343. https://doi.org/10.1002/hyp.7847

Johnston, M. B. 1990. *Estudio Preliminar de los Musgos Epipétricos, Terrestres y de los que crecen sobre Troncos en Descomposición de Fortuna (Proyecto Hidroeléctrico Fortuna – Fase II)* [Preliminary study of epipetric, terrestrial mosses and those that grow on decomposing logs of Fortuna (Fortuna Hydroelectric Project – phase II)]. BA thesis, University of Panama, Panama.

La Farge-England, C. 1998. The Infrageneric Phylogeny, Classification and Phytogeography of *Leucoloma* (Dicranaceae, Bryopsida). *Bryologist*, 101:181–220. https://doi.org/10.2307/3244199

Lee, G. E., and R. S. Gradstein. 2013. Distribution and Habitat of the Malaysian Species of *Lejeunea* (Marchantiophyta: Lejeuneaceae), with Description of *Lejeunea tamaspocsii* sp. nov. *Polish Botanical Journal*, 58:59–69. https://doi.org/10.2478/pbj-2013-0007

Longton, R. E., and R. M. Schuster. 1983. Reproductive Biology. In *New Manual of Bryology,* Vol. 1, ed. R. M. Schuster, pp. 386–462. Nichinan, Japan: Hattori Botanical Laboratory.

Magill, R. E. 2010. Moss Diversity: New Look at Old Numbers. *Phytotaxa*, 9:167–174. https://doi.org/10.11646/phytotaxa.9.1.9

Miller, N., and W. R. Buck. 2008. Bryological results of the 31st A. L. Andrews Foray in Rhode Island. *Evansia*, 25:47–52. https://doi.org/10.1639/0747-9859-25.2.47

Mayo, E., M. D. Correa, N. Escobar, and R. Dressler. 1977. Apéndice 2. Vegetación. In *Evaluación Ambiental y Efectos del Proyecto Hidroeléctrico Fortuna Informe Final* [Environmental assessment and effects of the Fortuna Hydroelectric Project. Final report], ed. A. J. Adames, pp. 159–222. Revista Lotería No. 254, 255, 256. Panama City: Lotería Nacional de Beneficencia.

Nadkarni, N. M., and R. Solano. 2002. Potential Effects of Climate Change on Canopy Communities in a Tropical Cloud Forest: An Experimental Approach. *Oecologia*, 131:580–586. https://doi.org/10.1007/s00442-002-0899-3

O'Shea, B. J. 1999. African Sematophyllaceae (Bryopsida) and a New Key to the Genera, Using Mainly Gametophytic Characters. *Bryobrothera*, 5:299–302.

Papaefthimiou, D., P. Hrouzek, M. A. Mugnai, A. Lukesova, S. Turicchia, U. Rasmussen, and S. Ventura. 2008. Differential Patterns of Evolution and Distribution of the Symbiotic Behaviour in Nostocacean Cyanobacteria. *International Journal of Systematic and Evolutionary Microbiology*, 58:553–564. https://doi.org/10.1099/ijs.0.65312-0

Patzak, S. D., M. A. M. Renner, A. Schäfer-Verwimp, K. Feldberg, M. M. Heslewood, D. F. Peralta, A. Matos de Souza, H. Schneider, and J. Heinrichs. 2016. A Phylogeny of Lophocoleaceae-Plagiochilaceae-Brevianthaceae and a Revised

Classification of Plagiochilaceae. *Organisms Diversity & Evolution*, 16: 481–495. https://doi.org/10.1007/s13127-015-0258-y

Pócs, T. 1971. Studies on the Mountain Bryoflora of the Ha-Giang Province (Democratic Republic of Vietnam): Hepaticae. *Botanicheskiy Zhurnal*, 56:670–677.

Pócs, T. 1980. The Epiphytic Biomass and Its Effect on the Water Balance of Two Rain Forests in the Uluguru Mountains (Tanzania, East Africa). *Acta Botanica Academiae Scientiarum Hungaricae*, 26:143–167.

Proctor, M. C. F. 2009. Physiological Ecology. In *Bryophyte Ecology*, ed. B. Goffinet and A. J. Shaw, pp. 236–268. Cambridge: Cambridge University Press.

Ramsay, H. P. 2012. Australian Mosses Online. 1. Sematophyllaceae: *Trichosteleum*. http://www.anbg.gov.au/abrs/Mosses_online/01_Sematophyllaceae/Semat_Trichosteleum.pdf.

Reese, W. D. 1987. World Ranges, Implications for Patterns of Historical Dispersal and Speciation, and Comments on Phylogeny of *Syrrhopodon* (Calymperaceae). In *Bryostephane Steereana: A Collection of Bryological Papers Presented to William Campbell Steere on the Occasion of his 80th Birthday*, ed. W. R. Buck, 426–445. Memoirs of the New York Botanical Garden, No. 45. New York: New York Botanical Garden Press.

Reese, W. D. 1993. *Calymperaceae*. Flora Neotropica Monograph, No. 58. Bronx: New York Botanical Garden Press.

Reiner-Drehwald, M. E., and A. L. Ilkiu-Borges. 2007. *Lejeunea huctumalcensis*, a Widely Distributed Lejeuneaceae from the Neotropics, and Its Relation to *Ceratolejeunea*. *Bryologist*, 110(3):465–474. https://doi.org/10.1639/0007-2745(2007)110[465:LHAWDL]2.0.CO;2

Renzaglia, K. S., J. C. Villarreal, and R. J. Duff. 2009. New Insights into the Morphology, Anatomy and Systematics of Hornworts. In *Bryophyte Biology II*, ed. B. Goffinet and J. A. Shaw, pp. 139–171. Cambridge: Cambridge University Press.

Renzaglia, K. S., J. C. Villarreal, and D. Garbary. 2018. Morphology Supports the Setaphyte Hypothesis: Mosses Plus Liverworts Form a Natural Group. *Bryophyte Diversity and Evolution*, 40:11–17. https://doi.org/10.11646/bde.40.2.1

Richards, P. W. 1984. The Ecology of Tropical Forest Bryophytes. In *New Manual of Bryology*, Vol. 2, ed. R. M. Schuster, pp. 1233–1270. Nichinan, Japan: Hattori Botanical Laboratory.

Rodríguez-Quiel, E., G. Mendieta-Leiva, and M. Y. Bader. 2019. Elevational Patterns of Bryophyte and Lichen Biomass Differ among Substrates in the Tropical Montane Forest of Baru Volcano, Panama. *Journal of Bryology*, 41:95–106. https://doi.org/10.1080/03736687.2019.1584433

Salazar Allen, N., C. Chung C., and J. A. Gudiño L. n.d. Tabla de las hepáticas registradas para BCI, Fortuna y Parque Nacional Altos de Campana [Table of the liverworts reported for BCI, Fortuna and Altos de Campana National Park].

Salazar Allen, N., C. Arrocha, and C. Chung C. 1991. The Mosses of Barro Colorado Island. *Bryologist*, 94:289–293. https://doi.org/10.2307/3243967

Salazar Allen, N., and C. Chung C. 1997. Primera aproximación al catálogo de briofitos del Parque Nacional de Coiba (Panamá). [First approach to the catalog of the bryophytes of Coiba National Park]. In Flora y Fauna del Parque Nacional de Coiba (Panamá). Inventario Preliminar [Flora and fauna of Coiba National Park (Panama). Preliminary survey.] ed. S. Castroviejo, pp. 221–243. Madrid: Agencia Española de Cooperación Internacional.

Salazar Allen, N., and C. Chung C. 2005. Briofitas (Antocerotes, Hepáticas y Musgos) de la Región de Bahía Honda (Veraguas, Panamá) [Bryophytes (anthocerotes, liverworts, and mosses) from the Bahía Honda region (Veraguas, Panama)]. In *Estudios sobre la Biodiversidad de la Región de Bahía Honda (Veraguas, Panamá)* [Studies on the biodiversity of the Bahía Honda region (Veraguas, Panama)], ed. S. Castroviejo and A. Ibáñez, pp. 95–175. Madrid: Consejo Superior de Investigaciones Científicas.

Santamaría E., D. 1991. *Estudio Preliminar de los Musgos Cortícolas de Fortuna, Provincia de Chiriquí (Proyecto Hidroeléctrico Fortuna – Fase II)* [Preliminary study of the corticultural mosses of Fortuna, province of Chiriquí (Fortuna Hydroelectric Project – Phase II)]. BA thesis, University of Panama, Panama.

Sastre-De Jesús, I. 1987. *A Revision of the Neckeraceae Schimp. and the Thamnobryaceae Marg. & Dur. in the Neotropics*. PhD Dissertation, City University of New York.

Schäfer-Verwimp, A. 2014. Towards a More Complete Knowledge of the Liverwort Flora of Panama. *Phytotaxa*, 172:201–234. https://doi.org/10.11646/phytotaxa.172.3.3

Schuster, R. M. 1992. *Frullania* Raddi. In *The Hepaticae and Anthocerotae of North America*, ed. R. M Schuster, pp. 13–269. East of the Hundredth Meridian, No. 5. Chicago: Field Museum of Natural History.

Seemann, B. 1852–1854. Flora of the Isthmus of Panama. In *Botany of Voyage of H.M.S. Herald, Under the Command of Captain Henry Kellett, R.N.N.,C.B., During the Years 1845–51*, pp. 57–254, pl. 1–60. London: Lovell Reeve Publishing Company.

Söderström, L., A. Hagborg, M. von Konrat, S. Bartholomew-Began, D. Bell, L. Briscoe, E. Brown(†), D. C. Cargill, D. P. Costa, B. J. Crandall-Stotler, E. D. Cooper, G. Dauphin, J. J. Engel, K. Feldberg, D. Glenny, S. R Gradstein, X. He, J. Heinrichs(†), J. Hentschel, A. L. Ilkiu-Borges, T. Katagiri, N. A. Konstantinova, J. Larraín, D. G. Long, M. Nebel, T. Pócs, F. Puche, E. Reiner-Drehwald, M. A. M. Renner, A. Sass-Gyarmati, A. Schäfer-Verwimp, J. G. Segarra Moragues, R. E. Stotler(†), P. Sukkharak, B. M. Thiers, J. Uribe, J. Váňa, J. C. Villarreal, M. Wigginton, L. Zhang, and R.-L. Zhu. 2016. World Checklist of Hornworts and Liverworts. *PhytoKeys*, 59:1–828. https://doi.org/10.3897/phytokeys.59.6261

Söderström, L., J. Váňa, B. Crandall-Stotler, R. E. Stotler, A. Hagborg, and M. von Konrat. 2013. Notes on Early Land Plants Today. 43. New Combinations in Lophocoleaceae (Marchantiophyta). *Phytotaxa*, 112:18–32. https://doi.org/10.11646/phytotaxa.112.1.4

Spörle, J. 1990. *Phytochemische Untersuchungen an Ausgewählten Panamaischen Lebermoosen* [Phytochemical studies on selected Panamanian liverworts]. PhD thesis, Fakultät der Universität de Saarlandes, Germany.

Stotler, R., N. Salazar Allen, S. R. Gradstein, W. McGuinness, A. Whittemore, and C. Chung. 1998. A Checklist of the Hepatics and Anthocerotes of Panama. *Tropical Bryology*, 15:167–195. https://doi.org/10.11646/bde.15.1.14

Suárez, G. M., M. M. Schiavone, and M. T. Colotti. 2014. The Genus *Holomitrium* (Dicranaceae, Bryophyta), New Record in Argentina and Uruguay. *Boletín de la Sociedad Argentina de Botánica*, 49:457–461. https://doi.org/10.31055/1851.2372.v49.n4.9823

Tsubota, H., H. Akiyama, T. Yamaguchi, and H. Deguchi. 2001. Molecular Phylogeny of the Sematophyllaceae (Hypnales, Musci) Based on Chloroplast *rbcL* Sequences. *Journal of the Hattori Botanical Laboratory*, 90:221–240.

Turetsky, M. R. 2003. The Role of Bryophytes in Carbon and Nitrogen Cycling. *Bryologist*, 106:395–409. https://doi.org/10.1639/05

Vanderpoorten, A., and B. Goffinet. 2009. *Introduction to Bryophytes*. Cambridge: Cambridge University Press.

van Zanten, B. O. 1978. Experimental Studies on Trans-Oceanic Long-Range Dispersal of Moss Spores in the Southern Hemisphere. *Journal of the Hattori Botanical Laboratory*, 44:455–482.

van Zanten, B. O., and T. Pócs. 1981, Distribution and Dispersal of Bryophytes. *Advances in Bryology*, 1:479–562.

Villarreal, J. C., N. Cusimano, and S. S. Renner. 2015. Biogeography and Diversification Rates in Hornworts: The Limitations of Diversification Modeling. *Taxon*, 64:229–238. https://doi.org/10.12705/642.7

Vitt, D. H., and H. P. Ramsay. 1985a. The *Macromitrium* Complex in Australasia (Orthotrichaceae: Bryopsida). Part I. Taxonomy and Phylogenetic Relationships. *Journal of the Hattori Botanical Laboratory*, 59:325–451.

Vitt, D. H., and H. P. Ramsay. 1985b. The *Macromitrium* Complex in Australasia (Orthotrichaceae: Bryopsida). Part II. Distribution, Ecology and Paleogeography. *Journal of the Hattori Botanical Laboratory*, 59:453–468.

Wei, Y.-M., R.-L. Zhu, and S. R. Gradstein, 2014. Notes on Early Land Plants Today. 49. On *Lejeunea huctumalcensis* Lindenb. & Gottsche and the Resurrection of *Otigoniolejeunea* (Spruce) Schiffn., an Older name for *Physantholejeunea* R. M. Schust. (Marchantiophyta, Lejeuneaceae). *Phytotaxa*, 162:236–238. https://doi.org/10.11646/phytotaxa.162.4.8

Ye, W., Y.-M. Wei, A. Schäfer-Verwimp, and R.-L. Zhu. 2015. Phylogenetic Position of *Oryzolejeunea* (Lejeuneaceae, Marchantiophyta): Evidence from Molecular Markers and Morphology. *Journal of Systematics and Evolution*, 51:468–475. https://doi.org/10.1111/j.1759-6831.2012.00238.x

Zotz, G., B. Büdel, A. Meyer, H. Zellner, and O. L. Lange. 1997. Water Relations and CO$_2$ Exchange of Tropical Bryophytes in a Lower Montane Rain Forest in Panama. *Botanica Acta*, 110:9–17. https://doi.org/10.1111/j.1438-8677.1997.tb00605.x

6. The Role of Epiphytes in Rainfall Interception by a Lower Montane Tropical Forest in Panama

Diana Carolina Gómez González,[1*] *Gerhard Zotz,*[2,3] *and Maaike Y. Bader*[4]

ABSTRACT. Lower montane tropical forests are typically characterized by substantial epiphyte loads. One of the important ecological roles of epiphytes in these forest systems is the interception of rainwater with a major impact on forest hydrology. Several morphological traits of epiphytes assure a dependable water supply and greatly increase the water-holding capacity of the forest canopy. We quantified the epiphyte water-holding capacity at the stand level and the effect of epiphytes on rainfall interception and stemflow in lower montane tropical forest at Fortuna Forest Reserve, western Panama. Specifically, we determined the water-holding capacity of all epiphytic matter from 22 tree trunks varying in diameter at breast height (DBH) and from 28 canopy branches. We extrapolated our data to the stand level on the basis of biomass–tree-size relationships and using tree DBH data from a nearby 1 ha plot. The stand-level epiphytic water-holding capacity was estimated at 2.5 mm. From rainfall, throughfall, and stemflow data, we estimated total canopy interception to be 40% of this value. Interception by epiphytes alone would be about 20% (0.5 mm d^{-1}) assuming water-holding capacity to be fully exchanged on a daily basis, but this measure decreases to much lower values considering that epiphytic matter in the forest studied normally maintains its capacity partially filled. We also compared stemflow from stem-halves with and without epiphytes of 12 of the 22 trees. Variation was large, but on average, epiphytes reduced stemflow, indicating a modest effect on water and probably nutrient fluxes through stemflow at the stand level. Epiphytes play a special role in the hydrology of the Fortuna forest, making it pertinent to understand their responses to ongoing climatic changes to predict changes in local and regional hydrological patterns.

INTRODUCTION

The abundance and diversity of epiphytes in tropical montane cloud forests (TMCFs) can strongly influence the hydrology of the entire forest (Darby et al., 2016; Gotsch et al., 2016; Hölscher et al., 2004; Köhler et al., 2007), as epiphytes can intercept large fractions of total precipitation because of their high water-holding capacity (Hölscher et al., 2004). Nonvascular epiphytes, in particular, have been shown to play a major role in forest hydrology, while the impact of vascular epiphytes seems to be generally modest (Zotz, 2016). For example, epiphytic mosses can hold several times their own mass in water (Frahm, 1990; Kürschner and Parolly, 2004; Pócs 1980), with typical values of up to 400% of their dry mass (Hölscher et al., 2004; Köhler et al., 2007) and records of >1,000% in some cushion mosses (Zotz et al., 1997). As mosses tend to be very abundant in TMCFs, these plants can thus significantly increase the overall water-holding capacity of the canopies of such forests (Hölscher et al., 2004; Köhler et al., 2007). The water-holding capacity of mosses at the stand level in a lower montane tropical forest (LMTF) in Costa Rica has been estimated to exceed 40,000 L ha^{-1} (Köhler et al., 2007). Although vascular epiphytes may not play as important a role hydrologically as nonvascular epiphytes, this may be different for tank bromeliads, which can hold considerable amounts

---

[1] Vicerrectoría de Investigación y Posgrado, Universidad Autónoma de Chiriquí.

[2] Functional Ecology, Institute of Biology and Environmental Sciences, University of Oldenburg, Germany.

[3] Smithsonian Tropical Research Institute, Apartado 0843-03092, Balboa, Ancon, Republic of Panama.

[4] Ecological Plant Geography, Faculty of Geography, University of Marburg, Germany.

* Correspondence: diana.gomez@unachi.ac.pa

of water in their overlapping leaf bases (Zotz et al., 1999). Still, existing estimates of their water-holding capacity do not reach the magnitude of bryophytes: the highest published value is 33,000 L ha^{-1} in a dwarf forest with very high tank-bromeliad density in Puerto Rico (Richardson et al., 2000).

The process in which rainfall is captured by the vegetation (including tree foliage, branches, and epiphytes) and returned directly to the atmosphere without reaching the ground is called *interception loss* (Bakar et al., 2012; Nadkarni and Sumera, 2004). Interception loss can be estimated as the difference between rainfall reaching the canopy and the sum of throughfall and stemflow under the canopy (Crockford and Richardson, 2000; McJannet et al., 2007). Throughfall is the water that reaches the soil as it drips off the plant canopy, and stemflow is the water that flows down the stems until it reaches the base of the plants (Garcia-Estringana et al., 2010). Estimates of rainfall interception in tropical montane forests vary considerably. For example, Veneklaas and Van Ek (1990) report 13% of interception loss in a tropical upper-montane cloud forest (TUMCF) in Colombia, whereas Ataroff and Rada (2000) report 51% for a TUMCF in Venezuela.

As epiphytes can modify canopy temperature and circulation patterns (Clark et al., 1998; Freiberg, 2001), they also affect canopy evaporation rates (Van Stan et al., 2016), so the effect on interception is not only through direct water capture. Intercepted water starts to evaporate immediately after or even during a rainfall event (Garcia-Estringana et al., 2010). Even though epiphytic matter (dead and alive epiphytic components) can have a large water-holding capacity, this capacity will affect total interception only if it is not already used, that is, if the epiphytes are not more or less saturated with water due to previous precipitation (Calder, 2001). Therefore, the realized interception will also strongly depend on rainfall dynamics as well as the canopy microclimate at each site (Gotsch et al., 2016; Zotz, 2016).

A recent review of stemflow studies (Levia and Germer, 2015) shows that the funneling of precipitation to the base of the tree stem significantly affects a number of ecohydrological processes in wooded ecosystems. Stemflow is likely to be higher on larger trees because their canopy leaf area is larger. Therefore, tree size should affect the amount of stemflow. This positive relationship was observed in *Picea sitchensis* plantations in southern Scotland (Ford and Deans, 1978). However, Johnson (1990) found that, despite the greater crown size, stemflow was inversely correlated with tree age and interception capacity in a forest in highland Scotland. Due to different crown architectures, tree-size–stemflow relationships are probably species-specific as well as dependent on forest canopy structure. For cloud forest trees, the relationship between stemflow and tree size is not known, but characteristics such as leaf pubescence, insertion angle of the leaves, rigidity of the branches, and structure of the tree canopy are determining factors for the water-storage capacity, both directly and by affecting the accumulation of epiphytic biomass (Garcia-Estrigana et al., 2010), and thus these factors also affect stemflow.

Stemflow begins at the base of branches. If something obstructs the path along the branch to the stem, drip points will occur, turning potential stemflow into throughfall (Williams, 2004). If the obstruction is capable of absorbing water, as in the case of a dry epiphyte, it may also turn potential stemflow into intercepted canopy water. Therefore, the presence of epiphytes on trunks should decrease stemflow. However, Fleischbein et al. (2005) and Oyarzún et al. (2011) addressed this question and found no such relationship in a lower montane forest in Ecuador and in forest in the Andes of south-central Chile, respectively.

Overall, there is substantial variation in currently available data on hydrological processes in forests, particularly in the tropics. The role of epiphytes in these processes is even less well understood, with widely varying results obtained in different studies. Thus, there is a need for more data to assess the roles of epiphytes on water cycling in tropical forests. The purposes of this study were (1) to estimate the water-holding capacity of different components of epiphytic matter at the stand level in the LMTF of the Fortuna Forest Reserve, (2) to assess the influence of vascular and nonvascular epiphytes on stemflow, (3) to calculate interception losses in this forest at the stand level, and (4) to estimate the relative contribution of epiphytes to total interception in this forest.

STUDY SITE AND CLIMATIC CONDITIONS

The study site was located in an LMTF in the Fortuna Forest Reserve (FFR), in western Panama, in the Quebrada Honda watershed (8°45′40″N, 82°14′22″W, 1,150 m above sea level [asl]). Important tree species at the location include *Oreomunnea mexicana*, *Quercus* sp., and genera including *Hedyosmum*, *Faramea*, *Trichilia*, *Guettarda*, *Ardisia*, and *Inga* (Gómez González et al., 2017). Long-term data (Prada et al., 2017) indicate annual precipitation of ~3,500 mm y^{-1}. Due to equipment failure, precipitation could be quantified only for part of the study period, from May to November 2014: 2,461 mm (HOBO RG3 data-logging rain gauge [Onset Computer Corp., Cape Cod, MA, USA] located ~20 m outside the forest). The mean temperature was 18°C according to recordings using HOBO data logging.

MATERIALS AND METHODS

Sampling of Epiphytic Matter

We sampled trunk and branch epiphytic matter (sensu Zotz, 2016), separating dead and live epiphytic components. Trees were climbed using single-rope techniques or were accessed with ladders in the case of smaller trees. Epiphytic matter of 22 trees of different DBHs and species was sampled from one-half of the entire tree trunk (from the beginning of the crown down to the base). Epiphytic matter in the tree crowns was estimated by sampling all epiphytes from 28 branches (2–11 cm basal diameter) from 15 trees after cutting and lowering the branches to the ground. This allowed us to establish the relationship between branch diameter and epiphytic matter and obtain an estimate of the epiphytic matter on the branches of the 22 sampled trees. Epiphytic matter per stand area was derived from the relationship between epiphytic matter and tree DBH and information on DBH distributions of all trees greater than 5 cm in a nearby 1 ha plot (Prada et al., 2017; see Gómez González et al., 2017, for details of the sampling and estimates of epiphytic matter).

Water-Holding Capacity of Epiphytic Matter

In the laboratory, the epiphytic matter was separated into five components: dead organic matter (DOM), lichens, bryophytes, vascular-plant epiphytes, and vascular-plant hemiepiphytes and nomadic vines (lumped into one group; for definitions of different life forms, see Zotz, 2016). Vascular plants were identified and voucher specimens were deposited in the herbaria of the University of Panama (PMA) and University of Chiriquí (UCH). For detailed results, see Gómez González et al. (2017).

Vascular plants were weighed within 2 h of collection to obtain fresh weights. Maximum water-holding capacity was determined gravimetrically after immersion in water for 5 h and subsequent draining for 30 min, and comparison was made of this saturated mass with sample fresh mass (for vascular plants; modified from Veneklaas and van Ek, 1990) or sample dry mass (for DOM and bryophytes; lichen biomass was negligible and not further considered). The different reference masses for the groups are related to the hydration dynamics of the groups: DOM and bryophytes can potentially dry out completely and thus absorb and release water relative to their dry weight, whereas vascular plants (except filmy ferns with negligible biomass in our samples) maintain a more or less constant internal water content, so that water is intercepted and released from their surface only, which scales with plant fresh weight.

Additionally, to account for the water impounded in tank bromeliads, we measured the maximum tank water content of 17 tank bromeliads of different species ranging in fresh mass from 0.005 to 1.00 kg. The water-holding capacity of these tank bromeliads was regressed against their fresh mass, and the function obtained was used to estimate the water-holding capacity of bromeliads at the stand level. This estimate was based on measurements of the total bromeliad fresh mass on the sampled trees (all species identified except one, which is relatively rare, are classified as tank bromeliads). These estimates were then extrapolated to the stand scale on the basis of the relationship between bromeliad fresh mass and tree DBH and the DBH distributions of all trees >5 cm in the nearby 1 ha plot.

After saturated weights were determined, all material was dried at 60°C, and dry mass was determined after a period of 48 h (for most of the living tissues) or 96 h in the case of some Araceae and Bromeliaceae (depending on their size and level of succulence) and dead organic matter (modified from Chen et al., 2010).

The total water-holding capacity for each group was determined as (saturated mass − dry mass) ÷ dry mass for DOM and bryophytes, and as (saturated mass − fresh mass) ÷ fresh mass for vascular epiphytes. The water-holding capacity was extrapolated to the stand level on the basis of the estimated dry mass and fresh mass, respectively, of these epiphytic matter components in the nearby 1 ha forest plot (Gómez González et al., 2017).

Stemflow, Throughfall, and Rainfall Measurement

Interception, throughfall, and stemflow are all related to plant morphology, structure, and biomass (Garcia-Estringana et al., 2010). We therefore measured throughfall and stemflow under trees of different species, varying in DBH and structural characteristics.

Stemflow was determined for 12 of the 22 trees from which we had previously removed the epiphytic matter. Each trunk had two distinct halves: one-half of the column with intact epiphyte cover and the other half without epiphytes. We compared the amount of stemflow between these two treatments using collectors made of polyurethane foam collars fitted around the trunks 1 m above the forest floor. Each collar was divided in two halves that collected the stemflow from each half, with and without epiphytes, separately and drained into separate water collectors (Stanton et al., 2014; Levia et al., 2010, modified). The amounts of collected stemflow water were determined weekly from May 2014 to May 2015.

There was no relationship between the amount of stemflow and DBH of the tree trunks for either treatment ($R^2 = 0.01$, $P > 0.05$, treatment with epiphytes; and $R^2 = 0.21$, $P > 0.05$, treatment without epiphytes). Therefore, to calculate total stemflow at the stand level, the mean annual stemflow per half-trunk (16.6 ± 0.4 L, $n = 12$; treatment with epiphytes) and (24.4 ± 0.6 L, $n = 12$; treatment without epiphytes) was multiplied by two, converting half-trunks into whole-trunks, and by the number of trees ≥5 cm DBH in the 1 ha plot ($n = 5{,}318$, Prada et al., unpublished data census 2013).

Throughfall collectors were placed 1 m above the ground to avoid overestimation by splash water. In total, 24 collectors with a reception area of 240 cm^2 each were placed in the understory below the crown of the 12 trees where stemflow was measured (2 collectors below each tree). Collectors consisted of circular funnels attached to water collectors via a hose. A polyethylene net with a 0.5 mm mesh was placed in every funnel in order to minimize measurement errors due to organic material or insects blocking the funnel entrance. Similar to stemflow, throughfall was also measured every week from May 2014 to May 2015. Throughfall was extrapolated to the stand level by simple extrapolation of the amount collected per area.

Rainfall was measured by a tipping-bucket rain gauge (HOBO RG3) with a resolution of 0.2 mm. The rain gauge was located ~20 m outside the forest in a large clearing. Data were recorded from May 2014 to November 2014, after which the rain gauge stopped working. Tipping events per week were summed up to obtain weekly rain values to be compared with the simultaneous stemflow and throughfall measurements.

Interception losses were estimated from total rainfall, throughfall, and stemflow over the 27 wk period when rainfall was accurately recorded. Unfortunately, we could not use the graphical method suggested by Leyton et al. (1967) to estimate the water-holding capacity of a canopy from the relationship between throughfall and rainfall because this method requires data for single rain events, whereas we had only weekly totals.

RESULTS

Water-Holding Capacity of Epiphytic Matter

The water-holding capacity of epiphytic matter at the stand level was estimated at 25,390 L ha^{-1}, or 2.5 mm (Table 6.1). Dead organic matter contributed most to this capacity, with 13,266 L ha^{-1} (1.3 mm). This was due to the high contribution of DOM to epiphytic matter (62%) and the relatively high water-holding capacity per unit weight: 131% of dry mass (Table 6.1). Even though bryophytes represented just 6% of epiphytic matter in the forest, their very high water-holding capacity (734% of dry weight) explains their important contribution of 7,428 L ha^{-1} (0.7 mm; Table 6.1).

The water-holding capacity of individual bromeliads increased linearly with fresh mass ($R^2 = 0.90$, $P < 0.001$) and ranged from 0.02 to 0.65 L (Figure 6.1). We found 311 bromeliads on the sampled trees and estimated the total fresh mass at 15,077 kg ha^{-1}. Using the linear relationship obtained, we estimated the stand-level water-holding capacity of all tank bromeliads at 2,700 L ha^{-1} (0.2 mm), that is, 10% of the total.

Stemflow, Throughfall, Rainfall, and Interception

Total rainfall from 15 May 2014 to 10 November 2014 was 2,461 mm. Throughfall during the same 27 wk period was 1,471 ± 26 mm (mean ± SD, $n = 24$), corresponding to 59% of rainfall. During this period, the average stemflow in the treatment without epiphytes was 18.2 ± 0.8 mm ($n = 12$) compared to 10.7 ± 0.4 mm ($n = 12$) with epiphytes. Stemflow thus represented 0.7% (treatment without epiphytes) and 0.4% (control with epiphytes) of rainfall. Based on these totals, interception loss was estimated at 40%.

The effect of epiphyte cover on stemflow was consistent through time, with average stemflow of trunk portions with epiphytes being nearly always similar to or lower than stemflow on those without (Figure 6.2). However, between trees, the effect of epiphyte cover was highly variable (Figure 6.3). In five trees with high stemflow, the half-trunks without epiphytes yielded more water, whereas in one tree with high stemflow, this pattern was reversed. In the trees with lower stemflow, the two patterns were equally frequent. There was no relationship between DBH and stemflow (Pearson correlation, $P > 0.05$).

Rainfall was variable during the study period, which was, of course, reflected in the amount of throughfall (Figure 6.4). The lowest throughfall occurred in weeks 40 and 46 of the study year, corresponding to January and February 2015, which is the drier season in Panama (Figure 6.4). However, even during the drier season, it rained enough to create substantial throughfall every week except one, and drier periods never lasted more than 2 weeks.

As expected, the variation in throughfall plus stemflow was linearly related to rainfall (Figure 6.5). Temporal fluctuations in rainfall, throughfall, and stemflow were clearly correlated, but there were also some conspicuous discrepancies in particular weeks. For example, most rainfall peaks (those of weeks 1, 6, 9, 12, 18, 20, and 22) resulted in clear peaks in throughfall and stemflow,

TABLE 6.1. Total epiphytic matter (dry mass of dead organic matter (DOM) and bryophytes, fresh mass for vascular plants), total water-holding capacity at stand level, and water-holding capacity per unit mass of epiphytic matter in a tropical montane cloud forest at 1,150 m above sea level at Quebrada Honda, Fortuna Forest Reserve, western Panama.

	Matter (*dry mass*) in forest (kg ha^{-1})	**Water-holding capacity (l ha^{-1})**	**Water-holding capacity (% of *dry* weight)**
DOM	10,136	13,266	131
Bryophytes	1,012	7,428	734
	Matter (*fresh* weight) in forest (kg ha^{-1})	**Water-holding capacity (l ha^{-1})**	**Water-holding capacity (% of *fresh* weight)**
Hemiepiphytes	1,481	363	25
Vascular plants	4,893	1,633	33
Tank bromeliads	15,077	2,700	50
Total	32,599	25,390	—

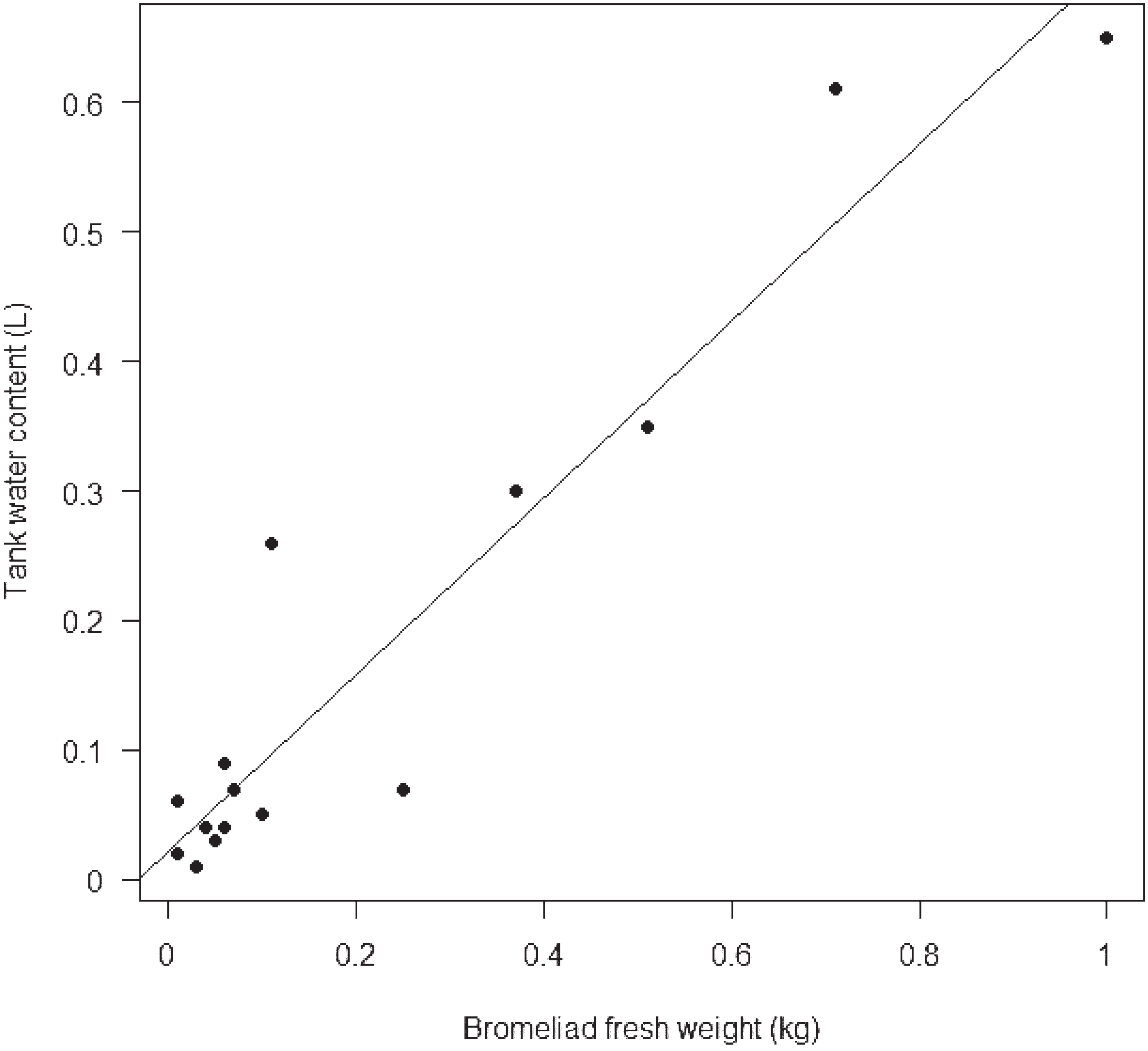

FIGURE 6.1. Relationship between the tank water-holding capacity and plant size of bromeliads (including different species) collected from a lower montane forest at Quebrada Honda, Fortuna Forest Reserve, western Panama (tank water content = 0.02 + 0.68 × bromeliad fresh weight, $R^2 = 0.90$, $P > 0.001$, Pearson regression model).

whereas the peaks in weeks 15 and 26 did not result in a response in either throughfall or stemflow (Figure 6.4). From week 28 onward, we have no data for rainfall, but despite peaks in throughfall between weeks 30 and 40, stemflow stayed low. Another interesting observation is that in weeks 24 to 39 (Figures 6.2 and 6.4), after and during a period of high rainfall, we found no difference between stem-halves with and without epiphytes.

DISCUSSION

Because of the irregularity of their water supply, many epiphytes are specialized to absorb and retain water very effectively, leading to the expectation of a large water-holding capacity of the epiphytes in the Fortuna forest. In our study, epiphytic matter was estimated at 16,439 kg ha^{-1} (Gómez González et al., 2017),

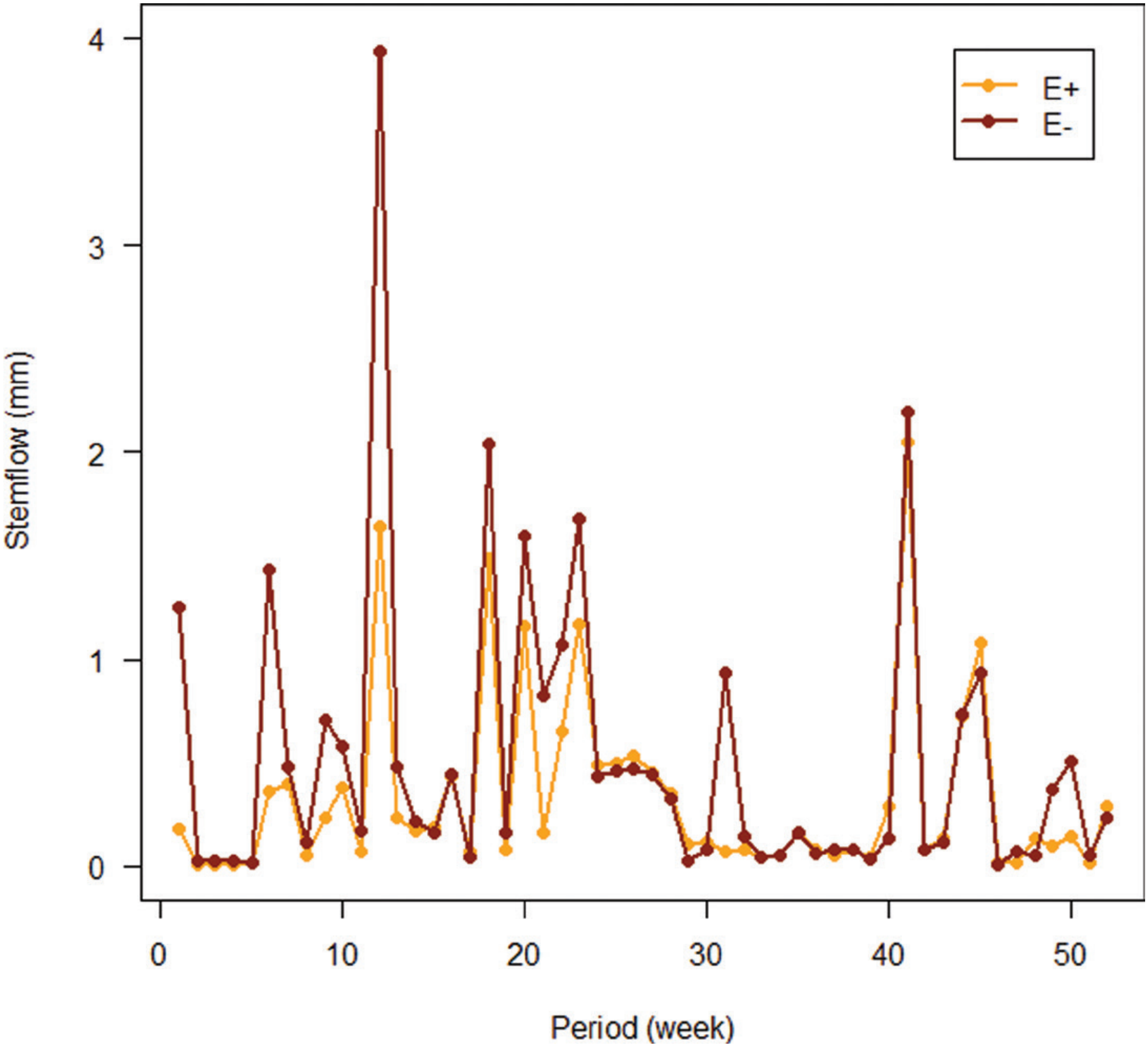

FIGURE 6.2. Average weekly stemflow (mm) from 12 half-trunks with epiphytes (E+) paired with half-trunks without epiphytes (E−) in a period of 52 weeks (May 2014-May 2015) in a lower montane tropical forest (1,150 m asl) in western Panama (Quebrada Honda, Fortuna).

which in turn could hold 25,390 l ha^{-1}, or 2.5 mm, of water. Theoretically, if this capacity were to be filled up daily, which would require a daily shower followed by desiccating conditions to return all water back to the atmosphere, it would result in an annual interception potential exceeding 900 mm. As total precipitation over 27 weeks was 2,461 mm, which could be extrapolated to ~4,700 mm y^{-1} rainfall (assuming relatively constant conditions), this would be equivalent to an interception of about 20% by epiphytic matter alone.

However, this daily filling and draining scenario is not realistic in Fortuna or any moist forest. Our data do not allow us to estimate the contribution of epiphytes to the 40% interception at the stand level, but it will certainly be much less than the theoretical maximum of 20% mentioned in the preceding

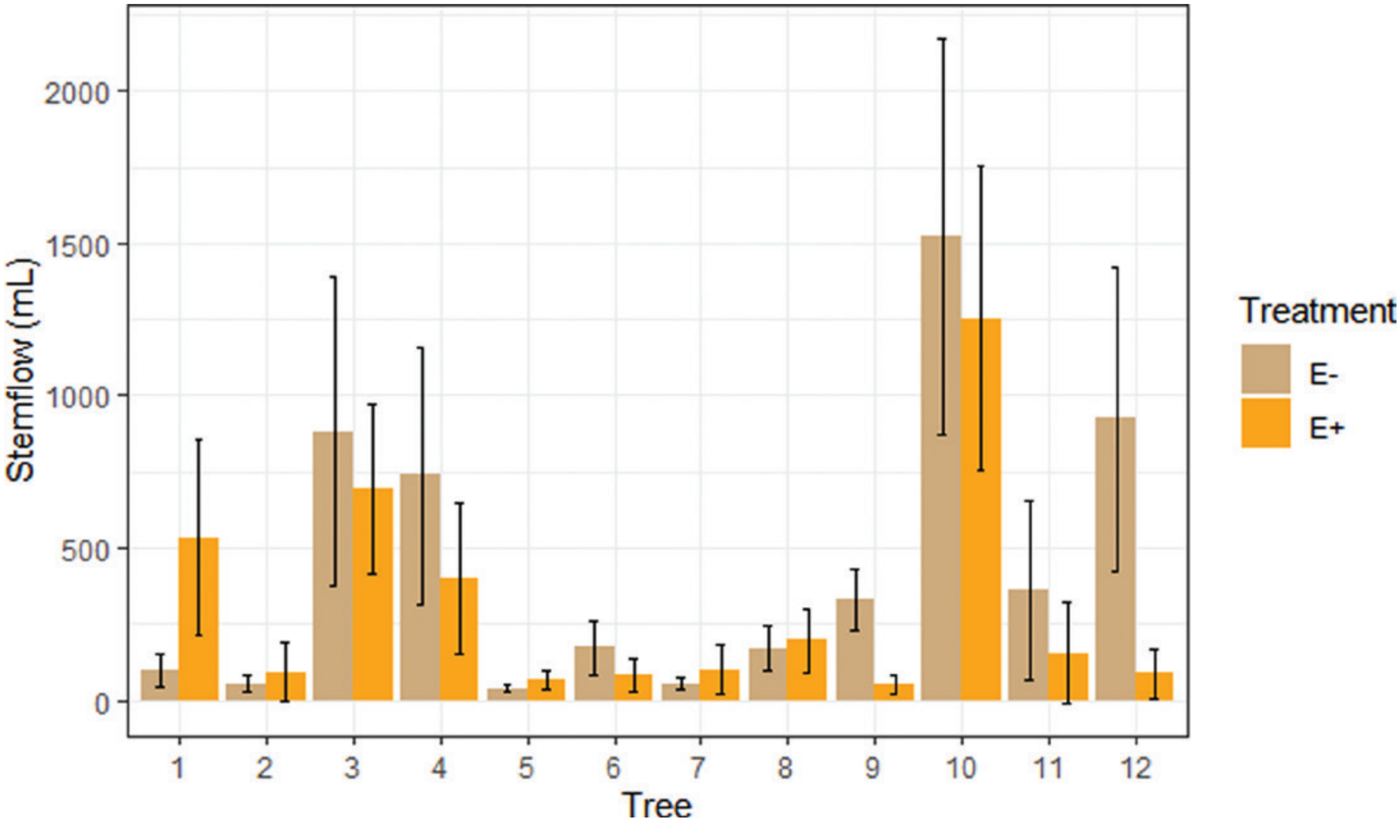

FIGURE 6.3. Mean total stemflow (ml) from 12 half-trunks with epiphytes (E+) paired with half-trunks without epiphytes (E–) with different diameter at breast height (ordered by DBH, from small, to large [cm]) over a period of 52 weeks (May 2014–May 2015) in a lower montane tropical forest (1,150 m asl) in western Panama (Quebrada Honda, Fortuna).

paragraph. Actual interception depends on how much of the water-holding capacity is already used, which in turn depends on temporal and spatial precipitation patterns, including occult or horizontal precipitation such as fog, and on evapotranspiration rates (Hölscher et al., 2004). These dependencies appear to be reflected in the temporal patterns of throughfall relative to rainfall, as shown in Figure 6.5, where in some weeks following a week with low rainfall (e.g., weeks 15 and 26), high rainfall was not associated with high throughfall. We suspect that, during this time, the canopy was relatively dry, and interception therefore was particularly high.

Our estimation of 2.5 mm of water-holding capacity at the stand level is within the range previously reported for tropical upper montane forests (2–5 mm) in studies using similar direct measurement methods (Hölscher et al., 2004; Köhler et al., 2007; Veneklaas and Van Ek, 1990). It agrees particularly well with the capacity of 2.6 mm calculated by Cavelier et al. (1997) for interception in a forest in another part of the Fortuna Forest Reserve. These authors based their estimate on the method of Leyton et al. (1967) using rainfall and throughfall data for individual rain events.

Likewise, the estimated canopy interception (40%) is within the range of values (Veneklaas and Van Ek, 1990; Ataroff and Rada, 2000) reported from other tropical montane forests (Cavelier et al., 1997; Hölscher et al., 2004; Oyarzun et al., 2011) and, again, almost identical to an estimated 37% for a nearby forest (Cavelier et al., 1997). These values may be due to the dense canopy and abundant epiphytes present. Still, the actual amount of water captured in the canopy may be even higher than suggested by this balance between rainfall and throughfall because of additional water inputs by fog, which is frequent in our study area. Intercepted water from passing clouds could even result in throughfall exceeding rainfall on some days, which would result in negative interception estimates. Even in less extreme cases, not accounting for fog input is likely to lead to an underestimation of canopy interception.

It has been suggested that the presence of epiphytes results in decreased stemflow and an increase in interception loss (Garcia-Estringana et al., 2010; Van Stan and Pypker, 2015). As stemflow can be an important source of nutrients for trees, this implies effects of epiphytes on nutrient fluxes (Stanton et al., 2014). However, differences between the amount of stemflow on trunks

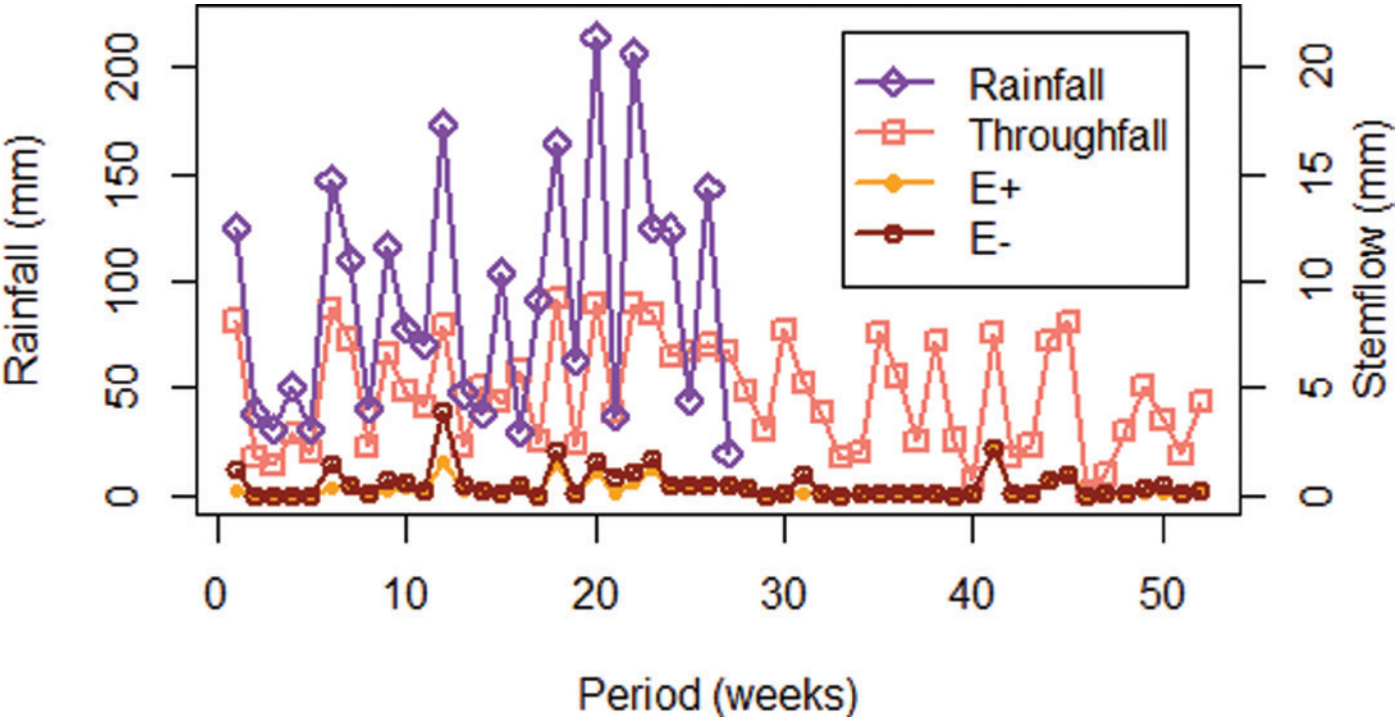

FIGURE 6.4. Weekly rainfall, throughfall (mean from 24 recipients with a 240 cm^2 each), and stemflow (means of 12 trunks with epiphytes [E+] and without epiphytes [E−]) in a lower montane tropical forest in western Panama (Quebrada Honda, Fortuna). Shown are weekly totals for 52 weeks (May 2014–May 2015) for throughfall and stemflow and 27 weeks (May–November 2014) for rainfall.

with and without epiphytes were inconsistent. Fleischbein et al. (2005) mentioned that the amount of stemflow decreases in the presence of bryophytes and lichens but tends to increase in the presence of vascular epiphytes in a tropical lower montane forest in the south Ecuadorian Andes. Such contrasting effects of vascular and nonvascular epiphytes may partly explain our results, because the epiphytic vegetation was composed of a mixture of both groups. There was a dominance of vascular epiphytes in terms of biomass, but we can expect a disproportionately large effect of bryophytes due to their larger water-holding capacity. Variation in stemflow between trunk-halves can also arise from local asymmetries in the canopy or inclination of the trunks. Overall, our data suggest a generally negative effect of epiphytes on stemflow. However, the large variation between trees requires that this experiment be repeated with a larger sample size. Conversely, the duration of the experiment can be reduced to cover only a few rainy weeks, because the differences between the treatments were quite consistent through time. It should also be considered that stemflow is initiated in the crown, so that manipulating only trunk epiphytes should not affect stemflow as much as a full canopy manipulation would.

According to Stanton et al. (2014), the presence of epiphytes affects host plants because epiphytes take up water that would otherwise reach the soil and benefit the tree. This may be the case in the coastal fog deserts of their study, because (1) canopies and epiphytes are frequently dry, and epiphytes can take up water according to their water-holding capacity; and (2) vegetation is strongly moisture limited. In our forest, however, neither condition was met, so that negative effects on host trees via hydrological changes are less likely. However, another observation by Stanton et al. (2014), the stabilization of the forest microclimate through the slow release of water, should be relevant in our study system as well, particularly for the epiphytes themselves.

In summary, rainfall interception was high in the studied forest of the Fortuna Forest Reserve (40%). This is partly related to the high water-holding capacity of the abundant epiphytic matter, even if the potential 20% interception by epiphytes is never reached because part of the capacity is always used in this environment with frequent rainfall and prevailing high humidity. The presence of epiphytes on tree trunks reduced the amount of stemflow not on every single tree but on average. This indicates that at the stand level, stem epiphytes affect stem water fluxes modestly but that, potentially more important, they may also affect nutrient fluxes. Even though we could not quantify all contributions of epiphytes to hydrological fluxes in detail, our study documents their role in increasing the water-holding capacity of the forest and in redirecting flows. These hydrological roles, as well as other ecosystem functions, such as carbon storage and habitat provision for other organisms, highlight the importance of monitoring and understanding the fate of these aerial plants to ongoing climatic changes.

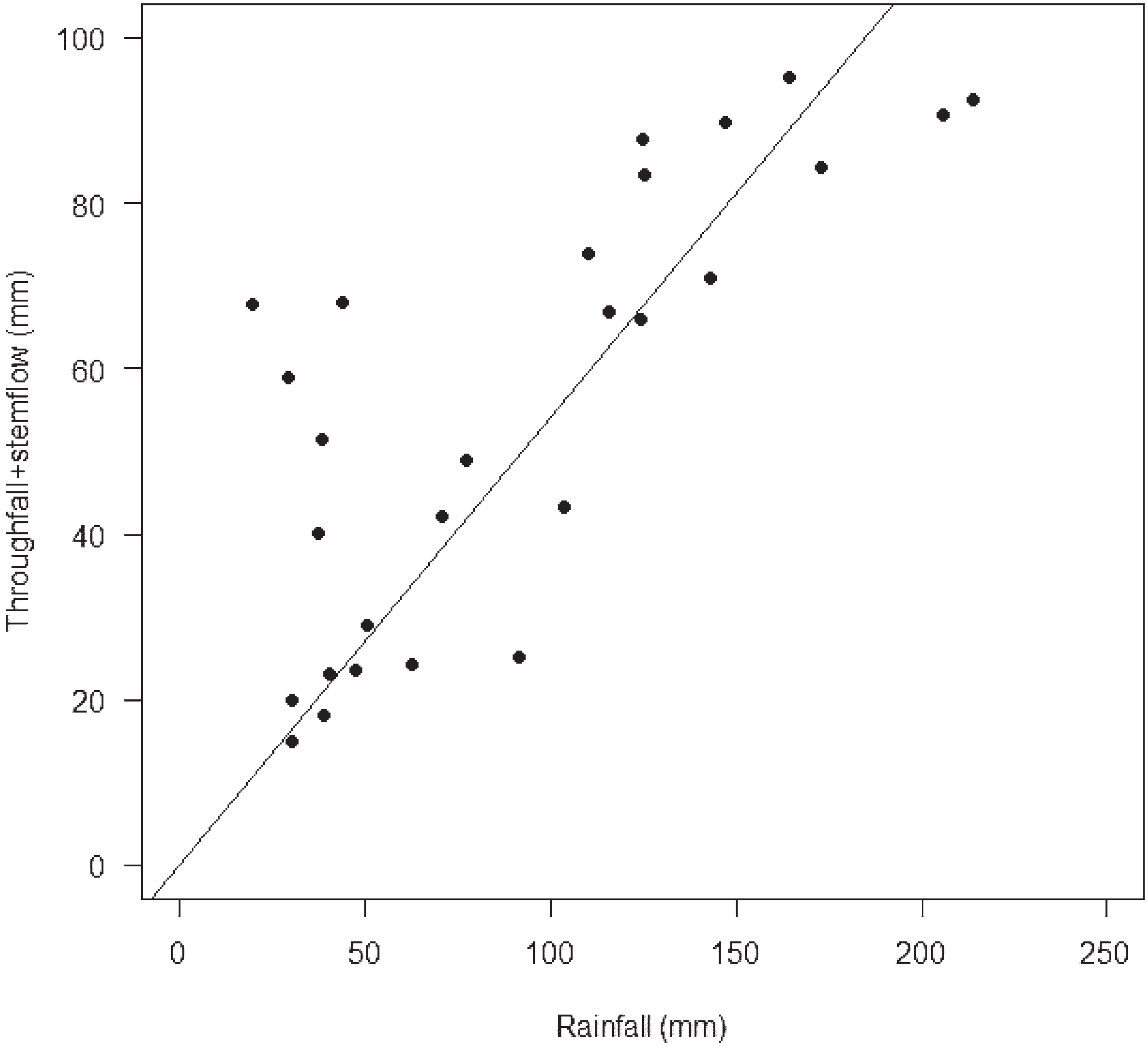

FIGURE 6.5. Relationship between weekly averages of throughfall + stemflow (mm) and rainfall (mm) for a period of 27 weeks in Quebrada Honda, Fortuna Forest Reserve, western Panama. The solid line gives the result of a linear regression (throughfall = 22.65 + 0.36 rainfall; $R^2 = 0.59$, $P < 0.0001$).

ACKNOWLEDGMENTS

We thank Jim Dalling, Katherine Heineman, and Margarita Prada at the University of Illinois Urbana-Champaign for sharing tree plot data. Many thanks also to René Araúz, Eduardo Gómez, Carolina González, and Carlos Espinoza for their help during fieldwork. This project was financially supported by SENACYT (Secretaría Nacional de Ciencia y Tecnología), Panamá.

REFERENCES

Ataroff, M., and F. Rada. 2000. Deforestation Impact on Water Dynamics in a Venezuelan Andean Cloud Forest. *Journal of the Human Environment*, 29:440–444. https://doi.org/10.1579/0044-7447-29.7.440

Bakar, A. A., A. Bin Bki, N. Bt Hamzah, Z. Bin Yusop, and M. K. Bin Khalil. 2012. Throughfall, Stemflow and Interception Loss of Artificial Tropical Forest. In *CHUSER 2012: 2012 IEEE Colloquium on Humanities, Science and Engineering*, ed. IEEE Malaysia Section, Power Electronics, Industrial Electronics, and Industrial Applications Joint Chapter, pp. 98–202. Piscataway, NJ: IEEE.

Calder, I. R. 2001. Canopy Processes: Implications for Transpiration, Interception and Splash Induced Erosion, Ultimately for Forest Management and Water Resources. *Plant Ecology*, 153:203–214. https://doi.org/10.1023/A:1017580311070

Cape, J. N., A. H. F. Brown, S. M. Robertson, G. Howson, and I. S. Paterson. 1991. Interspecies Comparisons of Throughfall and Stemflow at Three Sites in Northern Britain. *Forest Ecology and Management*, 46:165–177. https://doi.org/10.1016/0378-1127(91)90229-O

Cavelier, J., M., Jaramillo, D. Solis, and D. De León. 1997. Water Balance and Nutrient Inputs in Bulk Precipitation in Tropical Montane Cloud Forest in Panama. *Journal of Hydrology*, 193:83–96. https://doi.org/10.1016/S0022-1694(96)03151-4

Chen, L., W.-Y. Liu, and G.-S. Wang. 2010. Estimation of Epiphytic Biomass and Nutrient Pools in the Subtropical Montane Cloud Forest in the Ailao Mountains, South-Western China. *Ecological Research*, 25:315–325. https://doi.org/10.1007/s11284-009-0659-5

Clark, K. L., N. M. Nadkarni, and H. L. Gholz. 1998. Growth, Net Production, Litter Decomposition, and Net Nitrogen Accumulation by Epiphytic Bryophytes in a Tropical Montane Forest. *Biotropica*, 30:12–23. https://doi.org/10.1111/j.1744-7429.1998.tb00365.x

Crockford, R. H., and D. P. Richardson. 2000. Partitioning of Rainfall into Throughfall, Stemflow and Interception: Effect of Forest Type, Ground Cover and Climate. *Hydrological Processes*, 14:2903–2920. https://doi.org/10.1002/1099-1085(200011/12)14:16/17<2903::AID-HYP126>3.0.CO;2-6

Darby, A., D. Draguljic, A. Glunk, and S. G. Gotsch. 2016. Habitat Moisture Is an Important Driver of Patterns of Sap Flow and Water Balance in Tropical Montane Cloud Forest Epiphytes. *Oecologia*, 182:357–371. https://doi.org/10.1007/s00442-016-3659-5

Fleischbein, K., W. Wilcke, R. Goller, J. Boy, C. Valarezo, W. Zech, and K. Knoblich. 2005. Rainfall Interception in a Lower Montane Forest in Ecuador: Effects of Canopy Properties. *Hydrological Processes*, 19:1355–1371. https://doi.org/10.1002/hyp.5562

Ford, E. D., and J. D. Deans. 1978. The Effects of Canopy Structure on Stemflow, Throughfall and Interception Loss in a Young Sitka Spruce Plantation. *Journal of Applied Ecology*, 15:905–917. https://doi.org/10.2307/2402786

Frahm, J. P. 1990. Bryophyte Phytomass in Tropical Ecosystems. *Botanical Journal of the Linnean Society*, 104:23–33. https://doi.org/10.1111/j.1095-8339.1990.tb02209.x

Freiberg, M. 2001. The Influence of Epiphyte Cover on Branch Temperature in a Tropical Tree. *Plant Ecology*, 153:241–250. https://doi.org/10.1023/A:1017540629725

Garcia-Estringana, P., N. Alonso-Blazquez, and J. Alegre, 2010. Water Storage Capacity, Stemflow and Water Funneling in Mediterranean Shrubs. *Journal of Hydrology*, 389:363–372. https://doi.org/10.1016/j.jhydrol.2010.06.017

Gómez González, D. C., C. Rodríguez Quiel, G. Zotz, and M. Y. Bader. 2017. Species Richness and Biomass of Epiphytic Vegetation in a Tropical Montane Forest in Western Panama. *Tropical Conservation Science*, 10:1–17. https://doi.org/10.1177/1940082917698468

Gotsch, S. G., N. Nadkarni, and A. Amici. 2016. The Functional Roles of Epiphytes and Arboreal Soils in Tropical Montane Cloud Forests. *Journal of Tropical Ecology*, 32:455–468. https://doi.org/10.1017/S026646741600033X

Hölscher, D., L. Köhler, A. I. J. M. Van Dijk, and L. A. Bruijnzeel. 2004. The Importance of Epiphytes to Total Rainfall Interception by a Tropical Montane Rain Forest in Costa Rica. *Journal of Hydrology*, 292:308–322. https://doi.org/10.1016/j.jhydrol.2004.01.015

Johnson, R. C. 1990. The Interception, Throughfall and Stemflow in a Forest in Highland Scotland and the Comparison with Other Upland Forests in the U.K. *Journal of Hydrology*, 118:281–287. https://doi.org/10.1016/0022-1694(90)90263-W

Köhler, L., C. Tobón, K. F. A. Frumau, and L. A. Bruijnzeel. 2007. Biomass and Water Storage Dynamics of Epiphytes in Old-Growth and Secondary Montane Cloud Forest Stands in Costa Rica. *Plant Ecology*, 193:171–184. https://doi.org/10.1007/s11258-006-9256-7

Kürschner, H., and G. Parolly. 2004. Phytomass and Water-Storing Capacity of Epiphytic Rain Forest Bryophyte Communities in S Ecuador. *Botanische Jahrbücher*, 125:489–504. https://doi.org/10.1127/0006-8152/2004/0125-0489

Leyton, L., E. R. C. Reynolds, and F. B. Thompson. 1967. Rainfall Interception in Forest and Moorland. In *International Symposium on Forest Hydrology*, ed. E. Sopper and H. W. Lull, pp. 163–178. New York: Pergamon Press.

Levia, D. F., J. T. Van Stan II, S. M. Mage, and P. W. Kelley-Hauske. 2010. Temporal Variability of Stemflow Volume in a Beech-Yellow Poplar Forest in Relation to Tree Species and Size. *Journal of Hydrology*, 380:112–120. https://doi.org/10.1016/j.jhydrol.2009.10.028

Levia, D. F., and S. Germer. 2015. A Review of Stemflow Generation Dynamics and Stemflow-Environment Interactions in Forests and Shrublands. *Reviews of Geophysics*, 53:673–714. https://doi.org/10.1002/2015RG000479

Mcjannet, D., J. Wallace, and P. Reddell. 2007. Precipitation Interception in Australian Tropical Rainforests: I. Measurement of Stemflow, Throughfall and Cloud Interception. *Hydrological Processes*, 21:1692–1702. https://doi.org/10.1002/hyp.6347

Nadkarni, N. M., and M. M. Sumera. 2004. Old-Growth Forest Canopy Structure and Its Relationship to Throughfall Interception. *Forest Science*, 50:290–298.

Oyarzún, C. E., R. Godoy, J. Staelens, P. J. Donoso, and N. E. C. Verhoest. 2011. Seasonal and Annual Throughfall and Stemflow in Andean Temperate Rainforests. *Hydrological Processes*, 25:623–633. https://doi.org/10.1002/hyp.7850

Pócs, T. 1980. The Epiphytic Biomass and Its Effect on the Water Balance of Two Rain Forest Types in the Uluguru Mountains (Tanzania, East Africa). *Acta Botanica Academiae Scientiarum Hungaricae*, 26:143–167.

Prada, C. M., A. Morris, K. M. Andersen, B. L. Turner, P. Caballero, and J. W. Dalling. 2017. Soils and Rainfall Drive Landscape-Scale Changes in the Diversity and Functional Composition of Tree Communities in Premontane Tropical Forest. *Journal of Vegetation Science*, 28:859–870. https://doi.org/10.1111/jvs.12540

Richardson, B. A., M. J. Richardson, F. Scatena, and W. McDowell. 2000. Effects of Nutrient Availability and Other Elevational Changes on Bromeliad Populations and Their Invertebrate Communities in a Humid Tropical Forest in Puerto Rico. *Journal of Tropical Ecology*, 16:167–188. https://doi.org/10.1017/S0266467400001346

Stanton, D. E., J. Huallpa Chávez, L. Villegas, F. Villasante, J. Armesto, L. O Hedin, H. Horn, and J. Dalling. 2014. Epiphytes Improve Host Plant Water Use by Microenvironment Modification. *Functional Ecology*, 28:1274–1283. https://doi.org/10.1111/1365-2435.12249

Van Stan, J. T. I., E. D. Gutmann, E. Lewis, and T. E. Gay. 2016. Modeling Rainfall Interception Loss for an Epiphyte-Laden *Quercus virginiana* Forest Using Reformulated Static- and Variable-Storage Gash Analytical Models. *Journal of Hydrometeorology*, 17:1985–1997. https://doi.org/10.1175/JHM-D-16-0046.1

Van Stan, J. T. I., and T. G. Pypker. 2015. A Review and Evaluation of Forest Canopy Epiphyte Roles in the Partitioning and Chemical Alteration of Precipitation. *Science of the Total Environment*, 536:813–824. https://doi.org/10.1016/j.scitotenv.2015.07.134

Veneklaas, E. J., and R. Van Ek. 1990. Rainfall Interception in Two Tropical Montane Rain Forests, Colombia. *Hydrological Processes*, 4:311–326. https://doi.org/10.1002/hyp.3360040403

Williams, M. B. 2004. Investigating the Contribution of Stemflow to the Hydrology of a Forest Catchment. BS thesis, University of Southampton, United Kingdom.

Zotz, G. 2016. *Plants on Plants–The Biology of Vascular Epiphytes*. Cham, Switzerland: Springer International.

Zotz, G., B. Büdel, A. Meyer, H. Zellner, and O. L. Lange. 1997. Water Relations and CO_2 Exchange of Tropical Bryophytes in a Lower Montane Rain Forest in Panama. *Plant Biology*, 110:9–17. https://doi.org/10.1111/j.1438-8677.1997.tb00605.x

Zotz, G., and V. Thomas. 1999. How Much Water Is in The Tank? Model Calculations for Two Epiphytic Bromeliads. *Annals of Botany*, 83:183–192. https://doi.org/10.1006/anbo.1998.0809

7. The Orchids of Fortuna, Panama: A Checklist of Photosynthetic Pathways, Growth Habitat, and Resource Acquisition

Katia Silvera[1,2]

ABSTRACT. Tropical montane forests are sites of known high orchid diversity, but their number of species, population health, and resource acquisition remain understudied. The Fortuna Forest Reserve in western Panama harbors orchid species with broad distribution and shared origins with North and South America as well as endemic and endangered species. In this chapter, recorded data from herbarium specimens and values of leaf stable isotopic composition of carbon ($\delta^{13}C$) and nitrogen ($\delta^{15}N$) inform an updated inventory of the orchid flora for Fortuna and an evaluation of the diversity of resource use strategies and patterns of nutrient utilization with implications for tropical montane orchid conservation. These data indicate that orchids can integrate different nitrogen (N) sources at a local scale. Epiphytic orchids show negative $\delta^{15}N$ values compared to terrestrial, suggesting an atmospheric signal from wet deposition in the form of ammonium and nitrate. Terrestrial species with higher N content and higher $\delta^{15}N$ may allow for an increase in photosynthesis, especially on exposed sites or road banks where light intensity is expected to be higher. Orchid conservation programs at Fortuna can be accomplished by focusing on inventories to monitor the diversity of orchids and by targeting individual key species on the long-term basis. An integrated approach with local agencies is required for long-term sustainability.

INTRODUCTION

Orchidaceae is one of the largest and most widespread families of vascular plants, with 30,080 species reported worldwide (Plants of the World Online [POWO], n.d.). Tropical montane forests are known sites for high orchid diversity, especially miniature species, because high rainfall, moist environments, and humidity promote epiphytism, which in turn is linked to accelerated diversification rates (Gravendeel et al., 2004; Givnish et al., 2015). The Mesoamerican region, which includes the western volcanic region of Panama, is particularly rich in orchid diversity – nearly 10% of all orchid species are found here (Bogarín et al., 2013; Bogarín et al., 2014). Panama has 1,432 reported orchid species (POWO, n.d.) and has one of the largest lists of endemic species from all of Mesoamerica (Bogarín et al., 2013). The Fortuna Forest Reserve in western Panama is one of the largest mid-elevation cloud forest sites in Central America, with at least 20% of the plant diversity for the country and a significant portion of species being endemic to this region (Dalling et al., this volume).

Epiphytes are one of the most frequent life forms found in tropical montane cloud forests, with orchids being by far the most species-rich group (Gradstein, 2008; Gómez González et al., 2017). Epiphytic orchids may have the ability to colonize fine-scale niche sites because altitudinal variations in fog deposition and micro-conditions within the branches of tree canopies create a multifaceted array of suitable conditions (Givnish et al., 2015). Orchid diversity in Panama peaks at altitudinal ranges between 1,000 and 1,500 m above sea level (asl) (Silvera et al., 2009; Givnish et al., 2015). The diversity at

---

[1] Department of Botany and Plant Sciences, University of California Riverside, 2150 Batchelor Hall, Riverside, CA 92521, USA.

[2] Smithsonian Tropical Research Institute, Apartado 0843-03092, Balboa, Ancon, Republic of Panama.

the Fortuna Forest Reserve has a range from 700 to 2,000 m asl. Patterns of abundant species diversification and endemism at high-elevation sites are determined not only by combinations of climatic variables but also by historical and evolutionary processes and dispersal limitations (Gradstein, 2008; Kessler and Kluge, 2008). However, assessments of the quality and diversity of epiphytes in tropical montane forests remain sparse (Gómez González et al., 2017).

The orchid diversity for the Fortuna Forest Reserve in western Panama combines species that have broad distribution and shared origins with North and South America as well as species that are shared between Costa Rica and Panama and found nowhere else (35 out of 186 species; Table 7.1). In addition, at least 10 species that are endemic to Panama are present in Fortuna (Table 7.1 and appendix 7.1). The Jardín Botánico Lankester in Costa Rica and the Autonomous University of Chiriquí Herbarium (UCH) in Panama have joined efforts and established a long-term collaboration focused on the study of the Orchidaceae family (Bogarín et al., 2013; Bogarín et al., 2014). These efforts have produced inventories and vouchers, and new records for the orchid family, many of which have been documented through the database Epidendra, maintained by Jardín Botánico Lankester. A checklist for the Fortuna dam region in Chiriquí and Bocas del Toro, published by the Missouri Botanical Garden, lists 252 orchid species for this region (McPherson et al., 2010; for Fortuna orchid images, see https://fortuna.life.illinois.edu). In this analysis, recorded information from herbarium specimens and values of leaf isotopic composition of δ^{13}C and δ^{15}N are used to first provide an inventory of the orchid flora for the Fortuna Forest Reserve with emphasis on the two largest genera present in these records, *Maxillaria* and *Epidendrum*, and then to evaluate the diversity of resource use strategies and patterns of nutrient utilization with implications for tropical montane orchid conservation.

TABLE 7.1. Leaf carbon and nitrogen stable isotopic composition (δ^{13}C and δ^{15}N), growth form, %N, %C, and C:N ratio for 186 Fortuna orchid species collected from herbarium sheets. Species nomenclature follows the Plants of the World database managed by the Royal Botanic Gardens, Kew. Species names provided in parentheses correspond to the synonym names given in the herbarium sheet. Herbarium accession number and collection localities are provided in Table 7.2. Asterisk (*) = endemic species; dash (—) = no data.

Species name	Growth Form	δ^{13}C	%N	δ^{15}N	%C	C:N ratio
Acianthera glumacea (Lindl.) Pridgeon & M.W.Chase (*Pleurothallis alexandrae*)	Epiphytic	−30.01	0.95	−4.02	47.86	50.38
Acianthera sicaria (Lindl.) Pridgeon & M.W.Chase	Epiphytic	−22.89	—	—	51.85	—
Anathallis cuspidata (Luer) Pridgeon & M.W.Chase (*Pleurothallis cuspidata*)	Epiphytic	−28.69	0.98	−2.72	44.57	45.48
Barbosella dolichorhiza Schltr.	Epiphytic	−25.89	0.84	−2.64	54.18	64.50
Barbosella prorepens (Rchb.f.) Schltr.	Epiphytic	−26.92	1.43	−0.03	51.35	35.91
Baskervilla colombiana Garay	Terrestrial	−34.57	2.31	1.92	44.83	19.41
Brachionidium dressleri Luer	Terrestrial	−32.25	3.36	−2.63	47.05	14.00
Brassia chlorops Endrés & Rchb.f. (*Ada chlorops*)	Epiphytic	−27.25	—	—	50.56	—
Brassia chlorops Endrés & Rchb.f. (*Ada chlorops*)	Epiphytic	−26.82	1.31	−3.18	54.59	41.67
Brassia horichii (I.Bock) M.W.Chase (*Mesospinidium horichii*)	Epiphytic	−29.37	2.23	−0.33	50.03	22.43
Brassia horichii (I.Bock) M.W.Chase (*Mesospinidium horichii*)	Epiphytic	−28.73	—	—	49.98	—
Campylocentrum brenesii Schltr.	Epiphytic	−18.62	—	—	49.47	—
Coccineorchis bracteosa (Ames & C.Schweinf.) Garay	Terrestrial	−31.90	—	—	45.56	—
Coccineorchis warszewicziana Szlach., Rutk. & Mytnik	Terrestrial	−26.89	1.05	−0.89	42.23	40.22
Cyclopogon plantagineus Schltr.	Terrestrial	−30.01	4.39	3.42	45.47	10.36
Cyrtochiloides ochmatochila (Rchb.f.) N.H.Williams & M.W.Chase (*Oncidium ochmatochilum*)	Epiphytic	−29.68	—	—	49.72	—
Cyrtochiloides ochmatochila (Rchb.f.) N.H.Williams & M.W.Chase *(Oncidium ochmatochilum)*	Epiphytic	−24.69	1.32	—	53.57	40.58
Daiotyla crassa (Dressler) Dressler (*Chondrorhyncha crassa*)*	Epiphytic	−32.45	1.45	−3.09	42.09	29.03
Dichaea costaricensis Schltr.	Epiphytic	−28.82	1.40	−2.70	51.09	36.49

TABLE 7.1. (*Continued*)

Species name	Growth Form	$\delta^{13}C$	%N	$\delta^{15}N$	%C	C:N ratio
Dichaea dressleri Folsom*	Epiphytic	–31.36	1.51	–2.86	42.41	28.09
Diodonopsis erinacea (Rchb.f.) Pridgeon & M.W.Chase (*Masdevallia erinacea*)	Epiphytic	–31.06	0.87	–3.73	46.85	53.85
Echinosepala sempergemmata (Luer) Pridgeon & M.W.Chase (*Myoxanthus sempergemmatus*)	Epiphytic	–28.33	1.48	–3.58	51.08	34.51
Elleanthus glaucophyllus Schltr.	Epiphytic	–29.05	—	—	46.76	—
Elleanthus hymenophorus (Rchb.f.) Rchb.f.	Terrestrial	–30.19	1.84	—	35.16	19.11
Elleanthus jimenezii (Schltr.) C.Schweinf. (*Epilyna jimenezii*)	Epiphytic	–29.44	0.56	—	54.77	97.80
Elleanthus jimenezii (Schltr.) C.Schweinf. *(Epilyna jimenezii)*	Epiphytic	–28.61	—	—	52.77	—
Elleanthus poiformis Schltr.	Epiphytic	–29.83	1.16	0.38	51.18	44.12
Elleanthus stolonifer Barringer	Epiphytic	–29.52	1.44	—	49.85	34.62
Epidendrum allenii L.O.Williams	Epiphytic	–28.71	2.03	–2.83	45.62	22.47
Epidendrum exile Ames	Epiphytic	–29.12	—	—	47.23	—
Epidendrum exile Ames	Epiphytic	–28.25	—	—	47.47	—
Epidendrum fortunae Hágsater & Dressler (*Oerstedella fortunae*)*	Epiphytic	–30.41	1.69	—	50.36	29.80
Epidendrum intermixtum Ames & C.Schweinf.	Epiphytic	–27.79	2.32	–2.02	47.03	20.27
Epidendrum intermixtum Ames & C.Schweinf. (*Oerstedella intermixta*)	Epiphytic	–27.47	—	–3.17	—	—
Epidendrum jejunum Rchb.f.	Epiphytic	–26.98	—	—	42.72	—
Epidendrum lacustre Lindl.	Epiphytic	–34.44	—	—	43.40	—
Epidendrum lacustre Lindl.	Epiphytic	–27.88	—	—	44.43	—
Epidendrum muscicola Schltr.	Epiphytic	–28.44	—	—	50.49	—
Epidendrum muscicola Schltr.	Epiphytic	–27.79	—	—	50.14	—
Epidendrum muscicola Schltr.	Epiphytic	–27.26	—	—	53.92	—
Epidendrum notabile Schltr.	Epiphytic	–31.60	—	—	46.42	—
Epidendrum notabile Schltr.	Epiphytic	–30.20	—	—	46.53	—
Epidendrum notabile Schltr.	Epiphytic	–28.10	—	—	46.03	—
Epidendrum odontochilum Hágsater	Epiphytic	–25.36	—	—	44.60	—
Epidendrum paranthicum Rchb.f. (*Epidendrum sancti-ramoni*)	Epiphytic	–26.85	0.75	–3.15	52.97	70.63
Epidendrum phyllocharis Rchb.f.	Epiphytic	–32.52	—	—	45.13	—
Epidendrum platystigma Rchb.f.	Epiphytic	–29.60	—	—	51.32	—
Epidendrum pleurothalloides Hágsater	Epiphytic	–29.28	—	—	49.86	—
Epidendrum radicans Pav. ex Lindl.	Terrestrial	–15.39	—	—	49.55	—
Epidendrum sanchoi Ames	Epiphytic	–33.50	—	—	49.69	—
Epidendrum sanchoi Ames	Epiphytic	–30.36	—	—	49.05	—
Epidendrum selaginella Schltr.	Epiphytic	–33.93	—	—	46.05	—
Epidendrum talamancanum (J.T.Atwood) Mora–Ret. & García Castro	Epiphytic	–28.49	1.24	–3.92	53.02	42.76
Epidendrum turialvae Rchb.f.	Epiphytic	–31.60	—	—	43.62	—
Goodyera erosa (Ames & C.Schweinf.) Ames, F.T.Hubb. & C.Schweinf.	Terrestrial	–33.30	—	—	44.15	—

(*Continued*)

TABLE 7.1. (*Continued*)

Species name	Growth Form	δ^{13}C	%N	δ^{15}N	%C	C:N ratio
Goodyera striata Rchb.f.	Terrestrial	–33.09	—	—	44.96	—
Habenaria repens Nutt.	Terrestrial	–31.68	—	—	41.31	—
Jacquiniella globosa (Jacq.) Schltr.	Epiphytic	–27.57	—	—	50.04	—
Jacquiniella standleyi (Ames) Dressler	Epiphytic	–29.58	—	—	52.27	—
Jacquiniella teretifolia (Sw.) Britton & P.Wilson	Epiphytic	–25.93	0.77	–5.60	46.28	60.10
Kefersteinia excentrica Dressler & Mora–Ret.	Epiphytic	–26.57	2.06	–1.21	48.67	23.63
Kefersteinia lactea (Rchb.f.) Schltr.	Epiphytic	–29.14	1.93	–0.78	49.79	25.80
Kreodanthus sarcochilus E.A.Christ. sp. nov. ined.	Terrestrial	–31.53	2.29	–0.93	43.80	19.13
Lepanthes brunnescens Luer*	Epiphytic	–31.91	1.61	–3.26	43.36	26.93
Lepanthes wendlandii Rchb.f.	Epiphytic	–29.89	0.71	–7.04	47.09	66.32
Lycaste schilleriana Rchb.f.	Epiphytic	–30.32	1.11	–0.80	42.06	37.89
Lycaste schilleriana Rchb.f.	Epiphytic	–30.02	—	—	44.04	—
Macroclinium alleniorum Dressler & Pupulin	Epiphytic	–17.11	—	—	54.69	—
Malaxis excavata (Lindl.) Kuntze (*Malaxis hastilabia*)	Terrestrial	–35.56	—	—	47.98	—
Malaxis pandurata (Schltr.) Ames	Terrestrial	–33.36	3.01	4.15	43.57	14.48
Malaxis simillima (Rchb.f.) Kuntze	Terrestrial	–28.33	3.15	–1.08	46.83	14.87
Masdevallia chasei Luer	Epiphytic	–27.32	0.85	–1.77	43.14	50.75
Masdevallia nidifica Rchb.f.	Epiphytic	–30.53	2.18	–1.38	45.89	21.05
Maxillaria acervata Rchb.f.	Epiphytic	–31.74	—	—	51.00	—
Maxillaria adendrobium (Rchb.f.) Dressler (*Ornithidium adendrobium*)	Epiphytic	–27.19	—	—	50.54	—
Maxillaria angustissima Ames, F.T.Hubb. & C.Schweinf.*	Epiphytic	–32.36	1.22		46.07	37.76
Maxillaria angustissima Ames, F.T.Hubb. & C.Schweinf.*	Epiphytic	–29.28	—	–5.10	—	—
Maxillaria arachnitiflora Ames & C.Schweinf.	Epiphytic	–28.84	—	–3.49	—	—
Maxillaria bicallosa (Rchb.f.) Garay	Epiphytic	–28.63	1.07		49.16	45.94
Maxillaria biolleyi (Schltr.) L.O.Williams	Epiphytic	–26.10	—	–1.89	—	—
Maxillaria bracteata (Schltr.) Ames & Correll	Epiphytic	–28.64	—	–3.22	—	—
Maxillaria calcarata (Schltr.) Molinari (*Cryptocentrum calcaratum*)	Epiphytic	–22.95	1.66	–3.49	50.49	30.42
Maxillaria carinulata Rchb.f. (*Maxillaria amplifora*)	Epiphytic	–28.69	—	—	49.30	—
Maxillaria chionantha J.T.Atwood	Epiphytic	–30.03	1.48	—	50.02	33.80
Maxillaria costaricensis Schltr.	Epiphytic	–29.90	0.98	—	54.95	56.07
Maxillaria dendrobioides (Schltr.) L.O.Williams	Epiphytic	–28.25	1.22	—	54.00	44.26
Maxillaria diuturna Ames & C.Schweinf.	Epiphytic	–33.39	—	—	49.30	—
Maxillaria diuturna Ames & C.Schweinf.	Epiphytic	–28.99	—	–2.60	—	—
Maxillaria flava Ames, F.T.Hubb. & C.Schweinf. (*Camaridium ramonense*)	Epiphytic	–31.27	—	—	53.48	—
Maxillaria fulgens (Rchb.f.) L.O.Williams (*Ornithidium fulgens*)	Epiphytic	–28.08	—	—	49.58	—
Maxillaria fulgens (Rchb.f.) L.O.Williams (*Ornithidium fulgens*)	Epiphytic	–27.96	—	—	52.73	—
Maxillaria inaequisepala (C.Schweinf.) Molinari (*Cryptocentrum inaequisepalum*)	Epiphytic	–24.96	—	—	49.12	—

TABLE 7.1. (*Continued*)

Species name	Growth Form	$\delta^{13}C$	%N	$\delta^{15}N$	%C	C:N ratio
Maxillaria inaudita Rchb.f. (*Camaridium inauditum*)	Epiphytic	–33.85	—	—	45.78	—
Maxillaria inaudita Rchb.f. (*Camaridium inauditum*)	Epiphytic	–29.83	—	—	49.00	—
Maxillaria longicolumna J.T.Atwood*	Epiphytic	–28.70	1.43	–3.43	52.90	36.99
Maxillaria minus (Schltr.) L.O.Williams (*Maxillaria minor*)	Epiphytic	–28.74	—	–3.19	—	—
Maxillaria monteverdensis J.T.Atwood & Barboza (*Camaridium monteverdense*)	Epiphytic	–33.05	—	—	55.19	—
Maxillaria nutantiflora Schltr. (*Camaridium nutantiflorum*)*	Epiphytic	–28.00	—	—	49.78	—
Maxillaria ramonensis Schltr.	Epiphytic	–28.71	—	–3.13	—	—
Maxillaria reichenheimiana Endrés & Rchb.f.	Epiphytic	–33.47	—		42.68	—
Maxillaria scalariformis J.T.Atwood*	Epiphytic	–29.04	—	–2.14	—	—
Maxillaria standleyi (Ames) Molinari (*Cryptocentrum standleyi*)	Epiphytic	–31.38	—	—	46.79	—
Maxillaria trilobata Ames & Correll	Epiphytic	–30.12	—	–0.21	—	—
Maxillaria valerioi Ames & C.Schweinf.	Epiphytic	–27.79	—	–2.43	—	—
Maxillaria variabilis Bateman ex Lindl.	Epiphytic	–29.69	—	–2.91	—	—
Maxillaria wercklei (Schltr.) L.O.Williams	Epiphytic	–32.06	1.70	—	51.43	30.25
Microchilus nigrescens (Schltr.) Ormerod	Terrestrial	–27.30	—	—	42.87	—
Microchilus nigrescens (Schltr.) Ormerod (*Erythrodes killipii*)	Terrestrial	–33.81	—	—	43.33	—
Miltoniopsis warszewiczii (Rchb.f.) Garay & Dunst.	Epiphytic	–27.86	1.25	–3.53	50.56	40.45
Muscarella segregatifolia (Ames & C.Schweinf.) Karremans (*Pleurothallis segregatifolia*)	Epiphytic	–29.45	2.08	–1.07	43.66	20.99
Myoxanthus trachychlamys (Schltr.) Luer	Epiphytic	–28.30	0.72	–7.61	47.09	65.40
Octomeria costaricensis Schltr.	Epiphytic	–27.84	—	—	50.45	—
Oncidium bryolophotum Rchb.f.	Epiphytic	–30.20	3.40	—	49.27	14.49
Oncidium bryolophotum Rchb.f.	Epiphytic	–29.88	—	—	44.68	—
Oncidium cheirophorum Rchb.f.	Epiphytic	–26.85	1.72	—	53.00	30.81
Oncidium cheirophorum Rchb.f. (*Oncidium exauriculatum*)	Epiphytic	–27.57	0.91	—	46.97	51.62
Oncidium exalatum Hágsater*	Epiphytic	–28.80	1.10	—	51.08	46.44
Oncidium luteum Rolfe	Epiphytic	–27.52	1.92	—	47.32	24.65
Oncidium macrobulbon (Kraenzl.) M.W.Chase & N.H.Williams (*Sigmatostalix macrobulbon*)	Epiphytic	–28.81	1.87	—	47.34	25.32
Oncidium nebulosum Lindl. (*Oncidium klotzschianum*)	Epiphytic	–31.24	—	—	52.00	—
Oncidium schroederianum (O'Brien) Garay & Stacy	Epiphytic	–28.10	1.27	—	47.49	37.39
Oncidium warszewiczii Rchb.f.	Epiphytic	–31.20	—	—	50.20	—
Oncidium warszewiczii Rchb.f.	Epiphytic	–27.09	1.53	–2.79	49.65	32.45
Otoglossum chiriquense (Rchb.f.) Garay & Dunst.	Epiphytic	–27.82	1.50	–2.12	52.28	34.85
Otoglossum chiriquense (Rchb.f.) Garay & Dunst.	Epiphytic	–27.44	—	—	56.40	—
Palmorchis silvicola L.O.Williams	Epiphytic	–32.30	3.18	1.16	41.23	12.97
Palmorchis trilobulata L.O.Williams	Terrestrial	–33.31	3.99	–1.12	45.03	11.29
Palmorchis trilobulata L.O.Williams	Terrestrial	–32.57	—	—	41.58	—
Pescatoria cerina (Lindl. & Paxton) Rchb.f.	Terrestrial	–24.40	—	—	48.71	—
Phragmipedium caudatum (Lindl.) Rolfe	Epiphytic	–26.00	—	—	53.83	—

(*Continued*)

TABLE 7.1. (*Continued*)

Species name	Growth Form	δ^{13}C	%N	δ^{15}N	%C	C:N ratio
Phragmipedium warszewiczianum (Rchb.f.) Schltr.	Epiphytic	–26.89	2.09		55.62	26.61
Platystele aurea Garay (*Pleurothallis rubella*)	Epiphytic	–30.25	0.88	–5.20	45.57	51.78
Platystele caudatisepala (C.Schweinf.) Garay	Epiphytic	–33.20	—	—	49.01	—
Platystele lancilabris (Rchb.f.) Schltr.	Epiphytic	–30.34	—	—	46.28	—
Platystele ovalifolia (H.Focke) Garay & Dunst.	Epiphytic	–30.82	—	—	55.34	—
Platystele oxyglossa (Schltr.) Garay	Epiphytic	–31.08	1.07	–11.11	47.74	44.62
Platystele stenostachya (Rchb.f.) Garay	Epiphytic	–29.37	1.01	–5.76	45.66	45.21
Platystele stenostachya (Rchb.f.) Garay	Epiphytic	–29.21	—	—	46.30	—
Pleurothallis bivalvis Lindl. (*Pleurothallis angusta*)	Epiphytic	–28.86	1.05	–4.53	46.78	44.55
Pleurothallis bivalvis Lindl. (*Pleurothallis antonensis*)	Epiphytic	–30.19	0.88	–4.40	46.26	52.57
Pleurothallis coriacardia Rchb.f.	Epiphytic	–30.90	1.02	–1.41	46.50	45.59
Pleurothallis dentipetala Rolfe ex Ames	Epiphytic	–31.76	1.31	–0.03	46.62	35.59
Pleurothallis eumecocaulon Schltr.	Epiphytic	–28.08	0.86	–5.00	50.39	58.59
Pleurothallis palliolata Ames	Epiphytic	–28.96	1.43	1.02	48.84	34.15
Pleurothallis rectipetala Ames & C.Schweinf.	Epiphytic	–29.47	0.53	–7.15	44.42	83.81
Pleurothallis ruscifolia (Jacq.) R.Br.	Epiphytic	–29.02	0.79	–4.82	46.09	58.34
Pleurothallis titan Luer	Epiphytic	–26.38	1.07	–3.12	47.09	44.01
Pleurothallopsis ujarensis (Rchb.f.) Pridgeon & M.W.Chase (*Restrepiopsis ujarensis*)	Epiphytic	–25.53	0.91	–3.45	48.86	53.69
Ponthieva brenesii Schltr.	Epiphytic	–30.14	1.91	3.47	42.73	22.37
Psilochilus macrophyllus (Lindl.) Ames	Terrestrial	–28.73	2.58	–1.49	45.84	17.77
Psilochilus physurifolius (Rchb.f.) Løjtnant	Terrestrial	–30.03	—	—	45.85	—
Scaphosepalum microdactylum Rolfe	Epiphytic	–27.93	—	—	44.51	—
Scaphyglottis amparoana (Schltr.) Dressler	Epiphytic	–23.89	0.82	—	51.00	62.20
Scaphyglottis arctata (Dressler) B.R.Adams	Epiphytic	–27.36	1.04	–4.36	52.77	50.74
Scaphyglottis densa (Schltr.) B.R.Adams	Epiphytic	–26.66	—	—	51.28	—
Scaphyglottis gigantea Dressler	Epiphytic	–26.68	—	—	49.96	—
Scaphyglottis gigantea Dressler	Epiphytic	–24.90	1.19	—	49.45	41.55
Scaphyglottis modesta (Rchb.f.) Schltr.	Epiphytic	–30.52	—	—	44.76	—
Scaphyglottis prolifera (R.Br.) Cogn.	Epiphytic	–26.37	—	—	50.32	—
Scaphyglottis prolifera (R.Br.) Cogn.	Epiphytic	–25.66	—	—	48.29	—
Scaphyglottis sessiliflora B.R.Adams	Epiphytic	–31.79	1.88	—	49.39	26.27
Scaphyglottis sigmoidea (Ames & C.Schweinf.) B.R.Adams	Epiphytic	–32.17	1.51	—	49.10	32.52
Scaphyglottis sigmoidea (Ames & C.Schweinf.) B.R.Adams	Epiphytic	–29.10	—	—	49.03	—
Sobralia amabilis (Rchb.f.) L.O.Williams	Epiphytic	–28.63	0.97	—	54.09	55.76
Sobralia candida (Poepp. & Endl.) Rchb.f.	Epiphytic	–30.60	1.33	—	50.91	38.28
Sobralia carazoi C.H.Lank. & Ames	Epiphytic	–29.29	1.32	—	46.72	35.39
Sobralia chrysostoma Dressler	Terrestrial	–29.37	0.51	—	52.41	102.76
Sobralia kerryae Dressler	Epiphytic	–29.05	1.01	—	52.24	51.72
Sobralia leucoxantha Rchb.f.	Epiphytic	–27.51	—	—	50.90	—
Sobralia undatocarinata C.Schweinf.	Terrestrial	–32.22	2.02	—	43.21	21.39

TABLE 7.1. (*Continued*)

Species name	Growth Form	$\delta^{13}C$	%N	$\delta^{15}N$	%C	C:N ratio
Sobralia undatocarinata C.Schweinf.	Epiphytic	–31.63	1.09	—	47.79	43.84
Specklinia colombiana (Garay) Pridgeon & M.W.Chase (*Acostaea costaricensis*)	Epiphytic	–32.04	—	—	45.84	—
Stelis despectans Schltr.	Epiphytic	–29.74	0.55	—	46.21	84.02
Stelis gigantea Pridgeon & M.W.Chase (*Pleurothallis powellii*)	Epiphytic	–25.71	1.48	–2.03	45.13	30.49
Stelis microchila Schltr.	Epiphytic	–28.89	1.12	—	49.23	43.96
Stelis pilosa Pridgeon & M.W.Chase (*Pleurothallis amparoanum*)	Epiphytic	–27.05	1.00	–3.13	49.78	49.78
Stelis segoviensis (Rchb.f.) Pridgeon & M.W.Chase	Epiphytic	–29.78	—	—	47.73	—
Stelis storkii Ames	Epiphytic	–29.09	0.87	—	44.33	50.95
Stelis superbiens Lindl. (*Stelis leucopogon*)	Epiphytic	–29.55	0.89	—	42.58	47.84
Stellamaris pergrata (Ames) Mel.Fernández & Bogarín (*Trichosalpinx pergrata*)	Terrestrial	–33.51	1.49	—	42.71	28.66
Stenorrhynchos speciosum (Jacq.) Rich.	Epiphytic	–32.67	1.98	—	44.09	22.27
Systeloglossum panamense Dressler & N.H.Williams*	Epiphytic	–28.17	1.13	—	52.88	46.80
Trichosalpinx arbuscula (Lindl.) Luer	Epiphytic	–27.31	0.67	—	40.14	59.91
Trichosalpinx ciliaris (Lindl.) Luer	Epiphytic	–28.58	0.99	–4.44	43.59	44.03
Trichosalpinx dura (Lindl.) Luer (*Pleurothallis foliata*)	Epiphytic	–28.24	0.57	–7.64	47.69	83.67

Carbon and Nitrogen Leaf Isotopic Composition for Studying Functional Strategies in Orchids

How epiphytic orchids species without access to mineral soil nutrients manage to acquire nutrients remains poorly understood. Nitrogen is often considered a limiting nutrient in wet tropical montane forests (Vitousek, 1984; Tanner et al., 1998). Unraveling sources of nutrient and whether epiphytic tropical orchid species may rely solely on atmospheric deposition as their main source of nitrogen and terrestrial orchid species may take up nitrogen through roots that are in contact with soil is important to understand ecosystem nutrient dynamics. Many epiphytic orchid species can grow as terrestrial species whenever a thick mat of humid and not fully decomposed organic matter is concentrated near the top layer of the soil and roots are present but not entirely buried, such as in the case of *Epidendrum radicans* Pav. ex Lindl, a ground-dwelling species at the Fortuna Forest Reserve (Figure 7.1). Litter nutrients in montane forests may have higher total concentrations of N and lower C to N ratios (C:N) with decreased cycling of nutrients because of organic matter buildup due to incomplete decomposition and low soil temperature effects on nutrient mobilization and microbial activity (Körner, 1989; Tanner et al., 1998; Wegner, et al. 2003). Other sources of N for both terrestrial and epiphytic orchids may come from N_2 fixed by microorganisms and as a direct N transfer from various forms of mycorrhizae (Stewart et al., 1995; Hietz et al., 1999; Hietz et al., 2002). Studies that examine leaf N and C composition between growth forms such as epiphytes and terrestrial species at tropical montane cloud forests are few and sparse. The use of stable isotopes to measure $\delta^{13}C$ provides a quick and efficient way to identify which photosynthetic pathways is acquired (Bender, 1971; Santiago et al., 2005; Silvera et al., 2010; Silvera and Lasso, 2016). Similarly, the use of $\delta^{15}N$ and its signature can be helpful to determine preferential sources and pathways by which N is acquired by orchids, whether atmospheric or soil based sources (Stewart et al., 1995; Högberg, 1997; Hietz et al., 1999; Hietz et al., 2002). This chapter details an analysis conducted of N and C using stable isotopic composition of leaf tissue from orchids collected at different sites at the Fortuna Forest Reserve to understand if there are differences in nutrient source availability and to identify resource acquisition tendencies between terrestrial and epiphytic growth forms.

METHODS

Small fragments (2–5 mg) of dried leaf tissue were collected from herbarium sheets from 186 specimens encompassing 52 genera and 157 species of plants that were collected at different sites within the Fortuna Forest Reserve and deposited at five main herbaria known to host large numbers of Panamanian orchid species: Missouri Botanical Gardens Herbarium

FIGURE 7.1. *Epidendrum radicans* Pav. ex Lindl. A ground-rooting terrestrial orchid species with bright orange-red flowers commonly found on roadsides and grasslands. This species can grow as an epiphyte on lower-elevation sites. At the Fortuna Forest Reserve, plants are often found sprawling along the ground or climbing over grassland vegetation with stems usually erect. Plants are often vigorous and can withstand high winds and direct sunlight.

(MOBOT), Marie Selby Botanical Gardens Herbarium (SEL), University of Florida Herbarium (FLAS), University of Panama Herbarium (Universidad de Panama), and the Smithsonian Tropical Research Institute Herbarium (SCZ).

Values for $\delta^{13}C$ were determined for 186 leaf samples. From these, 174 were also analyzed for C concentration (%C), 99 for N concentration (%N), and 73 for $\delta^{15}N$ composition using an elemental analyzer (Europa ANCA-SL, Europa Scientific, Ltd., Crewe, UK) on a continuous-flow isotope ratio mass spectrometer (PDZ Europa 20/20 Mass Spectrometer, PDZ Europa Scientific, Ltd.; and the Finnigan-MAT DELTA Plus XL, Thermo Fisher Scientific, Waltham, MA, USA) at the Center for Stable Isotope Biogeochemistry, University of California Berkeley, or the Facility for Isotope Ratio Mass Spectrometry (FIRMS), University of California Riverside, using an elemental analyzer (Elemental Combustion System ECS 4010, Costech, Valencia, CA, USA) interfaced with an isotope ratio mass spectrometer (Delta V Advantage, Thermo Scientific, Bremen, Germany).

Both $\delta^{13}C$ and $\delta^{15}N$ are expressed in delta notation (‰) relative to the international standards for C (Pee Dee Belemnite standard *Belemnitella americana*) and N (atmospheric, N_2). Orchid nomenclature provided within each herbarium sheet was updated following the Plants of the World database managed by the Royal Botanic Gardens, Kew.

RESULTS

Leaf $\delta^{13}C$ values across all species ranged between a minimum of −35.56‰ for the terrestrial species *Malaxis excavata* (Lindl.) Kuntze and a maximum of −15.39‰ for the terrestrial species *Epidendrum radicans* (Table 7.1) with an average of −29.13‰. Leaf $\delta^{15}N$ values ranged between a minimum of −11.11‰ for the epiphytic species *Platystele oxyglossa* (Schltr.) Garayand and a maximum of 4.15‰ for the terrestrial species *Malaxis pandurata* (Schltr.) Ames (Table 7.1) with an average value of −2.63‰ across all 73 samples measured. Leaf N concentration ranged from a minimum of 0.51% to a maximum of 4.39%. Similarly, leaf C concentration ranged from a minimum of 35.16% to a maximum of 56.40% with an average value of 48.08%. The C:N ratio was significantly lower in terrestrial species compared to epiphytic species (Figure 7.2, top panel) (*t*-test, $p = 0.0002$) and showed no differences with increasing elevation (Figure 7.2, bottom panel). Leaf $\delta^{15}N$ was negatively correlated to $\delta^{13}C$ with terrestrial species tending to show higher and more positive $\delta^{15}N$ values compared to epiphytes (Figure 7.3; Figure 7.4, top panel). In addition to showing lower and more negative $\delta^{15}N$ values, epiphytes have lower concentrations of N compared to terrestrial species (Figure 7.4, top panel). There is a significant increase in C concentration with increasing $\delta^{13}C$ values ($p < 0.01$), and terrestrial species show lower C concentrations compared to epiphytes (Figure 7.4, bottom panel). Interestingly, an increase in N concentration with increased elevation was not found for epiphytes or terrestrial species, but terrestrial species tend to show a relatively higher concentration compared with epiphytes across different elevations (Figure 7.5).

DISCUSSION

Photosynthetic Pathways and Patterns of Resource Acquisition

Large surveys of $\delta^{13}C$ are useful to distinguish between different photosynthetic pathways because of differential enzyme-mediated discrimination against $^{13}CO_2$ during photosynthetic C assimilation between crassulacean acid metabolism (CAM) and C_3 photosynthesis (Bender et al., 1973; Osmond et al., 1973; Santiago et al., 2005; Silvera et al., 2005). The vast majority of orchid species at the Fortuna Forest Reserve use C_3 photosynthesis as their

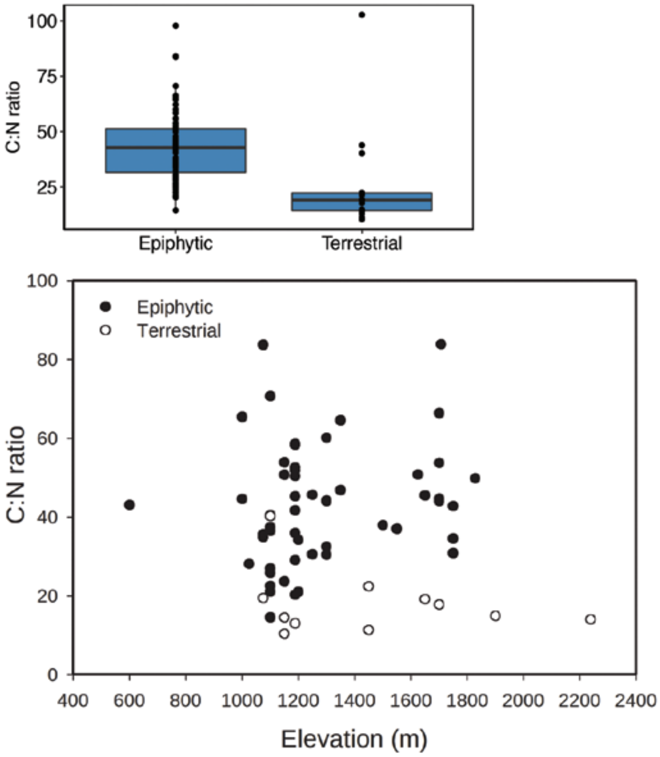

FIGURE 7.2. Distribution box plot of C:N ratios for 54 epiphytic and 11 terrestrial orchid species (top panel) and C:N ratios of 83 epiphytic and 16 terrestrial orchid species as a function of elevation (bottom panel). Closed circles represent epiphytic species, and open circles represent terrestrial species.

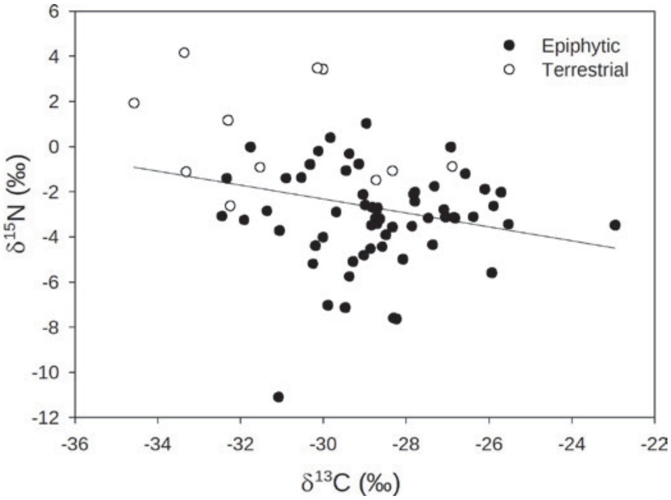

FIGURE 7.3. Dual isotope plot of carbon stable isotopic composition ($\delta^{13}C$) and nitrogen stable isotopic composition ($\delta^{15}N$) of photosynthetic tissue for 62 epiphytic and 11 terrestrial orchid species from samples derived from herbarium specimens collected at different sites within the Fortuna Forest Reserve, Panama. Closed circles represent epiphytic species, and open circles represent terrestrial species.

main photosynthetic pathway. From 186 species measured, only three showed $\delta^{13}C$ values less negative than −22‰ characteristic of the CAM pathway: *Campylocentrum brenesii* Schltr., *Macroclinium alleniorum* Dressler & Pupulin, and *Epidendrum radicans*. *Epidendrum radicans* is a commonly found terrestrial species growing by roadsides at the Fortuna Forest Reserve (Figure 7.1), but it can also grow as an epiphyte (Muthukumar and Shenbagam, 2017). Many species within *Epidendrum* and *Maxillaria* can be seen growing both as an epiphyte and as a terrestrial species at different sites. Leaf $\delta^{15}N$ can be used to discern patterns of resource acquisition between growth forms, even within the same species, opening new, interesting areas of research in orchid ecophysiology.

Differences in plant $\delta^{15}N$ found between growth forms are the result of differences in source $\delta^{15}N$ values. Epiphytes mainly use ^{15}N-depleted N sources (atmospheric deposition), with leaves showing negative $\delta^{15}N$ values compared to terrestrial species (Figure 7.3, Figure 7.4 top panel). Epiphytes source less N from the soil but can receive a small amount of soil-derived N from tree leaves. The position of individuals within the canopy and their unique physiologies could account for differences between $\delta^{15}N$ values among epiphytes (Hietz et al., 1999). For example, the $\delta^{15}N$ signal from epiphytes found at lower strata should be larger because these plants should receive more nutrients from runoff from branches and leaves of host trees. Epiphytes show negative $\delta^{15}N$ values compared to terrestrial, suggesting an atmospheric signal from wet deposition in the form of ammonium and nitrates. Terrestrial species with higher N content and higher $\delta^{15}N$ may allow for an increase in photosynthesis, especially on exposed sites or road banks where light intensity is expected to be higher.

Orchid species also differ in their requirements for N and C for seedling establishment. Epiphytes are generally exposed to high light levels at early stages of development compared to terrestrial species whose seeds would need to germinate symbiotically on leaf litter, with different demands for mycorrhiza-supplied carbon (Alghamdi, 2019). The dynamics of the epiphytic habitat can change throughout the lifetime of an orchid species because of the growth of the host tree or changes in the community (Bogarín et al., 2013). Seeds and seedling requirements for resources also differ between epiphytes and terrestrial orchid species in tropical montane cloud forests. Terrestrial species are non-photosynthetic at the early stages of development and rely completely on fungal symbionts for C acquisition.

The most unique species at Fortuna include *Sobralia chrysostoma* Dressler, a terrestrial species with a C:N ratio of 102.76 (Table 7.1, Figure 7.2), the largest C:N ratio of any species measured at the Fortuna Forest Reserve. *Sobralia* belongs to a group of ephemeral and delicate flowered species with flowers known to last just a few hours. *Sobralia chrysostoma* grows on open, windy, and exposed areas by roadsides, and plants of this species bloom

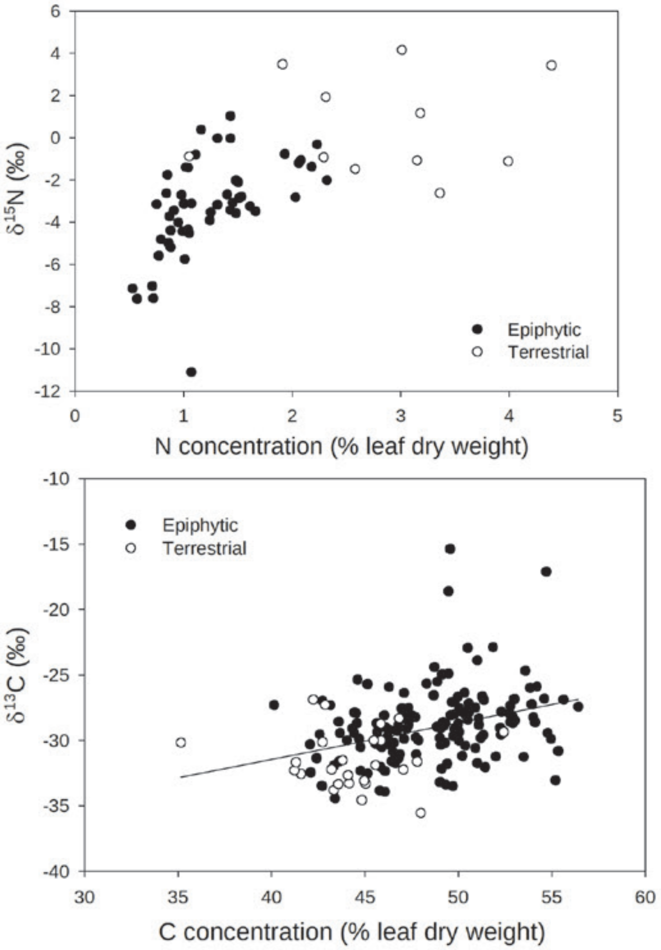

FIGURE 7.4. Plots of stable isotopic composition and nutrient content (% leaf dry weight) for nitrogen from 50 epiphytic and 11 terrestrial orchid species (top panel); and for carbon from 149 epiphytic and 25 terrestrial orchid species (bottom panel). Closed circles represent epiphytic species, and open circles represent terrestrial species.

gregariously across distant mountains at the Reserve. The views from this species flowering all at the same time in the early hours of the morning are spectacular (Figure 7.6). Leaves from *S. chrysostoma* are thick and sclerophyllous and therefore likely have a greater investment or allocation to C to withstand the strong winds of growing on exposed environments, and lower levels of nutrient uptake coupled with slow growth and low herbivory thus contribute to a higher foliar C:N ratio compared to other epiphyte or terrestrial orchid species. Another interesting species is *Elleanthus jimenezii* (Schltr.) C. Schweinf., an epiphytic species with a C:N ratio of 97.8. *Elleanthus* is closely related to *Sobralia* species, and plants are commonly found in high mountain areas at around 1,500 m of elevation (Szlachetko and Kolanowska, 2016).

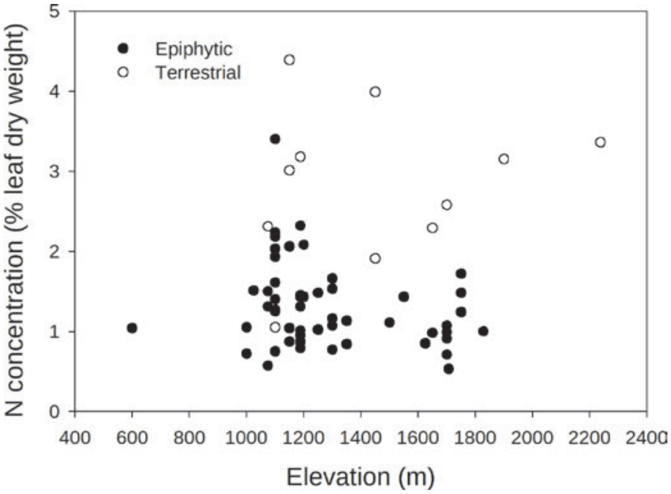

FIGURE 7.5. Nitrogen content as a function of elevation for 54 epiphytic and 11 terrestrial orchid species. Closed circles represent epiphytic species, and open circles represent terrestrial species.

Orchids can integrate different N sources at a local scale. At the Fortuna Forest Reserve, water availability and sources of atmospheric deposition are likely the main drivers of differences in δ^{15}N values, especially between epiphytic and terrestrial growth forms. In areas where N is relatively high, tissues can become ^{15}N enriched, but leaf δ^{15}N can decrease with increasing water availability (Amundson et al., 2003, Vitória et al., 2018). Terrestrial species can show mycorrhizal associations that can affect δ^{15}N values, especially at the seedling stage, and should be further investigated. Leaf isotopic composition provides information on plant responses to environmental changes and can be used as an indicator of ecological change, especially under current climate change scenarios (Vitória et al., 2018).

Orchid Diversity in the Fortuna Forest Reserve

The Fortuna Forest Reserve is one of the most extensive preserved tropical mountain cloud forests in Central America and harbors exceptionally high plant diversity, especially of species that thrive in environments with high humidity and lower light levels. The highest point of the reserve is Cerro Chorcha at 2,213 m, and the lowest point is found at 700 m. These differences in elevation and contrasting rugged terrain with constant high humidity, fog input, and cool weather create microhabitats suitable for orchid establishment. Table 7.1 lists 186 different orchid species from different contrasting sites. From these, *Maxillaria* and *Epidendrum* are the genera with the largest numbers of species (Figure 7.7).

Maxillaria is a Neotropical genus of approximately 646 species distributed in the American continent from South Florida and Northern Mexico to Central America and the Lesser Antilles to Colombia, Brazil, Bolivia, and northern Argentina (POWO, n.d.; Atwood and Mora de Retana, 1999; Pridgeon et al., 2009). *Maxillaria* species can be found from near sea level to up to

FIGURE 7.6. *Sobralia chrysostoma* Dressler. A common species on roadsides at the Fortuna Forest Reserve. Plants of this species bloom in synchronicity several miles apart, and flowers last just a few hours.

3,500 m of elevation (Pridgeon et al., 2009). Most *Maxillaria* species are epiphytes. However, in tropical montane cloud forests, *Maxillaria* species can show terrestrial growth patterns by growing on steep exposed slopes; for example, *Maxillaria inaudita* (Figure 7.8) is a cloud forest species that blooms from January to August and produces long, elongated clustered canes with monopodial growth (Atwood and Mora de Retana, 1999; Whitten and Blanco, 2011); and *Maxillaria fulgens* (Figure 7.9) is a robust shrublike orchid with bright orange flowers pollinated by hummingbirds that grows on road banks in Fortuna (Whitten and Blanco, 2011).

The large Neotropical genus *Epidendrum* has approximately 1,500 species. The majority of *Epidendrum* species at the Fortuna Forest Reserve are epiphytes, but terrestrial species are also common, especially growing on mountain slopes (Pinheiro and Cozzolino, 2013). *Epidendrum radicans* is a species of the *E. secundum* complex known to have weedy terrestrial habitats, with roots sprouting along the stems, and can grow on exposed and disturbed open areas and reproduce vegetatively (Bierzychudek, 1981; Hammel et al., 2003).

CONSERVATION APPROACHES TO PRESERVE ORCHID DIVERSITY AT THE FORTUNA FOREST RESERVE

Whenever orchid research and scientific findings inform legislation, conservation programs flourish. Orchid species are protected by international laws that regulate the trade of species across borders, especially wild-collected plants. The Convention on International Trade in Endangered Species of Wild Fauna and Flora (CITES, https://www.cites.org) ratified in 1975 and signed by more than 160 nations worldwide (including Panama), restricts and monitors the trade of orchid species under the premise that orchids are such a desired commodity that without such regulation, orchid species can become extinct in the future. Although these restrictions apply for regulating the trading of species across international borders, in situ efforts to maintain population health are urgently needed to truly conserve orchid biodiversity, especially in developing countries with large numbers of species. These efforts fall on each individual country, and local legislations that address management of fragile orchid populations can provide avenues for developing long-term solutions to maintaining orchid diversity. The first step is to establish protected areas such as national parks or natural reserves within each country to prevent habitat destruction through deforestation or fragmentation. Once protected areas exist, examples of efforts aimed at protecting orchid populations within these sites include providing subsidies to incentivize conservation efforts in local communities and promoting the genuine propagation of orchids by commercial nurseries, government agencies, or as alternative means of living for poor communities situated within or near orchid populations with the purpose of reducing the rate of removal of orchids from their natural habitat for selling purposes. These efforts should also be accompanied by sanctions to those who illegally extract orchids from the wild without the proper permits. Conservation can then be sustained first by focusing on inventories to monitor the diversity of a protected area such as the Fortuna Forest Reserve and second by targeting

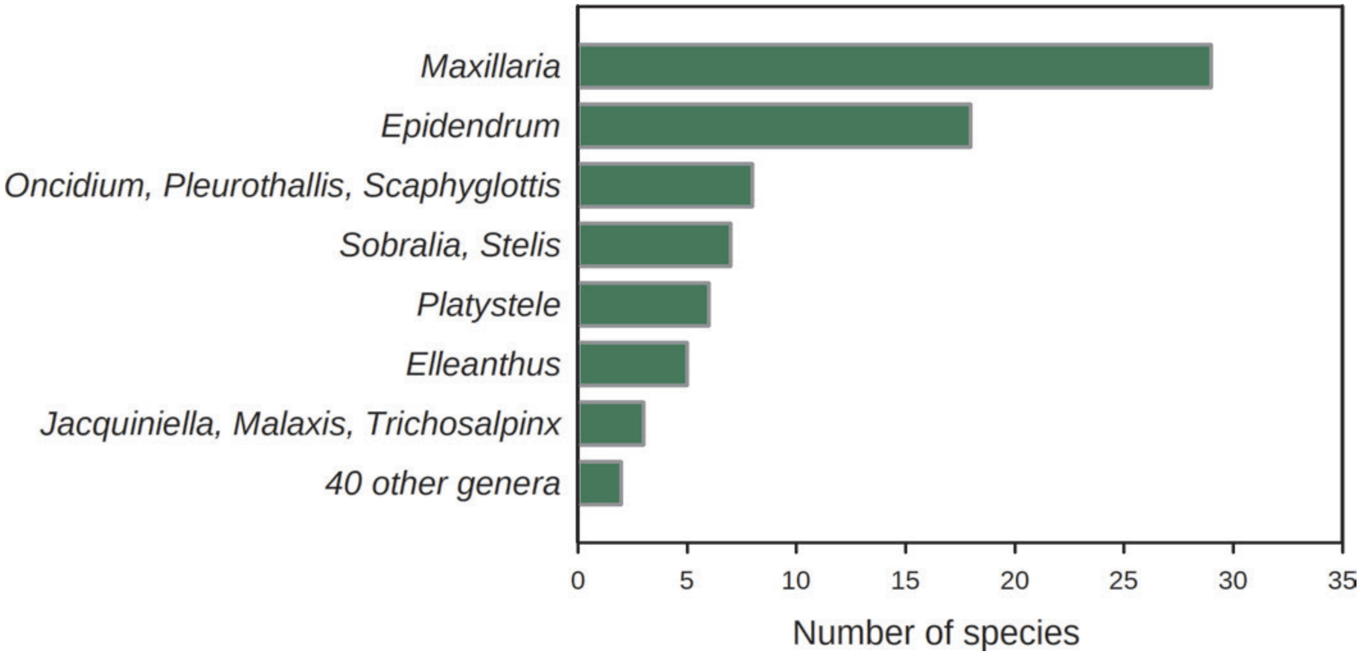

FIGURE 7.7. The most diverse orchid genera present at the Fortuna Forest Reserve. Bars represent the number of species per genus. Data was generated using 187 species from samples derived from herbarium specimens collected at different sites within the Fortuna Forest Reserve, Panama.

FIGURE 7.8. *Maxillaria inaudita* Rchb.f. growing on exposed soils with erect stems. Inflorescences carry fragrant whitish flowers. Photos by Gaspar Silvera.

FIGURE 7.9. *Maxillaria fulgens* (Rchb.f.) L. O. Williams growing on a road bank across the Continental Divide on the Fortuna Forest Reserve. Flowers of this species are produced in large bright clusters and are pollinated by hummingbirds.

FIGURE 7.10. *Phragmipedium longifolium* (Warsz. & Rchb.f.) Rolfe growing at the Smithsonian Tropical Research Institute facilities. Photos by Gaspar Silvera.

individual key species based on research that can be monitored on the long-term basis.

Conservation can apply methods informed by scientific findings. However, these avenues can work only if a thorough inventory has been conducted and species have been properly identified. Taxonomy for conservation relies on the idea that providing accurate identification and describing orchid diversity within particular sites provides an avenue to making genetic diversity a focus of conservation efforts (Schuiteman and de Vogel, 2003). This chapter provides an inventory of species for the Fortuna Forest Reserve that can be used for further research. The Smithsonian Tropical Research Institute (STRI) maintains a small research facility at the Fortuna Forest Reserve with an in situ collection of orchids that serves not only as a reference collection but also as a natural propagation garden within a forest reserve. For example, plants of the endangered terrestrial species *Phragmepedium longifolium* (Warsz. & Rchb.f.) Rolfe have been magnificently propagated within this living collection, consisting of large patches that can naturally propagate and produce several hundred inflorescences within a single flowering season (Figure 7.10). This species is particularly vulnerable to extinction because of massive extraction from its natural habitats and therefore has been placed in Appendix I of CITES and the Red List of Threatened Species of the International Union for Conservation of Nature (IUCN) (Pupulín, 2002; Muñoz et al., 2010). *Phragmepedium longifolium* usually grows in isolated patches near rivers or areas with high humidity, consisting of just a few individuals per population (Muñoz et al., 2010; Muñoz and Warner, 2016). There are no ecological or population data for this species in Panama. Maintaining living collections at a research facility provides an avenue for studying population dynamics or pollination studies in addition to a germplasm bank for conservation purposes. Researchers working on taxonomy, pollination biology, bioprospecting, and plant–animal interactions can use living collections for research and hypotheses testing. The living collection at the STRI Fortuna research station within the Fortuna Forest Reserve provides a helpful snapshot of orchids that are in bloom at any given month, and will likely be encountered in the field. For orchid research, this in situ collection is unique, highly valuable, and often overlooked.

FUTURE STUDIES

A comprehensive assessment of the orchid diversity at the Fortuna Forest Reserve is still needed, with monthly monitoring of populations and flowering times. Research regarding the role of mycorrhizal fungi associated with orchid seeds and their role in orchid nutrition and seedling survival would be a great area for future research. Research using leaf δ^{15}N as a tracer of N metabolism under current climate change scenarios can be useful to characterize physiological mechanisms utilized by different growth forms.

ACKNOWLEDGMENTS

I am grateful to Kent Perkins, Marc Frank, Mark Whitten, and Norris Williams from the University of Florida Herbarium; Bruce Holst from the Marie Selby Botanical Gardens; Jim Solomon from the Missouri Botanical Gardens Herbarium; and Mireya Correa from the University of Panama Herbarium for access to herbarium collections. I am grateful to Delores Lucero from the Facility for Isotope Ratio Mass Spectrometry (FIRMS) at the University of California Riverside and Stefania Mambelli from the Center for Stable Isotope Biogeochemistry at the University of California, Berkeley for assistance with isotopic analysis. Thanks to Louis Santiago for valuable suggestions to improve this manuscript and Gaspar Silvera for assistance with species identification and for providing images. This work was supported by NSF grant DEB 1442199 and the Smithsonian Tropical Research Institute.

APPENDIX 7.1

Herbarium accession number and collection site for 186 orchid species from the Fortuna Forest Reserve. Species nomenclature follows the Plants of the World database managed by the Royal Botanic Gardens, Kew. Species names provided in parentheses correspond to the synonym names given in the herbarium sheet. Asterisk (*) = endemic species.

Species name	Herbarium Collection Number	Collection site
Acianthera glumacea (Lindl.) Pridgeon & M.W.Chase (*Pleurothallis alexandrae*)	MOBOT 4273643	Chiriquí: Fortuna Hydroelectric Project on forested slope south side of river and upriver from camp
Acianthera sicaria (Lindl.) Pridgeon & M.W.Chase	FLAS Dressler-5451	Chiriquí: Camp Hornito, Fortuna dam, elev. 1,000–1,200 m
Anathallis cuspidata (Luer) Pridgeon & M.W.Chase (*Pleurothallis cuspidata*)	MOBOT 3326498	Chiriquí: Along trail to Cerro Pate Macho; forested slopes
Barbosella dolichorhiza Schltr.	MOBOT 5463884	Chiriquí: Camp Hornitos, Fortuna dam
Barbosella prorepens (Rchb.f.) Schltr.	MOBOT 5463907	Chiriquí: Near Vivero, 2–3 km S of Fortuna dam; Valle de Hornito
Baskervilla colombiana Garay	MOBOT 4273395	Chiriquí: Slope NW of confluence of Hornito and Chiriquí Rivers; cloud forest
Brachionidium dressleri Luer	MOBOT 2481263	Chiriquí: Cerro Hornitos, 40 km NW of Gualaca
Brassia chlorops Endrés & Rchb.f. (*Ada chlorops*)	FLAS Dressler-5514	Chiriquí: Camp Hornito, Fortuna dam, elev. 1,000–1,200 m
Brassia chlorops Endrés & Rchb.f. (*Ada chlorops*)	MOBOT 4272326	Chiriquí: Near Fortuna dam on slopes of Cerro Hornito above Los Planes; forested slopes
Brassia horichii (I.Bock) M.W.Chase (*Mesospinidium horichii*)	FLAS Dressler-5350	Chiriquí: Camp Hornito, Fortuna dam, elev. 1,000–1,200 m
Brassia horichii (I.Bock) M.W.Chase (*Mesospinidium horichii*)	MOBOT 4971080	Chiriquí: Camp Hornitos, Fortuna dam
Campylocentrum brenesii Schltr.	FLAS Dressler-5458	Chiriquí: Camp Hornito, Fortuna dam, elev. 1,000–1,200 m
Coccineorchis bracteosa (Ames & C.Schweinf.) Garay	FLAS Dressler-5395	Chiriquí: Camp Hornito, Fortuna dam to Cerro Fortuna, elev. 1,200–1,500 m

Species name	Herbarium Collection Number	Collection site
Coccineorchis warszewicziana Szlach., Rutk. & Mytnik	MOBOT 3659052	Chiriquí: Fortuna dam along Quebrada
Cyclopogon plantagineus Schltr.	MOBOT 3502879	Chiriquí: Near Fortuna dam along trail across valley of Quebrada Hornito
Cyrtochiloides ochmatochila (Rchb.f.) N.H.Williams & M.W.Chase (*Oncidium ochmatochilum*)	FLAS Dressler-5466	Chiriquí: Camp Hornito, Fortuna dam, elev. 1,000–1,200 m
Cyrtochiloides ochmatochila (Rchb.f.) N.H.Williams & M.W.Chase (*Oncidium ochmatochilum*)	MOBOT 3714801	Chiriquí: Near Fortuna dam along trail across Hornito River; forested slopes
Daiotyla crassa (Dressler) Dressler* (*Chondrorhyncha crassa*)	MOBOT 4622799	Chiriquí: Gualaca-Chiriquí Grande, near Lake Fortuna along trail to meteorological station on Hornito River departing from highway N side
Dichaea costaricensis Schltr.	MOBOT 4893570	Chiriquí: Camp Hornitos, Fortuna dam
Dichaea dressleri Folsom*	MOBOT 2928645	Chiriquí: Fortuna Hydroelectric Project along Chiriquí River upriver from camp and in cutover near camp
Diodonopsis erinacea (Rchb.f.) Pridgeon & M.W.Chase (*Masdevallia erinacea*)	MOBOT 3311771	Chiriquí: Between Fortuna dam and Continental Divide; forest on whitish ground
Echinosepala sempergemmata (Luer) Pridgeon & M.W.Chase (*Myoxanthus sempergemmatus*)	MOBOT 2623825	Chiriquí: Path from Linares farm ~1,400 m to top of Cerro Hornito at 1,750 m
Elleanthus glaucophyllus Schltr.	FLAS Dressler-6247	Chiriquí: Valle de Fortuna, S of dam near Quebrada Arena
Elleanthus hymenophorus (Rchb.f.) Rchb.f.	FLAS 205748	Chiriquí: Fortuna dam, trail to meteorological station of Hornito River
Elleanthus jimenezii (Schltr.) C.Schweinf. (*Epilyna jimenezii*)	FLAS Dressler-5341	Chiriquí: Camp Hornito, Fortuna dam, elev. 1,000–1,200 m
Elleanthus jimenezii (Schltr.) C.Schweinf. (*Epilyna jimenezii*)	FLAS Blanco2997	Chiriquí: Gualaca, near Lake Fortuna; Sendero Quebrada Alemán
Elleanthus poiformis Schltr.	MOBOT 5345800	Chiriquí: Valle de Fortuna, ~0.5 km N of dam
Elleanthus stolonifer Barringer	FLAS Blanco2934	Chiriquí: Gualaca, near Lake Fortuna
Epidendrum allenii L.O.Williams	MOBOT 3201936	Chiriquí: Fortuna dam along Quebrada Los Chornos to N of reservoir
Epidendrum exile Ames	FLAS Dressler-sn	Chiriquí: Camp Hornito, Fortuna dam, elev. 1,000–1,200 m
Epidendrum exile Ames	MOBOT 2937322	Chiriquí: Slope NW of confluence of Hornito and Chiriquí Rivers
Epidendrum fortunae Hágsater & Dressler (*Oerstedella fortunae*)*	MOBOT 2928625	Chiriquí: Fortuna Hydroelectric Project; in cloud forest on ridge behind camp
Epidendrum intermixtum Ames & C.Schweinf.	UPA 13388	Chiriquí: Protero de Pitty, S of Fortuna dam
Epidendrum intermixtum Ames & C.Schweinf. (*Oerstedella intermixta*)	SEL 56434	Chiriquí: Above Fortuna dam; wet montane forest

(*Continued*)

Species name	Herbarium Collection Number	Collection site
Epidendrum jejunum Rchb.f.	FLAS Dressler-sn	Chiriquí: Near Camp Hornito, Fortuna dam, elev. 1,000–1,200 m
Epidendrum lacustre Lindl.	MOBOT 3431736	Chiriquí: Near Fortuna dam along road N of lake on road bank
Epidendrum lacustre Lindl.	MOBOT 3032062	Chiriquí: Near Fortuna dam, lower slope of Cerro Fortuna; Fortuna Hydroelectric Project; premontane rainforest
Epidendrum muscicola Schltr.	FLAS Dressler-5363	Chiriquí: Camp Hornito, Fortuna dam, elev. 1,000–1,200 m
Epidendrum muscicola Schltr.	FLAS Dressler-5765	Chiriquí: Cerro Hornito, NNE of Gualaca, elev. 1,750–2,000 m
Epidendrum muscicola Schltr.	MOBOT 4622802	Chiriquí: Gualaca-Chiriquí Grande, near Lake Fortuna, along trail to meteorological station on Hornito River departing from highway N side, ~5 km S of science station.
Epidendrum notabile Schltr.	FLAS Dressler-5424	Chiriquí: Camp Hornito, Fortuna dam, elev. 1,200–1,500 m
Epidendrum notabile Schltr.	FLAS Dressler-5424	Chiriquí: Camp Hornito, Fortuna dam, elev. 1,200–1,500 m
Epidendrum notabile Schltr.	MOBOT 3431746	Chiriquí: Near Fortuna dam along trail across valley S of lake
Epidendrum odontochilum Hágsater	MOBOT 4305124	Chiriquí: Near Fortuna dam along trail near Hornito River
Epidendrum paranthicum Rchb.f. (*Epidendrum sancti-ramoni*)	MOBOT 2710890	Chiriquí: N of Fortuna dam in forest in front of camp at the other bank of Chiriquí River
Epidendrum phyllocharis Rchb.f.	FLAS Dressler-5360	Chiriquí: Camp Hornito, Fortuna dam, elev. 1,000–1,200 m
Epidendrum platystigma Rchb.f.	MOBOT 4298832	Bocas del Toro: NW ridge of Cerro Pate Macho from summit to Finca Serrano
Epidendrum pleurothalloides Hágsater	MOBOT 5781117	Chiriquí: Near Fortuna dam on slopes of Cerro Hornito above Los Planes; forested slopes
Epidendrum radicans Pav. ex Lindl.	MOBOT 3432782	Chiriquí: Los Llanos near Volcan. Tussock field
Epidendrum sanchoi Ames	FLAS Dressler-5326	Chiriquí: Camp Hornito, Fortuna dam, elev. 1,000–1,200 m
Epidendrum sanchoi Ames	FLAS Dressler-5326	Chiriquí: Camp Hornito, Fortuna dam, elev. 1,000–1,200 m
Epidendrum selaginella Schltr.	FLAS Dressler-5659	Chiriquí: Camp Hornito, Fortuna dam, elev. 1,000–1,200 m
Epidendrum talamancanum (J.T.Atwood) Mora-Ret. & García Castro	MOBOT 2623817	Chiriquí: Path from Linares farm ~1,400 m to top of Cerro Hornito at 1,750 m Flat heath-like area, a bald with a 3–5 m canopy
Epidendrum turialvae Rchb.f.	FLAS Dressler-5492	Chiriquí: Camp Hornito, Fortuna dam, elev. 1,000–1,200 m
Goodyera erosa (Ames & C.Schweinf.) Ames, F.T.Hubb. & C.Schweinf.	FLAS Dressler-5701	Chiriquí: Camp Hornito, Fortuna dam, elev. 1,000–1,200 m

Species name	Herbarium Collection Number	Collection site
Goodyera striata Rchb.f.	FLAS Dressler-5534	Chiriquí: Cerro Hornito, NNE of Gualaca, elev. 1,600–1,700 m
Habenaria repens Nutt.	FLAS Dressler-6258	Chiriquí: Valle de Fortuna, S of dam near STRI station, elev. 1,100–1,200 m
Jacquiniella globosa (Jacq.) Schltr.	FLAS Dressler-5438	Chiriquí: Camp Hornito, Fortuna dam, elev. 1,000–1,200 m
Jacquiniella standleyi (Ames) Dressler	FLAS Dressler-5332	Chiriquí: Camp Hornito, Fortuna dam, elev. 1,000–1,200 m
Jacquiniella teretifolia (Sw.) Britton & P.Wilson	MOBOT 2932836	Chiriquí: Fortuna dam project area, ~8 km N of main camp; step hillside, primary forest
Kefersteinia excentrica Dressler & Mora-Ret.	MOBOT 3716832	Chiriquí: Near Fortuna dam along trail across Hornito River; forested slopes
Kefersteinia lactea (Rchb.f.) Schltr.	MOBOT 4893548	Chiriquí: Camp Hornitos, Fortuna dam
Kreodanthus sarcochilus E.A.Christ. sp. nov. ined.	MOBOT 2908235	Bocas del Toro: NW ridge of Cerro Pate Macho from summit to Finca Serrano
Lepanthes brunnescens Luer*	MOBOT 3716824	Chiriquí: Near Fortuna dam along roadside and in forest between road and reservoir
Lepanthes wendlandii Rchb.f.	SEL 14782	Chiriquí: In elfin forest on Cerro Hornito; sepals orange, petals and lip red.
Lycaste schilleriana Rchb.f.	FLAS Dressler-5390	Chiriquí: Camp Hornito, Fortuna dam, elev. 1,000–1,200 m
Lycaste schilleriana Rchb.f.	MOBOT 2628639	Chiriquí: Area east of main camp at Fortuna dam
Macroclinium alleniorum Dressler & Pupulin	FLAS Dressler-5501	Chiriquí: Camp Hornito, Fortuna dam, elev. 1,000–1,200 m
Malaxis excavata (Lindl.) Kuntze (*Malaxis hastilabia*)	FLAS Dressler-6096	Chiriquí: Fortuna Valley, near pipeline, N of lake
Malaxis pandurata (Schltr.) Ames	MOBOT 3311774	Chiriquí: Near Fortuna dam along trail near forestry station toward river
Malaxis simillima (Rchb.f.) Kuntze	MOBOT 2908231	Chiriquí: SE slope and summit of Cerro Pate Macho; trail from Palo Alto River, 4 km NE of Boquete; cloud forest and elfin forest
Masdevallia chasei Luer	UPA 36026	Chiriquí: Along trail to Cerro Pate Macho; forested slopes
Masdevallia nidifica Rchb.f.	MOBOT 3201961	Chiriquí: Fortuna dam along Quebrada Bonito to W of road
Maxillaria acervata Rchb.f.	FLAS Dressler-5439	Chiriquí: Camp Hornito, Fortuna dam, elev. 1,000–1,200 m
Maxillaria adendrobium (Rchb.f.) Dressler (*Ornithidium adendrobium*)	FLAS 212831	Bocas del Toro: Road across Fortuna dam to Chiriquí Grande, elev. 1,111 m. Cultivated in roadside garden of Ms. Isabel Martinez
Maxillaria angustissima Ames, F.T.Hubb. & C.Schweinf.*	SEL 81901	Chiriquí: Valle de Fortuna, 1 km N of dam

(*Continued*)

Species name	Herbarium Collection Number	Collection site
Maxillaria angustissima Ames, F.T.Hubb. & C.Schweinf.*	FLAS 212844	Bocas del Toro: Road across Fortuna dam to Chiriquí Grande
Maxillaria arachnitiflora Ames & C.Schweinf.	SEL 56656	Chiriquí: Above Fortuna dam; wet montane forest
Maxillaria bicallosa (Rchb.f.) Garay	FLAS 212860	Bocas del Toro: Road across Fortuna dam to Chiriquí Grande
Maxillaria biolleyi (Schltr.) L.O.Williams	SEL 84898	Chiriquí: Fortuna dam region along trail to Cerro Hornito
Maxillaria bracteata (Schltr.) Ames & Correll	SEL 65933	Chiriquí: Near Fortuna dam
Maxillaria calcarata (Schltr.) Molinari (*Cryptocentrum calcaratum*)	MOBOT 2941738	Chiriquí: Along road between Gualaca and Fortuna dam
Maxillaria carinulata Rchb.f. (*Maxillaria amplifora*)	FLAS Dressler-5797	Chiriquí: Cerro Hornito, elev. 1,800–2,100 m
Maxillaria chionantha J.T.Atwood	FLAS 212884	Bocas del Toro: Road across Fortuna dam to Chiriquí Grande
Maxillaria costaricensis Schltr.	FLAS 212894	Chiriquí: Fortuna, without exact locality; collected and imported by Katia Silvera in 2001. Sympatric with *Oncidium cheirophorum*; flowered in cultivation at the University of Florida; Mark Whitten #1910 collection
Maxillaria dendrobioides (Schltr.) L.O.Williams	FLAS 212911	Bocas del Toro: Road across Fortuna dam to Chiriquí Grande; cultivated in roadside garden of Ms. Isabel Martinez
Maxillaria diuturna Ames & C.Schweinf.	SEL 45578	Chiriquí: East of Fortuna, main campsite
Maxillaria diuturna Ames & C.Schweinf.	FLAS 212921	Bocas del Toro: Road across Fortuna dam to Chiriquí Grande, elev. 1,111 m; cultivated in roadside garden of Ms. Isabel Martinez
Maxillaria flava Ames, F.T.Hubb. & C.Schweinf. (*Camaridium ramonense*)	FLAS Dressler-5441	Chiriquí: Camp Hornito, Fortuna dam, elev. 1,000–1,200 m
Maxillaria fulgens (Rchb.f.) L.O.Williams (*Ornithidium fulgens*)	FLAS Dressler-5452	Chiriquí: Camp Hornito, Fortuna dam, elev. 1,000–1,200 m
Maxillaria fulgens (Rchb.f.) L.O.Williams (*Ornithidium fulgens*)	FLAS 214869	Bocas del Toro: Road across Fortuna dam to Chiriquí Grande, elev. 1,111 m; cultivated in roadside garden of Ms. Isabel Martinez
Maxillaria inaequisepala (C.Schweinf.) Molinari (*Cryptocentrum inaequisepalum*)	FLAS Dressler-5453	Chiriquí: Camp Hornito, Fortuna dam, elev. 1,000–1,200 m
Maxillaria inaudita Rchb.f. (*Camaridium inauditum*)	FLAS Dressler-5586	Chiriquí: Cerro Fortuna, elev. 1,400–1,500 m
Maxillaria inaudita Rchb.f. (*Camaridium inauditum*)	FLAS Whitten-2763	Chiriquí: Road from Fortuna dam to Chiriquí Grande; flowered in cultivation
Maxillaria longicolumna J.T.Atwood*	MOBOT 2928592	Chiriquí: S slope of Cerro Pate Macho along Palo Alto River; montane wet forest
Maxillaria minus (Schltr.) L.O.Williams (*Maxillaria minor*)	SEL 71060	Chiriquí: Fortuna dam along Quebrada Arena
Maxillaria monteverdensis J.T.Atwood & Barboza (*Camaridium monteverdense*)	FLAS Dressler-5758	Chiriquí: Cerro Hornito, NNE of Gualaca, elev. 1,750–2,000 m
Maxillaria nutantiflora Schltr. (*Camaridium nutantiflorum*)*	FLAS Dressler-5786	Chiriquí: Cerro Fortuna, elev. 1,300–1,400 m
Maxillaria ramonensis Schltr.	SEL 56446	Chiriquí: Above Fortuna dam; wet montane forest

Species name	Herbarium Collection Number	Collection site
Maxillaria reichenheimiana Endrés & Rchb.f.	FLASDressler-5402	Chiriquí: Camp Hornito, Fortuna dam, to Cerro Fortuna, 1,200–1,500 m
Maxillaria scalariformis J.T.Atwood*	SEL 83980	Chiriquí: Gualaca-Chiriquí Grande; road over Fortuna Lake
Maxillaria standleyi (Ames) Molinari (*Cryptocentrum standleyi*)	FLAS Dressler-5496	Chiriquí: Camp Hornito, Fortuna dam, elev. 1,000–1,200 m
Maxillaria trilobata Ames & Correll	SEL 71468	Chiriquí: Fortuna dam along Quebrada Arena
Maxillaria valerioi Ames & C.Schweinf.	SEL 56324	Chiriquí: Fortuna dam area
Maxillaria variabilis Bateman ex Lindl.	SEL 61459	Chiriquí: Near Fortuna dam along Road N of Lake
Maxillaria wercklei (Schltr.) L.O.Williams	FLAS 213101	Bocas del Toro: Road across Fortuna dam to Chiriquí Grande; cultivated in roadside garden of Ms. Isabel Martinez
Microchilus nigrescens (Schltr.) Ormerod	FLAS Dressler-5339	Chiriquí: Camp Hornito, Fortuna dam
Microchilus nigrescens (Schltr.) Ormerod (*Erythrodes killipii*)	FLAS Dressler-5339	Chiriquí: Camp Hornito, Fortuna dam
Miltoniopsis warszewiczii (Rchb.f.) Garay & Dunst.	MOBOT 4272346	Chiriquí: Near Fortuna dam along roadside and in forest between road and reservoir
Muscarella segregatifolia (Ames & C.Schweinf.) Karremans (*Pleurothallis segregatifolia*)	MOBOT 2999583	Chiriquí: Quebrada Aleman, ~13 km N of Los Planes de Hornito, Fortuna Hydroelectric Project; premontane forest
Myoxanthus trachychlamys (Schltr.) Luer	SEL 15387	Chiriquí: Above camp at Fortuna dam; flowers white, odor of foul cheese
Octomeria costaricensis Schltr.	FLAS Dressler-5327	Chiriquí: Camp Hornito, Fortuna dam, elev. 1,000–1,200 m
Oncidium bryolophotum Rchb.f.	FLAS Dressler-6054	Chiriquí: Fortuna area, N side of Chiriquí River near Sierpe
Oncidium bryolophotum Rchb.f.	MOBOT 3201963	Chiriquí: Fortuna dam along Quebrada Bonito to W of road
Oncidium cheirophorum Rchb.f.	MOBOT 2627293	Chiriquí: Path from Linares farm ~1,400 m to top of Cerro Hornito at 1,750 m
Oncidium cheirophorum Rchb.f. (*Oncidium exauriculatum*)	FLAS 213117	Bocas del Toro: Road across Fortuna dam to Chiriquí Grande; cultivated in roadside garden of Ms. Isabel Martinez
Oncidium exalatum Hágsater*	MOBOT 2937525	Chiriquí: Along road to Fortuna dam site, N of Gualaca; 36.5 km beyond the bridge over the Esti River, 1,400 m, ~19 km N of Los Planes de Hornito, ~17 km N of junction to tunnel
Oncidium luteum Rolfe	MOBOT 3393412	Chiriquí: Along proposed route of road over Fortuna dam, N of lake; forested slopes 1,110–1,150 m
Oncidium macrobulbon (Kraenzl.) M.W.Chase & N.H.Williams (*Sigmatostalix macrobulbon*)	MOBOT 2894583	Chiriquí: Near Gualaca ~17 km from Planes de Hornito, La Fortuna on road to dam, elev. 1,200 m
Oncidium nebulosum Lindl. (*Oncidium klotzschianum*)	FLAS Dressler-5585	Chiriquí: Cerro Fortuna, elev. 1,400–1,500 m
Oncidium schroederianum (O'Brien) Garay & Stacy	MOBOT 3399704	Chiriquí: Camp Hornitos, Fortuna dam
Oncidium warszewiczii Rchb.f.	FLAS Dressler-5755	Chiriquí: Cerro Hornito, NNE of Gualaca, elev. 1,750–2,000 m

(*Continued*)

Species name	Herbarium Collection Number	Collection site
Oncidium warszewiczii Rchb.f.	MOBOT 4272328	Chiriquí: Near Fortuna dam on slopes of Cerro Hornito above Los Planes; forested slopes
Otoglossum chiriquense (Rchb.f.) Garay & Dunst.	FLAS Dressler-5584	Chiriquí: Cerro Fortuna, elev. 1,400–1,500 m
Otoglossum chiriquense (Rchb.f.) Garay & Dunst.	MOBOT 4273416	Chiriquí: Along highway between Gualaca and Chiriquí Grande, 1 km S of Continental Divide and Bocas del Toro boundary; virgin forest along highway
Pabstiella pleurothalloides (Cogn.) Luer (*Pleurothallis pleurothalloides*)	MOBOT 3772357	Bocas del Toro: Along road between Gualaca and Chiriquí Grande; ~9 km N of middle of bridge over Fortuna Lake along steep bank above road
Palmorchis silvicola L.O.Williams	UPA 17796	Chiriquí: SW from Camp Hornito, going up to Finca Pitti, bordering the forest and returning from S side of camp
Palmorchis trilobulata L.O.Williams	FLAS Dressler-5345	Chiriquí: Camp Hornito, Fortuna dam, elev. 1,000–1,200 m
Palmorchis trilobulata L.O.Williams	MOBOT 2628582	Chiriquí: Slope of hill above camp; at Fortuna dam
Pescatoria cerina (Lindl. & Paxton) Rchb.f.	FLAS Dressler-5442	Chiriquí: Camp Hornito, Fortuna dam, elev. 1,000–1,200 m
Phragmipedium caudatum (Lindl.) Rolfe	FLAS Dressler-6048	Chiriquí: Near Vivero, 2–3 km S of Fortuna dam, Valle de Hornito
Phragmipedium warszewiczianum (Rchb.f.) Schltr.	FLAS 149690	Chiriquí: La Fortuna, Chiriquí; plants epiphytic; flowered in cultivation; voucher, J.T.Atwood, Jr 782
Platystele aurea Garay (*Pleurothallis rubella*)	MOBOT 4273626	Chiriquí: Fortuna dam; forest area
Platystele caudatisepala (C.Schweinf.) Garay	FLAS Dressler-5462	Chiriquí: Camp Hornito, Fortuna dam, elev. 1,000–1,200 m
Platystele lancilabris (Rchb.f.) Schltr.	FLAS Dressler-5413	Chiriquí: Camp Hornito, Fortuna dam, to Cerro Fortuna, 1,200–1,500 m
Platystele ovalifolia (H.Focke) Garay & Dunst.	FLAS Dressler-5508	Chiriquí: Camp Hornito, Fortuna dam, elev. 1,000–1,200 m
Platystele oxyglossa (Schltr.) Garay	MOBOT 2623594	Chiriquí: Fortuna dam, top of mountain above camp to south
Platystele stenostachya (Rchb.f.) Garay	FLAS Dressler-5444	Chiriquí: Camp Hornito, Fortuna dam, elev. 1,000–1,200 m
Platystele stenostachya (Rchb.f.) Garay	SEL 79273	Chiriquí: Fortuna roadside forest 59 km N of Chiriquí; flowers yellow
Pleurothallis bivalvis Lindl. (*Pleurothallis angusta*)	MOBOT 3201975	Bocas del Toro: Pipeline road near Continental Divide, Fortuna dam
Pleurothallis bivalvis Lindl. (*Pleurothallis antonensis*)	MOBOT 2937577	Chiriquí: La Fortuna Hydroelectric Project on forested slope south side of river and upriver from camp
Pleurothallis coriacardia Rchb.f.	SEL 93279	Chiriquí: Fortuna reserve; lower montane forest; epiphyte on fallen branch; flowers translucent orange with red lines
Pleurothallis dentipetala Rolfe ex Ames	MOBOT 4273633	Chiriquí: Fortuna dam project area, slope NW of confluence of Hornito and Chiriquí Rivers; low cloud forest

Species name	Herbarium Collection Number	Collection site
Pleurothallis eumecocaulon Schltr.	MOBOT 4658642	Bocas del Toro: Epiphytic in forest between Fortuna and Chiriquí Grande, alt. elev. 1,180 m
Pleurothallis palliolata Ames	MOBOT 3224437	Chiriquí: Distrito Boquete, Fortuna dam; mostly collected along stream on white sandy soil with very thin humus layer
Pleurothallis rectipetala Ames & C.Schweinf.	MOBOT 2937272	Chiriquí: Cerro Hornito
Pleurothallis ruscifolia (Jacq.) R.Br.	MOBOT 4272349	Chiriquí: Near Fortuna dam along trail across Rio Hornito; forested slopes
Pleurothallis titan Luer	MOBOT 4273442	Chiriquí: Along road between Gualaca and Fortuna dam on Rio Chiriquí, 7.9 km NW of Los Planes Hornito, elev. 1,300 m
Pleurothallopsis ujarensis (Rchb.f.) Pridgeon & M.W.Chase (*Restrepiopsis ujarensis*)	SEL 15411	Chiriquí: On large tree trunk in cloud forest on Cerro Hornito; flowers pale green
Ponthieva brenesii Schltr.	MOBOT 2628583	Chiriquí: Slope of hill above camp; at Fortuna dam
Psilochilus macrophyllus (Lindl.) Ames	MOBOT 3608753	Chiriquí: Fortuna dam, top of mountain above camp to south
Psilochilus physurifolius (Rchb.f.) Løjtnant	FLAS Dressler-5391	Chiriquí: Camp Hornito, Fortuna dam, to Cerro Fortuna, elev. 1,200–1,500 m
Scaphosepalum microdactylum Rolfe	FLAS Dressler-5418	Chiriquí: Camp Hornito, Fortuna dam, elev. 1,000–1,400 m
Scaphyglottis amparoana (Schltr.) Dressler	FLAS 213157	Bocas del Toro: Road across Fortuna dam to Chiriquí Grande; cultivated in roadside garden of Ms. Isabel Martinez
Scaphyglottis arctata (Dressler) B.R.Adams	MOBOT 3311767	Chiriquí: Between Fortuna dam and Continental Divide; forest on whitish ground
Scaphyglottis densa (Schltr.) B.R.Adams	FLASDressler-5788	Chiriquí: Camp Hornito, Fortuna dam, elev. 1,000–1,200 m
Scaphyglottis gigantea Dressler	FLASDressler-5940	Chiriquí: Cerro Horqueta N of Boquete
Scaphyglottis gigantea Dressler	MOBOT 3772331	Chiriquí: Cerro Hornito, S facing slope approached from Los Planes de Hornito
Scaphyglottis modesta (Rchb.f.) Schltr.	FLAS Dressler-6286	Chiriquí: Valle de Fortuna
Scaphyglottis prolifera (R.Br.) Cogn.	FLAS Dressler-5440	Chiriquí: Camp Hornito, Fortuna dam, elev. 1,000–1,200 m
Scaphyglottis prolifera (R.Br.) Cogn.	FLAS Dressler-5440	Chiriquí: Camp Hornito, Fortuna dam, elev. 1,000–1,200 m
Scaphyglottis sessiliflora B.R.Adams	MOBOT 3303748	Chiriquí: Distrito Boquete, Fortuna dam, along trail following Continental Divide; cloud forest
Scaphyglottis sigmoidea (Ames & C.Schweinf.) B.R.Adams	FLAS Dressler-5760	Chiriquí: Cerro Hornito, NNE of Gualaca, elev. 1,750–2,000 m
Scaphyglottis sigmoidea (Ames & C.Schweinf.) B.R.Adams	MOBOT 5313064	Chiriquí: Cerro Hornito (Cerro Pata de Macho); southern rim of Fortuna dam and reserve watershed, ridge trail leading to the summit; dwarf cloud forest vegetation
Sobralia amabilis (Rchb.f.) L.O.Williams	MOBOT 4304243	Chiriquí: Fortuna dam, N of reservoir, ridge along Continental Divide and southward from Quebrada de Arena

(*Continued*)

Species name	Herbarium Collection Number	Collection site
Sobralia candida (Poepp. & Endl.) Rchb.f.	MOBOT 5345810	Bocas del Toro: Between Fortuna and Chiriquí Grande, elev. 1,000–1,050 m
Sobralia carazoi C.H.Lank. & Ames	MOBOT 4649925	Chiriquí: Fortuna dam area; Fortuna-Chiriquí Grande, ~1 km; NW of center of dam
Sobralia chrysostoma Dressler	MOBOT 5170269	Bocas del Toro: N of Continental Divide on road to Chiriquí Grande
Sobralia kerryae Dressler	MOBOT 5345793	Bocas del Toro: Between Fortuna and Chiriquí Grande, elev. 850 m
Sobralia leucoxantha Rchb.f.	FLAS Dressler-5494	Chiriquí: Camp Hornito, Fortuna dam, elev. 1,000–1,200 m
Sobralia undatocarinata C.Schweinf.	FLAS 204924	Chiriquí: Fortuna dam, N of reservoir, ridge along Continental Divide and southward from Quebrada de Arena
Sobralia undatocarinata C.Schweinf.	MOBOT 4951499	Chiriquí: Fortuna dam area, N of reservoir, ridge along Continental Divide and southward from Quebrada de Arena
Specklinia colombiana (Garay) Pridgeon & M.W.Chase (*Acostaea costaricensis*)	FLAS Dressler-5370	Chiriquí: Camp Hornito, Fortuna dam, elev. 1,000–1,200 m
Stelis despectans Schltr.	MOBOT 2623608	Chiriquí: Fortuna dam, top of mountain above camp to south
Stelis gigantea Pridgeon & M.W.Chase (*Pleurothallis powellii*)	MOBOT 3432755	Chiriquí: Near Fortuna dam; forested slopes along ridge at southern boundary of watershed
Stelis microchila Schltr.	MOBOT 4274940	Chiriquí: Near La Sierpe, ~0.5 km N of Rio Chiriquí, Fortuna Hydroelectric Project
Stelis pilosa Pridgeon & M.W.Chase (*Pleurothallis amparoanum*)	MOBOT 2928621	Chiriquí: Cerro Hornitos
Stelis segoviensis (Rchb.f.) Pridgeon & M.W.Chase	FLAS Dressler-5507	Chiriquí: Camp Hornito, Fortuna dam, elev. 1,000–1,200 m
Stelis storkii Ames	MOBOT 4274953	Chiriquí: Distrito de Boquete, Fortuna dam, Continental Divide; cloud forest
Stelis superbiens Lindl. (*Stelis leucopogon*)	MOBOT 2928671	Chiriquí: Along road between Gualaca and Fortuna dam, N of Gualaca on Chiriquí River; ~28 km beyond bridge over Esti River; 11.5 km beyond Los Planes de Hornito
Stellamaris pergrata (Ames) Mel.Fernández & Bogarín (*Trichosalpinx pergrata*)	MOBOT 2623595	Chiriquí: Fortuna dam, top of mountain above camp to south
Stenorrhynchos speciosum (Jacq.) Rich.	MOBOT 3032040	Chiriquí: Near Los Planes de Hornito along road to Fortuna dam; N of Gualaca on Rio Chiriquí, 2–3 km E of Finca Linares; high hills
Systeloglossum panamense Dressler & N.H.Williams*	MOBOT 4971081	Chiriquí: Camp Hornito, Fortuna dam, to Cerro Fortuna, 1,200–1,500 m
Trichosalpinx arbuscula (Lindl.) Luer	MOBOT 2637405	Chiriquí: Fortuna Hydroelectric Project; along Chiriquí River upriver from camp and in cutover near camp
Trichosalpinx ciliaris (Lindl.) Luer	SEL 18356	Chiriquí: In elfin cloud forest on Cerro Hornito; flowers purple
Trichosalpinx dura (Lindl.) Luer (*Pleurothallis foliata*)	MOBOT 3131353	Chiriquí: Slope NW of confluence of Hornito and Chiriquí Rivers; cloud forest

References

Alghamdi, S. A. 2019. Influence of Mycorrhizal Fungi on Seed Germination and Growth in Terrestrial and Epiphytic Orchids. *Journal of Biological Sciences*, 26:495–502. https://doi.org/10.1016/j.sjbs.2017.10.021

Amundson, R., A. T. Austin, E. A. G. Schuur, K. Yoo, V. Matzek, C. Kendall, A. Uebersax, D. Brenner, and W. T. Baisden. 2003. Global Patterns of the Isotopic Composition of Soil and Plant Nitrogen. *Global Biogeochemical Cycles*, 17:1–10. https://doi.org/10.1029/2002GB001903

Atwood, J. T., and D. E. Mora de Retana. 1999. Family #39 Orchidaceae: Tribe Maxillarieae: Subtribes Maxillariinae and Oncidiinae. *Fieldiana*, 40:1–182.

Bender, M. M. 1971. Variations in the ^{13}C/^{12}C Ratios of Plants in Relation to the Pathway of Photosynthetic Carbon Dioxide Fixation. *Phytochemistry*, 10:1239–1244. https://doi.org/10.1016/S0031-9422(00)84324-1

Bender, M. M., I. Rouhani, H. M. Vines, and C. C. Black. 1973. ^{13}C/^{12}C Ratio Changes in Crassulacean Acid Metabolism Plants. *Plant Physiology*, 52:427–430. https://doi.org/10.1104/pp.52.5.427

Bierzychudek, P. 1981. *Asclepias*, *Lantana*, and *Epidendrum*: A Floral Mimicry Complex? *Biotropica*, 13:54–58. https://doi.org/10.2307/2388070

Bogarín, D., F. Pupulín, C. Arrocha, and J. Warner. 2013. Orchids without Borders: Studying the Hotspot of Costa Rica and Panama. *Lankesteriana*, 13:13–26. https://doi.org/10.15517/lank.v0i0.11529

Bogarín, D., Z. Serracín, Z. Samudio, R. Rincón, and F. Pupulín. 2014. An Updated Checklist of the Orchidaceae of Panama. *Lankesteriana*, 14:135–364. https://doi.org/10.15517/lank.v14i3.17958

Dalling, J. W., C. M. Prada, K. D. Heineman, K. M. Andersen, A. Morris, J. Pardo, E. Hollenbeck, P. Caballero, C. Espinosa, E. García, and B. L. Turner. 2021. Introduction to the Fortuna Forest Reserve: Soil and Climate Effects on the Tree Communities of a Premontane Tropical Forest. In *The Fortuna Forest Reserve, Panama: Interacting Effects of Climate and Soils on the Biota of Wet Premontane Tropical Forest*, ed. J. W. Dalling and B. L. Turner, pp. 1–33. Smithsonian Contributions to Botany, No. 112. Washington, D.C.: Smithsonian Institution Scholarly Press.

Givnish, T. J., D. Spalink, M. Ames, S. P. Lyon, S. J. Hunter, A. Zuluaga, W. J. D. Iles, M. A. Clements, M. T. K. Arroyo, J. Leebens-Mack, L. Endara, R. Kriebel, K. M. Neubig, W. M. Whitten, N. H. Williams, and K. M. Cameron. 2015. Orchid Phylogenomics and Multiple Drivers of Their Extraordinary Diversification. *Proceedings. Biological Sciences*, 282:1–10. https://doi.org/10.1098/rspb.2015.1553

Gómez González, D. C., C. Rodríguez Quiel, G. Zotz, and M. Y. Bader. 2017. Species Richness and Biomass of Epiphytic Vegetation in a Tropical Montane Forest in Western Panama. *Tropical Conservation Science*, 10:1–17. https://doi.org/10.1177/1940082917698468

Gradstein, S. R. 2008. Epiphytes of Tropical Montane Forests: Impact of Deforestation and Climate Change. In *Tropical Mountain Forest: Patterns and Processes in a Biodiversity Hotspot*, ed. S. R. Gradstein, J. Homeier, and D. Gansert, pp. 51–65. Biodiversity and Ecology Series. Göttingen, Germany: Universitätsverlag Göttingen.

Gravendeel, B., A. Smithson, F. J. W. Slik, and A. Schuiteman. 2004. Epiphytism and Pollinator Specialization: Drivers for Orchid Diversity? *Philosophical Transactions of the Royal Society B: Biological Sciences*, 359:1523–1535. https://doi.org/10.1098/rstb.2004.1529

Hammel, B. E., M. H. Grayum, C. Herrera, and N. Zamora. 2003. *Manual de Plantas de Costa Rica. Volumen III. Monocotiledóneas (Orchidaceae-Zingiberaceae)* [Costa Rica plants manual. Vol. 3. Monocots (Orchidaceae-Zingiberaceae)]. St. Louis: Missouri Botanical Garden Press.

Hietz, P., W. Wanek, and M. Popp. 1999. Stable Isotopic Composition of Carbon and Nitrogen and Nitrogen Content in Vascular Epiphytes along an Altitudinal Transect. *Plant, Cell, & Environment*, 22:1435–1443. https://doi.org/10.1046/j.1365-3040.1999.00502.x

Hietz, P., W. Wanek, R. Wania, and N. M. Nadkarni. 2002. Nitrogen-15 Natural Abundance in a Montane Cloud Forest Canopy as an Indicator of Nitrogen Cycling and Epiphyte Nutrition. *Oecologia*, 131:350–355. https://doi.org/10.1007/s00442-002-0896-6

Högberg, P. 1997. ^{15}N Natural Abundance in Soil-Plant Systems. *New Phytologist*, 137:179–203. https://doi.org/10.1046/j.1469-8137.1997.00808.x

Kessler, M., and J. Kluge 2008. Diversity and Endemism in Tropical Montane Forests: From Patterns to Processes. In *Tropical Mountain Forest: Patterns and Processes in a Biodiversity Hotspot*, ed. S. R. Gradstein, J. Homeier, and D. Gansert, pp. 35–50. Biodiversity and Ecology Series. Göttingen, Germany: Universitätsverlag Göttingen.

Körner, Ch. 1989. The Nutritional Status of Plants from High Altitudes. *Oecologia*, 81:379–391. https://doi.org/10.1007/BF00377088

McPherson, G., M. Merello, and M. Fica. 2010. A Checklist of the Fortuna Dam Region, Chiriqui/Bocas Del Toro, Panama. http://www.mobot.org/MOBOT/Research/fortuna.shtml.

Muñoz, M., and J. Warner. 2016. Distribución de Poblaciones Silvestres y Descripción del Hábitat de *Phragmipedium* en Costa Rica [Distribution of wild populations and description of the *Phragmipedium* habitat in Costa Rica]. *Lankesteriana*, 7:66–70. https://doi.org/10.15517/lank.v7i1-2.18442

Muñoz, M., J. Warner, and F. J. Albertazzi. 2010. Genetic Diversity Analysis of the Endangered Slipper Orchid *Phragmipedium longifolium* in Costa Rica. *Plant Systematics and Evolution*, 290:217–223. https://doi.org/10.1007/s00606-010-0362-6

Muthukumar, T., and M. Shenbagam. 2017. Vegetative Anatomical Adaptations of *Epidendrum radicans* (Epidendroideae, Orchidaceae) to Epiphytic Conditions of Growth. *Modern Phytomorphology*, 11:117–130.

Osmond, C. B., W. G. Allaway, B. G. Sutton, J. H. Troughton, O. Queiroz, L. Ulrich, and K. Winter. 1973. Carbon Isotope Discrimination in Photosynthesis of CAM Plants. *Nature*, 246:41–42. https://doi.org/10.1038/246041a0

Pinheiro, F., and S. Cozzolino. 2013. *Epidendrum* (Orchidaceae) as a Model System for Ecological and Evolutionary Studies in the Neotropics. *Taxon*, 62:77–88. https://doi.org/10.1002/tax.621007

Plants of the World Online (POWO). n.d. Facilitated by the Royal Botanic Gardens, Kew. Accessed 6 September 2019. http://plantsoftheworldonline.org.

Pridgeon, A. M., P. J. Cribb, M. W. Chase, and F. N. Rasmussen. 2009. *Genera* Orchidacearum *Volume 5: Epidendroideae (Part II)*. New York: Oxford University Press.

Pupulín, F. 2002. Catálogo Revisado y Anotado de las Orchidaceae de Costa Rica [Revised and annotated catalog of the Orchidaceae of Costa Rica]. *Lankesteriana*, 4:1–88.

Santiago, L. S., K. Silvera, J. L. Andrade, and T. E. Dawson. 2005. El Uso de Isótopos Estables en Biología Tropical [The use of stable isotopes in tropical biology]. *Interciencia*, 30:536–542.

Schuiteman, A., and E. de Vogel. 2003. Taxonomy for Conservation. In *Orchid Conservation*, ed. K. W. Dixon, S. P. Kell, R. L. Barrett, and P. J. Cribb, pp. 55–68. Kota Kinabalu, Sabah: Natural History Publications.

Silvera, K., and E. Lasso. 2016. Ecophysiology and Crassulacean Acid Metabolism of Tropical Epiphytes. In *Tropical Tree Physiology: Adaptations and Responses in a Changing Environment*, *Tree Physiology*, ed. G. Goldstein and L. S. Santiago, pp. 25–43. Cham, Switzerland: Springer International.

Silvera, K., L. S. Santiago, and K. Winter. 2005. Distribution of Crassulacean Acid Metabolism in Orchids of Panama: Evidence of Selection for Weak and Strong Modes. *Functional Plant Biology*, 32:397–407. https://doi.org/10.1071/FP04179

Silvera, K., L. S. Santiago, J. C. Cushman, and K. Winter. 2009. Crassulacean Acid Metabolism and Epiphytism Linked to Adaptive Radiations in the Orchidaceae. *Plant Physiology*, 149:1838–1847. https://doi.org/10.1104/pp.108.132555

Silvera, K., L. S. Santiago, J. C. Cushman, and K. Winter. 2010. The Incidence of Crassulacean Acid Metabolism in Orchidaceae Derived from Carbon Isotope Ratios: A Checklist of the Flora of Panama and Costa Rica. *Botanical Journal of the Linnean Society*, 163:194–222. https://doi.org/10.1111/j.1095-8339.2010.01058.x

Stewart, G. R., S. Schmidt, L. L. Handley, M. H. Turnbull, P. D. Erskine, and C. A. Joly. 1995. ^{15}N Natural Abundance of Vascular Rainforest Epiphytes: Implications for Nitrogen Source and Acquisition. *Plant, Cell & Environment*, 18:85–90. https://doi.org/10.1111/j.1365-3040.1995.tb00547.x

Szlachetko, D. L., and M. Kolanowska. 2016. Notes on the Genus *Epilyna* (Orchidaceae), with the Description of Four New Species. *Annales Botanici Fennici*, 53:15–20. https://doi.org/10.5735/085.053.0203

Tanner, E. V. J., P. M. Vitousek, and E. Cuevas. 1998. Experimental Investigation of Nutrient Limitation of Forest Growth on Wet Tropical Mountains. *Ecology*, 79:10–22. https://doi.org/10.1890/0012-9658(1998)079[0010:EIONLO]2.0.CO;2

Vitória, A. P., E. Ávila-Lovera, T. de Oliveira Vieira, A. P. L. do Couto-Santos, T. J. Pereira, L. S. Funch, L. Freitas, L. A. P. de Miranda, P. J. F. P. Rodrigues, C. E. Rezende, and L. S. Santiago. 2018. Isotopic Composition of Leaf Carbon (δ^{13}C) and Nitrogen (δ^{15}N) of Deciduous and Evergreen Understorey Trees in Two Tropical Brazilian Atlantic Forests. *Journal of Tropical Ecology*, 34:145–156. https://doi.org/10.1017/S0266467418000093

Vitousek, P. M. 1984. Litterfall, Nutrient Cycling, and Nutrient Limitation in Tropical Forests. *Ecology*, 65:285–298. https://doi.org/10.2307/1939481

Wegner, C., M. Wunderlich, M. Kessler, and M. Schawe 2003. Foliar C:N Ratio of Ferns along an Andean Elevational Gradient. *Biotropica*, 35:486–490. https://doi.org/10.1111/j.1744-7429.2003.tb00605.x

Whitten, W. M., and M. Blanco. 2011. Defining Generic Limits in *Maxillaria*. *Orchids*, 80:104–113.

8. Diversity and Ecology of the Ferns in Fortuna

Jéssica L. Viana[1]* *and James W. Dalling*[1,2]

ABSTRACT. Ferns are the second-most diverse plant group, exhibiting a broad variety of habits from 1 mm floating herbs to 20 m tall tree ferns. Habitats with continually wet and warm environments, which are associated with mid-elevation tropical rainforests, harbor the highest fern diversity in the Neotropics. Here we describe the fern and lycophyte flora of the lower montane tropical rainforests of Fortuna Forest Reserve and adjacent Palo Seco Protected Forest and discuss the associations of their component species with environmental variables. As a result of extensive field collections, the current fern species list of Fortuna is extended, including two new distribution records for Panama. Floristic similarity across sites at Fortuna reflects similarities in underlying parent material and associated soil fertility, with several indicator taxa associated with particular soil nutrient conditions related to parent material type. Compositional variation among herbaceous ferns and tree ferns was remarkably similar with respect to parent material and soil variables. However, the abundance patterns of tree ferns diverged from those of herbaceous ferns in response to soil nutrient and light availability.

INTRODUCTION

The record of ferns on Earth is remarkably long. In the Late Devonian through Permian Periods (~400 million years [Ma] ago), the Coenopteridales are believed to have exhibited the first fernlike morphology and to have given rise to the earliest-emerging extant filicalean families, Gleicheniaceae and Osmundaceae (Phillips, 1974). They were characterized by laminar fronds, circinate venation, and foliar-borne annulate sporangia, morphological traits that characterize modern fern taxa. While the relatively invariant morphology prevalent in ferns seems to have failed to generate the evolutionary novelties of angiosperms, ferns have nevertheless succeeded by preserving their leaf as a functional photosynthetic and reproductive organ. As a bifunctional organ, leaves in ferns have also undergone a diversification in shape and form reflecting the ecological requirements of the species (Vasco et al., 2013; Watkins et al., 2016).

Phylogenetic studies employing chloroplast markers of living taxa for evolutionary inferences (Schneider et al., 2004; Schuettpelz and Pryer, 2009, 2007) suggest that ferns are a monophyletic lineage and the closest relative to the seed plants, with lycophytes being a sister group to ferns and seed plants. These studies imply a radiation event in the leptosporangiate ferns (i.e., ferns in which sporangia emerge from a single epidermal cell) during the Late Cretaceous. More recently, Testo and Sundue (2016) used chloroplast markers and fossil data calibration to suggest that the origin of all ferns – including both Equisetaceae and Psilotaceae families – took place during the Silurian (~440 Ma ago), and leptosporangiate ferns, during the Carboniferous. This is much earlier than previously hypothesized, suggesting that the most modern taxa arose in the Cretaceous and diversified during the Cenozoic (Schneider et al., 2004; Schuettpelz and Pryer, 2009). One concern

---

[1] Department of Plant Biology, University of Illinois at Urbana-Champaign, 265 Morrill Hall, 505 S. Goodwin Ave, Urbana, IL 61801, USA.

[2] Smithsonian Tropical Research Institute, Apartado 0843-03092, Balboa, Ancon, Republic of Panama.

* Correspondence: lira.phb@gmail.com

is that these studies (i.e., Schneider et al., 2004; Schuettpelz and Pryer, 2009) are based on plastid gene markers, which provide incomplete information on ancestry given their single linkage group and uniparental origin (Wolf et al., 2018). Furthermore, hybridization events, significant and recurrent in ferns, are missed in plastid phylogenetics. New approaches point toward the use of low-copy nuclear sequence data for acquiring multilocus nuclear-encoded genes, which should provide a better detection of signatures of complex evolutionary histories such as those of ferns.

With no major significant changes in their reproductive biology over millions of years, ferns preserve a remarkable and singular means of reproduction given their free-living gametophyte stage. Three types of sexual breeding systems are undertaken by ferns. Outcrossing and sporophytic selfing breeding types need eggs and sperm from different gametophytes, but for outcrossing types, gametophytes need to come from differing sporophyte parents, whereas in sporophytic selfing types, gametophytes can be derived from the same sporophyte individual. These breeding systems are equivalent to those of seed plants. The third type is gametophytic selfing, in which eggs and sperm derive from a single, bisexual gametophyte, a unique breeding system in homosporous fern lineages that enable their capacity for extreme inbreeding (Sessa et al., 2016). In the short term, gametophytic selfing reduces genetic variation, resulting in progeny that have identical pairs of genes for any given pair of hereditary characteristics. However, gametophytic selfing also increases the recruitment potential of homosporous ferns by enabling colonization following long-distance dispersal (Klekowski, 1979).

In addition to possessing these diverse breeding systems, ferns are set apart from bryophytes and seed plants by having sporophyte and gametophyte stages independent of one another. This singular dichotomy, found only in the life cycle of ferns, poses not only stimulating and demanding questions to future field-based ecological studies but also a concern about how to approach ferns when considering the effects of one distinct life stage on another. While the ecological distribution of sporophytes may be dependent on the capacity of gametophytes to acquire resources for growth and reproduction, gametophytes can also increase species ranges by occurring in areas where its sporophyte stage is absent (Greer and McCarthy, 1999; Nitta et al., 2016). Thus, it is imperative that upcoming ecological studies involving ferns consider how the biology of gametophytes might impact the fate of sporophytes, considering the advantages and disadvantages of having a flexible breeding system, as ferns do (Page, 2002; Sessa et al., 2016).

FERN DIVERSITY AND ENVIRONMENTAL GRADIENTS

After flowering plants, ferns are the most diverse vascular plant group in the world (Kreft et al., 2010). The highest diversity is associated with tropical mid-elevation forests and oceanic island habitats (Moran, 2008). Mountains with elevations of 800 to 2,000 m maintain the highest species richness and levels of endemism (Kluge and Kessler, 2006). Tropical forests featuring mid-elevation slopes usually experience higher precipitation rates and reduced seasonality when compared to lowland tropical forests, which coupled with frequent cloud cover provides the humid conditions for ferns to complete their life cycle. Although it is thought that water is essential for ferns, there are species with physiological and reproductive adaptations that enable ferns to cope with dry conditions (Holmlund et al., 2020; Paul et al., 1995). Furthermore, local habitat heterogeneity associated with slope, aspect, and soil variation on mountains may also contribute to the observed higher diversity at these sites. In an exploration of species microhabitat distributions and their elevational ranges, Jones et al. (2011) suggested that microhabitat requirements of mid-elevation fern species may differ from those of lowland forests.

Fortuna Forest Reserve and the adjacent southeastern part of the Palo Seco Protected Forest (henceforth Fortuna), are lower montane humid to superhumid rainforests (Holdridge, 1947) located in western Panama with altitude varying from 700 to 2,000 m above sea level (asl). Twelve one-hectare plots were established across the reserves to sample variation in climate and underlying parent material and soil characteristics (Figure 8.1; Prada et al., 2017; Dalling et al., this volume; Turner and Dalling, this volume). In this area, with elevations from 850 to 1,300 m, mean annual rainfall ranges from 4,400 to 6600 mm with increasing seasonality from the Caribbean to the Pacific slope. Both parent material and associated soil conditions and precipitation have been found to strongly influence canopy tree species and understory palm species distributions (Andersen et al., 2010; Prada et al., 2017). Here we focus on (1) describing the major floristic components of ferns and lycophytes in Fortuna and (2) characterizing habitat associations of terrestrial herbaceous ferns and tree ferns.

To examine the regional diversity of ferns in Fortuna, we considered the most prominent macroenvironmental features. These include (1) parent material, which consists of multiple distinct volcanically derived rocks: rhyolite, mafic-volcanic, dacite, basalt, and undifferentiated volcanics (Silva et al., this volume) that give rise to soils differing in nutrient availability (see Turner and Dalling, this volume); (2) annual and seasonal precipitation; and (3) light availability, given differences in canopy structure across Fortuna and the high frequency of low-level cloud cover in these lower montane forests (Dalling et al., this volume). The analysis of the fern community at Fortuna included an existing list of taxa compiled by McPherson et al. (2010) at the MOBOT projects webpage and in situ field collections. Field collections were focused mostly on terrestrial species at the 12 one-hectare plots. Specimens were also collected along the trails that lead to those plots. All specimens collected were identified and deposited in the Universidad de Panama Herbarium (PMA) and the Universidad Autónoma de Chiriquí (UNACHI). The Taxonomic Name Resolution Service (TNRS) was used to obtain standardized scientific names and to resolve synonyms (TNRS iPlant Collaborative, version 4.0, http://tnrs.iplantcollaborative.org).

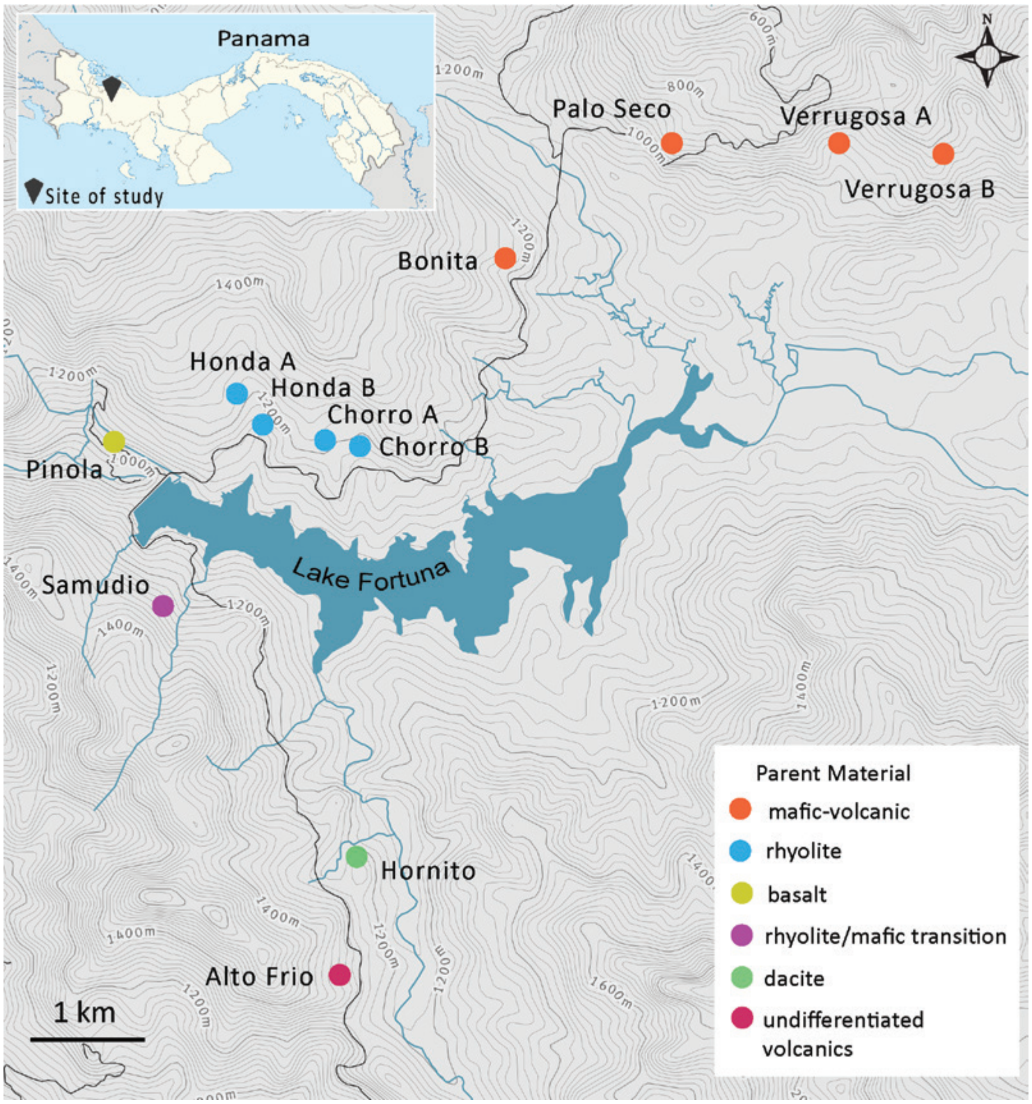

FIGURE 8.1. Location of the 12 one-hectare plots surveyed at Fortuna and Palo Seco forests.

FORTUNA FERN AND LYCOPHYTE COMPOSITIONAL DIVERSITY

From the species list retrieved from McPherson et al. (2010), a total of 265 species names were listed, including epiphytes, terrestrial herbaceous ferns, and tree fern taxa, of which 241 species names were accepted, 23 were synonyms, and one name was unresolved. We obtained 102 species during in situ field collections (appendix 8.1), of which 77 came from the 12 one-hectare plot surveys and 25 from surrounding access trails. These collections contributed an additional 48 taxa (of which 39 are terrestrial) to the McPherson list, resulting in a total of 289 fern and lycophyte species. These taxa represent 25 families and 81 genera. Dryopteridaceae (53 spp.) was the richest family (Figure 8.2). The genus *Elaphoglossum*, nested in this family, contributed more than half of the species (29 spp.), representing a large fraction of the epiphytic component of the flora of Fortuna. *Elaphoglossum* has also been reported as the most species-rich genus in a fern flora of a mid-elevation montane forest in Peru (Jones et al., 2011). Other families important at Fortuna include Polypodiaceae (39 spp.), containing mostly epiphytic species, and Hymenophyllaceae (22 spp.) with both epiphytic and terrestrial species. *Diplazium* (Athyriaceae) and *Asplenium* (Aspleniaceae) were the fourth-ranked genera with 19 species each. *Diplazium* is comprised exclusively of terrestrial species, whereas *Asplenium* exhibits varied habits. The genus *Cyathea* (15 spp.) and species from the family Thelypteridaceae (18 spp.) are also important components of the Fortuna fern flora. Thelypteridaceae are mostly terrestrial species, while *Cyathea* are tree continuation: from the family Cyatheaceae. Only 11% of the genera were represented by a single species. Lycophytes contributed an additional 21 species, with *Palhinhae* and *Selaginella* the most species-rich genera (9 spp. each). Terrestrial ferns represented 15.1% of the flora of Fortuna when considering only the vascular taxa censused in the plots.

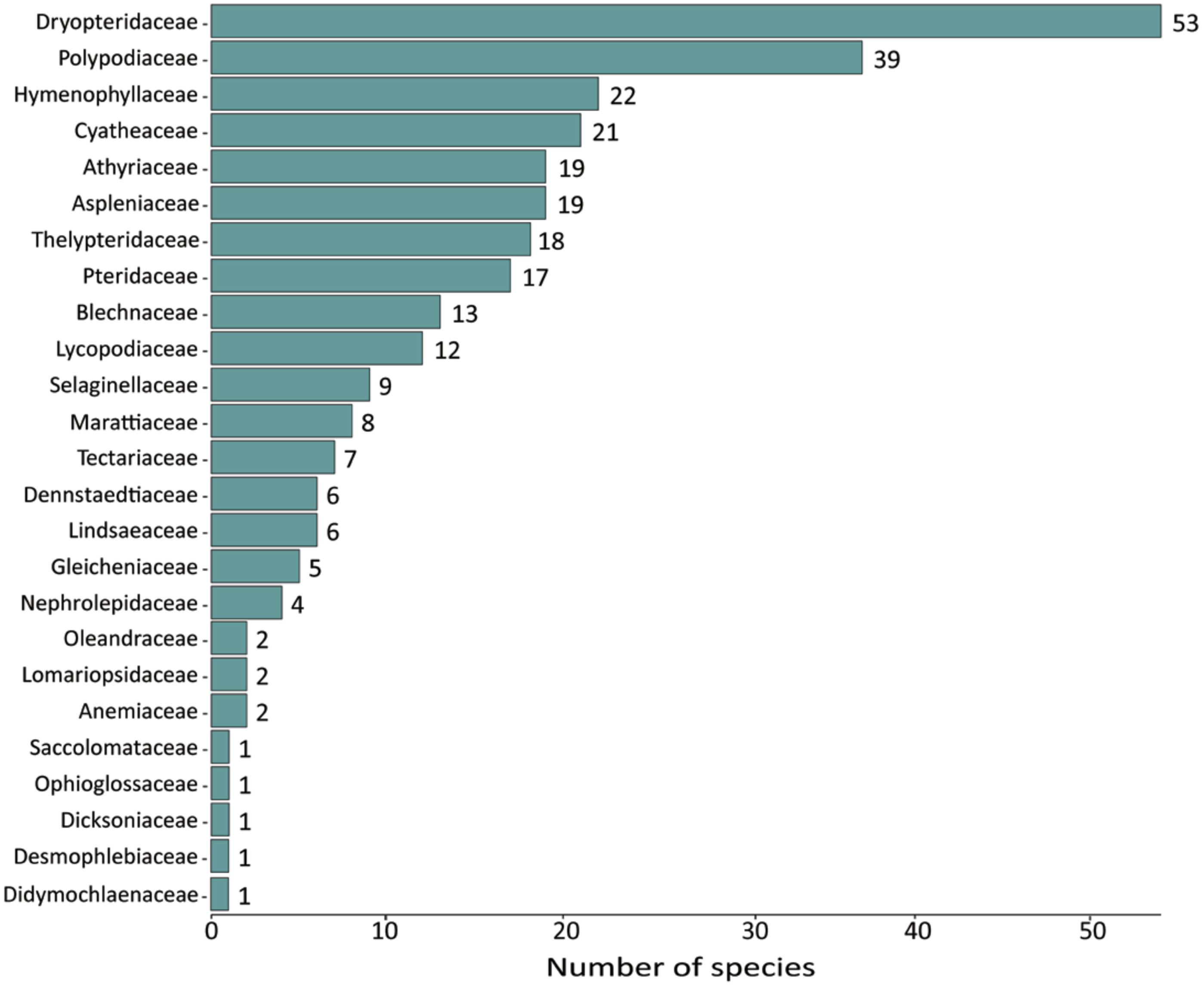

FIGURE 8.2. Species richness of Fortuna ferns species by family. Data source: McPherson et al. (2010) and Viana field collections.

An examination of different growth forms among fern species was conducted by consulting the online version of Flora Mesoamericana (http://legacy.tropicos.org/Project/FM), which provides detailed descriptions of species. Seven categories of growth form were listed for fern species: terrestrial, epiphyte, tree fern, hemiepiphyte, climbers, epiphyte/terrestrial/rupicolous (ETR), and epiphyte/terrestrial (ET). Fern species were distributed across growth forms as follows: 52.9% terrestrials, 35% epiphytes, 7.6% tree ferns, 2.1% ETR, 1.7% hemiepiphytes, 0.4% climbers (represented by a single species, *Salpichlaena volubilis*), and 0.4% ET, indicating that only a single species, *Asplenium harpeodes*, can adopt both growth forms. The low percentage of taxa assigned to the hemiepiphyte growth form might reflect the difficulty in documenting this habit in natural environments, although hemiepiphytism occurs in a diversity of families, including Blechnaceae, Hymenophyllaceae, Lomariopsidaceae, and Tectariaceae (Kramer and Green, 1990), which occur in Fortuna. Terrestrial and epiphytic ferns were the two most frequently encountered growth forms (Figure 8.3). The higher proportion of terrestrial ferns may not reflect actual richness differences at Fortuna but instead can be explained by field collectors who were focused primarily on terrestrial species.

Data on species collections from the 12 permanent plots (appendix 8.1) revealed that the overall abundance of terrestrial

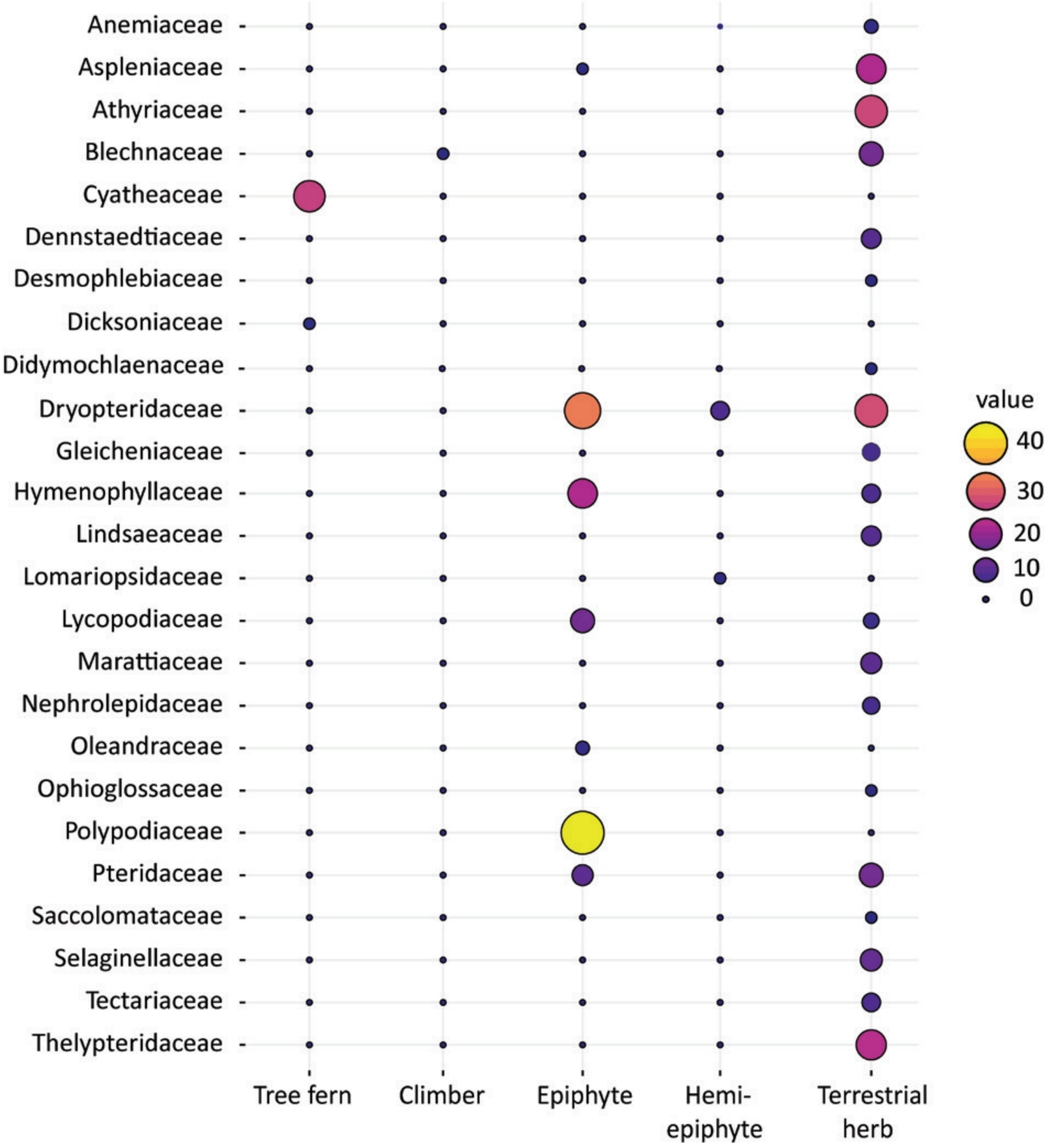

FIGURE 8.3. Distribution of fern species habits across fern families in Fortuna. Epiphyte/terrestrial/rupicolous species can adopt epiphytic, rupicolous, or terrestrial habits; epiphyte/terrestrial species can be epiphytic or terrestrial.

ferns peaks in sites with dacite and rhyolite-derived soils. Furthermore, when abundance is partitioned by growth form, tree ferns are more abundant in rhyolite sites that have soils characterized by a high total nitrogen to total phosphorus ratio (total N:P >16) and low pH (<5). In contrast, terrestrial herbaceous ferns are more abundant in dacite-derived soils associated with intermediate soil total N:P and effective cation exchange capacity (ECEC) (Viana et al., 2020). In contrast to abundance, the highest fern diversity and richness were obtained for two sites with mafic-volcanic-derived soils (Verrugosa A: Fisher's alpha diversity = 7.4; Bonita: richness = 25 species; Figure 8.4). Therefore, these patterns suggest that, at the regional scale, richness and diversity of

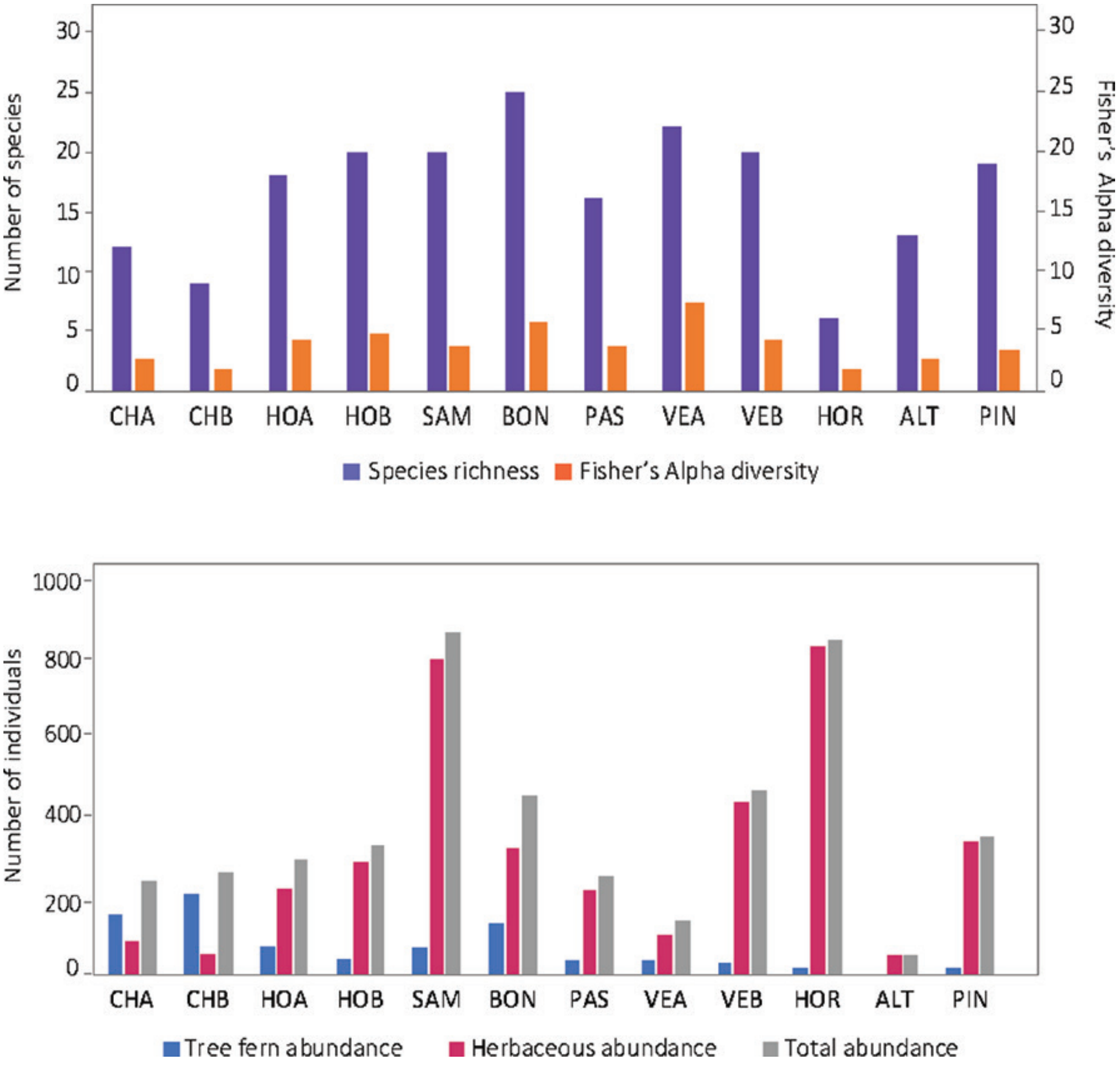

FIGURE 8.4. (Top) Species richness and Fisher's alpha diversity. (Bottom) Tree fern, herbaceous fern, and total fern abundance across 12 one-hectare plots at Fortuna. Sites were ordered from low-fertility sites on the left to high-fertility sites on the right (Prada et al., 2017). See Plates 8.1–8.13 for images of the floristic composition of fern species from Fortuna.

ferns appears to be greatest on sites with intermediate fertility, whereas abundance patterns might depend on growth form, with the highest abundance of tree ferns at low-fertility sites and with the highest abundance of herbaceous ferns at high-fertility sites.

LOCAL HABITAT ASSOCIATIONS OF TERRESTRIAL SPECIES

Fern biogeography in the Neotropics is well understood across precipitation and elevational gradients (Jones et al., 2013; Watkins et al., 2006). Beyond these broad-scale climatic effects on fern distributions, more localized habitat conditions, characterized by variation in soil and parent material, likely also play an important role. In lowland Amazonian forest where climatic conditions are relatively uniform, base cation concentration, soil clay content, pH, soil carbon to nitrogen ratio (C:N), and total phosphorus (P) and calcium (Ca) explain most of the variation in fern species composition (Tuomisto and Poulsen 1996; Jones et al., 2006; Jones et al., 2014; Jones et al., 2016; Zuquim et al., 2014). Steep gradients in the availability of key nutrients over short spatial scales, as occurs at Fortuna, could therefore provide new insights into the influence of soil variables on fern distribution and growth.

In this section, we describe the compositional associations of terrestrial ferns with environmental predictors by performing a nonmetric multidimensional scaling (NMDS) analysis. We used raw species abundances and standardized environmental data collected at 12 one-hectare plots established across distinct parent materials (Dalling et al., Table 1.1, this volume). Environmental data consisted of 19 soil variables, rainfall, and red to far-red light ratios (R:FR) measured at each plot. The compositional patterns of tree ferns and terrestrial herb fern species were analyzed together and then separately given the difference in habit and observed patterns in abundance across plots. A Procrustes analysis was performed to determine whether tree fern communities and herbaceous fern communities have similar or distinct configurations of ordination space. The significance of the Procrustes analysis was tested in 999 permutations. These ordination analyses are complementary to results presented in Viana et al. (2020), which contrasted all fern taxa and palm taxa at Fortuna. In addition, we report species associations with parent material and soil nutrient status based on an indicator species analysis (De Cáceres et al., 2010), which analyzes species associations with combinations of sites. Eleven 1 ha plots were selected and combined in three groups according to parent material: low-fertility rhyolite sites (Chorro A and B, Honda A and B); intermediate fertility mafic-volcanic sites (Bonita, Palo Seco, Verrugosa A and B); high-fertility basalt/dacite/undifferentiated-volcanic sites (Pinola, Hornito, Alto Frio). The Samudio site was excluded because it contains both rhyolite and mafic-volcanic microsites that are not mapped within the plot. Indicator species were identified using the *multipatt* function implemented using the package *indicspecies* in R (De Cáceres, 2013), which calculates an indicator value (IV) from the product of relative abundance and relative frequency of the species in the groups (Dufrêne and Legendre, 1997). We also repeated the analysis separating two rhyolite groups: the most infertile and deep rhyolite deposits (the two Chorro plots) and shallower rhyolite deposits (the two Honda plots). Significance was assessed by 999 random permutations with $p < 0.05$. In addition, species occurring in at least six plots, three site groups, and having greater than 150 individuals were classified as generalist taxa.

HERBACEOUS FERN HABITAT ASSOCIATIONS

Fern species composition was similar among plots within the same parent material group (Figure 8.5). Two distinct clusters formed in the NMDS space, one with all Rhyolite plots and another with all mafic-volcanic plots on the Caribbean slope (Palo Seco, Bonita, Verrugosa A and B). Plots with high soil fertility (Pinola, Alto Frio, and Hornito) did not cluster but were correlated with positive coordinates of the NMDS first dimension (NMDS1). Soil and light variables were significantly correlated with fern composition (appendix 8.2), notably soil moisture ($r^2 = 0.83$, $p < 0.01$), total N: P ($r^2 = 0.74$, $p < 0.01$) and total P ($r^2 = 0.73$, $p < 0.01$). Herbaceous and tree fern NMDS ordinations showed a high degree of concordance based on Procrustes analysis ($m^2 = 0.22$; $p < 0.001$; Procrustes rotation correlation = 0.88), indicating that species composition–environment relationships of herbaceous and tree ferns were significantly more similar to each other than expected at random.

Twelve species were identified as indicator taxa based on preferences for the three classes of soil fertility (Table 8.1). Low-fertility rhyolite sites provided seven species, of which three were restricted to Honda sites, two were restricted to Chorro sites, and two occurred on both Chorro and Honda sites. Intermediate fertility mafic-volcanic sites provided three species, and high-fertility basalt/dacite sites provided a single species. All seven species restricted to low-fertility sites belonged to three families: Lindsaeaceae (1 sp.), Cyatheaceae (4 spp.), and Blechnaceae (2 spp.). The four species from the intermediate-fertility sites were distributed into three families: Dryopteridaceae (2 spp.), Cyatheaceae (1 sp.), and Marattiaceae (1 spp.). The single species restricted to high-fertility sites belongs to the Athyriaceae family.

Numerous taxa that were not selected by the indicator analysis also had constrained distributions. *Desmophlebium lechleri* and *Thelypteris frigida* were relatively frequent at both Chorro A and B, while *Lindsaea imrayana* and *Danaea* sp. were restricted to Chorro B but were not abundant. *Parablechnum schiedeanum*§ (for species marked §, taxa were recorded at the site but not included in the plot survey) was also observed only at Chorro. In the Honda plots, we often found the generalist species *Olfersia cervina* and numerous juvenile individuals of *Cyathea nigripes*. Scattered aggregations of *Megalastrum biseriale*, and *Megalastrum pulverulentum* were restricted to Honda sites. At Samudio, the site that was excluded from the indicator species analysis, *Diplazium macrophyllum* dominates the understory where the canopy is open. Its occurrence was restricted to this site. *Dicksonia sellowiana* was also found only in Samudio despite its broad distribution across Central and South America. It is an endangered species and is reportedly found in areas with high rates of canopy change (Alfonso-Moreno et al., 2011). The presence of these two taxa at Samudio may reflect a large number of treefalls in the plot that occurred in 2005 to 2006.

All plots located on the Caribbean slope of the Continental Divide (Bonita, Palo Seco, Verrugosa A and B) are classified as having mafic-volcanic parent material, with total N:P ranging from 7.7 to 11.1, pH ranging from 4.5 to 5.1, and relative clay-rich soils lacking a developed organic layer (Andersen et al., 2010; Turner and Dalling, this volume). The filmy fern *Trichomanes elegans*, displaying iridescent blue leaves, was recorded in all mafic-volcanic sites except Palo Seco, although it was observed in shady and sloping microsites outside the plot. Tuomisto and Ruokolainen (1993) reported the restriction of *T. elegans* to clay soils in a rain forest in the Peruvian Amazonia. *Dracoglossum plantagineum* and *Mickelia hemiotis* occurred only at the Verrugosa A and B sites, and *Thelypteris gigantea* occurred only at Verrugosa A.

The two plots on the southern side of Fortuna, Hornito and Alto Frio, are the most fertile plots in terms of extractable cations and P availability. Both sites are markedly seasonal, with lower mean annual precipitation at Alto Frio (Dalling et al., this volume). Hornito maintains several species-rich genera, including

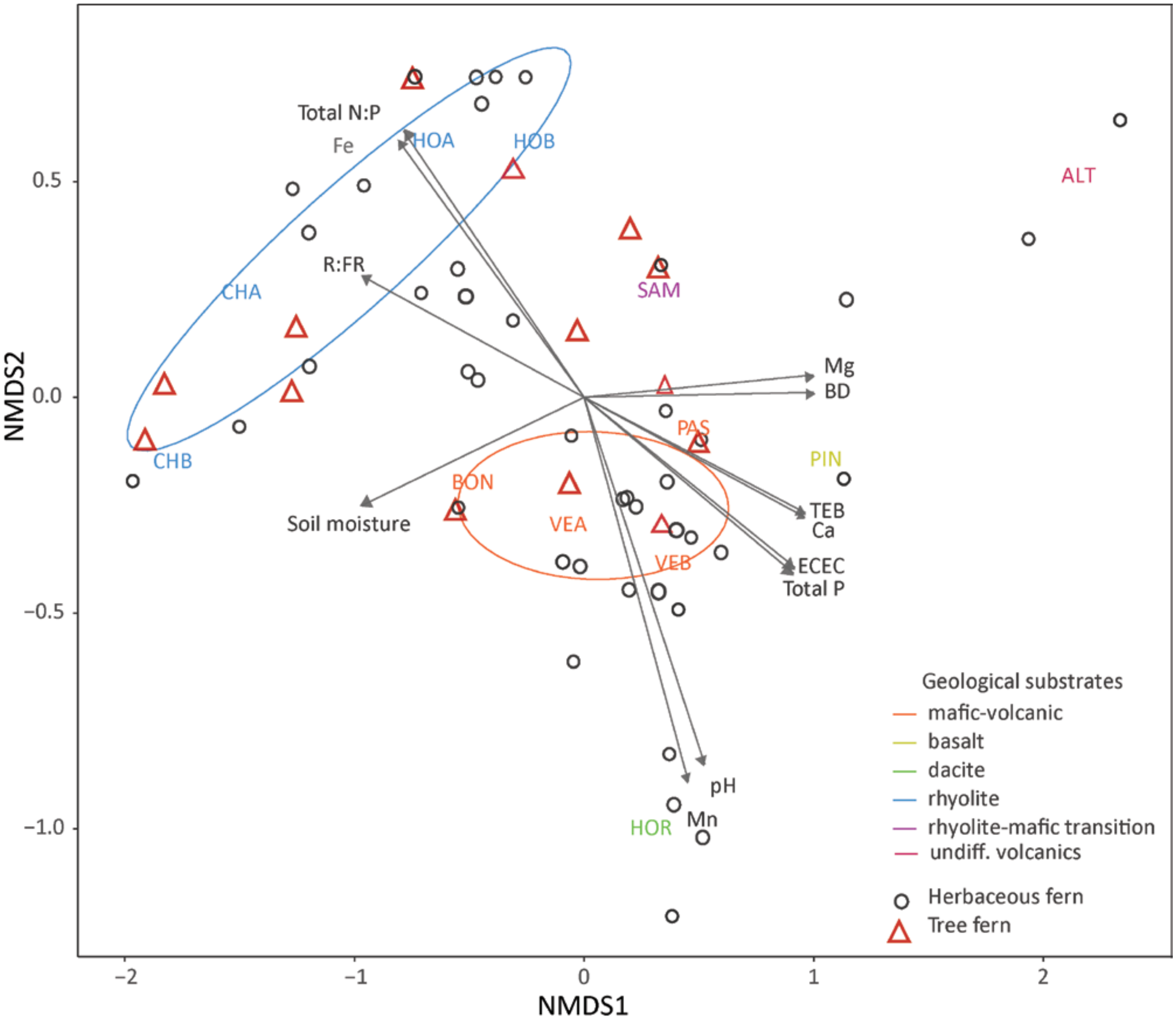

FIGURE 8.5. The first two dimensions of a nonmetric multidimensional scaling analysis of the floristic composition of 77 fern species collected from 12 one-hectare plots. Sites are color coded by geological substrate. Herbaceous and tree fern species scores are color and shape coded. Vectors indicate environmental variables significantly correlated with the fern community ($p \leq 0.05$). Confidence ellipses (95% confidence limit) are shown for geological substrates with more than three plots. Total N:P, total nitrogen to phosphorus ratio; Total P, total phosphorus; BD, bulk density; Mg, magnesium; ECEC, effective cation exchange capacity; TEB, total exchangeable bases; Ca, calcium; Mn, manganese; R:FR, red to far-red light ratios; Fe, iron.

Asplenium, *Thelypteris*, and *Tectaria*, while Alto Frio has only a species-poor assemblage. Species in common with other plots were *Adiantum tetraphyllum* and *Pteris altissima*. *Blechnum occidentale* and *Ctenitis submarginalis* were the most abundant species. *Phanerophlebia juglandifolia*§ and *Pteris quadriaurita* were found only at Alto Frio. Another high-fertility site, Pinola, with high rainfall and basalt parent material where soil total P is 618 µg cm^{-3}, had three taxa restricted to it: *Lastreopsis killipii*, *Diplazium striatastrum*, and *Thelypteris eggersii*.

While many taxa showed strong substrate or site preferences, we also found taxa that showed no evidence of an association with habitat. A key species that fits in this pattern was *Didymochlaena truncatula*, which occurred in most plots with high rainfall and well-drained soils. This species has a pantropical distribution (Garcia and Salino, 2008) and was relatively abundant at Fortuna. Farias et al. (2015) tested whether phenological patterns in *D. truncatula* were linked to temperature and rainfall in a lower montane forest in Brazil. No correlation was

TABLE 8.1. Indicator species analysis for terrestrial ferns in 11 one-hectare plots. Plots are divided into three groups based on parent material and associated soil fertility: rhyolite plots (Chorro A and B, Honda A and B), mafic-volcanic plots (Bonita, Palo Seco, Verrugosa A and B), and high-fertility plots (Pinola, Hornito, and Alto Frio). Generalist taxa are ordered by abundance. Observed IV = observed indicator value; *P* = significance values. —indicates no data available. See Plates 8.1–8.5 for images of indicator taxa.

Soil fertility conditions	Indicator species	Observed IV	*P*
Low fertility specialists (*rhyolite sites*)	*Lindsaea arcuata*	1.00	0.006
	Cyathea divergens	0.97	0.013
Chorro specialists	*Alsophila salvinii*	1.00	0.039
	Cyathea rojasiana	1.00	0.039
Honda specialists	*Austroblechnum stoloniferum*	1.00	0.032
	Blechnum binervatum	1.00	0.032
	Cyathea pinnula	0.99	0.031
Intermediate fertility specialists (mafic-volcanic sites)	*Danaea moritziana*	1.00	0.003
	Stigmatopteris heterophlebia	1.00	0.003
	Mickelia oligarchica	0.97	0.022
	Cyathea eggersii	0.87	0.048
High fertility specialists (basal, dacite and undifferentiated volcanic sites)	*Diplazium plantaginifolium*	0.816	0.049
Generalists	*Didymochlaena truncatula*	—	—
	Diplazium urticifolium	—	—
	Megalastrum atrogriseum	—	—
	Olfersia cervina	—	—

found between sterile or fertile leaf production and environmental factors, only leaf mortality and leaf growth per month were negatively correlated with rainfall. If phenological responses of *D. truncatula* are not correlated to specific environmental factors, further functional traits such as those regarding its gametophyte (e.g., longevity, drought resistance, or light requirements) may provide novel insights. Other species that exhibit no clear soil habitat association were *Megalastrum atrogriseum*, *Diplazium urticifolium*, both terrestrial herbs, and the tree ferns *Alsophila erinacea* and *Cyathea multiflora*.

Based on regression trees and indicator species analysis, Zuquim et al. (2014) found that *Adiantum* and *Pteris* species at a lowland forest located in Brazilian Amazonia were both associated with high-cation sites, in accordance with observations at Fortuna, where the only species of *Adiantum* occurred in dacite and basalt sites. In the same study, *Lindsaea* species were indicators of the poorer soils. Interestingly, distinct species from Lindsaeaceae were separated by soil type in Fortuna. *Lindsaea arcuata* and *L. imrayana* occurred exclusively on the infertile rhyolite plots, while *L. klotzschiana*[§] was observed only in a fertile site with dacite parent material. Furthermore, at both dacite and rhyolite plots, *Lindsaea* species were frequently found in association with *Oreomunnea mexicana* trees, one of the few ectomycorrhizal trees at Fortuna, and a species that forms monodominant stands characterized by a reduced availability of inorganic nitrogen (Corrales et al., 2016).

Overall, the observed species occurrences at Fortuna provide strong support for species edaphic preferences across the soil nutrient gradient. Determining the response of ferns to soil nutrients and other soil characteristics, such as particle size from plot-based plant and soil surveys, is useful because small-scale soil variation affecting plants is often absent from large-scale soil surveys (Zuquim et al., 2014). Furthermore, our knowledge of fern species and their soil associations provides a platform for future work to elucidate the functional basis of soil affinities of ferns, possibly focusing on mycorrhizal associations and/or physiological traits associated with distinct root morphologies. Seeking an explanation for how ferns have survived for more than 400 Ma might improve our understanding of other plant groups and their relationship with soils as well.

In this section, we have illustrated the predictive power of soil conditions over the composition of terrestrial fern species. The association of some epiphytic taxa with specific soil and site conditions has been already demonstrated (Tuomisto, 2006). At the community level, although it is anticipated that terrestrial ferns show greater habitat specialization than epiphytic ones, this prediction is yet to be tested.

Tree Fern Habitat Associations

Tree ferns are distinct from herbaceous ferns because of the development of a caudex, or trunk-like structure. This morphological feature likely gave tree ferns a competitive advantage over herbaceous plant groups in the light-limited understory. However, the character is not unique to the clade Cyatheaceae to which most tree ferns belong. Neither do all ferns in Cyatheaceae have a trunk-like habit (Large and Braggins, 2004). Cyatheaceae consists of 643 species (PPG 1, 2016), making them the most speciose family among the order Cyatheales. The family Cyatheaceae radiated during the late Jurassic (Korall and Pryer, 2014) and expanded its range across tropical, subtropical, and temperate regions.

With a broad latitudinal range (23°N to 50°S latitude), tree ferns are present in most rainforests around the world as an important compositional and structural unit (Brock et al., 2016). Most tree ferns are associated with tropical montane and premontane cloud forests that provide a combination of topographic and climatic features, including persistent orographic rainfall. Temperature is also a key factor explaining tree fern distribution. With the exception of a few New Zealand species, most tree ferns do not occur where temperatures drop below freezing (Brock et al., 2016).

The floristic survey of the 12 one-hectare plots yielded 814 individuals: 12 species and 1 morphospecies in the Cyatheaceae and a single species in the Dicksoniaceae family. *Cyathea rojasiana* accounted for 32% of all tree fern individuals. Only two plots (Chorro A and B; rhyolite parent material) accounted for all individuals of this species. In fact, from the 258 fern individuals recorded in Chorro B, 79% were tree ferns. In contrast, *Cyathea multiflora*, ranked as the second-most abundant tree fern, occurred in all but rhyolite sites and Alto Frio. *Cyathea divergens* and *Alsophila erinacea* were the third- and fourth-most abundant taxa.

Procrustes analysis of the NMDS ordination of herbaceous ferns and tree ferns showed that floristic distances among taxa in these groups were significantly more similar to each other than expected by chance. Environmental factors significantly correlated with tree fern floristic composition overlapped with those of herbaceous ferns. Moisture and total N:P obtained the highest correlation values for both tree ferns and herbaceous ferns (appendix 8.2). Exchangeable iron, the R:FR ratio, and total P obtained higher correlation values for tree fern composition, while total P, dry season rainfall, exchangeable calcium, total extractable base cations, and effective cation exchange capacity obtained higher correlation values for herbaceous fern composition. To compare visually the floristic patterns of herbaceous and tree ferns, we fitted soil fertility as a categorical variable into the NMDS ordination. Sites were assigned one of the three levels of soil fertility variable: low (four rhyolite sites), intermediate (four mafic-volcanics sites), and high (three sites: basalt, dacite, and undifferentiated volcanics). Samudio was excluded from this analysis. Soil fertility was significantly correlated with both herbaceous and tree ferns ($r^2 = 0.73$, $p = 0.001$ and $r^2 = 0.60$, $p = 0.023$). Soil fertility levels clustered similarly in both herbaceous and tree ferns (Figure 8.6).

Although herbaceous and tree ferns showed similar floristic association patterns, the two groups showed opposing abundance patterns in relation to total soil N:P and R:FR (Viana et al., 2020). Tree fern abundance was associated with low soil fertility sites and positively correlated with total soil N:P (and therefore associated with rhyolite sites), whereas herbaceous fern abundance was negatively correlated with high total N:P (and therefore associated with the dacite site). A similar response of these two groups was also obtained with R:FR. Differences in the abundance of herbaceous ferns and tree ferns across parent materials suggest that coexistence of these groups in the understory might in part reflect resource partitioning.

Interestingly, the direction of tree fern species associations with P availability may be ecosystem dependent. At Fortuna, high tree fern abundance is associated with relatively infertile, low soil P sites. Similarly, in Hawaiian tropical forests, tree fern cover is lower in sites with either high N or high P concentrations (Vitousek, 2004). In contrast, in cool-temperate rainforest systems in New Zealand, tree fern abundance is higher on alluvial terrain and the early stages of chronosequences characterized by N limitation of productivity (Coomes et al., 2013; Turner et al., 2018). Soil moisture conditions have also been associated with tree fern distributional patterns (Brock et al., 2016). However, there is still much to reveal about the ecology of tree ferns. For instance, we do not know whether the free-living gametophytes of tree ferns are influenced by by similar or distinct soil conditions.

NOTES ON SPECIES OCCURRENCE

Patterns of endemism in tropical ferns and lycophytes are similar to those of richness (Moran, 2008) characterized by a unimodal relationship with elevation. However, endemism peaks at a higher elevation than the peak species richness (Kessler, 2010). According to Moran and Riba (1995), 15% of Costa Rican and Panamanian ferns and lycophytes are endemic to the two countries. Of the five endemic fern species found at PILA, La Amistad International Park, a protected area that straddles the border and encompasses half of the Talamanca mountain range, only one, *Trichomanes consanguineum*, is found at Fortuna. Among lycophytes, *Selaginalla corraea* Valdespino is the only species endemic to Fortuna (Valdespino, 1993). It is described as a very small plant, much like a moss in appearance, and with an epipetric or terrestrial habit (Figure 8.7). *Selaginalla corraea* is associated with rhyolitic rocks; with soils on steep, forested slopes; and an elevation of 1,100 to 1,200 m (I. Valdespino, personal

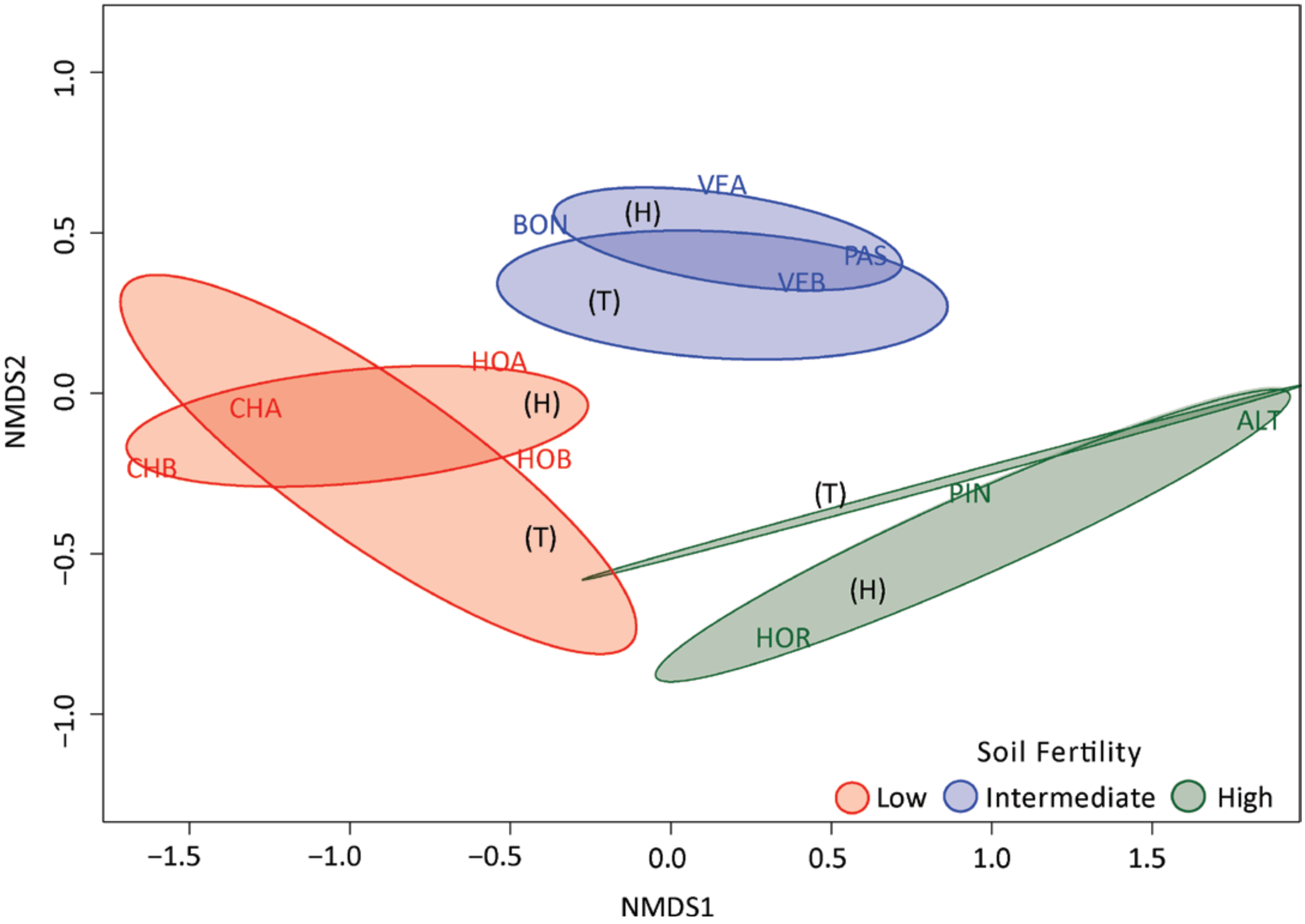

FIGURE 8.6. The first two dimensions of nonmetric multidimensional scaling analysis using raw abundance data. Confidence ellipses (95% confidence limit) were calculated for soil fertility categorical variables with three levels: low (rhyolite geological substrates), intermediate (mafic-volcanic), and high (basalt, dacite and undifferentiated volcanics). The Samudio plot, which includes both rhyolite and mafic microsites, was excluded. Confidence ellipses are shown for both tree ferns (T) and herbaceous ferns (H). Site scores are based on the floristic composition of the herbaceous ferns.

communication, 15 November 2018), an environmental description that fits the Honda and Chorro watersheds. The occurrence of *Cyathea rojasiana*, one of the few tree fern species endemic to Panama, is also restricted to very wet cloud forests. The type specimen used to describe the species was collected in the vicinity of Quebrada Bonito, one of the wettest parts of the Fortuna reserve.

Extensive field collections at Fortuna are likely to yield additional taxa. Based on recent field collections, we report new records for Panama of two fern species. The first is *Bolbitis hastata*, which had a previously known range that extended from Mexico to Costa Rica. This species was found in the Hornito plot in ephemeral streams beds. No other population of this species has been observed in the Fortuna reserve. The second is *Thelypteris hatchii*, which ranges from southern Mexico to northern Costa Rica. However, *T. hatchii* is common under high canopy forest and gentle slopes in Hornito plot, accounting for 22% of fern individuals in that plot. We also report the occurrence of *Diplazium* x *verapax* in this area, a rare rather than endemic hybrid species resulting from the interaction between *D. plantaginifolium* and *D. werckleanum*, its likely co-occurring parents (Testo et al., 2017). *Diplazium* x *verapax* is a peculiar-looking fern; it shows an intermediate appearance between its parental progenitors (Figure 8.8). *Diplazium plantaginifolium* has simple leaves, and

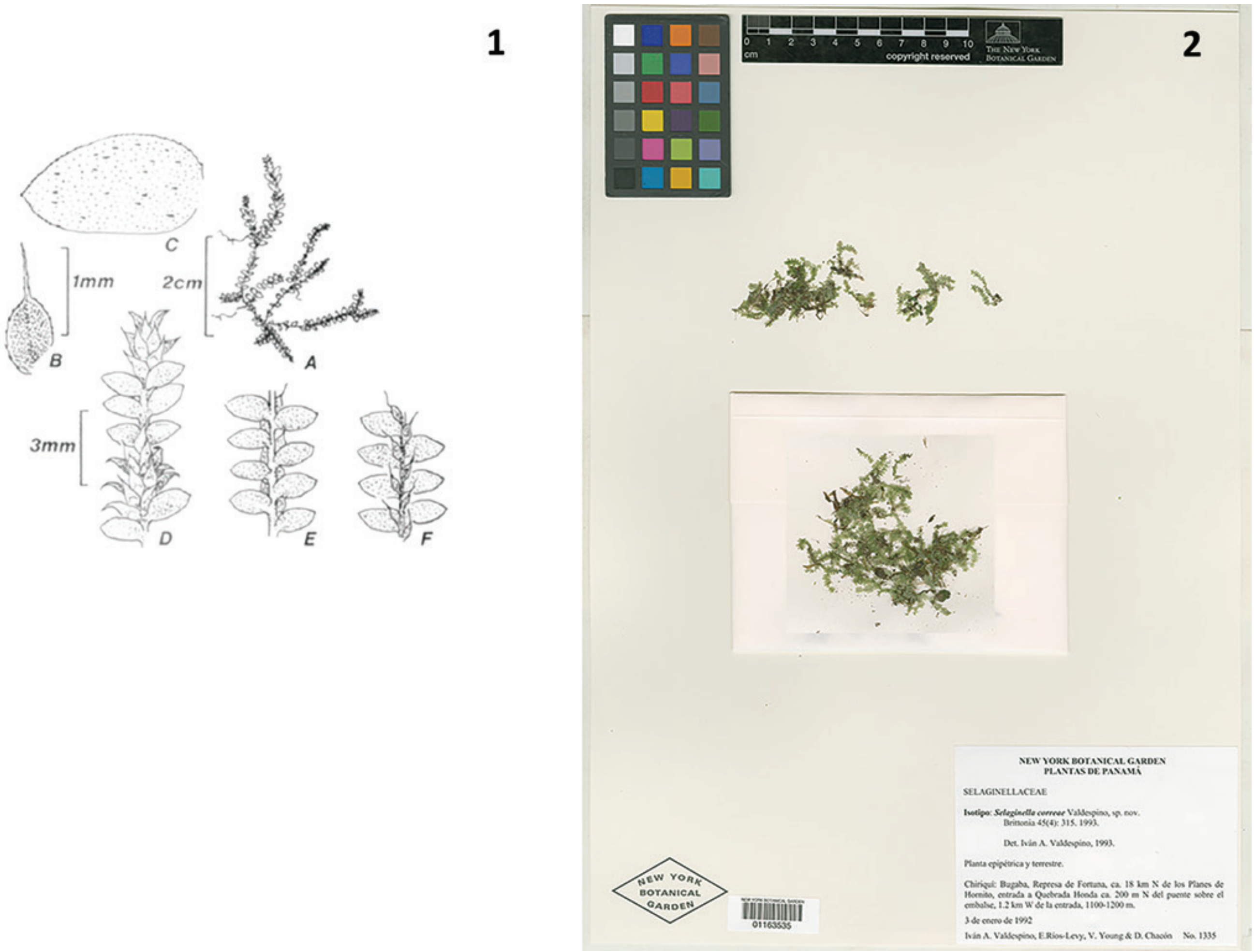

NEW YORK BOTANICAL GARDEN
PLANTAS DE PANAMÁ

SELAGINELLACEAE

Isotipo: ***Selaginella correae*** Valdespino, sp. nov.
Brittonia 45(4): 315. 1993.

Det. Iván A. Valdespino, 1993.

Planta epipétrica y terrestre.

Chiriquí: Bugaba, Represa de Fortuna, ca. 18 km N de los Planes de Hornito, entrada a Quebrada Honda ca. 200 m N del puente sobre el embalse, 1.2 km W de la entrada, 1100-1200 m.

3 de enero de 1992

Iván A. Valdespino, E.Ríos-Levy, V. Young & D. Chacón No. 1335

FIGURE 8.7. *Selaginella correae*, a lycophyte species endemic of Fortuna. Morphological features of *S. correae*. 1: (a) plant habit, (b) median leaf, (c) lateral leaf hairs, (d) fertile portions (strobili) of the stem, (e and f) lower and upper surface of stem. Modified from Valdespino (1993). 2: Exsiccate of the specimen collection from the New York Botanical Garden (I. A. Valdespino 1335 with E. Ríos-Levy, V. Young & D. Chacón, NY).

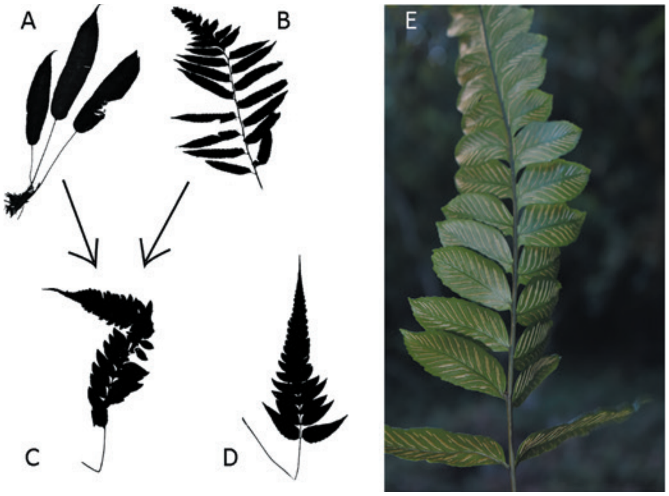

FIGURE 8.8. Silhouettes of four *Diplazium* taxa. (a) *Diplazium plantaginifolium* (G.J. Gastrony et al. 651,MO). (b) *Diplazium werckleanum* (I. deMartinez 58,MO). (c) *D.* x *verapax* (W.L. Testo 1045,NY). (d) *D. riedelianum* (E. Schmalz s.n.,VT). (e) Reproductive leaf of *D.* x *verapax* from a specimen collected at Fortuna.

D. werckleanum, pinnate leaves. This hybrid could be easily be confused with *D. riedelianum* (Bong. ex Kuhn) Kuhn ex C. Chr., although a recent treatment of these species restricted *D. riedelianum* to Argentina, Brazil, and Paraguay (200 to 800 m), whereas *D.* x *verapax* ranges from Mexico to Panama (650 to 1,690 m). Because hybrids are usually sterile, the only way to reproduce is by the means of buds located in the lamina, apparently the reason this hybrid is reported to be rare (Testo et al., 2017). Indeed, in Fortuna, *D.* x *verapax* is found only in the Hornito area.

SUMMARY

Fortuna forests are characterized by diverse fern and lycophyte taxa. The examination of a previous list of the fern flora combined with in situ collections resulted in a 19% increase in species number. A major floristic contribution comes from the family Dryopteridaceae, comprised of epiphytic and terrestrial genera, in which the epiphytic genus *Elaphoglossum* – the richest in species – is included. Polypodiaceae, the second-most species-rich family, contributes exclusively epiphytic taxa. Prominent diverse terrestrial genera are the herbaceous taxa *Diplazium* and *Thelypteris* and tree fern genus *Cyathea*, considered a key component of the vegetation of mid- and high-elevation cloud forests in the Neotropics.

Fern species show clear habitat association across the gradient in soil fertility and parent material at Fortuna, with 12 indicator species significantly associated with groups of sites based on parent material. Rhyolite sites provided the highest number of indicator species. Herbaceous and tree ferns showed similar compositional patterns, but their relationship with total N:P was distinct: tree ferns were related to infertile soils (high total N:P), while herbaceous ferns were related to fertile soils (low total N:P).

APPENDIX 8.1

Terrestrial fern species present in the Fortuna Forest Reserve and adjacent upland areas of the Palo Seco reserve. This table combines species from plot and floristic surveys, and from the Fortuna species list (http://www.mobot.org/MOBOT/fortuna/fortunaDropdown.aspx). Shading indicates parent material (R/M = rhyolite–mafic-volcanic transition; Undif. = undifferentiated volcanics). *n* = total number of individuals across all plots; asterisk (*) = species not recorded in the Fortuna species list; x = species that occur along plot trails or its surroundings.

	Rhyolite				R/M	Mafic-volcanic				Basalt	Dacite	Undif.	
Families and species	Cho.A	Cho.B	Hon.A	Hon.B	Samu.	Bonita	Palo	Ver.A	Ver.B	Pinola	Horn.	Alto.	*n*
Anemiaceae													
Anemia hirsuta	—	—	—	—	—	—	—	—	—	—	—	—	—
Anemia phyllitidis	—	—	—	—	—	—	—	—	—	—	—	x	—
Aspleniaceae	—	—	—	—	—	—	—	—	—	—	—	—	—
Asplenium auriculatum	—	—	—	—	—	—	—	—	—	—	—	—	—
Asplenium cirrhatum	—	—	—	—	—	—	—	—	6	—	28	—	34
Asplenium cristatum	—	—	—	—	—	—	—	—	—	—	17	—	17
*Asplenium delitescens**	—	—	—	—	—	—	—	—	—	—	x	—	—
Asplenium dissectum	—	—	—	—	—	—	—	—	—	—	—	—	—
Asplenium gomezianum	—	—	—	—	—	—	—	—	—	—	—	—	—
Asplenium harpeodes	—	—	—	—	—	—	—	—	—	—	—	—	—
Asplenium holophlebium	—	—	—	—	—	—	—	—	—	—	—	—	—
*Asplenium laetum**	—	—	—	—	—	—	3	—	—	—	—	—	3
Asplenium miradorense	—	—	—	—	—	—	—	—	—	—	—	—	—
Asplenium obtusifolium	—	—	—	—	—	—	—	—	—	—	4	—	4
Asplenium pteropus	—	—	—	—	—	—	—	—	—	—	x	—	—
Asplenium pululahuae	—	—	—	—	—	—	—	—	—	—	—	—	—
Asplenium radicans	—	—	—	—	—	—	—	—	—	—	17	—	17
Asplenium repandulum	—	—	—	—	—	—	—	—	—	—	—	—	—
Asplenium riparium	—	—	—	—	—	—	—	—	—	—	—	—	—
Asplenium rutaceum	—	—	—	—	—	—	—	—	—	—	—	—	—
Asplenium sulcatum	—	—	—	—	—	—	—	—	—	—	—	—	—
Asplenium sp.	—	—	—	—	—	5	—	—	—	—	—	—	5
Athyriaceae													
Diplazium atirrense	—	—	—	—	—	5	3	—	1	—	—	—	9
Diplazium cristatum	—	—	—	—	—	—	—	—	—	1	—	—	1
Diplazium gomezianum	—	—	—	—	—	—	—	—	—	—	—	—	—
Diplazium hammelianum	—	—	—	—	—	—	—	—	—	—	—	—	—
Diplazium lindbergii	—	—	—	—	—	—	—	—	—	—	—	—	—
Diplazium lonchophyllum	—	—	—	—	—	—	—	—	—	—	—	—	—
Diplazium macrophyllum	—	—	—	—	328	—	—	—	—	—	—	—	328
*Diplazium obscurum**	—	—	4	—	—	11	—	1	—	—	—	—	16
Diplazium palmense	—	—	—	1	—	17	—	—	—	—	—	—	18

	Rhyolite				R/M	Mafic-volcanic				Basalt	Dacite	Undif.	
Families and species	Cho.A	Cho.B	Hon.A	Hon.B	Samu.	Bonita	Palo	Ver.A	Ver.B	Pinola	Horn.	Alto.	*n*
Diplazium paucipinnum	—	—	—	—	—	—	—	—	—	—	—	—	—
*Diplazium plantaginifolium**	—	—	—	—	—	—	—	—	—	1	59	—	60
Diplazium prominulum	—	—	—	—	—	—	2	—	24	21	283	—	330
Diplazium seemannii	—	—	—	—	—	—	—	—	—	—	—	—	—
*Diplazium solutum**	—	—	—	—	—	21	—	—	—	—	—	—	21
*Diplazium striatastrum**	—	—	—	—	—	—	—	—	—	22	—	—	22
Diplazium subsilvaticum	—	—	—	59	51	—	—	—	—	—	—	—	110
Diplazium urticifolium	—	—	7	3	166	23	22	—	84	21	1	—	327
Diplazium werckleanum	—	—	—	—	—	—	—	—	—	—	—	—	—
Diplazium x *verapax**	—	—	—	—	—	—	—	—	—	—	x	—	—
Blechnaceae													
Austroblechnum divergens	14	3	2	2	102	9	—	—	—	—	—	—	132
Austroblechnum lherminieri	—	—	—	—	3	—	—	—	—	—	29	—	32
Austroblechnum stoloniferum	—	—	2	9	—	—	—	—	—	—	—	—	11
Blechnum binervatum	—	—	2	2	—	—	—	—	—	—	—	—	4
Blechnum falciforme	—	—	—	—	—	—	—	—	—	—	—	—	—
*Blechnum gracile**	—	—	—	—	—	—	—	—	—	—	x	—	—
*Blechnum occidentale**	—	—	—	—	—	—	—	—	—	—	—	22	22
Blechnum wardiae	—	—	—	—	—	—	—	—	—	—	—	—	—
Blechnum werckleanum	—	—	—	—	—	—	—	—	—	—	—	—	—
*Parablechnum schiedeanum**	x	x	x	—	—	—	—	—	—	—	—	—	—
Salpichlaena volubilis	—	—	x	x	—	—	—	—	—	—	x	—	—
Cyatheaceae													
Alsophila erinacea	—	—	17	18	18	15	3	2	1	1	2	—	77
*Alsophila firma**	—	—	—	—	—	—	—	x	—	—	—	—	—
Alsophila polystichoides	—	—	—	—	—	10	—	—	—	—	—	—	10
Alsophila salvinii	3	40	—	—	—	—	—	—	—	—	—	—	43
Cyathea bicrenata	—	—	—	—	—	—	—	—	—	—	—	—	—
Cyathea chiricana	12	1	—	—	—	14	—	2	—	—	—	—	29
Cyathea cocleana	—	—	—	—	—	—	—	—	—	—	—	—	—
Cyathea delgadii	—	—	—	—	—	—	1	—	—	—	—	—	1
Cyathea divergens	18	24	27	9	—	6	—	5	—	—	—	—	89
Cyathea eggersii	—	—	—	—	3	36	4	12	—	—	—	—	55

(*Continued*)

	Rhyolite				R/M	Mafic-volcanic				Basalt	Dacite	Undif.	
Families and species	Cho.A	Cho.B	Hon.A	Hon.B	Samu.	Bonita	Palo	Ver.A	Ver.B	Pinola	Horn.	Alto.	*n*
Cyathea fulva	—	—	—	—	—	—	—	—	—	—	—	—	—
Cyathea horrida	—	—	—	1	8	—	3	—	6	—	—	—	18
Cyathea multiflora	—	—	—	—	13	50	26	15	25	16	16	—	161
Cyathea mutica	—	—	—	—	—	—	—	—	—	—	—	—	—
Cyathea nigripes	—	—	3	—	—	—	—	—	—	—	—	—	3
Cyathea pinnula	—	—	22	13	1	—	—	—	—	—	1	—	37
*Cyathea rojasiana**	120	140	—	—	—	—	—	—	—	—	—	—	260
*Cyathea schiedeana**	—	—	—	—	—	—	—	—	—	—	—	—	—
Cyathea sp.	—	—	5	—	—	—	—	—	—	—	—	—	5
Cyathea williamsii	—	—	—	—	—	—	—	—	—	—	—	—	—
Sphaeropteris brunei	—	—	—	—	—	—	—	—	—	—	—	—	—
Dennstaedtiaceae													
Blotiella lindeniana	—	—	—	—	—	—	—	—	—	—	—	—	—
Dennstaedtia dissecta	—	—	—	—	—	1	—	1	—	—	1	—	3
Dennstaedtia wercklei	—	—	—	—	—	—	—	—	—	—	—	—	—
Hypolepis nigrescens	—	—	—	—	—	—	—	—	—	—	—	—	—
Hypolepis stuebelii	—	—	—	—	—	—	—	—	—	—	—	—	—
Hypolepis viscosa	—	—	—	—	—	—	—	—	—	—	—	—	—
Desmophlebiaceae													
Desmophlebium lechleri	26	—	—	11	—	2	—	—	—	—	—	—	39
Dicksoniaceae													
Dicksonia sellowiana	—	—	—	1	23	—	—	—	—	—	—	—	24
Didymochlaenaceae													
Didymochlaena truncatula	—	—	52	13	62	—	24	14	75	46	77	—	363
Dryopteridaceae													
*Arachniodes denticulata**	—	—	—	—	—	—	—	—	—	—	x	—	—
Arachniodes ochropteroides	—	—	—	—	—	—	—	—	—	—	—	—	—
*Bolbitis hastata**	—	—	—	—	—	—	—	—	—	—	7	—	7
Ctenitis hemsleyana	—	—	—	—	—	—	—	—	—	—	—	—	—
*Ctenitis submarginalis**	—	—	—	—	—	—	—	—	—	—	—	6	6
*Elaphoglossum lingua**	1	—	—	104	—	—	—	—	—	—	—	—	105
*Elaphoglossum phoras**	—	—	—	—	1	—	—	—	—	—	—	—	1
*Lastreopsis killipii**	—	—	—	—	—	—	—	—	—	69	—	—	69

	Rhyolite				R/M	Mafic-volcanic				Basalt	Dacite	Undif.	
Families and species	**Cho.A**	**Cho.B**	**Hon.A**	**Hon.B**	**Samu.**	**Bonita**	**Palo**	**Ver.A**	**Ver.B**	**Pinola**	**Horn.**	**Alto.**	*n*
Megalastrum atrogriseum	—	—	—	4	12	2	2	4	5	78	89	—	196
*Megalastrum biseriale**	—	—	56	—	—	—	—	—	—	—	—	—	56
Megalastrum pulverulentum	—	—	27	—	—	—	—	—	—	—	—	—	27
Mickelia hemiotis	—	—	—	—	—	—	—	33	78	—	—	—	111
Mickelia nicotianifolia	—	—	—	—	—	—	—	—	—	—	—	—	—
Mickelia oligarchica	—	—	—	2	1	26	1	1	3	—	—	—	34
Olfersia cervina	2	—	26	38	—	91	—	1	1	—	—	—	159
Phanerophlebia juglandifolia	—	—	—	—	—	—	—	—	—	—	x	—	—
*Polystichum platyphyllum**	—	—	—	—	—	—	—	—	—	—	—	—	—
Polybotrya polybotryoides	—	—	—	—	9	—	—	—	—	—	—	—	9
Polybotrya sp.	—	—	—	1	—	—	—	—	—	—	—	—	1
Stigmatopteris heterophlebia	—	—	—	—	—	4	28	12	4	—	—	—	48
Stigmatopteris lechleri	—	—	—	—	—	—	—	—	—	—	—	—	—
*Stigmatopteris longicaudata**	—	—	—	—	—	—	—	—	—	—	—	—	—
Gleicheniaceae													
Sticherus bifidus	—	—	—	—	—	—	—	—	—	—	—	—	—
Sticherus compactus	—	—	—	—	—	—	—	—	—	—	—	—	—
Sticherus hastulatus	—	—	—	—	—	—	—	—	—	—	—	—	—
Sticherus hypoleucus	—	—	—	—	—	—	—	—	—	—	—	—	—
*Sticherus intermedius**	—	—	—	—	3	—	—	x	x	—	—	—	3
Hymenophyllaceae													
Abrodictyum rigidum	5	—	—	—	—	19	—	—	—	—	—	—	24
Trichomanes crinitum	—	—	—	—	—	—	—	—	—	—	—	—	—
Trichomanes diversifrons	—	—	—	—	—	—	—	—	—	—	—	—	—
*Trichomanes elegans**	—	—	—	—	—	7	—	2	5	—	—	—	14
Trichomanes ludovicinum	—	—	—	—	—	—	—	—	—	—	—	—	—
Lindsaeaceae													
Lindsaea arcuata	7	2	17	43	—	—	—	—	—	—	—	—	69
Lindsaea imrayana	—	7	—	—	—	—	—	—	—	—	—	—	7
Lindsaea klotzschiana	—	—	—	—	—	—	—	—	—	—	x	—	—
Lindsaea pratensis	—	—	—	—	—	—	—	—	—	—	—	—	—
Lindsaea quadrangularis	—	—	—	x	—	—	—	—	—	—	—	—	—
Odontosoria gymnogrammoides	—	—	—	—	—	—	—	—	—	—	—	—	—

(Continued)

	Rhyolite				R/M	Mafic-volcanic				Basalt	Dacite	Undif.	
Families and species	Cho.A	Cho.B	Hon.A	Hon.B	Samu.	Bonita	Palo	Ver.A	Ver.B	Pinola	Horn.	Alto.	*n*
Lomariopsidaceae													
Dracoglossum plantagineum	—	—	—	—	—	—	—	8	123	—	—	—	131
Marattiaceae													
Danaea crispa	—	—	—	—	—	—	—	—	x	—	—	—	—
Danaea cuspidata	—	—	—	—	—	—	—	—	—	—	—	—	—
Danaea elliptica	—	—	—	—	—	—	—	—	—	—	—	—	—
*Danaea moritziana**	—	—	—	—	—	28	74	22	4	—	—	—	128
*Danaea nodosa**	—	—	—	—	—	—	58	—	27	—	3	—	88
Danaea sp.	—	2	—	—	—	—	—	—	—	—	—	—	2
Marattia excavata	—	—	—	—	—	—	—	—	—	—	—	—	—
Marattia interposita	1	—	2	—	—	—	—	—	—	—	—	—	3
Nephrolepidaceae													
Nephrolepis biserrata	—	—	—	—	—	—	—	—	—	—	—	—	—
Nephrolepis multiflora	—	—	—	—	—	—	—	—	—	—	—	—	—
Nephrolepis pectinata	—	—	—	—	—	—	—	2	—	—	—	—	2
*Nephrolepis rivularis**	—	—	—	—	x	—	—	—	—	—	—	—	—
Pteridaceae													
*Adiantum tetraphyllum**	—	—	—	—	—	—	—	—	—	1	—	2	3
Jamesonia flexuosa	—	—	—	—	—	—	—	—	—	—	—	—	—
Jamesonia glaberrima	—	—	—	—	—	—	—	—	—	—	—	—	—
Pityrogramma calomelanos	—	—	—	—	—	—	—	—	—	—	—	—	—
Pteris altissima	—	—	—	5	1	—	6	3	1	7	—	15	38
*Pteris praestantissima**	—	—	—	—	—	—	—	x	x	—	—	—	—
*Pteris quadriaurita**	—	—	—	—	—	—	—	—	—	—	—	3	3
Pteris speciosa	—	—	—	—	—	—	—	—	—	—	—	—	—
Pteris tripartita	—	—	—	—	—	—	—	—	—	—	—	—	—
*Pteris vittata**	—	—	—	—	—	—	—	—	—	x	—	—	—
Saccolomataceae													
Saccoloma inaequale	—	—	24	—	—	5	—	4	—	—	—	—	33
Tectaria chimborazensis	—	—	—	—	—	—	—	—	—	—	—	—	—
Tectaria murilloana	—	—	—	—	—	—	—	—	—	—	—	—	—
Tectaria nicaraguensis	—	—	—	—	—	—	—	—	—	—	—	—	—

	Rhyolite				R/M	Mafic-volcanic				Basalt	Dacite	Undif.	
Families and species	Cho.A	Cho.B	Hon.A	Hon.B	Samu.	Bonita	Palo	Ver.A	Ver.B	Pinola	Horn.	Alto.	*n*
Tectariaceae													
*Tectaria athyrioides**	—	—	—	—	—	—	—	x	x	—	—	—	—
Tectaria pilosa	—	—	—	—	—	—	—	—	3	—	—	—	3
Tectaria subebenea	—	—	—	—	—	—	—	—	—	—	—	2	2
Tectaria trifoliata	—	—	—	—	—	—	—	—	—	—	3	—	3
Thelypteridaceae													
*Macrothelypteris torresiana**	—	—	—	—		—	—	—	—	x	—	—	—
Steiropteris valdepilosa	—	—	—	—	—	—	—	—	x	—	—	—	—
Thelypteris andreana	—	—	—	—	—	—	—	—	x	—	—	—	—
Thelypteris atrovirens	—	x	—	—	—	—	—	—	—	—	—	—	—
Thelypteris balbisii	—	—	—	—	—	—	—	—	—	—	—	—	—
Thelypteris christensenii	—	—	—	—	—	—	—	—	—	—	—	—	—
*Thelypteris decussata**	—	—	10	—	5	10	—	2	—	—	—	—	27
*Thelypteris eggersii**	—	—	—	—	—	—	—	—	—	79	—	—	79
*Thelypteris frigida**	29	39	—	—	—	34	—	1	—	—	1	—	104
Thelypteris gigantea	—	—	—	—	—	—	—	3	—	—	—	—	3
Thelypteris glandulosa	—	—	—	—	—	—	—	—	—	—	—	—	—
*Thelypteris hatchii**	—	—	—	—	—	—	—	—	—	—	189	—	189
Thelypteris lepidula	—	—	—	—	—	—	—	—	—	—	—	—	—
Thelypteris leprieurii	—	—	—	—	—	—	—	—	—	—	—	—	—
*Thelypteris nicaraguensis**	—	—	—	—	—	—	—	—	1	—	—	—	1
Thelypteris resinifera	—	—	—	—	—	—	—	—	—	—	—	—	—
*Thelypteris tetragona**	x	x	—	—	—	—	—	—	—	—	—	—	—
Thelypteris villana	—	—	—	—	—	—	—	—	—	—	—	—	—

APPENDIX 8.2

Correlation coefficients of environmental variables fitted onto a nonmetric multidimensional scaling ordination of herbaceous and tree fern floristic composition. Variables displayed are statistically significant at $p \leq 0.05$.

	Correlation coefficient (r^2)	
Variables	*Tree fern*	*Herbaceous fern*
Soil moisture	0.90	0.88
Total nitrogen: total phosphorus	0.70	0.78
Iron	0.67	—
Red: far red	0.64	0.50
Total phosphorus	0.62	0.73
Bulk density	0.59	0.69
Sodium	0.50	—
Magnesium	0.49	0.67
Dry rainfall	—	0.73
Calcium	—	0.73
Total extractable bases	—	0.72
Effective cation exchange capacity	—	0.70
Manganese	—	0.62
Aluminum	—	0.58
Rainfall	—	0.52
pH	—	0.49

REFERENCES

Alfonso-Moreno, R. A., C. E., Cadena-Vargas, G. Morales, N. Peña, and B. Pérez. 2011. Conservación Integral de *Dicksonia sellowiana* Hook., en Bogotá D.C. y su Área de Influencia [Integral conservation of *Dicksonia sellowiana* Hook. in Bogotá D.C. and its area of influence]. *Revista de la Academia Colombiana de Ciencias Exactas, Físicas y Naturales*, 134(35):79–96.

Andersen, K. M., B. L. Turner, and J. W. Dalling. 2010. Soil-Based Habitat Partitioning in Understorey Palms in Lower Montane Tropical Forests. *Journal of Biogeography*, 37(2):278–292. https://doi.org/10.1111/j.1365-2699.2009.02192.x

Brock, J. M. R., G. L. W. Perry, W. G. Lee, and B. R. Burns. 2016. Tree Fern Ecology in New Zealand: A Model for Southern Temperate Rainforests. *Forest Ecology and Management*, 375:112–126. https://doi.org/10.1016/j.foreco.2016.05.030

Coomes, D. A., W. A. Bentley, A. J. Tanentzap, and L. E. Burrows 2013. Soil Drainage and Phosphorus Depletion Contribute to Retrogressive Succession along a New Zealand Chronosequence. *Plant and Soil*, 367(1–2):77–91. https://doi.org/10.1007/s11104-013-1649-5

Corrales, A., S. A. Mangan, B. L. Turner, and J. W. Dalling. 2016. An Ectomycorrhizal Nitrogen Economy Facilitates Monodominance in a Neotropical Forest. *Plant and Soil* 367(1–2):77–91. https://doi.org/10.1007/s11104-013-1649-5

Dalling, J. W., C. M. Prada, K. D. Heineman, K. M. Andersen, A. Morris, J. Pardo, E. Hollenbeck, P. Caballero, C. Espinosa, E. García, and B. L. Turner. 2021. Introduction to the Fortuna Forest Reserve: Soil and Climate Effects on the Tree Communities of a Premontane Tropical Forest. In *Fortuna Forest Reserve, Panama: Interacting Effects of Climate and Soils on the Biota of a Wet Premontane Tropical Forest*, ed. J. W. Dalling and B. L. Turner, pp. 1–33. Smithsonian Contributions to Botany, No. 112. Washington, D.C.: Smithsonian Institution Scholarly Press.

De Cáceres, M. 2013. How to Use the *indicspecies* Package (ver. 1.7.1). http://cran.r-project.org/web/packages/indicspecies/vignettes/indicspeciesTutorial.pdf

De Cáceres, M., P. Legendre, and M. Moretti. 2010. Improving Indicator Species Analysis by Combining Groups of Sites. *Oikos*, 119(10):1674–1684. https://doi.org/10.1111/j.1600-0706.2010.18334.x

Dufrêne, M., and P. Legendre. 1997. Species Assemblages and Indicator Species: The Need for a Flexible Asymmetrical Approach. *Ecological Monographs*, 67(3):345–366. https://doi.org/10.1890/0012-9615(1997)067[0345:SAAIST]2.0.CO;2

Farias, R. de P., L. E. N. Costa, I. A. A. Silva, and I. C. L. Barros. 2015. Phenological Studies of Selected Leaf and Plant Traits of *Didymochlaena truncatula* (Dryopteridaceae) in a Brazilian Submontane Tropical Rainforest. *Nordic Journal of Botany*, 33(2):249–255. https://doi.org/10.1111/njb.00656

Garcia, P. A., and A. Salino. 2008. Dryopteridaceae (Polypodiopsida) no Estado de Minas Gerais, Brasil [Dryopteridaceae (Polypodiopsida) in the state of Minas Gerais, Brazil]. *Lundiana*, 9(1):3–27.

Greer, G. K., and B. C. McCarthy. 1999. Gametophytic Plasticity among Four Species of Ferns with Contrasting Ecological Distributions. *International Journal of Plant Sciences*, 160(5):879–886. https://doi.org/10.1086/314188

Holdridge, L. 1947. Determination of World Plant Formations from Simple Climatic Data. *Science* 105:367–368. http://science.sciencemag.org/content/105/2727/367.short

Holmlund, H. I., S. D. Davis, F. W. Ewers, N. M. Aguirre, G. Sapes, A. Sala, and J. Pittermann. 2020. Positive Root Pressure is Critical for Whole-Plant Desiccation Recovery in Two Species of Terrestrial Resurrection Ferns. *Journal of Experimental Biology*, 71 (3):1139–50. https://doi.org/10.1111/nph.16067

Jones, M. M., D. Cicuzza, O. Van Straaten, E. Veldkamp, and M. Kessler 2014. Determinants of Fern and Angiosperm Herb Community Structure in Lower Montane Rainforest in Indonesia. *Journal of Vegetation Science*, 25:1216–1224. https://doi.org/10.1111/jvs.12181

Jones, M. M., S. Ferrier, R. Condit, G. Manion, S. Aguilar, and R. P. Erez. 2013. Strong Congruence in Tree and Fern Community Turnover in Response to Soils and Climate in Central Panama. *Journal of Ecology*, 101:506–516. https://doi.org/10.1111/1365-2745.12053

Jones, M. M., K. Ruokolainen, N. C. L. Martinez, and H. Tuomisto. 2016. Differences in Topographic and Soil Habitat Specialization Between Trees and Two Understorey Plant Groups in a Costa Rican Lowland Rain Forest. *Journal of Tropical Ecology*, 32(6):482–497. https://doi.org/10.1017/S0266467416000419

Jones, M. M., B. Szyska, and M. Kessler. 2011. Microhabitat Partitioning Promotes Plant Diversity in a Tropical Montane Forest. *Global Ecology and Biogeography*, 20:558–569. https://doi.org/10.1111/j.1466-8238.2010.00627.x

Jones, M. M., H. Tuomisto, D. B. Clark, and P. Olivas. 2006. Effects of Mesoscale Environmental Heterogeneity and Dispersal Limitation on Floristic Variation in Rain Forest Ferns. *Journal of Ecology*, 94:181–195. https://doi.org/10.1111/j.1365-2745.2005.01071.x

Kessler, M. 2010. Biogeography of Ferns. In *Fern Ecology*, ed. K. Mehltreter, L. R. Walker, and J. M. Sharpe, pp. 22–60. Cambridge: Cambridge University Press.

Klekowski, E. J. 1979. The Genetics and Reproductive Biology of Ferns. In *The Experimental Biology of Ferns*, ed. A. F. Dyer, pp. 133–170. London: Academic Press.

Kluge, J., and M. Kessler. 2006. Fern Endemism and Its Correlates: Contribution from an Elevational Transect in Costa Rica. *Diversity and Distribution*, 12(5):535–545. https://doi.org/10.1111/j.1366-9516.2006.00231.x

Korall, P., and K. M. Pryer. 2014. Global Biogeography of Scaly Tree Ferns (Cyatheaceae): Evidence for Gondwanan Vicariance and Limited Transoceanic Dispersal. *Journal of Biogeography*, 41(2):402–413. https://doi.org/10.1111/jbi.12222

Kramer, K. U., and P. S. Green. 1990. Pteridophytes and Gymnosperms. In *The Families and Genera of Vascular Plants*, ed. K. Kubitzki, vol. 1, pp. 1–404. Berlin: Springer-Verlag.

Kreft, H., W. Jetz, J. Mutke, and W. Barthlott 2010. Contrasting Environmental and Regional Effects on Global Pteridophyte and Seed Plant Diversity. *Ecography*, 33(2):408–419.

Large, M., and J. Braggins. 2004. *Tree Ferns*. Portland, OR: Timber Press.

McPherson, G., M. Merello, and M. Fica (2010). A Checklist of the Fortuna Dam Region, Chiriqui/Bocas Del Toro, Panama. Accessed 3 January 2019. http://www.mobot.org/MOBOT/fortuna/fortunaDropdown.aspx

Moran, R. C. 2008. Diversity, Biogeography, and Floristics. In *Biology and Evolution of Ferns and Lycophytes*, ed. T. A. Ranker and C. H. Haufler, pp. 367–394. Cambridge: Cambridge University Press.

Moran, R. C., and R. Riba 1995 *Flora Mesoamericana. Vol. 1. Psilotaceae a Salviniaceae* [Mesoamerican flora. Vol. 1. Psilotaceae to Salviniaceae]. Mexico City: Universidad Nacional Autónoma de Mexico.

Nitta, J. H., R. Taputuarai, J. Meyer, and C. C. Davis. 2016. Life Cycle Matters: DNA Barcoding Reveals Contrasting Community Structure between Fern Sporophytes and Gametophytes. *Ecological Monographs*, 87(2):278–296. https://doi.org/10.1002/ecm.1246

Page, C. 2002. Ecological Strategies in Fern Evolution: A Neopteridological Overview. *Review of Palaeobotany and Palynology*, 119:1–33.

Paul, S. K., K. W. Dixon, and B. P. Miller. 1995. The Persistence and Germination of Fern Spores in Fire-prone, Semi-arid Environments. *Australian Journal of Botany*, 62(6):518–527. https://doi.org/10.1071/BT14193

Phillips, T. L. 1974. Evolution of Vegetative Morphology in Coenopterid Ferns. *Annals of the Missouri Botanical Garden*, 61(2):427–461. https://doi.org/10.2307/2395067

PPG 1 2016. A Community-derived Classification for Extant Lycophytes and Ferns. *Journal of Systematics and Evolution*, 54(6):563–603. https://doi.org/10.1111/jse.12229

Prada, C. M., A. Morris, K. M. Andersen, B. T. Turner, P. Caballero, and J. W. Dalling. 2017. Soils and Rainfall Drive Landscape-Scale Changes in the Diversity and Functional Composition of Tree Communities in Premontane Tropical Forest. *Journal of Vegetation Science*, 28(4):859–870. https://doi.org/10.1111/jvs.12540

Schneider, H., E. Schuettpelz, K. M. Pryer, R. Cranfill, S. Magallón, and R. Lupia. 2004. Ferns Diversified in the Shadow of Angiosperms. *Nature*, 4286982:553–557. https://doi.org/10.1038/nature02361

Schuettpelz, E., and K. M. Pryer. 2007. Fern Phylogeny Inferred from 400 Leptosporangiate Species and Three Plastid Genes. *Proceedings of the National Academy of Sciences*, 106(27):11200–11205. https://doi.org/10.1073/pnas.0811136106

Schuettpelz, E., and K. M. Pryer. 2009. Evidence for a Cenozoic Radiation of Ferns in an Angiosperm-Dominated Canopy. *Proceedings of the National Academy of Sciences*, 106(27):11200–11205. https://doi.org/10.1073/pnas.0811136106

Sessa, E. B., W. L. Testo, and J. E. Watkins. 2016. On the Widespread Capacity for, and Functional Significance of, Extreme Inbreeding in Ferns. *New Phytologist*, 211(3):1108–1119. https://doi.org/10.1111/nph.13985

Silva, C., D. Cárdenas, L. Londoño, B. L. Turner, and C. Jaramillo. 2021. Geological Map of the Fortuna Forest Reserve. In *Fortuna Forest Reserve, Panama: Interacting Effects of Climate and Soils on the Biota of a Wet Premontane Tropical Forest*, ed. J. W. Dalling and B. L. Turner, pp. 35–46. Smithsonian Contributions to Botany, No. 112. Washington, D.C.: Smithsonian Institution Scholarly Press.

Testo, W. L., M. Sundue, and A. Vasco. 2017. *Diplazium* Hybrids Involving *D. plantaginifolium* and *D. ternatum* from Mexico and Central America. *Brittonia*, 69(3):295–306. https://doi.org/10.1007/s12228-017-9476-2

Testo, W., and Sundue, M. 2016. A 4000-Species Dataset Provides New Insight into the Evolution of Ferns. *Molecular Phylogenetics and Evolution*, 105:200–211. https://doi.org/10.1016/j.ympev.2016.09.003

Tuomisto, H. 2006. Edaphic Niche Differentiation among *Polybotrya* Ferns in Western Amazonia: Implications for Coexistence and Speciation. *Ecography*, 29(3):273–284. https://doi.org/10.1111/j.2006.0906-7590.04390.x

Tuomisto, H., and A. D. Poulsen. 1996. Influence of Edaphic Specialization on Pteridophyte Distribution in Neotropical Rain Forests. *Journal of Biogeography*, 23(3):283–293. http://www.jstor.org/stable/2845846

Tuomisto, H., and K. Ruokolainen. 1993. Distribution of Pteridophyta and Melastomataceae along an Edaphic Gradient in an Amazonian Rain Forest. *Journal of Vegetation Science*, 4(1):25–34. https://doi.org/10.2307/3235634

Turner, B. L., and J. W. Dalling. 2021. Soils of the Fortuna Forest Reserve. In *Fortuna Forest Reserve, Panama: Interacting Effects of Climate and Soils on the Biota of a Wet Premontane Tropical Forest*, ed. J. W. Dalling and B. L. Turner, pp. 47–135. Smithsonian Contributions to Botany, No. 112. Washington, D.C.: Smithsonian Institution Scholarly Press.

Turner, B. L., A. Wells, K. M. Andersen, and L. M. Condron. 2018. Consequences of the Physical Nature of the Parent Material for Pedogenesis, Nutrient Availability, and Succession in Temperate Rainforests. *Plant and Soil*, 423(1–2):533–548. https://doi.org/10.1007/s11104-017-3514-4

Valdespino, I. A. 1993. Notes on Neotropical *Selaginella* (Selaginellaceae), Including New Species from Panama. *Brittonia*, 45(4):315–327. https://doi.org/10.2307/2807605

Vasco, A., R. C. Moran, and B. A. Ambrose. 2013. The Evolution, Morphology, and Development of Fern Leaves. *Frontiers in Plant Science*, 4:1–16. https://doi.org/10.3389/fpls.2013.00345

Viana, J. L., B. L. Turner, and J. W. Dalling. 2020. Compositional Variation in Understory Fern and Palm Communities along a Soil Fertility and Rainfall Gradient in a Lower Montane Tropical Forest. *Journal of Vegetation Science* postprint. https://doi.org/10.1111/jvs.12947

Vitousek, P. M. 2004. *Nutrient Cycling and Limitation: Hawai'i as a Model System*. Princeton, NJ: Princeton University Press.

Watkins, J. E., C. Cardelús, R. K. Colwell, and R. C. Moran. 2006. Species Richness and Distribution of Ferns along an Elevational Gradient in Costa Rica. *American Journal of Botany*, 93(1):73–83. https://doi.org/10.3732/ajb.93.1.73

Watkins, J. E., A. C. Churchill, and N. Michele Holbrook. 2016. A Site for Sori: Ecophysiology of Fertile–Sterile Leaf Dimorphy in Ferns. *American Journal of Botany*, 103(5):845–855. https://doi.org/10.3732/ajb.1500505

Wolf, P. G., T. A. Robison, M. G. Johnson, M. A. Sundue, W. L. Testo, and C. J. Rothfels. 2018. Target Sequence Capture of Nuclear-Encoded Genes for Phylogenetic Analysis in Ferns. *Applications in Plant Sciences*, 6(5): e1148. https://doi.org/10.1002/aps3.1148

Zuquim, G., H. Tuomisto, M. M. Jones, J. Prado, F. O. G. Figueiredo, G. M. Moulatlet, F. R. C. Costa, C. A. Quesada, and T. Emilio. 2014. Predicting Environmental Gradients with Fern Species Composition in Brazilian Amazonia. *Journal of Vegetation Science*, 25(5):1195–1207. https://doi.org/10.1111/jvs.12174

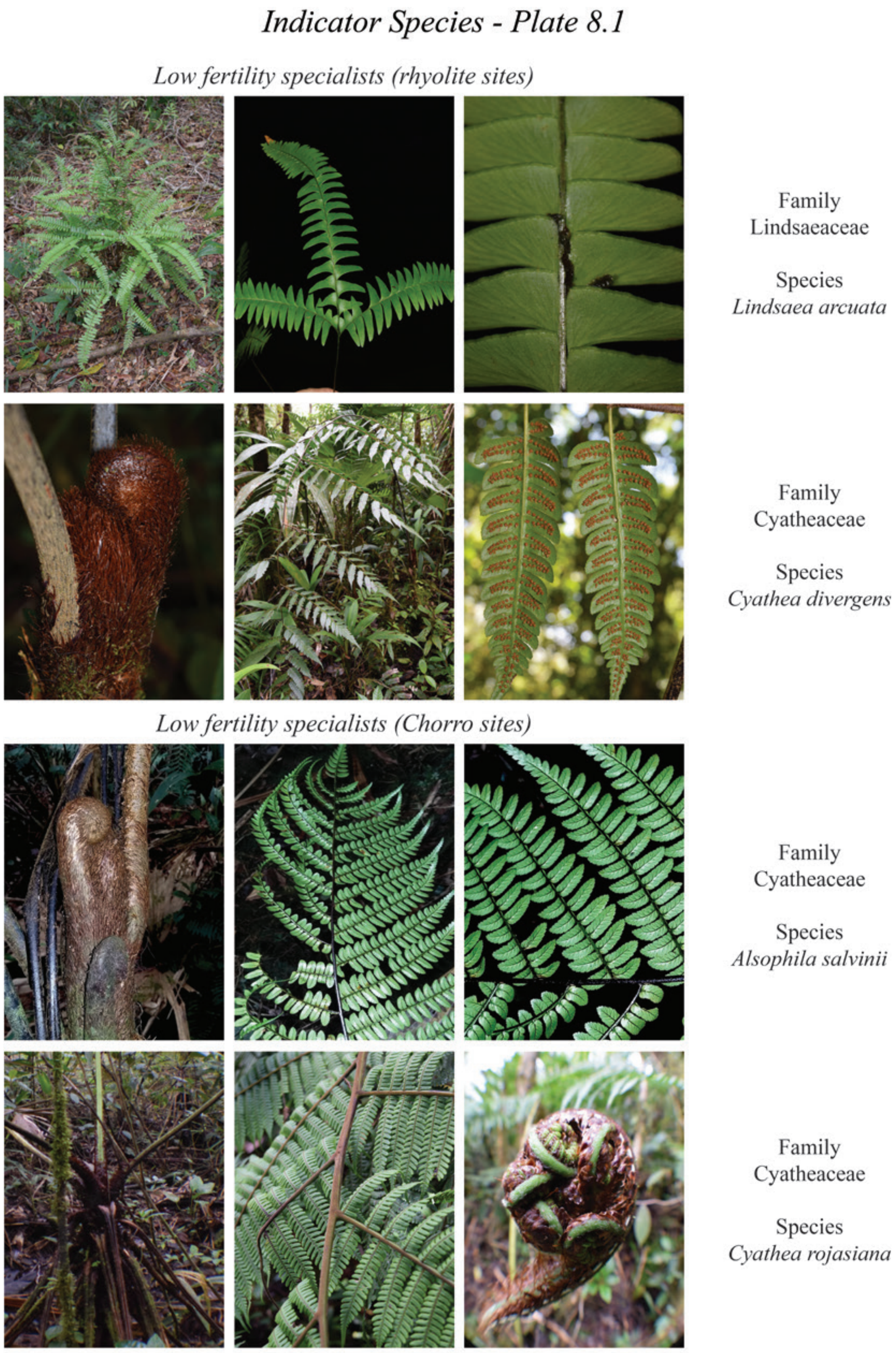

PLATES 8.1–8.5 display indicator species from Table 8.1. **Plates 8.6–8.13** display the most conspicuous terrestrial species of the flora of Fortuna, alphabetically organized by botanical family. Images show plant habit and detail of fertile leaves.

Indicator Species - Plate 8.2

Low fertility specialists (Honda sites)

Family
Blechnaceae

Species
Austroblechnum stoloniferum

Family
Blechnaceae

Species
Blechnum binervatum

Family
Cyatheaceae

Species
Cyathea pinnula

Intermediate fertility specialists (mafic volcanic sites)

Family
Marattiaceae

Species
Danaea moritziana

Indicator Species - Plate 8.3

Intermediate fertility specialists ***(mafic-volcanic sites)***

Family
Dryopteridaceae

Species
Stigmatopteris heterophlebia

Family
Dryopteridaceae

Species
Mickelia oligarchica

Family
Cyatheaceae

Species
Cyathea eggersii

High fertility specialists (basal, dacite and undif. volcanic sites)

Family
Athyriaceae

Species
Diplazium plantaginifolium

Indicator Species - Plate 8.4

Generalists

Family
Didymochlaenaceae

Species
Didymochlaena truncatula

Family
Athyriaceae

Species
Diplazium urticifolium

Family
Dryopteridaceae

Species
Megalastrum atrogriseum

Family
Dryopteridaceae

Species
Olfersia cervina

Fern Floristics - Plate 8.5

Fern Floristics - Plate 8.6

Athyriaceae


Diplazium lindbergii


Diplazium lindbergii


Diplazium macrophyllum


Diplazium macrophyllum


Diplazium obscurum


Diplazium palmense


Diplazium palmense


Diplazium solutum


Diplazium striatastrum


Diplazium striatastrum


Diplazium subsilvaticum


Diplazium subsilvaticum


Diplazium urticifolium


Diplazium urticifolium


Diplazium x verapax


Diplazium x verapax

Fern Floristics - Plate 8.7

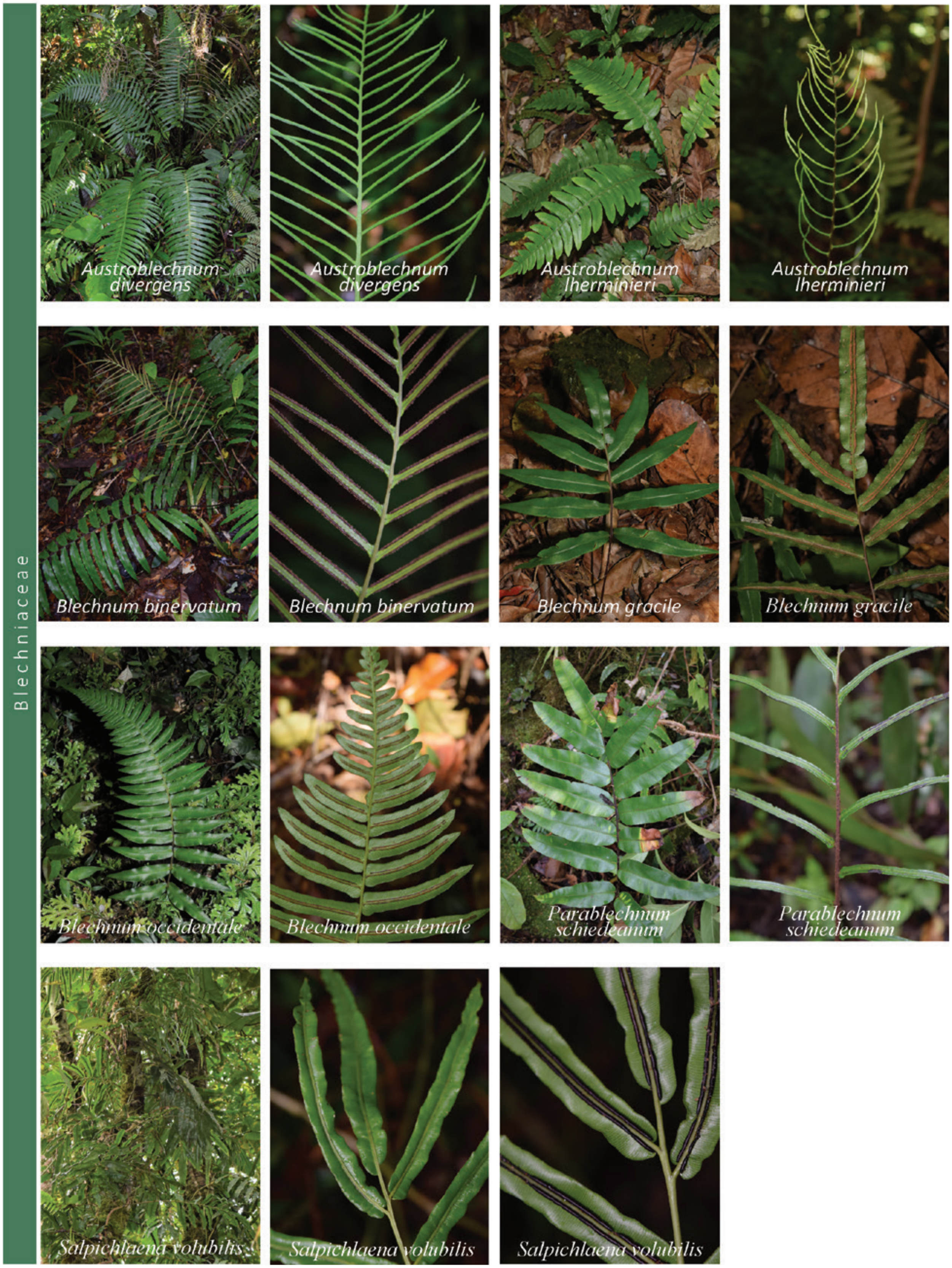

Fern Floristics - Plate 8.8

Cyatheaceae


Alsophila erinacea


Alsophila erinacea


Alsophila erinacea


Alsophila erinacea


Alsophila firma


Alsophila firma


Alsophila polystichoides


Alsophila polystichoides


Cyathea bicrenata


Cyathea bicrenata


Cyathea bicrenata


Cyathea mutica


Cyathea mutica


Cyathea pinnula

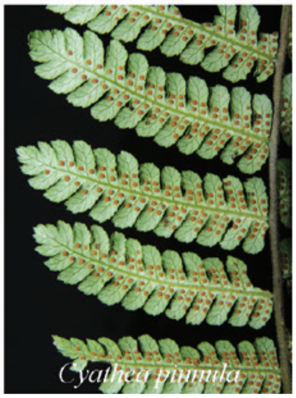
Cyathea pinnula

Fern Floristics - Plate 8.9

Fern Floristics - Plate 8.10

Arachniodes denticulata
Arachniodes denticulata
Bolbitis hastata
Bolbitis hastata
Ctenitis submarginalis
Ctenitis submarginalis
Lastreopsis killipii
Lastreopsis killipii
Megalastrum biseriale
Megalastrum biseriale
Mickelia hemiotis
Mickelia hemiotis
Phanerophlebia juglandifolia
Phanerophlebia juglandifolia
Stigmatopteris longicaudata
Stigmatopteris longicaudata

Fern Floristics - Plate 8.11

Fern Floristics - Plate 8.12

Marattiaceae


Danaea moritziana


Danaea moritziana


Danaea nodosa


Danaea nodosa

Nephrolepidaceae


Nephrolepis rivularis


Nephrolepis rivularis


Nephrolepis pectinata


Nephrolepis pectinata

Pteridaceae


Adiantum tetraphyllum


Adiantum tetraphyllum


Pteris altissima


Pteris altissima


Pteris praestantissima


Pteris praestantissima


Pteris quadriaurita


Pteris quadriaurita

Fern Floristics - Plate 8.13

9. Palm Flora and Drivers of Distributions in Fortuna Forest Reserve

Kelly M. Andersen

ABSTRACT. The palm family (Arecaceae) is a well-studied tropical plant group with high levels of diversity and abundance, making it a model for tropical forest ecology. The Fortuna Forest Reserve is a hotspot for diversity of understory palms in the Chamaedoreeae and Genomateae tribes of the palm family. This chapter provides a review of the Fortuna palm community, palm ecology, and mechanisms driving palm species distribution patterns. The strong soil nutrient gradient influences the palm community species distribution patterns, functional traits, and seedling performance. A series of experiments using seedlings of palm species with differing soil-based distribution patterns shows that key functional traits give species from low-nutrient sites a performance advantage over species associated with higher-nutrient soil types when growing on low-nutrient soils. Specifically, species from low-nutrient sites maintain high survival rates, high photosynthetic rates and photosynthetic nutrient use efficiency, high biomass allocation to leaves compared to roots, low herbivory rates, and low nitrogen-uptake rates when growing on low-nutrient soils. Thus, whole-plant strategies are important for understanding drivers for palm species distribution patterns along soil nutrient gradients. Furthermore, by using complementary experiments, direct and indirect relationships between soil nutrient availability and seedling performance could be distinguished. Specifically, soil nutrient availability, and nitrogen availability in particular, drives leaf physiological traits, but when growing under natural conditions, seedling growth is decoupled from leaf physiology due to an increase in herbivory rates and/or light limitation under high soil nutrient availability. Together, research on the Fortuna palm community provides testable hypotheses for how soil nutrients drive whole-plant strategies and species distribution patterns along soil nutrient gradients.

IMPORTANCE OF PALMS IN TROPICAL FORESTS

Palms are the quintessential tropical plant. Palms provide food, shelter, and other provisions for forest animal and humans, with some species, such as oil palm (*Elaeis guineensis*) and açai (*Euterpe oleracea*), reaching global commercial and socioeconomic importance (Cámara-Leret, Tuomisto, et al., 2017). Palms affect tropical forest community structure and regeneration of tree seedlings by altering environment conditions or through physical damage from falling fronds (Farris-Lopez et al., 2004; Peters et al., 2004; Wang and Augspurger, 2004). The prominence of the palm family, Arecaceae, across time and space in tropical biomes renders palms a model group for ecological and evolutionary research in tropical forests (Couvreur and Baker, 2013; Baker and Dransfield, 2016). Strong historical legacies, long-term climatic stability, and geological heterogeneity contribute to the current pantropical distribution and the high species richness of the palm family (Kissling et al., 2012). More than 2,600 palm species have been described (Dransfield et al., 2008; Baker and Dransfield, 2016). High rates of endemism and habitat associations are often linked to geological features that impose dispersal barriers and soil nutrient gradients (Clark et al., 1995; Eiserhardt et al., 2013; Cámara-Leret, Faurby,

---

Asian School of the Environment, Nanyang Technological University, Singapore, 639798.
Correspondence: kelly.andersen@ntu.edu.sg

et al., 2017). In Neotropical regions, uplift along the Andean corridor and Continental Divide provided opportunities for allopatric speciation, created habitat and environmental heterogeneity, and promoted diversification of many palm lineages (Gentry, 1982; Bacon et al., 2018).

This chapter focuses on two palm tribes, Chamaedoreeae and Geomateae, that are particularly diverse in the Fortuna Forest Reserve and surrounding forests. Specifically, it addresses potential mechanisms that may promote species diversity within and among forests on different soil types found within Fortuna and surrounding forests.

ROLE OF SOILS IN SPECIATION AND HABITAT ASSOCIATIONS IN PALMS

Palm–soil associations are well-studied across tropical ecosystems, although underlying mechanisms are seldom studied. One exemplary case study for palm–soil associations is the Lord Howe Island palms, where soil associations mediated speciation of two sympatric *Howea* palm species (Savolainen et al., 2006; Dunning et al., 2016; Osborne et al., 2017). Reproductive isolation is driven by differences in soil nutrient availability across a mosaic of volcanic and calcareous soil types (Savolainen et al., 2006). In western Amazonia, palm species show distinct distribution patterns with soil cation (calcium, magnesium, potassium) and phosphorus availability (Cámara-Leret, Faurby, et al., 2017; Muscarella et al., 2018). Furthermore, soils are implicated in driving phylogenetic community structure (Eiserhardt et al., 2013; Muscarella et al., 2018). Thus, palm communities can provide a model system for better understanding how closely related species coexist across soil and environmental gradients.

FORTUNA PALM COMMUNITY

Palms are an important component of the flora and structure of the Fortuna forest. Palm densities reach 41% relative abundance of the tree flora (*Colpothrinax aphenopetala*, *Wettinia quinaria*, *Euterpe precatoria* at the Chorro A site; Prada et al., 2017) and the density of non-spiny understory palms can exceed 25,000 individuals per hectare (at the Palo Seco site; Andersen, Turner, et al., 2010a). Over 25 understory palm species (Table 9.1, Plates 9.1–9.7) occurred in fifteen 5 × 5 m subplots in each of ten 1-hectare forest census plots across a soil nutrient gradient at Fortuna, including three (La Mina) to 14 (Palo Seco) species and 47 (Honda B) to 951 (Verrugosa) individuals (Table 2 in Andersen, Turner et al., 2010). Species accumulation curves for each of the 10 sites sampled across the soil nutrient gradient at Fortuna indicated that in most cases sampling efforts were sufficient to capture local species assemblages, despite the range in species richness and palm abundance surveyed (Figure 9.1). Furthermore, the shapes of the curves showed that La Mina and Frank sites contained fewer species that were relatively abundant, whereas Samudio, Casa Verde, and Honda A had similar overall palm abundances but higher species richness. In contrast, Palo Seco and Verrugosa had high palm abundances and high species richness.

Chamaedoreeae and Geonomateae are two tribes within the Arecoideae subfamily that are particularly diverse across the Fortuna Forest Reserve, with 14 and 9 species recorded, respectively. The most common understory palm species is *Geonoma cuneata* (Figure 9.2), occurring at nearly all studied sites and with the highest abundances at sites with overall high palm densities. In contrast, the most widespread palm species across sites is *Chamaedorea pinnatifrons*, but it generally occurs at low density. The majority of the understory palm species surveyed have restricted distribution patterns that are related to soil and environmental factors.

SOIL-BASED HABITAT ASSOCIATIONS OF FORTUNA PALMS

The consistent high rainfall and mosaic of soil types creating a strong soil nutrient gradient across the Fortuna Forest Reserve promotes an extraordinary palm flora with several endemic species (see Table 9.1). The distribution patterns of the understory palm communities are nonrandom across the different soil types at Fortuna (Andersen, Turner et al., 2010). Changes in palm community composition is related to shifts in soil nitrogen, cations, and aluminum. Furthermore, species can be grouped into three soil-based habitat associations based on soil type: dacitic, andesitic, rhyolitic. Although there is overlap in palm general morphological characteristics among species, there is evidence for functional trait differentiation among species within and among the soil-based habitat association groups. Note that the andesitic designation in previous publications (Andersen, Turner et al., 2010; Andersen et al., 2012; Andersen et al., 2014), based on coarse fragments in soil profile pits at the plots, is now classified as a mixed mafic-volcanics due to the difficulty in discriminating among the various mafic lithologies in the region (Silva et al., this volume).

TRAIT SPECTRUM OF FORTUNA PALMS

Functional traits were surveyed for 19 of the 25 understory palm species occurring along the soil nutrient gradient at Fortuna (Table 9.1; Turner and Dalling, this volume). Directional shifts in mean trait values along the soil nutrient gradient at Fortuna provides further evidence of soil-based niche partitioning among naturally occurring adult understory palms (Andersen et al., 2012). Foliar nutrient content and specific leaf area (SLA) increased with increasing soil nutrient availability (Andersen et al., 2012, fig. 3). Furthermore, species mean leaf trait values were related to species distribution patterns with soil nutrient

TABLE 9.1. Understory palm species recorded within the Fortuna Forest Reserve and/or used in seedling experiments at Fortuna. Species list and soil associations adapted from Andersen et al. (2010a, b, 2012). *Represent species endemic to Western Panama. Images are shown in Plates 1–7.

					Seedling experiments				
Tribe	Genus	Species	Species code	Soil association	Functional traits[1]	Field transplant[2]	Growing house[3]	Nitrogen addition[4]	Nitrogen tracer[5]
Reinhardtieae	*Reinhardtia*	*gracilis* (H. Wendl.) Drude ex Dammer	RG	Andesite	—	✓	—	—	—
Euterpeae	*Prestoea*	*longepetiolata* var. *roseospadix* L. H. Bailey	PL	Rhyolitic	✓	—	—	—	—
Geonomateae	*Asterogyne*	*martiana* (H. Wendl.) H. Wendl. Ex Hemsl.	AM	Andesite	—	—	—	—	—
	Calyptrogyne	*panamensis* var. *occidentalis* Henderson	CAP	Andesitic	✓	—	—	✓	—
	Geonoma	*congesta* H. Wendl. ex Spruce	GCO	Lowland	—	✓	—	—	—
	Geonoma	*cuneata* (H. Wendl. ex Spruce)	GC	Generalist	✓	✓	—	✓	✓
	Geonoma	*hugonis* Grayum and de Nevers*	GG	Rhyolitic	✓	✓	—	✓	—
	Geonoma	*deversa* (Poit.) Kunth	GD	Andesitic	—	—	—	—	—
	Geonoma	*interrupta* (Ruiz & Pav.) Mart.	GI	Andesitic	—	—	—	—	—
	Geonoma	*jussieuana* Mart.	GJ	Dacitic	✓	—	—	✓	—
	Geonoma	*lehmannii* subsp. *corrugata* Henderson	GS	Rhyolitic	✓	—	—	—	✓
	Geonoma	*undata* Klotzsch	GU	Rhyolitic	✓	—	—	—	—
	Pholidostachys	*pulchra* H. Wendl. ex Burret	PP	Andesitic	—	—	—	—	—
Chamaedoreeae	*Chamaedorea*	*costaricana* Oerst.	CC	Dacitic	✓	—	—	—	—
	Chamaedorea	*deckeriana* (Klotzsch) Hemsl.	CD	Andesitic	✓	✓	✓	✓	✓
	Chamaedorea	*microphylla* H. Wendl.*	CM	Dacitic	✓	—	—	—	—
	Chamaedorea	*palmeriana* Hodel & Uhl	CPA	Rhyolitic	✓	✓	—	—	✓
	Chamaedorea	*pinnatifrons* (Jacq.) Oerst.	CPI	Generalist	✓	✓	✓	✓	✓
	Chamaedorea	*recurvata* Hodel*	CRE	Rhyolitic	✓	✓	✓	✓	✓
	Chamaedorea	*robertii* Hodel & Uhl	CRO	Andesitic	✓	✓	✓	—	✓
	Chamaedorea	*scheryi* L. H. Bailey	CSC	Andesitic	✓	✓	—	—	—
	Chamaedorea	*pygmaea* H. Wendl.	CPY	Dacitic	✓	—	—	—	—
	Chamaedorea	*sullivaniorum* Hodel & Uhl	CSU	Andesitic	✓	✓	—	—	—
	Chamaedorea	*tepejilote* Liebm.	CT	Andesitic	✓	✓	✓	✓	✓
	Chamaedorea	*verecunda* Grayum & Hodel*	CV	Rhyolitic	—	—	—	—	—
	Chamaedorea	*woodsoniana* L. H. Bailey	CW	Dacitic	✓	✓	✓	✓	✓
	Synecanthus	*warscewiczianus* H. Wendl.	SW	Andesitic	—	—	—	—	—

[1] Andersen et al., 2012[2]; Andersen et al., 2014[3]; This chapter[4]; Andersen, Corre et al., 2010[5]; Andersen and Turner, 2013.

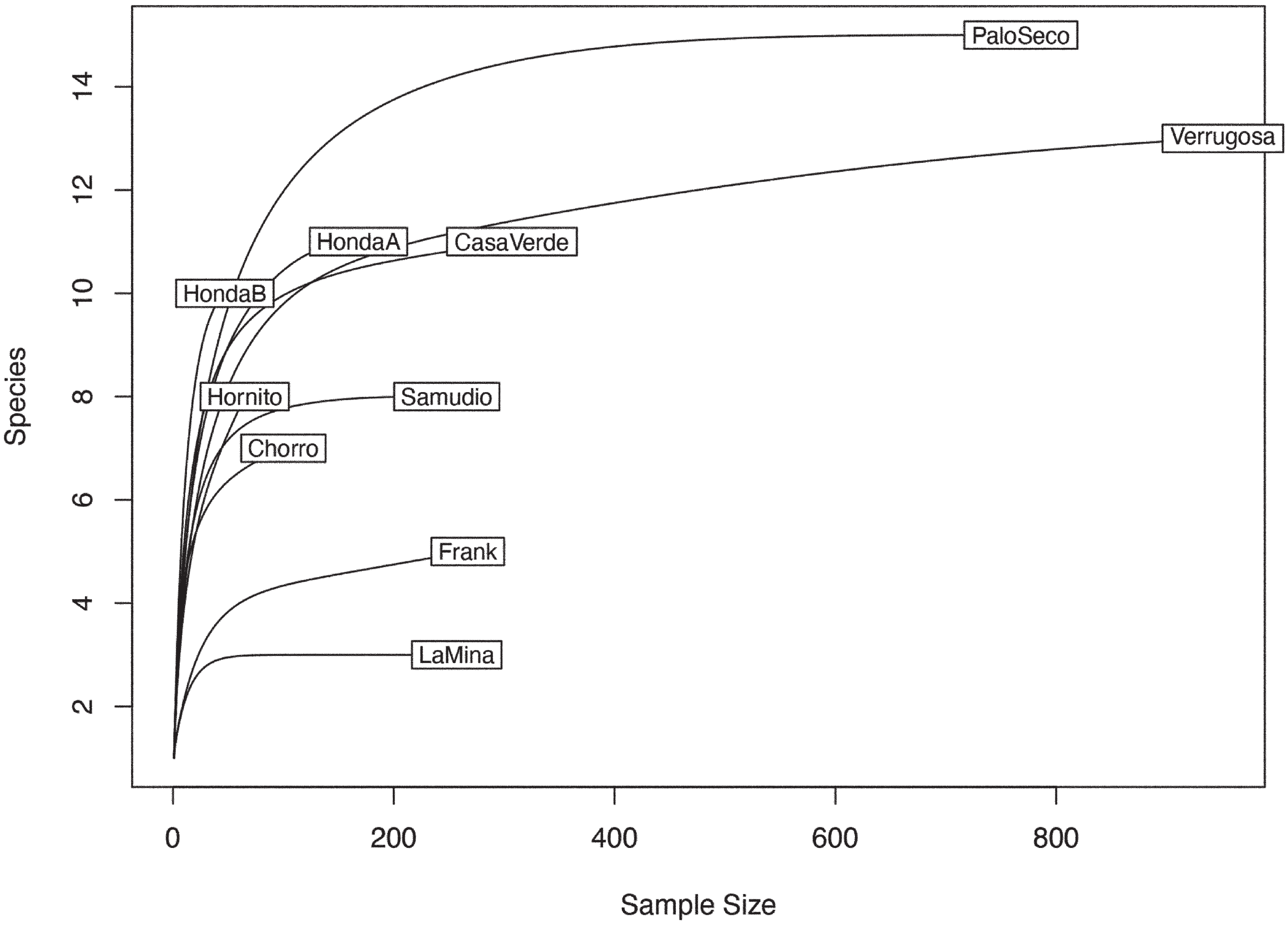

FIGURE 9.1. Species accumulation curves for the 10 sites sampled across the soil nutrient gradient in the Fortuna Forest Reserve and surrounding forests.

gradient (Andersen et al., 2012, fig. 2). More conservative traits were observed in species associated with low-nutrient rhyolitic soils, and leaf traits shifted toward more acquisitive leaf trait values as species distribution patterns were associated with increasing soil nutrient availability sites. Thus, habitat filtering, or the selection of species with similar traits specific to environmental conditions, appears to be an important factor structuring understory palm communities across the Fortuna soil nutrient gradient. However, there was evidence for significantly different leaf trait values among co-occurring species at a site, suggesting that niche differentiation, or competitive exclusion limiting the coexistence of similar species, was also an important mechanism structuring palm community at Fortuna. Seedling performance experiments helped to elucidate how these contrasting mechanisms shape the Fortuna palm communities.

SEEDLING PERFORMANCE OF UNDERSTORY PALMS

A series of field experiments were conducted to examine seedling performance in relation to palm species distribution patterns across soil gradient at Fortuna (Table 9.1): (1) seedling transplant experiment along the soil nutrient gradient to test potential niche-based mechanisms generating soil associations in understory palms (Andersen et al., 2014); (2) a greenhouse experiment to test the effect of soil type on seedling performance under controlled conditions; (3) a seedling transplant experiment in a nitrogen fertilization experiment to explicitly examine the role of nitrogen in driving soil associations (Andersen et al., 2012); (4) nitrogen isotope tracer experiments to test for partitioning of nitrogen chemical forms among palms and among

FIGURE 9.2. *Geonoma cuneata* var. *gracilis* is the most abundant palm in the Fortuna Forest Reserve.

sympatric species with contrasting root symbionts (Andersen and Turner, 2013; Andersen et al., 2017).

Seedling Transplant Experiment

The soil transplant experiment examined three growth trade-offs that have been shown to influence seedling performance between contrasting soil types and plant–soil associations in other tropical forests and which appear to shape the palm community across the Fortuna soil gradient. There may be a trade-off in biomass allocation, whereby allocation to roots is favorable at low-nutrient sites to maximize nutrient acquisition and allocation to leaves is favorable at high-nutrient sites to maximize growth (Chapin, 1980; Palmiotto et al., 2004; Baraloto et al., 2006). In contrast, growth trade-offs may be driven by physiological adaptations, whereby maximizing the amount of carbon fixed per unit of nutrient uptake is advantageous at low-nutrient sites, but maximizing carbon gain and overall growth rates are more favorable at the high-nutrient sites (Bloom and Chapin 1985; Wright et al., 2003; Baltzer et al., 2005). Alternatively, plant–soil interactions may be mediated by herbivores (Fine et al., 2004). It may be advantageous to invest in defense traits at low-nutrient sites where losing leaf tissue is costly, whereas at high-nutrient sites any leaf tissue lost to herbivores can be compensated by high growth rates (Coley et al., 1985; Fine et al., 2004). To assess these mechanisms in unison, a seedling transplant experiment was conducted at five sites along the Fortuna soil gradient. Seedlings of 13 species that differed in their distribution patterns across the sites were grown in common gardens that were either exposed to or protected from aboveground herbivores. Seedling survival was monitored over 21 months, after which leaf gas exchange and defense traits were surveyed. Seedlings were then harvested to assess biomass allocation, relative growth rates, and foliar nutrient contents and to quantify leaf area and leaf area damage.

Biomass allocation followed theoretical expectations with soil nutrient availability and species distribution patterns. Root mass ratios (RMR) decreased and leaf area ratio (LAR) increased with increasing soil nutrient availability. Furthermore, species from low-nutrient sites were able to maintain higher LAR and lower RMR at the low-nutrient Chorro site compared to species with different distribution patterns, suggesting biomass allocation trade-offs are important in determining seedling performance and species distribution patterns along soil nutrient gradients.

Physiological traits such as foliar nitrogen and phosphorus, photosynthetic rates, and photosynthetic nutrient use efficiency all changed accordingly along the soil nutrient gradient, with higher foliar nutrient contents and photosynthetic rates at sites with higher soil nutrient availability compared to low-nutrient sites. Species from the low-nutrient Chorro site maintained higher mass-based photosynthetic rates and high photosynthetic nutrient use efficiencies when grown at Chorro compared to species with different soil associations, suggesting that physiological traits and nutrient use efficiency are also important drivers of species distribution patterns.

An indirect cost of higher foliar nutrient content and photosynthetic rates was greater susceptibility to herbivore attack. A difference in pest pressure was related to soil nutrient availability and species distribution patterns where percentage of leaf area damage of seedlings increased with increasing soil nutrient availability among the sites, particularly for seedlings of naturally occurring species exposed to herbivores (Andersen et al., 2014). At the lowest-nutrient site, seedlings of locally occurring species had considerably lower leaf damage compared to the locally absent species, which were often necrotic or severely damaged. At the higher-nutrient sites, protection from herbivores significantly reduced leaf damage from insect herbivores.

Mortality was lower at low-nutrient sites and generally lower when the seedlings were protected from herbivores (Andersen et al., 2014, fig. 1). There was 100% survival for seedlings of naturally occurring species at Chorro when protected from herbivores. At high-nutrient sites, there were also survival advantages for naturally occurring species when protected from herbivores. In contrast, there was no effect of herbivore exclosure on growth performance, nor was there a consistent trend between growth rate and soil fertility, unlike responses to all other variables measured. However, two sites, Chorro and Palo Seco, showed growth advantages for locally occurring species.

The results from the palm transplant experiment showed that there were coordinated trait responses to soil fertility that were consistent with species distribution patterns rather than three distinct allocation trade-offs. Trait strategies were related to seedling performance and there were strong home-site advantages at the low-nutrient sites. “Home-field advantage” describes the idea that teams tend to perform better than expected at home than at away games. In an ecological context, this indicates that niche processes, or species-specific differences in their requirements for limiting resources, are important in shaping the understory palm community at Fortuna. However, factors such as light limitation were also implicated in explaining seedling growth performance along the soil nutrient gradient (Figure 9.3).

Greenhouse Bioassay Experiment

Transplant experiments are useful in determining species performance along environmental gradients. However, greenhouse bioassays can control for light, soil moisture, biotic interactions, and other factors that may influence seedling performance growing in different soils, as found in the seedling transplant experiment. A subset of the palm seedlings from the seeds collected from the transplant experiment were used in a growing house bioassay experiment. Seedlings were grown for 240 days in soils collected from each of the five field transplant experiment sites and mixed with washed sea sand (70:30 mix). Light conditions were adjusted to 3% light with shade cloth, and seedlings received rainfall with supplemental watering when necessary. Five *Chamaedorea* species with contrasting species distribution patterns along the soil nutrient gradient were used in the greenhouse experiment to determine the effect of soil type on seedling performance under controlled environmental conditions.

Results from the greenhouse experiment had similar patterns to those of the seedling transplant experiment, suggesting that soils were the main drivers of seedling performance in the field-based experiment. Relative growth rates were significantly lower for seedlings growing in soils collected from the low-nutrient Chorro site compared to all other sites ($F_{4,14.9} = 4.44$, $p < 0.05$; Figure 9.4). Species naturally occurring at the Chorro site had significantly greater relative growth rates compared to species locally absent from the low-nutrient site ($F_{1,19} = 26.87$, $p < 0.0001$). However, there were no other differences in growth

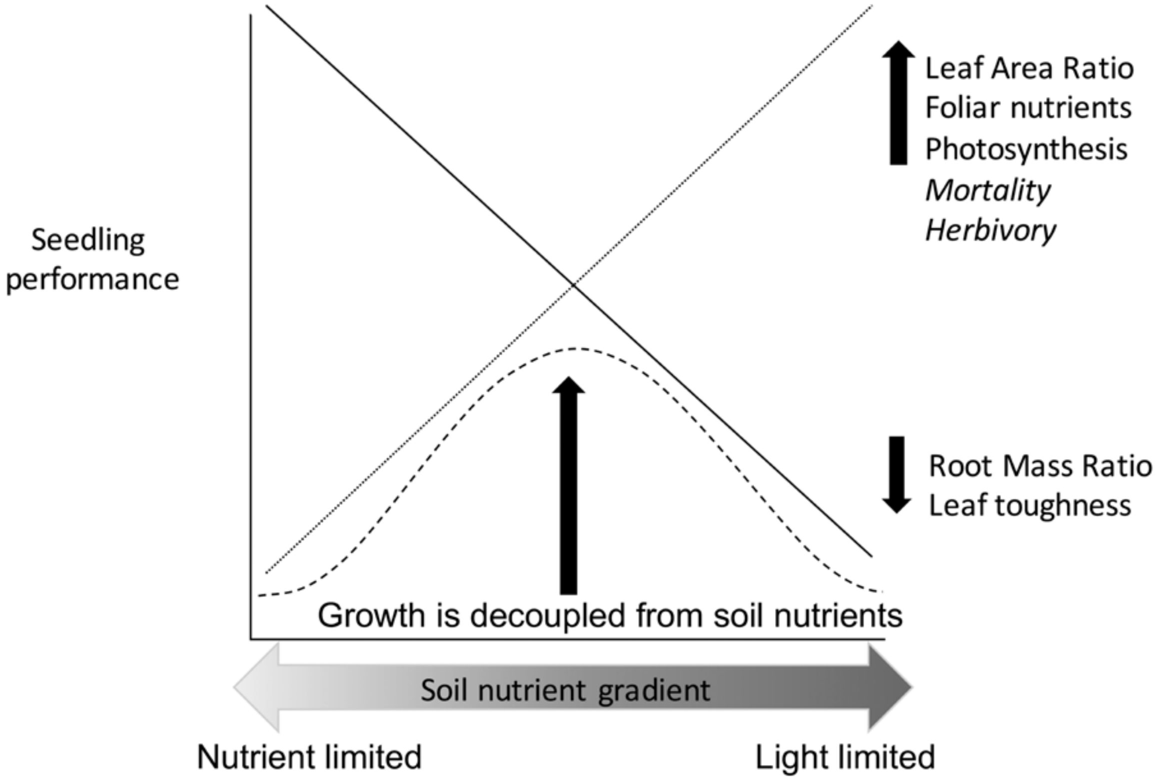

FIGURE 9.3. Conceptual diagram summarizing the findings from the seedling transplant experiment across the soil nutrient gradient in Fortuna. As soil nutrients increase, foliar nutrient content, photosynthetic capacity, and biomass allocation to leaves increase. At the same time, allocation to root biomass and defense against herbivore decrease. However, as leaf quality increases, herbivory levels increase correspondingly. As a result, survival and growth begin to decrease rather than increase at high soil nutrient availabilities. In addition, soil nutrient gradient was confounded by light availability, where low-nutrient sites had a more open canopy compared to high-nutrient sites. Therefore, optimal seedling performance is decoupled from the soil nutrient gradient and is expected to be highest at intermediate sites where soils and light levels are colimiting.

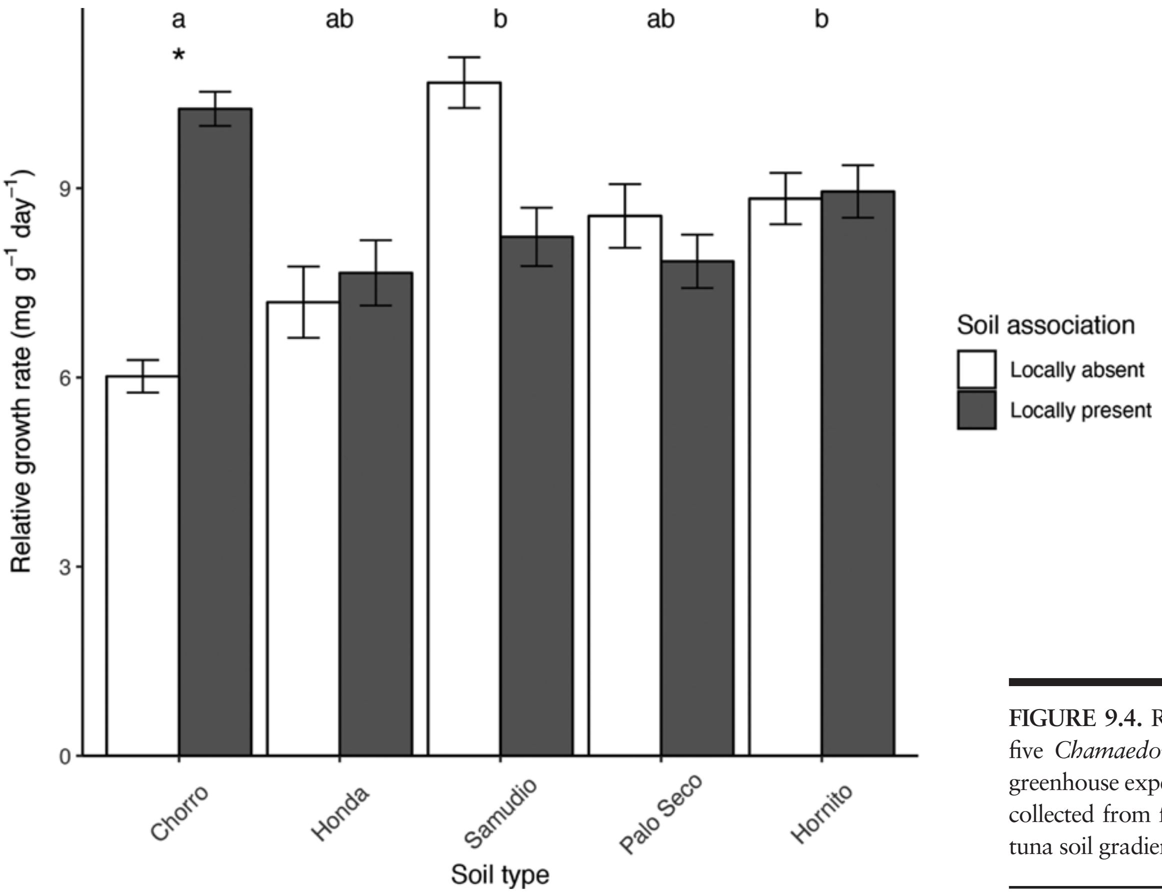

FIGURE 9.4. Relative growth rates of five *Chamaedorea* species used in the greenhouse experiment growing in soils collected from five sites along the Fortuna soil gradient.

performance between naturally occurring and absent species, unlike the transplant experiment where species naturally occurring at Palo Seco and species locally absent from the Samudio site had growth advantages (Andersen et al., 2014). This supports the hypothesis that home-site advantages of species from the Chorro site were likely driven by adaptations of these species to low-nutrient availability. The lack of a home-site advantage in the greenhouse experiment further supports confounding factors, such as light availability, in driving the home-site growth advantage of species from the Palo Seco site in the transplant experiment. Interestingly, the same pattern of higher growth rates of locally absent compared to naturally occurring species was found in the greenhouse experiment as in the transplant experiment, albeit the former was not significantly different, likely due to low sample size or differences in the species used across the experiments.

There was a strong positive relationship between relative growth rates and photosynthetic rates (Figure 9.5; RGR = 7.02 + 0.63(A_{max}), $F_{1,71.2}$ = 18.8, $p < 0.0001$), suggesting that leaf-level photosynthetic responses to soil type were a key driver of whole-plant growth. Furthermore, photosynthesis and relative growth rates generally increased with increasing nutrient availability of the soil types. Together, the results from the greenhouse experiment provide evidence for a direct physiological response determining seedling performance and, therefore, potential species distribution patterns along the soil nutrient gradient at Fortuna. In contrast, the transplant experiment results highlighted the interactive effects of light and herbivores in determining seedling performance under natural field conditions.

Seedling Responses to Nitrogen Addition

The greenhouse experiment showed the importance of soils in determining physiological controls on seedling performance but did not distinguish the roles of specific nutrients in driving the response to soil type. One of the key soil nutrients determining understory palm distribution patterns along the Fortuna soil nutrient gradient was soil nitrogen availability (Andersen, Turner et al., 2010). Large-scale nutrient addition experiments are necessary to disentangle biotic, abiotic, and other factors from the role of soil nitrogen in determining seedling performance and distribution patterns in Fortuna. To explicitly test the role of nitrogen in influencing understory palm seedling performance, and ultimately species distribution patterns, a common garden experiment (Andersen, Corre et al., 2010) was conducted within a large-scale nitrogen addition experiment, NITROF (Koehler et al., 2009; Corre et al., 2010; Adamek et al., 2010). The experiment took place in a low-nutrient site in the Honda catchment in a forest that was dominated by an ectomycorrhizal Juglandaceae tree species.

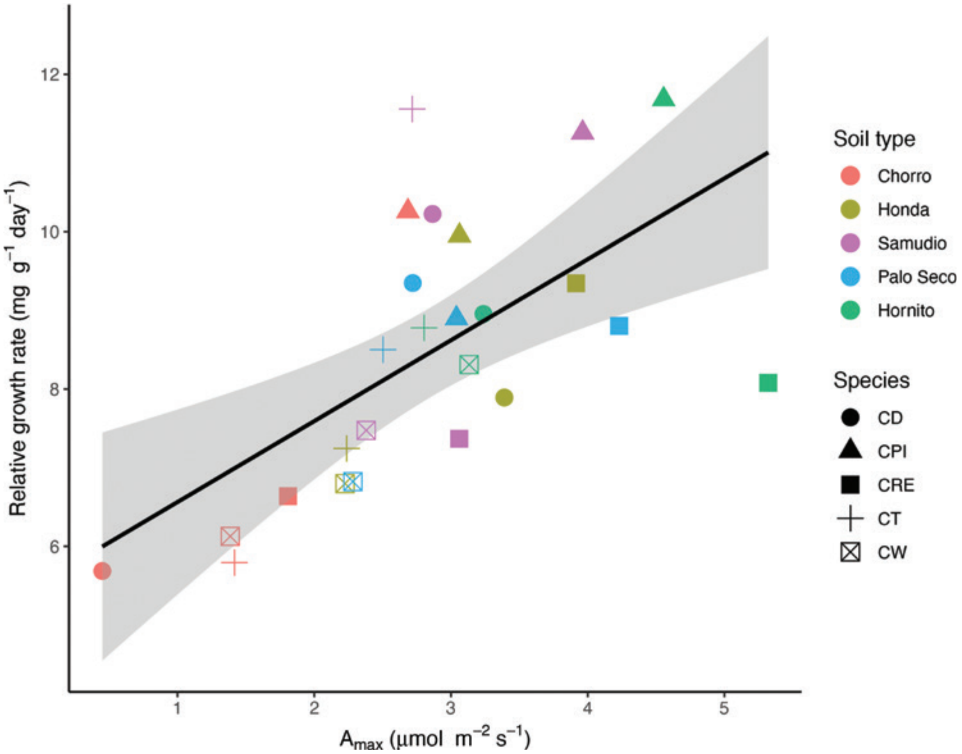

FIGURE 9.5. Relationship between area-based photosynthetic rates and relative growth rates of seedlings of five *Chamaedorea* species used in the greenhouse experiment. Soil type is listed in order of increasing soil nutrient availability and indicates the location from which the soil was collected.

Understory palm seedlings had higher leaf nitrogen content and photosynthetic rates with added nitrogen (Andersen, Corre et al., 2010). However, increased leaf quality (nutrient content and physiological processes) did not result in higher relative growth rate (Figure 9.6). Rather, leaf quality was related to an increase in leaf area lost to herbivores, which in turn results in a zero-sum game for the plant as a whole. There was no direct growth response or shifts in biomass allocation with nitrogen addition, which may have been mediated by herbivores, or alternatively, these traits are determined by other nutrient or environmental factors (Andersen, Corre et al., 2010).

There were differences in seedling responses to nitrogen addition among species–soil associations. Species from the higher nutrient dacitic soils had stronger increases in mass-based photosynthesis rates with added nitrogen compared to species with other soil-based habitat associations, suggesting that physiological traits are important in determining species distribution patterns along soil nitrogen gradients.

Nitrogen Uptake Patterns of Palm Seedlings

Nitrogen additions affected aboveground trait of palm seedlings, including carbon assimilation rates. However, nitrogen has also been shown to affect belowground traits related to nutrient acquisition strategies, including mycorrhizal associations, uptake rates, enzyme activity, and phenology (McKane et al., 2002; Houlton et al., 2007; Phillips et al., 2013). Nitrogen has multiple chemical forms that plants can access: inorganic or mineral forms (nitrate and ammonium) and organic nitrogen (simple amino acids) (Kielland, 1994; Schimel and Bennett, 2004; Houlton et al., 2007). Differences in the ability to take up nitrogen chemical forms can facilitate species coexistence in low-nitrogen ecosystems (McKane et al., 2002; Ashton et al., 2010). In tropical forests, plasticity in the forms of nitrogen taken up by the root might influence plant community structure by giving an advantage to species that can meet their nitrogen requirements with any nitrogen form found in their rhizosphere (Houlton et al., 2007; Andersen and Turner, 2013; Russo et al., 2013).

In two nitrogen tracer experiments, understory and canopy palms associated with low-nutrient rhyolitic soils had significantly lower nitrogen uptake rates compared to species with other distribution patterns with no uptake preferences among nitrogen forms (Andersen and Turner, 2013; Andersen et al., 2017). Thus, low nitrogen uptake rates and plasticity in the uptake of nitrogen forms may be important to meeting plant nitrogen demands at low-nutrient sites. Furthermore, nitrogen use was related to palm species distribution patterns across the soil gradient at Fortuna, whereby species found at higher nutrient sites had higher nitrogen uptake rates and natural abundance foliar $\delta^{15}N$ values (Andersen et al., 2012; Andersen and Turner, 2013). The combination of nitrogen tracer experiments and natural abundance of nitrogen isotopes in foliar tissue supports the hypothesis that flexibility in the use of nitrogen forms may alleviate competition for nitrogen within sites and along soil nutrient gradients, suggesting nitrogen acquisition strategies can influence plant communities in tropical forests.

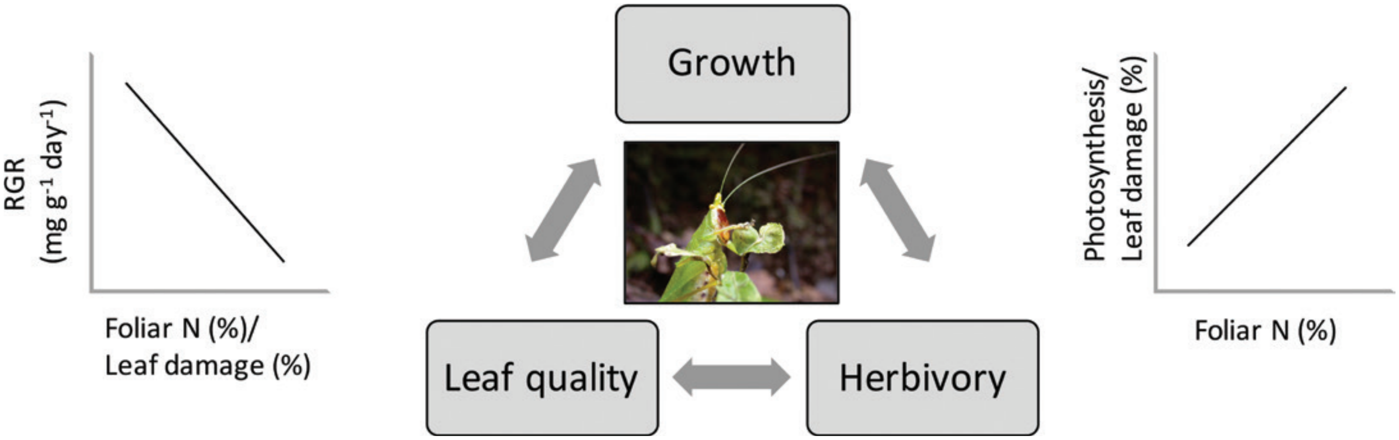

FIGURE 9.6. Conceptual relationships between leaf quality, herbivory, and growth. The strong positive relationship between leaf quality and herbivory results in negative relationships between leaf quality or herbivory and growth.

COMMON PATTERNS IN SEEDLING PERFORMANCE ACROSS EXPERIMENTS

Together, research on the Fortuna understory palm community highlighted the importance of coordinated shifts in aboveground and belowground functional traits and changes in community composition with soil fertility and established testable hypotheses for future research examining interactions between plant function and nutrient cycling. In all seedling experiments, rhyolitic species had home-site advantages at low-nutrient sites. Growing at their home site, understory palms specializing on rhyolitic soils are able to maintain higher leaf area and lower investment in roots compared to species with other soil associations. They are able to maximize photosynthetic capacity per unit leaf nitrogen, despite lower nitrogen uptake rates, and suffered lower rates of herbivory. Together, this suite of performance traits allowed them to minimize mortality and maintain higher growth rates compared to species with other soil associations. At the other end of the nutrient gradient, species distribution patterns may be driven by a combination of adaptations to low light availability and tolerance of higher herbivory rates. By using a group of closely related species, integrative frameworks that incorporate whole-plant strategies, including aboveground and belowground plant traits and biotic interactions, such as quantification of both antiherbivore defenses and herbivory rates, can improve our understanding of the drivers of species distribution patterns along soil nutrient gradients.

REFERENCES

Adamek, M., M. D. Corre, and D. Hölscher. 2009. Early Effect of Elevated Nitrogen Input on Above-Ground Net Primary Production of a Lower Montane Rain Forest, Panama. *Journal of Tropical Ecology*, 25:637–647. https://doi.org/10.1017/S0266467409990253

Andersen, K. M., M. Corre, B. L. Turner, and J. W. Dalling. 2010b. Plant-soil associations in a lower montane tropical forest: physiological acclimation and herbivore-mediated responses to nitrogen addition. *Functional Ecology* 24(6):1171–1180. https://dx.doi.org/10.1111/j.1365-2435.2010.01731.x

Andersen, K. M., and B. L. Turner. 2013. Preferences or Plasticity in Nitrogen Acquisition by Understorey Palms in a Tropical Montane Forest. *Journal of Ecology*, 101:819–825. https://doi.org/10.1111/1365-2745.12070

Andersen, K. M., M.-J. Endara, B. L. Turner, and J. W. Dalling. 2012. Trait-Based Community Assembly of Understory Palms along a Soil Nutrient Gradient in a Lower Montane Tropical Forest. *Oecologia*, 168:519–531. https://doi.org/10.1007/s00442-011-2112-z

Andersen, K. M., B. L. Turner, and J. W. Dalling. 2010a. Soil-Based Habitat Partitioning in Understory Palms in Lower Montane Tropical Forests. *Journal of Biogeography*, 37:278–292. https://doi.org/10.1111/j.1365-2699.2009.02192.x

Andersen, K. M., B. L. Turner, and J. W. Dalling. 2014. Seedling Performance Trade-Offs Influencing Habitat Filtering along a Soil Nutrient Gradient in a Tropical Forest. *Ecology*, 95:3399–3413. https://doi.org/10.1890/13-1688.1

Ashton, I., A. Miller, W. Bowman, and K. N. Suding. 2010. Niche Complementarity Due to Plasticity in Resource Use: Plant Partitioning of Chemical N Forms. *Ecology*, 91:3252–3260. https://doi.org/10.1890/09-1849.1

Bacon, C. D., F. J. Velásquez-Puentes, C. Hoorn, and A. Antonelli. 2018. Iriarteeae Palms Tracked the Uplift of Andean Cordilleras. *Journal of Biogeography*, 45:1653–1663. https://doi.org/10.1111/jbi.13350

Baker, W. J., and J. Dransfield. 2016. Beyond Genera Palmarum: Progress and Prospects in Palm Systematics. *Botanical Journal of the Linnean Society*, 182:207–233. https://doi.org/10.1111/boj.12401

Baltzer, J. L., S. C. Thomas, R. Nilus, and D. F. R. P. Burslem. 2005. Edaphic Specialization in Tropical Trees: Physiological Correlates and Responses to Reciprocal Transplantation. *Ecology*, 86:3063–3077. https://doi.org/10.1890/04-0598

Baraloto, C., D. Bonal, and D. E. Goldberg. 2006. Differential Seedling Growth Response to Soil Resource Availability among Nine Neotropical Tree Species. *Journal of Tropical Ecology*, 22:487–497. https://doi.org/10.1017/S0266467406003439

Bloom, A., F. S. Chapin III, and H. Mooney. 1985. Resource Limitation in Plants: An Economic Analogy. *Annual Review of Ecology and Systematics*, 16:363–392. https://doi.org/10.1146/annurev.es.16.110185.002051

Cámara-Leret, R., S. Faurby, M. J. Macía, H. Balslev, B. Goldel, J.-C. Svenning, W. D. Kissling, N. Rønsted, and C. H. Saslis-Lagoudakis. 2017. Fundamental Species Traits Explain Provisioning Services of Tropical American Palms *Nature Plants*, 3:1–7. https://doi.org/10.1038/nplants.2016.220

Cámara-Leret, R., H. Tuomisto, K. Ruokolainen, H. Balslev, and S. M. Kristiansen. 2017. Modelling Responses of Western Amazonian Palms to Soil Nutrients. *Journal of Ecology*, 105:367–381. https://doi.org/10.1111/1365-2745.12708

Chapin, F. S., III. 1980. The Mineral Nutrition of Wild Plants. *Annual Review of Ecology and Systematics*, 11:233–260. https://doi.org/10.1146/annurev.es.11.110180.001313

Clark, D. A., D. B. Clark, and M. R. Sandoval. 1995. Edaphic and Human Effects on Landscape-Scale Distributions of Tropical Rain Forest Palms. *Ecology*, 76:2581–2594. https://doi.org/10.2307/2265829

Coley, P. D., J. Bryant, and F. S. Chapin III. 1985. Resource Availability and Plant Antiherbivore Defense. *Science*, 230:895–899. https://doi.org/10.1126/science.230.4728.895

Corre, M. D., E. Veldkamp, J. Arnold, and S. J. Wright. 2010. Impact of Elevated N Input on Soil N Cycling and Losses in Old-Growth Lowland and Montane Forests in Panama. *Ecology*, 91:1715–1729. https://doi.org/10.1890/09-0274.1

Couvreur, T. L., and W. J. Baker. 2013. Tropical Rain Forest Evolution: Palms as a Model Group. *BMC Biology*, 11:48. https://doi.org/10.1186/1741-7007-11-48

Dransfield, J., N. W. Uhl, C. B. Asmussen, W. J. Baker, M. M. Harley, and C. E. Lewis. 2008. *Genera Palmarum: The Evolution and Classification of Palms*. London: Kew Publishing.

Dunning, L. T., H. Hipperson, W. J. Baker, R. K. Butlin, C. Devaux, I. Hutton, J. Igea, A. S. T. Papadopulos, X. Quan, C. M. Smadja, C. G. N. Turnbull, and V. Savolainen. 2016. Ecological Speciation in Sympatric Palms: 1. Gene Expression, Selection and Pleiotropy. *Journal of Evolutionary Biology*, 29:1472–1487. https://doi.org/10.1111/jeb.12895

Eiserhardt, W. L., J.-C. Svenning, W. J. Baker, T. L. P. Couvreur, and H. Balslev. 2013. Dispersal and Niche Evolution Jointly Shape the Geographic Turnover of Phylogenetic Clades across Continents. *Scientific Reports*, 3:1164. https://doi.org/10.1038/srep01164

Farris-Lopez, K., J. S. Denslow, B. Moser, and H. Passmore. 2004. Influence of a Common Palm, *Oenocarpus mapora*, on Seedling Establishment in a Tropical Moist Forest in Panama. *Journal of Tropical Ecology*, 20:429–438. https://doi.org/10.1017/S0266467404001531

Fine, P. V. A., I. Mesones, and P. D. Coley. 2004. Herbivores Promote Habitat Specialization by Trees in Amazonian Forests. *Science*, 305:663–665. https://doi.org/10.1126/science.1098982

Gentry, A. 1992. Tropical Forest Biodiversity: Distributional Patterns and Their Conservational Significance. *Oikos*, 63:19–28. https://doi.org/10.2307/3545512

Houlton, B. Z., D. M. Sigman, E. A. G. Schuur, and L. Hedin. 2007. A Climate-Driven Switch in Plant Nitrogen Acquisition within Tropical Forest Communities. *Proceedings of the National Academy of Sciences*, 104:8902–8906. https://doi.org/10.1073/pnas.0609935104

Kielland, K. 1994. Amino Acid Absorption by Arctic Plants: Implications for Plant Nutrition and Nitrogen Cycling. *Ecology*, 75:2373–2383. https://doi.org/10.2307/1940891

Koehler, B., and M. D. Corre. 2009. Chronic Nitrogen Addition Causes a Reduction in Soil Carbon Dioxide Efflux during the High Stem-Growth Period in a Tropical Montane Forest but No Response from a Tropical Lowland Forest in Decadal Scale. *Biogeosciences*, 6:8633–8660. https://doi.org/10.5194/bgd-6-8633-2009

McKane, R. B., L. C. Johnson, G. R. Shaver, K. J. Nadelhoffer, E. B. Rastetter, B. Fry, A. E. Giblin, K. Kielland, B. L. Kwiatkowski, J. A. Laundre, and G. Murray. 2002. Resource-Based Niches Provide a Basis for Plant Species Diversity and Dominance in Arctic Tundra. *Nature*, 415:68–71. https://doi.org/10.1038/415068a

Muscarella, R., C. D. Bacon, S. Faurby, A. Antonelli, S. M. Kristiansen, J.-C. Svenning, and H. Balslev. 2018. Soil Fertility and Flood Regime Are Correlated with Phylogenetic Structure of Amazonian Palm Communities. *Annals of Botany*, 10:135–15.

Osborne, O. G., R. De-Kayne, M. I. Bidartondo, I. Hutton, W. J. Baker, C. G. N. Turnbull, and V. Savolainen. 2017. Arbuscular Mycorrhizal Fungi Promote Coexistence and Niche Divergence of Sympatric Palm Species on a Remote Oceanic Island. *New Phytologist*, 186:281–13. https://doi.org/10.1111/nph.14850

Palmiotto, P., S. J. Davies, K. Vogt, M. Ashton, D. Vogt, and P. M. S. Ashton. 2004. Soil-Related Habitat Specialization in Dipterocarp Rain Forest Tree Species in Borneo. *Ecology*, 92:609–623. https://doi.org/10.1111/j.0022-0477.2004.00894.x

Peters, H. A., A. Pauw, M. R. Silman, and J. W. Terborgh. 2004. Falling Palm Fronds Structure Amazonian Rainforest Sapling Communities. *Proceedings of the Royal Society B: Biological Sciences*, 271(Suppl_5):S367–S369. https://doi.org/10.1098/rsbl.2004.0197

Phillips, R. P., E. Brzostek, and M. G. Midgley. 2013. The Mycorrhizal-Associated Nutrient Economy: A New Framework for Predicting Carbon-Nutrient Couplings in Temperate Forests. *New Phytologist*, 199:41–51. https://doi.org/10.1111/nph.12221

Prada, C. M., A. Morris, K. M. Andersen, B. L. Turner, P. Caballero, and J. W. Dalling. 2017. Soils and Rainfall Drive Landscape-Scale Changes in the Diversity and Functional Composition of Tree Communities in Premontane Tropical Forest. *Journal of Vegetation Science*, 28(4): 859–870. https://doi.org/10.1111/jvs.12540

Russo, S. E., A. Kochsiek, J. Olney, L. Thompson, A. E. Miller, and S. Tan. 2013. Nitrogen Uptake Strategies of Edaphically Specialized Bornean Tree Species. *Plant Ecology*, 214:1405–1416. https://doi.org/10.1007/s11258-013-0260-4

Savolainen, V., M.-C. Anstett, C. Lexer, I. Hutton, J. J. Clarkson, M. V. Norup, M. P. Powell, D. Springate, N. Salamin, and W. J. Baker. 2006. Sympatric Speciation in Palms on an Oceanic Island. *Nature*, 441:210–213. https://doi.org/10.1038/nature04566

Schimel, J., and J. Bennett. 2004. Nitrogen Mineralization: Challenges of a Changing Paradigm. *Ecology*, 85:591–602. https://doi.org/10.1890/03-8002

Silva, C., D. Cárdenas, L. Londoño, B. L. Turner, and C. Jaramillo. 2021. Geological Map of the Fortuna Forest Reserve. In *Fortuna Forest Reserve, Panama: Interacting Effects of Climate and Soils on the Biota of a Wet Premontane Tropical Forest*, ed. J. W. Dalling and B. L. Turner, pp. 35–46. Smithsonian Contributions to Botany, No. 112. Washington, D.C.: Smithsonian Institution Scholarly Press.

Turner, B. L., and J. W. Dalling. 2021. Soils of the Fortuna Forest Reserve. In *Fortuna Forest Reserve, Panama: Interacting Effects of Climate and Soils on the Biota of a Wet Premontane Tropical Forest*, ed. J. W. Dalling and B. L. Turner, pp. 47–135. Smithsonian Contributions to Botany, No. 112. Washington, D.C.: Smithsonian Institution Scholarly Press.

Wang, Y.-H., and C. Augspurger. 2004. Dwarf Palms and Cyclanths Strongly Reduce Neotropical Seedling Recruitment. *Oikos*, 107:619–633. https://doi.org/10.1111/j.0030-1299.2004.13328.x

Wright, I. J., P. B. Reich, and M. Westoby. 2003. Least-Cost Input Mixtures of Water and Nitrogen for Photosynthesis. *American Naturalist*, 161:98–111. https://doi.org/10.1086/344920

Palm Floristics - Plate 9.1

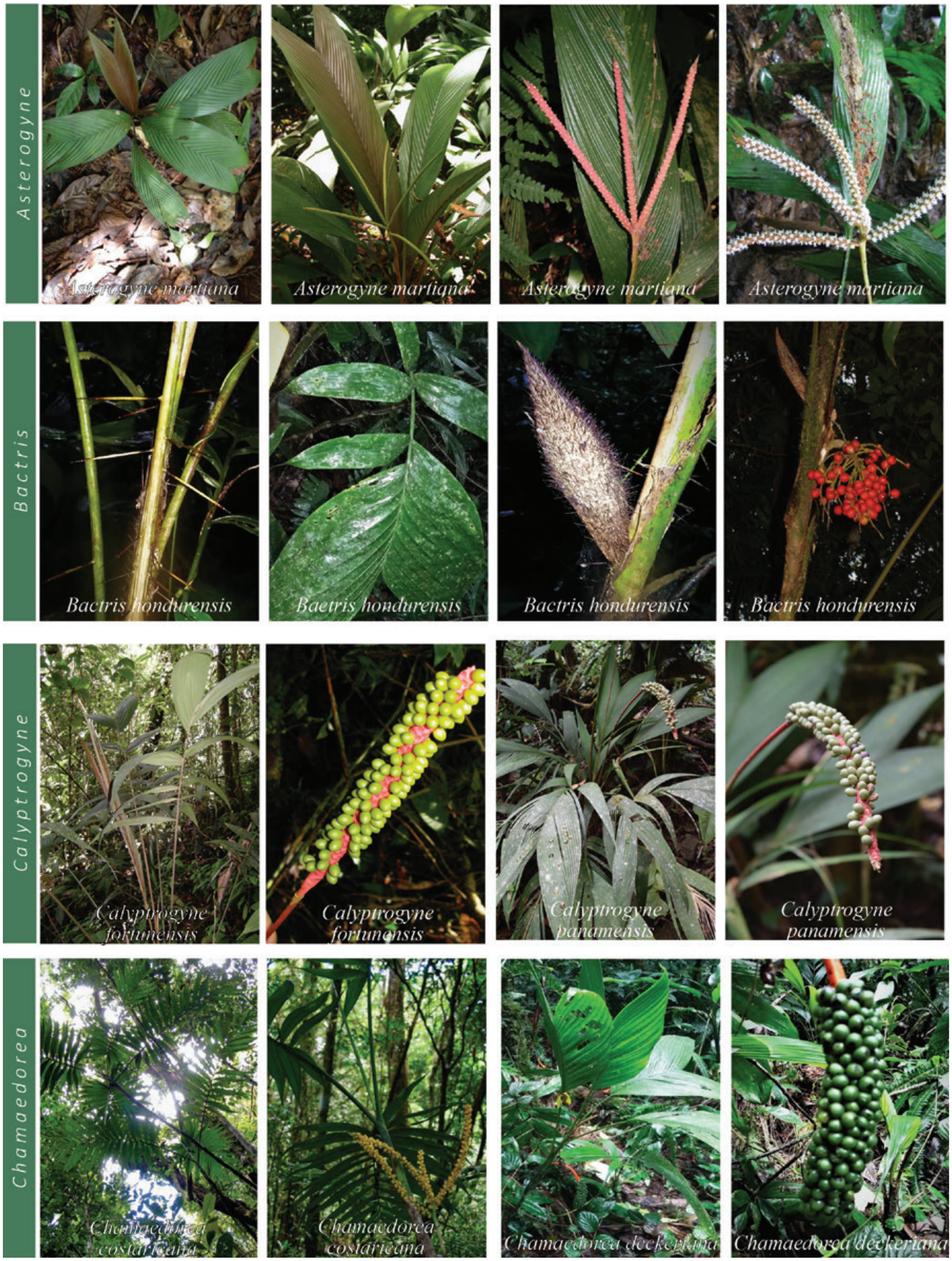

PLATES 9.1–9.7 display the most conspicuous understory and overstory palms species of the flora of Fortuna. Palm species are alphabetically organized by botanical family. Images show plant habit and details of the leaves, flowers, or fruits.

Palm Floristics - Plate 9.2

Palm Floristics - Plate 9.3

Chamaedorea

Colpothrinax

Palm Floristics - Plate 9.4

Palm Floristics - Plate 9.5

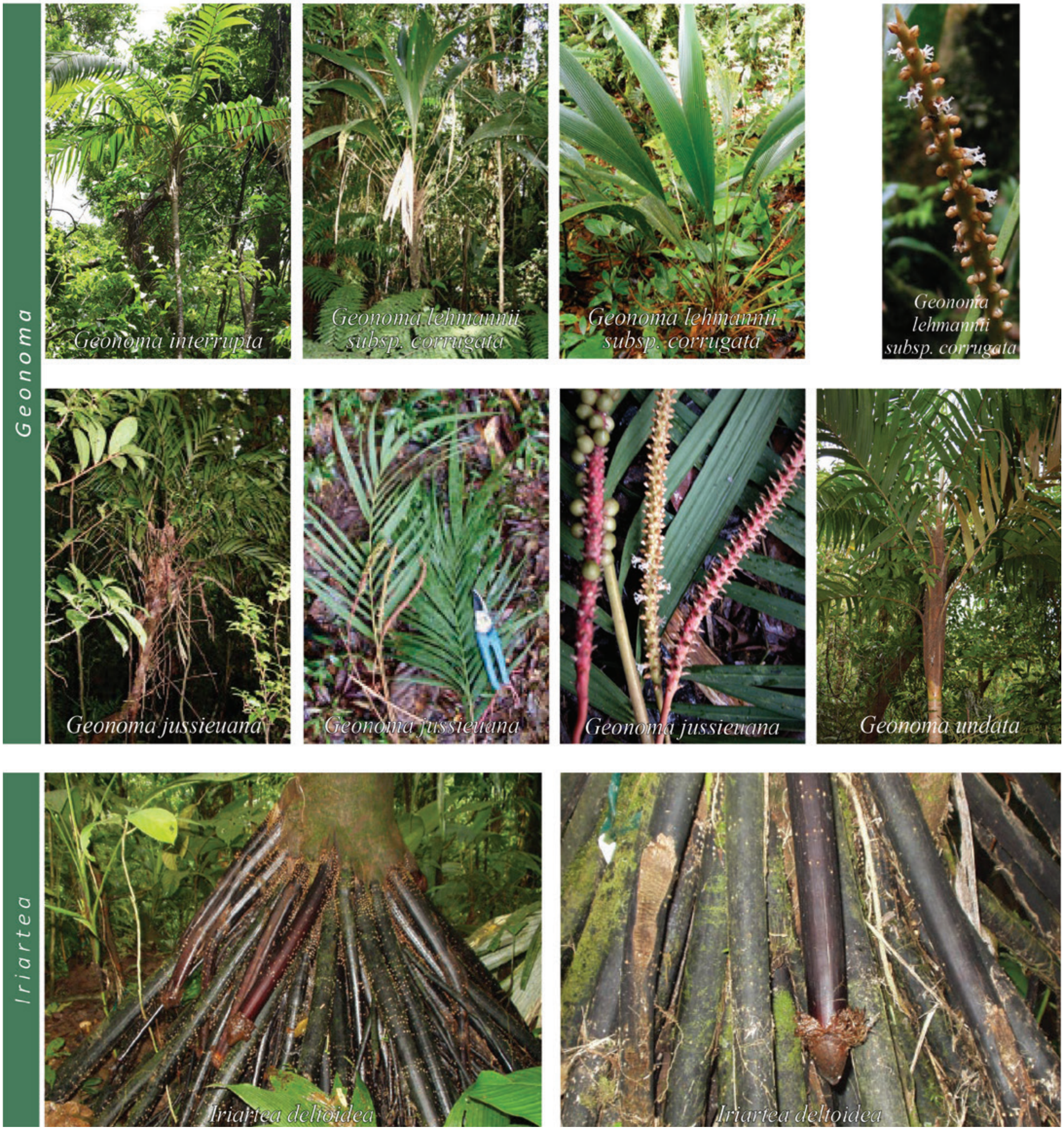

Palm Floristics - Plate 9.6

Palm Floristics - Plate 9.7

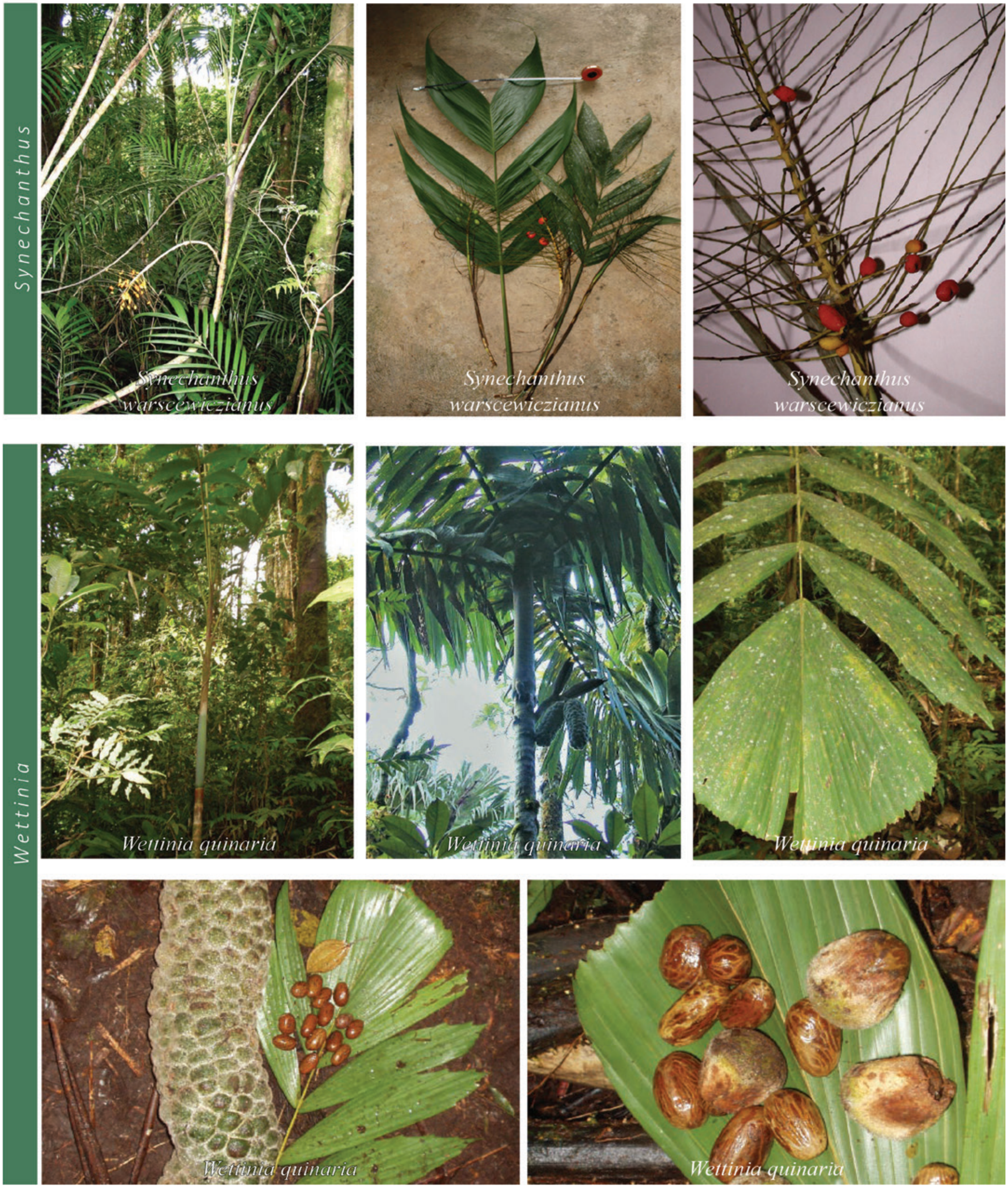

Index

Scientific Names Index

SUMMARY OF REQUIREMENTS FOR SMITHSONIAN CONTRIBUTIONS SERIES

For comprehensive guidelines and specifications, visit https://scholarlypress.si.edu.

ABSTRACTS must not exceed 300 words.

TEXT must be prepared in a recent version of Microsoft Word; use a Times font in 12 point for regular text; be double-spaced; and have 1" margins.

REQUIRED ELEMENTS are title page, abstract, table of contents, main text, and references.

FIGURES must be numbered sequentially (1, 2, 3, etc.) in the order called out; have components lettered consistently (in size, font, and style) and described in captions; include a scale bar or scale description, if appropriate; include any legends in or on figures rather than in captions. Figures must be original and must be submitted as individual TIF or EPS files.

FIGURE FILES must meet all required specifications in the Digital Art Preparation Guide. Color images should be requested only if required.

TAXONOMIC KEYS in natural history manuscripts should use the aligned-couplet form for zoology. If cross-referencing is required between key and text, do not include page references within the key, but number the keyed-out taxa, using the same numbers with their corresponding heads in the text.

SYNONYMY IN ZOOLOGY must use the short form (taxon, author, year:page), with full reference at the end of the manuscript under “References.”

REFERENCES should be in alphabetical order, and in chronological order for same-author entries. Each reference should be cited at least once in main text. Complete bibliographic information must be included in all citations. Examples of the most common types of citations can be found at SISP’s website under Resources/Guidelines & Forms.